

Hu · Wang

Dynamics  
of Controlled  
Mechanical Systems  
with Delayed Feedback

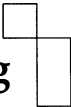


Springer

Hu • Wang

Dynamics of Controlled Mechanical Systems with Delayed Feedback

Springer-Verlag Berlin Heidelberg GmbH

**Engineering**  **ONLINE LIBRARY**

<http://www.springer.de/engine/>

المنارة للاستشارات

H. Y. Hu • Z. H. Wang

# Dynamics of Controlled Mechanical Systems with Delayed Feedback

With 74 Figures and 8 Tables



Springer

المنارة للاستشارات

Professor Haiyan Hu  
Nanjing University of Aeronautics and Astronautics  
Institute of Vibration Engineering Research  
210016 Nanjing  
P. R. China  
*e-mail: hhyae@nuaa.edu.cn*

Professor Zaihua Wang  
Nanjing University of Aeronautics and Astronautics  
Institute of Vibration Engineering Research  
210016 Nanjing  
P. R. China  
*e-mail: sjnj68@yahoo.com*

ISBN 978-3-642-07839-2

Library of Congress Cataloging-in-Publication-Data applied for

Die Deutsche Bibliothek – Cip-Einheitsaufnahme

Hu, Haiyan: Dynamics of controlled mechanical systems with delayed feedback :  
with 8 tables / H. Hu ; Z. Wang. - Berlin ; Heidelberg ; New York ; Barcelona ;  
Hong Kong ; London ; Milan ; Paris ; Tokyo : Springer 2002  
(Engineering online library)

ISBN 978-3-642-07839-2

ISBN 978-3-662-05030-9 (eBook)

DOI 10.1007/978-3-662-05030-9

This work is subject to copyright. All rights are reserved, whether the whole or part of the material is concerned, specifically the rights of translation, reprinting, reuse of illustrations, recitations, broadcasting, reproduction on microfilm or in any other way, and storage in data banks. Duplication of this publication or parts thereof is permitted only under the provisions of the German copyright Law of September 9, 1965, in its current version, and permission for use must always be obtained from Springer-Verlag. Violations are liable for prosecution under the German Copyright Law.

<http://www.springer.de>

© Springer-Verlag Berlin Heidelberg 2002

Originally published by Springer-Verlag Berlin Heidelberg New York in 2002

Softcover reprint of the hardcover 1st edition 2002

The use of general descriptive names, registered names trademarks, etc. in this publication does not imply, even in the absence of a specific statement, that such names are exempt from the relevant protective laws and regulations and therefore free for general use.

Typesetting: data delived by authors

Cover design: de'blik, Berlin

Printed on acid free paper SPIN: 10870766

62/3020/M - 5 4 3 2 1 0

المنارة للاستشارات

To Luna and Amanda  
for their love and support  
over the years

*Haiyan Hu*

To my wife Jun Shen  
and my daughter Jiayi  
for their love

*Zaihua Wang*

## Preface

Recent years have witnessed a rapid development of active control of various mechanical systems. With increasingly strict requirements for control speed and system performance, the unavoidable time delays in both controllers and actuators have become a serious problem. For instance, all digital controllers, analogue anti-aliasing and reconstruction filters exhibit a certain time delay during operation, and the hydraulic actuators and human being interaction usually show even more significant time delays. These time delays, albeit very short in most cases, often deteriorate the control performance or even cause the instability of the system, because the actuators may feed energy at the moment when the system does not need it. Thus, the effect of time delays on the system performance has drawn much attention in the design of robots, active vehicle suspensions, active tendons for tall buildings, as well as the controlled vibro-impact systems. On the other hand, the properly designed delay control may improve the performance of dynamic systems. For instance, the delayed state feedback has found its applications to the design of dynamic absorbers, the linearization of nonlinear systems, the control of chaotic oscillators, etc.

Most controlled mechanical systems with time delays can be modeled as the dynamic systems described by a set of ordinary differential equations with time delays. Finite as the number of unknowns in the ordinary differential equations is, the time delay implies that the change of a system state depends on the previous history of system. The solution space of such a set of delay differential equations, hence, is of infinite dimensions. This gives rise to a tough problem to the theoretical analysis of delayed dynamic systems. Over the past decades, numerous mathematicians have made great efforts to study the existence of solution, the oscillation property, the stability and the local bifurcation for delayed dynamic systems mainly in the frame of functional differential equations, and published a number of excellent monographs. Among them, the books such as (Hale 1977), (Qin et al. 1989), (Gopalsamy 1992), (Kuang 1993), (Hale and Lunel 1993) and (Diekmann et al. 1995) are a few to name.

From the viewpoint of an engineer, however, less attention has been paid to the practical problems associated with delayed dynamic systems, such as the modeling and parametric estimation, the stability analysis when some system parameters are to be designed, the dynamic performance of nonlinear delay systems, and so forth. Except for the works by (Stépán 1989) and (Moiola and Chen 1997), few monographs have been available for the engineers, who deal with various problems of control coming from mechanical engineering.

Motivated by the dynamics of controlled elastic structures, active vehicle suspensions and four-wheel-steering vehicles, the authors have been engaged in the dynamics of high dimensional mechanical systems with feedback time delays over the past five years. Summarized in this monograph are mainly recent advances of authors in the system modeling and simplification, the stability analysis of linear dynamic systems, the periodic vibration and bifurcation analysis of nonlinear dynamic systems, as well as the application of new approaches to controlled elastic structures and ground vehicles. The contents of the book are organized as following.

In Chapter 1, the models of a number of typical dynamic systems with time delays are presented first. Then, two parametric estimation techniques are given for the linear systems with short feedback time delays and the nonlinear systems with arbitrary feedback time delays, respectively. Afterwards, the identifiability problem of delayed dynamic systems is addressed.

Chapter 2 serves as an introduction to the theory of delay differential equations. It begins with the theorem of existence and uniqueness of a solution of initial value problem, and then outlines the fundamental properties of linear delay differential equations. Afterwards, it turns to the stability analysis of delay differential equations, offers a brief review for the important concepts and available methods, such as the Pontryakin theorem, the Hassard theorem, the Michailov criterion and the Nyquist diagram, with help of a number of illustrative examples.

The topics of Chapter 3 are the delay-independent stability of high dimensional linear systems with multiple time delays and the stability switches of high dimensional linear systems with an increase of a single time delay. Those high dimensional systems may have a number of parameters to be designed so that the stability analysis becomes a tough problem. On the basis of generalized Sturm theory, a simple, but systematic approach is presented to solve the tough problem. The approach is demonstrated through the stability analysis of a tall building model equipped with an active tendon, a quarter-car model of vehicle with an active suspension, as well as a four-wheel-steering vehicle with driver's delay.



Chapter 4 is devoted to the interval stability of high dimensional linear systems with a number of commensurate constant time delays. Based on the well-known edge theorem and the method of Dixon's resultant elimination, a new approach is presented for testing the interval Hurwitz stability of a non-polytopic family of quasi-polynomials. To demonstrate the approach, the interval Hurwitz stability is analyzed for a single-degree-of-freedom system with two commensurate time delays in the paths of displacement and velocity feedback, respectively.

In many applications, the time delays are much shorter than the shortest period of system vibration. If this is the case, the approximate approaches are preferable. Several approaches to the stability estimation are presented in Chapter 5, on the basis of perturbation of eigenvalues, for high dimensional linear systems with a short time delay in feedback. A criterion of interval stability is suggested by applying the Padé approximation to the exponential terms of time delay in the characteristic function of a linear system. In engineering, it is very natural and popular to simplify the controlled systems with a short time delay by replacing the delayed terms with their Taylor expansions. A detailed analysis in Chapter 5, together with the examples of both linear and nonlinear systems of single degree of freedom, indicates that this simplification must be implemented with great care.

From Chapter 6, the book turns to the nonlinear dynamics of controlled systems with time delays. To study the nonlinear dynamics of a system effectively, the mathematical model for the system should be as simple as possible. In Chapter 6, the theorem of central manifold and the theory of normal form are introduced first. Then, the central manifold theory is combined with the singular perturbation technique to simplify the nonlinear delay systems composed of a soft component and a rigid component. A typical example of this system is the quarter car model of vehicle with an active suspension.

For a nonlinear dynamic system, the periodic motion is usually the second most important topic, following the stability of equilibrium positions. Physically speaking, there are two important causes for the emergence of a periodic motion if the system is nonlinear. One is the well-known Hopf bifurcation at the equilibrium of an autonomous system, and the other is the either external or parametric periodic excitation in a non-autonomous system. In Chapter 7, the periodic motions owing to the two causes are discussed in detail. With help of the theory of the Hopf bifurcation, the periodic motions and their stability of an autonomous dynamic system under delayed control can be determined. Furthermore, if the gains of delayed feedback can be scaled as small parameters, the method of multiple scales can easily be used to analyze the dynamics of systems. In the case of strong feedback involving time delays, numerical analysis becomes a possibly unique,

but useful tool. The chapter presents a numerical approach to locate the periodic motion of nonlinear systems with a time delay.

In Chapter 8, the delayed control of nonlinear systems is outlined. As an example, the delayed resonator with velocity feedback is presented first to work as a vibration absorber. Then, the stabilization to a critically stable system is presented. Finally, controlling chaos, an interesting topic in the past two decades, is discussed through an example of the forced Duffing oscillator with delayed feedback.

The first author appreciates very much the kind host of Professors E. H. Dowell and L. N. Virgin to his sabbatical of 1996 in The Department of Mechanical Engineering and Material Science, Duke University, where he began to pay attention to the dynamics of mechanical systems with delayed control. Most results presented in this book come from the later projects supported in part by the National Natural Science Foundation of China under the Grants 59625511 and 19972025, and in part by the Ministry of Education under the Grant GG-130-10287-1593. The authors wish to acknowledge all of the help and encouragement they have received in the development of this book. Special thanks should be due to Dr. H. L. Wang and Dr. W. F. Zhang, who carefully read the manuscript of the book and made invaluable suggestions.

Haiyan Hu and Zaihua Wang  
Nanjing , March, 2002

# Contents

<b>1 Modeling of Delayed Dynamic Systems.....</b>	<b>1</b>
1.1 Mathematical Models .....	1
1.1.1 Dynamic Systems with Delayed Feedback Control .....	1
1.1.2 Dynamic Systems with Operator's Retardation .....	5
1.2 Experimental Modeling .....	9
1.2.1 Identification of Short Time Delays in Linear Systems .....	10
1.2.2 Identification of Arbitrary Time Delays in Nonlinear Systems.....	14
1.2.3 Discussions on Identifiability of Time Delays .....	21
<b>2 Fundamentals of Delay Differential Equations.....</b>	<b>27</b>
2.1 Initial Value Problems .....	27
2.1.1 Existence and Uniqueness of Solution .....	28
2.1.2 Solution of Linear Delay Differential Equations.....	33
2.2 Stability in the Sense of Lyapunov .....	37
2.2.1 The Lyapunov Methods.....	38
2.2.2 Method of Characteristic Function.....	42
2.2.3 Stability Criteria .....	47
2.3 Important Features of Delay Differential Equations.....	54
<b>3 Stability Analysis of Linear Delay Systems.....</b>	<b>59</b>
3.1 Delay-independent Stability of Single-degree-of-freedom Systems .....	60
3.1.1 Stability Criteria .....	61
3.1.2 Stability Criteria in Terms of Feedback Gains .....	66
3.2 The Generalized Sturm Criterion for Polynomials .....	70
3.2.1 Classical Sturm Criterion .....	70
3.2.2 Discrimination Sequence.....	72
3.2.3 Modified Sign Table.....	74
3.2.4 Generalized Sturm Criterion.....	75
3.3 Delay-independent Stability of High Dimensional Systems.....	76
3.4 Stability of Single-degree-of-freedom Systems with Finite Time Delays.....	86
3.4.1 Systems with Equal Time Delays.....	86
3.4.2 Systems with Unequal Time Delays.....	90
3.5 Stability Switches of High Dimensional Systems.....	91
3.5.1 Systems with a Single Time Delay.....	92
3.5.2 Systems with Commensurate Time Delays .....	98

3.6 Stability Analysis of an Active Chassis .....	102
3.6.1 A quarter Car Model of Suspension with a Delayed Sky-hook Damper ....	102
3.6.2 Four-wheel-steering Vehicle with a Time Delay in Drive's Response .....	109
<b>4 Robust Stability of Linear Delay Systems .....</b>	<b>115</b>
4.1 Robust Stability of a One-parameter Family of Quasi-polynomials .....	116
4.1.1 Non-convexity of the Set of Hurwitz Stable Quasi-polynomials .....	117
4.1.2 Sufficient and Necessary Conditions for Interval Stability .....	120
4.2 Edge Theorem for a Polytopic Family of Quasi-polynomials .....	124
4.2.1 Problem Formulation.....	125
4.2.2 Edge Theorem .....	127
4.2.3 Sufficient and Necessary Conditions .....	127
4.3 Dixon's Resultant Elimination .....	130
4.3.1 Dixon's Resultant Elimination.....	130
4.3.2 Robust $D$ -stability of One-parameter Family of Polynomials .....	136
4.4 Robust Stability of Systems with Uncertain Commensurate Delays .....	140
4.4.1 Problem Formulation.....	141
4.4.2 Stability of Vertex Quasi-polynomials .....	143
4.4.3 Stability of Edge Quasi-polynomials.....	145
4.4.4 A sufficient and Necessary Condition.....	147
4.4.5 An Illustrative Example .....	147
<b>5 Effects of a Short Time Delay on System Dynamics.....</b>	<b>151</b>
5.1 Stability Estimation of High Dimensional Systems.....	151
5.1.1 Distribution of Eigenvalues Subject to a Short Time Delay.....	152
5.1.2 Estimation of Eigenvalues.....	155
5.1.3 Illustrative Examples.....	158
5.1.4 A Relation of Orthogonality of Mode Shapes .....	167
5.2 Stability Test Based on the Padè Approximation .....	168
5.2.1 Test of Stability .....	168
5.2.2 Test of Interval Stability.....	176
5.3 Dynamics of Simplified Systems via the Taylor Expansion.....	179
5.3.1 Linear Systems with Delayed State Feedback.....	180
5.3.2 Nonlinear Systems with Delayed Velocity Feedback .....	182
<b>6 Dimensional Reduction of Nonlinear Delay Systems .....</b>	<b>189</b>
6.1 Decomposition of State Space of Linear Delay Systems.....	190
6.1.1 Spectrum of a Linear Operator .....	192
6.1.2 Decomposition of State Space.....	194
6.2 Dimensional Reduction for Stiff-soft Systems .....	198
6.2.1 A quarter Car Model as a Singularly Perturbed System.....	199
6.2.2 Center Manifold Reduction in Critical Cases.....	200
6.2.3 Reduction for Singularly Perturbed Differential Equations .....	202

6.3 Stability Analysis of an Active Suspension .....	205
6.3.1 Center Manifold Reduction .....	206
6.3.2 Computation of the Approximated Center Manifold.....	207
6.3.3 Stability Analysis .....	210
<b>7 Periodic Motions of Nonlinear Delay Systems .....</b>	<b>213</b>
7.1 The Hopf Bifurcation of Autonomous Systems.....	213
7.1.1 Theory of the Hopf Bifurcations .....	214
7.1.2 Decomposition of Bifurcating Solution.....	217
7.1.3 Bifurcating Solutions in Normal Form .....	219
7.2 Computation of Bifurcating Periodic Solutions .....	222
7.2.1 Method of the Fredholm Alternative .....	222
7.2.2 Stability of Bifurcating Periodic Solutions.....	227
7.2.3 Perturbation Method.....	230
7.3 Periodic Motions of a Duffing Oscillator with Delayed Feedback .....	234
7.3.1 Stability Switches of Equilibrium .....	235
7.3.2 Periodic Motion Determined by Method of Fredholm Alternative ..	237
7.3.3 Periodic Motion Determined by Method of Multiple Scales.....	243
7.4 Periodic Motions of a Forced Duffing Oscillator with Delayed Feedback ...	248
7.4.1 Primary Resonance.....	249
7.4.2 1/3 Subharmonic Resonance .....	254
7.5 Shooting Scheme for Locating Periodic Motions .....	259
7.5.1 Basic Concepts and Computation Scheme .....	259
7.5.2 Case Studies .....	262
<b>8 Delayed Control of Dynamic Systems.....</b>	<b>267</b>
8.1 Delayed Linear Feedback for Linear Systems .....	267
8.1.1 Delayed Linear Feedback and Artificial Damping .....	267
8.1.2 Delayed Resonator: A Tunable Vibration Absorber .....	269
8.2 Stabilization to Critically Stable Nonlinear Systems .....	272
8.2.1 Statement of Problem .....	274
8.2.2 Analysis on Stabilization .....	275
8.2.3 Case Studies .....	278
8.2.4 Discussions on Approximate Integrals .....	280
8.3 Controlling Chaotic Motion.....	282
8.3.1 Basic Idea .....	283
8.3.2 Choice of Feedback Gain .....	284
<b>References .....</b>	<b>287</b>
<b>Index .....</b>	<b>293</b>

# 1 Modeling of Delayed Dynamic Systems

Time delays may come from the retardation of either a controller or an actuator in controlled mechanical systems. In many cases, it is possible to establish the mathematical model for controlled mechanical systems with time delays from the principles of mechanics and the theory of control. However, this is not always the case. For a great number of practical systems, it is necessary to establish the model on the basis of experimental data. For instance, it would be impossible to establish the model for the retardation of human being if no experiments were made.

This chapter starts with a number of mathematical models for the controlled mechanical systems with feedback time delays to be studied in this book. Then, it presents two approaches to the parametric identification, including the estimation of time delays, of linear and nonlinear delayed dynamic systems respectively on the basis of experimental measurements, together with illustrative examples. As the identification of time delays is a tough problem, the chapter outlines the identifiability of time delays in some simple cases.

## 1.1 Mathematical Models

### 1.1.1 Dynamic Systems with Delayed Feedback Control

#### (1) *Linear dynamic systems*

The simplest physical model for controlled mechanical systems is a linear, time invariant system of single degree of freedom as shown in Fig. 1.1.1. The equation of motion of this system reads

$$m\ddot{x}(t)+c\dot{x}(t)+kx(t)=f(t)+g(t), \quad (1.1.1)$$

where the dot represents the derivative with respect to time  $t$ ,  $x(t)$  the displacement of system,  $f(t)$  the external force,  $g(t)$  the control force,  $m>0$  the mass coefficient,  $c\geq 0$  the damping coefficient and  $k>0$  the stiffness coefficient, respectively.

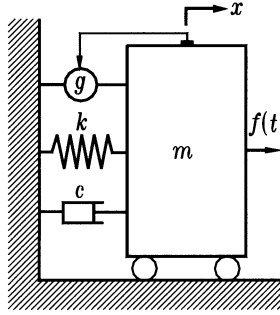


Fig. 1.1.1. A single degree of freedom system under feedback control

To improve the dynamic performance of the system, the control force  $g(t)$  is often designed as a linear state feedback as following

$$g(t) = \tilde{u}x(t) + \tilde{v}\dot{x}(t), \quad (1.1.2)$$

where  $\tilde{u}$  and  $\tilde{v}$  are constants, representing the feedback gains of displacement path and velocity path, respectively. Because of unavoidable time delays in both controllers and actuators, the actual control force should be modeled as

$$g(t) = \tilde{u}x(t - \tau_1) + \tilde{v}\dot{x}(t - \tau_2), \quad (1.1.3)$$

where  $\tau_1$  and  $\tau_2$  are the time delays in the paths of displacement and velocity feedback, respectively. Thus, Eq. (1.1.1) becomes

$$m\ddot{x}(t) + c\dot{x}(t) + kx(t) = \tilde{u}x(t - \tau_1) + \tilde{v}\dot{x}(t - \tau_2) + f(t). \quad (1.1.4)$$

In control engineering, the above dynamic equation is often cast as a set of first order differential equations with time delays, by using a state vector  $\mathbf{y} \equiv [x \quad \dot{x}]^T$ , as following

$$\dot{\mathbf{y}}(t) = \mathbf{A}_0\mathbf{y}(t) + \mathbf{A}_1\mathbf{y}(t - \tau_1) + \mathbf{A}_2\mathbf{y}(t - \tau_2) + \mathbf{f}(t), \quad (1.1.5)$$

where

$$\mathbf{A}_0 \equiv \begin{bmatrix} 0 & 1 \\ -k/m & -c/m \end{bmatrix}, \quad \mathbf{A}_1 \equiv \begin{bmatrix} 0 & 0 \\ \tilde{u}/m & 0 \end{bmatrix}, \quad \mathbf{A}_2 \equiv \begin{bmatrix} 0 & 0 \\ 0 & \tilde{v}/m \end{bmatrix}, \quad \mathbf{f}(t) \equiv \begin{bmatrix} 0 \\ f(t) \end{bmatrix}. \quad (1.1.6)$$

A more general form of Equation (1.1.5) reads

$$\dot{\mathbf{y}}(t) = \sum_{k=0}^l \mathbf{A}_k\mathbf{y}(t - \tau_k) + \mathbf{f}(t), \quad \mathbf{y} \in R^n, \quad (1.1.7)$$

where  $0 < \tau_1 < \dots < \tau_l$  are a set of time delays. This is a widely used model for linear systems in control engineering.

An example of Eq. (1.1.7) is the truncated modal equation of a tall structure equipped with *active tendon*, which is a new technique in structural control. As shown in (Zhang et al. 1993), the whole system can be modeled as a three-dimensional linear delay differential equation

$$\begin{cases} \dot{y}_1(t) = y_2(t), \\ \dot{y}_2(t) = -\omega_n^2 y_1(t) - 2\zeta\omega_n y_2(t) - y_3(t) + f(t), \\ \dot{y}_3(t) = -\alpha y_3(t) + \beta y_1(t - \tau_1) + \gamma y_2(t - \tau_2). \end{cases} \quad (1.1.8)$$

The first two differential equations in Eq. (1.1.8) govern the fundamental modal state of tall structure, while the third one governs the output of hydraulic actuator according to the modal state feedback. Here,  $y_1$  and  $y_2$  represent the fundamental modal displacement and velocity,  $y_3$  the control force,  $f(t)$  the external force,  $\omega_n > 0$  the fundamental natural frequency,  $\zeta > 0$  the corresponding damping ratio,  $\alpha > 0$  the time constant of hydraulic actuator,  $\beta$  and  $\gamma$  the feedback gains of modal displacement and modal velocity,  $\tau_1 > 0$  and  $\tau_2 > 0$  the time delays caused mainly by the hydraulic actuator, respectively. Equation (1.1.8) can be written in the form of Eq. (1.1.7) with

$$A_0 \equiv \begin{bmatrix} 0 & 1 & 0 \\ -\omega_n^2 & -2\zeta\omega_n & -1 \\ 0 & 0 & -\alpha \end{bmatrix}, \quad A_1 \equiv \begin{bmatrix} 0 & 0 & 0 \\ 0 & 0 & 0 \\ \beta & 0 & 0 \end{bmatrix}, \quad A_2 \equiv \begin{bmatrix} 0 & 0 & 0 \\ 0 & 0 & 0 \\ 0 & \gamma & 0 \end{bmatrix}, \quad f(t) \equiv \begin{bmatrix} 0 \\ f(t) \\ 0 \end{bmatrix}. \quad (1.1.9)$$

## (2) Nonlinear dynamic systems

In practice, a great number of dynamic models of controlled mechanical systems are nonlinear by nature. The nonlinearity may come from the flexible components undergoing large deformation, the backlash and the friction in the interface of two components, the saturation of controllers and actuators, and so on.

A simple, but widely used model for the nonlinear dynamic systems with delayed state feedback is the Duffing oscillator governed by

$$m\ddot{x}(t) + c\dot{x}(t) + kx(t) + \mu kx^3(t) = \tilde{u}x(t - \tau) + \tilde{v}\dot{x}(t - \tau) + f_0 \cos \omega t, \quad (1.1.10)$$

where  $\mu \neq 0$  characterizes the cubic nonlinearity, while other system parameters are similar to those in Eq. (1.1.4). This model, for instance, can be used to describe the single mode dynamics of a slender beam or a flexible plate with a piezoelectric pad equipped for vibration reduction when the beam or the plate undergoes a large deflection.



Because of the complexity of nonlinear dynamic analysis, the mathematical model of a nonlinear system should be as simple as possible. Hence, Eq. (1.1.10) is often re-scaled before the analysis. For example, the time  $t$  and the time delay  $\tau$  in Eq. (1.1.10) can be replaced, owing to  $m > 0$  and  $k > 0$ , with the dimensionless ones

$$\sqrt{\frac{k}{m}}t \rightarrow t, \quad \sqrt{\frac{k}{m}}\tau \rightarrow \tau \tag{1.1.11}$$

such that Equation (1.1.10) is recast as

$$\ddot{x}(t) + 2\zeta \dot{x}(t) + x(t) + \mu x^3(t) = ux(t-\tau) + v\dot{x}(t-\tau) + f \cos \lambda t, \tag{1.1.12}$$

where the dot represents the derivative with respect to the new time  $t$ , whereas all the parameters in Eq. (1.1.12) are also scaled to dimensionless ones as following

$$\zeta \equiv \frac{c}{2\sqrt{mk}}, \quad f \equiv \frac{f_0}{k}, \quad \lambda \equiv \omega \sqrt{\frac{m}{k}}, \quad u \equiv \frac{\tilde{u}}{k}, \quad v \equiv \frac{\tilde{v}}{\sqrt{mk}}. \tag{1.1.13}$$

Compared with Eq. (1.1.10), the number of system parameters in Eq. (1.1.12) has been decreased by two.

In vehicle engineering, the active control of vibration has found its application since 1980's when a number of contradictive requirements of performance, such as the ride comfort, suspension space and contact force of tires, should be met simultaneously for various road profiles. The *active suspension* compensates the motion of vehicle body through the use of hydraulic actuators and controllers. According to the design of load distribution, it is reasonable to look at the so-called *quarter car model* for the vertical vibration of active suspensions as shown in Fig. 1.1.2. In this model, the nonlinearity of tires is often taken into account so as to describe the system dynamics properly.

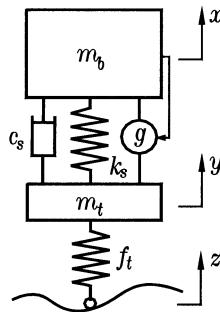


Fig. 1.1.2. A quarter car model of active suspension

The equation of motion of the quarter car model yields

$$\begin{cases} m_b \ddot{x}(t) + c_s [\dot{x}(t) - \dot{y}(t)] + k_s [x(t) - y(t)] + g = 0, \\ m_i \ddot{y}(t) + c_s [\dot{y}(t) - \dot{x}(t)] + k_s [y(t) - x(t)] + f_t(y(t) - z(t)) - g = 0, \end{cases} \quad (1.1.14)$$

where  $x$  represents the vertical displacement of vehicle body with mass  $m_b$ ,  $y$  the vertical displacement of the unsprung mass  $m_i$ ,  $z$  the road disturbance,  $k_s \geq 0$  and  $c_s \geq 0$  the coefficients of stiffness and damping of the suspension,  $f_t(\cdot)$  the restoring force of tire, which is a nonlinear function in the relative displacement  $y - z$ .

The simplest control strategy for active suspensions is based on the concept of *sky-hook damper*. That is, the control force should like the restoring force of a linear dashpot between the vehicle body and an imagined fixed frame such that

$$g = \tilde{v} \dot{x}(t - \tau), \quad (1.1.15)$$

where  $\tilde{v}$  is the feedback gain and  $\tau$  is the time delay owing to the controller and the hydraulic actuator. In some studies, Eq. (1.1.15) has been generalized to

$$g = \tilde{u} x(t - \tau) + \tilde{v} \dot{x}(t - \tau). \quad (1.1.16)$$

Substituting Eq. (1.1.15) or Eq. (1.1.16) into Eq. (1.1.14) gives a set of nonlinear delay differential equations.

As done in (Palkovics and Venhovens 1992), the quarter car model of active suspension can be further simplified to a forced Duffing oscillator if the unsprung mass, compared with the mass of vehicle body, is relatively small enough and can be neglected. In addition, the number of system parameters can also be reduced by re-scaling procedure.

An important feature of nonlinear dynamical systems is their possible chaotic outputs under deterministic inputs. To remove or utilize the chaotic motions of nonlinear systems, many active control strategies have been developed. Among them, the delayed linear feedback has proved itself a very powerful tool, see Section 8.3. The nonlinear systems equipped with this control should be certainly modeled by nonlinear delay differential equations.

### 1.1.2 Dynamic Systems with Operator's Retardation

If a dynamic system includes any interaction between a man and a machine, the retardation of operator has to be taken into account in the dynamic analysis when the time delay in retardation is not much shorter than the fundamental period of

machine. A well-known example is the steering dynamics of a vehicle at high speed. To deal with this sort of problems in later chapters, the mathematical model of a *four-wheel-steering vehicle*, or *4WS vehicle* for short, is established here with the time delay in driver's response taken into consideration.

The vehicle model shown in Fig. 1.1.3 includes a symmetric rigid body of mass  $m$  with two identical front wheels and two identical rear wheels. It is moving at a constant speed  $U$ . To study the steering dynamics of the vehicle moving at a constant speed, only the lateral and yaw dynamic equations of vehicle should be considered, while the longitudinal dynamic equation can be neglected.

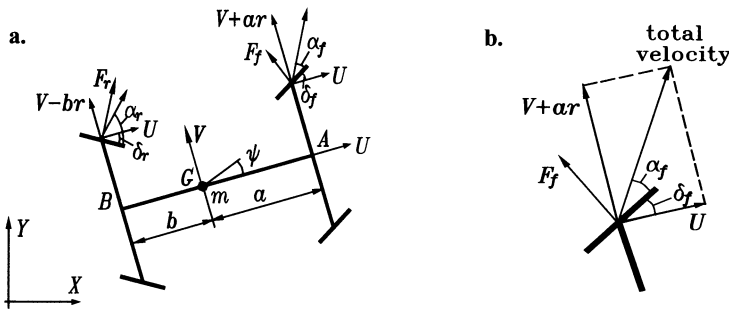


**Fig. 1.1.3.** A simple model for four-wheel-steering vehicles; **a.** vehicle in a fixed frame of coordinates, **b.** zoom view of a front wheel

Let  $G$  denote the center of mass, where a coordinate frame fixed on the vehicle body originates. The lateral velocity  $V$  and the yaw angular velocity  $r$  of the vehicle yield

$$\begin{cases} m(\dot{V} + rU) = 2F_f \cos \delta_f + 2F_r \cos \delta_r, \\ I_z \dot{r} = 2aF_f \cos \delta_f - 2bF_r \cos \delta_r, \end{cases} \quad (1.1.17)$$

where  $I_z$  is the inertia moment of rotation of the vehicle body with respect to the vertical axis  $z$ ,  $a$  and  $b$  are the distances from  $G$  to the front and rear axles,  $\delta_f$  and  $\delta_r$  are the steering angles applied on the front and rear wheels,  $F_f$  and  $F_r$  are the lateral forces due to the contact between the tyre and the road surface at each front and rear wheel. An interesting fact is that the dynamic equations of vehicle are independent of the width of vehicle if the vehicle and the road are assumed to be symmetric with respect to plane  $AB$ .

The lateral contact force is a function of the physical properties of the tyre and the corresponding side-slip angle  $\alpha_f$  or  $\alpha_r$ , observed on the front wheel or rear

wheel, respectively. These sideslip angles of wheels can be determined according to the simple geometric relations shown in Fig. 1.1.3 as follows

$$\alpha_f = \arctan\left(\frac{V+ar}{U}\right) - \delta_f, \quad \alpha_r = \arctan\left(\frac{V-br}{U}\right) - \delta_r. \quad (1.1.18)$$

The most popular tyre model is the truncated *Magic formula* proposed in (Pacejka 1989). Here, the third order truncation of the formula is used

$$F_f = -C_1\alpha_f + C_3\alpha_f^3, \quad F_r = -D_1\alpha_r + D_3\alpha_r^3, \quad (1.1.19)$$

where  $C_1$ ,  $C_3$ ,  $D_1$  and  $D_3$  are positive parameters.

Equations (1.1.17), (1.1.18) and (1.1.19) constitute a set of closed differential equations in unknown variables  $V$  and  $r$  to describe the lateral and yaw dynamics of the four-wheel-steering vehicle in the case of open loop. That is, the steering angles  $\delta_f$  and  $\delta_r$  are regarded as the independent input of the vehicle and the interaction of driver is not taken into account.

A popular control strategy is to steer the rear wheels on the basis of a pre-determined function as below

$$\delta_r = k_\delta \delta_f + k_r r. \quad (1.1.20)$$

There are two versions of this control strategy. One is the following linear strategy

$$k_\delta = \frac{-b + \frac{ma}{C_1(a+b)}U^2}{a + \frac{mb}{D_1(a+b)}U^2}, \quad k_r = 0. \quad (1.1.21)$$

It features that  $k_\delta \rightarrow -b/a < 0$  when  $U \rightarrow 0$  and  $k_\delta \rightarrow aD_1/bC_1 > 0$  when  $U \rightarrow +\infty$ . The other version is the bilinear strategy with the coefficients given by

$$k_\delta = \frac{C_1}{D_1} \neq 1, \quad k_r = \frac{2(aC_1 - bD_1) + mU^2}{2D_1U}. \quad (1.1.22)$$

An important feature of the bilinear strategy is the constant steering ratio  $k_\delta \neq 1$ .

The interaction between the driver and the vehicle should be studied in the fixed global frame of coordinates  $(x, y, \psi)$  as shown in Fig1.1.4, where  $(x, y)$  represents  $G$ , the mass center of vehicle, in driving and  $\psi$  the heading angle of vehicle. Obviously, the following relation holds

$$\begin{cases} \dot{y} = V \cos \psi + U \sin \psi, \\ \dot{\psi} = r. \end{cases} \quad (1.1.23)$$

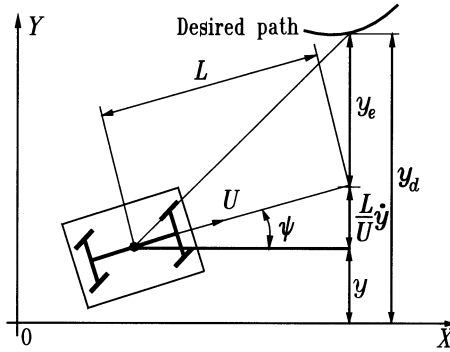


Fig. 1.1.4. The geometric relation in Eq. (1.1.24)

Many models have been proposed to describe the *perceptual delay* of the driver, who senses the deviation from the desired path and steers the vehicle to reduce the deviation. The simplest model in (Nagai and Mitschke 1987) reads

$$\begin{cases} y_e(t + \tau_p) = y_d(t + \tau_p) - y(t) - \frac{L}{U} \dot{y}(t), \\ \tau_s \dot{\delta}_f(t) + \delta_f(t) = K_m y_e(t - \tau_d). \end{cases} \quad (1.1.24)$$

Equation (1.1.24) describes the deviation from the desired path and the retard of both driver and steering mechanism, respectively. As shown in Fig. 1.1.4,  $L$  represents the preview distance,  $y_d$  the desired lateral displacement,  $y_e$  the error between desired and actual lateral displacement,  $\tau_s > 0$  the time delay of the steering mechanism,  $\tau_p > 0$  the preview time of the driver,  $\tau_d > 0$  the time delay of the driver,  $K_m$  the steering gain, respectively.

Substituting the first equation in Eq. (1.1.24) into the second one gives a linear delay differential equation in steering angle  $\delta_f$

$$\tau_s \dot{\delta}_f(t) + \delta_f(t) = K_m [y_d(t - \tau_d) - y(t - \tau) - \frac{L}{U} \dot{y}(t - \tau)], \quad (1.1.25)$$

where  $\tau = \tau_p + \tau_d > 0$  represents the total time delay of driver's retardation in the vehicle-driver system.

In summary, the motion of the four-wheel-steering vehicle-driver system yields a set of non-autonomous delay differential equations in five unknown state variables  $(V, r, y, \psi, \delta_f)$  as following



$$\left\{ \begin{array}{l} m\dot{V} = -mUr + 2F_f(V, r, \delta_f) \cos \delta_f + 2F_r(V, r, \delta_f) \cos(k_s \delta_f + k_r r), \\ I_z \dot{r} = 2aF_f(V, r, \delta_f) \cos \delta_f - 2bF_r(V, r, \delta_f) \cos(k_s \delta_f + k_r r), \\ \dot{y} = V \cos \psi + U \sin \psi, \\ \dot{\psi} = r, \\ \dot{\delta}_f = -\frac{\delta_f}{\tau_s} - \frac{K_m}{\tau_s} [y(t-\tau) + \frac{L}{U} V(t-\tau) \cos \psi(t-\tau) + L \sin \psi(t-\tau)] + f(t), \end{array} \right. \quad (1.1.26)$$

where  $F_f(V, r, \delta_f)$  and  $F_r(V, r, \delta_f)$  can be determined from Eqs. (1.1.18), (1.1.19) and (1.1.20), while

$$f(t) \equiv \frac{K_m}{\tau_s} y_d(t - \tau_d) \quad (1.1.27)$$

is regarded as an external excitation in the dynamic analysis.

## 1.2 Experimental Modeling

An important task in experimental modeling of delayed dynamic systems is to determine the time delays. Compared with the coefficients of inertial, stiffness and damping, as well as the feedback gains, the time delays should be regarded as the special system parameters in experimental modeling. Even for a linear, time invariant, delayed dynamic system, the identification of time delays from experimental data is always a tough problem of nonlinear parametric estimations, and hence, very sensitive to the noise in the measurements.

Most previous publications only dealt with the time delays in the input of a system. See, for example, (Liang and Christensen 1976), (Elnaggar et al. 1989), and (Ferretti et al. 1991, 1994). These studies were confined to the case when the ratio of time delay to be identified and sampling interval is an integer. To increase the accuracy of estimated time delays, the sampling interval should be short enough. However, the excessively short sampling intervals may produce the ill-conditioned problems in identification. Only a few studies were made to identify the feedback time delays, mainly the short time delays in linear systems. For example, (Tuch et al. 1994) studied the experimental modeling of a linear, time invariant system with short time delays. This section will be devoted to the identifi-

cation of time delays of both linear and nonlinear delayed systems, as well as the identifiability of time delays.

### 1.2.1 Identification of Short Time Delays in Linear Systems

#### (1) Approach based on frequency response function

The frequency response function of a linear, time invariant system involves a number of delay induced exponential functions, each of which can be approximated by a truncated Taylor expansion or a rational fraction, such as the Padé approximation in (Xu 1990). Hence, the frequency response function of the original system with time delays can be first approximated as the frequency response function of a delay free system of extended order, then the system parameters and time delays can be extracted.

To elucidate the above idea as simple as possible, we consider a linear delay system of single degree of freedom governed by Eq. (1.1.4). By performing the Fourier transform on both sides of Eq. (1.1.4), we have the frequency response function of system

$$H(\omega, \tau_1, \tau_2) = \frac{1}{k + ic\omega - m\omega^2 - ue^{-i\omega\tau_1} - iv\omega e^{-i\omega\tau_2}}, \quad (1.2.1)$$

where the conditions  $u < k$  and  $v < c$  are required for the stability of system free of time delays. Substituting the Euler formula for the exponential functions above yields

$$H(\omega, \tau_1, \tau_2) = \frac{1}{a(\omega, \tau_1, \tau_2) - m\omega^2 + ib(\omega, \tau_1, \tau_2)}, \quad (1.2.2)$$

where

$$\begin{cases} a(\omega, \tau_1, \tau_2) \equiv k - u\cos\omega\tau_1 - v\omega\sin\omega\tau_2, \\ b(\omega, \tau_1, \tau_2) \equiv c\omega + u\sin\omega\tau_1 - v\omega\cos\omega\tau_2. \end{cases} \quad (1.2.3)$$

If the time delays are short enough, the frequency range of concern yields the conditions  $0 < \omega\tau_1 \ll 1$  and  $0 < \omega\tau_2 \ll 1$ . In this case, the truncated Taylor expansion of Eq. (1.2.3) is

$$\left\{ \begin{aligned} a(\omega, \tau_1, \tau_2) &= k - u \left( 1 - \frac{1}{2} \omega^2 \tau_1^2 + \frac{1}{24} \omega^4 \tau_1^4 + \dots \right) - v \omega \left( \omega \tau_2 - \frac{1}{6} \omega^3 \tau_2^3 + \dots \right) \\ &= k - u + \omega^2 \left( \frac{u}{2} \tau_1^2 - v \tau_2 \right) - \frac{\omega^4}{6} \left( \frac{u}{4} \tau_1^4 - v \tau_2^3 \right) + \dots, \\ b(\omega, \tau_1, \tau_2) &= c \omega + u \left( \omega \tau_1 - \frac{1}{6} \omega^3 \tau_1^3 + \dots \right) - v \omega \left( 1 - \frac{1}{2} \omega^2 \tau_2^2 + \frac{1}{24} \omega^4 \tau_2^4 + \dots \right) \\ &= \omega \left( c + u \tau_1 - v \right) - \frac{\omega^3}{2} \left( \frac{u}{3} \tau_1^3 - v \tau_2^2 \right) + \frac{\omega^5}{24} \left( \frac{u}{5} \tau_1^5 - v \tau_2^4 \right) + \dots \end{aligned} \right. \quad (1.2.4)$$

Substituting the above equation into Eq. (1.2.2) gives an approximation of frequency response function

$$H(\omega, \tau_1, \tau_2) = \frac{1}{a_0 + (i\omega)a_1 + (i\omega)^2 a_2 + (i\omega)^3 a_3 + \dots}, \quad (1.2.5)$$

where

$$\left\{ \begin{aligned} a_0 &\equiv k - u, \end{aligned} \right. \quad (1.2.6a)$$

$$\left\{ \begin{aligned} a_1 &\equiv c + u \tau_1 - v, \end{aligned} \right. \quad (1.2.6b)$$

$$\left\{ \begin{aligned} a_2 &\equiv m - \frac{u}{2} \tau_1^2 + v \tau_2, \end{aligned} \right. \quad (1.2.6c)$$

$$\left\{ \begin{aligned} a_3 &\equiv \frac{u}{6} \tau_1^3 - \frac{v}{2} \tau_2^2. \end{aligned} \right. \quad (1.2.6d)$$

In practice, the parameters  $m$ ,  $c$  and  $k$  can first be extracted from a test of open-loop system. Then, the frequency response function of the closed-loop system is measured and used to fit Eq. (1.2.5) by using the technique of orthogonal polynomials so that the coefficients  $a_r$ ,  $r=0,1,2,3$  are extracted. Finally, the parameters  $u, v, \tau_1, \tau_2$  can be determined from Eq. (1.2.6) as following.

The first two equations in Eq. (1.2.6) give

$$u = k - a_0, \quad (1.2.7)$$

$$v = c + (k - a_0) \tau_1 - a_1. \quad (1.2.8)$$

Substituting these two equation into Eq. (1.2.6c) yields

$$\tau_2 = \frac{1}{c - a_1 + (k - a_0) \tau_1} \left( a_2 - m + \frac{k - a_0}{2} \tau_1^2 \right). \quad (1.2.9)$$

By substituting Eqs. (1.2.7), (1.2.8) and (1.2.9) into Eq. (1.2.6d), we have a polynomial equation in the unknown  $\tau_1$



$$\tau_1^4 + \frac{4(c-a_1)}{k-a_0} \tau_1^3 - \frac{12(a_2-m)}{k-a_0} \tau_1^2 - \frac{24a_3}{k-a_0} \tau_1 - \frac{24a_3(c-a_1)+12(a_2-m)^2}{(k-a_0)^2} = 0. \quad (1.2.10)$$

The minimal positive root  $\tau_1$  of Eq. (1.2.10) can easily be determined by using numerical techniques. Substituting  $\tau_1$  into Eqs. (1.2.8) and (1.2.9) gives  $v$  and  $\tau_2$ , respectively.

The feasibility of this approach is subject to the following three conditions. First, the time delays should satisfy  $0 < \omega\tau_1 \ll 1$  and  $0 < \omega\tau_2 \ll 1$  in the frequency range of curve fitting, usually in the frequency range of a dominant resonance. Second, the identification error of coefficients  $a_r$ ,  $r=0,1,2,3$  should be so small that Eq. (1.2.10) has positive real roots, or equivalently the following polynomial equation of order 8 has at least a pair of real roots

$$y^8 + \frac{4(c-a_1)}{k-a_0} y^6 - \frac{12(a_2-m)}{k-a_0} y^4 - \frac{24a_3}{k-a_0} y^2 - \frac{24a_3(c-a_1)+12(a_2-m)^2}{(k-a_0)^2} = 0. \quad (1.2.11)$$

The conditions for this fact can be derived according to the generalized Sturm criterion presented in Subsection 3.2.4. Finally, the stability of a practical system requires that the estimated coefficients yield the following inequalities  $a_r > 0$ ,  $r=0,1,2,3$ , see Subsection 5.3.1. If the system free of time delay is asymptotically stable, the first inequality holds. The second and the third inequalities also hold true provided that the time delays are short enough. Owing to the Taylor expansion, however, the last inequality  $a_3 > 0$  requires an extra condition

$$u\tau_1^3 - 3v\tau_2^2 > 0. \quad (1.2.12)$$

This is undoubtedly a shortcoming.

If the feedback gains  $u$  and  $v$  are known, it is possible to simplify the above procedure. From Eqs. (1.2.6b) and (1.2.6c), we have

$$\begin{cases} \tau_1 = \frac{a_1 + v - c}{u}, \\ \tau_2 = \frac{2(a_2 - m) + u\tau_1^2}{2v} = \frac{2u(a_2 - m) + (a_1 + v - c)^2}{2uv}. \end{cases} \quad (1.2.13)$$

The corresponding identifiability condition for time delays is

$$\begin{cases} u(a_1 + v - c) > 0, \\ uv[2u(a_2 - m) + (a_1 + v - c)^2] > 0. \end{cases} \quad (1.2.14)$$

If the feedback gains are unknown, but  $\tau_1 = \tau_2$  or  $\tau_1 = 0$  (or  $\tau_2 = 0$ ) holds true, the time delays can be determined from the first three equations in Eq. (1.2.6).

Finally, great care should be taken because this approach based on the truncated Taylor expansion with respect to short time delays has a number of shortcomings. First, the delay free model of extended orders may not be equivalent to the original system with time delays. The extra condition in Eq. (1.2.12) is an example. Second, the number of parameters to be identified increases with an increase of system order. This gives rise to the difficulty of both parametric identification and extraction of time delays from the identified parameters.

## (2) Approach based on modal parameters

Given the feedback gains, time delays can also be extracted from the modal parameters of closed-loop system. For this purpose, let  $a_3=0$  in Eq. (1.2.5). Then, the following natural frequency and damping ratio are defined for the system having the feedback free of time delays and the system with delayed feedback respectively

$$\begin{cases} \bar{\omega}_n \equiv \sqrt{\frac{k-u}{m}}, \\ \bar{\zeta} \equiv \frac{c-v}{2\sqrt{m(k-u)}}, \end{cases} \quad (1.2.15)$$

$$\begin{cases} \omega_n \equiv \sqrt{\frac{k-u}{m - \frac{u}{2}\tau_1^2 + v\tau_2}} \approx \bar{\omega}_n \left(1 + \frac{u}{4m}\tau_1^2 - \frac{v}{2m}\tau_2\right), \\ \zeta \equiv \frac{c+u\tau_1-v}{2\sqrt{(m - \frac{u}{2}\tau_1^2 + v\tau_2)(k-u)}} \approx \bar{\zeta} \left(1 + \frac{u}{c-v}\tau_1 - \frac{v}{2m}\tau_2\right). \end{cases} \quad (1.2.16)$$

Equation (1.2.16) can be rewritten as

$$\begin{cases} \frac{u}{4m}\tau_1^2 - \frac{v}{2m}\tau_2 + 1 - \frac{\omega_n}{\bar{\omega}_n} = 0, \\ \frac{u}{c-v}\tau_1 - \frac{v}{2m}\tau_2 + 1 - \frac{\zeta}{\bar{\zeta}} = 0. \end{cases} \quad (1.2.17)$$

Eliminating  $\tau_2$  from Eq. (1.2.17) gives

$$\frac{u}{4m}\tau_1^2 - \frac{u}{c-v}\tau_1 + \left(\frac{\zeta}{\bar{\zeta}} - \frac{\omega_n}{\bar{\omega}_n}\right) = 0. \quad (1.2.18)$$

Solving this equation for the minimal positive root  $\tau_1$  and substituting  $\tau_1$  into Eq. (1.2.17), we obtain  $\tau_2$ .

This approach has less accuracy than the approach based on the frequency response function since the condition  $a_3=0$  is imposed. However, it enables one to gain an insight into the effect of time delays on the system dynamics.

### 1.2.2 Identification of Arbitrary Time Delays in Nonlinear Systems

Consider an  $n$ -dimensional nonlinear system with delayed feedback

$$M\ddot{\mathbf{x}}(t) = \mathbf{f}(\mathbf{x}(t), \dot{\mathbf{x}}(t), \mathbf{x}(t-\tau_1), \dot{\mathbf{x}}(t-\tau_2), \mathbf{p}), \quad (1.2.19)$$

where  $M \in R^{n \times n}$  is the mass matrix,  $\mathbf{x} \in R^n$  the vector of generalized displacement,  $\mathbf{f} \in R^n$  the vector of generalized force,  $\tau_1$  and  $\tau_2$  the time delays in the displacement and velocity feedback,  $\mathbf{p} \in R^l$  the vector composed of  $l$  parameters to be identified. If the mass matrix  $M$ , the parametric vector  $\mathbf{p}$ , and the time delays  $\tau_1$  and  $\tau_2$  are replaced with the identified results  $\hat{M}$ ,  $\hat{\mathbf{p}}$ ,  $\hat{\tau}_1$  and  $\hat{\tau}_2$ , the residual error vector of Eq. (1.2.19) reads

$$\mathbf{e} \equiv \hat{M}\ddot{\mathbf{x}}(t) - \mathbf{f}(\mathbf{x}(t), \dot{\mathbf{x}}(t), \mathbf{x}(t-\hat{\tau}_1), \dot{\mathbf{x}}(t-\hat{\tau}_2), \hat{\mathbf{p}}). \quad (1.2.20)$$

To minimize the residual error, it is necessary to know the derivatives of generalized displacement  $\mathbf{x}$ . In order to avoid the numerical differentiation or integration, the  $r$ -th order derivative filter  $L_r(D)$  can be introduced to obtain the approximate displacement vector  $\mathbf{x}_f$ , the corresponding velocity vector  $\dot{\mathbf{x}}_f$  and acceleration vector  $\ddot{\mathbf{x}}_f$ , see (Zhang 2002). Thus, the residual error vector can be written as

$$\mathbf{e}_f \equiv \hat{M}\ddot{\mathbf{x}}_f(t) - \mathbf{f}(\mathbf{x}_f(t), \dot{\mathbf{x}}_f(t), \mathbf{x}_f(t-\hat{\tau}_1), \dot{\mathbf{x}}_f(t-\hat{\tau}_2), \hat{\mathbf{p}}). \quad (1.2.21)$$

If an objective function is defined as

$$J \equiv \sqrt{\sum_j \mathbf{e}_{fj}^T \mathbf{e}_{fj}}, \quad (1.2.22)$$

where  $\mathbf{e}_{fj}$  is the residual error vector at the moment  $t=t_j$ , the parametric identification can be regarded as a problem of minimization for  $\hat{M}$ ,  $\hat{\mathbf{p}}$ ,  $\hat{\tau}_1$  and  $\hat{\tau}_2$  in a given region of parametric space. This is a problem of global optimization with possible local optimizations.

Among the approaches to the global optimization, the *Genetic Algorithms*, often abbreviated as GA, have received great attention since 1980's because of their advantages superior in numbers. The genetic algorithms are based on the mechanism of natural selection and evolution. They combine the principle of survival of

the fittest individual among population with a structured and randomized information exchange to form a search algorithm with some of the innovative flair of human search.

The genetic algorithm starts from a set of random individuals of population and proceeds repeatedly from generation to generation through three basic genetic operators, i.e., reproduction, crossover and mutation, so that the quality of population is optimized step by step. Figure 1.2.1 shows the diagram of a typical genetic algorithm. The basic element processed by a genetic algorithm is the string formed by catenating sub-strings, each of which is the binary coding of a parameter. That is, each string represents a parameter. In what follows, the three basic genetic operators are outlined.

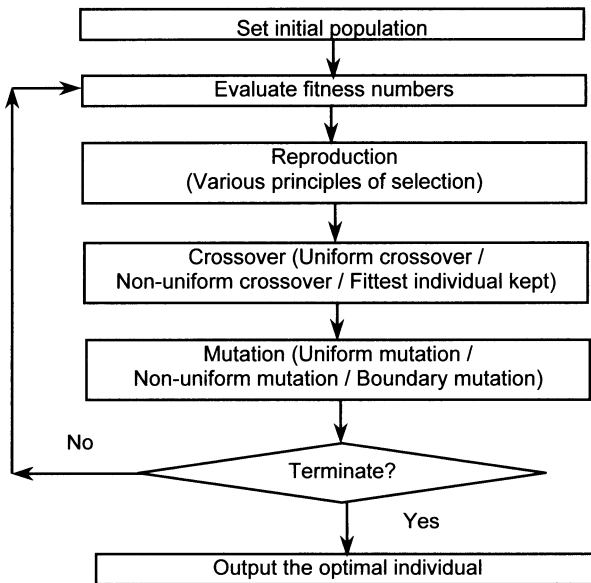


Fig. 1.2.1. A typical genetic algorithm

*Reproduction* is based on the principle of survival of the fittest. That is, the fittest individuals in the population should be first selected to reproduce their offspring. For this purpose, a positive number  $E_j$ , called the *fitness number*, is assigned to individual  $j$  in the population for all  $j$ , where a larger fitness number implies better fit of individual. In order to select the fittest individuals as the first choice, the probability  $p_j$  in selection is usually defined to be proportional to the fitness, say,

$$p_j = \frac{E_j}{\sum_{k=0}^N E_k}. \quad (1.2.23)$$

This way, two individuals with the largest probability will be first selected as a couple to reproduce their offspring.

*Crossover* is used to generate new individuals so that a new point in the parametric set is searched. In practice, two techniques of crossover are often used. One is the simple crossover, which exchanges the partial genes of two select chromosomes. And the other is the algorithm crossover. That is, the linear combination of two select chromosomes. The specific operator is to replace the parameters  $a$  and  $b$  of two individuals with  $a'$  and  $b'$ , satisfying  $a+b=a'+b'$ . Normally, the individual parameters of offspring yield

$$\begin{cases} a'=(1-\alpha)b+\alpha a, \\ b'=(1-\alpha)a+\alpha b, \end{cases} \quad (1.2.24)$$

where  $\alpha \in (0, 1)$  is a random parameter. In practice,  $\alpha$  can be set as a constant or a variable. The two cases correspond to the uniform crossover and the non-uniform crossover, respectively. To avoid missing the optimal individual and to increase the convergence, a new crossover operator is suggested as follows. Crossover the two parameters of parents, and then keep one of the parents fitter than the offspring, as well as the fitter individual of offspring. This operator can greatly speed up the convergence, but likely falls into a local optimization. Such a shortcoming can be removed by increasing the mutation probability.

The purpose of *mutation* is to introduce the genetic diversity into the population so that the almost uniform population, or the individuals of small fitness, undergoes a change. The mutation makes each new generation keep fresh individuals and avoid iteration stopping. The mutation may be uniform or non-uniform, too. The non-uniform mutation is as following. Take a random variable  $N_r$  from the set  $\{0,1\}$  and let

$$a' = \begin{cases} a + \delta(t, a_{\max} - a), & N_r = 0, \\ a - \delta(t, a - a_{\min}), & N_r = 1, \end{cases} \quad (1.2.25)$$

where  $\delta(t, y) = [z(1-t/T)]^b y$ ,  $T$  is the maximal number of generations,  $z$  a random variable on  $[0, 1]$ ,  $b$  a system parameter, representing the extent of non-uniformity. The value range of  $\delta(t, y)$  is  $[0, y]$ , and  $\delta(t, y) \rightarrow 0$  when  $t \rightarrow T$ .

To implement the genetic algorithm to minimize  $J$  in Eq. (1.2.22), a *fitness function* is introduced as following

$$E = \max(N - J), \quad (1.2.26)$$

where  $N$  is a sufficiently large positive number so that  $E > 0$  holds true during the parametric identification.

Compared with other optimization algorithms, the genetic algorithm does not depend on any gradient information of the objective function, and hence, meets the requirement of optimization of non-smooth and even discontinuous objective functions. The more important feature of a genetic algorithm is its ability of global optimization, because the genetic algorithm searches the best individual among the population, rather than a part of individuals, and emphasizes the information exchange among all individuals of population.

The efficacy and efficiency of a genetic algorithm mainly depends on the following choices. That is, the choice of reproduction, crossover and mutation, the choice of algorithm parameters such as the population probability, crossover probability and mutation probability, and the choice of fitness function. In the following two examples, several kinds of crossover and mutation were simultaneously used so as to improve the efficiency of genetic algorithm.

**Example 1.2.1** Consider the problem of parametric identification of a linear delay system of single degree of freedom governed by

$$m\ddot{x}(t) + c\dot{x}(t) + kx(t) = ux(t - \tau) + v\dot{x}(t - \tau) + f(t), \quad (1.2.27)$$

where  $m=1.0$ ,  $c=0.2$ ,  $k=1.0$ ,  $u=0.5$ ,  $v=0.1$  and  $\tau=0.025$ . In the numerical simulation of system response, the excitation  $f(t)$  was taken as a chirp sinusoidal excitation of unit amplitude, a very popular excitation for the parametric identification of linear dynamic systems, within the frequency range 0.01-10Hz. The system response was sampled at the rate of 0.02s. In the parametric identification, the number of individuals in original population was chosen as 80, and the mutation probability as 0.025. The crossover was taken as the operator of keeping the fittest individuals, and the mutation as the non-uniform operator.

As the first step, the open-loop test was made to identify the parameters  $m$ ,  $c$  and  $k$ . Then, the estimated  $m$ ,  $c$  and  $k$  were substituted into the closed-loop model to identify the feedback gains and time delay. The convergence of identification with respect to the number of iterations is shown in Figs. 1.2.2 and 1.2.3 respectively for different noise levels of measurement.

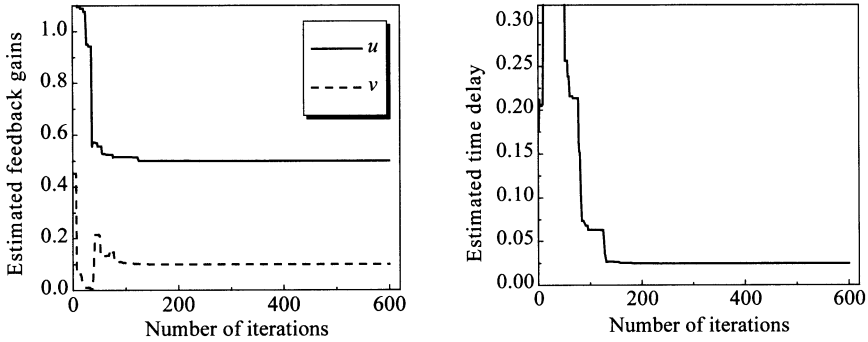


**Fig. 1.2.2.** Estimated feedback gains and time delay of a linear system when the measurement was free of noise

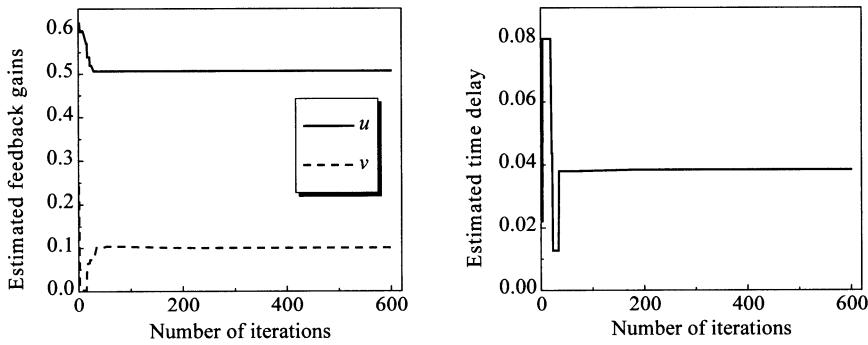


**Fig. 1.2.3.** Estimated feedback gains and time delay of a linear system when the measurement was contaminated by 5% noise

**Table 1.2.1.** Identification results of a linear dynamic system with delayed state feedback under different noise levels of measurement

Parameters	$m$	$k$	$c$	$u$	$v$	$\tau$
Search range	[0, 10]	[0, 10]	[0, 10]	[0, 10]	[0, 10]	[0, 0.5]
Exact value	1.0	1.0	0.2	0.5	0.1	0.025
Identification free of noise	1.00006	1.00009	0.19997	0.50002	0.09983	0.0247
Identification error (%)	0.006	0.009	0.015	0.004	0.17	1.12
Identification at 5% noise	1.00590	1.00605	0.19605	0.50655	0.10045	0.03836
Identification error (%)	0.59	0.61	1.98	1.31	0.45	53.44

As shown in Table 1.2.1 and Fig. 1.2.2, all the identified parameters approached the exact values if the sampled data were free of measurement noise. However, the identified time delay in Table 1.2.1 and Fig. 1.2.3 greatly deviated from the exact value and even had the relative error of 53.44% when only 5% white noise was added to the sampled data. The next example will show how to improve the applicability of the approach in the noisy case.

**Example 1.2.2** Consider a forced Duffing oscillator with linear delayed state feedback. As discussed in Subsection 1.1.1, the equation of motion of the system is governed by

$$\ddot{x}(t)+2\zeta\dot{x}(t)+x(t)+\mu x^3(t)=ux(t-\tau)+v\dot{x}(t-\tau)+f(t), \quad (1.2.28)$$

where  $\zeta=0.05$ ,  $\mu=0.05$ ,  $u=0.1$ ,  $v=-0.1$  and  $\tau=0.786$ . To get the system response, which well represents the nonlinear behavior of system under various intensity of excitation, the excitation of white noise with variance 0.1 was used in the numerical simulation of system response. The displacements of open-loop system and closed-loop system were sampled respectively at the rate of 0.01s. The open-loop parameters  $\zeta$  and  $\mu$  were first identified and then substituted into the closed-loop model. Afterwards,  $u$ ,  $v$  and  $\tau$  were identified.

**Table 1.2.2.** Identification results of a forced Duffing oscillator with delayed state feedback under different noise levels of measurement

Parameter	$\zeta$	$\mu$	$u$	$v$	$\tau$
Search range	[0, 1]	[0, 1]	[0, 1]	[-1, 0]	[0, 5]
Exact value	0.05	0.05	0.1	-0.1	0.786
Identification free of noise	0.05	0.05	0.09942	-0.1006	0.79997
Identification error (%)	0.00	0.00	0.58	0.60	1.78
Identification at 5% noise	0.051161	0.04956	0.11236	-0.09152	0.901977
Identification error	2.32	0.88	12.36	8.48	14.75
Identification at 10% noise	0.04826	0.04889	0.11518	-0.08950	0.92899
Identification error	3.48	2.22	15.18	10.50	18.19



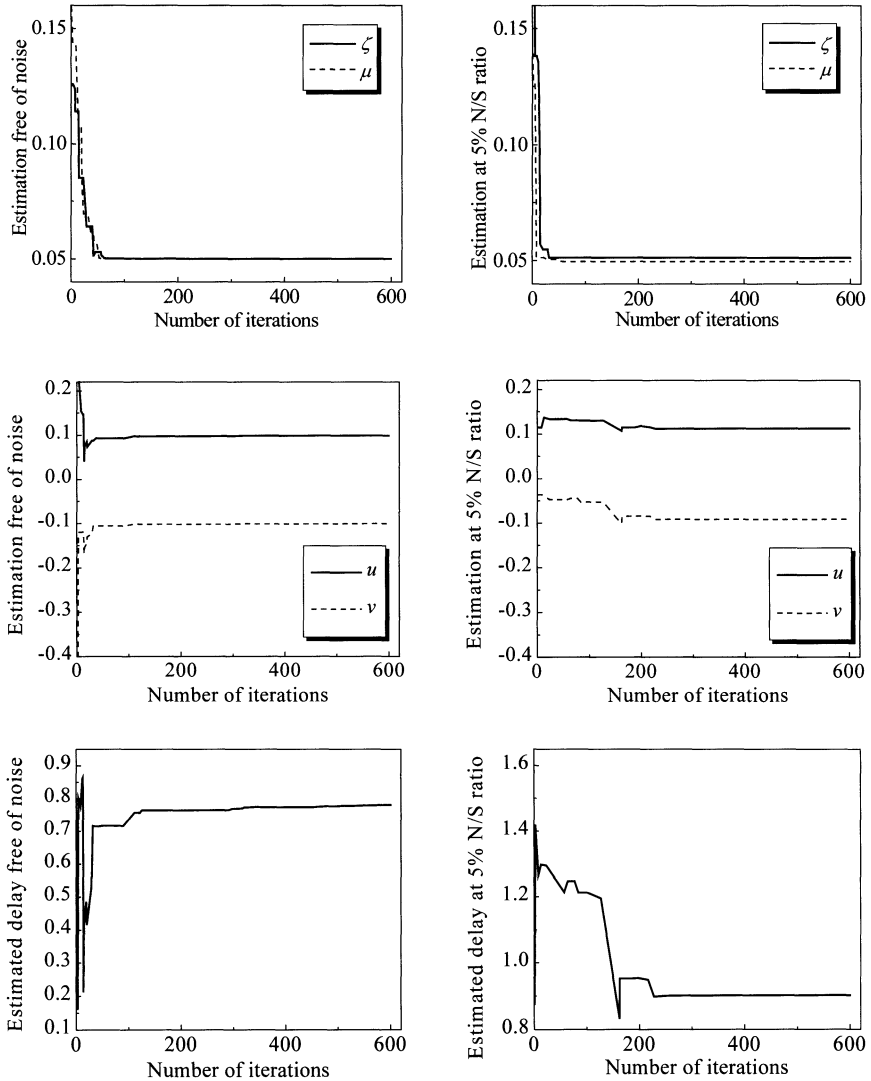


**Fig. 1.2.4.** Estimated parameters for a forced Duffing oscillator with delayed state feedback when the measurements were free of noise and contaminated by 5% noise, respectively

Similar to Example 1.2.1, the number of individuals in a population was chosen as 80, the crossover probability as 0.15, and the mutation probability as 0.075. Three case studies were made for the measurements without noise, with 5% and 10% white noise, respectively. To improve the identification process, several op-

erators of crossover and mutation, such as the algorithm crossover, uniform and non-uniform mutations, were used. Table 1.2.2 gives the identified parameters for different cases. Figure 1.2.4 shows the convergence procedure of parametric identification with an increase of iteration numbers. Obviously, the combination of crossover and mutation greatly improved the accuracy of identified parameters. For instance, the relative error of identified time delay was reduced from 53.44% in Example 1.2.1 to 14.75% when 5% noise was added into sampled data. The relative error of time delay was decreased to 18.19%, an acceptable percentage in engineering, even though the sampled data were contaminated by 10% white noise.

### 1.2.3 Discussions on Identifiability of Time Delays

As seen in previous subsections, it is not easy to extract the feedback time delays from the experimental data for a dynamic system, even for a linear dynamic system. A great number of failures in the identification of time delays urge one wonder whether the time delays in a dynamic system can be identified or not. In this subsection, a brief discussion will be made mainly on the identifiability of time delays of a linear dynamic system.

Consider again the frequency response function of a linear delay system of single degree of freedom given by Eq. (1.2.5) as following

$$H(\omega, \tau_1, \tau_2) = \frac{1}{a(\omega, \tau_1, \tau_2) - m\omega^2 + ib(\omega, \tau_1, \tau_2)}, \quad (1.2.29)$$

where

$$\begin{cases} a(\omega, \tau_1, \tau_2) \equiv k - u\cos\omega\tau_1 - v\omega\sin\omega\tau_2, \\ b(\omega, \tau_1, \tau_2) \equiv c\omega + u\sin\omega\tau_1 - v\omega\cos\omega\tau_2. \end{cases} \quad (1.2.30)$$

Obviously, both  $a(\omega, \tau_1, \tau_2)$  and  $b(\omega, \tau_1, \tau_2)$  are real functions in the time delays  $\tau_1$  and  $\tau_2$ , and has the same period  $2\pi/\omega$ . Hence, for any positive integers  $p$  and  $q$ , there exists the relation

$$\begin{cases} a(\omega, \tau_1 \pm \frac{2p\pi}{\omega}, \tau_2 \pm \frac{2q\pi}{\omega}) = a(\omega, \tau_1, \tau_2), \\ b(\omega, \tau_1 \pm \frac{2p\pi}{\omega}, \tau_2 \pm \frac{2q\pi}{\omega}) = b(\omega, \tau_1, \tau_2). \end{cases} \quad (1.2.31)$$

A specific case is

$$\begin{cases} a(\omega, \frac{2p\pi}{\omega}, \frac{2q\pi}{\omega})=a(\omega,0,0), \\ b(\omega, \frac{2p\pi}{\omega}, \frac{2q\pi}{\omega})=b(\omega,0,0). \end{cases} \quad (1.2.32)$$

Equation (1.2.31) implies that the identified time delays  $\hat{\tau}_1$  and  $\hat{\tau}_2$  may differ from the actual time delays  $\tau_1$  and  $\tau_2$  by  $2p\pi/\omega$  and  $2q\pi/\omega$  if only the harmonic excitation of frequency  $\omega$  is used in the test. For the system with identical time delays  $\tau_1=\tau_2$ , the identified results may yield  $\hat{\tau}_1-\hat{\tau}_2=2(p-q)\pi/\omega \neq 0$ . Equation (1.2.32) indicates that two distinct time delays  $\hat{\tau}_1=2p\pi/\omega$  and  $\hat{\tau}_2=2q\pi/\omega$  may even be identified for the system that does not have any time delays at all. As a result, it is impossible to extract the time delays properly from the response of system subject to a harmonic excitation of fixed frequency.

Now consider two distinct time delays  $\tau_1$  and  $\tau_2$ , as well as the time delays  $\hat{\tau}_1$  and  $\hat{\tau}_2$  identified from the experiment. Denote the corresponding frequency response functions by  $H(\omega, \tau_1, \tau_2)$  and  $H(\omega, \hat{\tau}_1, \hat{\tau}_2)$ , respectively. If they both are identical, Eqs. (1.2.29) and (1.2.30) lead to

$$\begin{cases} a(\omega, \hat{\tau}_1, \hat{\tau}_2) - a(\omega, \tau_1, \tau_2) \\ = u(\cos\omega\tau_1 - \cos\omega\hat{\tau}_1) + v\omega(\sin\omega\tau_2 - \sin\omega\hat{\tau}_2) = 0, \\ b(\omega, \hat{\tau}_1, \hat{\tau}_2) - b(\omega, \tau_1, \tau_2) \\ = u(\sin\omega\hat{\tau}_1 - \sin\omega\tau_1) - v\omega(\cos\omega\hat{\tau}_2 - \cos\omega\tau_2) = 0. \end{cases} \quad (1.2.33)$$

Equation (1.2.33) can be regarded as a set of linear equations in unknowns  $u$  and  $v\omega$ . The existence of non-zero solution of Eq. (1.2.33) is equivalent to the following necessary and sufficient condition

$$\begin{aligned} & (\cos\omega\tau_1 - \cos\omega\hat{\tau}_1)(\cos\omega\tau_2 - \cos\omega\hat{\tau}_2) \\ & + (\sin\omega\tau_1 - \sin\omega\hat{\tau}_1)(\sin\omega\tau_2 - \sin\omega\hat{\tau}_2) = 0. \end{aligned} \quad (1.2.34)$$

After simple manipulations on triangle functions, we arrive at

$$\sin\frac{\omega(\hat{\tau}_1 - \tau_1)}{2} \sin\frac{\omega(\hat{\tau}_2 - \tau_2)}{2} \cos\frac{\omega[(\hat{\tau}_1 + \tau_1) - (\hat{\tau}_2 + \tau_2)]}{2} = 0. \quad (1.2.35)$$

There follows the solution of Eq. (1.2.35)

$$\hat{\tau}_1 = \tau_1 \pm \frac{2p\pi}{\omega}, \quad \hat{\tau}_2 = \tau_2 \pm \frac{2q\pi}{\omega}, \quad (\hat{\tau}_1 + \tau_1) - (\hat{\tau}_2 + \tau_2) = \pm \frac{(2r+1)\pi}{\omega}, \quad (1.2.36)$$

where  $p$  and  $q$  are positive integers,  $r$  the non-negative integer.

The first two solutions in Eq. (1.2.36) indicate again that the identified time delays  $\hat{\tau}_1$  and  $\hat{\tau}_2$  may differ from the actual time delays  $\tau_1$  and  $\tau_2$  by  $2p\pi/\omega$

and  $2q\pi/\omega$ . The third solution implies that the identified results may be any pair of  $\hat{\tau}_1$  and  $\hat{\tau}_2$ , which yields the last equation of Eq. (1.2.36).

Now, we look at the comparison of frequency response functions  $H(\omega, \tau_1, \tau_2)$  and  $H(\omega, \hat{\tau}_1, \hat{\tau}_2)$ , as well as the amplitude of *impedance difference* defined as

$$\Delta(\omega) \equiv \sqrt{[a(\omega, \hat{\tau}_1, \hat{\tau}_2) - a(\omega, \tau_1, \tau_2)]^2 + [b(\omega, \hat{\tau}_1, \hat{\tau}_2) - b(\omega, \tau_1, \tau_2)]^2} \quad (1.2.37)$$

Figure 1.2.5 shows the amplitudes of  $H(\omega, 0, 0)$  and  $H(\omega, 4\pi, 6\pi)$ , and the amplitude of corresponding impedance difference. It is obvious that the two frequency functions are equal at the common values  $\omega=1, 2, 3, \dots$  for the frequency series  $\omega=2p\pi/|\hat{\tau}_1 - \tau_1| = p/2, p=1, 2, 3, \dots$  and  $\omega=2q\pi/|\hat{\tau}_2 - \tau_2| = q/3, q=1, 2, 3, \dots$ . Thus, it is impossible to identify whether or not the system has any time delays from the measured frequency response function at those frequencies.

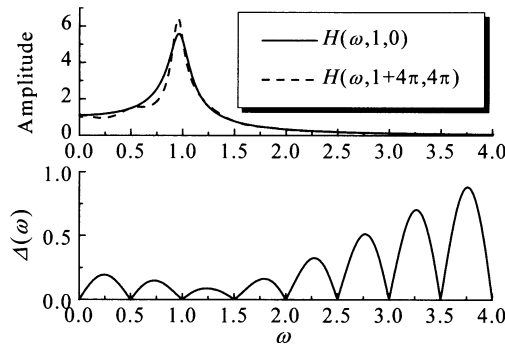


**Fig. 1.2.5.** Comparison of the frequency response functions  $H(\omega, 0, 0)$  and  $H(\omega, 4\pi, 6\pi)$ , together with the amplitude of  $\Delta(\omega)$

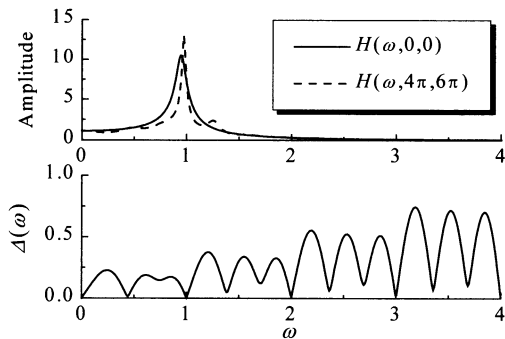


**Fig. 1.2.6.** Comparison of the frequency response functions  $H(\omega, 1, 0)$  and  $H(\omega, 1+4\pi, 4\pi)$ , together with the amplitude of  $\Delta(\omega)$

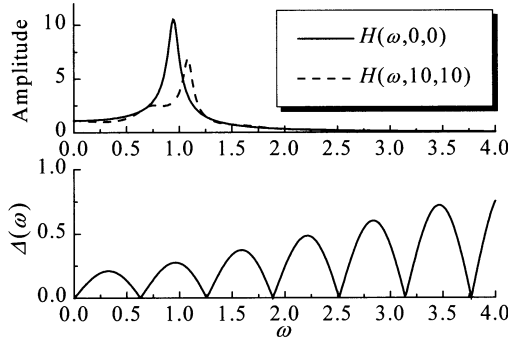


**Fig. 1.2.7.** Comparison of the frequency response functions  $H(\omega,0,0)$  and  $H(\omega,10,10)$ , together with the amplitude of  $\Delta(\omega)$

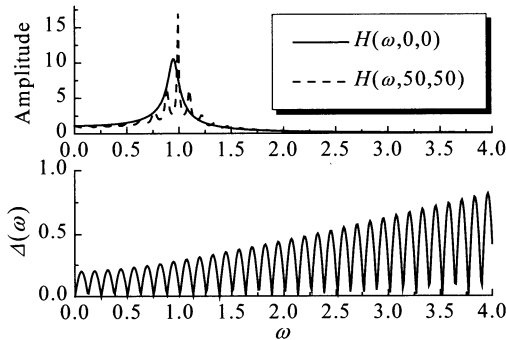


**Fig. 1.2.8.** Comparison of the frequency response functions  $H(\omega,0,0)$  and  $H(\omega,50,50)$ , together with the amplitude of  $\Delta(\omega)$

Similarly, the frequency response functions  $H(\omega,1,0)$  and  $H(\omega,1+4\pi,4\pi)$  in Fig. 1.2.6 are the same when  $\omega = p/2$ ,  $p=1,2,3,\dots$ . This case is also true if the time delays are arbitrary real numbers. In Fig. 1.2.7,  $H(\omega,0,0)$  and  $H(\omega,10,10)$  are identical when  $\omega = p\pi/5$ ,  $p=1,2,3,\dots$ , and so are  $H(\omega,0,0)$  and  $H(\omega,50,50)$  at  $\omega = p\pi/25$ ,  $p=1,2,3,\dots$  in Fig. 1.2.8.

As analyzed above, the identified time delays  $\hat{\tau}_1$  and  $\hat{\tau}_2$  may differ from the actual time delays  $\tau_1$  and  $\tau_2$  by  $2p\pi/\omega$  and  $2q\pi/\omega$ , where  $p$  and  $q$  are two integers. If the time delays to be identified are very short, it is easy to exclude the misidentified time delays. However, the dynamics of a system with short time delays is often quite close to the dynamics of a delay free system. In this case, the identification of short time delays may fail if the experimental data are contami-

nated by measurement noise. In what follows, the identifiability of short time delays is discussed for the second approach in Subsection 1.2.1.

From Eqs. (1.2.14) and (1.2.15), the sensitivities of modal parameters of closed-loop system with respect to the time delays can be derived

$$\frac{\partial \omega_n}{\partial \tau_1} = 0, \quad \frac{\partial \omega_n}{\partial \tau_2} = -\frac{\bar{\omega}_n v}{2m}, \quad \frac{\partial \zeta}{\partial \tau_1} = \frac{\bar{\zeta} u}{c-v}, \quad \frac{\partial \zeta}{\partial \tau_2} = -\frac{\bar{\zeta} v}{2m}. \quad (1.2.38)$$

As these sensitivities depend on the modal parameters of system without time delay, it is possible to determine what modal parameter is the best for the identification of time delays. For example, it is more difficult to identify  $\tau_1$  than  $\tau_2$  from the natural frequency  $\omega_n$ . If the condition  $2mu > v(c-v)$  holds, however, it may be easier to identify  $\tau_1$  than  $\tau_2$  from the estimated damping ratio.

**Example 1.2.3** Consider a linear delay system governed by Eq. (1.2.1) with following parameters

$$m=1.0, \quad c=0.2, \quad k=1.0, \quad u=0.1, \quad v=0.1, \quad \tau_1=0.2, \quad \tau_2=0.1. \quad (1.2.39)$$

The numerical simulation shows that if the input and output measurements of system were free of noise, the identified parameters coincided with the exact parameters at the first three digits. However, if the white noise of 1~5% was added to the sampled measurements, the accuracy of identified parameters became quite poor. From the experience of using the curve fitting technique of orthogonal polynomials, the accuracy of parameters  $a_0$  and  $a_2$  is relatively high since they both are related to the natural frequency. However, it is hard to identify an accurate  $a_1$  because it is associated with the modal damping. As a small parameter, the identified result of  $a_3$  does not have high accuracy, either.

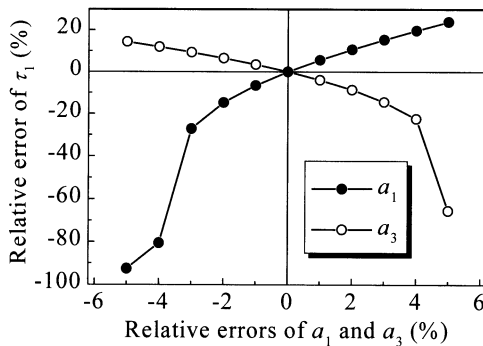


Fig. 1.2.9. Relative errors of identified parameters

In Fig. 1.2.9, the effect of estimation errors of  $a_1$  and  $a_3$  on the accuracy of identified time delays is given. The figure shows that only the fitting error of about 5% may give rise to the identification error of 80~90%. This indicates once more that it is indeed a tough and open problem to identify the time delays of a practical system from experimental data.

The identifiability of time delays from any nonlinear system is undoubtedly a tough problem, and can usually be discussed in time domain. To have a brief idea about the identifiability problem in time domain, consider the delayed state feedback

$$g(t) = ux(t - \tau_1) + v\dot{x}(t - \tau_2). \quad (1.2.40)$$

Applying the Lagrange mean value theorem to Eq. (1.2.40) yields

$$g(t) = u[x(t) - \tau_1\dot{x}(t - \theta\tau_1)] + v\dot{x}(t - \tau_2), \quad 0 \leq \theta(t) \leq 1. \quad (1.2.41)$$

Even though  $\theta(t)$  here is not a constant, the experimental data may offer great probability of  $\tau_2 \approx \theta(t)\tau_1$  such that

$$g(t) \approx ux(t) + (v - u\tau_1)\dot{x}(t - \tau_2). \quad (1.2.42)$$

If this is the case, the estimated results become

$$\hat{u} \approx u, \quad \hat{v} \approx v - u\tau_1, \quad \hat{\tau}_1 \approx 0, \quad \hat{\tau}_2 \approx \tau_2 \quad (1.2.43)$$

and totally deviate from the real values.

In general, the identifiability of dynamic systems with feedback time delays is still an open problem no matter whether the systems are linear or not. Nevertheless, it is better to keep the problem in mind when estimating the time delays from the experimental data or using the estimated time delays in system modeling.

## 2 Fundamentals of Delay Differential Equations

This chapter serves as a brief review of some theoretical results of delay differential equations in the form

$$\dot{x}(t) = f(t, x(t), x(t-\tau_1), x(t-\tau_2), \dots, x(t-\tau_l)), \quad x \in R^n, \quad (2.0.1)$$

where  $0 < \tau_1 \leq \tau_2 \leq \dots \leq \tau_l$  represent the time delays. The time delays are assumed to be constants hereinafter for simplicity, though it may be more reasonable, from the viewpoint of practice, to regard them as the functions in time  $t$ .

In addition, the time delays in a differential equation may appear in terms of the highest order derivative, for example,

$$\dot{x}(t) = ax(t) + b\dot{x}(t-\tau), \quad x \in R. \quad (2.0.2)$$

If this is the case, the delay differential equation is referred to as the *neutral type*, whereas Eq. (2.0.1) is called the *retarded type*. The delay differential equations of neutral type may behave quite different from those of retarded type. For mechanical systems, the displacement feedback and the velocity feedback are more popular than the acceleration feedback. Hence, the controlled mechanical systems with feedback time delays are usually modeled as Eq. (2.0.1), and the delay differential equations of neutral type will not be touched with in this book. As a result, the terminology “delay differential equation” used hereafter implies the delay differential equation of retarded type unless any further explanation is given.

For Eq. (2.0.1), the concepts of linear and nonlinear systems, autonomous and non-autonomous systems, orders or dimensions of systems, and so on will be used without special definition. What should be emphasized is that  $x(t)$  is not superior to any  $x(t-\tau_j)$ ,  $j=1,2,\dots,l$  in Eq. (2.0.1). They should be equally dealt with.

### 2.1 Initial Value Problems

For a dynamic system described by an ordinary differential equation, the state of system at any time  $t$  can be traced from an initial state at time  $t_0$  if the dynamic equation of system is given. However, this is not the case for any system governed



by a delay differential equation. To understand this fact, we consider the linear system of single degree of freedom with delayed state feedback given by Eq. (1.1.4). In the case of identical time delays, the initial value problem corresponding to Eq. (1.1.4) reads

$$\begin{cases} m\ddot{x}(t)+c\dot{x}(t)+kx(t)=ux(t-\tau)+\dot{x}(t-\tau)+f(t), & t>t_0, \\ x(t)=\phi(t), \quad \dot{x}(t)=\dot{\phi}(t), & t\in[t_0-\tau, t_0]. \end{cases} \quad (2.1.1)$$

That is, the initial state of system should be given by a continuous function  $\phi(t)$  and its continuous derivative  $\dot{\phi}(t)$  on the interval  $[t_0-\tau, t_0]$  in order to determine the state of system when  $t>t_0$ .

Because  $\tau_l$  is assumed to be the longest time delay in Eq. (2.0.1), the initial value problem of Eq. (2.0.1) should be stated as

$$\begin{cases} \dot{x}(t)=f(t, x(t), x(t-\tau_1), x(t-\tau_2), \dots, x(t-\tau_l)), & \mathbf{x}\in R^n, t>t_0, \\ x(t)=\phi(t), & t\in[t_0-\tau_l, t_0], \end{cases} \quad (2.1.2)$$

where  $\phi(t)\in C\equiv C([t_0-\tau_l, t_0], R^n)$  and  $C$  represents the Banach space of continuous functions mapping  $[t_0-\tau_l, t_0]$  into  $R^n$ . For each initial function  $\phi\in C$ , it is equipped with the norm

$$\|\phi\|_C \equiv \sup_{s\in[t_0-\tau_l, t_0]} \|\phi(s)\|, \quad (2.1.3)$$

where  $\|\cdot\|$  is an arbitrary norm in  $R^n$ . It is obvious that the space of initial state of Eq. (2.1.2) is infinite dimensional. This is one of the most important features of delay differential equations. When the dependence of  $\mathbf{x}(t)$  on the initial function  $\phi(t)$  ahead of the moment  $t=t_0$  needs to be emphasized, the symbol  $\mathbf{x}(t, t_0, \phi)$  will be used for  $\mathbf{x}(t)$  hereinafter.

### 2.1.1 Existence and Uniqueness of Solution

When an initial value problem of delay differential equation is to be solved, the most natural strategy is the *method of step-by-step*. For instance, it is possible to find out the solution  $\mathbf{x}(t)$  of Eq. (2.1.2) on  $[t_0, t_0+\tau_l]$ , where the right-hand side is in terms of given states  $\mathbf{x}(t-\tau_j)=\phi(t-\tau_j)$ ,  $j=1, 2, \dots, l$ . Then, Eq. (2.1.2) can be solved for  $\mathbf{x}(t)$  over  $[t_0+\tau_l, t_0+2\tau_l]$ , where the right-hand side is in terms of known solution found in the first step. Repeating this routine recurrently, it is feasible to determine  $\mathbf{x}(t)$  up to any desired interval.

**Example 2.1.1** Solve the initial value problem of a scalar delay differential equation

$$\begin{cases} \dot{x}(t) = -x(t-1), & t \geq 0, \\ x(t) = t, & t \in [-1, 0]. \end{cases} \tag{2.1.4}$$

On the interval  $[0, 1]$ , Eq. (2.1.4) becomes  $\dot{x}(t) = -(t-1)$ . Solving this ordinary differential equation gives a general solution  $x(t) = -(t-1)^2/2 + c_1$ , where  $c_1 = 1/2$  can be determined from the condition  $\phi(0) = 0$ . Hence, the solution of Eq. (2.1.4) on interval  $[0, 1]$  is  $x(t) = -(t-1)^2/2 + 1/2$ .

On the interval  $[1, 2]$ , Eq. (2.1.4) becomes  $\dot{x}(t) = (t-2)^2/2 - 1/2$  after  $x(t-1)$  is substituted. By integrating this equation under the condition  $x(1) = 1/2$ , we obtain  $x(t) = (t-2)^3/3! - t/2 + (1+1/3!)$ .

Repeating this routine recurrently gives the solution of Eq. (2.1.4)

$$x(t) = \begin{cases} t, & t \in [-1, 0], \\ -(t-1)^2/2 + 1/2, & t \in [0, 1], \\ (t-2)^3/3! - t/2 + (1+1/3!), & t \in [1, 2], \\ \dots \end{cases} \tag{2.1.5}$$

The corresponding time history is shown in Fig. 2.1.1.

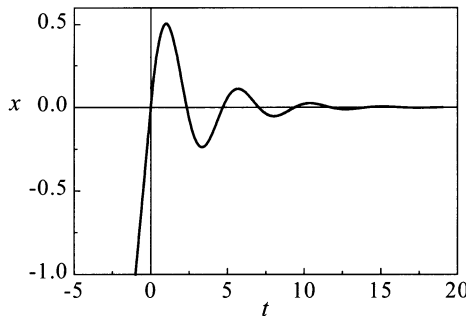


**Fig. 2.1.1.** Time history of solution of Eq. (2.1.4)

If multiple time delays are involved in a delay differential equation, the method of step-by-step is still valid, but may become very complicated. The method of step-by-step converts the initial value problem given by Eq. (2.1.2) into a series of initial value problems of ordinary differential equations, which may be successively solved. Using the idea of studying the existence and uniqueness for ordi-

nary differential equations leads to the corresponding conclusions for delay differential equations.

To briefly state the theorem of existence and uniqueness, consider Eq. (2.1.2) when  $l=1$  and rewrite it as

$$\begin{cases} \dot{\mathbf{x}} = \mathbf{f}(t, \mathbf{x}(t), \mathbf{x}(t-\tau)), & \mathbf{x} \in R^n, \quad t > t_0, \\ \mathbf{x}(t) = \boldsymbol{\phi}(t), & t \in [t_0 - \tau, t_0], \end{cases} \quad (2.1.6)$$

where  $\boldsymbol{\phi}(t)$  is continuous on  $[t_0 - \tau, t_0]$ . In addition, for  $\hat{t} \geq t_0$  and  $d > 0$ , we define two sets for the statement of following theorem

$$J \equiv [\hat{t}, +\infty), \quad D \equiv \{\mathbf{x} \in R^n \mid \|\mathbf{x}\| < d\}. \quad (2.1.7)$$

**Theorem 2.1.1** Assume that

(a)  $\mathbf{f}(t, \mathbf{x}(t), \mathbf{x}(t-\tau))$  is continuous in  $J \times D^2$ ;

(b)  $\mathbf{f}(t, \mathbf{x}(t), \mathbf{x}(t-\tau))$  is of local Lipschitz with respect to  $\mathbf{x}(t)$  and  $\mathbf{x}(t-\tau)$ , namely, there is a constant  $L_G > 0$  for  $G \subseteq J \times D^2$  such that for any  $(t, \boldsymbol{\xi}_1, \boldsymbol{\xi}_2)$  and  $(t, \boldsymbol{\eta}_1, \boldsymbol{\eta}_2) \in G$  the following inequality holds

$$\|\mathbf{f}(t, \boldsymbol{\xi}_1, \boldsymbol{\xi}_2) - \mathbf{f}(t, \boldsymbol{\eta}_1, \boldsymbol{\eta}_2)\| \leq L_G \sum_{j=1}^2 \|\boldsymbol{\xi}_j - \boldsymbol{\eta}_j\| \quad (\text{or } \leq L_G \max_{j=1,2} \|\boldsymbol{\xi}_j - \boldsymbol{\eta}_j\|). \quad (2.1.8)$$

Then, there exists a constant  $A > 0$  or  $A = +\infty$  such that Eq. (2.1.6) has a unique continuous solution  $\mathbf{x}(t, t_0, \boldsymbol{\phi})$  for  $t \in [t_0 - \tau, t_0 + A]$ .

**Proof** For a given initial function  $\boldsymbol{\phi}$ , we denote  $D_1 \equiv \{\boldsymbol{\psi} \mid \|\boldsymbol{\psi} - \boldsymbol{\phi}\|_c < d_1\}$  and  $\Omega \equiv [t_0, t_0 + A] \times D_1^2$ , and choose  $A > 0$  and  $d_1 \in (0, d)$  such that  $\Omega \subseteq J \times D^2$ . Furthermore, let  $\mathbf{x}_0(t) \in D$  be a continuous function defined by

$$\mathbf{x}_0(t) \equiv \begin{cases} \boldsymbol{\phi}(t), & t \in [t_0 - \tau, t_0], \\ \boldsymbol{\phi}(t_0), & t > t_0, \end{cases} \quad (2.1.9)$$

and then define  $\mathbf{x}_k(t)$  for  $k \geq 1$  recurrently by

$$\mathbf{x}_k(t) \equiv \begin{cases} \boldsymbol{\phi}(t), & t \in [t_0 - \tau, t_0], \\ \boldsymbol{\phi}(t_0) + \int_{t_0}^t \mathbf{f}(s, \mathbf{x}_{k-1}(s), \mathbf{x}_{k-1}(s-\tau)) ds, & t > t_0. \end{cases} \quad (2.1.10)$$

If  $\mathbf{x}_{k-1}(t) \in D$ ,  $M \equiv \sup_{\Omega} \|\mathbf{f}\|$  and  $d_0 \equiv \|\boldsymbol{\phi}(t_0)\|$  enable one to write

$$\begin{aligned}\|\mathbf{x}_k(t)\| &\leq \|\phi(t_0)\| + \int_{t_0}^t \|\mathbf{f}(s, \mathbf{x}_{k-1}(s), \mathbf{x}_{k-1}(s-\tau))\| ds \\ &\leq d_0 + M|t-t_0| \leq d_0 + MA.\end{aligned}\quad (2.1.11)$$

Thus,  $\mathbf{x}_k(t) \in D$  holds if  $A < (d-d_0)/2M$ . As a result,  $\mathbf{x}_k(t) \in D$  holds for all  $k \geq 1$ .

Now, we can claim that  $\mathbf{x}_k(t)$  converges uniformly on  $[t_0-\tau, t_0+A]$  as  $k \rightarrow +\infty$ . In fact, for  $t \in [t_0, t_0+A]$ , we have

$$\begin{aligned}\|\mathbf{x}_{k+1}(t) - \mathbf{x}_k(t)\| &\leq L \int_{t_0}^t [\|\mathbf{x}_k(s) - \mathbf{x}_{k-1}(s)\| + \|\mathbf{x}_k(s-\tau) - \mathbf{x}_{k-1}(s-\tau)\|] ds \\ &\leq 2L \int_{t_0}^t \|\mathbf{x}_k(s) - \mathbf{x}_{k-1}(s)\| ds,\end{aligned}\quad (2.1.12)$$

where  $L$  is the Lipschitz constant of  $\mathbf{f}(t, \mathbf{x}(t), \mathbf{x}(t-\tau))$  over  $\Omega$ . Because  $\mathbf{x}_k(t) - \mathbf{x}_{k-1}(t) \equiv 0$  holds for all  $t \in [t_0-\tau, t_0]$ , the above inequality is true for all  $t \in [t_0-\tau, t_0+A]$ . Using the inequality

$$\|\mathbf{x}_1(t) - \mathbf{x}_0(t)\| \leq M|t-t_0|, \quad t \in [t_0-\tau, t_0+A] \quad (2.1.13)$$

gives

$$\|\mathbf{x}_k(t) - \mathbf{x}_{k-1}(t)\| \leq \frac{M(2L)^{k-1}|t-t_0|^k}{k!}, \quad t \in [t_0-\tau, t_0+A], \quad k \geq 1. \quad (2.1.14)$$

This implies that  $\mathbf{x}_k(t)$  converges to a function  $\mathbf{x}(t) \equiv \mathbf{x}(t, t_0, \phi)$  uniformly on  $[t_0-\tau, t_0+A]$  as  $k \rightarrow +\infty$ . Imposing  $k \rightarrow +\infty$  in both sides of Eq. (2.1.10) gives

$$\mathbf{x}(t) = \begin{cases} \phi(t), & t \in [t_0-\tau, t_0], \\ \phi(t_0) + \int_{t_0}^t \mathbf{f}(s, \mathbf{x}(s), \mathbf{x}(s-\tau)) ds, & t > t_0. \end{cases} \quad (2.1.15)$$

To prove the uniqueness, it is assumed on contrary that there is another solution  $\mathbf{y}(t) = \mathbf{y}(t, t_0, \phi)$  of Eq. (2.1.6) on the interval  $[t_0-\tau, t_0+\tilde{A}]$  with  $\tilde{A} > 0$ . As done in the above part, we have

$$\|\mathbf{x}_{k+1}(t) - \mathbf{y}(t)\| \leq 2L \int_{t_0}^t \|\mathbf{x}_k(s) - \mathbf{y}(s)\| ds, \quad t \in [t_0-\tau, t_0 + \min(A, \tilde{A})] \quad (2.1.16)$$

and

$$\|\mathbf{x}_0(t) - \mathbf{y}(t)\| \leq M|t-t_0|, \quad t \in [t_0-\tau, t_0 + \min(A, \tilde{A})]. \quad (2.1.17)$$

There follows

$$\|\mathbf{x}_k(t) - \mathbf{y}(t)\| \leq \frac{M(2L)^k |t - t_0|^{k+1}}{(k+1)!}, \quad t \in [t_0 - \tau, t_0 + \min(A, \tilde{A})], \quad k \geq 0. \quad (2.1.18)$$

Equation (2.1.18) implies that  $\|\mathbf{x}_k(t) - \mathbf{y}(t)\| \rightarrow 0$  when  $k \rightarrow +\infty$ . Hence,  $\mathbf{x}(t) \equiv \mathbf{y}(t)$  holds for all  $t \in [t_0 - \tau, t_0 + \min(A, \tilde{A})]$ . This completes the proof.

Obviously, the proof of Theorem 2.1.1 is a natural extension of Picard's idea in studying the existence and uniqueness of a solution of ordinary differential equation. As done in the case of ordinary differential equations, it is also possible to prove that the solution depends continuously on the initial function under proper conditions. In addition, the solution of a delay differential equation can be extended toward the positive direction of  $t$ , first from  $[t_0 - \tau, t_0)$  to  $[t_0 - \tau, t_0 + A_1)$  with  $A_1 > 0$ , then to a larger  $[t_0 - \tau, t_0 + A_1 + A_2)$  with  $A_1 > 0$  and  $A_2 > 0$ , and repeatedly up to the maximal interval where the solution exists. However, it is very difficult and even impossible to extend the solution of a delay differential equation toward the negative direction of  $t$ , see (Hale 1977).

Worthy of mention is that, unlike the case of autonomous ordinary differential equations where the uniqueness means that the solutions starting from different initial conditions do not intersect with each other, the solutions of Eq. (2.1.6) from different initial conditions may intersect with each other. They may intersect even infinite many times, but do not destroy their own uniqueness because the intersections come from the project of different solutions in an infinite dimensional space into a finite dimensional space.

**Example 2.1.2** It is obvious that the linear delay differential equation

$$\dot{x}(t) = -x\left(t - \frac{\pi}{2}\right), \quad x \in R \quad (2.1.19)$$

has two distinct solutions  $x_1(t) = \sin t$  and  $x_2(t) = \cos t$ . They intersect with each other infinite number of times at  $t = \pi(k + 1/4)$ ,  $k = 0, 1, 2, \dots$

For Eq. (2.1.6), if  $f(t, \mathbf{x}(t), \mathbf{x}(t - \tau))$  is differentiable up to a sufficiently high order, the  $k$ -th order derivative  $\mathbf{x}^{(k)}(t)$  of solution  $\mathbf{x}(t)$  may be discontinuous at  $t_0 + (k - 1)\tau$ , but all  $\mathbf{x}^{(j)}(t)$ ,  $j < k$  are continuous at  $t_0 + (k - 1)\tau$ . For example, it is easy to see from the method of step-by-step that  $\mathbf{x}(t_0) = \mathbf{x}(t_0 + 0) = \mathbf{x}(t_0 - 0) = \boldsymbol{\phi}(t_0)$ . Nevertheless,  $\dot{\mathbf{x}}(t_0 + 0) = \dot{\mathbf{x}}(t_0 - 0) = \dot{\boldsymbol{\phi}}(t_0 - 0)$  may not hold. At  $t = t_0 + \tau$ ,  $\dot{\mathbf{x}}(t)$  is continuous because of the continuity of the right-hand side  $f(t, \mathbf{x}(t), \mathbf{x}(t - \tau))$ . According to

$$\begin{aligned} \ddot{x}(t) = & \frac{\partial f(t, x(t), x(t-\tau))}{\partial t} + D_{x(t)} f(t, x(t), x(t-\tau)) \dot{x}(t) \\ & + D_{x(t-\tau)} f(t, x(t), x(t-\tau)) \dot{x}(t-\tau), \end{aligned} \quad (2.1.20)$$

$\ddot{x}(t)$  may be discontinuous at  $t=t_0+\tau$  since  $\dot{x}(t-\tau)$  may not be continuous there as explained above. As  $t$  increases, the solution  $x(t)$  becomes more and more smooth. This property, usually referred to as the *flatness of solution*, results in some good behaviors of delay differential equations.

### 2.1.2 Solution of Linear Delay Differential Equations

For the initial value problem of a linear delay differential equation, the conditions of existence and uniqueness of its solution always hold true. As done for linear differential equations, the linear delay differential equations can be solved by means of the Laplace transformation. To present this technique as simple as possible, this subsection is confined to the scalar delay differential equations, even though all the results are true in the case of higher dimensions.

Consider the initial value problem of a linear scalar delay differential equation

$$\begin{cases} \dot{x} = ax + bx(t-\tau) + f(t), & x \in R, \quad t > 0, \\ x(t) = \phi(t), & t \in [-\tau, 0], \end{cases} \quad \begin{matrix} (2.1.21a) \\ (2.1.21b) \end{matrix}$$

where  $a, b \in R$  are constants,  $f(t)$  is a continuous function. In order to perform the Laplace transform on Eq. (2.1.21), it is essential to establish an exponential estimation for the solution first. To this end, we need the famous *Gronwall inequality* as following.

**Lemma 2.1.1** Suppose that  $u(t)$  and  $\alpha(t)$  are two real continuous functions on interval  $[c, d]$ , and  $\beta(t) \geq 0$  is an integrable function on  $[c, d]$ . Furthermore,  $\alpha(t)$  is non-decreasing on  $[c, d]$ . If

$$u(t) \leq \alpha(t) + \int_c^t \beta(s)u(s)ds, \quad (2.1.22)$$

then

$$u(t) \leq \alpha(t) \exp\left[\int_c^t \beta(s)ds\right]. \quad (2.1.23)$$

**Proof** Let  $R(t) \equiv \int_c^t \beta(s)u(s)ds$ , then Eq. (2.1.22) becomes  $u(t) \leq \alpha(t) + R(t)$ . It is easy from this inequality to derive

$$\frac{dR(t)}{dt} = \beta(t)u(t) \leq \beta(t)[\alpha(t) + R(t)] \quad (2.1.24)$$

and

$$\frac{d}{ds} \{R(s) \exp[-\int_c^s \beta(\xi) d\xi]\} \leq \alpha(s) \beta(s) \exp[-\int_c^s \beta(\xi) d\xi]. \quad (2.1.25)$$

Integrating Eq. (2.1.25) from  $a$  to  $t$  yields

$$R(t) \leq \int_c^t \alpha(s) \beta(s) \exp[\int_s^t \beta(\xi) d\xi] ds. \quad (2.1.26)$$

Because  $\alpha(t)$  is non-decreasing on  $[c, d]$ , substituting Eq. (2.1.26) into Eq. (2.1.22) gives

$$\begin{aligned} u(t) &\leq \alpha(t) + \alpha(t) \int_c^t \beta(s) \exp[\int_s^t \beta(\xi) d\xi] ds \\ &= \alpha(t) - \alpha(t) \int_c^t d \{ \exp[\int_s^t \beta(\xi) d\xi] \} = \alpha(t) \exp[\int_c^t \beta(s) ds]. \end{aligned} \quad (2.1.27)$$

This completes the proof of the lemma.

Applying the Gronwall inequality to Eq. (2.2.21) gives the following theorem.

**Theorem 2.1.2** For the unique solution  $x(t, 0, \phi)$  of Eq. (2.1.21), there exist two positive constants  $\alpha$  and  $\beta$  such that

$$|x(t, 0, \phi)| \leq \alpha e^{\beta t} [\|\phi\| + \frac{1}{\alpha} \int_0^t |f(s)| ds], \quad t > -\tau. \quad (2.1.28)$$

**Proof** Equation (2.1.21) is equivalent to

$$x(t) = \begin{cases} \phi(0) + \int_0^t [ax(s) + bx(s-\tau) + f(s)] ds, & t > 0, \\ \phi(t), & t \in [-\tau, 0]. \end{cases} \quad (2.1.29)$$

Hence, the following inequality holds for  $t \geq -\tau$

$$\begin{aligned} |x(t)| &\leq \max_{t \in [-\tau, 0]} |\phi(t)| + \int_0^t [|a| \cdot |x(s)| + |b| \cdot |x(s-\tau)| + |f(s)|] ds \\ &= \|\phi\| + \int_0^t |a| \cdot |x(s)| ds + \int_0^t |b| \cdot |\phi(s)| ds + \int_t^\tau |b| \cdot |x(s)| ds + \int_0^t |f(s)| ds \\ &\leq [(1+|b|\tau)\|\phi\| + \int_0^t |f(s)| ds] + \int_0^t (|a|+|b|)|x(s)| ds \\ &= \alpha [\|\phi\| + \frac{1}{\alpha} \int_0^t |f(s)| ds] + \int_0^t \beta |x(s)| ds, \end{aligned} \quad (2.1.30)$$

where  $\alpha \equiv 1 + |b|\tau$  and  $\beta \equiv |a| + |b|$ . Applying the Gronwall inequality to Eq. (2.1.30) yields Eq. (2.1.28). This completes the proof of Theorem 2.1.2.

Having had the exponential estimation for the solution  $x(t)$ , we can perform the Laplace transform on Eq. (2.1.21) so that

$$X(\lambda) = \Delta^{-1}(\lambda) [\phi(0) + be^{-\lambda\tau} \int_{-\tau}^0 \phi(s)e^{-\lambda s} ds + F(\lambda)], \quad (2.1.31)$$

where

$$\Delta(\lambda) \equiv \lambda - a - be^{-\lambda\tau}, \quad X(\lambda) \equiv \int_0^{+\infty} x(t)e^{-\lambda t} dt, \quad F(\lambda) \equiv \int_0^{+\infty} f(t)e^{-\lambda t} dt. \quad (2.1.32)$$

Here,  $\Delta(\lambda)$  is the *characteristic function* of Eq. (2.1.21a). Let

$$h(t) \equiv \int_{\Gamma} \Delta^{-1}(\lambda) e^{\lambda t} d\lambda, \quad (2.1.33)$$

where  $\Gamma$  is a contour on the complex plane with  $\text{Re}\lambda > \beta$ . Obviously,  $h(t)$  serves as the *impulse response function* since it is the response of the system governed by Eq. (2.1.21a) subject to a Dirac impulse  $f(t) = \delta(t)$  and the initial condition  $\phi(t) \equiv 0$  on  $t \in [-\tau, 0]$ .

Applying the inverse Laplace transform to Eq. (2.1.31) yields

$$x(t) = h(t)\phi(0) + \int_{\Gamma} \Delta^{-1}(\lambda) e^{\lambda t} [be^{-\lambda\tau} \int_{-\tau}^0 \phi(s)e^{-\lambda s} ds + F(\lambda)] d\lambda. \quad (2.1.34)$$

By using the theorem of convolution, Eq. (2.1.34) can be simplified to

$$x(t) = h(t)\phi(0) + b \int_{-\tau}^0 h(t-\tau-s)\phi(s) ds + \int_0^t h(t-s)f(s) ds. \quad (2.1.35)$$

The first two terms in the right-hand side of Eq. (2.1.35) are composed of the *general solution* of the homogeneous equation corresponding to Eq. (2.1.21a) under the initial condition (2.1.21b). Denoting this solution by  $x(t, 0, \phi)$ , we arrive at the following formula of variation-of-constants.

**Theorem 2.1.3** The general solution of Eq. (2.1.21) is in the form

$$x(t) = x(t, 0, \phi) + \int_0^t h(t-s)f(s) ds, \quad (2.1.36)$$

where  $x(t, 0, \phi)$  is the general solution of Eq. (2.1.21a) under the initial condition (2.1.21b) when  $f(t) \equiv 0$ .

Theorem 2.1.3 shows that linear delay differential equations have the same structure of solutions as linear ordinary differential equations. That is, the solution



consists of two parts. One is proportional to the non-zero initial function  $\phi(t)$  for  $t \in [-\tau, 0]$ , and the other is to the non-zero input  $f(t)$  for  $t > 0$ .

Finally, we look at the solution structure of the homogeneous equation corresponding to Eq. (2.1.21a). Let  $\lambda_0$  be a root of the characteristic function  $\Delta(\lambda)$  and define it as the *characteristic root* of Eq. (2.1.21a). According to the definition of  $\Delta(\lambda)$  in Eq. (2.1.32),  $x_0(t) \equiv e^{\lambda_0 t}$  is obviously a solution of Eq. (2.1.21a) when  $f(t) \equiv 0$ . As for all the characteristic roots of Eq. (2.1.21a), each of them corresponds to a solution of Eq. (2.1.21a) when  $f(t) \equiv 0$ . All these solutions are referred to as the *fundamental solutions* of the homogeneous equation of Eq. (2.1.21a). Obviously, any linear combination of the fundamental solutions is also a solution of the corresponding homogeneous equation of Eq. (2.1.21a). This property is quite similar to that of ordinary differential equations, but the number of fundamental solutions here is usually infinite.

If  $\lambda_0$  is a repeated root of  $\Delta(\lambda)$ , counted by multiplicity  $m$ , the fundamental solutions corresponding to  $\lambda_0$  will be  $x_k(t) \equiv t^k e^{\lambda_0 t}, k=0, 1, \dots, m-1$ . To verify this assertion, substitute  $x_k(t)$  into Eq. (2.1.21a) under  $f(t) \equiv 0$  and use the binomial formula to expand  $(t-\tau)^k$ , then we have

$$\begin{aligned} \dot{x}_k(t) - ax_k(t) - bx_k(t-\tau) &= [\lambda_0 t^k + kt^{k-1} - at^k - b(t-\tau)^k] e^{\lambda_0 t} \\ &= e^{\lambda_0 t} \sum_{j=0}^k \binom{k}{j} t^{k-j} \Delta^{(j)}(\lambda_0), \quad k=0, 1, \dots, m-1, \end{aligned} \tag{2.1.37}$$

where  $\Delta^{(0)}(\lambda_0) \equiv \Delta(\lambda_0)$  and  $\Delta^{(j)}(\lambda_0)$  represents the  $j$ -th derivative of  $\Delta(\lambda)$  at  $\lambda_0$ . Because  $\Delta^{(k)}(\lambda_0) = 0, k=0, 1, \dots, m-1$ , all  $x_k(t) = t^k e^{\lambda_0 t}, k=0, 1, \dots, m-1$  are the solutions of Eq. (2.1.21a) when  $f(t) \equiv 0$ .

Moreover, it has been shown, in (Diekmann et al. 1995) on the basis of theory of residues, that any solution of the homogeneous equation corresponding to Eq. (2.1.21a) under some conditions is in the form

$$x(t) = \sum_j q_j(t) e^{\lambda_j t}, \tag{2.1.38}$$

where  $\lambda_j, j=1, 2, \dots$  are the characteristic roots and  $q_j(t), j=1, 2, \dots$  are polynomials. In general, the solution of the homogeneous equation corresponding to Eq. (2.1.21a) is in the form

$$x(t) = \sum_j q_j(t) e^{\lambda_j t} + \int, \tag{2.1.39}$$

where the integral approaches to zero as  $t \rightarrow +\infty$ .

## 2.2 Stability in the Sense of Lyapunov

The stability in the sense of Lyapunov has been widely used to evaluate the performance of dynamic systems no matter whether any time delays are involved or not. Compared with the dynamic systems free of time delays, the stability analysis for delayed dynamic systems, of course, is much more complicated in general. Following the similar routine as done for ordinary differential equations, it can be shown that there exists a kind of delay differential equations whose stability of zero solutions depends on the initial time  $t_0$ , see (Qin et al. 1989). The engineering systems governed by such a kind of delayed differential equations is dangerous and should be considered to be unstable. For the autonomous dynamic systems with constant time delays, however, the stability of the zero solutions is independent of the choice of initial time  $t_0$ .

The theme of this book is confined to the study on the dynamic systems with constant time delays. For example, we consider a set of autonomous delay differential equations with constant time delays  $0 < \tau_1 \leq \tau_2 \leq \dots \leq \tau_l$  as following

$$\begin{cases} \dot{y}(t) = \tilde{f}(y(t), y(t-\tau_1), y(t-\tau_2), \dots, y(t-\tau_l)), & y \in R^n, \quad t > t_0, \\ y(t) = \tilde{\phi}(t), & t \in [t_0 - \tau_l, t_0], \end{cases} \quad (2.2.1)$$

where  $\tilde{\phi}(t)$  is continuous on  $[t_0 - \tau_l, t_0]$ . Assume that Eq. (2.2.1) satisfies the conditions of existence and uniqueness of solution, and denote its unique solution by  $\tilde{y}(t) \equiv \tilde{y}(t, t_0, \tilde{\phi})$ .

As in the case of ordinary differential equations, the stability problem of a non-zero solution can always be transformed into that of a zero solution. In fact, a perturbed solution  $\hat{y}(t) \equiv \hat{y}(t, t_0, \tilde{\phi})$  should be studied to check the stability of non-zero solution  $\tilde{y}(t)$ . Let  $x(t) \equiv \hat{y}(t) - \tilde{y}(t)$ , then we have

$$\begin{cases} \dot{x}(t) = \tilde{f}(x(t) + \tilde{y}(t), x(t-\tau_1) + \tilde{y}(t-\tau_1), \dots, x(t-\tau_l) + \tilde{y}(t-\tau_l)) \\ \quad - \tilde{f}(\tilde{y}(t), \tilde{y}(t-\tau_1), \dots, \tilde{y}(t-\tau_l)), & t > t_0, \\ x(t) = \phi(t) \equiv \hat{\phi}(t) - \tilde{\phi}(t), & t \in [t_0 - \tau_l, t_0] \end{cases} \quad (2.2.2a)$$

or simply denote it by

$$\begin{cases} \dot{x}(t) = f(x(t), x(t-\tau_1), \dots, x(t-\tau_l)), & t > t_0, \\ x(t) = \phi(t), & t \in [t_0 - \tau_l, t_0]. \end{cases} \quad (2.2.2b)$$

Obviously, Eq. (2.2.2) has a zero solution starting from  $\phi(t) \equiv 0, t \in [t_0 - \tau, t_0]$ .

**Definition 2.2.1** The zero solution of Eq. (2.2.2b) is said to be *stable* if for any  $\varepsilon > 0$ , there exists  $\delta > 0$  such that any solution  $x(t, t_0, \phi)$  of Eq. (2.2.2b) satisfies  $\|x(t, t_0, \phi)\| < \varepsilon$  provided that  $\|\phi\|_c < \delta$ .

**Definition 2.2.2** The zero solution of Eq. (2.2.2) is said to be *asymptotically stable* if it is stable and there is a sufficiently small  $\delta' > 0$  such that  $\|x(t, t_0, \phi)\| \rightarrow 0$  as  $t \rightarrow +\infty$  provided that  $\|\phi\|_c < \delta'$ .

In general, the concepts of uniformly asymptotic stability, exponential asymptotic stability and global asymptotic stability can also be introduced as in the case of ordinary differential equations. Anyway, the widely used concept in engineering is the asymptotic stability. The analysis of asymptotic stability for autonomous delayed differential equations will be discussed in detail in this book.

There are basically two important kinds of methods to study the stability of delay differential equations. One is the Lyapunov method, and the other is the method of characteristic function. The pertinent advantage of the Lyapunov method is its applicability to both linear and nonlinear delay differential equations. However, it has great difficulty in both constructing the Lyapunov function and estimating the derivative of the Lyapunov function along the solution of a delay differential equation. In addition, the results obtained by the Lyapunov method are usually conservative. What will be mainly discussed in this book is the method of characteristic function. Though this method works only for linearized delay differential equations, it offers some useful sufficient and necessary conditions.

## 2.2.1 The Lyapunov Methods

In this subsection, a few examples are presented to demonstrate how to check the stability of delay differential equations by using the Lyapunov method. For detailed discussions on this topic, it is referred to see (Qin et al. 1989).

### (1) Method of Lyapunov function

Most results, on the basis of the Lyapunov function, about the stability of zero solution for ordinary differential equations can be extended to delay differential equations. For example, if there is a positive definite function  $V$  in the system state such that the total derivative of  $V$ , i.e., the derivative of  $V$  with respect to time  $t$  along the solution of a delay differential equation, is non-positive definite or negative definite, the zero solution is stable or asymptotically stable.

**Example 2.2.1** Consider a delay differential equation

$$\dot{x}(t) = -x(t)x^2(t-\tau), \quad x \in R. \quad (2.2.3)$$

Let the positive definite Lyapunov function be  $V(x) \equiv x^2/2$ , then the total derivative of  $V(x)$  reads

$$\left. \frac{dV}{dt} \right|_{\text{Eq.(2.2.3)}} = x(t)\dot{x}(t) = -x^2(t)x^2(t-\tau) \leq 0. \quad (2.2.4)$$

Thus, the zero solution of Eq. (2.2.3) is stable.

In many cases, great difficulty may be encountered in estimating the total derivative of  $V$  by a direct use of the method of Lyapunov function. To avoid the difficulty, Razumikhin proposed a useful condition as following. In order that the zero solution is asymptotically stable, it is necessary to require that the total derivative of  $V$  is negative definite when

$$|x(t-\tau)| \leq |x(t)| \quad \text{for } t \geq t_0. \quad (2.2.5)$$

This inequality is usually called the *Razumikhin condition*. The idea behind this condition is quite simple. To ensure the zero solution asymptotically stable, the solution of an initial value problem should have a tendency of decreasing. If the inequality  $|x(t)| < |x(t-\tau)|$  holds for all  $t \geq t_0$ , the solution is undoubtedly asymptotically stable. So, it is necessary to check the stability for the case of  $|x(t-\tau)| \leq |x(t)|$  only. This implies that the Razumikhin condition does not strengthen the stability conditions, but reduce the unnecessary complexities.

**Example 2.2.2** Check the stability of a linear delay differential equation

$$\dot{x}(t) = -2x(t) - x(t-\tau), \quad x \in R. \quad (2.2.6)$$

Let  $V(x) \equiv x^2/2$ , then the total derivative of  $V(x)$  reads

$$\left. \frac{dV}{dt} \right|_{\text{Eq.(2.2.4)}} = -2x^2(t) - x(t)x(t-\tau). \quad (2.2.7)$$

Applying the Razumikhin condition to Eq. (2.2.7) gives

$$\left. \frac{dV}{dt} \right|_{\text{Eq.(2.2.4)}} \leq -2x^2(t) + |x(t)| \cdot |x(t-\tau)| \leq -x^2(t). \quad (2.2.8)$$

The zero solution of Eq. (2.2.6) is asymptotically stable because  $-x^2$  is negative definite.

**Example 2.2.3** Find out the asymptotic stability conditions for the following  $n$ -dimensional linear system with a time delay

$$\dot{x}(t) = Ax + Bx(t-\tau), \quad x \in R^n. \quad (2.2.9)$$

We first assume that the matrix  $A$  is *Hurwitz stable*. That is, all the characteristic roots of  $A$  have negative real parts. Then, we suppose that the positive definite matrix  $P$  is a unique solution of the following matrix equation

$$A^T P + PA = -2Q \quad (2.2.10)$$

with a given positive definite matrix  $Q$ . Let the Lyapunov function be defined as

$$V = \mathbf{x}^T(t) P \mathbf{x}(t) + \int_{t-\tau}^t \mathbf{x}^T(t) Q \mathbf{x}(t) dt. \quad (2.2.11)$$

Along the solution of Eq. (2.2.9), we have

$$\left. \frac{dV}{dt} \right|_{\text{Eq.(2.2.9)}} = -\mathbf{x}^T(t) Q \mathbf{x}(t) + 2\mathbf{x}^T(t) P B \mathbf{x}(t-\tau) - \mathbf{x}^T(t-\tau) Q \mathbf{x}(t-\tau). \quad (2.2.12)$$

Applying the Cauchy inequality to the second term in the right-hand side of Eq. (2.2.12) yields

$$\begin{aligned} 2\mathbf{x}^T(t) P B \mathbf{x}(t-\tau) &= 2\mathbf{x}^T(t) P B Q^{-1/2} Q^{1/2} \mathbf{x}(t-\tau) \\ &\leq \mathbf{x}^T(t) P B Q^{-1} B^T P \mathbf{x}(t) + \mathbf{x}^T(t-\tau) Q \mathbf{x}(t-\tau). \end{aligned} \quad (2.2.13)$$

Thus,

$$\begin{aligned} \left. \frac{dV}{dt} \right|_{\text{Eq.(2.2.9)}} &\leq -\mathbf{x}^T(t) Q \mathbf{x}(t) + \mathbf{x}^T(t) P B Q^{-1} B^T P \mathbf{x}(t) \\ &\leq -\mathbf{x}^T(t) Q^{1/2} (I - Q^{-1/2} P B Q^{-1} B^T P Q^{-1/2}) Q^{1/2} \mathbf{x}(t). \end{aligned} \quad (2.2.14)$$

Let  $\lambda_{\max}(C)$  and  $\lambda_{\min}(C)$  be the maximal and minimal characteristic roots of matrix  $C$ , and  $\sigma_{\max}(C)$  and  $\sigma_{\min}(C)$  be the maximal and minimal singular values of  $C$ . The total derivative of  $V$  is negative definite if

$$1 - \lambda_{\max}(Q^{-1/2} P B Q^{-1} B^T P Q^{-1/2}) > 0. \quad (2.2.15)$$

In order that Eq. (2.2.15) holds, it is sufficient that

$$1 - \sigma_{\max}^2(Q^{-1/2} P B Q^{-1/2}) > 0. \quad (2.2.16)$$

This is true if

$$1 - \sigma_{\max}^2(Q^{-1/2} P) \sigma_{\max}^2(B Q^{-1/2}) > 0, \quad (2.2.17)$$

or

$$1 - \frac{\sigma_{\max}^2(Q^{-1/2} P) \|B\|_2^2}{\sigma_{\min}^2(Q^{1/2})} > 0. \quad (2.2.18)$$

Therefore, if all entries in matrix  $B$  are small enough such that

$$\|B\|_2 < \frac{\sigma_{\min}(Q^{1/2})}{\sigma_{\max}(Q^{-1/2}P)} \tag{2.2.19}$$

holds, the zero solution of Eq. (2.2.9) is asymptotically stable. This is a quite natural conclusion when Eq. (2.2.9) is regarded as a slightly perturbed equation from a set of linear ordinary differential equations with the coefficient matrix  $A$  being Hurwitz stable.

**(2) Method of Lyapunov functional**

In mathematics, the delay differential equations are classified into the catalogue of functional differential equations. Thus, the general frame for the stability analysis of delay differential equations is based upon the method of Lyapunov functional. This method can be demonstrated through an example as follows.

For a given real number  $r > 0$ , let  $C \equiv C([-r, 0], R^n)$  be the Banach space of continuous functions mapping  $[-r, 0]$  into  $R^n$ , and each  $\phi \in C$  be equipped with the norm  $\|\phi\|_C = \sup_{s \in [-r, 0]} \|\phi(s)\|$ , where  $\|\cdot\|$  is any norm in  $R^n$ . If  $x_t(s) \equiv x(t+s)$  is defined for  $s \in [-r, 0]$ , then the delay differential equation with initial condition  $x(t) = \phi(t)$  for  $t \in [\sigma - r, \sigma]$  can be recast in the form of functional differential equation

$$\begin{cases} \dot{x} = f(t, x_t), \\ x_\sigma = \phi. \end{cases} \tag{2.2.20}$$

For instance, the scalar delay differential equation  $\dot{x}(t) = -cx(t)[1+x(t-1)]$  can be written as  $\dot{x} = f(t, x_t)$ , where  $f(t, \psi) = -c\psi(0)[1+\psi(-1)]$ . Similarly, if  $f(t, \psi) = g(t, \psi(0), \psi(-\tau))$ , then  $\dot{x} = f(t, x_t)$  gives  $\dot{x}(t) = g(t, x(t), x(t-\tau))$ .

**Example 2.2.4** Consider the scalar differential equation with a time delay

$$\dot{x}(t) = ax(t) + bx(t-\tau), \tag{2.2.21}$$

namely,

$$\dot{x}(t) = ax_t(0) + bx_t(-\tau). \tag{2.2.22}$$

Let the Lyapunov functional  $V$  be defined as

$$V(x_t) = \frac{1}{2} x_t^2(0) + \mu \int_{-\tau}^0 x_t^2(s) ds, \quad \mu > 0, \tag{2.2.23}$$

which is positive definite. The total derivative of  $V$  is

$$\begin{aligned} \frac{dV}{dt} \Big|_{\text{Eq.(2.2.22)}} &= (a+\mu)x_t^2(0) + bx_t(0)x_t(-\tau) - \mu x_t^2(-\tau) \\ &= \begin{bmatrix} x_t(0) & x_t(-\tau) \end{bmatrix} \begin{bmatrix} a+\mu & b/2 \\ b/2 & -\mu \end{bmatrix} \begin{bmatrix} x_t(0) \\ x_t(-\tau) \end{bmatrix}. \end{aligned} \quad (2.2.24)$$

In order that the total derivative of  $V$  is negative definite, it is sufficient and necessary that the following two inequalities hold

$$a+\mu < 0, \quad -4(a+\mu)\mu - b^2 > 0. \quad (2.2.25)$$

This fact is true if  $\mu = -a/2$  and  $a^2 - b^2 > 0$ . In other words, the zero solution is asymptotically stable if  $a < 0$  and  $|b| < -a$ . In this case, the stability is independent of the time delay.

It is certainly possible to check the results of Example 2.2.3 by using the Lyapunov functional, too. In fact, the Lyapunov function  $V$  defined in Eq. (2.2.11) is essentially a Lyapunov functional as following

$$V(x_t) = x_t^T(0)Px_t(0) + \int_{-\tau}^0 x_t^T(s)Qx_t(s)ds, \quad (2.2.26)$$

and the total derivative of  $V$  now becomes

$$\begin{aligned} \frac{dV}{dt} \Big|_{\text{Eq.(2.2.9)}} &= -x_t^T(0)Qx_t(0) + 2x_t^T(0)PBx_t(-\tau) - x_t^T(-\tau)Qx_t(-\tau) \\ &= - \begin{bmatrix} x_t(0) \\ x_t(-\tau) \end{bmatrix}^T \begin{bmatrix} Q & -PB \\ -B^T P & Q \end{bmatrix} \begin{bmatrix} x_t(0) \\ x_t(-\tau) \end{bmatrix}. \end{aligned} \quad (2.2.27)$$

In order that Eq. (2.2.27) is negative definite, it is sufficient and necessary that the coefficient matrix in the right-hand side of Eq. (2.2.27) is positive definite. This is definitely true if  $\|B\|_2$  is small enough.

Finally, it is worthy to point out the possibility of determining whether or not the zero solution of a delay differential equation is unstable by means of the Lyapunov method, see, for example, (Hale 1977).

## 2.2.2 Method of Characteristic Function

Consider an  $n$ -dimensional linear delay system governed by

$$\dot{x} = Ax + \sum_{j=1}^l B_j x(t-\tau_j), \quad x \in R^n, \quad A, B_j \in R^{n \times n}, \quad (2.2.28)$$

where  $0 < \tau_1 < \dots < \tau_l$  are the time delays. Substituting the candidate solution  $\mathbf{x}(t) = \mathbf{a}e^{\lambda t}$  with a constant  $\lambda$  and a constant vector  $\mathbf{a}$  into Eq. (2.2.28) yields

$$\det(\lambda \mathbf{I} - \mathbf{A} - \sum_{j=1}^l \mathbf{B}_j e^{-\lambda \tau_j}) = 0, \tag{2.2.29}$$

where  $\mathbf{I} \in R^{n \times n}$  is the identity matrix. Eq. (2.2.29) is called the *characteristic equation* of Eq. (2.2.28), and its roots are called the *characteristic roots* of Eq. (2.2.28). Furthermore, Eq. (2.2.29) can be recast as following

$$p(\lambda) \equiv \lambda^n + d_1(\lambda)\lambda^{n-1} + \dots + d_{n-1}(\lambda)\lambda + d_n(\lambda) = 0, \tag{2.2.30}$$

where  $d_j(\lambda)$  are the polynomials with respect to  $e^{-\lambda \tau_1}$ ,  $e^{-\lambda \tau_2}$ , ... and  $e^{-\lambda \tau_l}$ . In particular,

$$d_1(\lambda) = -e^{-\lambda \tau_1} \text{tr}(\mathbf{B}_1) - e^{-\lambda \tau_2} \text{tr}(\mathbf{B}_2) - \dots - e^{-\lambda \tau_l} \text{tr}(\mathbf{B}_l), \tag{2.2.31}$$

where  $\text{tr}(\mathbf{B}_j)$  is the trace of matrix  $\mathbf{B}_j$ . The characteristic function  $p(\lambda)$  in Eq. (2.2.30) is usually called a *quasi-polynomial* or emphatically characteristic quasi-polynomial since  $d_j(\lambda)$  may include a number of exponential functions in  $\lambda$ . The method of characteristic function is to study the system stability by investigating the root allocation of  $p(\lambda)$ .

Equation (2.2.30) gives the asymptotic behavior of  $p(\lambda)$

$$p(\lambda) = \lambda^n + O(|\lambda|^{n-1}), \tag{2.2.32}$$

as  $|\lambda| \rightarrow +\infty$  under the condition  $\text{Re} \lambda \geq 0$ . This implies that the roots (if any) of  $p(\lambda)$  must lie in a sufficiently large disk. If this is not the case,  $p(\lambda)$  should have an infinite number of roots on the open right half-plane. Then, there is a root sequence  $\{\lambda_j\}$  such that  $p(\lambda_j) = 0$  and  $|\lambda_j| \rightarrow +\infty$  as  $j \rightarrow +\infty$ . This gives a contradictory equation

$$0 = \frac{p(\lambda_j)}{\lambda_j^n} \rightarrow 1 + o(1). \tag{2.2.33}$$

On the other hand, the quasi-polynomial  $p(\lambda)$  is a non-constant, analytic function in  $\lambda$  on the entire complex plane, so the roots of  $p(\lambda)$  are isolated, and only a finite number of roots lie in any compact set of the complex plane. The above two facts can be summarized as a lemma.

**Lemma 2.2.1** The quasi-polynomial  $p(\lambda)$  in Eq. (2.2.30) has only a finite number of roots on the right half-plane defined by  $\text{Re} \lambda \geq 0$ .

Moreover, we have the following claim.



**Lemma 2.2.2** The number of roots of  $p(\lambda)$  in any given strip  $\{\lambda = x + iy \mid a \leq x \leq b\}$  is finite.

**Proof** Assume on the contrary that there are an infinite number of roots  $\{\lambda_j\}$  of  $p(\lambda)$  in the given strip. Because only a finite number of roots lie in a compact set of the complex plane, we have  $|\lambda_j| \rightarrow +\infty$  subject to  $a \leq \operatorname{Re} \lambda_j \leq b$  as  $j \rightarrow +\infty$ . This results in the contradictory Eq. (2.2.33) again. The proof is completed.

Lemma 2.2.2 reveals an important feature of delay differential equation, which is essential for the stability analysis.

**Lemma 2.2.3** If all the roots of  $p(\lambda)$  have negative real parts, then, there exists a positive number  $\alpha$  such that  $\operatorname{Re} \lambda \leq -\alpha$  holds true for all roots of  $p(\lambda)$ .

**Proof** Assume on the contrary that there is a root sequence  $\{\lambda_j\}$  of  $\lambda = re^{i\theta}$  on the open left half-plane such that  $\operatorname{Re} \lambda_j \rightarrow 0$  when  $j \rightarrow +\infty$ . Then, we must have  $|\lambda_j| \rightarrow +\infty$  as  $j \rightarrow +\infty$  since only a finite number of roots lie in a compact set of the complex plane. This again gives the contradictory Eq. (2.2.33).

**Example 2.2.5** Consider the simple quasi-polynomial  $p(\lambda) = \lambda - a - be^{-\lambda\tau}$ . If  $b \neq 0$ ,  $p(\lambda)$  has an infinite number of roots. Assume that  $\{\lambda_j\}$  is a sequence of roots of  $p(\lambda)$ , then

$$|\lambda_j - a| = |b| e^{-\tau \operatorname{Re} \lambda_j}. \quad (2.2.34)$$

If  $|\lambda_j| \rightarrow +\infty$ , then  $\operatorname{Re} \lambda_j \rightarrow -\infty$  as  $j \rightarrow +\infty$ . This implies that there exists a real number  $\alpha$  such that  $\operatorname{Re} \lambda < \alpha$  holds for all roots  $\lambda$  of  $p(\lambda)$ . Because  $p(\lambda)$  is analytic on the entire complex plane, the roots must be isolated, and the number of roots in any compact regions of the complex plane is finite. Moreover, the number of roots on the right half-plane is finite. In fact, the roots in the strip  $\{\lambda = x + iy \mid 0 \leq x \leq \alpha\}$  must lie in some bounded rectangle. Otherwise, there is a sequence of roots  $\{\lambda_j\}$  with  $|\lambda_j| \rightarrow +\infty$  and  $0 \leq \operatorname{Re} \lambda_j < \alpha$  as  $j \rightarrow +\infty$ . This contradicts Eq. (2.2.34). Thus, the number of roots with  $\operatorname{Re} \lambda \geq 0$  must be finite.

Assume that all the roots of  $p(\lambda)$  are  $\{\lambda_j\}$  counted by multiplicity  $m_j$ . As pointed out in Subsection 2.1.2, any solution of a linear homogeneous delay differential equation can be expressed as a linear combination of the fundamental solutions such as  $t^k e^{\lambda_j t}$ ,  $k = 0, 1, \dots, m_j$ ,  $j = 1, 2, \dots, +\infty$ . Thus, we have the following assertions for the stability of delay differential equation.

**Theorem 2.2.1** The zero solution of Eq. (2.2.28) is asymptotically stable if and only if all the roots of Eq. (2.2.30) have negative real parts.

**Theorem 2.2.2** Assume that  $p(\lambda)$  in Eq. (2.2.30) has a finite number of simple pure imaginary roots and all the other roots of  $p(\lambda)$  have real parts less than a negative number, then the zero solution of Eq. (2.2.28) is stable.

**Theorem 2.2.3** If  $p(\lambda)$  in Eq. (2.2.30) has any repeated pure imaginary roots or any roots with positive real parts, the zero solution of Eq. (2.2.28) is unstable.

The proofs of the above theorems are based on the estimation techniques for contour integral, see (Qin et al. 1989) for more details.

As for the analysis of asymptotic stability, the *Pontryakin Theorem* stated below serves as a very powerful tool.

**Theorem 2.2.4** Let  $R(\omega) \equiv \text{Re}[p(i\omega)]$  and  $S(\omega) \equiv \text{Im}[p(i\omega)]$ , then the zero solution of Eq. (2.2.28) is asymptotically stable if and only if  $R(\omega)$  and  $S(\omega)$  have real, simple and interlacing roots, and the following inequality holds for all real  $\omega$

$$R(\omega)S'(\omega) - S(\omega)R'(\omega) > 0, \quad (2.2.35a)$$

where the prime represents the derivative with respect to  $\omega$ .

The proof of this theorem is not presented here since it is rather lengthy. To understand the theorem intuitively, we note that Eq. (2.2.35a) is equivalent to

$$\frac{d}{d\omega} \arg p(i\omega) = \frac{S'(\omega)R(\omega) - R'(\omega)S(\omega)}{R^2(\omega) + S^2(\omega)} > 0. \quad (2.2.35b)$$

Thus, a quasi-polynomial  $p(\lambda)$  is asymptotically stable if and only if  $R(\omega)$  and  $S(\omega)$  have real, simple and interlacing roots, and the phase angle of  $p(i\omega)$  increases monotonously with an increase of  $\omega$ .

If the time delays are regarded as system parameters, a root of  $p(\lambda)$  is continuous with respect to the time delays. This fact leads to the following theorem.

**Theorem 2.2.5** As the time delays vary, the multiplicity summation of roots of  $p(\lambda)=0$  on the open right half-plane can change only if a root appears on or crosses the imaginary axis.

**Proof** For the sake of simplicity, the proof is given for the case of a single time delay. To look at the effect of the time delay, denote  $p(\lambda)$  by  $p(\lambda, \tau)$ . Lemma 2.2.1 shows that the multiplicity summation of roots of  $p(\lambda, \tau)$  on the open right half-plane is finite. Suppose that the multiplicity summation changes, but no roots appear on or cross the imaginary axis. This can occur only when a root appears at infinity. In fact, let  $\lambda = \lambda(\tau)$  be a root of  $p(\lambda, \tau) = 0$ . For a small circular disk around  $\lambda(\tau)$  and any  $\tau'$  sufficiently close to  $\tau$ , the multiplicity summation of roots in the disk is equal to the multiplicity of  $\lambda(\tau)$ . From the Rouché's theorem in complex analysis, a root  $\lambda(\tau)$  is not able to appear or disappear, or change its multiplicity all of a sudden at any finite point on the complex plane. Hence, there exists a time delay  $\hat{\tau}$  and a root  $\lambda(\tau)$  of  $p(\lambda, \tau) = 0$  such that  $|\lambda| \rightarrow +\infty$  as  $\tau \rightarrow \hat{\tau} + 0$  or  $\tau \rightarrow \hat{\tau} - 0$  for  $\text{Re} \lambda \geq 0$ . However,

$$\frac{p(\lambda(\tau), \tau)}{\lambda^n(\tau)} = 1 + o(1) \quad (2.2.36)$$

holds for  $\operatorname{Re} \lambda \geq 0$  when  $\tau \rightarrow \hat{\tau} + 0$  or  $\tau \rightarrow \hat{\tau} - 0$  since  $|e^{-\tau \lambda(\tau)}| \leq 1$ . Equation (2.2.36) contradicts the fact that  $p(\lambda, \tau) = 0$ . Then, as  $\tau$  varies, the multiplicity summation of roots of  $p(\lambda, \tau) = 0$  on the open right half-plane can change only if a root appears on or crosses the imaginary axis. This completes the proof of Theorem 2.2.5.

From this proof, the same result holds true when the roots of  $p(\lambda)$  are considered as functions with respect to the coefficients of  $p(\lambda)$ .

A quasi-polynomial usually has an infinite number of roots, so it is hard and even impossible to find out all the roots. Hence, Theorem 2.2.1 can only be used directly to deal with a few simple cases such as the so-called delay-independent stability of a scalar delay differential equation.

**Definition 2.2.3** The solution of a delay differential equation is said to be *delay-independent stable* if it is asymptotically stable for any given time delays.

The following theorem is obviously true.

**Theorem 2.2.6** Equation (2.2.28) is delay-independent stable if and only if the following two conditions hold.

(a) Equation (2.2.28) is asymptotically stable when all the time delays disappear.

(b) The marginal stability condition  $p(i\omega) = 0$  has no real root  $\omega$  for all given time delays.

**Example 2.2.6** Study the condition of delay-independent stability of a linear delay differential equation as following

$$\dot{x}(t) + ax(t) + bx(t - \tau) = 0, \quad x \in R. \quad (2.2.37)$$

The corresponding characteristic function of Eq. (2.2.37) is

$$p(\lambda) = \lambda + a + be^{-\lambda\tau}. \quad (2.2.38)$$

When  $\tau = 0$ , we have  $p(\lambda) = \lambda + a + b$ , and  $a + b$  must be positive to guarantee the Hurwitz stability of the system without time delay. If  $\tau > 0$ , the marginal stability condition  $p(i\omega) = 0$  leads to  $|i\omega + a| = |b|$ . It yields  $\omega^2 + a^2 - b^2 = 0$ . Conversely, if there exists  $\omega > 0$  satisfying this equation, then  $|i\omega + a|^2 = |b|^2$  holds. Thus, there is a real number  $\theta \in [0, 2\pi)$  so that  $i\omega + a = be^{i\theta}$ . So we have  $\tau = \theta/\omega$  such that  $p(i\omega) = 0$ . If  $a^2 - b^2 = 0$  then  $p(0) = a + b = 2a \neq 0$  since  $a + b > 0$ . Hence, for all given delay  $\tau$ ,  $p(i\omega) \neq 0$  holds for all real  $\omega$  if and only if  $\omega^2 + a^2 - b^2 = 0$  does not have any real root  $\omega$  other than zero. This fact is true if  $a^2 - b^2 \geq 0$ .

Thus, Eq. (2.2.37) is delay-independent stable if and only if both  $a+b>0$  and  $a^2 - b^2 \geq 0$  hold true.

### 2.2.3 Stability Criteria

To testify the asymptotically stability of a linear delay differential equation, it is sufficient to investigate the allocation of characteristic roots as analyzed in Subsection 2.2.2. Because a quasi-polynomial usually has an infinite number of roots, it is hard, and even impossible, to find out all the roots. So, it is highly demanded to develop some practical stability criteria. This subsection focuses on the stability criterion for the linear delay differential equation with following characteristic quasi-polynomial

$$p(\lambda) \equiv \lambda^n + d_1(\lambda)\lambda^{n-1} + \dots + d_{n-1}(\lambda)\lambda + d_n(\lambda) = 0, \quad (2.2.39)$$

where  $d_j(\lambda)$  are polynomials with respect to  $e^{-\lambda\tau_1}$ ,  $e^{-\lambda\tau_2}$ , ... and  $e^{-\lambda\tau_l}$ , and  $\tau_j$  are the time delays. The main result of this subsection is the Hassard theorem as following.

**Theorem 2.2.7** Assume that the characteristic quasi-polynomial  $p(\lambda)$  of a linear delay differential equation has no roots on the imaginary axis. Let  $M(\omega) \equiv \text{Re}[i^{-n} p(i\omega)]$ ,  $N(\omega) \equiv \text{Im}[i^{-n} p(i\omega)]$ , and  $\rho_1 \geq \rho_2 \geq \dots \geq \rho_m > 0$  be the positive roots, counted by multiplicity, of  $M(\omega)$ . Then, the delay differential equation is asymptotically stable if and only if

- (a)  $p(0) \neq 0$ ,
- (b)  $N(\rho_j) \neq 0$  for all  $j=1, 2, \dots, m$ ,
- (c)  $\frac{n}{2} + \frac{1}{2}(-1)^m \text{sgn} N(0) + \sum_{j=1}^m (-1)^{j-1} \text{sgn} N(\rho_j) = 0$ .

As  $p(\lambda)$  is assumed to have no roots on the imaginary axis, condition (a) in Theorem 2.2.7 is certainly satisfied. Thus, it requires verifying conditions (b) and (c) only. Before the proof of the theorem, two simple examples are presented to demonstrate how to use Theorem 2.2.7 to complete the stability analysis.

**Example 2.2.7** As shown in Example 2.2.6, the system governed by the quasi-polynomial  $p(\lambda) = \lambda + 2 - e^{-\lambda\tau}$  is delay-independent stable. Now, we verify this result by using Theorem 2.2.7. Here  $n=1$ ,  $p(0) = 1 \neq 0$ ,  $M(\omega) = \omega + \sin\omega\tau$  and  $N(\omega) = -2 + \cos\omega\tau$ . Because  $M(\omega)$  has no positive roots for any given  $\tau$ , so  $m=0$ . Condition (c) in Theorem 2.2.7 is  $n/2 + \text{sgn} N(0)/2 = 0$ , which is definitely true because  $N(0) = -1 < 0$ . This completes the verification.

**Example 2.2.8** Consider the stability of  $p(\lambda)=\lambda^2+2\lambda+e^{-\lambda\tau}$  when  $\tau=1$  and  $\tau=4$ . We have  $n=2$ ,  $p(0)=1\neq 0$ ,  $M(\omega)=2\omega-\sin\omega\tau$  and  $N(\omega)=\omega^2-\cos\omega\tau$ . When  $\tau=1$ ,  $M(\omega)$  has no positive roots and  $m=0$ , and  $N(0)=-1<0$  holds true. Thus,  $n/2+(-1)^m\text{sgn}N(0)/2=0$ . When  $\tau=4$ ,  $M(\omega)$  has a positive root  $\rho_1=0.4739$ , and  $N(\rho_1)=0.5436$ . This fact, together with  $m=1$  and  $N(0)=-1$ , gives  $n/2-\text{sgn}N(0)/2+\text{sgn}N(\rho_1)+0$ . Thus, all the conditions in Theorem 2.2.7 also hold for  $\tau=4$ . The system corresponding to  $p(\lambda)=\lambda^2+2\lambda+e^{-\lambda\tau}$  is asymptotically stable for both  $\tau=1$  and  $\tau=4$ .

To prove Theorem 2.2.7, three lemmas are required. These lemmas are related to a contour  $\Gamma \equiv \Gamma_1 \cup \Gamma_2$  for any given  $r>0$  as shown in Fig. 2.2.1, where

$$\Gamma_1 = \{ \lambda = re^{i\theta}, \theta: -\pi/2 \rightarrow \pi/2 \}, \tag{2.2.40a}$$

$$\Gamma_2 = \{ \lambda = i\omega, \omega: r \rightarrow 0 \rightarrow -r \}. \tag{2.2.40b}$$

Here,  $r$  is chosen to be large enough such that  $\Gamma$  encircles all the roots of  $p(\lambda)$  on the right half-plane  $\text{Re}\lambda \geq 0$ .

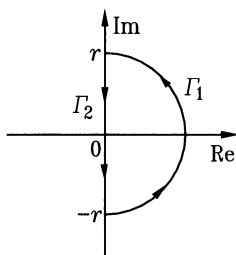


**Fig. 2.2.1.** Contour  $\Gamma$  for Theorem 2.2.7

**Lemma 2.2.4** Under the conditions of Theorem 2.2.7, the number of roots, counted by multiplicity, of  $p(\lambda)$  with  $\text{Re}\lambda \geq 0$  is  $(2\pi i)^{-1} \oint_{\Gamma} [p'(\lambda)/p(\lambda)]d\lambda$ .

**Proof** Because  $p(\lambda)$  is an entire function, there is a non-zero entire function  $q(\lambda)$  on  $\Gamma$  and in its interior such that

$$p(\lambda) = q(\lambda) \prod_{j=1}^N (\lambda - z_j)^{k_j}, \tag{2.2.41}$$

where  $z_j$  are the roots of  $p(\lambda)$  encircled in  $\Gamma$ . Then, we have

$$\frac{p'(\lambda)}{p(\lambda)} = \frac{d[\ln p(\lambda)]}{d\lambda} = \sum_{j=1}^N \frac{k_j}{\lambda - z_j} + \frac{q'(\lambda)}{q(\lambda)}. \tag{2.2.42}$$

The Cauchy theorem in complex analysis implies that

$$\oint_{\Gamma} \frac{q'(\lambda)}{q(\lambda)} d\lambda = 0. \tag{2.2.43}$$

By using the theorem of residue, we have

$$\oint_{\Gamma} \frac{1}{\lambda - z_j} d\lambda = 2\pi i, \quad j=1,2,\dots,N. \tag{2.2.44}$$

Substituting Eqs. (2.2.44) and (2.2.43) into the contour integral of Eq. (2.2.43) on  $\Gamma$  concludes that Lemma 2.2.4 is true.

Now, we start the analysis of next lemma. The property of the contour integral on  $\Gamma_1$  is considerably simple. In fact, noting the asymptotic behavior

$$p(\lambda) = \lambda^n + d_1(\lambda)\lambda^{n-1} + O(|\lambda|^{n-2}) \tag{2.2.45}$$

and

$$p'(\lambda) = [n + d_1'(\lambda)]\lambda^{n-1} + O(|\lambda|^{n-2}), \tag{2.2.46}$$

we have

$$\frac{p'(\lambda)}{p(\lambda)} = \lambda^{-1} [n + d_1'(\lambda)] + O(|\lambda|^{-2}), \tag{2.2.47}$$

as  $|\lambda| \rightarrow +\infty$  with  $\text{Re} \lambda \geq 0$ . Thereby, we obtain

$$\frac{1}{2\pi i} \int_{\Gamma_1} \frac{p'(\lambda)}{p(\lambda)} d\lambda = \frac{1}{2\pi} \int_{-\pi/2}^{\pi/2} [n + d_1'(re^{i\theta})] d\theta + O(r^{-1}). \tag{2.2.48}$$

However,  $d_1(\lambda)$  is a linear combination of the exponential functions  $e^{-\lambda\tau_1}$ ,  $e^{-\lambda\tau_2}$ , ... and  $e^{-\lambda\tau_l}$  with  $\tau_i > 0$ , so  $|d_1'(re^{i\theta})|$  is bounded and  $\lim_{r \rightarrow +\infty} d_1'(re^{i\theta}) = 0$ . Applying the dominated convergence theorem to Eq. (2.2.28) yields

$$\lim_{r \rightarrow +\infty} \frac{1}{2\pi i} \int_{\Gamma_1} \frac{p'(\lambda)}{p(\lambda)} d\lambda = \frac{n}{2}. \tag{2.2.49}$$

On  $\Gamma_2$ , the following two asymptotic expressions hold

$$M(\omega) = \omega^n + O(|\omega|^{n-1}), \quad N(\omega) = O(|\omega|^{n-1}). \tag{2.2.50}$$

For sufficiently large  $\omega > 0$ ,  $M(\omega) > 0$  and  $N(\omega) = o(M(\omega))$  are true. As it is assumed that  $p(i\omega) \neq 0$  holds for real  $\omega$ , there exist  $A(\omega) > 0$  and real  $\phi(\omega)$  such that

$$M(\omega) + iN(\omega) = A(\omega)e^{i\phi(\omega)}. \quad (2.2.51)$$

Then, we have

$$\frac{M'(\omega) + iN'(\omega)}{M(\omega) + iN(\omega)} = \frac{A'(\omega)}{A(\omega)} + i\phi'(\omega), \quad (2.2.52)$$

and

$$\frac{1}{2\pi i} \int_{r_2} \frac{p'(\lambda)}{p(\lambda)} d\lambda = \frac{1}{2\pi i} \int_r^{-r} \left[ \frac{A'(\omega)}{A(\omega)} + i\phi'(\omega) \right] d\omega. \quad (2.2.53)$$

From the definition of  $M(\omega)$  and  $N(\omega)$ , one of them is an even function and the other is an odd function. So,  $A'(\omega)/A(\omega) = [M^2(\omega) + N^2(\omega)]' / [2(M^2(\omega) + N^2(\omega))]$  is an odd function and  $\phi'(\omega) = [M(\omega)N'(\omega) - N(\omega)M'(\omega)] / [M^2(\omega) + N^2(\omega)]$  is an even function. As a result, we have

$$\lim_{r \rightarrow \infty} \frac{1}{2\pi i} \int_{r_2} \frac{p'(\lambda)}{p(\lambda)} d\lambda = \lim_{r \rightarrow \infty} \frac{1}{\pi} [\phi(0) - \phi(r)] = \frac{\phi(0)}{\pi}. \quad (2.2.54)$$

The above facts can be summarized as the following lemma.

**Lemma 2.2.5** Under the conditions of Theorem 2.2.7, the number of roots, counted by multiplicity, of  $p(\lambda)$  with  $\text{Re} \lambda \geq 0$  is  $n/2 + \phi(0)/\pi$ .

**Lemma 2.2.6**

$$\frac{\phi(0)}{\pi} = \frac{1}{2} (-1)^m \text{sgn} N(0) + \sum_{j=1}^m (-1)^{j-1} \text{sgn} N(\rho_j). \quad (2.2.55)$$

**Proof** As  $M(0) + iN(0) \neq 0$ , and either  $M(\omega)$  or  $N(\omega)$  is an odd function, exactly one of the following four cases holds true. (a)  $M(0) = 0$  and  $N(0) > 0$ , (b)  $M(0) = 0$  and  $N(0) < 0$ , (c)  $M(0) > 0$  and  $N(0) = 0$ , (d)  $M(0) < 0$  and  $N(0) = 0$ .

If  $M(\omega)$  has no positive roots, the curve  $M(\omega) + iN(\omega)$  for  $\omega \geq 0$  starts at a point satisfying one of the conditions (a), (b) and (c), traces a path on the half-plane  $M(\omega) > 0$ , and  $N(\omega) = o(M(\omega))$  as  $\omega \rightarrow +\infty$ . Thus, the change in  $\phi(\omega)$  on the interval  $[0, +\infty)$  is  $-\pi/2$ ,  $\pi/2$  or  $0$ , depending on the conditions of (a), (b) or (c). As a result, we have

$$0 - \phi(0) = -\frac{\pi}{2} \text{sgn} N(0). \quad (2.2.56)$$

In general, let  $\rho_1 \geq \rho_2 \geq \dots \geq \rho_m > 0$  be the positive roots, counted by multiplicity, of  $M(\omega)$ . We can show that  $m$  must be finite as in the proof of Lemma 2.2.1 because of Eq. (2.2.50). Thus, we have

$$\phi(\rho_m) - \phi(0) = \frac{\pi}{2} [\operatorname{sgn} N(\rho_m) - \operatorname{sgn} N(0)] \cdot \operatorname{sgn} M\left(\frac{\rho_m}{2}\right), \quad (2.2.57a)$$

$$\phi(\rho_j) - \phi(\rho_{j+1}) = \frac{\pi}{2} [\operatorname{sgn} N(\rho_j) - \operatorname{sgn} N(\rho_{j+1})] \cdot \operatorname{sgn} M\left(\frac{\rho_j + \rho_{j+1}}{2}\right),$$

$$j=1, 2, \dots, m, \quad (2.2.57b)$$

where  $\rho_{m+1} \equiv 0$ , and

$$0 - \phi(\rho_1) = -\frac{\pi}{2} \operatorname{sgn} N(\rho_1). \quad (2.2.57c)$$

Summing up both sides of the above equations and noting that

$$\operatorname{sgn} M\left(\frac{\rho_j + \rho_{j+1}}{2}\right) = \begin{cases} 0, & \rho_j = \rho_{j+1}, \\ (-1)^j, & \rho_{j+1} < \rho_j, \end{cases} \quad (2.2.58)$$

we arrive at

$$\phi(0) = \pi \left[ \frac{1}{2} (-1)^m \operatorname{sgn} N(0) + \sum_{j=1}^m (-1)^{j-1} \operatorname{sgn} N(\rho_j) \right]. \quad (2.2.59)$$

This completes the proof of Lemma 2.2.6.

At this stage, Theorem 2.2.7 can be immediately proved by a direct use of the above three lemmas. As shown in (Hassard 1997), this theorem can also be extended to the case when  $p(\lambda)$  has a finite number of pure imaginary roots.

Let  $R(\omega) \equiv \operatorname{Re}[p(i\omega)]$  and  $S(\omega) \equiv \operatorname{Im}[p(i\omega)]$  again, it is easy to show that

$$\frac{S'(\omega)R(\omega) - R'(\omega)S(\omega)}{R^2(\omega) + S^2(\omega)} = \frac{N'(\omega)M(\omega) - M'(\omega)N(\omega)}{M^2(\omega) + N^2(\omega)}. \quad (2.2.60)$$

Noting that

$$\begin{aligned} \frac{d}{d\omega} \arg[i^{-n} p(i\omega)] &= \frac{d}{d\omega} \arctan \frac{N(\omega)}{M(\omega)} = \frac{N'(\omega)M(\omega) - M'(\omega)N(\omega)}{M^2(\omega) + N^2(\omega)} \\ &= \frac{d}{d\omega} \arg p(i\omega), \end{aligned} \quad (2.2.61)$$

we obtain

$$\arg p(i\omega) \Big|_0^{+\infty} = \arg[i^{-n} p(i\omega)] \Big|_0^{+\infty}. \quad (2.2.62)$$

From the proof of Lemma 2.2.6, the variation of  $\arg[i^{-n} p(i\omega)]$  is just  $\phi(\infty) - \phi(0) = -\phi(0)$  when  $\omega$  varies from zero to the positive infinity. Now, We are in the position to state the *Michailov's criterion* as following.



When  $p(\lambda)$  has no root on the imaginary axis, all the roots of  $p(\lambda)$  stay on the open left half-plane if and only if the variation of  $\arg p(i\omega)$  is  $n\pi/2$  when  $\omega$  increases from zero to the positive infinity, namely,

$$\arg p(i\omega) \Big|_0^{+\infty} = \frac{n\pi}{2}. \quad (2.2.63)$$

However, it is not easy to verify Eq. (2.2.63) in practice. So, the following criterion in integral form is more preferable.

**Theorem 2.2.8** Assume that  $p(\lambda)$  has no root on the imaginary axis, then, all the roots of  $p(\lambda)$  stay on the open left half-plane if and only if

$$\int_0^{+\infty} Z(\omega) d\omega = \frac{n\pi}{2}, \quad (2.2.64)$$

where

$$Z(\omega) \equiv \frac{d[\arg p(i\omega)]}{d\omega} = \frac{R(\omega)S'(\omega) - S(\omega)R'(\omega)}{R^2(\omega) + S^2(\omega)}. \quad (2.2.65)$$

**Remark 2.2.1** In order to check Eq. (2.2.64), it is sufficient to verify

$$\int_0^s Z(\omega) d\omega > \frac{(n-1)\pi}{2} \quad (2.2.66)$$

if a positive number  $s$  is chosen such that  $\int_s^{+\infty} Z(\omega) d\omega < \pi/2$ .

**Example 2.2.9** Consider again the quasi-polynomial  $p(\lambda) = \lambda + 2 - e^{-\lambda\tau}$  in Example 2.2.7. The function  $Z(\omega)$  now is in the form

$$Z(\omega) = \frac{2 - \tau + (1 - 2\tau)\cos\omega\tau + \omega\tau\sin\omega\tau}{\omega^2 + 4\cos\omega\tau - 2\omega\sin\omega\tau + 5}. \quad (2.2.67)$$

By integrating  $Z(\omega)$  numerically, we find  $\int_0^{+\infty} Z(\omega) d\omega = \pi/2 \approx 1.5708$ . According to Theorem 2.2.8, all the roots of  $p(\lambda)$  stay on the open left-half plane for any given time delay.

**Example 2.2.10** Check the stability of a delay differential equation with the following characteristic quasi-polynomial

$$p(\lambda) \equiv 0.1\lambda^2 + 0.3\lambda + 0.5 + (0.1\lambda + 0.2)e^{-\lambda\tau_1} + (0.2\lambda + 0.3)e^{-\lambda\tau_2}. \quad (2.2.68)$$

Now, we check whether  $\int_0^{+\infty} Z(\omega) d\omega = \pi \approx 3.1416$  holds by using numerical integration. The computation shows that  $p(\lambda)$  is asymptotically stable when  $\tau_1 = 3$  and  $\tau_2 = 1.5$ , and is unstable for  $\tau_1 = 2.5$  and  $\tau_2 = 2$ .

In control engineering, an effective and popular method for testifying the stability of linear delay systems is the graphic method of the *Nyquist diagram*. The method is based on the following theorem.

**Theorem 2.2.9** A linear dynamic delay system with Eq. (2.2.39) being the characteristic quasi-polynomial is asymptotically stable if and only if the Nyquist diagram of  $W(i\omega)$ , where

$$W(\lambda) \equiv \frac{p(\lambda)}{(\lambda+1)^n}, \tag{2.2.69}$$

does not encircle the origin of the complex plane.

**Proof** It is easy to see from the Cauchy theorem in complex analysis that

$$\frac{1}{2\pi i} \oint_{\Gamma} \frac{W'(\lambda)}{W(\lambda)} d\lambda = \frac{1}{2\pi i} \oint_{\Gamma} \left[ \frac{p'(\lambda)}{p(\lambda)} - \frac{n}{\lambda+1} \right] d\lambda = \frac{1}{2\pi i} \oint_{\Gamma} \frac{p'(\lambda)}{p(\lambda)} d\lambda, \tag{2.2.70}$$

since  $n/(\lambda+1)$  is analytic within  $\Gamma$ . From Lemma 2.2.4, the left-hand side of Eq. (2.2.70) also counts the number of roots of  $p(\lambda)$  with  $\text{Re}\lambda \geq 0$ . Substituting

$$W(\lambda) = |W(\lambda)|e^{i\theta} \tag{2.2.71}$$

into the right-hand side of Eq. (2.2.70) gives

$$\begin{aligned} \frac{1}{2\pi i} \oint_{\Gamma} \frac{W'(\lambda)}{W(\lambda)} d\lambda &= \frac{1}{2\pi i} \oint_{\Gamma} d[\ln W(\lambda)] = \frac{1}{2\pi i} \oint_{\Gamma} [d\ln|W(\lambda)| + id\theta] \\ &= \frac{\theta_2 - \theta_1}{2\pi}. \end{aligned} \tag{2.2.72}$$

where  $\theta_1$  and  $\theta_2$  are the initial and final values of phase angle of  $W(\lambda)$  when  $\lambda$  moves along  $\Gamma$  in the counter-clockwise direction exactly one circle. Because  $W(\lambda) \rightarrow 1+0 \cdot i$  as  $|\lambda| \rightarrow +\infty$  with  $\text{Re}\lambda \geq 0$ , the quasi-polynomial  $p(\lambda)$  has no roots with  $\text{Re}\lambda \geq 0$ , or equivalently  $\theta_2 - \theta_1 = 0$ , if and only if the Nyquist diagram of  $W(i\omega)$  does not encircle the origin of the complex plane.

**Example 2.2.11** Confirm the stability of  $p(\lambda)$  in Eq. (2.2.68) by using Theorem 2.2.8. As shown in Fig. 2.2.2a, the Nyquist diagram of  $p(i\omega)/(i\omega+1)^2$  with  $\tau_1=3$  and  $\tau_2=1.5$  does not encircle the origin of the complex plane. Thus, the quasi-polynomial  $p(\lambda)$  is asymptotically stable. As for  $\tau_1=2.5$  and  $\tau_2=2$ ,  $p(\lambda)$  is unstable because the origin stays in the region bounded by the Nyquist diagram  $p(i\omega)/(i\omega+1)^2$  shown in Fig. 2.2.2b.



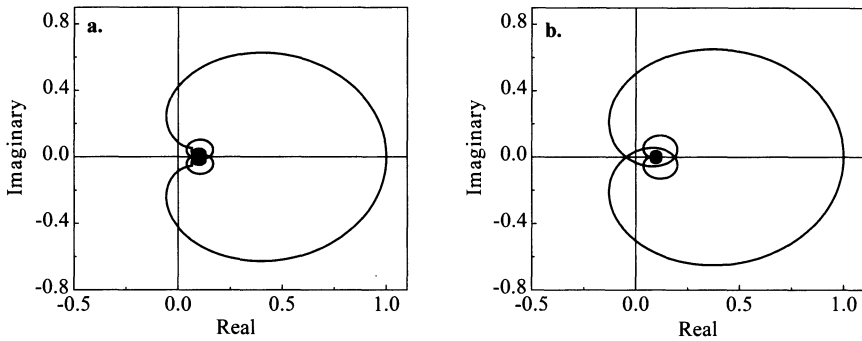


**Fig. 2.2.2.** The Nyquist diagrams of  $p(i\omega)/(i\omega+1)^2$ ; **a.**  $\tau_1=3$  and  $\tau_2=1.5$ , **b.**  $\tau_1=2.5$  and  $\tau_2=2$

### 2.3 Important Features of Delay Differential Equations

As shown in the previous sections, the delay differential equations can be studied in a similar way for ordinary differential equations in many aspects, and some results are also similar to those for ordinary differential equations. However, the delay differential equations are indeed different from ordinary differential equations. Example 2.1.2, for instance, indicates that the uniqueness of the solution of a delay differential equation does not exclude the possible cases where different solutions may intersect with each other. This is not the case for ordinary differential equations.

The most notable feature of a delay differential equation is the infinite dimensions of both state space and solution space. The state space of a delay differential equation is an infinite-dimensional Banach space, rather than the Euclidean space for ordinary differential equations. As stated in the beginning of Section 2.1, the state of a dynamic system with a time delay  $\tau$  can only be determined if its initial state is given as a function vector  $\phi(t)$  in the Banach space  $C([t_0-\tau, t_0], R^n)$ , instead of a constant state vector of finite dimensions in the Euclidean space. The solution space of a delay differential equation, no matter what dimensions the equation has, is always infinite-dimensional, whereas the solution space of an ordinary differential equation is of finite dimensions. This fact can be alternatively understood as following. The characteristic function of a linear delay differential equation includes at least one exponential term due to time delays, and hence may have an infinite number of characteristic roots, while an ordinary differential equation of order  $n$  has just  $n$  characteristic roots. This difference is the essential

cause that may give rise to great difference between these two kinds of differential equations.

Though the time delays are often very short in applications, they should be neglected or simplified with a great care. In what follows, a number of simple, but interesting examples will be given to demonstrate the effect of time delays on the system dynamics. They will lead readers to the latter chapters of the book.

**(1) Effect of time delays on the uniqueness of solutions**

**Example 2.3.1** Consider a nonlinear delay differential equation

$$\dot{x}(t)=[x(t-\tau)-K]^{1/3}, \quad x \in R, \tag{2.3.1}$$

where  $K$  is a constant. When  $\tau=0$ , Eq. (2.3.1) becomes an ordinary differential equation

$$\dot{x}(t)=[x(t)-K]^{1/3}. \tag{2.3.2}$$

Under the initial condition  $x(0)=K$ , Eq. (2.3.2) has two solutions. One is  $x(t)=K$  and the other is  $x(t)=K+2\sqrt{2}t^{3/2}/(3\sqrt{3})$ . Using the method of step-by-step, however, we can show that the solution of Eq. (2.3.1) is unique under any continuous initial functions if  $\tau>0$ .

**Example 2.3.2** Consider again a nonlinear delay differential equation

$$\dot{x}(t)=[x(t)-x(t-\tau)]^{1/3}, \quad x \in R. \tag{2.3.3}$$

When  $\tau=0$ , this equation degenerates to  $\dot{x}=0$ , the existence and uniqueness of the solution hold true under any initial condition. If the initial function  $x(t)=\phi(t)\equiv K$  is assumed for  $t \in [-\tau, 0]$ , Eq. (2.3.3) has at least two solutions  $x(t)\equiv K$  and  $x(t)=K+2\sqrt{2}t^{3/2}/(3\sqrt{3})$  when  $t \in [0, \tau]$ .

**(2) Effect of time delays on the stability of solutions**

**Example 2.3.3** Consider a set of linear delay differential equations

$$\begin{cases} \dot{x}(t)=y(t-\tau), & x, y \in R, \\ \dot{y}(t)=-x(t-\tau). \end{cases} \tag{2.3.4}$$

When  $\tau=0$ , the zero solution of Eq. (2.3.4) is stable. For a sufficiently short time delay  $\tau$ , however, it is easy to show that the zero solution of Eq. (2.3.4) is unstable. In fact, the characteristic equation of Eq. (2.3.4) is

$$\lambda^2 + e^{-2\lambda\tau} = 0. \tag{2.3.5}$$

Let the root of Eq. (2.3.5) be a function in  $\tau$  and denote it by  $\lambda(\tau)$ , we can readily verify that

$$\lambda(0) = \pm i, \quad \left. \frac{d(\operatorname{Re}\lambda)}{d\tau} \right|_{\tau=0} = 1. \quad (2.3.6)$$

Thereby, Eq. (2.3.5) has a pair of conjugate characteristic roots with positive real parts when the time delay  $\tau$  is a sufficiently small, positive number.

**Example 2.3.4** Consider a set of linear delay differential equations

$$\dot{\mathbf{x}}(t) = \mathbf{A}\mathbf{x}(t) + \mathbf{B}\mathbf{x}(t-\tau), \quad (2.3.7)$$

where

$$\mathbf{A} = \begin{bmatrix} 0 & 1 & 0 \\ -1 & 1 & 0 \\ 0 & 0 & -1 \end{bmatrix}, \quad \mathbf{B} = \begin{bmatrix} 0 & 0 & 0 \\ 1 & -1 & 0 \\ 0 & 0 & 0 \end{bmatrix}. \quad (2.3.8)$$

The corresponding characteristic equation reads

$$p(\lambda) = (\lambda+1)[\lambda^2 - \lambda + 1 + (\lambda-1)e^{-\lambda\tau}] = 0. \quad (2.3.9)$$

When  $\tau=0$ , Eq. (2.3.9) has a repeated root  $\lambda=0$  and the zero solution is unstable. For  $\tau>0$ , we find that  $\lambda=0$  is a simple characteristic root and all other characteristic roots have negative real parts. Thus, the zero solution is asymptotically stable.

As time delays often produce great difficulty in the dynamic analysis, it is certainly beneficial to simplify the delay terms in a delay differential equation before it is analyzed or solved. A natural idea is to use the truncated Taylor expansion for the delay terms in a delay differential equation. The following example, however, indicates that the abuse of Taylor's expansion may give a wrong prediction of the system dynamics.

**Example 2.3.5** Consider a linear delay differential equation

$$\dot{x}(t) = -2x(t) + x(t-\tau), \quad x \in R. \quad (2.3.10)$$

According to Example 2.2.6, the zero solution of Eq. (2.3.10) is delay-independent stable. For any short time delay  $\tau$  satisfying  $0 < \tau \ll 1$ , substituting the first order Taylor expansion  $x(t-\tau) \approx x(t) - \tau\dot{x}(t)$  into Eq. (2.3.10) yields

$$(\tau+1)\dot{x}(t) + x(t) = 0. \quad (2.3.11)$$

The approximated differential equation is asymptotically stable since  $\tau > -1$ . If the second order Taylor expansion  $x(t-\tau) \approx [x(t) - \tau \dot{x}(t) + \tau^2 \ddot{x}(t)/2]$  is substituted into Eq. (2.3.10), the result is a second order ordinary differential equation

$$\tau^2 \ddot{x}(t) - 2(\tau+1)\dot{x}(t) - 2x(t) = 0. \quad (2.3.12)$$

It is easy to verify, from the Routh-Hurwitz criterion, that the zero solution of Eq. (2.3.12) is unstable. This example shows that great care must be taken when the Taylor approximation of higher orders is used to simplify the delay terms. The efficacy of the Taylor expansion of delay terms will be analyzed in detail in Section 5.3.

It is also worthy to notice that the stability criteria of delay differential equations of neutral type are quite different from those for retarded type. For example, the zero solution of a delay differential equation of retarded type is asymptotically stable if and only if all the characteristic roots have negative real parts, but this may not be the case for a delay differential equation of neutral type. That is, the zero solution of a delay differential equation of neutral type may not be asymptotically stable even if all the characteristic roots have negative real parts. As stated in (Kolmanovskii and Myshkis 1999), all the characteristic roots of the following delay differential equation of neutral type

$$\dot{x}(t) = -x(t) - \dot{x}(t-\tau), \quad x \in R \quad (2.3.13)$$

lie on the left half-plane, but an infinite number of them are closely accumulated to the imaginary axis so that the zero solution of Eq. (2.3.13) is unstable.

### (3) Effect of time delays on the periodicity of solutions

**Example 2.3.6** Consider the delay differential equation

$$\ddot{x}(t) + x(t-\tau) = 0, \quad x \in R, \quad (2.3.14)$$

which serves as the simplest model for delayed linear oscillators. Equation (2.3.14) has a periodic solution if  $\tau = 0$ . For any  $\tau > 0$ , however, Eq. (2.3.14) has no periodic solution at all because the corresponding characteristic equation  $\lambda^2 + e^{-\lambda\tau} = 0$  has no pure imaginary roots. Intuitively speaking, the truncated Taylor expansion of the delayed stiffness term  $x(t-\tau) \approx x(t) - \tau \dot{x}(t)$  produces a negative damping term  $-\tau \dot{x}(t)$  when  $\tau$  is sufficiently short. This term even renders the system unstable.

**Example 2.3.7** Consider the delay differential equation

$$\ddot{x}(t) + c\dot{x}(t) + x(t-\tau) = 0, \quad x \in R, \quad (2.3.15)$$

where  $c > 0$ . This is a simple model for the damped linear oscillators with a time delay  $\tau$  in the stiffness term  $x(t)$ . If  $\tau = 0$ , Eq. (2.3.15) has no periodic solution and any perturbed motion of the oscillator from its equilibrium  $x \equiv 0$  is damped out. When  $\tau > 0$ , however, Eq. (2.3.15) may have a periodic solution because the corresponding characteristic equation has a pair of pure imaginary roots for a proper choice of  $(c, \tau)$ . For instance, when  $c = 0.0998$  and  $\tau = 0.1$ , the characteristic equation of Eq. (2.3.15) has a pair of conjugate imaginary roots  $\pm 0.9975i$ . In this case, the effect of damping term  $c\dot{x}(t)$  is approximately balanced off by  $-\ddot{x}(t)$  owing to the delayed stiffness term  $x(t-\tau)$ . Hence, the harmonic oscillation becomes possible.

### 3 Stability Analysis of Linear Delay Systems

From the viewpoint of mathematicians, the stability problem of a linear delay dynamic system has been solved because a number of sufficient and necessary conditions have been available for the stability analysis when the time delays are given. See, for example, (Stépán 1989), (Qin et al. 1989) and (Hassard 1997). As presented in Section 2.2, however, these conditions do not show any explicit relationship among the system parameters that the engineers are interested in. When those conditions are used, the stability test usually involves very tedious computation such as solving transcendental equations or computing the spectrum of operators.

The stability criteria for linear delayed dynamic systems can be classified into two catalogues according to whether the stability of system depends on the time delays or not. In the latter case, the system is asymptotically stable for arbitrary time delays. That is, the system stability is independent of time delays. In this case, the stability criteria are relatively simple. If the stability criteria for given time delays are considered, things become much more complicated.

This chapter is devoted to the stability analysis, which can be completed by using computer algebra, for the linear dynamic systems with single or multiple time delays in state feedback. At first, the analysis of delay-independent stability of single-degree-of-freedom systems with two time delays is presented as an illustrative example. Then, the analysis is made for the delay-independent stability of high dimensional systems with two time delays on the basis of generalized Sturm criterion for polynomials. Afterwards, the stability switch is analyzed in detail for high dimensional systems with an increase of a single time delay. To show the effectiveness of the approaches to high dimensional systems, the stability analysis is made for various examples in engineering, including a model of tall building with an active tendon for vibration reduction, an active suspension of ground vehicle and a four-wheel-steering vehicle with driver's retardation taken into account.



### 3.1 Delay-independent Stability of Single-degree-of-freedom Systems

This section deals with the single-degree-of-freedom systems with delayed state feedback discussed in Subsection 1.1.1. For simplicity, we can first re-scale Eq. (1.1.4) by using the same procedure from Eq. (1.1.10) to Eq. (1.1.12), and then study the dynamic equation of system as following

$$\ddot{x}(t) + 2\zeta\dot{x}(t) + x(t) = u x(t - \tau_1) + v \dot{x}(t - \tau_2) + f(t), \quad (3.1.1)$$

where  $\zeta \geq 0$  is the damping ratio as usual,  $u$  and  $v$  the dimensionless feedback gains,  $\tau_1 \geq 0$  and  $\tau_2 \geq 0$  the dimensionless time delays in the displacement feedback and velocity feedback, respectively.

To check the asymptotic stability of the steady-state motion  $x(t)$ , it is sufficient to study the variational equation that governs the small perturbation  $\Delta x(t)$  near  $x(t)$

$$\Delta \ddot{x}(t) + 2\zeta \Delta \dot{x}(t) + \Delta x(t) = u \Delta x(t - \tau_1) + v \Delta \dot{x}(t - \tau_2). \quad (3.1.2)$$

Substituting the candidate solution  $\Delta x(t) = a e^{\lambda t}$  into Eq. (3.1.2) yields the following characteristic equation

$$D(\lambda, \tau_1, \tau_2) \equiv \lambda^2 + 2\zeta\lambda + 1 - u e^{-\lambda\tau_1} - v \lambda e^{-\lambda\tau_2} = 0. \quad (3.1.3)$$

Given two time delays  $\tau_1$  and  $\tau_2$ , Eq. (3.1.2) is asymptotically stable if and only if all the roots of Eq. (3.1.3) have negative real parts.

If there is no time delay in the state feedback, Eq. (3.1.3) becomes a quadratic equation in  $\lambda$

$$D(\lambda, 0, 0) = \lambda^2 + (2\zeta - v)\lambda + (1 - u) = 0. \quad (3.1.4)$$

In this case, the asymptotic stability condition given by the Routh-Hurwitz criterion is

$$u < 1, \quad v < 2\zeta. \quad (3.1.5)$$

Except for this trivial case, Eq. (3.1.3) is transcendental. It is almost impossible to check the system stability by solving Eq. (3.1.3) for the infinite number of roots. Thus, it is not an easy task to give simple stability criteria for the delay differential equations like Eq. (3.1.1).

In general, the criteria of delay-independent stability are much simpler than those for the stability of a system with given time delays. Hence, they have re-

ceived much attention over the past decades, see, for example, (Qin et al. 1989) and (Gopalsamy 1992). As the simplest case, the dynamic systems with a single time delay have been intensively studied and the delay-independent stability criteria in terms of pure mathematical parameters have been given in (Qin et al. 1989) and (Mori and Kokame 1989). Yet, fewer successful studies have been made for the dynamic systems with multiple time delays and no practical stability criterion has been available. For instance, the sufficient condition given in (Wang and Wang 1993) requires very tedious computation for exponential matrices, while the concise criterion proposed in (Wang and Wang 1996) is not applicable to the dynamic systems with multiple time delays.

A practical problem in the design of feedback controllers is how to select the appropriate feedback gains  $u$  and  $v$  such that the controlled dynamic systems are asymptotically stable if any time delays exist in the controllers and actuators. Sometimes, the feedback gains  $u$  and  $v$  might have been designed according to a control strategy, say, LQG, but the time delays in the controller and actuators were not taken into consideration in the previous design. One may wonder whether the controlled dynamic system is asymptotically stable and robust with respect to the variation of the feedback gains. However, the archival publications dealt with the stability criteria in terms of pure mathematical parameters only, instead of the feedback gains.

The aim of this section is to find the practical criteria of delay-independent stability for the damped vibrating systems governed by Eq. (3.1.1) when two time delays appear in the state feedback. A sufficient and necessary algebraic condition of delay-independent stability is derived first. Then, an equivalent condition of delay-independent stability in terms of feedback gains  $u$  and  $v$  is discussed and the region of delay-independent stability on the plane of  $(u, v)$  is given.

### 3.1.1 Stability Criteria

As stated in Theorem 2.2.6, Eq. (3.1.1) is delay-independent stable if all the roots of  $D(\lambda, 0, 0)$  have negative real parts and the critical condition  $D(i\omega, \tau_1, \tau_2) = 0$  has no real root  $\omega$  for any given  $\tau_1$  and  $\tau_2$ . In what follow, we look for the necessary and sufficient condition, under which  $D(i\omega, \tau_1, \tau_2) = 0$  has no real root  $\omega$  for any given  $\tau_1$  and  $\tau_2$ .

It is obvious from Eq. (3.1.3) that  $D(i\omega, \tau_1, \tau_2) = 0$  gives

$$|1 - \omega^2 + 2i\zeta\omega|^2 = |u \exp(i\omega\tau_2 - i\omega\tau_1) + iv\omega|^2, \quad (3.1.6a)$$

or

$$\left|1-\omega^2+2i\zeta\omega\right|^2=\left|u+iv\omega\exp(i\omega\tau_1-i\omega\tau_2)\right|^2. \quad (3.1.6b)$$

Both Eqs. (3.1.6a) and (3.1.6b) have the same form

$$(1-\omega^2)^2+(2\zeta\omega)^2=u^2+(v\omega)^2+2uv\omega\sin(\omega\tau_2-\omega\tau_1), \quad (3.1.7)$$

namely,

$$\omega^4+(4\zeta^2-2-v^2)\omega^2+1-u^2=2uv\omega\sin[\omega(\tau_2-\tau_1)]. \quad (3.1.8)$$

If  $D(i\omega,\tau_1,\tau_2)=0$  has real root  $\omega$  for some  $\tau_1$  and  $\tau_2$ , so does Eq. (3.1.8).

Conversely, if there are  $\omega \neq 0$ ,  $\tau_1$  and  $\tau_2$  satisfying Eq. (3.1.8), then either Eq. (3.1.6a) or Eq. (3.1.6b) holds. Thus, there exists a non-negative number  $\theta \in R$  such that either

$$1-\omega^2+2i\zeta\omega=\exp(-i\omega\theta)\{u\exp[i\omega(\tau_2-\tau_1)]+iv\omega\}, \quad \theta+\tau_1-\tau_2 \geq 0 \quad (3.1.9a)$$

or

$$1-\omega^2+2i\zeta\omega=\exp(-i\omega\theta)\{u+iv\omega\exp[i\omega(\tau_1-\tau_2)]\}, \quad \theta+\tau_2-\tau_1 \geq 0 \quad (3.1.9b)$$

is true. This fact leads to  $D(i\omega,\theta-\tau_2+\tau_1,\theta)=0$  or  $D(i\omega,\theta,\theta-\tau_1+\tau_2)=0$ . That is, for given time delays  $\hat{\tau}_1=\theta+\tau_1-\tau_2 \geq 0$ ,  $\hat{\tau}_2=\theta$  or  $\hat{\tau}_1=\theta$ ,  $\hat{\tau}_2=\theta+\tau_1-\tau_2 \geq 0$ ,  $D(i\omega,\hat{\tau}_1,\hat{\tau}_2)=0$  holds and gives a contradiction. If  $\omega=0$  satisfies Eq. (3.1.8), then  $u=-1$ . There follows  $D(0,\tau_1,\tau_2)=2 \neq 0$ .

The above analysis can be summarized as the following conclusion.

**Theorem 3.1.1** Given two time delays  $\tau_1 \geq 0$  and  $\tau_2 \geq 0$ ,  $D(i\omega,\tau_1,\tau_2)=0$  has no real root  $\omega$  if and only if Eq. (3.1.8) has no real root  $\omega$  other than zero.

As both sides of Eq. (3.1.8) are even functions in  $\omega$ , it is sufficient hereinafter to study the case of  $\omega \geq 0$  only.

### (1) The case of equal time delays

When  $\tau_1=\tau_2=\tau$ , Eq. (3.1.8) becomes

$$\omega^4+p\omega^2+q=0, \quad (3.1.10)$$

where

$$p \equiv 4\zeta^2-2-v^2, \quad q \equiv 1-u^2. \quad (3.1.11)$$

Equation (3.1.10) has four roots in the form

$$\omega_{1,2} = \sqrt{\frac{1}{2}(-p \mp \sqrt{p^2 - 4q})}, \quad \omega_{3,4} = -\sqrt{\frac{1}{2}(-p \mp \sqrt{p^2 - 4q})}. \quad (3.1.12)$$

The number of real roots among them depends on the combination of parameters  $p$  and  $q$  as follows.

- (a)  $p^2 - 4q < 0$  : none of the roots is real.
- (b)  $p^2 - 4q \geq 0, p > 0, q > 0$  : none of the roots is real.
- (c)  $p^2 - 4q \geq 0, p < 0, q \geq 0$  : all of the roots are real.
- (d)  $p^2 - 4q \geq 0, q < 0$  : the roots  $\omega_2$  and  $\omega_4$  are real.

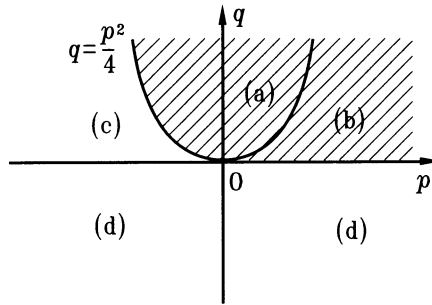


**Fig. 3.1.1.** Delay-independent stable region, containing the non-negative half  $p$ -axis, on the plane of  $(p, q)$  when  $\tau_1 = \tau_2$ .

These cases are shown on the plane of  $(p, q)$  in Fig. 3.1.1, where the shaded region represents the parameter combinations that guarantee the system stability independent of time delays. Remind that Eq.(3.1.10) could have a solution  $\omega = 0$ , we see that the delay-independent stability conditions can be simplified to

$$p \geq 0, \quad q \geq 0 \quad \text{or} \quad p < 0, \quad p^2 - 4q < 0. \quad (3.1.13)$$

**(2) The case of unequal time delays**

To study the case when  $\tau_1 \neq \tau_2$ , three functions are defined as following

$$\begin{cases} g(\omega) \equiv \omega^4 + p\omega^2 + q - r\omega \sin[\omega(\tau_2 - \tau_1)], \\ \underline{g}(\omega) \equiv \omega^4 + p\omega^2 + q - |r|\omega, \\ \bar{g}(\omega) \equiv \omega^4 + p\omega^2 + q + |r|\omega, \end{cases} \quad (3.1.14)$$

where  $r = 2uv$ . It is obvious that  $\underline{g}(0) = g(0) = \bar{g}(0) = q$  and for all  $\omega \geq 0$

$$\underline{g}(\omega) \leq g(\omega) \leq \bar{g}(\omega). \quad (3.1.15)$$

In the analysis of delay-independent stability, the time delays  $\tau_1$  and  $\tau_2$  can be arbitrary non-negative numbers. So, they can be chosen such that  $g(\omega)=\bar{g}(\omega)$  or  $g(\omega)=\underline{g}(\omega)$  for any given  $\omega \geq 0$ . Thus,  $g(\omega)$  has no root on  $(0, +\infty)$  if  $\underline{g}(\omega) > 0$  for all  $\omega \geq 0$ , or  $\bar{g}(\omega) < 0$  for all  $\omega \geq 0$ . However, the second case is obviously impossible since the leading coefficient of  $\bar{g}(\omega)$  is positive, which implies that  $\bar{g}(\omega) > 0$  holds for sufficiently large positive  $\omega$ .

Now, we derive a condition for checking  $\underline{g}(\omega) > 0$  subject to  $\omega \geq 0$ . The derivative of  $\underline{g}(\omega)$  with respect to  $\omega$  reads

$$\underline{g}'(\omega) = 4\omega^3 + 2p\omega - |r|. \quad (3.1.16)$$

To look at the roots of this cubic polynomial, a new parameter is introduced as following

$$\delta = \left(\frac{p}{6}\right)^3 + \left(\frac{r}{8}\right)^2. \quad (3.1.17)$$

The solution of polynomial  $\underline{g}(\omega)$  falls into one of the cases.

(a) If  $\delta > 0$ ,  $\underline{g}'(\omega) = 0$  has one real root and a pair of conjugate complex roots

$$\omega_1 = \alpha + \beta, \quad \omega_2 = \alpha\theta_1 + \beta\theta_2, \quad \omega_3 = \alpha\theta_2 + \beta\theta_1, \quad (3.1.18)$$

where

$$\alpha = \sqrt[3]{\frac{|r|}{8} + \sqrt{\delta}}, \quad \beta = \sqrt[3]{\frac{|r|}{8} - \sqrt{\delta}}, \quad \theta_1 = \frac{-1 + i\sqrt{3}}{2}, \quad \theta_2 = \frac{-1 - i\sqrt{3}}{2}. \quad (3.1.19)$$

(b) If  $\delta = 0$ ,  $\underline{g}'(\omega) = 0$  has three real roots

$$\omega_1 = 2\sqrt[3]{\frac{|r|}{8}}, \quad \omega_2 = \omega_3 = -\sqrt[3]{\frac{|r|}{8}}. \quad (3.1.20)$$

(c) If  $\delta < 0$ , then  $p < 0$  and  $\underline{g}'(\omega) = 0$  has three real roots

$$\omega_1 = 2\sqrt{-\frac{p}{6}} \cos\left(\frac{\gamma}{3}\right), \quad \omega_2 = 2\sqrt{-\frac{p}{6}} \cos\left(\frac{\gamma + 2\pi}{3}\right), \quad \omega_3 = 2\sqrt{-\frac{p}{6}} \cos\left(\frac{\gamma + 4\pi}{3}\right), \quad (3.1.21)$$

where  $0 < \gamma < \pi$  is defined by

$$\cos \gamma = -\frac{|r|}{8} / \left(\frac{p}{6} \sqrt{-\frac{p}{6}}\right). \quad (3.1.22)$$

In this case, both  $\omega_2 < 0$  and  $\omega_3 < 0$  are true since we have  $\gamma/3 + 2\pi/3 \in (2\pi/3, \pi)$  and  $\gamma/3 + 4\pi/3 \in (4\pi/3, 5\pi/3)$ .

The above analysis indicates that only the root  $\omega_1$  is positive in these cases. This fact, together with the inequality  $\underline{g}'(0) = -|r| \leq 0$ , leads to

$$\underline{g}'(\omega) < 0 \text{ for } \omega \in (0, \omega_1) \text{ and } \underline{g}'(\omega) > 0 \text{ for } \omega \in (\omega_1, +\infty). \quad (3.1.23)$$

This implies that  $\underline{g}(\omega_1)$  is the minimum of  $\underline{g}(\omega)$  on  $[0, +\infty)$ . Hence,  $\underline{g}(\omega) > 0$  holds true for all  $\omega \geq 0$  provided that  $\underline{g}(\omega_1) > 0$ . If this is the case,  $g(\omega) > 0$  holds for all  $\omega \geq 0, \tau_1, \tau_2 \geq 0$ .

In summary, the delay-independent stability criterion can be stated as follows.

**Theorem 3.1.2** Equation (3.1.1) is delay-independent stable for any time delays  $\tau_1$  and  $\tau_2$  if and only if either of the following two sets of inequalities holds

$$p \geq 0, \quad q \geq 0, \quad \underline{g}(\omega_1) > 0, \quad (3.1.24a)$$

$$p < 0, \quad p^2 - 4q < 0, \quad \underline{g}(\omega_1) > 0, \quad (3.1.24b)$$

where  $\underline{g}(\omega)$  is defined in Eq. (3.1.14) and

$$\omega_1 = \begin{cases} \sqrt[3]{\frac{|r|}{8} + \sqrt{\delta}} + \sqrt[3]{\frac{|r|}{8} - \sqrt{\delta}}, & \delta \geq 0, \\ 2\sqrt{\frac{p}{6} \cos \frac{\gamma}{3}}, & \delta < 0. \end{cases} \quad (3.1.25)$$

Given a system, the stability test based on Theorem 3.1.1 is an easy task including simple algebraic computation only. Table 3.1.1 shows 4 examples.

**Table 3.1.1.** Delay-independent stability of 4 illustrative examples

Example	System Parameter	Stability Test	Conclusion
3.1.1	$\zeta = 0.10$	$p = -1.963, q = 0.9900$	Delay-independent stable
	$u = 0.10$	$p^2 - 4q = -0.1086$	
	$v = 0.05$	$\underline{g}(\omega_1) = 0.0172$	
3.1.2	$\zeta = 0.10$	$p = -1.963, q = 0.9100$	Not delay-independent stable
	$u = 0.30$	$p^2 - 4q = 0.2114$	
	$v = 0.05$	$\underline{g}(\omega_1) = 0.0826$	
3.1.3	$\zeta = 0.50$	$p = -1.250, q = 0.7500$	Not delay-independent stable
	$u = 0.50$	$p^2 - 4q = -1.436$	
	$v = 0.50$	$\underline{g}(\omega_1) = -0.0584$	
3.1.4	$\zeta = 0.50$	$p = -1.090, q = 0.6400$	Delay-independent stable
	$u = 0.60$	$p^2 - 4q = -1.372$	
	$v = 0.30$	$\underline{g}(\omega_1) = 0.0637$	

### 3.1.2 Stability Criteria in Terms of Feedback Gains

In this subsection, we study all possible combinations of feedback gains that guarantee the delay-independent stability of Eq. (3.1.1). Let  $D$  denote the region of those combinations on the plane of  $(u, v)$ , and  $D_0$  the region where the corresponding system with identical time delays is delay-independent stable. For simplicity, we refer to these regions as the regions of delay-independent stability. It is obvious that  $(0,0) \in D \subset D_0$  if  $\zeta > 0$ .

#### (1) The case of equal time delays

By substituting Eq. (3.1.11) into Eq. (3.1.13), we have

$$p = 4\zeta^2 - 2 - v^2 \geq 0, \quad q = 1 - u^2 \geq 0, \quad (3.1.26a)$$

or

$$p = 4\zeta^2 - 2 - v^2 < 0, \quad p^2 - 4q = (4\zeta^2 - 2 - v^2)^2 - 4(1 - u^2) < 0; \quad (3.1.26b)$$

namely,

$$u^2 \leq 1, \quad v^2 \leq 4\zeta^2 - 2, \quad (3.1.27a)$$

or

$$v^2 > 4\zeta^2 - 2, \quad 4u^2 + (v^2 + 2 - 4\zeta^2)^2 < 4. \quad (3.1.27b)$$

The second inequality in Eq. (3.1.27a) and the first inequality in Eq. (3.1.27b) are a pair of contradictory bounds for  $v^2$ . To gain an insight into the second inequality in Eq. (3.1.27b), we can find all intersections of the curve

$$P(u, v) \equiv 4u^2 + (v^2 + 2 - 4\zeta^2)^2 - 4 = 0 \quad (3.1.28)$$

with the axes of  $u$  and  $v$ . They are

$$u=0, \quad v = \begin{cases} \pm 2\zeta, \\ \pm 2\sqrt{\zeta^2 - 1}, \end{cases} \quad (3.1.29a)$$

$$v=0, \quad u = \pm 2\zeta \sqrt{1 - \zeta^2}. \quad (3.1.29b)$$

From Eq. (3.1.29), it is easy to see that this curve, like an ellipse, has a pair of intersections on the  $u$  and  $v$  axes respectively, if and only if the system is under-damped in the usual sense. Once the system is over-damped, the curve has no in-

tersection on the  $u$  axis, but four intersections on the  $v$  axis. In fact, two separated ellipses appear in this case. Imposing

$$\frac{\partial P(u,v)}{\partial v} = 4v(v^2 + 2 - 4\zeta^2) = 0, \tag{3.1.30}$$

we can determine the extreme values of  $u$  on these two ellipses

$$u = \pm 1. \tag{3.1.31}$$

From the above analysis, the criterion for delay-independent stability is determined for different damping ratios as following and the corresponding regions of delay-independent stability is shown in Fig. 3.1.2.

(a) If  $0 \leq \zeta \leq 1/\sqrt{2}$ ,  $D_0$  is surrounded by an ellipse. That is,

$$4u^2 + (v^2 + 2 - 4\zeta^2)^2 < 4. \tag{3.1.32}$$

(b) If  $1/\sqrt{2} < \zeta \leq 1$ , the boundary of  $D_0$  is composed of two arcs of an ellipse and two sides of a rectangular, which are described by

$$u^2 \leq 1, \quad v^2 \leq 4\zeta^2 - 2, \tag{3.1.33a}$$

or

$$4u^2 + (v^2 + 2 - 4\zeta^2)^2 < 4, \quad v^2 > 4\zeta^2 - 2. \tag{3.1.33b}$$

(c) If  $\zeta > 1$ , the boundary of  $D_0$  consists of two sides of a rectangular and two arcs from two ellipses governed by Eq. (3.1.33), too.

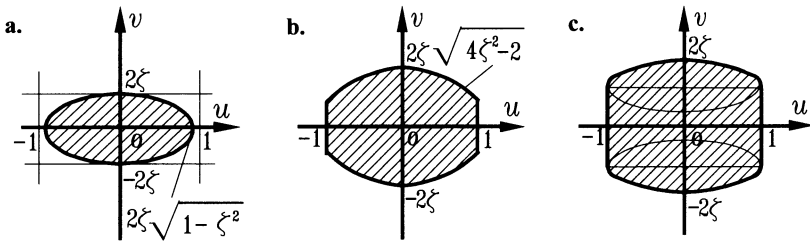


**Fig.3.1.2.** Regions of delay-independent stability on the plane of  $(u,v)$  for different damping ratios when  $\tau_1 = \tau_2$ ; **a.**  $0 \leq \zeta \leq 1/\sqrt{2}$ , **b.**  $1/\sqrt{2} < \zeta \leq 1$ , **c.**  $\zeta > 1$

**Theorem 3.1.3** The region  $D_0$  of delay-independent stability of Eq. (3.1.1) with equal time delays is symmetric with respect to both  $u$  and  $v$  axes and is connected and bounded in the rectangle  $\{(u,v) \mid |u| \leq 1, |v| \leq 2\zeta\}$ .

Hence, it is the damping that makes the delay-independent stability possible.



**(2) The case of unequal time delays**

If  $\tau_1 \neq \tau_2$ , the boundary of  $D$  yields  $\underline{g}(\omega_1)=0$ . However, it is almost impossible to solve  $\underline{g}(\omega_1)=0$  for the explicit expression of the boundary. Thus, a qualitative analysis of region  $D$  is made here. As  $p, q, |r|, p^2-4q, \gamma$  and  $\underline{g}(\omega_1)$  are even functions in  $u$  and  $v$ , the region  $D$  should be symmetric with respect to both  $u$  and  $v$  axes. So, attention is paid only to the first quadrant of  $(u, v)$  plane.

For  $u \geq 0$  and  $v \geq 0$ , it is easy to verify that

$$\begin{cases} \frac{\partial p}{\partial u} = 0, & \frac{\partial q}{\partial u} = -2u \leq 0, & \frac{\partial}{\partial u}(4q - p^2) = -8u \leq 0, \\ \frac{\partial p}{\partial v} = -2v \leq 0, & \frac{\partial q}{\partial v} = 0, & \frac{\partial}{\partial v}(4q - p^2) = 4pv \leq 0 \text{ with } p < 0 \end{cases} \quad (3.1.34)$$

and

$$\begin{cases} \frac{\partial}{\partial u} \underline{g}(\omega_1) = \underline{g}'(\omega_1) \frac{\partial \omega_1}{\partial u} + \omega_1^2 \frac{\partial p}{\partial u} + \frac{\partial q}{\partial u} - \omega_1 \frac{\partial |r|}{\partial u} = -2(u + v\omega_1) \leq 0, \\ \frac{\partial}{\partial v} \underline{g}(\omega_1) = \underline{g}'(\omega_1) \frac{\partial \omega_1}{\partial v} + \omega_1^2 \frac{\partial p}{\partial v} + \frac{\partial q}{\partial v} - \omega_1 \frac{\partial |r|}{\partial v} = -2\omega_1(u + v\omega_1) \leq 0, \end{cases} \quad (3.1.35)$$

since  $\underline{g}'(\omega_1)=0$ . These inequalities imply that if a given system with  $\zeta, u_0$  and  $v_0$  is delay-independent stable, so is the system with  $\zeta, v_0$  and  $0 \leq u \leq u_0$  or with  $\zeta, u_0$  and  $0 \leq v \leq v_0$ .

**Example 3.1.5** As testified in Example 3.1.1, the system with  $\zeta=0.1, u=0.1$  and  $v=0.05$  is delay-independent stable. According to the analysis above, the system with  $\zeta=0.1, v=0.05$  and  $0 \leq u \leq 0.1$ , or with  $\zeta=0.1, u=0.1$  and  $0 \leq v \leq 0.05$  is delay-independent stable, too.

Moreover, Eq. (3.1.35) leads to

$$\left. \frac{dv}{du} \right|_{\underline{g}(\omega_1)=0} = - \frac{\frac{\partial}{\partial u} \underline{g}(\omega_1)}{\frac{\partial}{\partial v} \underline{g}(\omega_1)} = - \frac{1}{\omega_1} < 0. \quad (3.1.36)$$

Hence, the boundary defined by  $\underline{g}(\omega_1)=0$  on the first quadrant of  $(u, v)$  plane is a simple curve. Along the boundary,  $v$  decreases with an increase of  $u$ .

From the above analysis on  $D$ , another stability criterion independent of time delays is also available.

**Theorem 3.1.4** The region  $D$  of delay-independent stability of Eq. (3.1.1) with unequal time delays is also symmetric with respect to both  $u$  and  $v$  axes and is

connected in the bounded  $D_0$ . Let  $U=\{(u,v)||u|\leq a_1,|v|\leq a_2\}$ , then it is sufficient to check  $(a_1,a_2)\in D$  in order to make sure that  $U\subset D$  holds.

**Example 3.1.6** Consider a system with  $\zeta=0.5$ . From Theorem 3.1.2 and Example 3.1.4, it is obvious that  $[-0.6, 0.6]\times[-0.3, 0.3]\subset D$  holds. This rectangular can be broadened in  $D$  by further numerical tests. For example, we can first fix  $u=0.6$  and choose a  $v$  larger than 0.3, say  $v=0.5$ . Direct computation gives  $p=-1.250$ ,  $q=0.64$ ,  $p^2-4q=-0.9975$  and  $\bar{g}(\omega_1)=-0.2567$ . This indicates that the system is not delay-independent stable and such a choice of  $v$  is too large. If a  $v$  less than 0.5, say  $v=0.34$ , is taken as the second try, then  $p=-1.1156$ ,  $q=0.6400$ ,  $p^2-4q=-1.3154$  and  $\bar{g}(\omega_1)=0.0073$ . Thus, the system is delay-independent stable and a larger rectangular  $[-0.6, 0.6]\times[-0.34, 0.34]\subset D$  is obtained.

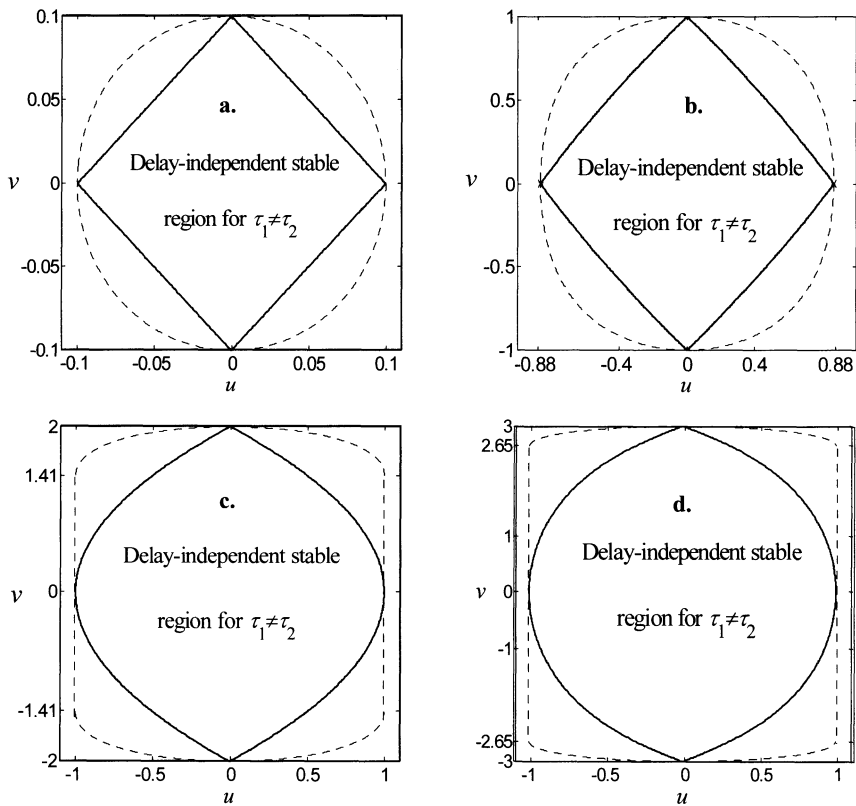


**Fig. 3.1.3.** Regions of delay-independent stability on the plane of  $(u,v)$  for different damping ratios; a.  $\zeta=0.05$ , b.  $\zeta=0.5$ , c.  $\zeta=1.0$ , d.  $\zeta=1.5$

For a given system, the region of delay-independent stability can be determined by using a simple short routine involving similar tests in Example 3.1.6. The typical regions of delay-independent stability for two under-damped systems, the critically damped system and an over-damped system are shown in Fig. 3.1.3, where the regions bounded by solid lines and curves are for distinct time delays and those with dashed boundaries are for equal time delays, respectively.

## 3.2 The Generalized Sturm Criterion for Polynomials

As shown in Subsection 3.1.1, the key step in testing the delay-independent stability of a system is to determine the number of real roots of a polynomial. Given a real polynomial with constant coefficients, the classical Sturm criterion gives a full answer to this problem. However, it does not work if the polynomial of order larger than 3 involves any unknown parameters. This case often happens when the delay-independent stability of a high dimensional system is analyzed in the design phase. Fortunately, the complete discrimination system for polynomials recently developed in (Yang et al. 1996a, 1996b), and is called the generalized Sturm criterion hereafter, offers a powerful tool to determine the number of a polynomial with unknown parameters. To acquire a good understanding of the theory, a brief review is made to the classical Sturm criterion first, and then some basic facts about the generalized Sturm criterion are presented in this section.

### 3.2.1 Classical Sturm Criterion

**Definition 3.2.1** Given a real number sequence  $l_1, l_2, \dots, l_n$  under the condition  $l_1 l_2 \dots l_n \neq 0$ , the sequence  $[s_1, s_2, \dots, s_n]$  with  $s_i \equiv \text{sgn}(l_i)$ ,  $i=1, 2, \dots, n$  is called the *sign table of the sequence*. The number of variation of signs of the sequence is the number of negative pairs in  $l_1 l_2, l_2 l_3, \dots, l_{n-1} l_n$ .

As a simple example, the sign table of the sequence 1, 3, -2, 1, -4, -10, -1, 4, 2 is [1, 1, -1, 1, -1, -1, 1, 1], and the number of variation of signs of is 4.

If a sequence contains any zeros, the number of variation of signs is defined as the number of variation of a new sequence revised by removing the zeros. For instance, the number of variation of signs of sequence -3, -5, 0, 3, 0, 2, -6, 0 is 2, while the number of variation of signs of sequence 0, -3, 2 is 1.

**Definition 3.2.2** Suppose that  $f(x)$  is a real polynomial without repeated roots. A sequence of real polynomials

$$f_0(x) \equiv f(x), f_1(x), \dots, f_s(x) \tag{3.2.1}$$

is called the *Sturm sequence* of polynomial  $f(x)$  if the following four conditions hold.

- (a) Any two neighboring polynomials in Eq. (3.2.1) have no common roots.
- (b) The last polynomial  $f_s(x)$  has no real roots.
- (c) If there exists an integer  $k$  yielding  $1 \leq k \leq s-1$  such that  $f_k(\alpha) = 0$ , then  $f_{k-1}(\alpha)f_{k+1}(\alpha) < 0$ ;
- (d) If  $f(\alpha) = 0$ , then, there exists a sufficiently small positive number  $\varepsilon$  such that  $f_0(k)f_1(k) < 0$  for  $k \in (\alpha - \varepsilon, \alpha)$ , and  $f_0(k)f_1(k) > 0$  for  $k \in (\alpha, \alpha + \varepsilon)$ .

Upon the basis of these concepts, the famous classical *Sturm criterion* can be stated as following.

**Theorem 3.2.1** Assume that a real polynomial  $f(x)$  has no repeated roots and has  $p$  real roots on the interval  $(\alpha, \beta)$ , satisfying  $f(\alpha)f(\beta) \neq 0$ . If the numbers of variation of signs of the sequences

$$f_0(\alpha), f_1(\alpha), \dots, f_s(\alpha) \tag{3.3.2a}$$

$$f_0(\beta), f_1(\beta), \dots, f_s(\beta) \tag{3.2.2b}$$

are  $v(\alpha)$  and  $v(\beta)$  respectively, then  $p = v(\alpha) - v(\beta)$ .

Some rules are available to construct the Sturm sequence of a polynomial without repeated roots. What follows is the most popular way. Let  $f_0(x) \equiv f(x)$ , and  $f_1(x) \equiv f'(x)$  be the derivative of  $f(x)$ . Dividing  $f(x)$  by  $f_1(x)$  gives the polynomial  $f_2(x)$  from  $f_0(x) = f_1(x)q_1(x) - f_2(x)$ . The other polynomials in the Sturm sequence can be constructed in the same way, namely,

$$f_k(x) = f_{k+1}(x)q_{k+1}(x) - f_{k+2}(x), \quad 0 \leq k < s-2, \tag{3.2.3}$$

except for the last one by  $f_{s-1}(x) = f_s(x)q_s(x)$ .

Because only the signs of the Sturm sequence are used in the applications of the Sturm criterion, all the positive factors can be dropped out at each step of constructing a Sturm sequence.

**Example 3.2.1** Consider a real polynomial

$$f(x) = x^5 + 5x^4 + 5x^3 - 5x^2 - 5x - 7. \tag{3.2.4}$$

The corresponding Sturm sequence can be constructed as follows. Let

$$f_0(x) \equiv f(x) = x^5 + 5x^4 + 5x^3 - 5x^2 - 5x - 7, \tag{3.2.5a}$$

$$f_1(x) \equiv f'(x)/5 = x^4 + 4x^3 + 3x^2 - 2x - 1. \tag{3.2.5b}$$

Dividing  $f_0(x)$  by  $f_1(x)$ , we arrive at  $f_0(x)=f_1(x)(x+1)-2(x^2+1)(x+3)$ . Because  $2(x^2+1)$  is a positive factor, we can take

$$f_2(x)=x+3. \quad (3.2.5c)$$

Dividing  $f_1(x)$  by  $f_2(x)$ , we have  $f_1(x)=f_2(x)(x^3+x^2-2)-(-5)$ . There follows

$$f_3(x)=-5. \quad (3.2.5d)$$

As a result, the Sturm sequence of  $f(x)$  consists of four polynomials  $f_0(x)$ ,  $f_1(x)$ ,  $f_2(x)$ ,  $f_3(x)$ .

To look at the relation between the real roots of  $f(x)$  in Eq. (3.2.4) and the number of variation of signs of its Sturm sequence, some cases are listed in Table 3.2.1. The Sturm criterion enables one to see that  $f(x)$  has only one real root on  $(-\infty, +\infty)$  and the root falls into the interval  $(1, 2)$ .

**Table 3.2.1.** The sign tables of the Sturm sequence of Eq. (3.2.4)

$x$	$f_0(x)$	$f_1(x)$	$f_2(x)$	$f_3(x)$	$v$
$-\infty$	-1	1	-1	-1	2
0	-1	-1	1	-1	2
1	-1	1	1	-1	2
2	1	1	1	-1	1
$+\infty$	1	1	1	-1	1

If  $f(x)$  has any repeated roots, the last polynomial  $f_s(x)$  in the Sturm sequence is the (non-constant) greatest common divisor of  $f_0(x)$  and  $f_1(x)$ . That is,  $f_s(x)=d(x)g_s(x)$ , where  $d(x)\equiv \text{g.c.d.}(f(x), f'(x))$  and the leading coefficient is set to be 1, while  $g_s(x)$  is the leading coefficient of  $f_s(x)$ . Let

$$f_k(x)\equiv d(x)g_k(x), \quad k=0,1,2,\dots,s. \quad (3.2.6)$$

Then,  $g_0(x)$  is a real polynomial without repeated roots, and  $g_0(x), g_1(x), \dots, g_s(x)$  is the Sturm sequence of  $g_0(x)$ . Therefore, the Sturm criterion still works for the polynomials with repeated roots in the sense that each of the repeated roots is counted only once.

### 3.2.2 Discrimination Sequence

In the generalized Sturm theory, the discrimination sequence plays the same role as the Sturm sequence in the classical Sturm criterion. The discrimination se-

quence can be constructed by using the so-called Bezout matrix, which is a useful concept in the theory of polynomials and can be defined in different ways.

To introduce the concept of the Bezout matrix, two real polynomials of order  $n$  are considered as following

$$f(x) \equiv a_0x^n + a_1x^{n-1} + \dots + a_{n-1}x + a_n, \tag{3.2.7a}$$

$$g(x) \equiv b_0x^n + b_1x^{n-1} + \dots + b_{n-1}x + b_n. \tag{3.2.7b}$$

They can be recast in the form

$$f(x) = f_{i1}(x)x^i + f_{i2}(x), \quad g(x) = g_{i1}(x)x^i + g_{i2}(x) \tag{3.2.8}$$

where

$$\begin{aligned} f_{i1}(x) &\equiv a_0x^{n-i} + a_1x^{n-1-i} + \dots + a_{n-i}, \\ f_{i2}(x) &\equiv a_{n-i+1}x^{i-1} + a_{n-i+2}x^{i-2} + \dots + a_n, \\ g_{i1}(x) &\equiv b_0x^{n-i} + b_1x^{n-1-i} + \dots + b_{n-i}, \\ g_{i2}(x) &\equiv b_{n-i+1}x^{i-1} + b_{n-i+2}x^{i-2} + \dots + b_n. \end{aligned} \tag{3.2.9}$$

Furthermore, a polynomial is introduced as following

$$p_i(x) \equiv \begin{vmatrix} f_{i1}(x) & f_{i2}(x) \\ g_{i1}(x) & g_{i2}(x) \end{vmatrix} \equiv \sum_{j=1}^n d_{ij}x^{n-j}. \tag{3.2.10}$$

The *Bezout matrix* is defined as the coefficient matrix of  $n$  polynomials  $p_{n-i+1}(x)$ ,  $i=1,2,\dots,n$  in the form

$$\begin{bmatrix} d_{11} & d_{12} & \dots & d_{1n} \\ d_{21} & d_{22} & \dots & d_{2n} \\ \vdots & \vdots & \ddots & \vdots \\ d_{n1} & d_{n2} & \dots & d_{nn} \end{bmatrix}. \tag{3.2.11}$$

**Definition 3.2.3** The *discrimination matrix* of  $f(x)$  is the Bezout matrix of  $f(x)$  and  $g(x) = 0 \cdot x^n + f'(x)$ , and denoted by  $discr(f)$ .

The discrimination matrix of  $f(x)$  can be proved in an explicit form as below

$$\begin{aligned} discr(f) &\equiv (c_{n-i,j-1}), \quad i, j = 1, \dots, n, \\ c_{ij} &\equiv [n - \max(i, j)] a_i a_j - \sum_{p=0}^{\min(i,j)-1} (i+j-2p) a_p a_{i+j-p}, \end{aligned} \tag{3.2.12}$$

where  $a_k \equiv 0$  if  $k < 0$  or  $k > n$ .

**Definition 3.2.4** The *discrimination sequence* of  $f(x)$  is defined as the principal sub-determinant sequence taken in order and denoted by

$$D_1(f), D_2(f), \dots, D_n(f). \quad (3.2.13)$$

**Algorithm 3.2.1** The following short MAPLE routine *discr* suggested in (Yang et al. 1996b) can be used to derive the discrimination sequence of a polynomial automatically.

```
> discr:=proc(poly,var)
>   local f, g, tt, d, bz, i, ar, j, mm, dd:
>     f:=expand(poly): d:=degree(f,var):
>     g:=tt*var^d+diff(f,var):
>     with(linalg):
>     bz:=subs(tt=0,bezout(f,g,var): ar:=[ ]:
>     for i to d do
>       ar:=[op(ar),row(bz,d+1-i..d+1-i)] od:
>     mm:=matrix(ar): dd:=[ ]:
>     for j to d do
>       d:=[op(dd),det(submatrix(mm,1..j,1..j))] od:
>     dd:=map(primpart,dd)
> end:
```

The repeated roots of a polynomial  $f(x)$  are determined exactly by the greatest common divisor of  $f(x)$  and  $f'(x)$ . The *sequence of sub-resultants* of  $f(x)$  and  $f'(x)$  are defined as the sequence of multiple order factors of  $f(x)$ , and is denoted by  $\Delta_0(f), \Delta_1(f), \dots, \Delta_{n-1}(f)$ .

### 3.2.3 Modified Sign Table

To state the generalized Sturm criterion in a compact form, it is helpful to introduce the concept of modified sign table first.

**Definition 3.2.5** Given a real number sequence  $l_1, l_2, \dots, l_n$  with  $l_1 \neq 0$ . The *modified sign table*  $[\varepsilon_1, \varepsilon_2, \dots, \varepsilon_n]$  of  $[s_1, s_2, \dots, s_n]$  with  $s_i = \text{sgn}(l_i)$ ,  $i=1, 2, \dots, n$  is a table generated in line with the rules as following.

(a) For any segment  $[s_i, s_{i+1}, s_{i+2}, \dots, s_{i+j}]$  of a given sign table with  $s_i \neq 0$ ,  $s_{i+1} = s_{i+2} = s_{i+3} = \dots = s_{i+j-1} = 0$  and  $s_{i+j} \neq 0$ ,  $[s_{i+1}, s_{i+2}, \dots, s_{i+j-1}]$  is replaced by  $[-s_i, -s_i, s_i, s_i, -s_i, -s_i, s_i, s_i, \dots]$ .

(b) All the other entries in the sign table are unchanged.

For example, the modified sign table of  $[1, -1, 0, 0, 0, 0, 1, 0, 0, 0, -1, 0]$  should be  $[1, -1, 1, 1, -1, -1, 1, -1, -1, 1, -1, 0]$  according to these two rules.

### 3.2.4 Generalized Sturm Criterion

On the basis of discrimination sequence and the corresponding modified sign table, the *generalized Sturm criterion* can be summarized as following, see (Yang et al. 1996b).

**Theorem 3.2.2** Let  $f(x)$  be a polynomial of order  $n$ ,  $D_1(f), D_2(f), \dots, D_n(f)$  be the corresponding discrimination sequence, and  $\sigma_i = D_{q_i}$ ,  $i=1, 2, \dots, k$  be the  $i$ -th nonzero term of the discrimination sequence, where  $\sigma_0 = 1$ . Let  $q_0 = 0$ ,  $r_i = q_{i+1} - q_i - 1$ ,  $i=0, 1, 2, \dots, k-1$ . Assume that the number of variation of signs in the modified sign table is  $s$ . If  $D_l(f) \neq 0$  and  $D_m(f) = 0$ ,  $m > l$ , then the following facts are true.

- (a) The number of distinct pairs of conjugate complex roots of  $f(x)$  is  $s$ .
- (b) The number of distinct real roots of  $f(x)$  is  $l - 2s$ , which satisfies

$$l - 2s = \sum_{i=0, r_i \text{ are even}}^{k-1} (-1)^{r_i/2} \operatorname{sgn}\left(\frac{\sigma_{i+1}}{\sigma_i}\right). \tag{3.2.14}$$

(c)  $\alpha$  is a root of  $f(x)$  with multiplicity  $p$  if and only if it is a root of  $\Delta_{n-i}(f)$  with multiplicity  $p-1$ .

(d) Except for some positive factors,  $D_1(f), D_2(f), \dots, D_l(f)$  is the discrimination sequence of polynomial  $f/\operatorname{g.c.d}(f, f')$ , which has no repeated roots.

**Example 3.2.2** Let  $f(x) = x^{18} - x^{16} + 2x^{15} - x^{14} - x^5 + x^4 + x^3 - 3x^2 + 3x - 1$ . The sign table of the corresponding discrimination sequence is  $[1, 1, -1, -1, -1, 0, 0, 0, -1, 1, 1, -1, -1, 1, -1, -1, 0, 0]$ . Thus, the modified sign table is  $[1, 1, -1, -1, -1, 1, 1, -1, -1, 1, 1, -1, -1, 1, -1, -1, 0, 0]$ , and the number of variation of signs is 7. As a result, the polynomial  $f(x)$  has two distinct real roots and 7 distinct pairs of conjugate complex roots. Note the fact that  $\operatorname{g.c.d}(f, f') = x^2 - x + 1$ , the remaining two roots of  $f(x)$  are a pair of conjugate complex roots repeated to one of the above 7 pairs.

**Example 3.2.3** To ensure that a polynomial of order 6 with positive leading coefficient has no real roots, it is necessary to make sure that one of the 14 cases in Table 3.2.2 holds true.





**Table 3.2.2.** 14 possible modified sign tables of the discrimination sequence of a polynomial of order 6 with positive leading coefficient

$D_1(f)$	$D_2(f)$	$D_3(f)$	$D_4(f)$	$D_5(f)$	$D_6(f)$	$l=2s$
1	-1	0	0	0	0	$s=1$
1	-1	1	1	0	0	
1	-1	-1	1	0	0	$s=2$
1	1	-1	1	0	0	
1	-1	1	1	1	-1	
1	-1	-1	-1	1	-1	
1	1	1	-1	1	-1	
1	-1	1	1	-1	-1	
1	-1	-1	1	1	-1	$s=3$
1	1	-1	1	1	-1	
1	1	-1	-1	1	-1	
1	-1	-1	1	-1	-1	
1	-1	1	-1	-1	-1	
1	1	-1	1	-1	-1	

Theorem 3.2.2 gives full information about the numbers of real roots and complex roots of a polynomial. It is the case of  $l=2s$  for  $s=1,2,\dots$  that serves the purpose of analysis of delay-independent stability.

### 3.3 Delay-independent Stability of High Dimensional Systems

Now, consider the delay-independent stability of a linear dynamic system with two time delays, the characteristic equation of which takes the following form

$$D(\lambda, \tau_1, \tau_2) \equiv P(\lambda) + Q_1(\lambda)e^{-\lambda\tau_1} + Q_2(\lambda)e^{-\lambda\tau_2} = 0, \tag{3.3.1}$$

where  $\tau_1 \geq 0$  and  $\tau_2 \geq 0$  are the time delays,  $P(\lambda)$ ,  $Q_1(\lambda)$  and  $Q_2(\lambda)$  are the real polynomials under the conditions  $\deg(P) = n > \deg(Q_j)$ ,  $j=1,2$ . The system of concern is delay-independent stable if and only if each of its characteristic roots has negative real part for all given  $\tau_1 \geq 0$  and  $\tau_2 \geq 0$ . Since  $D(\lambda, \tau_1, \tau_2)$  is analytic with respect to  $\lambda$ ,  $\tau_1$  and  $\tau_2$ . Thus, any root  $\lambda = \lambda(\tau_1, \tau_2)$  of  $D(\lambda, \tau_1, \tau_2)$  is continuous with respect to  $\tau_1$  and  $\tau_2$ . These facts lead to the following theorem.

**Theorem 3.3.1** The linear delayed dynamic system governed by Eq. (3.3.1) is delay-independent stable if and only if the following two conditions hold true.

(a) The polynomial  $P(\lambda)+Q_1(\lambda)+Q_2(\lambda)$ , corresponding to the case  $\tau_1=\tau_2=0$ , has only the roots with negative real parts.

(b) Equation  $D(i\omega,\tau_1,\tau_2)=0$  has no real root  $\omega$  for all  $\tau_1\geq 0$  and  $\tau_2\geq 0$ .

In general, the Routh-Hurwitz criterion is available to examine the first condition. What follows is to discuss how to check the second condition. Let

$$\begin{cases} P_R(\omega)\equiv\text{Re}[P(i\omega)], & P_I(\omega)\equiv\text{Im}[P(i\omega)], \\ Q_{jR}(\omega)\equiv\text{Re}[Q_{jR}(i\omega)], & Q_{jI}(\omega)\equiv\text{Im}[Q_{jI}(i\omega)], \quad j=1,2. \end{cases} \quad (3.3.2)$$

Eq. (3.3.1) has no roots  $\pm i\omega \neq 0$  for all  $\tau_1\geq 0$  and  $\tau_2\geq 0$  if and only if

$$\begin{aligned} &P_R^2(\omega)+P_I^2(\omega)-[Q_{1R}^2(\omega)+Q_{1I}^2(\omega)+Q_{2R}^2(\omega)+Q_{2I}^2(\omega)] \\ &\quad -2[Q_{1R}(\omega)Q_{2I}(\omega)-Q_{1I}(\omega)Q_{2R}(\omega)]\sin[\omega(\tau_2-\tau_1)] \\ &\quad -2[Q_{1I}(\omega)Q_{2I}(\omega)+Q_{1R}(\omega)Q_{2R}(\omega)]\cos[\omega(\tau_2-\tau_1)]=0 \end{aligned} \quad (3.3.3)$$

has no non-negative root  $\omega$  for all  $\tau_1\geq 0$  and  $\tau_2\geq 0$ . The two harmonic terms above can be combined into the one with a phase shift  $\varphi$  so that Eq. (3.3.3) becomes

$$\begin{aligned} &P_R^2(\omega)+P_I^2(\omega)-[Q_{1R}^2(\omega)+Q_{1I}^2(\omega)+Q_{2R}^2(\omega)+Q_{2I}^2(\omega)] \\ &\quad -2\sqrt{[Q_{1R}(\omega)Q_{2I}(\omega)-Q_{1I}(\omega)Q_{2R}(\omega)]^2+[Q_{1I}(\omega)Q_{2I}(\omega)+Q_{1R}(\omega)Q_{2R}(\omega)]^2} \\ &\quad \quad \quad \sin[\omega(\tau_2-\tau_1)+\varphi]=0. \end{aligned} \quad (3.3.4)$$

As  $P_R(\omega)$ ,  $Q_{jR}(\omega)$ ,  $j=1,2$  are even functions and  $P_I(\omega)$ ,  $Q_{jI}(\omega)$ ,  $j=1,2$  are odd functions respectively, we have

$$D(0, \tau_1, \tau_2) = P_R(0) + Q_{1R}(0) + Q_{2R}(0) \quad (3.3.5)$$

If  $\omega = 0$  satisfies Eq. (3.3.4), then  $P_R^2(0) - [Q_{1R}^2(0) + Q_{2R}^2(0)] = 0$ . If in addition we assume that  $D(0, \tau_1, \tau_2) = 0$ , then  $P_R(0) = Q_{1R}(0) = Q_{2R}(0) = 0$ , which contradicts the Hurwitz stability of  $P(\lambda) + Q_1(\lambda) + Q_2(\lambda)$ . Thus  $D(0, \tau_1, \tau_2) \neq 0$  for all given delays  $\tau_1$  and  $\tau_2$ .

Thus, if  $\tau_1 = \tau_2 = \tau$ ,  $D(i\omega,\tau_1,\tau_2)=0$  has no real root  $\omega$  for all  $\tau \geq 0$  if and only if the left-hand side of Eq. (3.3.3), denoted by  $F(\omega)$ ,

$$F(\omega)\equiv\omega^{2n}+b_1\omega^{2(n-1)}+b_2\omega^{2(n-2)}+\dots+b_{n-1}\omega^2+b_n \quad (3.3.6a)$$

has no real roots other than zero. If  $\tau_1 \neq \tau_2$ , an even function  $G(\omega)$  is defined as

$$G(\omega) \equiv P_R^2(\omega) + P_I^2(\omega) - [Q_{1R}^2(\omega) + Q_{1I}^2(\omega) + Q_{2R}^2(\omega) + Q_{2I}^2(\omega)] \\ - 2\sqrt{[Q_{1R}(\omega)Q_{2I}(\omega) - Q_{1I}(\omega)Q_{2R}(\omega)]^2 + [Q_{1I}(\omega)Q_{2I}(\omega) + Q_{1R}(\omega)Q_{2R}(\omega)]^2} \quad (3.3.6b)$$

Hence by following the same routine in the proof of Theorem 3.1.1, we see that Eq. (3.3.4) has no non-negative roots for all  $\tau_1 \geq 0$  and  $\tau_2 \geq 0$  if and only if  $G(\omega)$  has no positive roots or  $G(0) = 0$ , namely,  $G(\omega^2)$  has no real roots other than zero. Obviously,  $G(\omega)$  may not be a polynomial for some systems. This is the case for some systems with delayed feedback control.

So we arrive at an important theorem for the delay-independent stability.

**Theorem 3.3.2**  $D(i\omega, \tau_1, \tau_2) = 0$  has no real root  $\omega$  for all  $\tau_1 \geq 0$  and  $\tau_2 \geq 0$  if and only if the polynomial  $F(\omega)$  or  $G(\omega^2)$  has no real root  $\omega$  other than zero.

As a result of direct application of the generalized Sturm criterion, Theorem 3.3.2 can be more specifically stated below.

**Theorem 3.3.3**  $D(i\omega, \tau_1, \tau_2) = 0$  has no real root  $\omega$  for all  $\tau_1 \geq 0$  and  $\tau_2 \geq 0$  if and only if  $F(0) = 0$  ( $G(0) = 0$ ), or the modified sign table of  $F(\omega)$  (or  $G(\omega^2)$ ) is subject to the condition  $l = 2s$  for  $s = 1, 2, \dots, n$  or  $2n$ , where  $l$  and  $s$  are the number of non-zero terms and the number of variation of signs in the corresponding discrimination sequence, respectively.

Based on the above analysis, an approach to the delay-independent stability can be summarized as below.

**Algorithm 3.3.1**

- (a) Work out Eq. (3.3.3) and the corresponding polynomial  $F(\omega)$  or  $G(\omega^2)$ .
- (b) Determine the discrimination sequence corresponding to  $F(\omega)$  or  $G(\omega^2)$  by using the MAPLE routine *discr*.
- (c) Justify the stability. The system is delay-independent stable if and only if  $P(\lambda) + Q_1(\lambda) + Q_2(\lambda)$  is Hurwitz stable, and  $F(0) = 0$  ( $G(0) = 0$ ) or the condition  $l = 2s$  holds for some  $s = 1, 2, 3, 4, \dots, n$  or  $2n$ .

**Remark 3.3.1** The computation in stability test can be greatly reduced if the terms in the discrimination sequence are factorized.

In practice, especially in the design phase of a controlled system, it is often desirable to know the delay-independent stable region in a space spanned by the design parameters. Once the discrimination sequence is obtained and each term is factorized, each factor can be set to be zero and the corresponding graph can be plotted. These graphs divide the parameter space into several sub-regions. Each of them can be easily determined to be or not to be the delay-independent stability region by checking the corresponding modified sign table. The points satisfy

$F(0) = 0$  (or  $G(0) = 0$ ) may be on the boundary of the stable region. This procedure will be demonstrated through a few examples.

**Example 3.3.1** Consider again the single-degree-of-freedom system with two distinct time delays in the paths of displacement feedback and velocity feedback, respectively. As shown in Section 3.1, the characteristic equation of the system is

$$\lambda^2 + 2\zeta\lambda + 1 - ue^{-\lambda\tau_1} - v\lambda e^{-\lambda\tau_2} = 0, \quad \tau_1 \neq \tau_2. \quad (3.3.7)$$

Comparing Eq. (3.3.7) with Eq. (3.3.1) gives

$$P(\lambda) = \lambda^2 + 2\zeta\lambda + 1, \quad Q_1(\lambda) = -u, \quad Q_2(\lambda) = -v\lambda. \quad (3.3.8)$$

According to Eq. (3.3.6), we have

$$G(\omega^2) = \omega^8 + p\omega^4 + r\omega^2 + q, \quad (3.3.9)$$

where

$$p \equiv 4\zeta^2 - v^2 - 2, \quad q \equiv 1 - u^2, \quad r \equiv -2|uv|. \quad (3.3.10)$$

We assume hereinafter that  $v < 2\zeta$  and  $u < 1$ . These two inequalities are the sufficient and necessary conditions for the asymptotic stability of systems free of time delay. In order that the system is delay-independent stable, it is sufficient and necessary to make sure that Eq. (3.3.9) has no real roots.

By using MAPLE routine *discr*, we obtain the discrimination sequence of  $G(\omega^2)$  as following

$$1, d_0, d_0d_1, d_1d_2, d_2d_3, d_3d_4, d_4d_5, d_5^2d_6, \quad (3.3.11)$$

where

$$\begin{aligned} d_0 &\equiv 0, \quad d_1 \equiv -p, \quad d_2 \equiv -p^2, \quad d_3 \equiv -(2p^3 - 8pq + 9r^2), \\ d_4 &\equiv (4p^3 - 48pq + 27r^2)r, \quad d_6 \equiv q, \\ d_5 &\equiv -(27r^4 + 4p^3r^2 - 144pqr^2 - 16p^4q + 128p^2q^2 - 256q^3). \end{aligned} \quad (3.3.12)$$

Because the expressions of  $d_i$ ,  $i=0, 1, \dots, 6$  are even functions with respect to  $u$  and  $v$ , it is sufficient to study the case for positive  $u$  and  $v$  only. When the second term and the third term in the discrimination sequence vanish, the first three terms of the modified sign tables must be 1, -1, -1. If the number of variation of signs in the modified sign table is 2, the non-zero terms in the modified sign table has 4 entries to ensure that the system is delay-independent stable. Hence, the modified sign table of the discrimination sequence should be [1, -1, -1, 1, 0, 0, 0, 0]. When the number of variation of signs in the modified sign table is 3, the sixth

entry in the modified sign table must be negative to guarantee the delay-independent stability. Therefore, there are three cases for the modified sign tables corresponding to the delay-independent stability. They are  $[1, -1, -1, 1, -1, -1, 0, 0]$ ,  $[1, -1, -1, 1, 1, -1, 0, 0]$  and  $[1, -1, -1, -1, 1, -1, 0, 0]$ . In the case when the signs in the modified sign table changes 4 times, the eighth term in the modified sign table should be positive for delay-independent stability, and there are totally 10 cases. Hence, the system is delay-independent stable if and only if the modified sign table of its discrimination sequence is one of the 14 cases listed in Table 3.3.1.

**Table 3.3.1.** 14 possible modified sign tables of the discrimination sequence of  $G(\omega^2)$  in the case of delay-independent stability

$D_1(f)$	$D_2(f)$	$D_3(f)$	$D_4(f)$	$D_5(f)$	$D_6(f)$	$D_7(f)$	$D_8(f)$	$l=2s$
1	-1	-1	1	0	0	0	0	$s=2$
1	-1	-1	1	-1	-1	0	0	$s=3$
1	-1	-1	1	1	-1	0	0	
1	-1	-1	-1	1	-1	0	0	
1	-1	-1	1	-1	-1	-1	1	$s=4$
1	-1	-1	-1	1	-1	-1	1	
1	-1	-1	-1	-1	1	-1	1	
1	-1	-1	1	1	-1	-1	1	
1	-1	-1	-1	1	1	-1	1	
1	-1	-1	1	-1	1	1	1	
1	-1	-1	1	1	1	-1	1	
1	-1	-1	1	-1	-1	1	1	
1	-1	-1	-1	1	-1	1	1	
1	-1	-1	1	1	-1	1	1	

In what follows, two case studies are presented to illustrate the analysis of delay-independent stability.

**Case 1**  $\zeta=0.25$ . Substituting  $\zeta=0.25$  into Eqs. (3.3.9) and (3.3.10) gives

$$d_0 = 0, \quad d_1 = 1.75 + v^2 > 0, \quad d_2 = -d_1^2 < 0,$$

$$d_3 = 2v^6 + 10.5v^4 + (10.375 - 28u^2)v^2 + 14u^2 - 3.2813,$$

$$d_4 = |uv| [8v^6 + 42v^4 + (-22.5 + 120u^2)v^2 + (-125.13 + 168u^2)],$$

$$\begin{aligned}
d_5 &= 16v^8 + (112 - 28u^2)v^6 + (166 - 467u^2 + 16u^4)v^4 + \\
&(-105 - 369.25u^2 + 560u^4)v^2 + 14.063 - 134.06u^2 + 376u^4 - 256u^6, \\
d_6 &= 1 - u^2.
\end{aligned} \tag{3.3.13}$$

The curve determined by  $d_3=0$  is ellipse-like, as shown in Fig. 3.3.1. The inside of the “ellipse” is governed by  $d_3<0$ , while the outside by  $d_3>0$ . The graph of  $d_4=0$  is hyperbola-like, the corresponding sub-region containing the origin is governed by  $d_4<0$ , the other parts by  $d_4>0$ . The graph of  $d_5=0$  consists of four lines, the w-like region and the m-like region are determined by  $d_5<0$ , and the other parts by  $d_5>0$ . Following the present approach, it is possible to see that only the combination  $(u,v)$  in the rhombus-like region that makes the system delay-independent stable. For example, in the rhombus-like region, we have  $d_1=0$ ,  $d_1>0$ ,  $d_2<0$ ,  $d_3<0$ ,  $d_4<0$ ,  $d_5>0$  and  $d_6>0$ . Thus, the sign table of the discrimination sequence is [1, 0, 0, -1, 1, 1, -1, 1]. There follows the modified sign table [1, -1, -1, -1, 1, 1, -1, 1]. This fact indicates that  $G(\omega^2)$  has no real roots and thus the system is delay-independent stable if the combination of  $(u,v)$  falls into this region. In the region inside the ellipse-like region but outside the rhombus-like region, we have  $d_1=0$ ,  $d_1>0$ ,  $d_2<0$ ,  $d_3<0$ ,  $d_4<0$ ,  $d_5<0$  and  $d_6>0$ . Hence, the corresponding modified sign table is [1, -1, -1, -1, 1, 1, 1, 1]. Therefore, the polynomial  $G(\omega^2)$  has  $4=8-2\times 2$  real roots and the system is not delay-independent stable.

**Case 2**  $\zeta=0.75$ . This damping ratio results in

$$\begin{aligned}
d_0 &= 0, \quad d_1 = v^2 - 0.25, \quad d_2 = -d_1^2 < 0, \\
d_3 &= 2v^6 - 1.5v^4 - (28u^2 + 7.625)v^2 - 2u^2 + 1.9688, \\
d_4 &= |uv| [8v^6 - 6v^4 - (120u^2 + 94.5)v^2 + (43.875 - 24u^2)], \\
d_5 &= 16v^8 + (4u^2 - 16)v^6 + (16u^4 - 323u^2 - 122)v^4 \\
&+ (63 + 16.75u^2 - 80u^4)v^2 + 248.06 - 752.06u^2 + 760u^4 - 256u^6, \\
d_6 &= 1 - u^2.
\end{aligned} \tag{3.3.14}$$

As analyzed in the previous case, the delay-independent stable region on the plane of  $(u,v)$  can be easily determined by checking the modified sign tables of the discrimination sequence and shown as the biggest rhombus in Fig. 3.3.2. For example, in the smallest rhombus-like region, we have  $d_1=0$ ,  $d_1<0$ ,  $d_2<0$ ,  $d_3>0$ ,  $d_4>0$ ,  $d_5>0$  and  $d_6>0$ . Hence, the sign table of the discrimination sequence is

[1, 0, 0, 1, -1, 1, 1, 1]. There follows the modified sign table [1, -1, -1, 1, -1, 1, 1, 1]. This indicates that  $G(\omega^2)$  has no real roots and the system is delay-independent stable if a parametric combination falls into this region. In the region inside the biggest rhombus-like region subject to  $0.5 < |v| < 1$ , we have  $d_1=0$ ,  $d_1 > 0$ ,  $d_2 < 0$ ,  $d_3 < 0$ ,  $d_4 < 0$ ,  $d_5 > 0$  and  $d_6 > 0$ . Hence, the sign table of the discrimination sequence is [1, 0, 0, -1, 1, 1, -1, 1] and the modified sign table is [1, -1, -1, -1, 1, 1, -1, 1]. Thus, the polynomial  $G(\omega^2)$  has no real roots and the system is delay-independent stable. In the region with the boundary composed of the rhombus-like curves, we have  $d_1=0$ ,  $d_1 < 0$ ,  $d_2 < 0$ ,  $d_3 < 0$ ,  $d_4 > 0$ ,  $d_5 > 0$  and  $d_6 > 0$ . Thus, the sign table of the discrimination sequence is [1, 0, 0, 1, 1, -1, 1, 1], the modified sign table is [1, -1, -1, 1, 1, -1, 1, 1] and  $s=4$ . Thus,  $G(\omega^2)$  has no real roots and the system is delay-independent stable if the parameter combination falls into this region. On the curves plotted by  $d_2=0$  or  $d_3=0$  or  $d_4=0$ , the sign table is [1, 0, 0, 0, 0, 1, -1, 1] or [1, 0, 0, 1, 0, 0, -1, 1] or [1, 0, 0, 1, 1, 0, 0, 1]. There follow the modified sign tables [1, -1, -1, 1, 1, 1, -1, 1] or [1, -1, -1, 1, -1, -1, -1, 1] or [1, -1, -1, 1, 1, -1, -1, 1], respectively. Hence, the system is also delay-independent stable on these curves. As a result, the system is delay-independent stable in the whole biggest rhombus-like region.

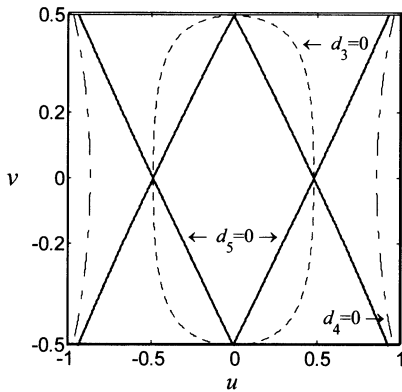


**Fig. 3.3.1.** The rhombus-like region of delay-independent stability on the plane of  $(u, v)$  when  $\zeta = 0.25$

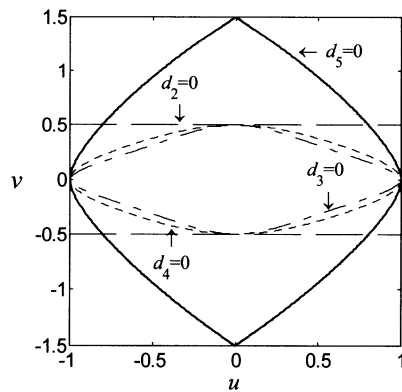


**Fig. 3.3.2.** The delay-independent stable region on the plane of  $(u, v)$  is the biggest rhombus-like region when  $\zeta = 0.75$ .

**Example 3.3.2** A set of delay differential equations has been presented in Subsection 1.1.1 to describe the dynamics of a tall structure equipped with an active

tendon. If the time delays are assumed as  $\tau_1 = \tau_2 = \tau$  and the fundamental natural frequency is scaled as  $\omega_n = 1$ , the equations are simplified to

$$\begin{cases} \dot{x}_1(t) = x_2(t), \\ \dot{x}_2(t) = -x_1(t) - 2\zeta x_2(t) - x_3(t) + f(t), \\ \dot{x}_3(t) = \alpha\gamma x_1(t - \tau) + \alpha\delta x_2(t - \tau) - \alpha x_3(t), \end{cases} \quad (3.3.15)$$

where  $x_1$  is the modal displacement,  $x_2$  the modal velocity,  $x_3$  the control force,  $\zeta$  the damping ratio,  $\alpha > 0$  the time constant of hydraulic actuator,  $\gamma$  and  $\delta$  the feedback gains of displacement and velocity,  $f(t)$  the external force, respectively. The corresponding characteristic equation is

$$\lambda^3 + (\alpha + 2\zeta)\lambda^2 + (1 + 2\alpha\zeta)\lambda + \alpha + \alpha(\delta\lambda + \gamma)e^{-\lambda\tau} = 0. \quad (3.3.16)$$

### (1) General case

When  $\tau = 0$ , the system is asymptotically stable if and only if the following Routh-Hurwitz stability conditions hold

$$\alpha + 2\zeta > 0, \quad 1 + \gamma > 0, \quad (\alpha + 2\zeta)(\alpha\delta + 2\alpha\zeta + 1) > \alpha(1 + \gamma). \quad (3.3.17)$$

The first inequality here is always true since  $\alpha$  and  $\zeta$  are positive.

When  $\tau > 0$ , it is easy to find that  $F(\omega)$  in Eq. (3.3.6a) reads

$$F(\omega) = \omega^6 + b_1\omega^4 + b_2\omega^2 + b_3, \quad (3.3.18)$$

where

$$b_1 \equiv \alpha^2 + 4\zeta^2 - 2, \quad b_2 \equiv 1 - 2\alpha^2 - \alpha^2\delta^2 + 4\alpha^2\zeta^2, \quad b_3 \equiv \alpha^2(1 - \gamma^2). \quad (3.3.19)$$

The polynomial  $F(\omega)$  has no real roots other than zero only when  $|\gamma| \leq 1$ . By using the MAPLE routine *discr*, we obtain the discrimination sequence

$$\begin{aligned} & 1, \quad -b_1, \quad 3b_1b_2 - b_1^3, \quad -7b_1^2b_2^2 - 9b_1b_2b_3 + b_1^4b_2 + 3b_1^3b_3 + 12b_2^3, \\ & -8b_1^2b_2^4 + 37b_1^3b_2^2b_3 - 84b_1b_2^3b_3 + 27b_1^2b_2b_3^2 + b_1^4b_2^3 - 4b_1^5b_2b_3 \\ & -12b_1^4b_3 - 81b_1b_3^3 + 16b_2^5 + 108b_2^2b_3^2, \\ & b_3(-16b_1^6b_3 + 8b_1^5b_2^3b_3 - b_1^4b_2^4 + 144b_1^4b_2b_3^2 - 216b_1^3b_3^3 - 68b_1^3b_2^3b_3 \\ & + 8b_1^2b_2^5 - 270b_1^2b_2^2b_3^2 + 144b_1b_2^4b_3 + 972b_1b_2b_3^3 - 729b_3^4 - 16b_2^6 - 216b_2^3b_3^2). \end{aligned} \quad (3.3.20)$$

To reduce the computation, it is beneficial to factorize the above six polynomials as following



$$1, d_0, d_0d_1, d_1d_2, d_2d_3, d_3^2d_4, \quad (3.3.21)$$

where

$$\begin{aligned} d_0 &= -b_1, \quad d_1 = b_1^2 - 3b_2, \quad d_2 = b_1^2b_2 + 3b_1b_3 - 4b_2^2, \\ d_3 &= -(4b_1^3b_3 - b_1^2b_2^2 - 18b_1b_2b_3 + 4b_2^3 + 27b_3^2), \\ d_4 &= -b_3. \end{aligned} \quad (3.3.22)$$

That is, the sign tables of Eq. (3.3.20) can be obtained by computing the signs of  $d_i, i=0, 1, 2, 3, 4$ , instead of computing the polynomials in Eq. (3.3.20).

According to Theorems 3.3.1 and 3.3.3, as well as Example 3.2.3, the system is delay-independent stable if and only if (a) the inequalities in Eq. (3.3.17) hold true, and (b) the modified sign tables of the discrimination coincides one of the 14 cases of listed in Table 3.2.2.

## (2) Case studies

Now, attention is paid to the case when  $\alpha=2$ . Substituting  $\alpha=2$  into Eqs. (3.3.19) and (3.3.22) gives

$$\begin{aligned} d_0 &= -2 - 4\zeta^2 < 0, \quad d_1 = 25 + 12\delta^2 - 32\zeta^2 + 16\zeta^4, \\ d_2 &= -64\delta^4 + (-64\zeta^4 + 448\zeta^2 - 240)\delta^2 - 200 \\ &\quad + 896\zeta^2 - 880\zeta^4 - 24\gamma^2 - 48\zeta^2\gamma^2 + 256\zeta^6, \\ d_3 &= 256\delta^6 + (256\zeta^4 - 2816\zeta^2 + 1408)\delta^4 \\ &\quad + [(1152\zeta^2 + 576)\gamma^2 - 2048\zeta^6 + 11136\zeta^4 - 11520\zeta^2 + 2000]\delta^2 \\ &\quad + 4096\zeta^8 - 16896\zeta^6 + 22800\zeta^4 - 10000\zeta^2 \\ &\quad + (1024\zeta^6 - 3072\zeta^4 + 480\zeta^2 + 2000)\gamma^2 - 432\gamma^4, \\ d_4 &= 4\gamma^2 - 4. \end{aligned} \quad (3.3.23)$$

When  $\zeta=0$ , it is easy to know that  $d_0 < 0$ ,  $d_1 > 0$ ,  $d_2 < 0$ ,  $d_3 > 0$  and  $d_4 < 0$ . Thus, the number of variation of signs in the modified sign table  $[1, -1, -1, -1, -1, -1]$  of the discrimination sequence is 1. This implies that the system is not delay-independent stable since  $F(\omega)$  has  $4(=6-2 \times 1)$  real roots. This fact shows again that only damping makes the delay-independent stability possible.

For the case when  $\zeta=0.02$  studied in (Zhang et al. 1993), we have

$$b_1 = 2.0016, \quad b_2 = -6.9936 - 4\delta^2, \quad b_3 = 4(1 - \gamma^2) \in [0, 4]. \quad (3.3.24)$$

Hence,

$$\begin{aligned}
 d_0 &= -2.0016 < 0, \quad d_1 = 2.4987 \times 10 + 12\delta^2 > 0, \\
 d_2 &= -64\delta^4 - 2.3982 \times 10^2 \delta^2 - 2.4019 \times 10\gamma^2 - 1.9964 \times 10^2 < 0, \\
 d_3 &= 256\delta^6 + 1.4069 \times 10^3 \delta^4 + (5.7646 \times 10^2 \gamma^2 + 1.9954 \times 10^3) \delta^2 + \\
 &\quad 2.0002 \times 10^3 \gamma^2 - 432\gamma^4 - 3.9964 \\
 d_4 &= -b_3 < 0.
 \end{aligned}
 \tag{3.3.25}$$

If  $d_3 > 0$  or  $d_3 = 0$ , the sign table of the discrimination sequence in Eq. (3.3.21) is  $[1, -1, -1, -1, -1, -1]$  or  $[1, -1, -1, -1, 0, 0]$ . In both cases, the number of variation of signs is 1. Thus,  $F(\omega)$  has  $4=6-2 \times 1$  or  $2=4-2 \times 1$  real roots such that the system is not delay-independent stable. Hence, the system is delay-independent stable if and only if the feedback gains of control satisfy

- (a)  $d_3 < 0$ ,
- (b)  $-1 < \gamma, (2 + 2 \times 0.02)(2\delta + 2 \times 2 \times 0.02 + 1) > 2(1 + \gamma)$ .

Because the straight line  $1.02(2\delta + 5.08) = 1 + \gamma$  on the plane of  $(\gamma, \delta)$  does not intersect the boundary  $d_3 = 0$ , the delay-independent stable region is governed by  $d_3 < 0$  only and shown in Fig. 3.3.3.

Another case study can be similarly made for  $\zeta = 0.5$  and the corresponding region of delay-independent stability is shown in Fig. 3.3.4.

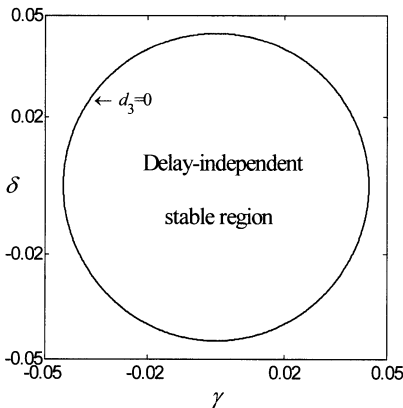


Fig. 3.3.3. The delay-independent stable region of a tall structure with active tendon on the plane of  $(\gamma, \delta)$  when  $\alpha = 2$  and  $\zeta = 0.02$

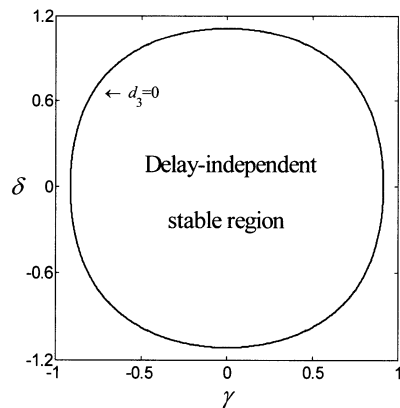


Fig. 3.3.4. The delay-independent stable region of a tall structure with active tendon on the plane of  $(\gamma, \delta)$  when  $\alpha = 2$  and  $\zeta = 0.5$

### 3.4 Stability of Single-degree-of-freedom Systems with Finite Time Delays

As analyzed in Sections 3.1 and 3.3, it is very restrictive for a controlled system to be delay-independent stable. For instance, the region of delay-independent stability of Eq. (3.1.1) is always bounded in the rectangular  $\{(u, v) \mid |u| \leq 1, |v| \leq 2\zeta\}$  on the plane of  $(u, v)$ . The region is very small since most mechanical systems are slightly damped. In practice, the stability of many controlled systems is only required for bounded time delays, especially for the short time delays on a bounded interval.

This section, therefore, deals with the system stability when two finite time delays are given. By separating the real and imaginary parts of the critical condition  $D(i\omega, \tau_1, \tau_2) = 0$ , we have

$$\begin{cases} \operatorname{Re}[D(i\omega, \tau_1, \tau_2)] \equiv 1 - \omega^2 - u \cos \omega \tau_1 - v \omega \sin \omega \tau_2 = 0, \\ \operatorname{Im}[D(i\omega, \tau_1, \tau_2)] \equiv 2\zeta \omega + u \sin \omega \tau_1 - v \omega \cos \omega \tau_2 = 0. \end{cases} \quad (3.4.1)$$

Solving Eq. (3.4.1) for  $u$  and  $v$  yields

$$\begin{cases} u = \frac{(1 - \omega^2) \cos \omega \tau_2 - 2\zeta \omega \sin \omega \tau_2}{\cos[\omega(\tau_1 - \tau_2)]}, \\ v = \frac{(1 - \omega^2) \sin \omega \tau_1 + 2\zeta \omega \cos \omega \tau_1}{\omega \cos[\omega(\tau_1 - \tau_2)]}. \end{cases} \quad (3.4.2)$$

On the plane of  $(u, v)$ , Eq. (3.4.2) gives the transition set where at least one characteristic root of Eq. (3.1.3) changes the sign of real part. As both  $u$  and  $v$  are even functions in frequency  $\omega$ , the transition set will be discussed on the semi-infinite interval  $\omega \in [0, +\infty)$  only.

#### 3.4.1 Systems with Equal Time Delays

If  $\tau_1 = \tau_2 \equiv \tau$ , Eq. (3.4.2) becomes

$$\begin{cases} u = [(1 - \omega^2) \cos \omega \tau - 2\zeta \omega \sin \omega \tau], \\ v = [(1 - \omega^2) \sin \omega \tau + 2\zeta \omega \cos \omega \tau] / \omega. \end{cases} \quad (3.4.3)$$

Thus, the transition set is a continuous curve  $C_\tau$  on the plane of  $(u, v)$  when the parameter  $\omega$  varies on  $[0, +\infty)$ . It is easy to find from Eq. (3.4.3) that the curve  $C_\tau$  starts from the point  $A = (1, 2\zeta + \tau)$  on the plane of  $(u, v)$ . As shown in Fig.

3.4.1, the curve  $C_\tau$  becomes complicated and intersects itself if the time delay is long enough.

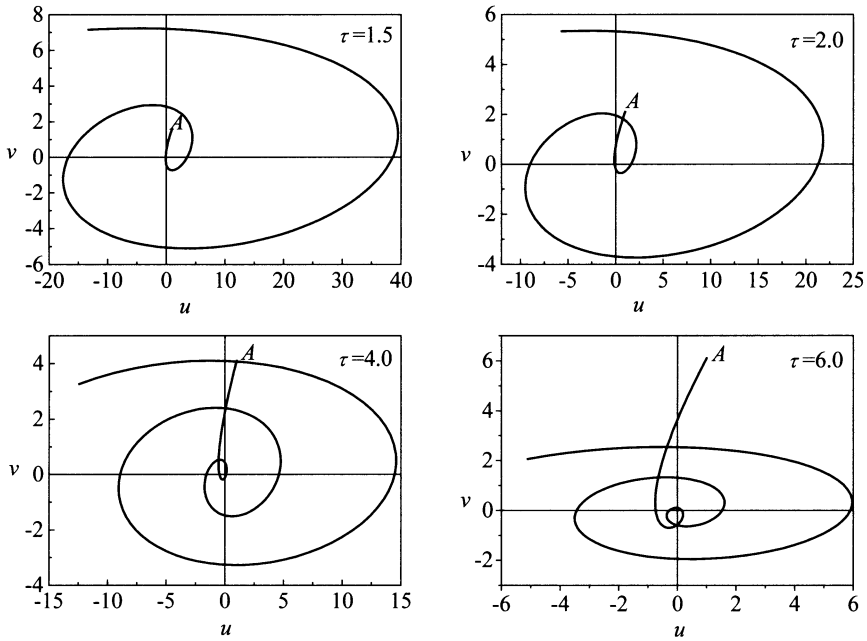


Fig. 3.4.1. Transition sets on the plane of  $(u, v)$  at  $\zeta=0.05$  for various equal time delays

From the viewpoint of an engineer, one may wonder the critical time delay  $\tau_m$ , with which the curve  $C_\tau$  just intersects itself at  $(1, 2\zeta + \tau_m)$  on the plane of  $(u, v)$ . According to Eq. (3.4.3), such a time delay yields

$$\begin{cases} (1-\omega^2)\cos\omega\tau_m - 2\zeta\omega\sin\omega\tau_m = 1, \\ (1-\omega^2)\sin\omega\tau_m + 2\zeta\omega\cos\omega\tau_m = (2\zeta + \tau_m)\omega. \end{cases} \quad (3.4.4)$$

This condition can be recast as

$$\tan(\omega\tau_m + \varphi) = (2\zeta + \tau_m)\omega, \quad \varphi = \tan^{-1} \frac{2\zeta\omega}{1-\omega^2}. \quad (3.4.5)$$

In addition, the self-intersection of curve  $C_\tau$  at  $(1, 2\zeta + \tau_m)$  implies that Eq. (3.1.10) has two different positive roots when  $u=1$  and  $v=2\zeta + \tau_m$ . From Eqs. (3.1.11) and (3.1.12), these two roots are

$$\omega_1 = 0, \quad \omega_2 = \sqrt{-p} = \sqrt{\tau_m^2 + 4\zeta\tau_m + 2}. \quad (3.4.6)$$

Substituting  $\omega$  in Eq. (3.4.5) with  $\omega_2$  yields

$$\begin{cases} \tan(\tau_m \sqrt{\tau_m^2 + 4\zeta\tau_m + 2} + \varphi) = (2\zeta + \tau_m) \sqrt{\tau_m^2 + 4\zeta\tau_m + 2}, \\ \varphi = \tan^{-1} \frac{2\zeta \sqrt{\tau_m^2 + 4\zeta\tau_m + 2}}{1 - (\tau_m^2 + 4\zeta\tau_m + 2)}. \end{cases} \quad (3.4.7)$$

Solving Eq. (3.4.7) numerically for the minimal positive root, we obtain the critical time delay for given damping ratio. As shown in Fig. 3.4.2, the critical time delay decreases with an increase of the damping ratio.

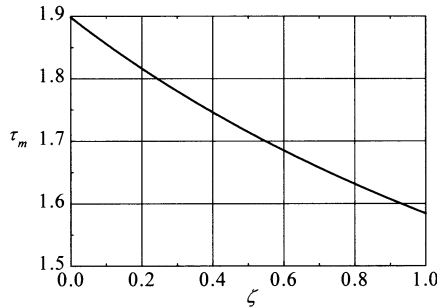


Fig. 3.4.2. Critical time delay versus damping ratio

Given a time delay  $\delta < \tau_m$ , the transition set  $C_\delta$  shown in Fig. 3.4.3 does not intersect itself. This curve, together with the lines of  $u=1$  and  $v=2\zeta$ , surrounds a shaded region denoted by  $D_\delta^1$  in Fig. 3.4.3. According to  $(0,0) \in D_\delta^1$ , all combinations of  $(u,v) \in D_\delta^1$  guarantee the system stability for equal time delays  $\tau_1 = \tau_2 = \delta$ . This region will be called the stability region hereafter for short.

It should be emphasized that  $D_\delta^1$  in Fig. 3.4.3 is the unique stability region where the feedback gains guarantee the system stability for any equal time delays  $\tau_1 = \tau_2 = \tau \leq \delta$ . What follows is an intuitive proof of this assertion.

By differentiating Eq. (3.4.3) with respect to  $\omega$ , we have the tangent of  $C_\tau$  at the starting location

$$\begin{aligned} \frac{dv}{du} &= \frac{\frac{\partial v}{\partial \omega}}{\frac{\partial u}{\partial \omega}} = \frac{\frac{\tau(1-\omega^2)}{\omega} \cos \omega \tau + \left(\frac{\omega^2-1}{\omega^2} - 2 - 2\zeta\tau\right) \sin \omega \tau}{-2\omega(1+\zeta\tau) \cos \omega \tau + (\tau\omega^2 - \tau - 2\zeta) \sin \omega \tau} \\ &\approx \frac{2\tau + 2\zeta\tau^2}{2 + 4\zeta\tau + \tau^2} = \tau + O(\tau). \end{aligned} \quad (3.4.8)$$

If  $0 \leq \tau < \delta$ , the curves  $C_\tau$  and  $C_\delta$  intersect each other near  $(0, 2\zeta)$  as shown in Fig. 3.4.3. According to the analysis in Subsection 3.1.2, only the parameter combination  $(u, v)$  under the conditions  $p^2 - 4q \geq 0$ ,  $p < 0$ ,  $q \geq 0$  enables Eq. (3.1.10) to have two positive roots. The third inequality here implies that  $C_\tau$  and  $C_\delta$  intersect each other only in the region of  $|u| < 1$ . Thus,  $C_\tau$  can not enter into the stability region  $D_\delta^1$  if  $u < -1$ . As a result, the combination of feedback gains  $(u, v) \in D_\delta^1$  ensures that the system is asymptotically stable for any equal time delays  $\tau_1 = \tau_2 = \tau \leq \delta$ .

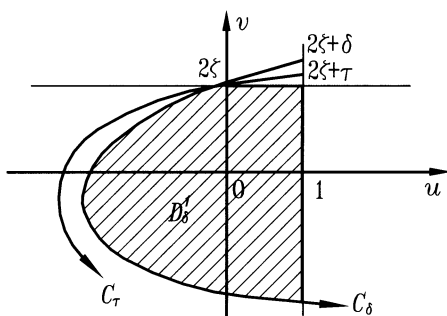


Fig. 3.4.3. Stability region  $D_\delta^1$  on the plane of  $(u, v)$  for  $\tau_1 = \tau_2 = \tau \leq \delta$

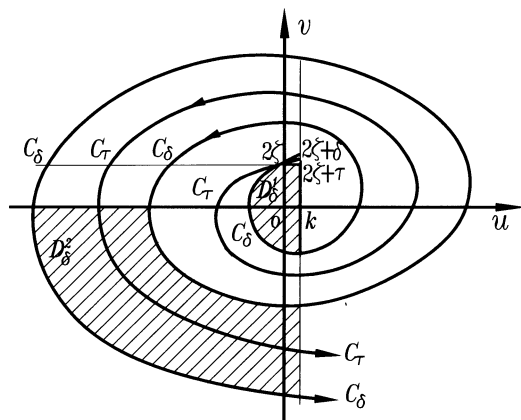


Fig. 3.4.4. Transition sets  $C_\delta$  and  $C_\tau$  on the plane of  $(u, v)$  for equal time delays

Then, it is easy to see that the system is unstable for any  $0 < \tau \leq \delta$  if the combination of feedback gains  $(u, v)$  falls into other shaded regions, say  $D_\delta^2$  in Fig. 3.4.4, where the roots of Eq. (3.1.3) seem to have the negative real parts again with variation of  $(u, v)$ . In fact, even for a very short time delay  $\tau$ , the corresponding spiral  $C_\tau$  will enter into  $D_\delta^2$  as long as the frequency  $\omega$  is high enough.

This implies that the system will undergo instability if the disturbance  $\Delta x(t)$  involves any harmonic components of sufficiently high frequency. As a result, the assertion, made in (Palkovics and Venhovens 1992), that there exist other stability regions on the plane of  $(u, v)$  is not true.

### 3.4.2 Systems with Unequal Time Delays

In the case of  $\tau_1 \neq \tau_2$ , let  $\Delta\tau = |\tau_1 - \tau_2|$ . It is obvious that both  $u$  and  $v$  in Eq. (3.4.2) will approach to the infinity when  $\omega\Delta\tau \rightarrow n\pi/2, n=1,3,5,\dots$ . Thus, the transition set given by Eq. (3.4.2) in this case is no longer a continuous curve. It consists of infinite number of curves defined by the parametric equation in  $\omega$  on the intervals  $[0, \pi/2\Delta\tau), (\pi/2\Delta\tau, 3\pi/2\Delta\tau)$ , and so on. As analyzed in the previous subsection, the boundary of the stability region is a small part of the transition set corresponding to the lower frequency  $\omega$ . So, we focus on the transition set in the frequency range  $\omega \in [0, \pi/2\Delta\tau)$ .

Consider first the case when  $0 < \tau_1 < \tau_2$ . The transition set is a curve starting from  $(1, 2\zeta + \tau_1)$  on the plane of  $(u, v)$  and approaches to the infinity when  $\omega(\tau_2 - \tau_1) \rightarrow \pi/2$ . It is easy to find that the tangent of the asymptotic line reads

$$\begin{aligned} \frac{v}{u} &\rightarrow \frac{(1-\omega^2)\sin\omega\tau_1 + 2\zeta\omega\cos\omega\tau_1}{\omega[(1-\omega^2)\cos\omega(\tau_1 + \pi/2) - 2\zeta\omega\sin\omega(\tau_1 + \pi/2)]} \\ &= -\frac{1}{\omega} = \frac{\pi}{2(\tau_1 - \tau_2)} < 0. \end{aligned} \quad (3.4.9)$$

Obviously, if  $\Delta\tau$  is small, the curve will spiral one or more rounds and go to the infinity on the second quadrant or the fourth quadrant. Otherwise, it goes to the infinity on the fourth quadrant. These two cases are shown in Fig. 3.4.5a and 3.4.5b, respectively.

If  $0 < \tau_2 < \tau_1$ , we similarly find the tangent of the asymptotic line

$$\begin{aligned} \frac{v}{u} &\rightarrow \frac{(1-\omega^2)\sin\omega(\tau_2 + \pi/2) + 2\zeta\omega\cos\omega(\tau_2 + \pi/2)}{\omega[(1-\omega^2)\cos\omega\tau_2 - 2\zeta\omega\sin\omega\tau_2]} \\ &= \frac{1}{\omega} = \frac{\pi}{2(\tau_1 - \tau_2)} > 0, \end{aligned} \quad (3.4.10)$$

when  $\omega(\tau_1 - \tau_2) \rightarrow \pi/2$ . The transition set will approach to the infinity on the first quadrant or the third quadrant if  $\Delta\tau$  is small. Otherwise, it goes to the infinity on the third quadrant. These two cases are shown in Fig. 3.4.5c and 3.4.5d, respectively.

Noting the marginal stability conditions in Eq. (3.4.2) for a system without time delays in feedback, we can determine the stability regions shown as the shaded ones in Fig. 3.4.5. Fig. 3.4.5d shows that the stability region shrinks to a very small one if  $0 < \tau_2 \ll \tau_1$ . This is the most dangerous case that should be avoided in practice.

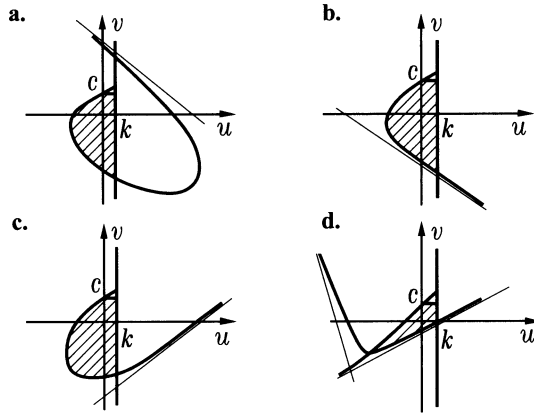


**Fig. 3.4.5.** Transition sets and stability regions on the plane of  $(u, v)$  for unequal time delays; **a.**  $\tau_1 < \tau_2$ , small  $\Delta\tau$ , **b.**  $\tau_1 < \tau_2$ , large  $\Delta\tau$ , **c.**  $\tau_1 > \tau_2$ , small  $\Delta\tau$ , **d.**  $\tau_1 > \tau_2$ , large  $\Delta\tau$

### 3.5 Stability Switches of High Dimensional Systems

As the delay-independent stable region of a practical system is often a very small part in the parameter space of the system, a question is aroused as following. What stability properties does a system have if the system parameters are chosen out of the delay-independent stable region in the parameter space?

To answer this question, the characteristic roots of a delayed dynamic system are taken as the functions of time delay. If the system parameters do not fall into the delay-independent stable region, the real part of at least one characteristic root changes its sign when the time delay varies. That is, the stability of system can not keep unchanged with an increase of time delay. Such a change with increase of time delay has been referred to as the *stability switch* in (Kuang 1993) and (Marshall et al. 1992). The concept of stability switch is not new, still, it is an open problem if some uncertain parameters of the system are involved in the design phase.



The objective of this section is to gain an insight into the system stability in the parameter space and to give a simple approach so as to complete the stability analysis as done by using the method of  $D$ -subdivision.

### 3.5.1 Systems with a Single Time Delay

We first analyze the stability of a delayed dynamic system of single degree of freedom to give a guide of the analysis of stability switches.

**Example 3.5.1** Consider the system with the characteristic equation

$$D(\lambda, \tau) \equiv \lambda^2 + \lambda + 4 + 2e^{-\lambda\tau} = 0. \quad (3.5.1)$$

Suppose that  $\lambda = i\omega$  and  $\omega \geq 0$  is a root of  $D(\lambda, \tau) = 0$  for  $\tau > 0$ . From  $D(i\omega, \tau) = 0$ , thus, we have  $|(i\omega)^2 + i\omega + 4| = 2$ . There follows

$$\omega^4 - 7\omega^2 + 12 = 0. \quad (3.5.2)$$

This equation has four roots  $\omega_{1,3} = \pm 2$  and  $\omega_{2,4} = \pm\sqrt{3}$ .

Substituting  $\lambda = i\omega_1 = 2i$  into Eq. (3.5.1) gives  $\cos\omega_1\tau = 0$  and  $\sin\omega_1\tau = 1$ . Then, we have

$$\tau_{1,k} = k\pi + \frac{\pi}{4} \quad \text{and} \quad \tau_{1,k+1} - \tau_{1,k} = \pi, \quad k = 0, 1, 2, \dots \quad (3.5.3)$$

At  $\omega_2 = \sqrt{3}$ , we have  $2\cos\omega_2\tau = -1$  and  $2\sin\omega_2\tau = \sqrt{3}$ , as well as

$$\tau_{2,k} = [(2k+1)\pi - \frac{\pi}{3}]/\sqrt{3} \quad \text{and} \quad \tau_{2,k+1} - \tau_{2,k} = 2\pi/\sqrt{3}, \quad k = 0, 1, 2, \dots \quad (3.5.4)$$

It is obvious that  $D(\lambda, 0)$  is asymptotically stable. As the characteristic roots are continuous with respect to  $\tau$ , the system keeps stable until  $\tau$  arrives at  $\pi/4$ , the minimum of critical time delays which may destroy the stability of system, from the left side. To see whether the stability of system changes, we check the sign of  $d[\text{Re}(\lambda)]/d\tau$  as  $\tau$  is crossing  $\pi/4$ . Straightforward computation shows that  $d[\text{Re}(\lambda)]/d\tau > 0$  when  $\tau = \pi/4$ . Hence, the characteristic equation of system has a pair of conjugate complex roots with positive real part when  $\tau$  is a little bit larger than  $\pi/4$  so that the system becomes unstable. The system keeps unstable until  $\tau$  reaches the next critical time delay  $2\pi/(3\sqrt{3})$  from the left side. At the second critical time delay,  $d[\text{Re}(\lambda)]/d\tau < 0$  holds. Thus, the characteristic equation decreases a pair of conjugate complex roots with positive real part and the system becomes stable again. As the time delay increases further, the characteris-

tic equation increases a pair of characteristic roots with the positive real part when  $\tau$  is crossing  $\tau_{1,k}$ , and decreases such a pair when  $\tau$  is crossing  $\tau_{2,k}$ . With an increase of time delay, therefore, the system changes the status from stability to instability, and then from instability to stability, and so on. The stability exchange happens one by one provided that  $\tau_{1,k+1} - \tau_{2,k} > 0$  holds. However, the relation  $\tau_{1,k+1} - \tau_{1,k} = \pi < 2\pi/\sqrt{3} = \tau_{2,k+1} - \tau_{2,k}$  indicates that the condition  $\tau_{1,k+1} - \tau_{2,k} > 0$  must be destroyed with an increase of  $k$ . Thus, the exchange of stability has to stop eventually and permanent instability occurs.

This example shows that the analysis of stability switches of a delayed dynamic system includes two steps. That is, to find out the possible vibration frequencies and possible critical values of time delay first, then to check the sign of differentiation of the characteristic roots with respect to the time delay at the critical values. The second step tells if the time delay stabilizes or destabilizes the system.

Now we consider the stability switches of a high dimensional, linear dynamic system with a single time delay governed by the following characteristic equation

$$D(\lambda, \tau) \equiv P(\lambda) + Q(\lambda)e^{-\lambda\tau} = 0, \tag{3.5.5}$$

where  $\tau \geq 0$  is the time delay,  $P(\lambda)$  and  $Q(\lambda)$  are two polynomials of real coefficients with  $\deg(P) = n > \deg(Q)$ . Without loss of generality, we assume that both polynomials  $P(\lambda)$  and  $Q(\lambda)$  have no common pure imaginary roots.

To study the marginal stability when  $D(i\omega, \tau) = 0$ , let

$$\begin{aligned} P_R(\omega) &\equiv \text{Re}[P(i\omega)], & P_I(\omega) &\equiv \text{Im}[P(i\omega)], \\ Q_R(\omega) &\equiv \text{Re}[Q(i\omega)], & Q_I(\omega) &\equiv \text{Im}[Q(i\omega)], \end{aligned} \tag{3.5.6}$$

where  $P_R(\omega)$  and  $Q_R(\omega)$  are even functions, whereas  $P_I(\omega)$  and  $Q_I(\omega)$  are odd functions. Hence, the equivalent form of  $D(i\omega, \tau) = 0$  reads

$$\begin{cases} Q_R(\omega)\cos\omega\tau + Q_I(\omega)\sin\omega\tau = -P_R(\omega), \\ Q_I(\omega)\cos\omega\tau - Q_R(\omega)\sin\omega\tau = -P_I(\omega). \end{cases} \tag{3.5.7}$$

In order that Eq. (3.5.5) has a pair of pure imaginary roots  $\pm i\omega$  for  $\tau \geq 0$ , it is necessary that  $|P(i\omega)| = |Q(i\omega)|$ , that is,

$$P_R^2(\omega) + P_I^2(\omega) - [Q_R^2(\omega) + Q_I^2(\omega)] = 0, \tag{3.5.8}$$

has a positive root  $\omega$ . As the case of  $\tau_1 = \tau_2$  in Section 3.3, the left side of above equation can simply be recast in an explicit form

$$F(\omega) \equiv \omega^{2n} + b_1\omega^{2(n-1)} + b_2\omega^{2(n-2)} + \dots + b_{n-1}\omega^2 + b_n. \tag{3.5.9}$$

Thus, we have the following theorem.



**Theorem 3.5.1** In order that the quasi-polynomial  $D(\lambda, \tau)$  has pure imaginary roots  $\lambda = \pm i\omega$ , it is necessary that  $\omega$  is a real positive root of  $F(\omega)$ .

Because  $P(i\omega)$  and  $Q(i\omega)$  do not share any real root,  $Q_R^2(\omega) + Q_I^2(\omega) \neq 0$  must hold. Otherwise, Eq. (3.5.8) gives  $P_R(\omega) = 0$ ,  $P_I(\omega) = 0$ ,  $Q_R(\omega) = 0$  and  $Q_I(\omega) = 0$ . They are in contradiction with the assumption. Once a positive root  $\omega$  of  $F(\omega)$  is found, the critical time delays are given by

$$\tau_k = \frac{\theta}{\omega} + \frac{2k\pi}{\omega}, \quad k = 1, 2, \dots \tag{3.5.10}$$

where  $\theta \in [0, 2\pi)$  yields a set of triangle equations

$$\begin{cases} \sin\theta = \frac{Q_R(\omega)P_I(\omega) - P_R(\omega)Q_I(\omega)}{Q_R^2(\omega) + Q_I^2(\omega)}, \\ \cos\theta = -\frac{P_R(\omega)Q_R(\omega) + Q_I(\omega)P_I(\omega)}{Q_R^2(\omega) + Q_I^2(\omega)}. \end{cases} \tag{3.5.11}$$

If  $F(\omega)$  has no positive roots, the system does not undergo any stability switch. That is, the system is delay-independent stable if it is asymptotically stable when the time delay disappears, or unstable for an arbitrary time delay if the system free of time delay is unstable.

If  $F(\omega)$  has any positive roots, the root  $\lambda$  of Eq. (3.5.5) can be regarded as a function of  $\tau$  and is denoted by  $\lambda(\tau)$ . Once a pair of pure imaginary characteristic roots  $\pm i\omega$  is found and the corresponding critical values of time delay in Eq. (3.5.10) are determined, the variation direction of its real part with respect to the time delay  $\tau$  can be studied through  $S \equiv \text{sgn}[d(\text{Re}\lambda)/d\tau|_{\lambda=i\omega}]$ . The following theorem enables one to avoid complicated computation.

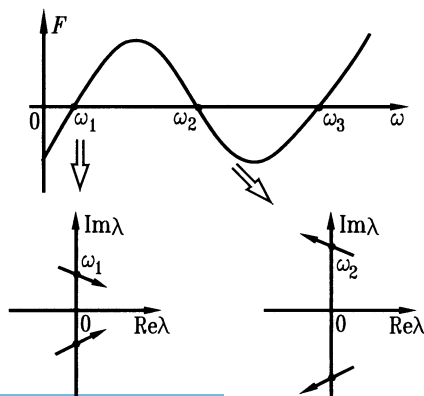


Fig. 3.5.1. Explanation of Theorem 3.5.2

**Theorem 3.5.2**  $S = \text{sgn} F'(\omega)$ .

**Proof** Differentiating Eq. (3.5.5) with respect to  $\tau$  yields

$$\frac{d\lambda}{d\tau} = \frac{\lambda Q(\lambda)}{P'(\lambda)e^{\lambda\tau} + Q'(\lambda) - \tau Q(\lambda)}. \quad (3.5.12)$$

In order that this derivative is properly defined at  $\lambda = \pm i\omega$ , it should be required that  $P'(i\omega)\exp(i\omega\tau) + Q'(i\omega) - \tau Q(i\omega) \neq 0$ , i.e.,  $\pm i\omega$  are not a pair of repeated characteristic roots. Noting the following two relations

$$\text{sgn}\left[\text{Re}\left(\frac{1}{a+ib}\right)\right] = \text{sgn}\left(\frac{a-ib}{a^2+b^2}\right) = \text{sgn}[\text{Re}(a+ib)], \quad a, b \in R, \quad (3.5.13)$$

$$\left(\frac{d\lambda}{d\tau}\right)^{-1} = -\frac{P'(\lambda)}{\lambda P(\lambda)} + \frac{Q'(\lambda)}{\lambda Q(\lambda)} - \frac{\tau}{\lambda}, \quad (3.5.14)$$

we have

$$\begin{aligned} S &= \text{sgn}\left[\left.\frac{d(\text{Re}\lambda)}{d\tau}\right|_{\lambda=i\omega}\right] = \text{sgn}\left[\left.\text{Re}\left(\frac{d\lambda}{d\tau}\right)\right|_{\lambda=i\omega}\right] = \text{sgn}\left[\left.\text{Re}\left(\frac{d\lambda}{d\tau}\right)^{-1}\right|_{\lambda=i\omega}\right] \\ &= \text{sgn}\left\{\text{Re}\left[-\frac{P'(i\omega)}{i\omega P(i\omega)} + \frac{Q'(i\omega)}{i\omega Q(i\omega)} - \frac{\tau}{i\omega}\right]\right\} \\ &= \text{sgn}\left\{\text{Im}\left[\frac{Q'(i\omega)\bar{Q}(i\omega)}{\omega|Q(i\omega)|^2} - \frac{P'(i\omega)\bar{P}(i\omega)}{\omega|P(i\omega)|^2}\right]\right\} \\ &= \text{sgn}\left\{\text{Im}[Q'(i\omega)\bar{Q}(i\omega) - P'(i\omega)\bar{P}(i\omega)]\right\}, \end{aligned} \quad (3.5.15)$$

where the bar denotes the operation of complex conjugate. Substituting

$$\begin{aligned} &\text{Im}[Q'(i\omega)\bar{Q}(i\omega) - P'(i\omega)\bar{P}(i\omega)] \\ &= P_R(\omega)P'_R(\omega) + P_I(\omega)P'_I(\omega) - Q_R(\omega)Q'_R(\omega) - Q_I(\omega)Q'_I(\omega), \quad (3.5.16) \\ &= \frac{1}{2}F'(\omega) \end{aligned}$$

into Eq. (3.5.15) yields

$$S = \text{sgn} F'(\omega). \quad (3.5.17)$$

This completes the proof.

Furthermore, two cases are discussed as following. The first case is that the polynomial  $F(\omega)$  has one positive simple root  $\omega_0$  with the critical values  $\tau_k, k=1,2,\dots$  of time delay given by Eq. (3.5.10). Because the leading coefficient of polynomial  $F(\omega)$  is positive, we have  $F(\omega) > F(\omega_0) = 0$  for all  $\omega > \omega_0$  and  $F(\omega) < F(\omega_0) = 0$  for  $\omega \in [0, \omega_0)$ . There follows  $F'(\omega_0) > 0$ . This fact indicates

that each crossing of the real part of characteristic roots at a critical value  $\tau_k$  of time delay corresponding to  $\pm i\omega_0$  must be from the left to the right. Thus, the characteristic equation of system has a new pair of conjugate roots with positive real parts when the time delay is crossing a critical value  $\tau_k$  of time delay, and the number of characteristic roots with positive real part can not decrease as the time delay increases. Hence, if the system without time delay is asymptotically stable, the numbers of characteristic roots with positive real part are  $0, 2, 4, \dots, 2i, \dots$  on the intervals  $[0, \tau_0), (\tau_0, \tau_1), (\tau_1, \tau_2), \dots, (\tau_{i-1}, \tau_i), \dots$ , respectively. This means that the system is asymptotically stable for  $\tau \in [0, \tau_0)$ , and unstable for  $\tau \in [\tau_0, +\infty)$ . If the system free of time delay is unstable, then there exists at least one pair of conjugate characteristic roots with positive real part for  $\tau \in [0, \tau_0)$ . Thus, the system is unstable for any given time delay.

In the second case, the polynomial  $F(\omega)$  has a number of simple, positive roots denoted by  $\omega_1 > \omega_2 > \dots > \omega_p > 0$ . The difference between two critical values of time delay corresponding to a given pair of roots  $\pm i\omega_j$  satisfies

$$\tau_{j,k+1} - \tau_{j,k} = \frac{2\pi}{\omega_j} < \frac{2\pi}{\omega_{j+1}} = \tau_{j+1,k+1} - \tau_{j+1,k}, \quad k=1, 2, \dots, j=1, 2, \dots, p-1. \quad (3.5.18)$$

The crossing of real parts of characteristic roots at two adjacent simple roots  $\omega_j$  and  $\omega_{j+1}$  must be in opposite directions, since  $F'(\omega_j)$  and  $F'(\omega_{j+1})$  have opposite signs. In fact, it is easy to see that both  $\text{sgn}[F'(\omega_{2j-1})] > 0$  and  $\text{sgn}[F'(\omega_{2j})] < 0, j \geq 1$  are true since  $F(\omega) > F(\omega_1) = 0$  holds for all  $\omega \in (\omega_1, +\infty)$  and all possible  $\omega \in (\omega_{2k+1}, \omega_{2k})$ , and  $F(\omega) < F(\omega_1) = 0$  for all possible  $\omega \in (\omega_{2k}, \omega_{2k-1})$ . That is, the crossing real parts of characteristic roots at  $\tau_{2j-1,k}$  corresponding to  $\pm i\omega_{2j-1}$  must be from the left to the right, and the crossing at  $\tau_{2j,k}$  corresponding to  $\pm i\omega_{2j}$  must be from the right to the left. Therefore, as the time delay varies from zero to the positive infinity, the characteristic equation of system always adds a new pair of conjugate roots with positive real parts for each crossing at  $\tau_{2j-1,k}$ , but reduces such a pair for each crossing at  $\tau_{2j,k}$ . Given a long time delay  $\hat{\tau}$ , Eq. (3.5.18) indicates that the interval  $[0, \hat{\tau}]$  includes more  $\tau_{1,k}$  corresponding to  $\pm i\omega_1$  than  $\tau_{2,l}$  to  $\pm i\omega_2$ . Hence, more characteristic roots change their sign of real parts from the negative to the positive at  $\tau_{1,k}$  than those changing the sign of real parts from the negative to the positive at  $\tau_{2,l}$  with an increase of time delay in the interval  $[0, \hat{\tau}]$ . A similar assertion holds also true for the time delay crossing at  $\tau_{3,m}$  and  $\tau_{4,n}$  corresponding to  $\pm i\omega_3$  and  $\pm i\omega_4$ , and so forth. Hence, the characteristic equation of system must have eventually some roots with positive real parts when the time delay is long enough. As a result, the system

must become unstable with an increase of time delay and the number of stability switches is finite.

The above analysis can be summarised as following.

**Theorem 3.5.3** Assume that Eq. (3.5.5) has no pure imaginary characteristic roots  $i\omega$  such that  $Q(i\omega)=0$ .

(a) If the polynomial  $F(\omega)$  has no positive root, the system is delay-independent stable or unstable for any given time delay, depending on whether or not the system free of time delay is stable.

(b) Suppose that  $F(\omega)$  has only one simple positive root  $\omega$ . If the system free of time delay is asymptotically stable, there exists exactly one critical time delay  $\tau_0 > 0$  such that the system remains asymptotically stable when  $\tau \in [0, \tau_0)$ , and becomes unstable when  $\tau \geq \tau_0$ . If the system is unstable for  $\tau = 0$ , it is unstable for an arbitrary time delay  $\tau$ .

(c) If  $F(\omega)$  has at least two positive roots  $\omega_1 > \omega_2 > \dots > \omega_p > 0$  and the roots are simple, a finite number of stability switches may occur as the time delay  $\tau$  increases from zero to the positive infinity, and the system becomes unstable at last.

If the order of a system is one or two, the analysis on the number of real roots of  $F(\omega)$  is relatively easy. If the system is of high order and includes some parameters to be designed, however, pure numerical consideration is time consuming. In this case, the generalized Sturm criterion serves as an effective tool for analysing the stability switches.

**Theorem 3.5.4** Assume that Eq. (3.5.5) has no pure imaginary characteristic roots satisfying  $Q(i\omega)=0$  and the roots of  $F(\omega)$  are simple. Let  $l$  and  $s$  be the number of non-zero terms and the number of variation of signs in the modified sign table of the discrimination sequence of  $F(\omega)$ , then following facts are true.

(a) If  $l-2s=0$ , the system is delay-independent stable or unstable for any time delay, depending on whether the system free of time delay is asymptotically stable or not.

(b) If  $l-2s=2$  and the system free of time delay is asymptotically stable, there exists a critical time delay  $\tau_0 > 0$  such that the system remains asymptotically stable when  $\tau \in [0, \tau_0)$ , and becomes unstable when  $\tau \geq \tau_0$ . If  $l-2s=2$  and the system is unstable for  $\tau = 0$ , it keeps unstable for an arbitrary time delay  $\tau$ .

(c) If  $l-2s > 2$ , a finite number of stability switches occurs as the time delay  $\tau$  increases and the system becomes unstable at last.

Based on Theorem 3.5.1 and the generalized Sturm criterion, the stability analysis for a dynamic system with uncertain parameters and an uncertain time delay can be completed as follows.

**Algorithm 3.5.1**

- (a) Find polynomial  $F(\omega)$  corresponding to the characteristic function.  
 (b) Run the MAPLE routine *discr* to get the discrimination sequence of  $F(\omega)$  and the factors  $d_i, i=0, 1, \dots$ .  
 (c) Divide the parameter region of concern into some sub-regions by drawing the graphs of  $d_i, i=0, 1, \dots$  and the curves determined by the Routh-Hurwitz stability conditions of system when  $\tau=0$ .  
 (d) Use Theorem 3.2.2 to check the number of real roots of  $F(\omega)$  in each sub-region of the parameter region and use Theorem 3.5.1 to predict the stability switches.

This algorithm will be demonstrated in Section 3.6 via analysing the stability switches of a quarter model of active suspension and a four-wheel-steering vehicle, respectively.

**3.5.2 Systems with Commensurate Time Delays**

In this subsection, the problem of stability switches is studied for a more general linear dynamic system, which has multiple commensurate time delays. As we shall see, a similar result can be obtained as in the case of single time delay.

Consider the characteristic quasi-polynomial of system in the form

$$P(\lambda, z) \equiv \sum_{k=0}^m q_k(\lambda) z^k, \quad (3.5.19)$$

where  $z=e^{-\lambda\tau}$  and  $\tau>0$ . We define first

$$P^{(1)}(\lambda, z) \equiv q_0(-\lambda)P(\lambda, z) - q_m(\lambda)z^m P(-\lambda, 1/z). \quad (3.5.20a)$$

It is easy to see that  $P^{(1)}(\lambda, z)$  can be written as

$$P^{(1)}(\lambda, z) = \sum_{k=0}^{m-1} q_k^{(1)}(\lambda) z^k, \quad (3.5.20b)$$

since it does not contain the term  $z^m$ . Repeating the same procedure, we have

$$P^{(j)}(\lambda, z) \equiv \sum_{k=0}^{m-j} q_k^{(j)}(\lambda) z^k, \quad j=1, 2, \dots, m. \quad (3.5.21)$$

Obviously, if  $(\lambda, z)=(i\omega, e^{-i\omega\tau})$  is a root of  $P(\lambda, z)=0$ , so is it for  $P(-\lambda, 1/z)=0$  since the coefficients in  $P(\lambda, z)$  are real. Moreover,  $(\lambda, z)=(i\omega, e^{-i\omega\tau})$  is a com-

mon root of all  $P^{(j)}(\lambda, z)=0$  and  $P^{(j)}(-\lambda, 1/z)=0, j=1, 2, \dots, m$ . Notice that  $P^{(m)}(\lambda, z)=q_0^{(m)}(\lambda)$  is independent of  $z$ , it must be in the form of polynomial  $F(\omega^2)$  because  $q_0^{(m)}(\pm\lambda)=0$  at each root  $(\lambda, z)=(i\omega, e^{-i\omega\tau})$  of  $P(\lambda, z)$ .

**Theorem 3.5.5** In order that  $P(\lambda, z)$  has a pair of pure imaginary roots  $\lambda=\pm i\omega$ ,  $\omega$  must be a root of  $F(\omega^2)$ .

**Remark 3.5.1** From the concept of resultant for two polynomials of a single variable, the polynomial  $F(\omega^2)$  is in fact the resultant of polynomial  $P(\lambda, z)$  and polynomial  $z^m P(-\lambda, 1/z)$  with respect to  $z$  except for a non-zero constant.

Once a positive root  $\omega$  of  $F(\omega^2)$  is found, it is possible solve  $P(i\omega, z)=0$  for  $z$  under the condition of  $|z|=1$  and then determine the critical values of time delay. For the analysis of stability switches, the variation direction of real part of characteristic roots should be determined as  $\tau$  is varied. That is,  $S=\text{sgn}(d\text{Re}\lambda/d\tau)|_{\lambda=i\omega}$  needs to be computed.

For brevity, denote the quasi-polynomials by  $Q(\lambda, \tau)\equiv P(\lambda, z)$  and  $Q^{(j)}(\lambda, \tau)\equiv P^{(j)}(\lambda, z)$  for  $j=1, 2, \dots, m$ . Assume that  $(\lambda, \tau)=(i\omega_0, \tau_0)$  yields both  $Q(i\omega_0, \tau_0)=0$  and  $Q^{(1)}(i\omega_0, \tau_0)=0$ . Let  $\tau$  be slightly perturbed to  $\tau=\tau_0+\delta\tau$ ,  $\delta\lambda$  and  $\delta\lambda_1$  be the small perturbations of  $\lambda$  from  $i\omega_0$  such that

$$\begin{cases} Q(i\omega_0+\delta\lambda, \tau_0+\delta\tau)=0, \\ Q^{(1)}(i\omega_0+\delta\lambda_1, \tau_0+\delta\tau)=0. \end{cases} \tag{3.5.22}$$

We need to know when  $\text{Re}\delta\lambda \cdot \text{Re}\delta\lambda_1 > 0$  and when  $\text{Re}\delta\lambda \cdot \text{Re}\delta\lambda_1 < 0$ . Expanding the above two equations and neglecting the high order terms with respect to small perturbations  $\delta\tau$ ,  $\delta\lambda$  and  $\delta\lambda_1$ , we have

$$\begin{cases} Q_\lambda(i\omega_0, \tau_0)\delta\lambda + Q_\tau(i\omega_0, \tau_0)\delta\tau = 0, \\ Q_\lambda^{(1)}(i\omega_0, \tau_0)\delta\lambda_1 + Q_\tau^{(1)}(i\omega_0, \tau_0)\delta\tau = 0, \end{cases} \tag{3.5.23}$$

where the subscripts  $\lambda$  and  $\tau$  represent the corresponding partial derivatives of the functions. Straightforward computation gives

$$\begin{aligned} Q_\lambda^{(1)}(i\omega_0, \tau_0) &= q_0(-i\omega_0)Q_\lambda(i\omega_0, \tau_0) + q_m(i\omega_0)z_0^m Q_\lambda(-i\omega_0, \tau_0), \\ Q_\tau^{(1)}(i\omega_0, \tau_0) &= q_0(-i\omega_0)Q_\tau(i\omega_0, \tau_0) - q_m(i\omega_0)z_0^m Q_\tau(-i\omega_0, \tau_0), \end{aligned} \tag{3.5.24}$$

where  $z_0^m = e^{-i\omega_0\tau_0}$ . Thus,

$$\begin{aligned} & q_0(-i\omega_0)[Q_\lambda(i\omega_0, \tau_0)\delta\lambda_1 + Q_\tau(i\omega_0, \tau_0)\delta\tau] \\ & + q_m(i\omega_0)z_0^m [Q_\lambda(-i\omega_0, \tau_0)\delta\lambda_1 - Q_\tau(-i\omega_0, \tau_0)\delta\tau] = 0. \end{aligned} \tag{3.5.25}$$



Now, we eliminate  $Q_\lambda(\pm i\omega_0, \tau_0)$  and  $Q_\tau(\pm i\omega_0, \tau_0)$ . To this end, imposing the complex conjugate on the first equation in Eq. (3.5.23) yields

$$Q_\lambda(-i\omega_0, \tau_0)\delta\bar{\lambda} + Q_\tau(-i\omega_0, \tau_0)\delta\bar{\tau} = 0. \quad (3.5.26)$$

This, together with Eq. (3.5.25), leads to

$$\begin{aligned} q_0(-i\omega_0)Q_\lambda(i\omega_0, \tau_0)(\delta\lambda_1 - \delta\lambda) \\ + q_m(i\omega_0)z_0^m Q_\lambda(-i\omega_0, \tau_0)(\delta\lambda_1 + \delta\bar{\lambda}) = 0. \end{aligned} \quad (3.5.27)$$

Imposing the complex conjugate on the above equation, we have

$$\begin{aligned} q_0(i\omega_0)Q_\lambda(-i\omega_0, \tau_0)(\delta\bar{\lambda}_1 - \delta\bar{\lambda}) \\ + q_m(-i\omega_0)z_0^{-m} Q_\lambda(i\omega_0, \tau_0)(\delta\bar{\lambda}_1 + \delta\lambda) = 0. \end{aligned} \quad (3.5.28)$$

Eliminating  $Q_\lambda(\pm i\omega_0, \tau_0)$  from Eqs. (3.5.27) and (3.5.28) gives

$$\begin{aligned} q_0(i\omega_0)q_\lambda(-i\omega_0)(\delta\lambda_1 - \delta\lambda)(\delta\bar{\lambda}_1 - \delta\bar{\lambda}) \\ = q_m(i\omega_0)q_m(-i\omega_0)(\delta\lambda_1 + \delta\bar{\lambda})(\delta\bar{\lambda}_1 + \delta\lambda). \end{aligned} \quad (3.5.29)$$

Let  $\delta\lambda = x + iy$  and  $\delta\lambda_1 = x_1 + iy_1$ . Then, we can rewrite Eq. (3.5.29) as

$$\begin{aligned} [q_0(i\omega_0)q_0(-i\omega_0) - q_m(i\omega_0)q_m(-i\omega_0)](x^2 + x_1^2 + (y - y_1)^2) \\ = 2xx_1[q_0(i\omega_0)q_0(-i\omega_0) + q_m(i\omega_0)q_m(-i\omega_0)]. \end{aligned} \quad (3.5.30)$$

Thereby,  $\text{Re}\delta\lambda \cdot \text{Re}\delta\lambda_1 > 0$  holds if and only if

$$q_0^{(1)}(i\omega_0) = q_0(i\omega_0)q_0(-i\omega_0) - q_m(i\omega_0)q_m(-i\omega_0) > 0. \quad (3.5.31)$$

This implies that as the time delays increase, the direction of crossing by a root of  $Q(\lambda, \tau)$ , namely  $P(\lambda, z)$ , is the same as that of the corresponding root of  $Q^{(1)}(\lambda, \tau)$ , namely  $P^{(1)}(\lambda, z)$ , if and only if  $q_0^{(1)}(i\omega_0) > 0$ , and is opposite if and only if  $q_0^{(1)}(i\omega_0) < 0$ .

The same procedure can be repeatedly applied to

$$\begin{cases} Q^{(i)}(i\omega_0 + \delta\lambda_i, \tau_0 + \delta\tau) = 0, \\ Q^{(i+1)}(i\omega_0 + \lambda_{i+1}, \tau_0 + \delta\tau) = 0, \quad i = 1, 2, \dots, m-2. \end{cases} \quad (3.5.32)$$

Therefore, the direction of crossing by a root of  $Q^{(i)}(\lambda, \tau)$ , namely  $P^{(i)}(\lambda, z)$ , is the same as that of the corresponding root of  $Q^{(i+1)}(\lambda, \tau)$ , namely  $P^{(i+1)}(\lambda, z)$ , if and only if  $q_0^{(i+1)}(i\omega_0) > 0$ , and is opposite if and only if  $q_0^{(i+1)}(i\omega_0) < 0$ , where

$$q_0^{(i+1)}(i\omega_0) = q_0^{(i)}(i\omega_0)q_0^{(i)}(-i\omega_0) - q_{m-i}^{(i)}(i\omega_0)q_{m-i}^i(-i\omega_0). \quad (3.5.33)$$

In the final step, namely the simplification from  $Q^{(m-1)}(\lambda, \tau) = q_0^{(m-1)}(\lambda) + q_1^{(m-1)}(\lambda)z$  to  $Q^{(m)}(\lambda) = q_0^{(m-1)}(\lambda)q_0^{(m-1)}(-\lambda) - q_1^{(m-1)}(\lambda)q_1^{(m-1)}(-\lambda)$ , Theorem 3.5.2 can be used. Then, we have the following theorem.

**Theorem 3.5.6** Let  $\Pi(\lambda) \equiv q_0(\lambda)q_0^{(1)}(\lambda) \cdots q_0^{(m-1)}(\lambda)$ , then

$$S \equiv \operatorname{sgn} \left[ \frac{d(\operatorname{Re} \lambda)}{d\tau} \Big|_{\lambda=i\omega_0} \right] = \operatorname{sgn} \left[ \Pi(i\omega_0) \frac{dF(\omega^2)}{d(\omega^2)} \Big|_{\omega=\omega_0} \right]. \quad (3.5.34)$$

**Example 3.5.2** Study the stability switch of

$$P(\lambda, z) = m\lambda^2 + c\lambda + k - uz^2 - v\lambda z \quad \text{with } z = e^{-\lambda\tau}. \quad (3.5.35)$$

We have

$$q_0(\lambda) = m\lambda^2 + c\lambda + k, \quad q_1(\lambda) = -v\lambda, \quad q_2(\lambda) = -u. \quad (3.5.36)$$

The analysis on the stability switches includes five steps as following.

(a) Computation of  $P^{(1)}(\lambda, z)$ : We have

$$\begin{aligned} P^{(1)}(\lambda, z) &= q_0(-\lambda)P(\lambda, z) - q_2(\lambda)z^2P(-\lambda, 1/z) \\ &= m^2\lambda^4 + (2mk - c^2)\lambda^2 + k^2 - u^2 + [-mv\lambda^3 + cv\lambda^2 + (u - k)v\lambda]z, \end{aligned} \quad (3.5.37)$$

and then

$$q_0^{(1)}(\lambda) = m^2\lambda^4 + (2mk - c^2)\lambda^2 + k^2 - u^2, \quad (3.5.38)$$

$$q_1^{(1)}(\lambda) = -mv\lambda^3 + cv\lambda^2 + (u - k)v\lambda. \quad (3.5.39)$$

(b) Computation of  $P^{(2)}(\lambda, z)$ : We derive

$$\begin{aligned} P^{(2)}(\lambda, z) &= q_0^{(1)}(-\lambda)P^{(1)}(\lambda, z) - q_1^{(1)}(\lambda)zP^{(1)}(-\lambda, 1/z) \\ &= m^4\lambda^8 + c_1\lambda^6 + c_2\lambda^4 + c_3\lambda^2 + c_4, \end{aligned} \quad (3.5.40)$$

where

$$\begin{aligned} c_1 &= m^2(2c^2 - 4mk - v^2), \\ c_2 &= c^4 + 6m^2k^2 + 2mkv^2 - 2m^2u^2 - c^2v^2 - 2muv^2 - 4mc^2k, \\ c_3 &= 2c^2k^2 + 4mku^2 + 2kuv^2 - k^2v^2 - 4mk^3 - u^2v^2 - 2c^2u^2, \\ c_4 &= (k^2 - u^2)^2. \end{aligned} \quad (3.5.41)$$

(c) Computation of the critical times: Solve

$$F(\omega^2) = m^4\omega^8 + c_1\omega^6 + c_2\omega^4 + c_3\omega^2 + c_4 \quad (3.5.42)$$

for positive roots first. Then, find out the complex values of  $z$  from  $P(i\omega, z)=0$  such that  $|z|=1$  and in turn find out the critical time delays.

(d) At each pair of critical values of  $\omega$  and  $\tau$ , determine the sign of  $q_0^{(1)}(i\omega)F'(\omega^2)$ . If the sign is positive, then the system increases a pair of characteristic roots with positive real part as the time delays cross the critical value. If the sign is negative, the system decreases such a pair of characteristic roots with positive real parts.

(e) Determine the stability for the system free of time delays. This, together with the conclusions obtained in step (d), enables one to determine the number of interchange of stability. We must pay attention to the condition that guarantees the occurrence of interchanges.

### 3.6 Stability Analysis of an Active Chassis

In this section, the stability of equilibrium of two models of advanced ground vehicles is analyzed to demonstrate how to investigate the stability switches of delayed dynamic systems with undetermined system parameters and time delays. One is the quarter car model of ground vehicle equipped with a sky-hook damper, and the other is a four-wheel-steering car with a time delay in driver's response taken into account. The stability of equilibrium of these two models has been reported in a number of previous publications, but mainly limited to relatively simple cases. For example, the stability of equilibrium of an undamped quarter car model of vehicle with active suspension was analyzed for a given time delay in (Palkovics and Venhovens 1992) by using the method of  $D$ -subdivision. Numerical analysis was made in (Hu and Wu 2000) to investigate the stability and the Hopf bifurcation for the four-wheel-steering car with driver's delay taken into consideration when the vehicle parameters were given. In what follows, attention will be paid to the stability switches of the equilibrium of those two models under different parameter combinations.

#### 3.6.1 A quarter Car Model of Suspension with a Delayed Sky-hook Damper

This subsection deals with the stability switches of the equilibrium of a quarter car model equipped with an active suspension. As discussed in Subsection 1.1.1, the equation of motion of the linearized system at the equilibrium yields

$$\begin{cases} m_b \ddot{x}(t) + c_s [\dot{x}(t) - \dot{y}(t)] + k_s [x(t) - y(t)] + \tilde{v} \dot{x}(t - \tau) = 0, \\ m_t \ddot{y}(t) - c_s [\dot{x}(t) - \dot{y}(t)] - k_s [x(t) - y(t)] + k_t [y(t) - z(t)] - \tilde{v} \dot{x}(t - \tau) = 0, \end{cases} \quad (3.6.1)$$

where  $x$  presents the vertical displacement of the vehicle body  $m_b$ ,  $y$  the vertical displacement of the unsprung mass  $m_t$ ,  $z$  the road disturbance,  $c_s$  and  $k_s$  the damping coefficient and the stiffness coefficient of suspension, and  $k_t$  the linear stiffness of tire,  $\tilde{v}$  the feedback gain of velocity,  $\tau$  the time delay in the feedback control of sky-hook damper.

In the following study, the system parameters are taken from a real car model. They are  $m_b = 290$  kg,  $m_t = 59$  kg,  $k_s = 16,812$  N/m,  $k_t = 190,000$  N/m,  $c_s = 0 \sim 980$  Ns/m,  $v = -2,000 \sim 2,000$  Ns/m.

To simplify the analysis, both the time  $t$  and the time delay  $\tau$  are substituted with the dimensionless ones

$$\sqrt{\frac{k_s}{m_b}} t \rightarrow t, \quad \sqrt{\frac{k_s}{m_b}} \tau \rightarrow \tau. \quad (3.6.2)$$

With help of the following dimensionless parameters

$$\begin{aligned} m &\equiv \frac{m_b}{m_t} = 4.9153, & k &\equiv \frac{k_t}{k_s} = 11.301, \\ c &\equiv \frac{c_s}{\sqrt{m_b k_s}} \in [0, 0.4438], & v &\equiv \frac{\tilde{v}}{\sqrt{m_b k_s}} \in [0, 0.9078], \end{aligned} \quad (3.6.3)$$

Equation (3.6.1) can be recast as

$$\begin{cases} \ddot{x}(t) + c[\dot{x}(t) - \dot{y}(t)] + [x(t) - y(t)] + v\dot{x}(t - \tau) = 0, \\ \ddot{y}(t) - mc[\dot{x}(t) - \dot{y}(t)] - m[x(t) - y(t)] + mky(t) - mv\dot{x}(t - \tau) = 0, \end{cases} \quad (3.6.4)$$

where the dot represents the derivative with respect to the new time  $t$ , and the road disturbance  $z$  is neglected since it does not play any role in the stability of a linear system.

The characteristic equation of Eq. (3.6.4) reads

$$D(\lambda, \tau) \equiv \lambda^4 + c(1+m)\lambda^3 + (1+m+mk)\lambda^2 + mck\lambda + mk + v\lambda(\lambda^2 + mk)e^{-\lambda\tau} = 0, \quad (3.6.5)$$

and gives

$$D(\lambda, 0) = \lambda^4 + [c(1+m) + v]\lambda^3 + (1+m+mk)\lambda^2 + mk(c+v)\lambda + mk = 0. \quad (3.6.6)$$

The Routh-Hurwitz criterion indicates that the system free of time delay is asymptotically stable if and only if

$$\begin{cases} v+c(1+m)>0, \\ v(1+m)+c[(m+1)^2+m^2k]>0, \\ v^2+c[m(1+k)+1]v+mkc^2>0. \end{cases} \quad (3.6.7)$$

When  $\tau > 0$ , the polynomial  $F(\omega)$  defined by Eq. (3.3.5) reads

$$F(\omega) = \omega^8 + b_1\omega^6 + b_2\omega^4 + b_3\omega^2 + b_4, \quad (3.6.8)$$

where

$$\begin{cases} b_1 \equiv c^2 - v^2 - 2 + 2m(c^2 - k - 1) + m^2c^2, \\ b_2 \equiv 1 + m(2kv^2 - 2kc^2 + 4k + 2) + m^2(k^2 - 2kc^2 + 2k + 1), \\ b_3 \equiv -2mk + m^2k(kc^2 - kv^2 - 2k - 2), \\ b_4 \equiv m^2k^2. \end{cases} \quad (3.6.9)$$

By using the MAPLE routine *discr*, we obtain the discrimination sequence

$$1, d_0, d_0d_1, d_1d_2, d_2d_3, d_3d_4, d_4d_5, d_5^2d_6, \quad (3.6.10)$$

where

$$\begin{aligned} d_0 &\equiv -b_1, & d_1 &\equiv -8b_2 + 3b_1^2, & d_2 &\equiv b_1^2b_2 + 3b_1b_3 - 4b_2^2, \\ d_3 &\equiv -3b_1^3b_3 + b_1^2b_2^2 - 6b_1^2b_4 + 14b_1b_2b_3 - 4b_2^3 + 16b_2b_4 - 18b_3^2, \\ d_4 &\equiv -b_1^2b_2^2b_3 - 18b_1b_2b_3^2 + 7b_1^2b_3b_4 + 12b_1b_2^2b_4 - 48b_2b_3b_4 \\ &\quad + 4b_2^3b_3 + 16b_1b_4^2 + 27b_3^3 + 4b_1^3b_3^2 - 3b_1^3b_2b_4, \\ d_5 &\equiv -27b_1^4b_4^2 + 18b_1^3b_2b_3b_4 - 4b_1^3b_3^3 - 4b_1^2b_2^3b_4 + b_1^2b_2^2b_3^2 \\ &\quad + 144b_1^2b_2b_4^2 - 6b_1^2b_3^2b_4 - 80b_1b_2^2b_3b_4 + 18b_1b_2b_3^3 - 192b_1b_3b_4^2 \\ &\quad + 16b_2^4b_4 - 4b_2^3b_3^2 - 128b_2^2b_4^2 + 144b_2b_3^2b_4 + 256b_4^3 - 27b_3^4, \\ d_6 &\equiv b_4 > 0. \end{aligned} \quad (3.6.11)$$

In what follows, the stability switches of this quarter car model of active suspension are discussed for different combinations of dimensionless damping ratio  $c$  and feedback gain  $v$ .

### (1) General results

Consider the parameter region defined by

$$\Omega \equiv \{(v, c) \mid |v| < 0.9, 0 < c < 0.45\}. \quad (3.6.12)$$

When  $c$  varies from 0 to 0.45, the inequalities  $d_0 > 0$ ,  $d_1 > 0$  and  $d_6 > 0$  always hold true. As shown in Fig. 3.6.1, the curves, symmetrical to the  $c$ -axis, are given by  $d_2 = 0$ ,  $d_3 = 0$ ,  $d_4 = 0$  and  $d_5 = 0$  on the plane of  $(v, c)$ . The dashed curve is given by  $d_2 = 0$ , the dotted curve by  $d_3 = 0$ , the lowest thick curve (broad V-shaped curve) by  $d_4 = 0$ , while the curve determined by  $d_5 = 0$  consists of two parts, the narrow V-shaped and the broad V-shaped curves. As a result, the region  $\Omega$  is divided into 10 sub-regions, which are numbered by I, II, ..., X, from the left to the right and from the top to the bottom, respectively.

From Eq. (3.6.7) we know that the left part of the narrow V-shaped curve is also the boundary of the region determined by the Routh-Hurwitz stability conditions. That is, the system free of time delay is asymptotically stable when the parameters are chosen from the sub-regions II, III, V, VI, VIII, and X, and is unstable when the parameter combinations are taken from the sub-regions I, IV, VII and IX.

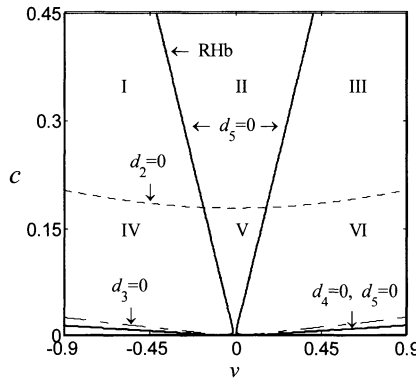


**Fig. 3.6.1.** Parameter division for the stability of a quarter car model of active suspension, where the four sub-regions in lower part are numbered as VII, VIII, IX and X

As shown in Table 3.6.1, the number of variation of signs in the modified sign tables of the discrimination sequence is 4 when a pair of parameters  $(v, c)$  falls into the narrow V-shaped region, namely, sub-regions II and V. In this case, the polynomial  $F(\omega)$  has no real roots ( $0 = 8 - 2 \times 4$ ). On the boundary of sub-regions II and V, the sign table of the discrimination sequence is  $[1, 1, 1, 0, 0, 1, -1, 1]$  and the modified sign table is  $[1, 1, 1, -1, -1, 1, -1, 1]$ , so the number of variation of signs is also 4. This means that the polynomial has no real roots. In other sub-regions, the number of variation of signs is 2 and the polynomial  $F(\omega)$  has exactly 2  $(= (8 - 2 \times 2) / 2)$  distinct positive roots. Thus, the system is delay-

independent stable in the narrow V-shape region, namely, sub-regions II and V, and it may exhibit a finite number of stability switches in other sub-regions.

**Table 3.6.1.** Sign tables of the discrimination sequence in the stability analysis of a quarter car model of active suspension

Sub-region	$d_0$ $d_1$ $d_2$ $d_3$ $d_4$ $d_5$ $d_6$	$D_1$ $D_2$ $D_3$ $D_4$ $D_5$ $D_6$ $D_7$ $D_8$	$l-2s$
I, III	+ + + - - - +	1 1 1 1 -1 1 1 1	4
II	+ + + - - + +	1 1 1 1 -1 1 -1 1	0
IV, VI	+ + - - - - +	1 1 1 -1 1 1 1 1	4
V	+ + - - - + +	1 1 1 -1 1 1 -1 1	0
VII, VIII	+ + - + - + +	1 1 1 -1 -1 -1 1 1	4
IX, X	+ + - + + + +	1 1 1 -1 -1 1 1 1	4

We can find that only when a pair of parameters  $(v, c)$  falls to the boundary of two V-shaped regions, can the polynomial  $F(\omega)$  have repeated real roots. On the other common boundaries outside the narrow V-shaped region, the polynomial  $F(\omega)$  has 2 distinct simple positive roots. For example, on the common boundary, determined by  $d_2=0$ , of sub-regions III and IV the modified sign table of the discrimination sequence is [1, 1, 1, -1, -1, 1, 1, 1] since the sign table of the discrimination sequence is [1, 1, 1, 0, 0, 1, 1, 1]. Thus, the number of variation of signs in the modified sign table is 2 and  $F(\omega)$  has 2 distinct simple positive roots. On the curve determined by  $d_3=0$ , the modified sign table of the discrimination sequence is [1, 1, 1, -1, 1, 1, 1, 1], for the sign table of the discrimination sequence is [1, 1, 1, -1, 0, 0, 1, 1]. So, the number of variation of signs in the modified sign table is 2 and  $F(\omega)$  has also 2 distinct simple positive roots. Thus, the system possesses a finite number of stability switches when the parameters are chosen from the common boundaries except for the two V-shaped curves.

Though all the sub-regions, except for those numbered as II and V, make the polynomial  $F(\omega)$  have 2 distinct positive roots, the dynamic behaviors of the system do have differences in these sub-regions. Let the time delay increase from zero to the positive infinity. When the parameters are chosen from sub-regions I, IV, VII and IX, the system undergoes a finite number of stability exchanges from instability to stability, then to instability and so on, and eventually becomes unstable. However, if the parameters are taken from sub-regions III, VI, VIII and X, the system first remains stable, then becomes unstable, and then turns to be stable, and

so on, and becomes unstable at last. This fact will be demonstrated through a few case studies as follows.

## (2) Case studies

**Case 1**  $\nu = 0.6$  and  $c = 0.4$ . This parametric combination falls into the sub-region III in Fig. 3.6.1. In this case, the system free of time delay is asymptotically stable. It is easy to know that the polynomial  $F(\omega)$  has 2 distinct real roots  $\omega_1 = 1.2077$  and  $\omega_2 = 0.7681$ , satisfying  $F'(\omega_1) > 0$  and  $F'(\omega_2) < 0$ , respectively. The corresponding critical values of time delay are

$$\tau_{1,0} = 1.8112, \quad \tau_{1,1} = 7.0136, \quad \tau_{1,2} = 12.2161, \quad \tau_{1,3} = 17.4185, \dots \quad (3.6.13a)$$

$$\tau_{2,0} = 5.2456, \quad \tau_{2,1} = 13.4262, \quad \tau_{2,2} = 21.6068, \quad \tau_{2,3} = 29.7874, \dots \quad (3.6.13b)$$

They can be ranked as

$$\tau_{1,0} < \tau_{2,0} < \tau_{1,1} < \tau_{1,2} < \tau_{2,1} < \tau_{1,3} < \tau_{2,2} < \dots \quad (3.6.14)$$

This sequence of critical time delays shows that the system is asymptotically stable for  $\tau \in [0, \tau_{1,0})$ , unstable for  $\tau \in [\tau_{1,0}, \tau_{2,0}]$ , asymptotically stable again for  $\tau \in (\tau_{2,0}, \tau_{1,1})$ , and eventually unstable for  $\tau \geq \tau_{1,1}$ .

The conclusions for the stability in the first three intervals lie in the facts that  $F'(\omega_1) > 0$  and  $F'(\omega_2) < 0$  hold, and that the system is asymptotically stable for  $\tau = 0$ . To show the conclusion for  $\tau \geq \tau_{1,1}$ , we observe that in Eq. (3.6.14)  $\tau_{1,1}$  is followed immediately by  $\tau_{1,2}$ , but any  $\tau_{2,k}$  cannot be followed by  $\tau_{2,k+1}$  since  $\tau_{1,k+1} - \tau_{1,k} = 2\pi/\omega_+ < 2\pi/\omega_- = \tau_{2,k+1} - \tau_{2,k}$  and  $\tau_{1,0} < \tau_{2,0}$ . Hence, the system has at least one pair of characteristic roots with positive real part if  $\tau > \tau_{1,1}$ . This implies that the equilibrium of system is unstable as long as  $\tau > \tau_{1,1}$  holds.

Now, the case when  $\tau > \tau_{1,2}$  should draw special attention. In this case, we can not simply follow the conditions  $F'(\omega_+) > 0$  and  $F'(\omega_-) < 0$  to conclude that the system is asymptotically stable for  $\tau \in (\tau_{2,1}, \tau_{1,3})$ ,  $(\tau_{2,2}, \tau_{1,4})$ , and so on. This fact can be verified when  $\tau = 15 \in (\tau_{2,1}, \tau_{1,3})$  is taken as an example. Let  $M(\omega) \equiv \text{Re}[i^{-4}D(i\omega, \tau)]$  and  $N(\omega) \equiv \text{Im}[i^{-4}D(i\omega, \tau)]$ . Then,  $M(\omega)$  has four positive roots  $\rho_1 = 7.7727$ ,  $\rho_2 = 1.0301$ ,  $\rho_3 = 0.7872$  and  $\rho_4 = 0.7235$ , which yield  $N(\rho_1) = 11.7883$ ,  $N(\rho_2) = 35.1676$ ,  $N(\rho_3) = -12.2723$  and  $N(\rho_4) = -917.0734$ . Thus, we have

$$\sum_{k=1}^4 (-1)^{k-1} \text{sgn}[N(\rho_k)] = 1 - 1 - 1 + 1 = 0. \quad (3.6.15)$$



Because  $n=4$  and  $N(0)=0$ , Eq. (3.6.15) contradicts the stability condition given by Theorem 2.2.7 as following

$$\frac{n}{2} + \frac{1}{2}(-1)^4 N(0) + \sum_{k=1}^4 (-1)^{k-1} \operatorname{sgn}[N(\rho_k)] = 0. \quad (3.6.16)$$

This result can also be verified by using the Nyquist diagram. The system, therefore, is unstable for  $\tau \in (\tau_{2,1}, \tau_{1,3})$ ,  $(\tau_{2,2}, \tau_{1,4})$ , ..., and then unstable for all  $\tau \geq \tau_{1,1}$ . As a result, the number of stability switches is 3.

**Case 2**  $\nu = 0.3$  and  $c = 0.1$ . In this case, the polynomial  $F(\omega)$  has 2 distinct real roots  $\omega_1 = 1.0979$  and  $\omega_2 = 0.8361$  so that  $F'(\omega_1) > 0$  and  $F'(\omega_2) < 0$  hold, respectively. The corresponding critical values of time delay are

$$\tau_{1,0} = 1.7053, \quad \tau_{1,1} = 7.4280, \quad \tau_{1,2} = 13.1506, \quad \tau_{1,3} = 18.8733, \dots \quad (3.6.17a)$$

$$\tau_{2,0} = 5.2560, \quad \tau_{2,1} = 12.7708, \quad \tau_{2,2} = 20.2856, \quad \tau_{2,3} = 27.8004, \dots \quad (3.6.17b)$$

which are ranked as

$$\tau_{1,0} < \tau_{2,0} < \tau_{1,1} < \tau_{2,1} < \underline{\tau_{1,2} < \tau_{1,3}} < \tau_{2,2} < \tau_{1,4} < \tau_{2,3} < \dots \quad (3.6.18)$$

It can be similarly found that the system is asymptotically stable for  $\tau \in [0, \tau_{1,0})$ ,  $(\tau_{2,0}, \tau_{1,1})$  and  $(\tau_{2,1}, \tau_{1,2})$ , and unstable for  $\tau \in [\tau_{1,0}, \tau_{2,0}]$ ,  $[\tau_{1,1}, \tau_{2,1}]$  and  $[\tau_{1,2}, +\infty)$ . Hence, the system exhibits 5 stability switches.

**Case 3**  $\nu = -0.5$  and  $c = 0.2$ . This parameter combination gives 2 distinct real roots  $\omega_1 = 1.1961$  and  $\omega_2 = 0.7690$  of polynomial  $F(\omega)$ , satisfying  $F'(\omega_1) > 0$  and  $F'(\omega_2) < 0$ , as well as the critical values of time delay

$$\tau_{1,0} = 4.2369, \quad \tau_{1,1} = 9.4898, \quad \tau_{1,2} = 14.7427, \quad \tau_{1,3} = 19.9956, \dots \quad (3.6.19a)$$

$$\tau_{2,0} = 1.5375, \quad \tau_{2,1} = 9.7085, \quad \tau_{2,2} = 17.8796, \quad \tau_{2,3} = 26.0506, \dots \quad (3.6.19b)$$

They are ranked as

$$\tau_{2,0} < \underline{\tau_{1,0} < \tau_{1,1}} < \tau_{2,1} < \tau_{1,2} < \tau_{2,2} < \dots \quad (3.6.20)$$

Now, the system free of time delays is unstable, but becomes stable for  $\tau \in (\tau_{2,0}, \tau_{1,0})$ , and then goes to unstable again for  $\tau \in (\tau_{1,0}, +\infty)$ . Hence, the system undergoes the stability switch twice.

**Case 4**  $\nu = 0.05$  and  $c = 0.01$ . This is a case when the stability of the system changes many times with an increase of the time delay. In fact, this parameter combination gives 2 distinct real roots  $\omega_1 = 0.9806$  and  $\omega_2 = 0.9356$  of polynomial  $F(\omega)$ , satisfying  $F'(\omega_1) > 0$  and  $F'(\omega_2) < 0$ . The critical values of time delay cor-

responding to  $\omega_1=0.9806$  are 1.7892, 8.1965, 14.6039, 21.0113, 27.4186, 33.8260, 40.2333, 46.6407, 53.0481, 59.4554, 65.8628, 72.2701, 78.67750, ..., while those corresponding to  $\omega_2=0.9356$  are 4.8387, 11.5545, 18.2703, 24.9860, 31.7018, 38.4175, 45.1333, 51.8490, 58.5648, 65.2806, 71.9963, 78.7121, 85.4278, and so forth. In accordance with the notations used above, we have  $\tau_{2,10} < \tau_{1,11} < \tau_{1,12} < \tau_{2,11}$ . As a result, the system undergoes 23 stability switches as the time delay increases!

These numerical examples illustrate that, in the sense of stability switches, the stability behavior of the quarter car model of active suspension with a delayed sky-hook damper is very complicated. The system may change its stability many, but finite, times as the time delay increases. If all the critical values of time delay are increasingly ranked, then the change of stability must terminate as soon as any  $\tau_{1,k}$  is followed by  $\tau_{1,k+1}$  in the sequence of critical time delays, and the system is unstable as long as  $\tau > \tau_{1,k}$ . The increase in time delay usually results in instability of the system, but it also offers the probability of stabilizing an unstable system free of time delay as demonstrated in Case 3.

### 3.6.2 Four-wheel-steering Vehicle with a Time Delay in Drive's Response

Now consider the model established in Subsection 1.1.2 for four-wheel-steering vehicles. Let  $V$  be the lateral velocity,  $r$  the yaw angular velocity,  $y$  the vertical coordinate in a fixed frame,  $\psi$  the heading angle of the vehicle,  $\delta_f$  and  $\delta_r$  the steering angles applied on the front and rear wheels respectively. When the time delay in driver's response is taken into account, the motion of system is described by a set of five-dimensional differential equations with a time delay as following

$$\begin{cases} m\dot{V}(t) = -mUr(t) + 2F_f \cos\delta_f(t) + 2F_r \cos\delta_r(t), \\ I_z \dot{r}(t) = 2aF_f \cos\delta_f(t) - 2bF_r \cos\delta_r(t), \\ \dot{y}(t) = V(t)\cos\psi(t) + U\sin\psi(t), \\ \dot{\psi}(t) = r(t), \\ \dot{\delta}_f(t) = -\frac{1}{\tau_s}\delta_f(t) - \frac{K_m}{\tau_s}[y(t-\tau) + \frac{L}{U}V(t-\tau)\cos\psi(t-\tau) + L\sin\psi(t-\tau)] + f(t), \end{cases} \quad (3.6.21)$$

where  $U$  is the constant moving speed of the vehicle,  $I_z$  the inertia moment of rotation of the vehicle body with respect to the vertical axis,  $a$  and  $b$  the distances from the center of mass to the front and rear axles respectively,  $F_f$  and  $F_r$  the lateral forces generated by the contact between the tire and the road surface at each of front wheel and rear wheel respectively,  $L$  the preview distance of the driver,  $\tau$  the time delay in driver's response, and  $f(t)$  the external disturbance.

As discussed in Subsection 1.1.2, the tyre forces are described by means of the truncated Magic formula

$$\begin{cases} F_f = -C_1 \left[ \arctan\left(\frac{V+ar}{U}\right) - \delta_f \right] + C_3 \left[ \arctan\left(\frac{V+ar}{U}\right) - \delta_f \right]^3, \\ F_r = -D_1 \left[ \arctan\left(\frac{V-br}{U}\right) - \delta_r \right] + D_3 \left[ \arctan\left(\frac{V-br}{U}\right) - \delta_r \right]^3, \end{cases} \quad (3.6.22)$$

where  $C_1$ ,  $C_3$ ,  $D_1$  and  $D_3$  are positive parameters. In addition, the bilinear control strategy between the front and rear steering angles is implemented

$$\delta_r = k_\delta \delta_f + k_r r, \quad (3.6.23)$$

where

$$k_\delta = -\frac{C_1}{D_1} \neq 1, \quad k_r = \frac{2(aC_1 - bD_1) + mU^2}{2D_1U}. \quad (3.6.24)$$

The vehicle is said to be *under-steered* or *over-steered* if  $aC_1 - bD_1$  is negative or positive, respectively. In what follows, the system parameters are taken as  $m = 1,300$  kg,  $I_z = 3,000$  kgm<sup>2</sup>,  $a = 1.0$  m,  $b = 1.6$  m,  $C_1 = 44,400$  N/rad,  $D_1 = 43,600$  N/rad for under-steered case or 25,600 N/rd for over-steered case,  $C_3 = 44,400$  N/rad<sup>3</sup>,  $D_3 = 44,400$  N/rad<sup>3</sup>,  $\tau_s = 0.2$ s and  $K_m = 0.02$ .

As studied in (Hu and Wu 2000), this four-wheel-steering vehicle has 9 steady state motions, including a trivial one. After some necessary manipulations, we can get the characteristic function of the linearized equations corresponding to the trivial solution as follows

$$\begin{aligned} D(\lambda, \tau) &\equiv \lambda^5 + a_4 \lambda^4 + a_3 \lambda^3 + a_2 \lambda^2 + a_1 \lambda + a_0 \\ &= \lambda^5 + c_{04} \lambda^4 + c_{03} \lambda^3 + c_{02} \lambda^2 + (c_{13} \lambda^3 + c_{12} \lambda^2 + c_{11} \lambda + c_{10}) e^{-\lambda \tau}, \end{aligned} \quad (3.6.25)$$

where

$$a_i \equiv c_{0i} + c_{1i} e^{-\lambda \tau}, \quad i = 0, 1, 2, 3, 4,$$

$$c_{00} = 0, \quad c_{01} = 0,$$

$$\begin{aligned}
c_{02} &= \frac{2}{m\tau_s I_z U^2} [mU^2 (bD_1 - aC_1) + 2C_1 D_1 (a+b)(a+b+k_r U)], \\
c_{03} &= \frac{2}{m\tau_s I_z U^2} [I_z U (C_1 + D_1) + m\tau_s U^2 (bD_1 - aC_1) + mU (a^2 C_1 + b^2 D_1) \\
&\quad + bk_r D_1 mU^2 + 2\tau_s C_1 D_1 (a+b)^2 + 2\tau_s k_r C_1 D_1 U (a+b)], \\
c_{04} &= \frac{1}{m\tau_s U I_z} [2m\tau_s (a^2 C_1 + b^2 D_1) + mU I_z + 2\tau_s I_z (C_1 + D_1) + 2\tau_s bk_r D_1 mU], \\
c_{10} &= \frac{4K_m C_1 D_1 (a+b)(1-k_\delta)}{m\tau_s I_z}, \\
c_{11} &= \frac{4K_m C_1 D_1 (a+b)[b+2L+k_r U+k_\delta(a-2L)]}{m\tau_s I_z U}, \\
c_{12} &= \frac{2K_m}{m\tau_s I_z U^2} [2abC_1 D_1 (1+k_\delta)L + 2(a+b)k_r C_1 D_1 LU + 2(a^2 k_\delta + b^2)LC_1 D_1], \\
c_{13} &= 0, \quad c_{14} = 0.
\end{aligned} \tag{3.6.26}$$

According to the Routh-Hurwitz criterion, the trivial solution for  $\tau=0$  is asymptotically stable if and only if

$$\begin{aligned}
a_0 > 0, \quad a_4 > 0, \quad a_4 a_3 - a_2 > 0, \quad a_4 a_3 a_2 - a_4^2 a_1 - a_2^2 + a_4 a_0 > 0, \\
a_4 a_3 a_2 a_1 - a_4 a_3^2 a_0 - a_4^2 a_1^2 + 2a_4 a_1 a_0 - a_2^2 a_1 + a_3 a_2 a_1 - a_0^2 > 0.
\end{aligned} \tag{3.6.27}$$

It is easy to derive the polynomial  $F(\omega)$  defined by Eq. (3.3.5)

$$\begin{aligned}
F(\omega) &= \omega^{10} + (c_{04}^2 - 2c_{03})\omega^8 + (c_{03}^2 - c_{13}^2 - 2c_{04}c_{02})\omega^6 + \\
&\quad (c_{02}^2 - c_{12}^2 + 2c_{13}c_{11})\omega^4 + (2c_{12}c_{10} - c_{11}^2)\omega^2 - c_{10}^2.
\end{aligned} \tag{3.6.28}$$

It has at least one positive root since  $F(0) = -c_{10}^2 < 0$  and  $F(+\infty) \rightarrow +\infty$ . Thus, the system can not be delay-independent stable. Using the MAPLE routine *discr* gives the discrimination sequence of  $F(\omega)$  as following

$$1, d_0, d_0 d_1, d_1 d_2, \dots, d_6 d_7, d_7^2 d_8. \tag{3.6.29}$$

As the expressions of  $d_6$  and  $d_7$  are lengthy, the terms of the discrimination sequence are not presented here. In what follows, attention will be paid to the following parameter combinations

$$\Delta \equiv \{(L, U) \mid 5\text{m/s} < U < 40\text{m/s}, 10\text{m} < L < 120\text{m}\}. \tag{3.6.30}$$

When the vehicle is under-steered, it is easy to know that the Routh-Hurwitz stability conditions are true in the whole region  $\Delta$  given by Eq. (3.6.30). That is, the vehicle is asymptotically stable for  $\tau=0$ . When  $\tau>0$ , we can readily find that  $d_0<0, d_1>0, d_3>0, d_5>0, d_6<0, d_7>0$  and  $d_8>0$ . By plotting the graphs of  $d_2=0$  and  $d_4=0$ , we divide the region  $\Delta$  on the plane of  $(L,U)$  into 5 sub-regions as shown in Fig. 3.6.2a, where  $d_4=0$  determines the curves  $c_1$  and  $c_2$ , and  $d_2=0$  gives  $c_3$ . Table 3.6.2 lists the sign tables of the discrimination sequence and indicates that the numbers of variation of signs in all sign tables are equal to 4. Thus, for each parameter combination in the given region,  $F(\omega)$  has exactly 1 ( $= (10-2 \times 4)/2$ ) simple positive root. Once this positive root is found, it is easy to obtain the minimal time delay  $\tau_0$  satisfying Eqs. (3.5.6) and (3.5.7). As a result, the system remains asymptotically stable when  $0 \leq \tau < \tau_0$ , and becomes unstable when  $\tau \geq \tau_0$ .

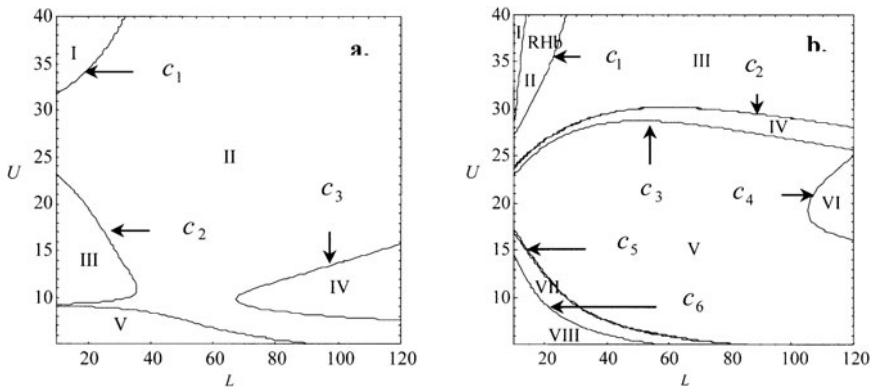


**Fig. 3.6.2.** Parameter divisions on the plane of  $(L, U)$  for stability analysis of a four-wheel-steering vehicle; **a.** the under-steered case, **b.** the over-steered case

**Table 3.6.2.** Sign tables of the discrimination sequence in the stability analysis of a four-wheel-steering vehicle in under-steered case

Sub-region	$d_0$ $d_1$ ... $d_7$ $d_8$	$D_1$ $D_2$ ... $D_9$ $D_{10}$	$l-2s$
I, III, V	- + + + - + - + +	1 -1 -1 1 1 -1 -1 -1 1	2
II	- + + + + + - +	1 -1 -1 1 1 1 1 -1 -1 1	2
VII	- + - + + + - + +	1 -1 -1 -1 -1 1 1 -1 -1 1	2

**Table 3.6.3.** Sign tables of the discrimination sequence in the stability analysis of a four-wheel-steering vehicle in over-steered case

Sub-region	$d_0$ $d_1$ $\dots$ $d_7$ $d_8$	$D_1$ $D_2$ $\dots$ $D_9$ $D_{10}$	$l-2s$
I, II, VIII	- + + + - + - + +	1 -1 -1 1 1 -1 -1 -1 1	2
III, VII	- + + + - + - + +	1 -1 -1 1 1 1 1 -1 -1 1	2
VI	- + + + + + - + +	1 -1 -1 1 1 1 1 1 -1 1	2
V	- + + + - + + - +	1 -1 -1 1 1 1 -1 -1 -1 1	2
VI	- + - + + - + - +	1 -1 -1 -1 -1 1 -1 -1 -1 1	2

When the vehicle is over-steered, the region  $\Delta$  is divided into 8 sub-regions, which are numbered by I, II, ..., VIII, from the top to the bottom, respectively as shown in Fig. 3.6.2b. The curve RHb here denotes the boundary determined by the Routh-Hurwitz stability conditions for the system without time delay. The graph of  $d_4=0$  here consists of two curves  $c_1$  and  $c_6$ . The graph of  $d_5=0$  is composed of two curves  $c_3$  and  $c_5$ . The graph of  $d_6=0$  is the same as that of  $d_7=0$ , and is composed of two curves  $c_2$  and  $c_5$ . The curve  $c_4$  is the graph of  $d_2=0$ . The sub-region I is the region where the system is unstable when  $\tau=0$ , and the other sub-regions are those that ensure the asymptotic stability of system without time delay. Table 3.6.3 shows the sign tables of the discrimination sequence, and indicates that the polynomial  $F(\omega)$  has only 1 ( $= (10-2 \times 4)/2$ ) simple positive root in all sub-regions, except for the parameter combinations on the two common boundaries between sub-regions III and IV, as well as V and VII, where  $F(\omega)$  has repeated roots. In sub-region I, therefore, the system is unstable for any time delay. In the other sub-regions, for almost all the parameter combinations, there exists a  $\tau_0$  depending on the parameters so that the system is asymptotically stable for  $\tau \in [0, \tau_0]$  and unstable for all  $\tau \in (\tau_0, +\infty)$ .

Here are two case studies: (a)  $U=30\text{m/s}$  and  $L=40\text{m}$ , (b)  $U=30\text{m/s}$  and  $L=60\text{m}$ , corresponding to the under-steered and over-steered cases, respectively. In the under-steered case, the critical time delays are  $\tau_0=0.2899$  and  $0.2108$ , and the corresponding frequencies are  $\omega=2.4586$  and  $3.3027$ , respectively. In the over-steered case, the critical time delays are  $\tau_0=0.1943$  and  $0.1412$ , while the corresponding frequencies are  $\omega=2.6654$  and  $3.4454$ , respectively.

In summary, for the four-wheel-steering vehicle with a time delay in driver's response taken into account, the stability behavior of the system is relatively simple. As the time delay increases from zero to the positive infinity, there are only two possible cases. If the system free of time delay is unstable, it is unstable for any

time delay. Or, there exists a critical time delay  $\tau_0 > 0$  such that the system remains asymptotically stable when  $\tau \in [0, \tau_0)$  and becomes unstable as long as  $\tau \geq \tau_0$  if the system free of time delay is asymptotically stable. As shown by the numerical examples, the critical time delays are usually very short. Thus, the delay response of a driver may induce undesirable instability of a four-wheel-steering vehicle.

## 4 Robust Stability of Linear Delay Systems

Difference always exists between a real dynamic system and its mathematical model because of the simplification in modeling, the measurement errors of system parameters, and so on. It is very natural, hence, to study the dynamic systems governed by differential equations involving a number of uncertain parameters. In practice, a dynamic system should be robust stable. The problem of *robust stability* of linear dynamic systems can be roughly stated as follows. Given a family  $\Omega$  of linear dynamic systems and a set  $D$  on the complex plane, how to construct a computationally tractable technique to determine whether the characteristic roots of every system in  $\Omega$  fall into  $D$ . This problem is usually referred to as the *D-stability* of  $\Omega$ . For the stability analysis of a continuous-time dynamic system,  $D$  should be the open left half-plane of the complex plane, whereas  $D$  should be an open unite circular disk on the complex plane for the stability analysis of a discrete-time dynamic system. As a special, but very important case of *D-stability*, a system is said to be *interval stable* if it is asymptotically stable under all parameter combinations when some uncertain parameters vary on their pre-specified intervals respectively.

The robust stability of linear dynamic systems has been intensively studied over the past decade. As well known, the robust stability of a linear dynamic system can be also determined by checking the location of its characteristic roots. For the dynamic system described by a set of linear ordinary differential equations, an important discovery on the interval stability was made in (Kharitonov 1979). It was proved that the interval stability of a family of characteristic polynomials, whose coefficients vary independently in corresponding intervals, is governed by the stability of four special characteristic polynomials. Afterwards, the so-called *Edge theorem* was established in (Bartlett et al. 1988) for the *D-stability* of a polytope  $\Omega$  generated by the convex hull of a finite number of polynomials. The edge theorem states that given a simply connected set  $D$  on the complex plane, a polytope  $\Omega$  of real polynomials, namely the convex hull of a finite number of real polynomials, is *D-stable* if and only if the set of exposed edges of  $\Omega$  is *D-stable*. The methods for robust stability analysis of polynomials under parametric



uncertainties have been comprehensively described in (Bhattacharyya et al. 1995). However, no finite testing set, like that in the Kharitonov theorem in (Huang 1992), exists for the  $D$ -stability in general.

As for delay differential systems, the edge theorem was extended to the  $D$ -stability of a polytopic family of quasi-polynomials in (Fu et al. 1989), where an effective graphical method, based on the Nyquist diagram of frequency response, was also presented for the  $D$ -stability. A similar problem was studied in (Barmish and Shi 1989) by means of a different frequency domain technique. The interval stability for differential equations with a single uncertain time delay was dealt with in (Tsyppkin and Fu 1993) by using the Nyquist diagram of frequency response. A numerical algorithm was suggested in (Kogan and Leizarowitz 1995) to testify the interval stability of delayed dynamic systems through the use of the zero-exclusion criterion. In (Kharitonov and Zhabko 1994), the problem of selecting the test sets for the robust stability was discussed for some special families of quasi-polynomials.

In this chapter, some stability criteria are first presented for the one-parameter family of quasi-polynomials generated by the convex hull of two quasi-polynomials. Then the edge theorem for polytopic family of quasi-polynomials is introduced and some stability criteria are given. Afterwards, the robust stability is analyzed for a linear system with uncertain commensurate time delays, but the coefficients of corresponding characteristic quasi-polynomial depend linearly on some other uncertain parameters. As pointed out in (Blondel and Tsitsiklis 2000), this problem of robust stability is an NP-hard problem due to the uncertainty of time delays. The term "NP-hard" is usually interpreted as an indication of inherent intractability. With help of Dixon's resultant elimination, the sufficient and necessary conditions are derived for the robust stability of this type of delayed dynamic systems, and then a graphic test for the robust stability is presented.

## 4.1 Robust Stability of a One-parameter Family of Quasi-polynomials

This section deals with the robust stability of a one-parameter family of quasi-polynomials generated by the convex combination of two quasi-polynomials  $p_1(\lambda)$  and  $p_2(\lambda)$  of the same order  $n$  defined as

$$\Omega \equiv \text{conv}\{p_1(\lambda), p_2(\lambda)\} \equiv \{p_{12}(\lambda, \mu) \equiv (1-\mu)p_1(\lambda) + \mu p_2(\lambda) \mid \mu \in [0, 1]\} \quad (4.1.1)$$

It is essential to test the robust stability of this one-parameter family in applying the edge theorem to be discussed in the next section. For simplicity, the family  $\Omega$  is said to be *Hurwitz stable* if every element of  $\Omega$  is Hurwitz stable, namely, the roots of every quasi-polynomial in  $\Omega$  have negative real parts. Obviously,  $\Omega$  is Hurwitz stable if and only if the value set  $\{p_{12}(\lambda, \mu) \mid p_{12} \in \Omega, \operatorname{Re} \lambda \geq 0, \mu \in [0, 1]\}$  does not contain zero. That is the zero-exclusion criterion.

#### 4.1.1 Non-convexity of the Set of Hurwitz Stable Quasi-polynomials

In general, the stability of both  $p_1(\lambda)$  and  $p_2(\lambda)$  can not guarantee the stability of the whole family  $\Omega$ . This fact will be demonstrated through the following two examples.

**Example 4.1.1** According to the Routh-Hurwitz criterion, it is easy to know that the polynomial

$$p(\lambda) \equiv a_0 \lambda^3 + a_1 \lambda^2 + a_2 \lambda + a_3 \quad (4.1.2)$$

with a positive leading coefficient  $a_0$  is Hurwitz stable if and only if

$$a_1 > 0, \quad a_3 > 0, \quad a_1 a_2 - a_0 a_3 > 0. \quad (4.1.3)$$

Thus, the following two polynomials are Hurwitz stable

$$p_1(\lambda) \equiv 0.5 \lambda^3 + \lambda^2 + \lambda + 1.7, \quad p_2(\lambda) \equiv 1.7 \lambda^3 + \lambda^2 + \lambda + 0.5, \quad (4.1.4)$$

because  $a_1 a_2 - a_0 a_3 = 0.5 > 0$  holds for both polynomials. However, the following linear combination of these two polynomials

$$p_{12}(\lambda) \equiv 0.5 p_1(\lambda) + 0.5 p_2(\lambda) = 1.1 \lambda^3 + \lambda^2 + \lambda + 1.1 \quad (4.1.5)$$

is not Hurwitz stable since  $a_1 a_2 - a_0 a_3 = -0.21 < 0$  holds.

**Example 4.1.2** We first consider a quasi-polynomial

$$q(\lambda) = \lambda + e^{-\lambda}. \quad (4.1.6)$$

Using Theorem 2.2.7, we have  $M(\omega) = \omega - \sin \omega$ , and  $N(\omega) = -\cos \omega$ . The unique root of  $M(\omega)$  is  $\omega = 0$ , so  $m = 0$ . Hence, all the conditions in Theorem 2.2.7 hold, i.e.,  $q(0) \neq 0$ ,  $1/2 + 1/2 \operatorname{sgn} N(0) = 0$ . We can also confirm the Hurwitz stability of Eq. (4.1.6) from Fig. 4.1.1, where the Nyquist diagram of  $q(i\omega)/(i\omega + 1)$  does not encircle the origin of the complex plane.

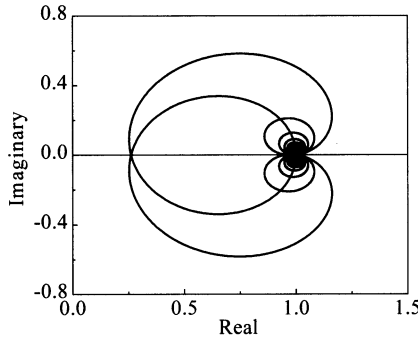


Fig. 4.1.1. The Nyquist diagram of  $q(i\omega)/(i\omega+1)$

Now, we check the Hurwitz stability of the following quasi-polynomial

$$p(\lambda,k) \equiv q^2(\lambda) + k, \quad k \geq 0. \tag{4.1.7}$$

It is easy to see that  $p(\lambda,0)$  is Hurwitz stable. Furthermore, we can show that the stability of  $p(\lambda,k)$  changes as  $k$  increases from zero. Separating the real and imaginary parts of the marginal stability condition  $p(i\omega,k)=0$  gives two sets of equations

$$\begin{cases} \cos^2 \omega + k = 0, \\ \sin \omega - \omega = 0, \end{cases} \tag{4.1.8a}$$

or

$$\begin{cases} \omega^2 \pm 2\omega + 1 - k = 0, \\ \cos \omega = 0, \quad \sin \omega = \mp 1. \end{cases} \tag{4.1.8b}$$

Obviously, Eq. (4.1.8a) is not true for any  $k > 0$ . Solving Eq. (4.1.8b) for  $\omega$  and  $k$  yields

$$\omega = \omega_n \equiv \frac{\pi}{2} + n\pi, \quad k = k_n \equiv \left[ \frac{\pi}{2} + n\pi - (-1)^n \right]^2, \quad n = 0, 1, 2, \dots \tag{4.1.9}$$

Direct computation shows that

$$\operatorname{sgn} \left[ \frac{d(\operatorname{Re} \lambda)}{dk} \Big|_{(\omega_n, k_n)} \right] = (-1)^n. \tag{4.1.10}$$

Thus, with an increase of  $k$ , the crossing of a characteristic root at  $k_{2l}$ ,  $l = 0, 1, 2, \dots$  must be from the left to the right. That is,  $p(\lambda,k)$  always increases a new pair of conjugate characteristic roots with positive real part for each crossing at

values of  $k_{2l}$ . On the contrary, the crossing of a characteristic root at  $k_{2l+1}$ ,  $l = 0, 1, 2, \dots$  must be from the right to the left with an increase of  $k$  and  $p(\lambda, k)$  decreases such a pair of characteristic roots for each crossing at values of  $k_{2l+1}$ . As a result,  $p(\lambda, k)$  changes its stability as  $k$  is crossing  $k_n$ . That is, it is Hurwitz stable for  $k \in [0, k_0), (k_1, k_2), \dots, (k_{2l+1}, k_{2l+2}), \dots$ , but unstable for  $k \in (k_0, k_1), (k_2, k_3), \dots, (k_{2l}, k_{2l+1}), \dots$ . Choosing  $20 \in (k_0, k_1)$  and  $40 \in (k_1, k_2)$ , we know that  $p(\lambda, 20)$  is unstable and  $p(\lambda, 40)$  is stable. The Nyquist diagrams in Figs. 4.1.2 and 4.1.3 show alternatively the instability of  $p(\lambda, 20)$  and the stability of  $p(\lambda, 40)$ .

Let  $p_1(\lambda) = p(\lambda, 0)$  and  $p_2(\lambda) = p(\lambda, 40)$ , then the Hurwitz stability of  $p_1(\lambda)$  and  $p_2(\lambda)$  can not guarantee the robust Hurwitz stability of the whole family  $\Omega \equiv \{p_{12}(\lambda, \mu) \equiv (1 - \mu)p_1(\lambda) + \mu p_2(\lambda) \mid \mu \in [0, 1]\}$  since  $p_{12}(\lambda, 1/2) = p(\lambda, 20) \in \Omega$  is not Hurwitz stable.

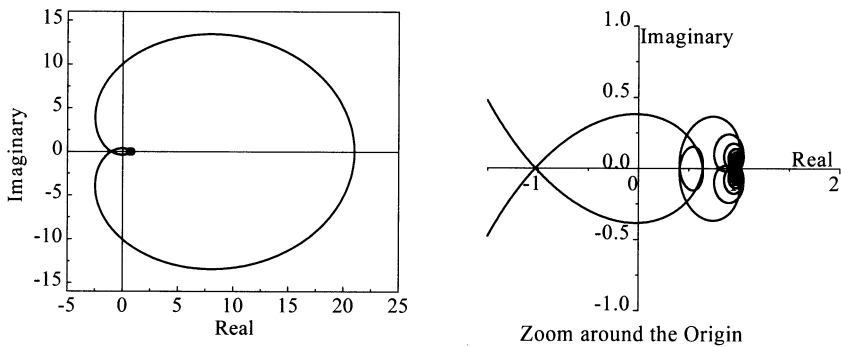


Fig. 4.1.2. The Nyquist diagram of  $p(i\omega, 20)/(i\omega+1)^2$ , where  $20 \in (k_0, k_1)$

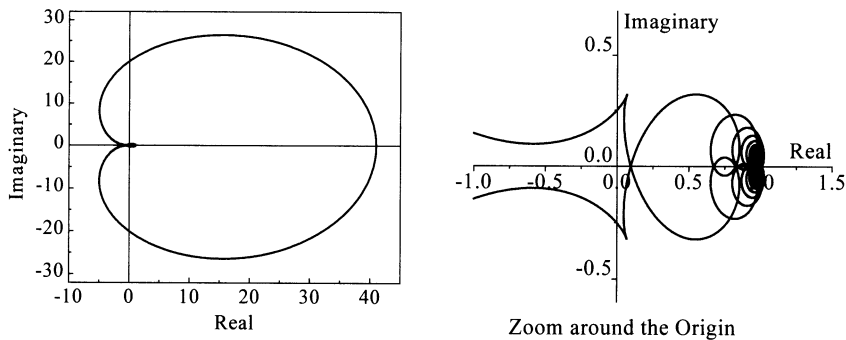


Fig. 4.1.3. The Nyquist diagram of  $p(i\omega, 40)/(i\omega+1)^2$ , where  $40 \in (k_1, k_2)$

### 4.1.2 Sufficient and Necessary Conditions for Interval Stability

The fact that each root  $\lambda(\mu)$  of  $p(\lambda, \mu)$  depends continuously on parameter  $\mu$  leads to the following theorem.

**Theorem 4.1.1** The family  $\mathcal{Q}$  is Hurwitz stable if and only if

- (a)  $p_1(\lambda)$  or  $p_2(\lambda)$  is Hurwitz stable,
- (b)  $p_{12}(i\omega, \mu) \neq 0$  holds for all  $\omega \in \mathbb{R}$  and all  $\mu \in [0, 1]$ .

**Proof** The necessity is obvious, so only the sufficiency is to be proved. Because  $p(\lambda, \mu)$  is analytic with respect to  $\lambda$  and  $\mu$ , the sum of the multiplicity of roots of  $p(\lambda, \mu) = 0$  on the open right half-plane can change only if a root appears on or crosses the imaginary axis as  $\mu$  varies. Noting that  $p_1(\lambda)$  or  $p_2(\lambda)$  is Hurwitz stable and  $p_{12}(i\omega, \mu) \neq 0$  holds true for all  $\omega \in \mathbb{R}$  and all  $\mu \in [0, 1]$ , we make sure that the sum of the multiplicity of roots of  $p_{12}(\lambda, \mu) = 0$  on the open right half-plane remains unchanged and equals to zero as  $\mu$  varies. That is,  $p(\lambda, \mu)$  is Hurwitz stable for all  $\mu \in [0, 1]$ . This completes the proof.

**Remark 4.1.1** The inequality  $p_{12}(i\omega, \mu) \neq 0$  holds true for sufficiently large  $\omega > \omega_0$ . Thus, it is required checking the inequality only on a finite domain  $[0, \omega_0] \times [0, 1]$ .

Next, let

$$R_j(\omega) \equiv \operatorname{Re}[p_j(i\omega)], \quad S_j(\omega) \equiv \operatorname{Im}[p_j(i\omega)], \quad j=1,2. \quad (4.1.11)$$

If there is any pair  $(\omega, \mu) \in [0, \omega_0] \times [0, 1]$  such that  $p_{12}(i\omega, \mu) = 0$ , then

$$\begin{cases} (1-\mu)R_1(\omega) + \mu R_2(\omega) = 0, \\ (1-\mu)S_1(\omega) + \mu S_2(\omega) = 0. \end{cases} \quad (4.1.12)$$

The fact that  $1-\mu$  and  $\mu$  does not vanish at the same time results in

$$\det \begin{bmatrix} R_1(\omega) & R_2(\omega) \\ S_1(\omega) & S_2(\omega) \end{bmatrix} = R_1(\omega)S_2(\omega) - R_2(\omega)S_1(\omega) = 0. \quad (4.1.13)$$

If Eq. (4.1.13) has no root for  $(\omega, \mu) \in [0, \omega_0] \times [0, 1]$ , then  $p_{12}(i\omega, \mu) \neq 0$  holds true on this region.

**Theorem 4.1.2** The polytope  $\mathcal{Q}$  defined in Eq. (4.1.1) is Hurwitz stable if and only if the following two conditions hold.

- (a) The quasi-polynomial  $p_1(\lambda)$  is Hurwitz stable.
- (b) For any root  $\omega_0 \in \mathbb{R}$  of Eq. (4.1.13), if  $R_1(\omega_0)R_2(\omega_0) \neq 0$ , then

$$R_1(\omega_0)R_2(\omega_0) > 0. \quad (4.1.14a)$$

If Eq. (4.1.13) has a non-negative root  $\omega_0 \geq 0$  such that  $R_1(\omega_0)=0$  or  $R_2(\omega_0)=0$ , then Eq. (4.1.14a) should be replaced by the following

$$S_1(\omega_0)S_2(\omega_0) > 0. \tag{4.1.14b}$$

**Proof** We first look at the necessity. Condition (a) is obviously necessary. To prove the necessity of condition (b), we first consider the case  $R_1(\omega_0)R_2(\omega_0) \neq 0$ . Assume on the contrary that the following inequality holds

$$R_1(\omega_0)R_2(\omega_0) < 0. \tag{4.1.15}$$

Then, we have  $R_1(\omega_0)/R_2(\omega_0) < 0$  and  $1 - R_1(\omega_0)/R_2(\omega_0) > 1$ . There follows

$$0 < \frac{R_2(\omega_0)}{R_2(\omega_0) - R_1(\omega_0)} = \frac{1}{1 - R_1(\omega_0)/R_2(\omega_0)} < 1, \tag{4.1.16}$$

namely,

$$\frac{R_2(\omega_0)}{R_2(\omega_0) - R_1(\omega_0)} \in (0, 1). \tag{4.1.17}$$

Denote the value of the expression in Eq. (4.1.17) by  $1 - \mu_0$ , where  $\mu_0 \in (0, 1)$ . Then, we have

$$(1 - \mu_0)R_1(\omega_0) + \mu_0 R_2(\omega_0) = 0. \tag{4.1.18}$$

According to Eq. (4.1.13), it is also true that

$$(1 - \mu_0)S_1(\omega_0) + \mu_0 S_2(\omega_0) = 0. \tag{4.1.19}$$

Combining Eq. (4.1.18) with Eq. (4.1.19) gives

$$(1 - \mu_0)p_1(i\omega_0) + \mu_0 p_2(i\omega_0) = 0. \tag{4.1.20}$$

When  $R_1(\omega_0)=0$  or  $R_2(\omega_0)=0$ , the same procedure for the case  $R_1(\omega_0)R_2(\omega_0) \neq 0$  can also be applied to show that there exists a  $\mu_0 \in [0, 1]$  such that Eq. (4.1.19) holds, and in turn Eq. (4.1.20) holds true if we assume on the contrary that  $S_1(\omega_0)S_2(\omega_0) \leq 0$  holds. Eq. (4.1.20) means that at least one of the quasi-polynomials in the polytope  $\Omega$  has a root on the imaginary axis. This assertion contradicts the Hurwitz stability of polytope  $\Omega$ . Therefore, condition (b) is necessary.

To prove the sufficiency, assume that  $p_1(\lambda)$  is Hurwitz stable and condition (b) holds. Note that Eq. (4.1.14) is equivalent to

$$\frac{R_2(\omega_0)}{R_2(\omega_0) - R_1(\omega_0)} \notin [0, 1] \quad \text{or} \quad \frac{S_2(\omega_0)}{S_2(\omega_0) - S_1(\omega_0)} \notin [0, 1]. \tag{4.1.21}$$

This indicates that for each  $\mu \in [0, 1]$ , any solution  $\omega_0$  of Eq. (4.1.13) does not satisfy Eq. (4.1.18) or correspondingly Eq. (4.1.19). Hence, we have  $(1-\mu)p_1(i\omega_0) + \mu p_2(i\omega_0) \neq 0$ , namely, Eq. (4.1.20) holds for all  $\mu \in [0, 1]$ . Thus, the roots of  $(1-\mu)p_1(\lambda) + \mu p_2(\lambda)$  do not cross the imaginary axis as  $\mu$  varies. As all the roots of  $p_1(\lambda)$  stay on the open left half-plane of the complex plane, so do the roots of all  $(1-\mu)p_1(\lambda) + \mu p_2(\lambda)$  for all  $\mu \in [0, 1]$ . This fact implies that all the quasi-polynomials in the convex combination generated by  $p_1(\lambda)$  and  $p_2(\lambda)$  are Hurwitz stable. This completes the proof of Theorem 4.1.2.

Because Eq. (4.1.13) is independent of  $\mu$ , all the roots of Eq. (4.1.13) can always be figured out numerically. Then, the stability analysis can be easily completed.

The robust Hurwitz stability of  $\Omega$  can also be analyzed by using the functions of phase angle defined as following

$$\varphi_j(\omega) \equiv \arg[p_j(i\omega)], \quad j=1, 2. \quad (4.1.22)$$

**Theorem 4.1.3** The family  $\Omega$  is robust Hurwitz stable if and only if

- (a)  $p_1(\lambda)$  and  $p_2(\lambda)$  are Hurwitz stable,
- (b)  $\varphi_1(\omega) - \varphi_2(\omega) \neq \pm\pi$  for any  $\omega \in [0, +\infty)$ .

**Proof** To prove the necessity, assume that  $\Omega$  is robust Hurwitz stable, but, on the contrary, there exists an  $\omega_0 \in R$  such that

$$\varphi_1(\omega_0) - \varphi_2(\omega_0) = \pm\pi. \quad (4.1.23)$$

If  $R_1(\omega_0) = 0$  or  $R_2(\omega_0) = 0$ , Eq. (4.1.23) obviously results in  $S_1(\omega_0)S_2(\omega_0) < 0$ . When  $R_1(\omega_0)R_2(\omega_0) \neq 0$ , Eq. (4.1.23) gives  $\tan\varphi_1(\omega_0) = \tan\varphi_2(\omega_0)$ , namely,

$$\frac{S_1(\omega_0)}{R_1(\omega_0)} = \frac{S_2(\omega_0)}{R_2(\omega_0)}. \quad (4.1.24)$$

This equation is equivalent to Eq. (4.1.13). In addition, Eq. (4.1.23) leads to the inequality  $R_1(\omega_0)R_2(\omega_0) < 0$ . Both cases contradict condition (b) in Theorem 4.1.2. Hence, condition (b) is necessary.

On the other hand, if condition (b) is true, Eqs. (4.1.23), (4.1.24) and (4.1.13) do not hold. Hence,  $p_{12}(i\omega, \mu) \neq 0$  holds for all  $(\omega, \mu) \in [0, \omega_0] \times [0, 1]$ . In other words, the stability of one-parameter family can not change as  $\mu$  varies on  $[0, 1]$ . Because  $p_1(\lambda)$  and  $p_2(\lambda)$  are Hurwitz stable,  $\Omega$  must be Hurwitz stable. This completes the proof of Theorem 4.1.3.

Besides the functions of phase angle, the Nyquist diagrams can also be used to analyze the robust Hurwitz stability of family  $\Omega$  as shown in the following theorem.

**Theorem 4.1.4** The family  $\Omega$  is robust Hurwitz stable if and only if

- (a) the Nyquist diagram of  $p_1(i\omega)/(i\omega+1)^n$  does not encircle the origin,
- (b) the Nyquist diagram of  $p_2(i\omega)/p_1(i\omega)$  does not intersect the non-positive part of the real axis.

**Proof** As stated in Theorem 2.2.11, the Nyquist diagram of  $p_1(i\omega)/(i\omega+1)^n$  does not encircle the origin if and only if  $p_1(\lambda)$  is Hurwitz stable. Assume that  $p_1(\lambda)$  is Hurwitz stable, it is required proving that condition (b) is necessary and sufficient for the Hurwitz stability of  $p_{12}(\lambda, \mu)$  when  $\mu \in (0, 1]$ .

To see the necessity, note that the Hurwitz stability of  $p_{12}(\lambda, \mu)$  implies

$$(1-\mu)p_1(i\omega) + \mu p_2(i\omega) \neq 0 \tag{4.1.25}$$

for all  $\omega \in \mathbb{R}$  and  $\mu \in [0, 1]$ . As  $p_1(\lambda)$  is Hurwitz stable,  $p_1(i\omega) \neq 0$  holds for all  $\omega \in \mathbb{R}$ . From this fact and  $\mu > 0$ , we can recast Eq. (4.1.25) as

$$\frac{1-\mu}{\mu} + \frac{p_2(i\omega)}{p_1(i\omega)} \neq 0. \tag{4.1.26}$$

Observing that  $(1-\mu)/\mu$  takes values on  $[0, +\infty)$  when  $\mu$  varies on  $(0, 1]$ , we conclude that condition (b) is necessary for the stability of  $p(\lambda, \mu)$ ,  $\mu \in (0, 1]$ .

To prove the sufficiency of condition (b), suppose, on the contrary, that there exists a positive number  $\hat{\mu} \in (0, 1]$  such that  $p_{12}(\lambda, \hat{\mu})$  is not Hurwitz stable even though condition (b) holds. Then,  $p_{12}(\lambda, \hat{\mu})$  has a root  $\lambda(\mu)$ , which depends continuously on  $\mu$  and has a non-negative real part when  $\mu = \hat{\mu}$ . As  $p_1(\lambda)$  is Hurwitz stable,  $\lambda(0)$  has negative real part. Hence, there must exist a positive number  $\tilde{\mu} \in (0, \hat{\mu}]$  such that  $\text{Re}[\lambda(\tilde{\mu})] = 0$ . This fact gives

$$p_{12}(i\omega, \tilde{\mu}) = (1-\tilde{\mu})p_1(i\omega) + \tilde{\mu}p_2(i\omega) = 0. \tag{4.1.27}$$

Equation (4.1.27) implies that  $p_2(i\omega)/p_1(i\omega) < 0$  since  $\tilde{\mu} > 0$  and  $1-\tilde{\mu} > 0$  hold. This is in contradiction with condition (b). Therefore, condition (b) is sufficient for the stability of  $p_{12}(\lambda, \mu)$  for any  $\mu \in (0, 1]$ . The proof is completed.

**Example 4.1.3** Check the robust Hurwitz stability of

$$\Omega \equiv \text{conv}\{p(\lambda, 0), p(\lambda, 0.32)\} \equiv \{p(\lambda, k) = q^2(\lambda) + k \mid k \in [0, 0.32]\}. \tag{4.1.28}$$

As shown in Example 4.1.2,  $p(\lambda, 0)$  is Hurwitz stable. Now, Fig. 4.1.4 indicates that the Nyquist diagram of  $p(i\omega, 0.32)/(i\omega+1)^2$  does not encircle the origin of the



complex plane. Hence, the quasi-polynomial  $p(\lambda, 0.32)$  is Hurwitz stable. In Fig. 4.1.5, the Nyquist diagram of  $p(i\omega, 0.32)/p(i\omega, 0)$  does not intersect the non-positive part of the real axis. According to Theorem 4.1.4, the family  $\Omega$  is robust Hurwitz stable.

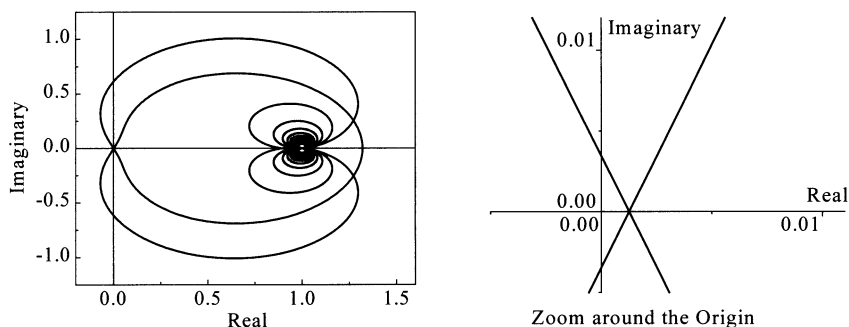


Fig. 4.1.4. The Nyquist diagram of  $p(i\omega, 0.32)/(i\omega+1)^2$

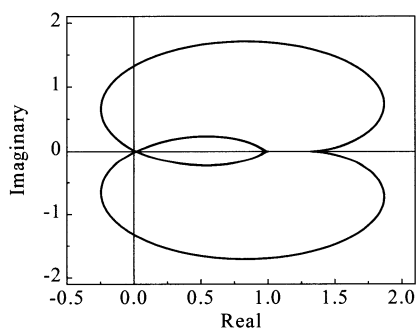


Fig. 4.1.5. The Nyquist diagram of  $p(i\omega, 0.32)/p(i\omega, 0)$

## 4.2 Edge Theorem for a Polytopic Family of Quasi-polynomials

This section is devoted to the robust Hurwitz stability of a polytope of quasi-polynomials. Roughly speaking, a *polytope* is the convex hull of a finite number of quasi-polynomials, which are called the *vertex quasi-polynomials*. What we are concerned with is to determine whether or not every member of the polytope is Hurwitz stable. As seen in Subsection 4.1.1, the stability of the vertex quasi-polynomials is not able to guarantee the robust stability of the whole family in

general. The edge theorem, which will be presented later in this section, shows that the stability of the entire family is governed by the edge quasi-polynomials, which are defined as the convex combination of two vertex quasi-polynomials.

### 4.2.1 Problem Formulation

Consider a type of linear dynamic systems with multiple time delays

$$B\dot{x}(t) = \sum_{j=0}^l A_j(\mathbf{q})x(t-\tau_j), \quad x \in R^n, \tag{4.2.1}$$

where  $0 = \tau_0 < \tau_1 < \dots < \tau_l$  represent the constant time delays,  $B \in R^{n \times n}$  is a nonsingular matrix, and  $A_j(\mathbf{q}) \in R^{n \times n}$ ,  $j=0,1,\dots,l$  are the constant matrices with an uncertain parametric vector  $\mathbf{q}$ , which falls into a given box of dimension(s)  $s$

$$\mathbf{q} \in Q \equiv \{(q_1, q_2, \dots, q_s) \mid \underline{q}_i \leq q_i \leq \bar{q}_i, 1 \leq i \leq s\} \subset R^s. \tag{4.2.2}$$

The uncertainties mentioned above may come from the simplification in system modeling, or the measurement errors of system parameters and time delays.

The characteristic function of Eq. (4.2.1) is a quasi-polynomial of order  $n$

$$\begin{aligned} p(\lambda) &\equiv \det[\lambda B - \sum_{j=0}^l e^{-\tau_j \lambda} A_j(\mathbf{q})] \\ &= a_{00}(\mathbf{q})\lambda^n + [\sum_{k=1}^N a_{1k}(\mathbf{q})e^{-h_k \lambda}] \lambda^{n-1} + \dots + \sum_{k=1}^N a_{nk}(\mathbf{q})e^{-h_k \lambda}, \end{aligned} \tag{4.2.3}$$

where  $a_{00} \neq 0$ ,  $0 = \tau_0 < \tau_1 < \dots < \tau_l$  are linear combinations of  $\tau_j$ , and the coefficients  $a_{ij}(\mathbf{q})$  may depend linearly or nonlinearly on  $\mathbf{q}$ . Of course,  $a_{00} = 1$  can be set if  $p(\lambda)$  is replaced by  $p(\lambda) = \det[\lambda I - \sum_{j=0}^l e^{-\tau_j \lambda} B^{-1} A_j(\mathbf{q})]$ . It is of interest to check the robust Hurwitz stability of the system for all admissible parametric perturbations.

Mathematically speaking, we study the interval Hurwitz stability of a family of quasi-polynomials of order  $n$  as following

$$\Omega \equiv \{p(\lambda) = a_{00}(\mathbf{q})\lambda^n + \sum_{j=1}^n [\sum_{k=1}^N a_{jk}(\mathbf{q})e^{-h_k \lambda}] \lambda^{n-j} \mid a_{00} \neq 0, \mathbf{q} \in Q \subset R^s\}. \tag{4.2.4}$$

The family  $\Omega$  of quasi-polynomials is said to be Hurwitz stable if and only if all the roots of each member of  $\Omega$  stay on the open left half-plane.

If the coefficients  $a_{ij}(\mathbf{q})$  are assumed to depend linearly on  $\mathbf{q}$ , then the family  $\Omega$  defined above can be regarded as a polytope generated by the convex combi-

nations of a number of quasi-polynomials  $p_1(\lambda), p_2(\lambda), \dots, p_r(\lambda)$  of order  $n$  in Eq. (4.2.3). That is,

$$\Omega \equiv \text{conv}\{p_1(\lambda), p_2(\lambda), \dots, p_r(\lambda)\}. \quad (4.2.5)$$

Here, the quasi-polynomials  $p_j(\lambda), j=1, \dots, r$  are called the *vertex quasi-polynomials*, or the *generators*, of  $\Omega$ .

Let  $E[\Omega]$  denote the set of all edges of the polytope  $\Omega$ . An *edge of polytope*  $\Omega$  is a one-dimensional, closed segment  $[x, y] \equiv \text{conv}\{x, y\}$  in  $\Omega$  such that for any open segment  $(x_0, y_0) = \text{conv}\{x_0, y_0\} \setminus \{x_0, y_0\}$  in  $\Omega$  intersecting  $[x, y]$ , we have  $[x_0, y_0] \subset [x, y]$ . An edge of  $\Omega$  is in the form of  $\text{conv}\{p_i(\lambda), p_j(\lambda)\}$ , but not all such closed segments are necessarily the edges. Given two quasi-polynomials  $p_1(\lambda) \neq p_2(\lambda)$ , for example,  $\text{conv}\{p_3(\lambda), p_2(\lambda)\}$  is not an edge if  $p_3(\lambda)$  is chosen as  $[p_1(\lambda) + p_2(\lambda)]/2$ .

For a quasi-polynomial  $p(\lambda)$  of order  $n$  given by Eq. (4.2.3), let the coefficient vector of  $p(\lambda)$  be defined by

$$\mathbf{p} \equiv [a_{00} \ a_{10} \ \dots \ a_{1N} \ \dots \ a_{n0} \ \dots \ a_{nN}]^T. \quad (4.2.6)$$

Obviously, there is a one-to-one relation between the set of quasi-polynomials in Eq. (4.2.4) and the set of their coefficient vectors. For a complex number  $\lambda$ , the real and imaginary parts of  $p(\lambda)=0$  can be expressed in terms of two linear equations with respect to vector  $\mathbf{p}$ . Then, it is straightforward to show that  $\lambda$  is a root of  $p(\lambda)$  if and only if

$$\mathbf{K}(\lambda)\mathbf{p}=0, \quad \mathbf{K}(\lambda) \in R^{2 \times (nN+n+1)}, \quad (4.2.7)$$

where the entries of matrix  $\mathbf{K}(\lambda)$  are in terms of  $\text{Re}(e^{-h_i\lambda} \lambda^{n-j})$  and  $\text{Im}(e^{-h_i\lambda} \lambda^{n-j})$ .

For a polytope  $\Omega$  of quasi-polynomials of order  $n$  given by Eq. (4.2.4) and a complex number  $\xi$ , the *value set* of  $\Omega$  with respect to  $\xi$  is defined as

$$V(\Omega, \xi) \equiv \{\mathbf{K}(\xi)\mathbf{p} \mid p(\lambda) \in \Omega\}. \quad (4.2.8)$$

For a polytope  $\Omega$  of quasi-polynomials and a fixed  $\xi$ ,  $V(\Omega, \xi)$  is a polytope on the complex plane. The following lemma is obviously true.

**Lemma 4.2.1** A given polytope  $\Omega$  of quasi-polynomials in Eq. (4.2.5) is Hurwitz stable if and only if  $V(\Omega, \xi)$  with  $\text{Re}\xi \geq 0$  does not contain any zeros.

For all  $p(\lambda) \in \Omega$  and  $\text{Re}\lambda \geq 0$ ,  $p(\lambda) = a_{00}\lambda^n + O(\lambda^{n-1})$  holds as  $|\lambda| \rightarrow +\infty$ . Thus, there exists a sufficiently large constant  $M > 0$  such that  $0 \notin V(\Omega, \lambda)$  for all  $\lambda$  with  $\text{Re}\lambda \geq 0$  and  $|\lambda| \geq M$ .

### 4.2.2 Edge Theorem

**Theorem 4.2.1** A polytope  $\Omega$  of quasi-polynomials of order  $n$  given by Eq. (4.2.4) is Hurwitz stable if and only if  $E[\Omega]$ , the set of all edges of  $\Omega$ , is Hurwitz stable.

The following lemma is essential in the proof, and also helpful in the understanding, of Theorem 4.2.1.

**Lemma 4.2.2** Consider a polytope  $\Omega$  of quasi-polynomials of order  $n$  given by Eq. (4.2.4) and  $V(\Omega, \xi)$  defined in Eq. (4.2.8). For any  $\text{Re}\xi \geq 0$ , we have

$$E[V(\Omega, \xi)] \subset V(E[\Omega], \xi), \quad (4.2.9)$$

where  $E[V]$  represents the set of all edges of  $V$ , respectively.

The proof of Theorem 4.2.1 and Lemma 4.2.2 are not given in this book because it requires much knowledge about convex analysis.

**Remark 4.2.1** Though the above statements are made for the Hurwitz stability, they are also valid in a more general frame of  $D$ -stability. For details, it is referred to (Fu et al. 1989).

### 4.2.3 Sufficient and Necessary Conditions

On the basis of the edge theorem, the key step in the stability analysis of a polytope of quasi-polynomials is to check the robust Hurwitz stability of the edge generated by two quasi-polynomials. Each edge generated by two quasi-polynomials  $p_i(\lambda)$  and  $p_j(\lambda)$  corresponds to a one-parameter family of quasi-polynomials as following

$$p_{ij}(\lambda, \mu) \equiv (1 - \mu)p_i(\lambda) + \mu p_j(\lambda), \quad \mu \in [0, 1]. \quad (4.2.10)$$

Let  $R_j(\omega) \equiv \text{Re}[p_j(i\omega)]$  and  $S_j(\omega) \equiv \text{Im}[p_j(i\omega)]$ , then, using Theorem 4.1.2, Theorem 4.1.3 and Theorem 4.1.4 gives the following theorems.

**Theorem 4.2.2** The polytope  $\Omega$  defined in Eq. (4.2.5) is Hurwitz stable if and only if the following two conditions hold true.

- All vertex quasi-polynomials of  $\Omega$  are Hurwitz stable.
- For each edge between  $p_i(\lambda)$  and  $p_j(\lambda)$ , if there is an  $\omega_0 \in R$  such that

$$R_i(\omega_0)S_j(\omega_0) - R_j(\omega_0)S_i(\omega_0) = 0, \quad (4.2.11)$$

then either

$$R_i(\omega_0)R_j(\omega_0) > 0 \quad (4.2.12a)$$

holds for  $R_i(\omega_0)R_j(\omega_0) \neq 0$ , or

$$S_i(\omega_0)S_j(\omega_0) > 0 \quad (4.2.12b)$$

is true when  $R_i(\omega_0)R_j(\omega_0) = 0$ .

**Theorem 4.2.3** The family  $\Omega$  defined in Eq. (4.2.5) is Hurwitz stable if and only if the following two conditions hold.

- (a) All vertex quasi-polynomials of  $\Omega$  are Hurwitz stable.
- (b) For each edge between  $p_i(\lambda)$  and  $p_j(\lambda)$ , the phase functions satisfy

$$\varphi_i(\omega) - \varphi_j(\omega) \neq \pm\pi. \quad (4.2.13)$$

**Theorem 4.2.4** Let  $E_1, E_2, \dots, E_r$  be the edges of the polytope defined in Eq. (4.2.5),  $p_{k0}(\lambda)$  and  $p_{k1}(\lambda)$  be the vertex quasi-polynomials of  $E_k$ . Then,  $\Omega$  is Hurwitz stable if and only if the following two conditions hold for each edge  $E_k$ .

(a) The Nyquist diagram of  $p_{k0}(i\omega)/(i\omega+1)^n$  does not encircle the origin of the complex plane.

(b) The Nyquist diagram of  $p_{k1}(i\omega)/p_{k0}(i\omega)$  does not cross the non-negative part of the real axis.

The testing procedure of vertex quasi-polynomials can be organized this way. First, check the Hurwitz stability on an arbitrarily chosen vertex, say,  $p_{10}(\lambda)$ . Then, check the robust Hurwitz stability of the edges, which contain  $p_{10}(\lambda)$ , according to condition (b) mentioned above. Afterwards, testify the stability of the edges that share a vertex with one of the previous edges, and so on. Because the set of edges of a polytope is connected, the robust Hurwitz stability of all edges can be verified this way in a finite number of steps.

By the way, some results are available to reduce the number of edge quasi-polynomials to be testified in the stability analysis. See, for example, (Kharitonov and Zhabko 1994).

**Example 4.2.1** Study the robust Hurwitz stability of a polytope of quasi-polynomials as following

$$\begin{aligned} \Omega &= \{p(\lambda, k, h) \mid k \in [-0.0144, -0.0029], h \in [0.739, 2.58]\} \\ &= \text{conv}\{p_0(\lambda), p_1(\lambda), p_2(\lambda), p_3(\lambda)\}, \end{aligned} \quad (4.2.14)$$

where

$$\begin{aligned} p(\lambda, k, h) &= h\lambda^3 + (6h+1)\lambda^2 + (13.75h+6+1.82he^{-0.165\lambda} + 0.42he^{-0.33\lambda})\lambda \\ &\quad + 13.75+1.82e^{-0.165\lambda} + (0.42-1305k)e^{-0.33\lambda}, \end{aligned}$$

$$\begin{aligned}
 p_0(\lambda) &= p(\lambda, -0.0144, 0.739), \quad p_1(\lambda) = p(\lambda, -0.0144, 2.58), \\
 p_2(\lambda) &= p(\lambda, -0.0029, 2.58), \quad p_3(\lambda) = p(\lambda, -0.0029, 0.739). \quad (4.2.15)
 \end{aligned}$$

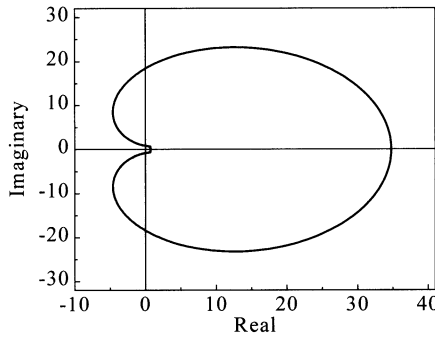


Fig. 4.2.1. The Nyquist diagram for the stability test of the vertex quasi-polynomial  $p_0(\lambda)$

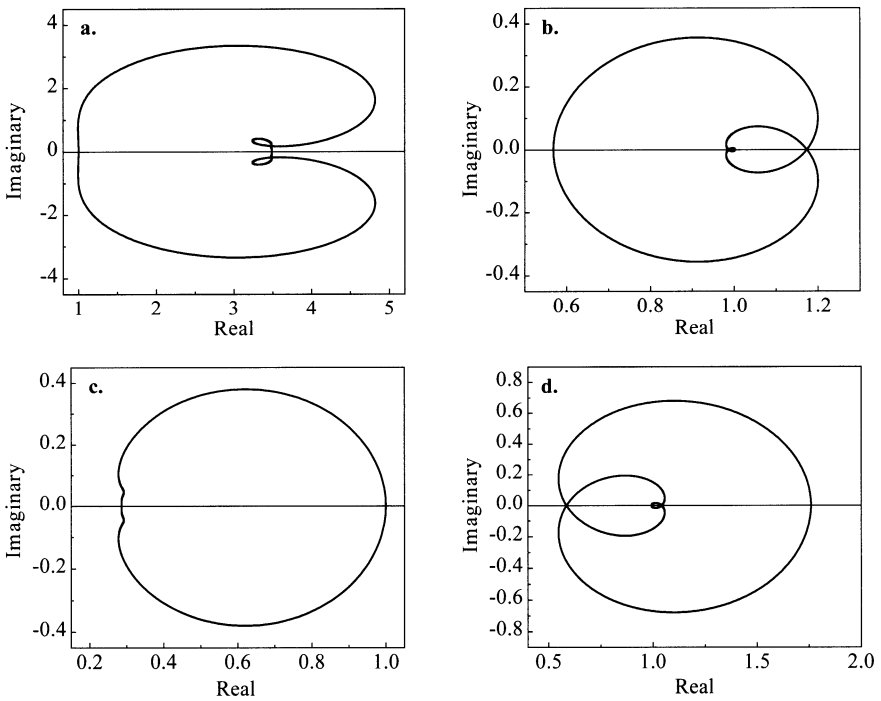


Fig. 4.2.2. The Nyquist diagrams for the stability test of edge quasi-polynomials; **a.**  $p_1(i\omega)/p_0(i\omega)$ , **b.**  $p_2(i\omega)/p_1(i\omega)$ , **c.**  $p_3(i\omega)/p_2(i\omega)$ , **d.**  $p_0(i\omega)/p_3(i\omega)$

From Theorem 4.2.3, we see that  $\Omega$  is robust Hurwitz stable due to the following two facts.

(a) The Nyquist diagram of  $p_0(i\omega)/(i\omega+1)^3$  does not encircle the origin of the complex plane as shown in Fig. 4.2.1. This implies that the vertex quasi-polynomial of  $p_0(\lambda)$  is Hurwitz stable.

(b) As shown in Fig. 4.2.2, the Nyquist diagrams of  $p_1(i\omega) / p_0(i\omega)$ ,  $p_2(i\omega) / p_1(i\omega)$ ,  $p_3(i\omega) / p_2(i\omega)$  and  $p_0(i\omega) / p_3(i\omega)$  do not intersect with the non-negative real axis so that the four edge quasi-polynomials are robust Hurwitz stable. For instance, the Nyquist diagrams of  $p_1(i\omega) / p_0(i\omega)$  indicates that the edge quasi-polynomial generated by  $p_0(\lambda)$  and  $p_1(\lambda)$  is robust Hurwitz stable.

### 4.3 Dixon's Resultant Elimination

In order to determine the condition of marginal stability when a system has a number of commensurate time delays, one usually needs to solve two polynomial equations. Dixon's resultant elimination, see (Dixon 1908) and (Yang et al. 1996b), is one of the most effective algorithms to solve polynomial equations though these polynomial equations may not have any solutions in closed form. The basic principle of resultant elimination includes two steps. First, a set of polynomial equations is constructed from the given polynomial equations and regarded as a set of linear equations with respect to the different powers of unknown variables. Then, the original polynomial equations are studied on the basis of theory of linear matrix equation. The Dixon's resultant elimination can be used to the stability analysis of polynomials and quasi-polynomials.

#### 4.3.1 Dixon's Resultant Elimination

To acquire a good understanding of the Dixon's resultant elimination, we first consider two polynomials  $f(x)$  and  $g(x)$  of order  $n$ , and define

$$\delta(x, \alpha) \equiv \frac{1}{x-\alpha} \det \begin{bmatrix} f(x) & g(x) \\ f(\alpha) & g(\alpha) \end{bmatrix} = \frac{f(x)g(\alpha) - f(\alpha)g(x)}{x-\alpha}. \quad (4.3.1)$$

Obviously,  $\delta(x, \alpha)$  is a polynomial of order  $n-1$  with respect to  $x$  and  $\alpha$ , respectively. At any common root  $x_0$  of  $f(x)$  and  $g(x)$ , the polynomial  $\delta(x, \alpha)$  vanishes for any value  $\alpha$ . Hence, the coefficients  $c_i(x_0)$ ,  $i=0, 1, \dots, n-1$  of  $\delta(x, \alpha)$  with respect to  $\alpha$  also vanish. That is,

$$c_i(x_0)=0, \quad i=0, 1, \dots, n-1. \quad (4.3.2)$$

Let the distinct powers of  $x$  be denoted by  $e_1=x^{n-1}, \dots, e_{n-1}=x, e_n=x^0=1$ , then we can rewrite the equations in Eq. (4.3.2) in the form of linear matrix equation

$$\mathbf{M} \begin{bmatrix} e_1 \\ e_2 \\ \vdots \\ e_n \end{bmatrix} = \begin{bmatrix} 0 \\ 0 \\ \vdots \\ 0 \end{bmatrix}. \quad (4.3.3)$$

The determinant of coefficient matrix  $\mathbf{M}$ , which is the Bezout resultant of  $f(x)$  and  $g(x)$ , must be zero since Eq. (4.3.3) has non-zero solution. That is to say,  $\det \mathbf{M}=0$  if  $f(x)$  and  $g(x)$  has common roots.

If the degrees of  $f(x)$  and  $g(x)$  satisfy  $\deg(f, x)=n > m = \deg(g, x)$ , this procedure can also be performed with  $f(x)$  and  $0 \cdot x^n + \dots + 0 \cdot x^{m+1} + g(x)$ .

Now we consider three polynomial equations in two unknowns  $x$  and  $y$

$$PS: f_1(x, y)=0, \quad f_2(x, y)=0, \quad f_3(x, y)=0, \quad (4.3.4)$$

and introduce Dixon's resultant. Though it is possible to elucidate the method of Dixon's resultant elimination in a more general frame, the following results are enough for the purpose of stability analysis. We first define a polynomial in new variables  $\alpha$  and  $\beta$  in the form of a determinant

$$\Delta(x, y; \alpha, \beta) \equiv \det \begin{bmatrix} f_1(x, y) & f_2(x, y) & f_3(x, y) \\ f_1(\alpha, y) & f_2(\alpha, y) & f_3(\alpha, y) \\ f_1(\alpha, \beta) & f_2(\alpha, \beta) & f_3(\alpha, \beta) \end{bmatrix}. \quad (4.3.5)$$

Because  $\Delta(x, y; \alpha, \beta)=0$  and  $\Delta(x, \beta; \alpha, \beta)=0$ ,  $\Delta(x, y; \alpha, \beta)$  must possess a factor  $(x-\alpha)(y-\beta)$ . Thus, we introduce a new polynomial

$$\delta(x, y; \alpha, \beta) \equiv \frac{\Delta(x, y; \alpha, \beta)}{(x-\alpha)(y-\beta)} \quad (4.3.6)$$

and refer to it as the *Dixon's reduced polynomial* of  $PS$ . Similar to the above simple case, this reduced polynomial serves as a bridge to express Eq. (4.3.4) in terms of linear matrix equation. If we expand  $f_i(x, y)$  as

$$f_k(x, y) = \sum_{i=0}^p \sum_{j=0}^q c_{ij}^{(k)} x^i y^j, \quad k = 1, 2, 3 \quad (4.3.7)$$

then we have



$$\delta(x, y; \alpha, \beta) = \sum_{k=0}^{2p-1} \sum_{l=0}^{q-1} \sum_{i=0}^{p-1} \sum_{j=0}^{2q-1} d_{ijkl} x^i y^j \alpha^k \beta^l. \quad (4.3.8)$$

**Example 4.3.1** Consider three polynomials in two variables  $s$  and  $t$

$$\begin{aligned} p_1(s, t) &\equiv (s^2 + s^2 t)x - s^2 t + t + s^2 + 1, \\ p_2(s, t) &\equiv (s^2 + s^2 t)y - s^2 t - s + t, \\ p_3(s, t) &\equiv (s^2 + s^2 t)z - 2s^2 + 2t + 2. \end{aligned} \quad (4.3.9)$$

Straightforward computation gives

$$\begin{aligned} \Delta(s, t; \alpha, \beta) &= \det \begin{bmatrix} p_1(s, t) & p_2(s, t) & p_3(s, t) \\ p_1(\alpha, t) & p_2(\alpha, t) & p_3(\alpha, t) \\ p_1(\alpha, \beta) & p_2(\alpha, \beta) & p_3(\alpha, \beta) \end{bmatrix} \\ &= \det \begin{bmatrix} p_1(s, t) - p_1(\alpha, t) & p_2(s, t) - p_2(\alpha, t) & p_3(s, t) - p_3(\alpha, t) \\ p_1(\alpha, t) - p_1(\alpha, \beta) & p_2(\alpha, t) - p_2(\alpha, \beta) & p_3(\alpha, t) - p_3(\alpha, \beta) \\ p_1(\alpha, \beta) & p_2(\alpha, \beta) & p_3(\alpha, \beta) \end{bmatrix} \\ &= (s - \alpha)(t - \beta)(c_1 \alpha^3 + c_2 \alpha^2 + c_3 \alpha + c_4). \end{aligned} \quad (4.3.10)$$

Thus, the Dixon's reduced polynomial is

$$\delta(s, t; \alpha, \beta) = c_1 \alpha^3 + c_2 \alpha^2 + c_3 \alpha + c_4, \quad (4.3.11a)$$

where

$$\begin{aligned} c_1 &\equiv (2x + 2z - 2)s + (6y - 4x - z - 2)t + 6y - 2x + z - 4, \\ c_2 &\equiv (6y - 4x - z - 2)st + (6y - 2x + z - 4)s + (2x - z - 2)t + 2x - z - 2, \\ c_3 &\equiv (2x - z - 2)st + (2x - z + 4)s + (2x - z - 2)t + 2x + z - 4, \\ c_4 &\equiv (2x - z - 2)st + (2x - z + 4)s. \end{aligned} \quad (4.3.11b)$$

Here,  $p = 2, q = 1$ , so the distinct powers of  $\alpha$  and  $\beta$  are  $\alpha^3, \alpha^2, \alpha$  and 1, while the distinct powers in  $\delta$  with respect to  $s$  and  $t$  are  $st, s, t$  and 1. The number of distinct powers of  $\delta$  with respect to  $\alpha$  and  $\beta$  is the same as that of distinct powers of  $\delta$  with respect to  $s$  and  $t$ . That is, they are  $2pq = 4$ .

We assume that different terms have different powers. Let  $c_j(x, y)$ ,  $j = 1, 2, \dots, 2pq$ , denote the coefficients of  $\delta(x, y; \alpha, \beta)$  with respect to the distinct powers of  $\alpha$  and  $\beta$  in a properly given order of the powers. If  $(x_0, y_0)$  is a

common root of  $PS$ , then  $\delta(x_0, y_0; \alpha, \beta) = 0$  holds true for any  $\alpha$  and  $\beta$ . As  $\alpha$  and  $\beta$  are free variables,  $(x_0, y_0)$  must satisfy

$$c_1(x, y) = 0, \quad c_2(x, y) = 0, \quad \dots, \quad c_{2pq}(x, y) = 0. \quad (4.3.12)$$

These equations are called the set of *Dixon's reduced polynomial equations* from  $PS$ . Let the distinct powers be  $e_1, e_2, \dots, e_{2pq-2} \equiv x, e_{2pq-1} \equiv y$ , and  $e_{2pq} \equiv 1$ , respectively, Eq. (4.3.12) can be recast as a linear matrix equation like Eq. (4.3.3). If  $PS$  has any common real roots, then Eq. (4.3.3) has non-zero solution since  $e_{2pq} = 1 \neq 0$ . Thus, the determinant  $J = \det \mathbf{M}$ , which is called the *Dixon's resultant* of  $PS$ , must vanish if  $PS$  has any real common root. The above analysis can be summarized as the following theorem.

**Theorem 4.3.1** If the set of polynomial equations  $PS$  has a real solution, it is necessary that the Dixon's resultant vanishes. Conversely, if Eq. (4.3.3) has a non-zero solution which is compatible to the powers  $(e_1, e_2, \dots, e_{2pq})$ , then  $PS$  has a solution.

The Gauss elimination makes it possible to solve Eq. (4.3.3) recurrently by transforming  $\mathbf{M}$  into an upper-triangle matrix. If the solution of Eq. (4.3.3) is compatible to the powers  $(e_1, e_2, \dots, e_{2pq})$ , it is easy to determine the corresponding  $x$  and  $y$ . Note that it is not necessary that all the terms in Eq. (4.3.7) appear in stability analysis. Though some "zero" coefficients can be added to  $f_k(x, y)$  in this case to achieve such a complete form as mentioned in (Kapur et al. 1994), a linear matrix equation like Eq. (4.3.3) is usually enough for our purpose.

**Example 4.3.2** Consider the characteristic equation corresponding to a dynamic system with two commensurate time delays

$$p(\lambda, \tau) \equiv \lambda^3 + (\alpha + 2\xi)\lambda^2 + (1 + 2\alpha\xi + \alpha\delta e^{-\tau\lambda})\lambda + \alpha\gamma e^{-2\tau\lambda} + \alpha = 0, \quad (4.3.13)$$

where  $\alpha > 0$ ,  $\xi > 0$  and  $\tau > 0$ . The system free of time delays is asymptotically stable if and only if the following Routh-Hurwitz stability conditions are true

$$\gamma + 1 > 0, \quad \alpha\gamma - \alpha(\alpha - 2\xi)\delta - 2\xi - 2\alpha^2\xi - 4\alpha\xi^2 < 0. \quad (4.3.14)$$

When  $\tau > 0$ , the marginal stability condition  $p(i\omega, \tau) = 0$  can be cast as

$$PS: \begin{cases} f_1(x, y) \equiv -\omega^2(\alpha + 2\xi) + \alpha\delta\omega y + 2\alpha\gamma x^2 + \alpha(1 - \gamma) = 0, \\ f_2(x, y) \equiv -\omega^3 + \omega + 2\alpha\xi\omega + \alpha\delta\omega x - 2\alpha\gamma xy = 0, \\ f_3(x, y) \equiv x^2 + y^2 - 1 = 0, \end{cases} \quad (4.3.15)$$

where  $x \equiv \cos\omega\tau$  and  $y \equiv \sin\omega\tau$ . The Dixon's reduced polynomial equations can be derived and classified into two groups

$$\begin{aligned} \text{G1: } g_i(x,y) &= 0, \quad i=1,2,3,4, \quad g_{s_1}(x,y)=0, \\ \text{G2: } g_i(x,y) &= 0, \quad i=1,2,3,4, \quad g_{s_2}(x,y)=0, \end{aligned} \quad (4.3.16)$$

where

$$\begin{aligned} g_1 &\equiv (1+\gamma-\omega^2)\alpha - 2\omega^2\xi + \alpha\delta\omega y - 2\alpha\gamma y^2, \\ g_2 &\equiv \omega^3 - \omega - 2\alpha\xi\omega - \alpha\delta\omega x + 2\alpha\gamma xy, \\ g_3 &\equiv [-2\alpha\delta\gamma\omega y + (-2\alpha\gamma - 4\gamma\xi + \alpha\delta^2)\omega^2 + 2\alpha\gamma(\gamma+1)]x \\ &\quad + 2\gamma\omega[\omega^2 - (1+2\alpha\xi)]y - \delta\omega^4 + \delta\omega^2(1+2\alpha\xi), \\ g_4 &\equiv 2\gamma\omega[\omega^2 - (1+2\alpha\xi)]x - 2\alpha\gamma\delta\omega y^2 + [(\alpha\delta^2 + 4\xi\gamma + 2\alpha\gamma)\omega^2 \\ &\quad - 2\alpha\gamma(1+\gamma)]y - (\alpha+2\xi)\delta\omega^3 + \alpha\delta(1-\gamma)\omega, \\ g_{s_1} &\equiv \delta\omega - 2\gamma y, \\ g_{s_2} &\equiv \omega(1+2\alpha\xi - \omega^2)x + [-(\alpha+2\xi)\omega^2 + \alpha(1-\gamma)]y + \alpha\delta\omega. \end{aligned} \quad (4.3.17)$$

For G1 in Eq. (4.3.16), let the distinct powers of  $x$  and  $y$  be denoted by  $e_1 \equiv y^2$ ,  $e_2 \equiv xy$ ,  $e_3 \equiv x$ ,  $e_4 \equiv y$  and  $e_5 \equiv 1$ , then we have a linear matrix equation  $\mathbf{M}[e_1 \dots e_5]^T = 0$ . We find, through direct computation, that the corresponding Dixon's resultant is not zero and reads (up to a non-zero factor)

$$\begin{aligned} J(\omega) &= \omega[\omega^6 + (\alpha^2 + 4\xi^2 - 2)\omega^4 \\ &\quad + (4\alpha^2\xi^2 + 1 - 2\alpha^2 - 2\gamma\alpha^2 - 4\alpha\gamma\xi)\omega^2 + (\gamma+1)^2\alpha^2]. \end{aligned} \quad (4.3.18)$$

For G2, we can show that the corresponding Dixon's resultant yields  $J(\omega)=0$ . Using the Gauss elimination transfers the corresponding Dixon's matrix  $\mathbf{M}$  into the following form

$$\mathbf{M} \rightarrow \tilde{\mathbf{M}} = \begin{bmatrix} * & * & * & * & * \\ 0 & * & * & * & * \\ 0 & 0 & a_{21} & a_{22} & a_{23} \\ 0 & 0 & 0 & a_{12} & a_{13} \\ 0 & 0 & 0 & 0 & 0 \end{bmatrix}. \quad (4.3.19)$$

This gives a set of linear equations in unknowns  $x$  and  $y$

$$\begin{cases} a_{21}x + a_{22}y + a_{23} = 0, \\ a_{12}y + a_{13} = 0. \end{cases} \quad (4.3.20)$$

Solving Eq. (4.3.20) for  $x$  and  $y$ , and then substituting them into  $x^2 + y^2 = 1$ , we have a polynomial  $\tilde{J}(\omega)$  with even order terms only

$$\tilde{J}(\omega) = \omega^{12} + a_1 \omega^{10} + a_2 \omega^8 + a_3 \omega^6 + a_4 \omega^4 + a_5 \omega^2 + a_6, \quad (4.3.21)$$

where

$$\begin{aligned} a_1 &\equiv -4 + 2\alpha^2 + 8\xi^2, \\ a_2 &\equiv 16\alpha^2 \xi^2 - \alpha^2 \delta^2 - 8\alpha^2 + \alpha^4 + 6 - 16\xi^2 + 16\xi^4, \\ a_3 &\equiv (8\xi^2 - \delta^2 - 4)\alpha^4 + 2[6 + 16\xi^2(\xi^2 - 1) + \delta^2(1 - 2\xi^2) - \delta^2]\alpha^2 + 4(2\xi^2 - 1), \\ a_4 &\equiv 2[(\gamma + 1 - 2\xi^2)\delta^2 + 8\xi^2(\xi^2 - 1) + 3 - \gamma^2]\alpha^4 + 4\alpha^3 \delta^2 \gamma \xi \\ &\quad + [-\delta^2 + 8(2 - \gamma^2)\xi^2 + 4(\gamma^2 - 2)]\alpha^2 + 1, \\ a_5 &\equiv \alpha^2 \{[-(1 + \gamma)^2 \delta^2 + 4(1 - \gamma^2)(2\xi^2 - 1)]\alpha^2 + 2(1 - \gamma^2)\}, \\ a_6 &\equiv \alpha^4 (1 - \gamma^2)^2. \end{aligned} \quad (4.3.22)$$

In order that  $PS$  has common real roots,  $\omega$  must be a real root of  $J(\omega)$  or  $\tilde{J}(\omega)$ . For any given  $\alpha$ ,  $\delta$ ,  $\gamma$  and  $\xi$ , we can determine whether  $J(\omega)$  or  $\tilde{J}(\omega)$  has real roots or not and find numerically all the real roots of  $J(\omega) = 0$  or  $\tilde{J}(\omega) = 0$  if there are any.

The stability switches of a linear system with a single time delay have been discussed in Subsection 3.5.1 by using the generalized Sturm criterion, which enables one to determine whether the system exhibits no stability switch, exact one stability switch or more than one stability switch under certain parameter combinations. If the system undergoes more than one stability switch, however, we have to find out numerically the critical values of time delay to obtain detailed information. When commensurate time delays are involved in a system, the method of Dixon's resultant elimination is effective for analyzing the stability switch.

As seen in Subsection 3.5.1, three main steps are involved in the analysis of stability switches. First, find out all the possible critical frequencies and the corresponding critical values of time delays. Then, determine the sign of the derivative of real part of each characteristic root with respect to the time delay. Finally, rank the critical values of time delays and count the number of stability switches.

**Example 4.3.3** Check the stability switches of the dynamic system with two commensurate time delays governed by Eq. (4.3.13) when

$$\alpha = 2, \quad \xi = 0.02, \quad \gamma = 0.3, \quad \delta = 0.5. \quad (4.3.23)$$

It is easy to know that  $\omega=0$  is the unique root of  $J(\omega)$ , and the corresponding polynomial Eq. (4.3.15) has no common real roots. The real roots of  $\tilde{J}(\omega)$  can be numerically found out. They are  $\omega=\pm 0.6428$  and  $\omega=\pm 1.1893$ . When  $\omega=\pm 1.1893$ , the critical values of time delay  $\tau$  are 0.5234, 5.807, 11.09, 16.37, 21.66, 26.94, 32.22, ..., and  $d(\text{Re}\lambda)/d\tau > 0$  at each pair of such  $(\omega, \tau)$ , whereas  $\omega=\pm 0.6428$  gives the critical values of  $\tau$  such as 2.816, 12.59, 22.37, 32.14, 41.91, 51.69, 61.46, ..., and  $d(\text{Re}\lambda)/d\tau < 0$  at each pair of such  $(\omega, \tau)$ . The critical values of  $\tau$  can be ranked as following

$$0.5234 < 2.816 < \underline{5.807} < 11.09 < 12.59 < 16.37 \dots \quad (4.3.24)$$

Noting that 5.807 and 11.09 are two critical values of  $\tau$  corresponding to the same frequency  $\omega=1.1893$ , we conclude as done in Subsection 3.5.1 that the system is Hurwitz stable when  $\tau \in [0, 0.5234)$  and  $(2.816, 5.807)$ , but unstable for  $\tau \in (0.5234, 2.816)$  and  $(5.807, +\infty)$ . As a result, the number of stability switches is 3.

#### 4.3.2 Robust $D$ -stability of One-parameter Family of Polynomials

As a direct application of Dixon's resultant elimination, the  $D$ -stability is discussed for a special one-parameter family of polynomials in this subsection. For this purpose, let  $D$  be a simply connected domain given on the complex plane with the boundary  $\partial D$  governed by a polynomial equation  $b(x, y)=0$ . As mentioned in the introduction of this chapter,  $D$  should be taken as the open unit disk on the complex plane in analyzing the *Schur stability* of discrete-time dynamic systems. Thus,  $\partial D$  is governed by  $b(x, y) \equiv x^2 + y^2 - 1 = 0$ . For the analysis of the Hurwitz stability of continuous-time dynamic systems,  $D$  should be the open left half-plane and  $b(x, y) \equiv x = 0$ . A family of polynomials is  $D$ -stable if and only if all the roots of each member of the family stay in  $D$ .

Now consider the  $D$ -stability of a one-parameter family of polynomials generated by two polynomials  $p_1(\lambda)$  and  $p_2(\lambda)$  as following

$$p_{12}(\lambda, \mu) \equiv (1-\mu)p_1(\lambda) + \mu p_2(\lambda), \quad \mu \in [0, 1]. \quad (4.3.25)$$

Obviously,  $p_{12}(\lambda, \mu)$  is analytic with respect to  $\lambda$  and  $\mu$ . The root  $\lambda(\mu)$  of  $p_{12}(\lambda, \mu)$  is continuous with respect to  $\mu$  and can not suddenly appear or disappear, or change its multiplicity at a finite point on the complex plane. With an increase of  $\mu$ , thus, the sum of multiplicity of all roots of  $p_{12}(\lambda, \mu) = 0$  in  $D^c$ , the

complement of set  $D$ , can change only if a root appears on or crosses the boundary  $\partial D$ . Thus, we have the following theorem.

**Theorem 4.3.2** The one-parameter family  $p_{12}(\lambda, \mu)$  defined in Eq. (4.3.25) is  $D$ -stable if and only if the following two conditions hold true.

- (a) At least either  $p_1(\lambda)$  or  $p_2(\lambda)$  has all characteristic roots in  $D$ .
- (b) The inequality  $p_{12}(x+iy, \mu) \neq 0$  holds for all  $\mu \in [0, 1]$  and all  $(x, y) \in \partial D$ .

The Dixon's resultant elimination enables one to check condition (b) without any difficulty. We first consider a special case, i.e., the robust Hurwitz stability. The marginal stability condition  $p_{12}(iy, \mu) = 0$  indicates that the real and imaginary parts satisfy  $R_{12}(y, \mu) = 0$  and  $S_{12}(y, \mu) = 0$ . Thus, the resultant  $J_{12}(\mu)$  of polynomials  $R_{12}(y, \mu)$  and  $S_{12}(y, \mu)$  in  $y$  is a polynomial with respect to  $\mu$  and must be zero. That is,

$$J_{12}(\mu) \equiv \text{Resultant}(R_{12}, S_{12}, y) = 0. \quad (4.3.26)$$

It is always feasible to find out numerically all the roots  $\mu \in A_{12} \subset [0, 1]$  of this polynomial  $J_{12}(\mu)$ . The robust Hurwitz stability of  $p_{12}(\lambda, \mu)$  for  $\mu \in [0, 1]$  is governed by the stability of  $p_1(\lambda)$  and  $p_2(\lambda)$  plus the polynomials  $p_{12}(\lambda, \mu)$  corresponding to  $\mu \in A_{12} \subset [0, 1]$ , namely by the polynomial set

$$T_{12} = \{p_{12}(\lambda, \mu) \mid \mu = 0, 1, \mu \in A_{12}\}. \quad (4.3.27)$$

This means that the test of robust Hurwitz stability of family  $p_{12}(\lambda, \mu)$  can be simplified to the test of robust Hurwitz stability of  $T_{12}$ .

Similar to the above simple case, we need to find out the testing set of polynomials for the general case. Separate the real and imaginary parts of  $p_{12}(x+iy, \mu)$  and denote them by  $R_{12}(x, y, \mu)$ ,  $S_{12}(x, y, \mu)$ , respectively. Then, condition (b) in Theorem 4.3.3 holds if and only if the following set of polynomial equations

$$PS: \begin{cases} f_1(x, y) \equiv R_{12}(x, y, \mu) = 0, \\ f_2(x, y) \equiv S_{12}(x, y, \mu) = 0, \\ f_3(x, y) \equiv b(x, y) = 0 \end{cases} \quad (4.3.28)$$

has no real common solutions. Thus, we get the testing set if the critical values of parameter  $\mu \in [0, 1]$  render  $p_{12}(\lambda, \mu)$  marginal stable. Let  $J_{12}(\mu)$  denote the corresponding Dixon's resultant. Then,  $J_{12}(\mu)$  is a polynomial of finite order with respect to  $\mu$  and must be zero if  $PS$  has any common roots. If  $J_{12}(\mu)$  is not always zero, then  $PS$  has common roots only when  $\mu$  reaches the roots of  $J_{12}(\mu)$  from Theorem 4.3.2. These roots can be numerically located and denoted as  $A_{12} \subset [0, 1]$ . Otherwise, when  $J_{12}(\mu)$  equals identically to zero, it was proved in

(Kapur et al. 1994) that there exists a non-zero condition  $\tilde{J}_{12}(\mu)=0$  for which  $PS$  has common roots. Or directly, solving Eq. (4.3.3) for  $x$  and  $y$  with help of the Gauss elimination and substituting them into the boundary condition  $b(x,y)=0$  we can also obtain a polynomial  $\tilde{J}_{12}(\mu)=0$  and find out all, if any, real roots  $\tilde{\Lambda}_{12} \subset [0, 1]$  of  $\tilde{J}_{12}(\mu)$ . With an increase of  $\mu$  from 0 to 1, therefore, the sum of multiplicity of all roots of  $p_{12}(\lambda,\mu)=0$  in the complement  $D^c$  of  $D$  can change only if  $\mu$  reaches the zeros of  $J_{12}(\mu)$  or  $\tilde{J}_{12}(\mu)$  in  $[0, 1]$ . Let  $T_{12}$  be the union set of  $p_1(\lambda)$ ,  $p_2(\lambda)$  and all the polynomials  $p_{12}(\lambda,\mu)$  corresponding to  $\mu \in \Lambda_{12}$  or  $\mu \in \tilde{\Lambda}_{12}$ , namely,

$$T_{12} = \{p_{12}(\lambda,\mu) \mid \mu=0,1, \mu \in \Lambda_{12} \text{ or } \mu \in \tilde{\Lambda}_{12}\}. \tag{4.3.29}$$

Then, it is obvious that the one-parameter family  $p_{12}(\lambda,\mu)$  is  $D$ -stable if and only if  $T_{12}$  is  $D$ -stable. Hence, the above analysis can be summarized as following.

**Theorem 4.3.3** The one-parameter family  $p_{12}(\lambda,\mu)$  of polynomials is  $D$ -stable if and only if  $T_{12}$  is  $D$ -stable.

The theorem indicates that  $T_{12}$  serves as a testing set that governs the robust  $D$ -stability of the whole family of polynomials  $p_{12}(\lambda,\mu)$  for all  $\mu \in [0, 1]$ . This is important because the number of elements of  $T_{12}$  is finite.

We note that  $PS$  has no real common solution if and only if one of the following cases occur: (a)  $J_{12}(\mu)$  or  $\tilde{J}_{12}(\mu)$  has no real zeros in  $[0, 1]$ ; or (b) at each  $\mu \in \Lambda_{12}$  or  $\mu \in \tilde{\Lambda}_{12}$ , Eq. (4.3.3) has no real solution; or (c) Eq. (4.3.3) has a solution  $z_0$  which gives a pair values of  $x = x_0, y = y_0$  but it is not compatible to the powers in  $z = z_0$ . Thus in practice, the stability test can be carried out easily by computing the Dixon's resultant and solving some linear matrix equations.

In what follows, two simple examples are given to demonstrate the Dixon's resultant approach. Because the testing set for the robust Hurwitz stability can be easily obtained by using the resultant in general sense, the following two examples are all about the robust Schur stability.

**Example 4.3.4** Consider first a simple polynomial  $p(\lambda) \equiv \lambda^2 + a_1\lambda + a_2$ . It is easy to verify that the roots of  $p(\lambda)$  stay in  $D$ , the open unit circular disk on the complex plane when  $a_1 = -21/20$  and  $a_2 = 27/100$ . Now, we study the robust Schur stability of the family

$$\begin{aligned} \Omega &\equiv \{p(\lambda) = \lambda^2 + a_1\lambda + \frac{27}{100} \mid -\frac{21}{20} \times 1.2 \leq a_1 \leq -\frac{21}{20} \times 0.8\} \\ &= \text{conv}\{\lambda^2 - \frac{63}{50}\lambda + \frac{27}{100}, \lambda^2 - \frac{21}{25}\lambda + \frac{27}{100}\}, \end{aligned} \tag{4.3.30}$$

when  $a_1$  is subject to a variation of  $\pm 20\%$ . It is easy to find that the two vertex polynomials are Schur stable. We require checking whether the polynomial family

$$p_{12}(\lambda, \mu) = \lambda^2 + \left(-\frac{63}{50} + \frac{21}{50}\mu\right)\lambda + \frac{27}{100} \quad (4.3.31)$$

has no roots on or outside  $D$  for all  $\mu \in [0, 1]$ . Straightforward computation gives the Dixon's resultant of the real and imaginary parts  $R(x, y, \mu)$  and  $S(x, y, \mu)$  of  $p_{12}(\lambda, \mu)$ , as well as the boundary polynomial  $b(x, y) = x^2 + y^2 - 1$ , as following

$$J(\mu) = (42\mu + 1)(42\mu - 253). \quad (4.3.32)$$

Here  $J(\mu)$  is determined except for a non-zero constant factor. Obviously,  $J(\mu)$  has no real root  $\mu \in [0, 1]$ . As a result, all the characteristic roots of family  $p_{12}(\lambda, \mu)$  stay in  $D$ . Thus, the polytope  $\Omega$  is robust Schur stable.

**Example 4.3.5** Consider now the following one-parameter family  $\Omega$

$$\begin{aligned} \Omega &\equiv \left\{ p(\lambda) = \lambda^3 + a\lambda^2 + \frac{1}{5}\lambda - \frac{1}{60} \mid -\frac{47}{60}(1+r) \leq a \leq -\frac{47}{60}(1-r) \right\} \\ &= \text{conv} \left\{ \lambda^3 - \frac{47}{60}(1+r)\lambda^2 + \frac{1}{5}\lambda - \frac{1}{60}, \lambda^3 - \frac{47}{60}(1-r)\lambda^2 + \frac{1}{5}\lambda - \frac{1}{60} \right\} \end{aligned} \quad (4.3.33)$$

with a variation of  $r=20\%$ . It is also easy to know that the two vertex polynomials are Schur stable. What follows is to check whether all the roots of family

$$p_{12}(\lambda, \mu) = \lambda^3 + \left(-\frac{47}{50} + \frac{47}{150}\mu\right)\lambda^2 + \frac{1}{5}\lambda - \frac{1}{60}, \quad \mu \in [0, 1] \quad (4.3.34)$$

fall into  $D$ .

Straightforward computation shows that the Dixon's reduced polynomial  $\delta$ , derived from  $R(x, y, \mu)$ ,  $S(x, y, \mu)$  and  $b(x, y) = x^2 + y^2 - 1$ , has 11 terms, a common factor  $y$  exists apparently in some of the reduced polynomials, and two of the reduced polynomials are apparently proportional to  $b(x, y)$ . Hence, we need to study the case when  $y=0$  and  $x=\pm 1$ . If there exists a  $\mu \in [0, 1]$  such that  $R(1, 0, \mu)=0$  and  $S(1, 0, \mu)=0$ , or  $R(-1, 0, \mu)=0$  and  $S(-1, 0, \mu)=0$ , then the polytope is not robust Schur stable. It is easy to see that this is not the case. After eliminating one apparent redundant polynomial and the common factor  $y$ , we can write the set of Dixon's reduced polynomial equations in the form

$$\hat{M}z = 0, \quad z = [y^4 \quad x^2 y^2 \quad xy^2 \quad y^2 \quad x^2 \quad x \quad y \quad 1]^T. \quad (4.3.35)$$

Using the Gauss elimination, we transform  $\hat{M}$  into the following form



$$\hat{M} \rightarrow \begin{bmatrix} * & * & * & * & * & * & * & * & * \\ 0 & * & * & * & * & * & * & * & * \\ 0 & 0 & * & * & * & * & * & * & * \\ 0 & 0 & 0 & * & * & * & * & * & * \\ 0 & 0 & 0 & 0 & 0 & -1 & 0 & 24 & * \\ 0 & 0 & 0 & 0 & 0 & 0 & 0 & -14677 + 94\mu & * \\ 0 & 0 & 0 & 0 & 0 & 0 & 0 & 0 & * \\ 0 & 0 & 0 & 0 & 0 & 0 & 0 & 0 & * \\ 0 & 0 & 0 & 0 & 0 & 0 & 0 & 0 & * \\ 0 & 0 & 0 & 0 & 0 & 0 & 0 & 0 & * \end{bmatrix}. \quad (4.3.36)$$

Then, Eq. (4.3.35), together with Eq. (4.3.36), gives

$$-14677 + 94\mu = 0, \quad -x + 24 = 0. \quad (4.3.37)$$

The solution of Eq. (4.3.37) does not fall into the demanded intervals  $\mu \in [0, 1]$  and  $x \in [-1, 1]$ . Thus, the set of Dixon's reduced polynomials derived from  $R(x, y, \mu)$ ,  $S(x, y, \mu)$  and  $b(x, y)$  has no common real roots at all. Therefore, the inequality  $p_{12}(x + iy, \mu) \neq 0$  holds true for all  $\mu \in [0, 1]$ . As a result, the polytope given in Eq. (4.3.33) is robust Schur stable.

#### 4.4 Robust Stability of Systems with Uncertain Commensurate Time Delays

This section deals with the robust Hurwitz stability of a linear system with uncertain commensurate time delays. It is actually the problem of robust Hurwitz stability of a non-polytopic family of quasi-polynomials. Though the intensive studies have been made on the robust stability of a polytope of quasi-polynomials, the test of robust stability for a non-polytopic family of quasi-polynomials is still an open problem. On the basis of the edge theorem, the section will present a necessary and sufficient condition for the robust Hurwitz stability of the whole family. The condition gives an effective procedure of graphic testing for the Hurwitz stability of the family. One may not favor the graphic method at first, but enjoys its effectiveness later, especially after understanding the difficulty in checking the robust stability of quasi-polynomials. In fact, the graphic test has to be made even in the case when the time delays are fixed.

#### 4.4.1 Problem Formulation

We assume that the time delays in the dynamic system of concern to be commensurate so that the characteristic equation of system is in the form of a quasi-polynomial

$$p(\lambda) \equiv \lambda^n + \sum_{k=0}^m \sum_{j=0}^{n-1} a_{jk}(\mathbf{q}) e^{-k\lambda\tau} \lambda^{n-1-j} = 0, \quad (4.4.1)$$

where  $\tau$  is a positive, uncertain constant and yields

$$0 < \underline{\tau} \leq \tau \leq \bar{\tau}, \quad (4.4.2)$$

and the uncertain parametric vector  $\mathbf{q}$  falls into a given box of dimension(s)  $s$

$$\mathbf{q} \in Q \equiv \{(q_1, q_2, \dots, q_s) \mid \underline{q}_i \leq q_i \leq \bar{q}_i, 1 \leq i \leq s\} \subset R^s. \quad (4.4.3)$$

The uncertainties mentioned above may come from the simplification in system modeling, the measurement errors of system parameters and time delays, etc.

The quasi-polynomial in Eq. (4.4.1) under conditions (4.4.2) and (4.4.3) can be written as a family of quasi-polynomials

$$\Pi \equiv \{ p(\lambda) = \lambda^n + \sum_{k=0}^m \sum_{j=0}^{n-1} a_{jk}(\mathbf{q}) e^{-k\tau\lambda} \lambda^{n-1-j} \mid \mathbf{q} \in Q, \underline{\tau} \leq \tau \leq \bar{\tau} \}. \quad (4.4.4)$$

In many applications, it is required that the system should be robust Hurwitz stable under all possible parameter combinations. That is, the roots of any member in family  $\Pi$  should have negative real parts under all desired parameter combinations.

The aim of this subsection is to present a new approach to testifying the robust stability of the family  $\Pi$  of quasi-polynomials. It is assumed hereinafter that the coefficients  $a_{jk}(\mathbf{q})$  in Eq. (4.4.1) depend linearly on the uncertain parametric vector  $\mathbf{q}$ . Of course,  $\Pi$  is not polytopic provided that any uncertainty exists in the common factor  $\tau$  of commensurate time delays, but it is truly a polytope for any fixed  $\tau$ . Thus, the test of robust stability can be completed on the basis of edge theorem. As a result, a sufficient and necessary condition for the robust Hurwitz stability of the entire polytope of quasi-polynomials is derived. This condition gives a very simple and effective graphic testing approach that determines whether the family  $\Pi$  of quasi-polynomials is robust Hurwitz stable or not.

Given a  $\tau \in [\underline{\tau}, \bar{\tau}]$ , a polytope with parameter  $\tau$  is defined as

$$\Omega_\tau \equiv \{ p(\lambda) = \lambda^n + \sum_{k=0}^m \sum_{j=0}^{n-1} a_{jk}(\mathbf{q}) e^{-k\tau\lambda} \lambda^{n-1-j} \mid \mathbf{q} \in Q \}, \quad (4.4.5)$$

which is generated by the convex hull of a set of quasi-polynomials  $p_1(\lambda, \tau), p_2(\lambda, \tau), \dots, p_r(\lambda, \tau)$  corresponding to the corner of parametric box  $Q$ , namely,

$$\Omega_\tau \equiv \text{conv} \{ p_1(\lambda, \tau), p_2(\lambda, \tau), \dots, p_r(\lambda, \tau) \}. \quad (4.4.6)$$

Obviously, the family  $\Pi$  in Eq. (4.4.5) can be written as

$$\Pi = \bigcup \{ \Omega_\tau \mid \underline{\tau} \leq \tau \leq \bar{\tau} \}. \quad (4.4.7)$$

The family  $\Pi$  is robust Hurwitz stable if and only if  $\Omega_\tau$  is robust Hurwitz stable for any given  $\tau \in [\underline{\tau}, \bar{\tau}]$ . Moreover, the edge theorem in (Fu et al. 1989) indicates that the polytope  $\Omega_\tau$  is robust Hurwitz stable if and only if all the edge quasi-polynomials are robust Hurwitz stable.

Each edge, generated by the vertex polynomials  $p_i(\lambda, \tau)$  and  $p_j(\lambda, \tau)$  of the polytope  $\Omega_\tau$ , corresponds to a two-parameter family of quasi-polynomials

$$p_{ij}(\lambda, \tau, \mu) \equiv (1-\mu)p_i(\lambda, \tau) + \mu p_j(\lambda, \tau), \quad \mu \in [0, 1], \tau \in [\underline{\tau}, \bar{\tau}]. \quad (4.4.8)$$

Because  $p_i(\lambda, \tau)$  and  $p_{ij}(\lambda, \tau, \mu)$  are analytic with respect to  $\lambda$ ,  $\tau$  and  $\mu$  as well, any root  $\lambda = \lambda(\tau)$  of  $p_i(\lambda, \tau) = 0$ , and  $\lambda = \lambda(\tau, \mu)$  of  $p_{ij}(\lambda, \tau, \mu) = 0$  can not suddenly appear or disappear, or change its multiplicity at a finite point on the complex plane. With an increase of  $\mu$  or  $\tau$ , therefore, the sum of the multiplicity of roots of  $p_i(\lambda, \tau) = 0$  or  $p_{ij}(\lambda, \tau, \mu) = 0$  on the right half-plane can change only if a root appears on or crosses the imaginary axis. The above fact can be summarized as the following theorem.

**Theorem 4.4.1** The non-polytopic family  $\Pi$  of quasi-polynomials is robust Hurwitz stable if and only if the following two statements are true.

(a) At least either of the one-parameter families of vertex quasi-polynomials  $p_i(\lambda, \tau)$  and  $p_j(\lambda, \tau)$  is robust Hurwitz stable. That is, there exists a common factor  $\tau_0 \in [\underline{\tau}, \bar{\tau}]$  of commensurate time delays such that  $p_i(\lambda, \tau)$  (or  $p_j(\lambda, \tau)$ ) is Hurwitz stable, and  $p_i(i\omega, \tau) \neq 0$  (or  $p_j(i\omega, \tau) \neq 0$ ) is true for any  $\tau \in [\underline{\tau}, \bar{\tau}]$  and  $\omega \geq 0$ .

(b) For each member of the two-parameter families of edge quasi-polynomials  $p_{ij}(\lambda, \tau, \mu)$  defined in Eq. (4.4.8), the inequality  $p_{ij}(i\omega, \tau, \mu) \neq 0$  holds true for any  $\mu \in [0, 1]$ ,  $\tau \in [\underline{\tau}, \bar{\tau}]$  and  $\omega \geq 0$ .

As the inequalities  $p_i(i\omega, \tau) \neq 0$  (or  $p_j(i\omega, \tau) \neq 0$ ) and  $p_{ij}(i\omega, \tau, \mu) \neq 0$  hold true for sufficiently large  $\omega$ , the stability test of the parametric families of quasi-polynomials can be checked within a finite range of  $\omega$ .

Now, a number of criteria are available to testify the Hurwitz stability of a given quasi-polynomial, see, for example, Theorem 2.2.7 and Theorem 2.2.11. However, these criteria do not work for checking condition (a) or (b). Very tedious computation is usually involved in testing procedures when the current methods are implemented. This subsection, thus, is devoted to developing the simple condition that governs the robust Hurwitz stability of the whole family of quasi-polynomials, as well as an effective method to complete the robust stability test.

The marginal stability condition  $p(i\omega, \tau) = 0$  is a transcendental equation in two unknowns  $\omega$  and  $\tau$ . If the characteristic function in Eq. (4.4.1) is in the form  $p(\lambda, \tau) \equiv P(\lambda) + Q(\lambda)e^{-\lambda\tau}$  with  $\deg P > \deg Q$ , the equation  $p(i\omega, \tau) = 0$  gives two linear equations with respect to  $\cos\omega\tau$  and  $\sin\omega\tau$ . Solving  $p(i\omega, \tau) = 0$  for  $\cos\omega\tau$  and  $\sin\omega\tau$ , and substituting the solutions into  $\cos^2\omega\tau + \sin^2\omega\tau - 1 = 0$ , we have a polynomial equation independent of  $\tau$ . Thus, we can numerically determine the critical values of  $\omega$ , and then figure out the corresponding critical values of  $\tau$ .

In order to solve the equation  $p(i\omega, \tau) = 0$  in a more complicated form for  $\omega$  and  $\tau$ , it is necessary to solve two polynomial equations simultaneously for unknowns  $\cos\omega\tau$  and  $\sin\omega\tau$ , rather than two linear equations, because we can expand  $\cos(k\omega\tau)$  and  $\sin(k\omega\tau)$  to the polynomials with respect to  $\cos\omega\tau$  and  $\sin\omega\tau$ . This problem has no closed-form solutions, whereas pure numerical procedures usually involve an infinite number of computational steps. It is natural, thus, to develop a computationally traceable procedure for calculating the maximal delay factor. For this purpose, the Dixon's resultant elimination is helpful.

#### 4.4.2 Stability of Vertex Quasi-polynomials

To check whether the inequality  $p_k(i\omega, \tau) \neq 0$ ,  $k = i, j$  holds true or not for any  $\tau \in [\underline{\tau}, \bar{\tau}]$  and  $\omega \geq 0$ , we consider a set of polynomial equations in two unknowns  $x = \cos\omega\tau$  and  $y = \sin\omega\tau$  as following

$$PS_k : \begin{cases} f_1(x, y) \equiv R_k(x, y, \omega) = 0, \\ f_2(x, y) \equiv S_k(x, y, \omega) = 0, \\ f_3(x, y) \equiv x^2 + y^2 - 1 = 0, \end{cases} \quad (4.4.9)$$

where  $R_k(x,y,\omega) \equiv \text{Re}[p_k(i\omega,\tau)]$  and  $S_k(x,y,\omega) \equiv \text{Im}[p_k(i\omega,\tau)]$ , whereas  $\omega$  is taken as a parameter. The real and imaginary parts  $R_k(x,y,\omega)$  and  $S_k(x,y,\omega)$  are two polynomials in  $x$ ,  $y$  and  $\omega$  since we can expand  $\cos(k\omega\tau)$  and  $\sin(k\omega\tau)$  to the polynomials with respect to  $\cos\omega\tau$  and  $\sin\omega\tau$ . Obviously,  $p(i\omega,\tau)=0$  has a real root  $(\omega^*,\tau^*) \in [0, +\infty) \times [\underline{\tau}, \bar{\tau}]$  if and only if  $PS_k$  has a real common root  $(\cos\omega^*\tau^*, \sin\omega^*\tau^*, \omega^*)$ .

Let  $J_k(\omega)$  denote the Dixon's resultant of  $PS_k$ . Then,  $J_k(\omega)$  is a polynomial with respect to  $\omega$ . As stated in Theorem 4.3.2,  $J_k(\omega)$  must be zero if  $PS_k$  has a real common root. That is,  $\omega^*$  must be a positive root of  $J_k(\omega)$ . Though  $J_k(\omega)$  may keep being zero for all  $\omega \geq 0$ , we can always find a solution in the form of  $x \equiv \cos\omega\tau = x^0(\omega)$  and  $y \equiv \sin\omega\tau = y^0(\omega)$  of  $PS_k$  by using Dixon's resultant elimination in Subsection 4.3.2 if the solution of corresponding Dixon's reduced linear equation is compatible to  $PS_k$ . Substituting them into  $x^2 + y^2 - 1 = 0$  gives a polynomial  $\tilde{J}_k(\omega)$ . Then,  $\omega^*$  must be the positive roots of  $\tilde{J}_k(\omega)$ . By using the following two sets corresponding to  $PS_k$

$$\Gamma_k \equiv \{ \omega \geq 0 \mid J_k(\omega) = 0 \text{ or } \tilde{J}_k(\omega) = 0 \}, \tag{4.4.10a}$$

$$T_k \equiv \{ \tau \in [\underline{\tau}, \bar{\tau}] \mid \cos\omega\tau = x^0(\omega), \sin\omega\tau = y^0(\omega), \omega \in \Gamma_k \}, \tag{4.4.10b}$$

we are in the position to summarize the following theorem.

**Theorem 4.4.2** The one-parameter family  $p_k(\lambda,\tau)$  is robust Hurwitz stable for any  $\tau \in [\underline{\tau}, \bar{\tau}]$  if and only if the following two statements are true.

- (a)  $p_k(\lambda,\underline{\tau})$  is Hurwitz stable;
- (b) One of the following three conditions holds. (i)  $\Gamma_k$  is null. (ii)  $\Gamma_k$  is not null, but the solution of Dixon's reduced linear equation is not compatible to  $PS_k$ . (iii)  $T_k$  is null.

Now, we can easily derive a polynomial  $R_k^0(\omega) (\leq R_k(x,y,\omega))$  with positive leading coefficient or  $R_k^0(\omega) (\geq R_k(x,y,\omega))$  with negative leading coefficient by replacing  $\cos\omega\tau$  and  $\sin\omega\tau$  in  $R_k(x,y,\omega)$  with 1 or  $-1$ . Thus, it is possible to solve the polynomial  $R_k^0(\omega)$  numerically for the maximal real root  $\omega_0$ . If  $\omega > \omega_0$ , either  $R_k(x,y,\omega) \geq R_k^0(\omega) > 0$  or  $R_k(x,y,\omega) \leq R_k^0(\omega) < 0$  holds. In order that the condition  $p_k(i\omega,\tau) \neq 0$  holds for  $(\omega,\tau) \in [0, +\infty) \times [\underline{\tau}, \bar{\tau}]$ , it is necessary to check the conditions in Theorem 4.4.2 on the region  $[0, \omega_0] \times [\underline{\tau}, \bar{\tau}]$ .

On the basis of Theorem 4.4.2, the robust stability analysis of vertex quasi-polynomials can be completed with help of the computer algebra platforms such as MAPLE and MATLAB. In practice, the MAPLE command "implicitplot" or better "algcurves[plot\_real\_curve]", or MATLAB command "ezplot" provides an

effective graphical tool to testify if  $p_k(i\omega, \tau) \neq 0$  is true on  $[0, \omega_0] \times [\underline{\tau}, \bar{\tau}]$ . Graphically, we need to check whether the graphs of  $\cos\omega\tau = x^0(\omega)$  and  $\sin\omega\tau = y^0(\omega)$  intersect with each other on  $[0, \omega_0] \times [\underline{\tau}, \bar{\tau}]$ , or even more directly to check whether the graphs of  $\text{Re}[p_k(i\omega, \tau)] = 0$  and  $\text{Im}[p_k(i\omega, \tau)] = 0$  intersect with each other on  $[0, \omega_0] \times [\underline{\tau}, \bar{\tau}]$ .

#### 4.4.3 Stability of Edge Quasi-polynomials

Now, we check whether the inequality  $p_j(i\omega, \tau, \mu) \neq 0$  holds true for any  $\mu \in [0, 1]$ ,  $\tau \in [\underline{\tau}, \bar{\tau}]$  and  $\omega \geq 0$  according to Theorem 4.4.1. This task is equivalent to check whether the following polynomial equation

$$z^2 p_i(i\omega, \tau) + p_j(i\omega, \tau) = 0 \quad (4.4.11)$$

has no real root  $z$  for any  $\tau \in [\underline{\tau}, \bar{\tau}]$  and  $\omega \geq 0$ , where  $z^2 = (1 - \mu)/\mu$  takes all the non-negative values with an increase of  $\mu$  in  $[0, 1]$ .

Let

$$R_i(\omega, \tau) \equiv \text{Re}[p_i(i\omega, \tau)], \quad S_i(\omega, \tau) \equiv \text{Im}[p_i(i\omega, \tau)], \quad i=1, 2, \dots, r. \quad (4.4.12)$$

Then, we write Eq. (4.1.11) as

$$[z^2 R_i(\omega, \tau) + R_j(\omega, \tau)]^2 + [z^2 S_i(\omega, \tau) + S_j(\omega, \tau)]^2 = 0, \quad (4.4.13)$$

namely,

$$az^4 + bz^2 + c = 0, \quad (4.4.14)$$

where

$$\begin{cases} a \equiv a(\omega, \tau) \equiv R_i^2(\omega, \tau) + S_i^2(\omega, \tau) \geq 0, \\ b \equiv b(\omega, \tau) \equiv 2[R_i(\omega, \tau)R_j(\omega, \tau) + S_i(\omega, \tau)S_j(\omega, \tau)], \\ c \equiv c(\omega, \tau) \equiv R_j^2(\omega, \tau) + S_j^2(\omega, \tau) \geq 0. \end{cases} \quad (4.4.15)$$

From the elementary algebra, the following statement is obviously true.

**Lemma 4.4.1** For  $a > 0$ ,  $az^4 + bz^2 + c = 0$  has no real roots if and only if either of the following two conditions holds

- (a)  $b \geq 0$ ,  $c > 0$ ;
- (b)  $b < 0$  and  $b^2 - 4ac < 0$ .

The Hurwitz stability of  $p_i(\lambda, \tau)$  and  $p_j(\lambda, \tau)$  implies that  $a > 0$  and  $c > 0$ . This fact, together with Lemma 4.4.1, leads to the following theorem.

**Theorem 4.4.3** Assume that the vertex quasi-polynomials  $p_i(\lambda, \tau)$  and  $p_j(\lambda, \tau)$  are robust Hurwitz stable for any  $\tau \in [\underline{\tau}, \bar{\tau}]$ . Then the two-parameter family  $p_{ij}(\lambda, \tau, \mu)$  is robust Hurwitz stable for  $\tau \in [\underline{\tau}, \bar{\tau}]$  and  $\mu \in [0, 1]$  if and only if either of the following conditions holds true for any  $\tau \in [\underline{\tau}, \bar{\tau}]$  and  $\omega \geq 0$ .

- (a)  $b \geq 0$ .
- (b)  $b < 0$  and  $b^2 - 4ac < 0$ .

According to the definition of  $b = b(\omega, \tau)$  in Eq. (4.4.15), the coefficient  $b$  is a polynomial with respect to  $\omega$ ,  $\cos\omega\tau$  and  $\sin\omega\tau$ . The leading coefficient with respect to  $\omega$  is positive and independent of  $\cos\omega\tau$  and  $\sin\omega\tau$ . It is easy to get a polynomial  $b_0(\omega) (\leq b(\omega, \tau))$  with positive leading coefficient by replacing  $\cos\omega\tau$  and  $\sin\omega\tau$  in  $b(\omega, \tau)$  with 1 or  $-1$ . Thus, it is possible to find out the maximal root  $\omega_0$  for polynomial  $b_0(\omega)$  numerically. If  $\omega > \omega_0$ , then  $b = b(\omega, \tau) \geq b_0(\omega) > 0$ . Thus, we only need to check the conditions of Theorem 4.4.3 on the rectangle  $[0, \omega_0] \times [\underline{\tau}, \bar{\tau}]$ . From Theorem 4.4.3, the following theorem is obviously true.

**Theorem 4.4.4** Assume that the vertex quasi-polynomials  $p_i(\lambda, \tau)$  and  $p_j(\lambda, \tau)$  are robust Hurwitz stable for any  $\tau \in [\underline{\tau}, \bar{\tau}]$ . If

$$\min_{[0, \omega_0] \times [\underline{\tau}, \bar{\tau}]} b(\omega, \tau) \geq 0 \quad \text{or} \quad \max_{[0, \omega_0] \times [\underline{\tau}, \bar{\tau}]} (b^2 - 4ac) < 0, \quad (4.4.16)$$

the two-parameter family  $p_{ij}(\lambda, \tau, \mu)$  is robust Hurwitz stable for any  $\tau \in [\underline{\tau}, \bar{\tau}]$  and  $\mu \in [0, 1]$ .

Suppose that  $b(\hat{\omega}, \hat{\tau}) \equiv \min_{[0, \omega_0] \times [\underline{\tau}, \bar{\tau}]} b(\omega, \tau)$ , then we have

$$\frac{\partial}{\partial \omega} b(\omega, \tau) \Big|_{(\hat{\omega}, \hat{\tau})} = 0 \quad \text{and} \quad \frac{\partial}{\partial \tau} b(\omega, \tau) \Big|_{(\hat{\omega}, \hat{\tau})} = 0, \quad (4.4.17)$$

where  $\partial b / \partial \omega$  and  $\partial b / \partial \tau$  are the polynomials with respect to  $\omega$ ,  $\cos\omega\tau$  and  $\sin\omega\tau$ . Using the Dixon's resultant elimination here again, we can find out the extreme points  $(\hat{\omega}, \hat{\tau})$  and the corresponding extreme values. It is easy to complete the same work for  $b^2 - 4ac$ .

Once the extreme point of  $b(\omega, \tau)$  or  $b^2 - 4ac$  is in hand, we need to check the conditions in Theorem 4.4.3 only on the sub-regions near the extreme points rather than the whole rectangle  $[0, \omega_0] \times [\underline{\tau}, \bar{\tau}]$ . This may greatly reduce the unnecessary computation.

In practice, the robust stability test for the edge quasi-polynomials can be graphically completed as follows.

#### Algorithm 4.4.1

- (a) Compute the coefficients  $a(\omega, \tau)$ ,  $b(\omega, \tau)$ ,  $c(\omega, \tau)$  and the polynomial  $b_0(\omega)$  with maximal root  $\omega_0$ .

(b) Plot the graphs of  $b(\omega, \tau) = 0$  and  $b^2(\omega, \tau) - 4a(\omega, \tau)c(\omega, \tau) = 0$  on the rectangle  $[0, \omega_0] \times [\underline{\tau}, \bar{\tau}]$ . These two graphs usually divide  $[0, \omega_0] \times [\underline{\tau}, \bar{\tau}]$  into several sub-regions.

(c) Check the stability. If there exist any sub-regions where conditions  $b \leq 0$  and  $b^2 - 4ac \geq 0$  are true, then the edge family is not robust Hurwitz stable there. Otherwise, the edge family is robust Hurwitz stable.

#### 4.4.4 A sufficient and Necessary Condition

In summary, the main result of this section can be stated as a sufficient and necessary condition that governs the robust Hurwitz stability of the entire family.

**Theorem 4.4.5** The family  $\mathcal{II}$  of quasi-polynomials is robust Hurwitz stable if and only if the following two conditions hold true.

(a) For each vertex quasi-polynomial family  $p_k(\lambda, \tau)$ , (i) the quasi-polynomial  $p_k(\lambda, \underline{\tau})$  is Hurwitz stable and  $\Gamma_k$  is null; or (ii)  $\Gamma_k$  is not null, but the solution of Dixon's reduced linear equation from  $PS_k$  is not compatible to  $PS_k$ ; or (iii)  $T_k$  is null.

(b) For each edge generated by  $p_i(\lambda, \tau)$  and  $p_j(\lambda, \tau)$ , the condition  $b \geq 0$  or the condition  $b < 0$  and  $b^2 - 4ac < 0$  holds true on the rectangle  $[0, \omega_0] \times [\underline{\tau}, \bar{\tau}]$ .

The test of robust Hurwitz stability on the basis of Theorem 4.4.5 requires testing the Hurwitz stability of some fixed quasi-polynomials, some one-parameter quasi-polynomials and two-parameter quasi-polynomials only. Here, the stability test of any family of quasi-polynomials can be made by means of the Dixon's resultant elimination for polynomial equations. In addition, the condition of Theorem 4.4.5 gives a combined analytical and numerical procedure, which can be completed effectively by combining the Nyquist diagrams and the parametric plots. As a result, the robust Hurwitz stability for the non-polytopic family  $\mathcal{II}$  can be completed if the analytical procedures and numerical routines, or the Nyquist diagrams and the parametric plots, are implemented together.

#### 4.4.5 An Illustrative Example

To demonstrate the proposed approach, the robust Hurwitz stability of a single-degree-of-freedom system with two commensurate time delays in the state feedback is considered. The motion of the system is governed by

$$\ddot{x} + 0.05\dot{x} + x = ux(t - 2\tau) + 0.5\dot{x}(t - \tau), \quad (4.4.18)$$



or alternatively by the characteristic equation

$$p(\lambda, u, \tau) \equiv \lambda^2 + 0.05\lambda + 1 - ue^{-2\lambda\tau} - 0.5\lambda e^{-\lambda\tau} = 0. \quad (4.4.19)$$

The robust Hurwitz stability is checked for a family  $\Pi$  of quasi-polynomials

$$\Pi \equiv \{p(\lambda, u, \tau) \mid u \in [0.375, 0.625], \tau \in [0.675, 1.125]\}. \quad (4.4.20)$$

The straightforward computation based on the proposed approach shows that the zero solution of the non-polytopic family is robust Hurwitz stable. For the sake of brevity, we only look at the graphic results, instead of the analytic and numeric procedures of test.

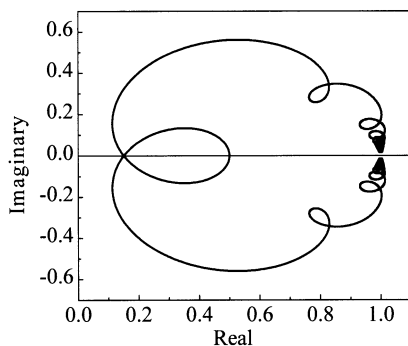


Fig. 4.4.1. The Nyquist diagram of  $p(i\omega, 0.5, 0.9)/(i\omega + 1)^2$

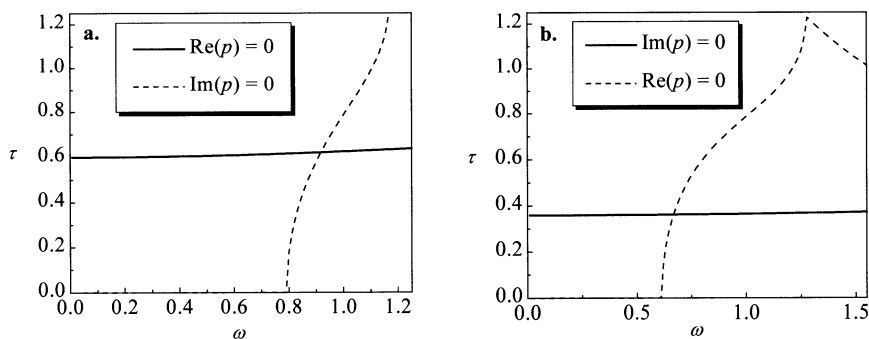
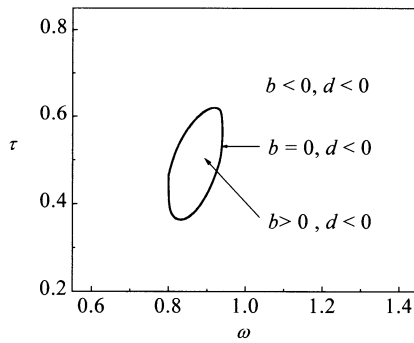


Fig. 4.4.2. Real and imaginary parts; a.  $p(i\omega, 0.375, \tau) = 0$ , b.  $p(i\omega, 0.625, \tau) = 0$



**Fig. 4.4.3.** The graph of  $b(\omega, \tau) = 0$

Figure 4.4.1 shows that the quasi-polynomial  $p(\lambda, 0.5, 0.9)$  is Hurwitz stable since the Nyquist diagram does not contain the origin of the complex plane. Figure 4.4.2 indicates that the real and imaginary parts do not reach zero simultaneously on the rectangle  $[0, \omega_0] \times [\underline{\tau}, \bar{\tau}]$ , and then the two vertex quasi-polynomials  $p(\lambda, 0.375, \tau)$  and  $p(\lambda, 0.625, \tau)$  satisfy the inequalities  $p(i\omega, 0.375, \tau) \neq 0$  and  $p(i\omega, 0.625, \tau) \neq 0$  respectively on the rectangle  $[0, \omega_0] \times [\underline{\tau}, \bar{\tau}]$ . Thus,  $p(\lambda, 0.375, \tau)$  and  $p(\lambda, 0.625, \tau)$  are Hurwitz stable for any  $\tau \in [0.675, 1.125]$ . In Fig. 4.4.3, the graph of  $b(\omega, \tau) = 0$  divides the corresponding rectangle  $[0, \omega_0] \times [\underline{\tau}, \bar{\tau}]$  into two parts by, while  $b^2 - 4ac$  is negative and does not appear in Fig. 4.4.3. Therefore, Eq. (4.4.14) corresponding to Eq. (4.4.20) has no real root  $z$ . As a result,  $\Pi$  is robust Hurwitz stable.

## 5 Effects of a Short Time Delay on System Dynamics

In many controlled mechanical systems, the unavoidable time delays are much shorter than the shortest period of system vibration. If this is the case, the controllers are usually designed according to well-developed control strategies, say optimal control, neglecting the time delays in the controllers and actuators. After the design, one may wonder whether the controlled system is still asymptotically stable if any short time delays appear in the feedback, whether the system stability is robust with respect to the small variation of feedback gains, and so forth. These questions have been answered in part in previous chapters when the system is of single degree of freedom. Nevertheless, tremendous computational efforts have to be made when the system dimension increases. To reduce the computational cost, hence, approximate approaches are preferable in practice.

This chapter presents several approximate approaches to estimating the stability and the robust stability of linear systems with a short feedback time delay, respectively. Then, it discusses the validity of the Taylor expansion of delay terms through the examples of both linear and nonlinear oscillators when they are equipped with the feedback involving a short time delay.

### 5.1 Stability Estimation of High Dimensional Systems

Consider a linear, time-invariant system of  $n$  degrees of freedom under the state feedback control with a bounded time delay  $0 \leq \tau \leq \rho$ . The motion of the system yields

$$M\ddot{x}(t) + C\dot{x}(t) + Kx(t) = f(t) + Ux(t-\tau) + V\dot{x}(t-\tau), \quad (5.1.1)$$

where  $x \in R^n$  is the vector of displacement,  $M \in R^{n \times n}$ ,  $C \in R^{n \times n}$ ,  $K \in R^{n \times n}$  are the matrices of mass, damping and stiffness in the usual sense,  $U \in R^{n \times n}$  and  $V \in R^{n \times n}$  are the feedback gain matrices for the displacement and the velocity paths, respectively. In general, these matrices, especially those of feedback gains, are not necessarily symmetric. In contrast to the Hamiltonian description, i.e., the state description, of controlled systems in most publications, the Lagrangian description

here will enable one to simplify computation and to gain an insight into the system dynamics as well.

Let  $C^n$  denote the complex space of  $n$  dimensions. Substituting the candidate solution  $x(t)=ae^{\lambda t}$ , where  $\lambda \in C^1$  and  $a \in C^n$ , into Eq. (5.1.1) yields a transcendental eigenvalue problem

$$D(\lambda, \tau)a=0, \tag{5.1.2}$$

with

$$D(\lambda, \tau) \equiv \lambda^2 M + \lambda C + K - e^{-\lambda \tau} (U + \lambda V) \in C^{n \times n}. \tag{5.1.3}$$

The system is asymptotically stable if and only if all the eigenvalues of Eq. (5.1.2) have negative real parts.

Meanwhile, we have the adjoint eigenvalue problem of Eq. (5.1.2)

$$b^* D(\lambda, \tau) \equiv \bar{b}^T D(\lambda, \tau) = 0, \quad b \in C^n, \tag{5.1.4}$$

Hereinafter, the asterisk always represents the transpose and conjugate operator. Even though Eq. (5.1.4) does not offer any new information on the system dynamics, it will be helpful to simplify the algebraic manipulation later.

### 5.1.1 Distribution of Eigenvalues Subject to a Short Time Delay

The characteristic function corresponding to Eq. (5.1.2) reads

$$D(\lambda, \tau) \equiv \det D(\lambda, \tau) = \det[\lambda^2 M + \lambda C + K - e^{-\lambda \tau} (U + \lambda V)]. \tag{5.1.5}$$

A controlled system is usually designed to be stable when the time delay in the state feedback vanishes. Henceforth, we assume that all the  $2n$  roots of  $D(\lambda, 0)$  have negative real parts throughout this section.

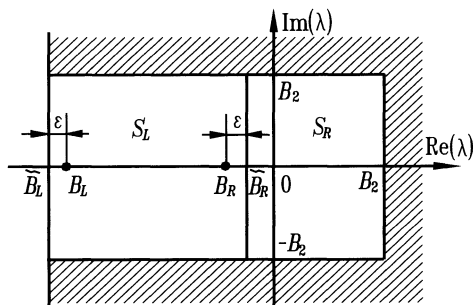


Fig. 5.1.1 Existence region of the roots of  $D(\lambda, \tau)$  on the complex plane

As shown in Fig. 5.1.1, let  $B_L < 0$  and  $B_R < 0$  be the smallest real part and the largest real part of these roots respectively, and  $B_I > 0$  be the bound of all imaginary parts of the roots in absolute value. Moreover, two bounds are defined for later use

$$\tilde{B}_L \equiv B_L - \varepsilon < 0, \quad \tilde{B}_R \equiv B_R + \varepsilon < 0, \tag{5.1.6}$$

where  $\varepsilon$  is a small positive number, that ensures the above inequalities. In what follows, we study the effect of a short time delay on the number and the distribution of the roots of Eq. (5.1.5) on the complex plane spanned. We shall show that Eq. (5.1.5) has only  $2n$  roots near those of  $D(\lambda, 0)$  if the time delay is short enough.

We first exclude the roots of Eq. (5.1.5) from the shaded region in Fig. 5.1.1. Equation (5.1.5) can be written as

$$D(\lambda, \tau) = p_0(\lambda^{2n} + p_1\lambda^{2n-1} + \dots + p_{2n}) = 0, \quad p_0 \neq 0. \tag{5.1.7}$$

where  $p_j, j=0, 1, \dots, 2n$  are the polynomials in terms of the entries of matrices  $M, C, K, U$  and  $V$ , as well as  $e^{-\lambda\tau}$ . It is easy to see that on the right half-plane  $\text{Re}(\lambda) > \tilde{B}_L$ , the following inequality holds

$$|e^{-\lambda\tau}| = e^{-\text{Re}(\lambda)\tau} < e^{-\tilde{B}_L\tau} \quad \text{for } 0 \leq \tau \leq \rho. \tag{5.1.8}$$

Thus,  $p_j, j=0, 1, \dots, 2n$  are bounded in absolute value. This fact enables one to define two bounds

$$B_1 \equiv \max_{1 \leq j \leq 2n} |p_j| \quad \text{for } \text{Re}(\lambda) > \tilde{B}_L, \quad 0 \leq \tau \leq \rho, \tag{5.1.9}$$

$$B_2 \equiv \max\{1, B_1, (2n+1)B_1\}. \tag{5.1.10}$$

There follows the inequality

$$\begin{aligned} |D(\lambda, \tau)| &= |p_0| \left| \lambda^{2n} + p_1\lambda^{2n-1} + \dots + p_{2n} \right| \geq |p_0| |\lambda|^{2n} \left( 1 - \frac{|p_1|}{|\lambda|} - \dots - \frac{|p_{2n}|}{|\lambda|^{2n}} \right) \\ &\geq |p_0| B_2^{2n} \left( 1 - \frac{2nB_1}{B_2} \right) > |p_0| B_2^{2n} \left( 1 - \frac{2n}{2n+1} \right) > 0. \end{aligned} \tag{5.1.11}$$

This inequality implies that none of the roots of Eq. (5.1.5) exists in the shaded region in Fig. 5.1.1 if  $0 \leq \tau \leq \rho$ .

Next, we analyze the possibility of the roots of  $D(\lambda, \tau)$  falling into the right closed rectangle  $S_R \equiv \{ \lambda \mid \tilde{B}_R \leq \text{Re}(\lambda) \leq B_2, \text{Im}(\lambda) \leq B_2 \}$ . For this purpose, rewrite  $D(\lambda, \tau)$  in  $S_R$  as

$$D(\lambda, \tau) = D(\lambda, 0) + Q(\lambda, \tau), \quad \text{with } Q(\lambda, 0) \equiv 0. \quad (5.1.12)$$

It is obvious that no root of  $D(\lambda, 0)$  exists in the closed rectangle  $S_R$ , thereby

$$B_3 \equiv \min_{\lambda \in S_R} |D(\lambda, 0)| > 0. \quad (5.1.13)$$

From the continuity of  $D(\lambda, \tau)$  with respect to  $\tau$ , there exists a small, positive number  $\delta_R = \delta(\varepsilon) < \rho$  such that

$$\max_{\lambda \in S_R} |Q(\lambda, \tau)| < B_3, \quad 0 \leq \tau < \delta_R. \quad (5.1.14)$$

Consequently, we have

$$|D(\lambda, \tau)| > |D(\lambda, 0)| - |Q(\lambda, \tau)| > B_3 - \max_{\lambda \in S_R} |Q(\lambda, \tau)| > 0, \quad 0 \leq \tau < \delta_R, \quad (5.1.15)$$

which excludes the roots of  $D(\lambda, \tau)$  from the closed rectangle  $S_R$ .

Finally, we study the number of roots of  $D(\lambda, \tau)$  in the left closed rectangular region  $S_L \equiv \{\lambda \mid \tilde{B}_L \leq \text{Re}(\lambda) \leq \tilde{B}_R, \text{Im}(\lambda) \leq B_2\}$ , where  $D(\lambda, \tau)$  can be written as Eq. (5.1.12) again. The definitions of bounds  $\tilde{B}_L$ ,  $\tilde{B}_R$  and  $B_2$  ensure that there is no root of  $D(\lambda, 0)$  on the boundary  $\Gamma$  of the closed region  $S_L$ , namely

$$B_4 \equiv \min_{\lambda \in \Gamma} |D(\lambda, 0)| > 0. \quad (5.1.16)$$

Also from the continuity of  $D(\lambda, \tau)$  with respect to  $\tau$ , there exists a small, positive number  $\delta_L = \delta(\varepsilon) < \rho$  such that

$$\max_{\lambda \in \Gamma} |Q(\lambda, \tau)| < B_4, \quad 0 \leq \tau < \delta_L. \quad (5.1.17)$$

According to the Rouché's theorem in complex analysis, the number of roots of  $D(\lambda, \tau)$  in the closed rectangle  $S_L$  is the same as that of  $D(\lambda, 0)$  in  $S_L$  provided that  $0 \leq \tau < \delta_L$ . The above analysis can be summarized as a useful theorem.

**Theorem 5.1.1** Given  $\varepsilon > 0$ , there exists a bound  $\delta(\varepsilon) = \min(\delta_L(\varepsilon), \delta_R(\varepsilon))$  for the time delay  $\tau$  such that  $D(\lambda, \tau)$  continues to have  $2n$  roots in the closed rectangle  $S_L$  if  $0 < \tau < \delta(\varepsilon)$ . However, the region of distribution of these roots on the complex plane may become slightly larger.

Without loss of generality, we can assume that the roots with the largest real part are a pair of complex roots of  $D(\lambda, 0)$  and distinct from the other roots of  $D(\lambda, 0)$ . Let  $\tilde{B}_L$  be greater than the second largest real part of the roots, we can similarly prove that  $D(\lambda, \tau)$  has a pair of complex roots only in the narrow strip  $S_L$  when  $0 < \tau < \delta(\varepsilon)$ . In this case, the real part of this pair of complex roots is bounded within  $[\tilde{B}_L, \tilde{B}_R]$ . We can therefore estimate the stability of the system

with delayed feedback simply from the variation of a single pair of roots of  $D(\lambda,0)$ , provided that the time delay is sufficiently short. This pair of roots will be referred to as “the most dangerous eigenvalues” hereafter for simplicity.

### 5.1.2 Estimation of Eigenvalues

Should there exist no time delay in the state feedback, Eqs. (5.1.2) and (5.1.4) would become a pair of adjoint, quadratic eigenvalue problems, the solutions of which yield

$$\begin{cases} D(\lambda_r,0)\mathbf{a}_r = [\lambda_r^2 \mathbf{M} + \lambda_r (\mathbf{C}-\mathbf{V}) + (\mathbf{K}-\mathbf{U})]\mathbf{a}_r = 0, \\ \mathbf{b}_r^* D(\lambda_r,0) = \mathbf{b}_r^* [\lambda_r^2 \mathbf{M} + \lambda_r (\mathbf{C}-\mathbf{V}) + (\mathbf{K}-\mathbf{U})] = 0, \end{cases} \quad r=1,2,\dots,2n, \quad (5.1.18)$$

where  $\lambda_r \in \mathbb{C}^1$  and  $\lambda_{n+r} = \bar{\lambda}_r \in \mathbb{C}^1$ ,  $r=1,2,\dots,n$  are  $n$  pairs of conjugate complex eigenvalues,  $\mathbf{a}_r \in \mathbb{C}^n$ ,  $\mathbf{a}_{r+n} = \bar{\mathbf{a}}_r \in \mathbb{C}^n$ ,  $\mathbf{b}_r \in \mathbb{C}^n$  and  $\mathbf{b}_{r+n} = \bar{\mathbf{b}}_r \in \mathbb{C}^n$ ,  $r=1,2,\dots,n$  are the corresponding eigenvectors. Specifically, all the eigenvectors are scaled to

$$\mathbf{a}_r^* \mathbf{a}_r = \mathbf{b}_r^* \mathbf{b}_r = 1, \quad r=1,2,\dots,2n. \quad (5.1.19)$$

When the feedback control involves a short time delay, there exists an eigenvalue  $\tilde{\lambda}_r$  near the eigenvalue  $\lambda_r$ . Similarly there is a corresponding eigenvector  $\tilde{\mathbf{a}}_r$  near  $\mathbf{a}_r$ . In this subsection, we study how to determine  $\tilde{\lambda}_r$  and  $\tilde{\mathbf{a}}_r$  for a specific time delay  $\tau$  when  $\lambda_r$  and  $\mathbf{a}_r$  are given, whereas

$$\tilde{\lambda}_r = \lambda_r + \Delta\lambda_r, \quad \tilde{\mathbf{a}}_r = \mathbf{a}_r + \Delta\mathbf{a}_r, \quad \tilde{\mathbf{a}}_r^* \mathbf{a}_r = 1. \quad (5.1.20)$$

#### (1) Approach based on truncated perturbation of an eigenvalue

Substituting the first two equations in Eq. (5.1.20) into Eq. (5.1.2) and dropping the higher order terms of  $\Delta\lambda_r$ ,  $\Delta\lambda_r \Delta\mathbf{a}_r$  and so on., we have

$$D(\lambda_r, \tau)(\mathbf{a}_r + \Delta\mathbf{a}_r) - \Delta\lambda_r E(\lambda_r, \tau)\mathbf{a}_r = 0, \quad (5.1.21)$$

where

$$E(\lambda_r, \tau) \equiv -\frac{d}{d\lambda} D(\lambda, \tau)|_{\lambda=\lambda_r} = -\{2\lambda_r \mathbf{M} + \mathbf{C} + e^{-\lambda_r \tau} [(U + \lambda_r V)\tau - V]\} \in \mathbb{C}^{n \times n}. \quad (5.1.22)$$

To solve Eq. (5.1.21) for  $\Delta\lambda_r$  and  $\Delta\mathbf{a}_r$ , we construct a set of linear equations in the unknown complex vector  $\mathbf{p}_r$

$$D(\lambda_r, \tau)\mathbf{p}_r = E(\lambda_r, \tau)\mathbf{a}_r. \quad (5.1.23)$$

Because  $\lambda_r$  is not the eigenvalue of Eq. (5.1.2) when  $\tau > 0$ , the matrix  $\mathbf{D}(\lambda_r, \tau)$  in Eq. (5.1.23) is invertible. Besides,  $\mathbf{E}(\lambda_r, \tau)\mathbf{a}_r$  must be a non-zero vector. Otherwise Eq. (5.1.21) implies that  $\lambda_r$  is the eigenvalue of Eq. (5.1.2). The solution of Eq. (5.1.23) thus is a unique non-zero vector  $\mathbf{p}_r$ . Comparing Eq. (5.1.23) with Eq. (5.1.21) yields

$$\tilde{\mathbf{a}}_r = \mathbf{a}_r + \Delta\mathbf{a}_r = \Delta\lambda_r \mathbf{p}_r, \tag{5.1.24}$$

Namely,  $\mathbf{p}_r$  is an eigenvector associated with the eigenvalue  $\tilde{\lambda}_r$  of Eq. (5.1.2).

Following the idea of the Rayleigh quotient, we have

$$\frac{\mathbf{p}_r^* \mathbf{D}(\lambda_r, \tau) \mathbf{p}_r}{\mathbf{p}_r^* \mathbf{E}(\lambda_r, \tau) \mathbf{p}_r} = \frac{\frac{\tilde{\mathbf{a}}_r^* \mathbf{E}(\lambda_r, \tau) \mathbf{a}_r}{\Delta\tilde{\lambda}_r}}{\frac{\tilde{\mathbf{a}}_r^* \mathbf{E}(\lambda_r, \tau) (\mathbf{a}_r + \Delta\mathbf{a}_r)}{\Delta\lambda_r \Delta\tilde{\lambda}_r}} = \Delta\lambda_r [1 - \frac{\tilde{\mathbf{a}}_r^* \mathbf{E}(\lambda_r, \tau) \Delta\mathbf{a}_r}{\tilde{\mathbf{a}}_r^* \mathbf{E}(\lambda_r, \tau) \mathbf{a}_r} + \dots]. \tag{5.1.25}$$

There follows an explicit expression for  $\Delta\lambda_r$

$$\Delta\lambda_r \approx \frac{\mathbf{p}_r^* \mathbf{D}(\lambda_r, \tau) \mathbf{p}_r}{\mathbf{p}_r^* \mathbf{E}(\lambda_r, \tau) \mathbf{p}_r} = \frac{\mathbf{p}_r^* [\lambda_r^2 \mathbf{M} + \lambda_r \mathbf{C} + \mathbf{K} - e^{-\lambda_r \tau} (\mathbf{U} + \lambda_r \mathbf{V})] \mathbf{p}_r}{\mathbf{p}_r^* \{2\lambda_r \mathbf{M} + \mathbf{C} + e^{-\lambda_r \tau} [(\mathbf{U} + \lambda_r \mathbf{V})\tau - \mathbf{V}]\} \mathbf{p}_r}. \tag{5.1.26}$$

Substituting Eqs. (5.1.26) and (5.1.24) into Eq. (5.1.21), we have the new eigenvalue and the eigenvector.

### (2) Simplified approach based on truncation of a very short time delay

If the time delay  $\tau$  is so short that the delay phase  $|\lambda_r \tau| \ll 1$ , we can write the matrices  $\mathbf{D}(\lambda_r, \tau)$  and  $\mathbf{E}(\lambda_r, \tau)$  as a truncated Taylor expansion at  $\lambda_r$  with respect to  $\lambda_r \tau$  and then have

$$\begin{cases} \mathbf{D}(\lambda_r, \tau) \approx \mathbf{D}(\lambda_r, 0) + \lambda_r \tau (\mathbf{U} + \lambda_r \mathbf{V}), \\ \mathbf{E}(\lambda_r, \tau) \approx \mathbf{E}(\lambda_r, 0) = -(2\lambda_r \mathbf{M} + \mathbf{C} - \mathbf{V}). \end{cases} \tag{5.1.27}$$

Substituting Eq. (5.1.27) into Eq. (5.1.21) yields

$$\mathbf{D}(\lambda_r, 0) \Delta\mathbf{a}_r + \lambda_r \tau (\mathbf{U} + \lambda_r \mathbf{V}) \mathbf{a}_r - \Delta\lambda_r \mathbf{E}(\lambda_r, 0) \mathbf{a}_r = 0. \tag{5.1.28}$$

Premultiplying Eq. (5.1.28) by the left eigenvector  $\mathbf{b}_r^*$  associated with eigenvalue  $\lambda_r$ , we have

$$\lambda_r \tau \mathbf{b}_r^* (\mathbf{U} + \lambda_r \mathbf{V}) \mathbf{a}_r - \Delta\lambda_r \mathbf{b}_r^* \mathbf{E}(\lambda_r, 0) \mathbf{a}_r = 0. \tag{5.1.29}$$

As proved in Subsection 5.1.4,  $\mathbf{a}_r$  and  $\mathbf{b}_r^*$  satisfy



$$\mathbf{b}_r^* \mathbf{E}(\lambda_r, 0) \mathbf{a}_r = -\mathbf{b}_r^* (2\lambda_r \mathbf{M} + \mathbf{C} - \mathbf{V}) \mathbf{a}_r \neq 0. \quad (5.1.30)$$

Therefore, the simplified explicit expression for  $\Delta\lambda_r$  reads

$$\Delta\lambda_r = \frac{\lambda_r \mathbf{b}_r^* (\mathbf{U} + \lambda_r \mathbf{V}) \mathbf{a}_r}{\mathbf{b}_r^* \mathbf{E}(\lambda_r, 0) \mathbf{a}_r} \tau = -\frac{\lambda_r \mathbf{b}_r^* (\mathbf{U} + \lambda_r \mathbf{V}) \mathbf{a}_r}{\mathbf{b}_r^* (2\lambda_r \mathbf{M} + \mathbf{C} - \mathbf{V}) \mathbf{a}_r} \tau. \quad (5.1.31)$$

It is easy to verify that Eq. (5.1.31) is identical to the result obtained by the first order perturbation with respect to the small parameter  $\tau$ .

From Eq. (5.1.31), the sensitivity of the eigenvalue module with respect to the time delay can be defined as

$$\mu(\lambda_r) \equiv \left| \frac{\Delta\lambda_r}{\lambda_r \tau} \right| = \left| \frac{\mathbf{b}_r^* (\mathbf{U} + \lambda_r \mathbf{V}) \mathbf{a}_r}{\mathbf{b}_r^* (2\lambda_r \mathbf{M} + \mathbf{C} - \mathbf{V}) \mathbf{a}_r} \right|. \quad (5.1.32)$$

Then, the following two limits hold true

$$\lim_{\lambda_r \rightarrow 0} \mu(\lambda_r) = \left| \frac{\mathbf{b}_r^* \mathbf{U} \mathbf{a}_r}{\mathbf{b}_r^* (\mathbf{C} - \mathbf{V}) \mathbf{a}_r} \right|, \quad \lim_{\lambda_r \rightarrow +\infty} \mu(\lambda_r) = \left| \frac{\mathbf{b}_r^* \mathbf{V} \mathbf{a}_r}{2\mathbf{b}_r^* \mathbf{M} \mathbf{a}_r} \right|. \quad (5.1.33)$$

It is worth noting that the sensitivity is independent of the system stiffness matrix  $\mathbf{K}$ . Keeping these relations in mind, we can estimate the relative change of the eigenvalues owing to a very short time delay.

### (3) Discussions

Presented above are two forms of the new approach for estimating an eigenvalue of the system with delayed feedback. The difference between these forms is the truncation of higher order terms, which consequently effect accuracy and computational effort. If the time delay is so short that  $|\lambda_r \tau| \ll 1$  holds, Eq. (5.1.31) provides an accurate and efficient estimate. If this inequality does not hold, yet  $|\Delta\lambda_r|/|\lambda_r|$  is still a small quantity, the eigenvalue can be estimated from Eq. (5.1.26), where the eigenvector  $\mathbf{p}_r$  has to be determined from a set of  $n$ -dimensional, complex, linear equations in advance.

Even though  $\lambda_r$  is denoted as the eigenvalue of the delay-free system, none of the eigenvalue properties of the delay-free system are used during the analysis. Thus,  $\lambda_r$  can be taken as an initial estimate of the eigenvalue of the delay system and repeatedly use Eq. (5.1.26) as a Newton-Raphson iteration if  $|\Delta\lambda_r|/|\lambda_r|$  is not small. If the time delay  $\tau$  is considered as a parameter, Eq. (5.1.26) can repeatedly be used as a continuation technique to trace the variation of an eigenvalue

with increase in time delay  $\tau$ . This is the third form of the present approach to the case of long time delay and will be demonstrated in the next subsection.

In addition, it is interesting to apply these estimates to an underdamped, single-degree-of-freedom system with delayed feedback. Now Eq. (5.1.26) reads

$$\Delta\lambda_1 = \frac{D(\lambda_1, \tau)}{E(\lambda_1, \tau)} = \frac{\lambda_1^2 m + \lambda_1 c + k - e^{-\lambda_1 \tau} (u + \lambda_1 v)}{2\lambda_1 m + c + e^{-\lambda_1 \tau} [(u + \lambda_1 v)\tau - v]}, \quad (5.1.34)$$

where  $m$ ,  $c$ ,  $k$ ,  $u$  and  $v$  are the scalar parameters corresponding to the matrices in Eq. (5.1.1), and

$$\lambda_1 = \frac{v-c}{2m} + i \frac{\sqrt{4m(k-u) - (c-v)^2}}{2m}. \quad (5.1.35)$$

Similarly, Eq. (5.1.31) in this case becomes

$$\Delta\lambda_1 = \frac{D(\lambda_1, \tau)}{E(\lambda_1, \tau)} = -\frac{\lambda_1 u + \lambda_1^2 v}{2\lambda_1 m + c - v} \tau. \quad (5.1.36)$$

Substituting Eq. (5.1.34) into Eq. (5.1.35) yields

$$\text{Re}(\Delta\lambda_1) = -\frac{mu + v^2 - cv}{2m^2} \tau. \quad (5.1.37)$$

It is worthy to note again that the variation of the real part of the eigenvalue is independent of the system stiffness.

### 5.1.3 Illustrative Examples

#### (1) A 2-DOF system with delayed state feedback

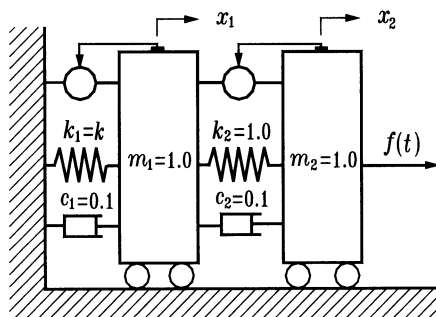


Fig. 5.1.2. A dual-mass system under the state feedback with equal time delays

To demonstrate the merits of the above approaches, consider the stability of the steady-state motion of a dual-mass system with a delayed feedback as shown in Fig. 5.1.2. The motion of the system yields Eq. (5.1.1), where

$$\mathbf{M} = \begin{bmatrix} 1 & 0 \\ 0 & 1 \end{bmatrix}, \quad \mathbf{C} = \begin{bmatrix} 0.2 & -0.1 \\ -0.1 & 0.1 \end{bmatrix}, \quad \mathbf{K} = \begin{bmatrix} k+1 & -1 \\ -1 & 1 \end{bmatrix}, \quad (5.1.38)$$

whereas the stiffness coefficient  $k$  and the feedback gain matrices  $\mathbf{U}$  and  $\mathbf{V}$  will be variously specified in different case studies. As a base comparison, the eigenvalues for a given time delay  $\tau$  in each case were first determined from the intersections of the curves  $\text{Re}[D(\lambda, \tau)] = 0$  and  $\text{Im}[D(\lambda, \tau)] = 0$  plotted numerically on the complex plane of  $\lambda$  by using MAPLE. These eigenvalues are taken as the exact numerical results in what follows. For the sake of simplicity, the terms ST, DT and NR will be used hereafter for the approach based on Single Truncation of eigenvalues, the approach based on Double Truncations of both eigenvalues and the time delay, and the Newton-Raphson iteration on the basis of ST, respectively. Also,  $\tau_r$  will be used to denote the shortest time delay when the  $r$ -th order mode of the delay-free system goes unstable, and referred to as the  $r$ -th critical time delay for short.

**Case 1** As the first and the simplest case, a state feedback was introduced to the system from the right mass to the connection only, so that

$$k=2.0, \quad \mathbf{U} = \begin{bmatrix} 0.0 & 1.0 \\ 0.0 & -1.0 \end{bmatrix}, \quad \mathbf{V} = \begin{bmatrix} 0.0 & 0.1 \\ 0.0 & -0.1 \end{bmatrix}. \quad (5.1.39)$$

The variation of the real and imaginary parts of two eigenvalues with an increase of time delay  $\tau$  is shown in Fig. 5.1.3, where the real parts of two pairs of conjugate eigenvalues vanished when the time delay arrived at the critical values  $\tau_1 \approx 0.396$  and  $\tau_2 \approx 0.418$ , respectively. The results of NR in Fig. 5.1.3 were identical to the exact results represented by circles. Both ST and DT gave good estimates of  $\tau_r$ . The relative errors were -0.1% and 1.5% for the first pair of conjugate eigenvalues, and 3.1% and -0.96% for the second, respectively. As DT provides a linear relationship between an eigenvalue and the time delay, the estimation error, especially that of the second pair of conjugate eigenvalues, became unacceptable when the time delay was longer.

Shown in Fig. 5.1.4 are the curves of  $\text{Re}[D(\lambda, \tau)] = 0$  and  $\text{Im}[D(\lambda, \tau)] = 0$  on the upper half-plane for two specific time delays  $\tau = 0.1$  and  $\tau = 2.5$ , corresponding to a stable status and an unstable status of the system, respectively. Each intersection point of these curves indicates an eigenvalue of Eq. (5.1.2) on the complex plane.

The new eigenvalues emerged in the figure only when the time delay was long enough. It is this fact that makes it possible to analyze the system stability according to the evolution of eigenvalues of the delay-free system.

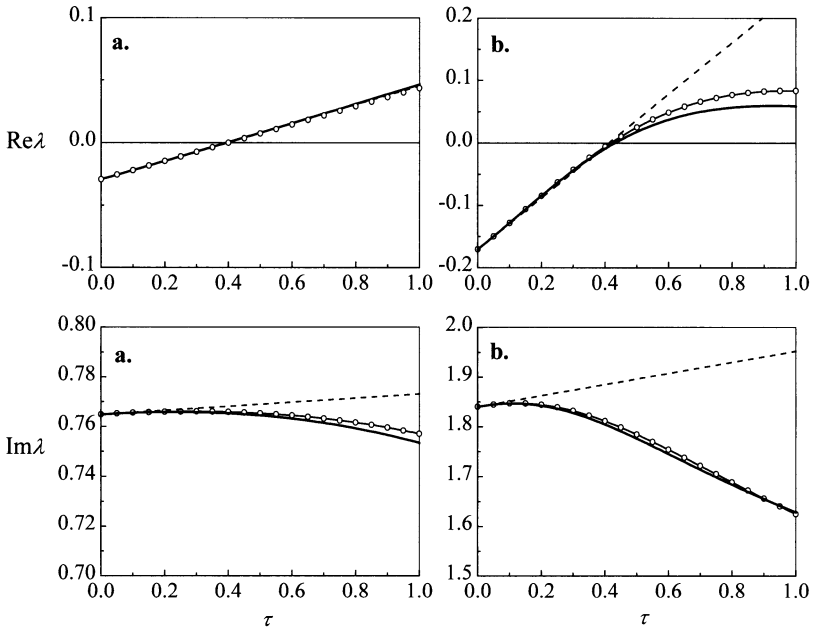


**Fig. 5.1.3.** Variation of the eigenvalues with an increase of time delay in Case 1; **a.** The first eigenvalue, **b.** The second eigenvalue; Key:  $\circ$ — NR, — ST, --- DT

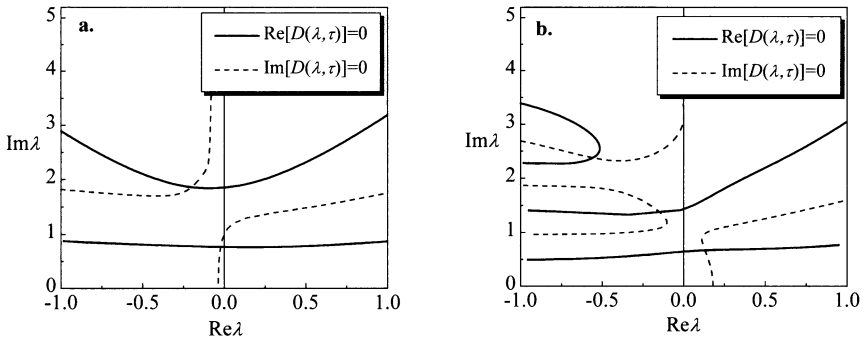


**Fig. 5.1.4.** Distribution of eigenvalues of Eq. (5.1.3) in Case 1; **a.**  $\tau=0.1$ , **b.**  $\tau=2.5$

**Case 2** The type of feedback was kept the same as that in Case 1 and only the velocity feedback gains were increased from  $\pm 0.1$  in Case 1 to  $\pm 1.0$  here. That is,

$$k=2.0, \quad U = \begin{bmatrix} 0.0 & 1.0 \\ 0.0 & -1.0 \end{bmatrix}, \quad V = \begin{bmatrix} 0.0 & 1.0 \\ 0.0 & -1.0 \end{bmatrix}. \quad (5.1.40)$$

The negative velocity feedback reduced the real part of the eigenvalues of the delay-free system, and hence increased the critical time delays. Intuitively speaking, it would appear more difficult to estimate eigenvalues in this case. In Fig. 5.1.5 are shown the variations of the real and imaginary parts of the two pairs of conjugate eigenvalues with increase in time delay, which reached the critical values respectively at  $\tau_1=1.135$  and  $\tau_2=0.644$ , much longer than those in Case 1. Here again the results of NR were the same as the exact results. As shown in Fig. 5.1.5, both ST and DT offered good estimations of the critical time delay  $\tau_1$  with relative errors of  $-1.76\%$  and  $0.44\%$ , respectively. For the estimation of the second critical time delay  $\tau_2$ , ST gave an under-estimation  $\tau_2=0.51$ . However, DT totally failed because of the non-monotonic trend of  $\text{Re}\lambda_2$  with an increase of the time delay. In this case, NR is the more appealing approach even though it required a few iterations. It is important to note that even though  $\lambda_1$  was the "most dangerous eigenvalue" when the system did not involve time delay,  $\text{Re}\lambda_2$  became positive earlier than  $\text{Re}\lambda_1$  when the time delay increased. Hence, the "most dangerous eigenvalue" can change for a sufficiently long time delay.

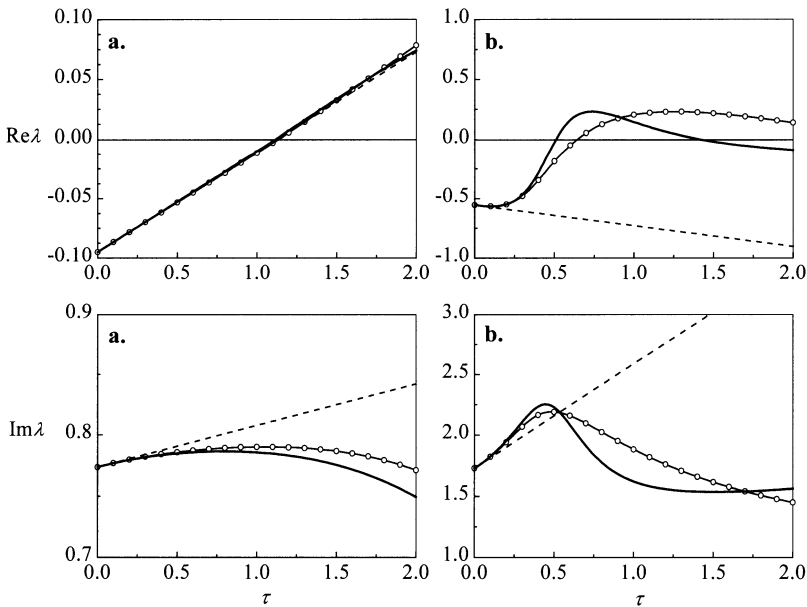


**Fig. 5.1.5.** Variation of the eigenvalues with an increase of time delay in Case 2; **a.** The first eigenvalue, **b.** The second eigenvalue; Key:  $\circ$  NR,  $—$  ST,  $---$  DT

**Case 3** To test the efficacy of the approach, the system was intentionally designed to be more complicated by introducing a stronger displacement feedback from both masses, namely

$$k=2.0, \quad U = \begin{bmatrix} -2.0 & 3.0 \\ 0.0 & -3.0 \end{bmatrix}, \quad V = \begin{bmatrix} 0.0 & 1.0 \\ 0.0 & -1.0 \end{bmatrix}. \quad (5.1.41)$$

As shown in Fig. 5.1.6, the real parts of the first and the second eigenvalues vanished at  $\tau_1=0.139$  and  $\tau_2=0.298$ , respectively. Both ST and DT again gave good estimations for the critical time delay  $\tau_1$  with relative errors of -0.07% and 0.94%, respectively. For more difficult estimation of the second critical time delay  $\tau_2$ , the relative errors of ST and DT were -6.7% and 76%, respectively.

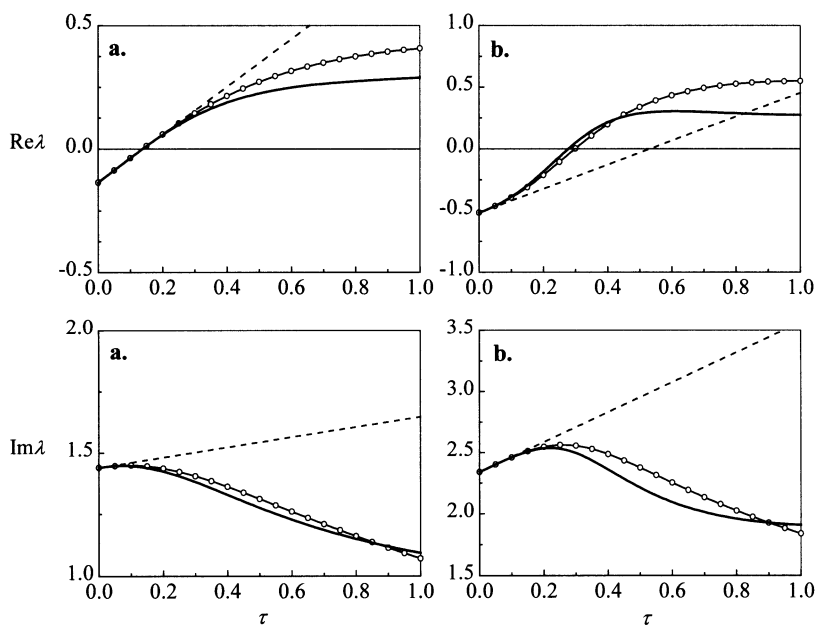


**Fig. 5.1.6.** Variation of the eigenvalues with an increase of time delay in Case 3; **a.** The first eigenvalue, **b.** The second eigenvalue; Key:  $\circ$ — NR, — ST, --- DT

**Case 4** Compared with Case 3, the system was rendered even more complicated by adding the velocity feedback from the left mass to itself, i.e.,

$$k=2.0, \quad U = \begin{bmatrix} -2.0 & 3.0 \\ 0.0 & -3.0 \end{bmatrix}, \quad V = \begin{bmatrix} -1.0 & 1.0 \\ 0.0 & -1.0 \end{bmatrix}. \quad (5.1.42)$$

As shown in Fig. 5.1.7, even though DT failed to estimate accurately the critical time delays for either eigenvalue in this case, both NR and ST worked successfully. For the two critical time delays  $\tau_1=0.383$  and  $\tau_2=0.365$ , the relative errors of ST were respectively 9.1% and 13.8%. Here again the real part of the "nominally less dangerous" eigenvalue  $\lambda_2$  of the delay-free system became positive a little bit earlier than that of the "most dangerous" one when the time delay increased.

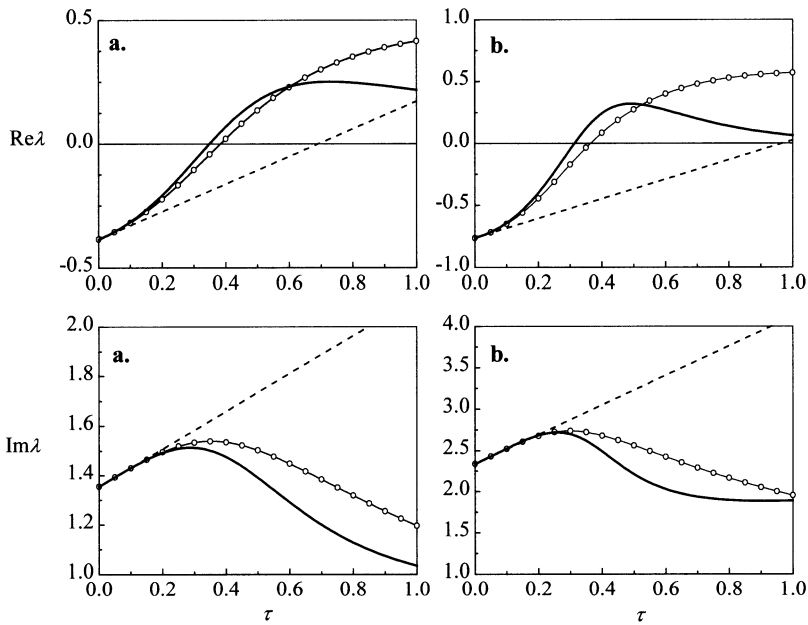


**Fig. 5.1.7.** Variation of the eigenvalues with an increase of time delay in Case 4; **a.** The first eigenvalue, **b.** The second eigenvalue; Key:  $\circ$ — NR, — ST, --- DT

**Case 5** In the final case, the right spring in the system was replaced with an extremely stiff one, while the state feedback was kept the same as that in Case 3, namely

$$k=399.0, \quad U = \begin{bmatrix} -2.0 & 3.0 \\ 0.0 & -3.0 \end{bmatrix}, \quad V = \begin{bmatrix} 0.0 & 1.0 \\ 0.0 & -1.0 \end{bmatrix}. \quad (5.1.43)$$

Figure 5.1.8 shows that the first mode of the system became unstable when the time delay reached  $\tau_1=0.316$ , whereas the second mode remained stable no matter how long the time delay became. Not surprisingly, ST predicted the oscillation of the second eigenvalue with respect to the time delay as accurately as NR did, but

DT gave a totally wrong prediction. This example demonstrates again the premise that ST and DT work well only within the ranges  $|\Delta\lambda_r/\lambda_r| \ll 1$  and  $|\lambda_r\tau| \ll 1$ , respectively.

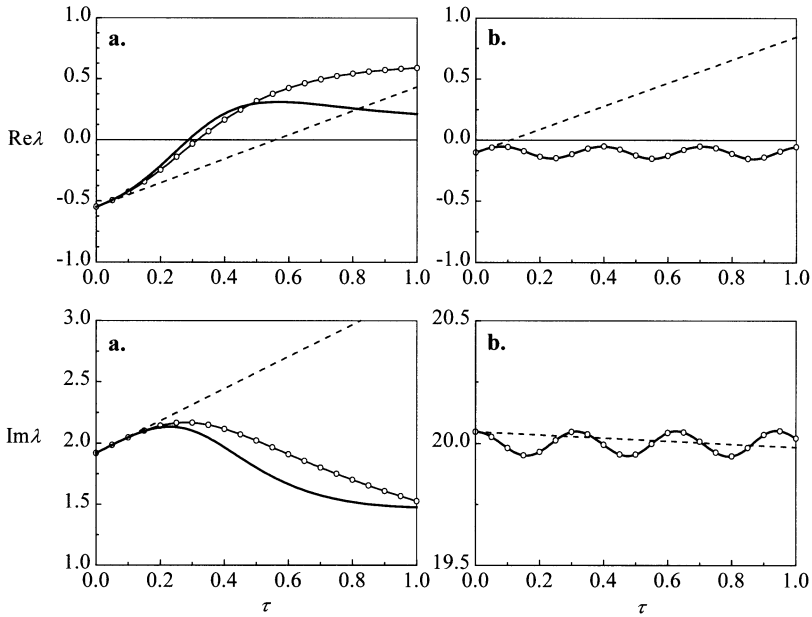


**Fig. 5.1.8.** Variation of the eigenvalues with an increase of time delay in Case 5; **a.** The first eigenvalue, **b.** The second eigenvalue; Key:  $\circ\text{---}\circ$  NR,  $\text{---}$  ST,  $\text{---}$  DT

**(2) A 10-DOF system with delayed velocity feedback**

In order to demonstrate the applicability of the new approach to the stability estimation of high dimensional systems with delayed feedback, a numerical study was made on an undamped chain system of 10 degrees of freedom as shown in Fig. 5.1.9, where

$$m_r=1.0, \quad k_r=1.0, \quad r=1,2,\dots,10. \tag{5.1.44}$$

To increase the damping of the system artificially, one channel of velocity feedback was introduced with the feedback gain  $v_{11}=-1.0$ .

If there was no time delay in the feedback, the 10 pairs of conjugate eigenvalues of system could be solved by using any commercially available codes for eigenvalue problems. The real parts and the imaginary parts of these eigenvalues are



listed in Table 5.1.1 according to the absolute value of their imaginary parts, from the minimum to the maximum. In this case, the dangerous eigenvalue was  $\lambda_1$ .

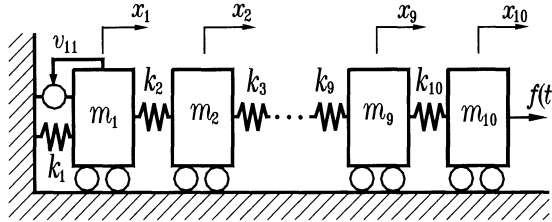


Fig.5.1.9. A 10-DOF system with a delayed velocity feedback

Table 5.1.1. Real and imaginary parts of eigenvalues of the delay free system and corresponding critical time delays

$r$	$Re\lambda_r$	$Im\lambda_r$	$\tau_r$
1	-0.0021	0.1497	10.375
2	-0.0165	0.4506	3.425
3	-0.0383	0.7500	2.064
4	-0.0660	1.0416	1.501
5	-0.2136	1.3013	0.732
6	-0.0877	1.3555	1.201
7	-0.0431	1.5927	1.023
8	-0.0215	1.7688	0.909
9	-0.0089	1.8964	0.839
10	-0.0022	1.9740	0.799

When the feedback had a time delay in the feedback, the stability analysis of the high dimensional system became very complicated. For example, the numerical approaches proposed in (Su et al. 1994) and (Chen 1995) involve very lengthy algebraic manipulations including the decomposition of singular values and so forth. However, the new approach written in a few lines of FORTRAN and incorporated with standard subroutines of linear algebra completed the analysis within a few seconds on a PC of Pentium-III. The critical time delays for all pairs of eigenvalues determined by NR are listed as the last column in Table 5.1.1.

Intuitively speaking, the higher a natural frequency, the shorter the critical time delay. So, it was expected that the most dangerous eigenvalue” should be  $\lambda_{10}$  with an increase of time delay since the real part of  $\lambda_{10}$  was the second smallest when there was no time delay in the feedback. Nevertheless, the most safe eigenvalue”

$\lambda_5$  became dangerous first with an increase of time delay, and its real part vanished at  $\tau_5=0.732$ . Figure 5.1.10 shows the evolution of eigenvalues  $\lambda_5$  and  $\lambda_{10}$  with increase of the time delay. This example indicates that care must be taken when the feedback of a high dimensional system involves any time delay.

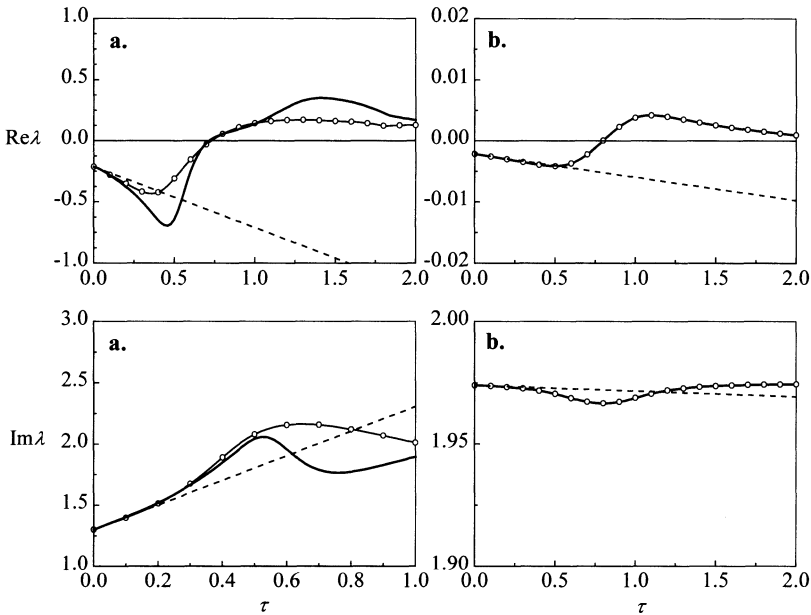


**Fig. 5.1.10.** Variation of two eigenvalues with an increase of time delay; **a.**  $\lambda_5$ , **b.**  $\lambda_{10}$ ; Key:  $-\circ-$ , NR,  $—$  ST,  $---$  DT.

In summary, the stability of a linear  $n$ -degree-of-freedom system with a single feedback time delay is governed by the evolution of the  $2n$  eigenvalues of the delay-free system with increase in the time delay, provided that the time delay in the state feedback is sufficiently short. To study the stability of the system involving feedback time delay, a perturbation approach is proposed so as to estimate efficiently the evolution of these eigenvalues. The approach can be used in three forms according to the length of time delay. If the time delay  $\tau$  is so short that the eigenvalue  $\lambda_r$  of concern yields  $|\lambda_r \tau| \ll 1$ , the simplest form of the approach gives an expression, similar to the Rayleigh quotient, for the variation of  $\lambda_r$  proportional to  $\tau$ . When the time delay is not so short, two alternative forms of the approach enable one to trace the variation of  $\lambda_r$  by solving a set of linear algebraic equations or by using Newton-Raphson iteration. The later form gives the exact numerical evolution of the eigenvalues with increase of time delay.

Worthy of mention finally is that it is straightforward to generalize the analysis and the assertions here for the following  $n$ -degree-of-freedom system with asynchronous time delays in different feedback channels

$$\sum_{j=1}^n [m_{ij}\ddot{x}_j(t) + c_{ij}\dot{x}_j(t) + k_{ij}x_j(t)] = f_j(t) + \sum_{j=1}^n [u_{ij}x_j(t - \tau_{ij}) + v_{ij}\dot{x}_j(t - \eta_{ij})]. \quad (5.1.45)$$

As the truncation in Eq. (5.1.21) requires only the small variation of eigenvalues due to the time delay, the approach described here can be directly used to analyze the stability of this kind of system also. However, much more computational efforts are required in tracing the evolution of eigenvalues if a system involves many different time delays as in Eq. (5.1.45).

#### 5.1.4 A Relation of Orthogonality of Mode Shapes

This subsection is an appendix for Subsection 5.1.2, presenting the proof of Eq. (5.1.30). Consider the following equation of the  $r$ -th eigenvalue and its eigenvector in the state space

$$(A - \lambda_r I) \mathbf{u}_r \equiv \begin{bmatrix} 0 & I \\ -M^{-1}(K - U) & -M^{-1}(C - V) \end{bmatrix} - \lambda_r I \begin{bmatrix} \mathbf{u}_{r1} \\ \mathbf{u}_{r1} \end{bmatrix} = 0. \quad (5.1.46)$$

Comparing this equation with the first one in Eq. (5.1.18), we can readily find

$$\mathbf{u}_{r1} = \mathbf{a}_r, \quad \mathbf{u}_{r2} = \lambda_r \mathbf{a}_r. \quad (5.1.47)$$

The adjoint relation of Eq. (5.1.46) reads

$$\mathbf{v}_r^* (A - \lambda_r I) \equiv [\mathbf{v}_{r1}^* \quad \mathbf{v}_{r2}^*] \begin{bmatrix} 0 & I \\ -M^{-1}K & -M^{-1}C \end{bmatrix} - \lambda_r I = 0, \quad (5.1.48)$$

whereby we obtain

$$\begin{cases} \lambda_r^2 \mathbf{v}_{r2}^* + \lambda_r \mathbf{v}_{r2}^* M^{-1} C + \mathbf{v}_{r2}^* M^{-1} K = 0, \\ \mathbf{v}_{r1}^* = \mathbf{v}_{r2}^* (\lambda_r + M^{-1} C). \end{cases} \quad (5.1.49)$$

From the comparison of the first equation in Eq. (5.1.48) with the second equation in Eq. (5.1.18), we have

$$\mathbf{v}_{r2}^* = \mathbf{b}_r^* M, \quad \mathbf{v}_{r1}^* = \mathbf{b}_r^* (\lambda_r M + C). \quad (5.1.50)$$

Noting the orthogonality relation of adjoint eigenvectors

$$\mathbf{v}_r^* \mathbf{u}_r = \mathbf{v}_{r1}^* \mathbf{u}_{r1} + \mathbf{v}_{r2}^* \mathbf{u}_{r2} \neq 0 \quad (5.1.51)$$

and substituting Eqs. (5.1.47) and (5.1.50) into Eq. (5.1.51), we obtain

$$2\lambda_r b_r^* M a_r + b_r^* (C - V) a_r \neq 0. \quad (5.1.52)$$

This completes the proof of Eq. (5.1.30).

## 5.2 Stability Test Based on the Padè Approximation

In this section, the Padè approximation, instead of the truncated Taylor expansion, is used to simplify the delayed dynamic systems to those described by the ordinary differential equation with its orders increased. The primary reason of using the Padè approximation comes from its higher accuracy and numerical stability, see, for example, (Xu 1990). To make the exposition as simple as possible, the study will be confined to a linear, single-degree-of-freedom system with two time delays in the feedback paths of both displacement and velocity, though the extension to higher dimensional systems is quite straightforward.

The dynamic equation of system of concern is

$$m\ddot{x}(t) + c\dot{x}(t) + kx(t) = ux(t - \tau_1) + v\dot{x}(t - \tau_2) + f(t), \quad (5.2.1)$$

where  $m > 0$ ,  $c \geq 0$  and  $k \geq 0$  are the coefficients of mass, damping and stiffness,  $u$  and  $v$  the feedback gains,  $\tau_1 \geq 0$  and  $\tau_2 \geq 0$  the time delays,  $f(t)$  the external excitation, respectively. The characteristic function of Eq. (5.2.1) reads

$$D(\lambda, \tau_1, \tau_2) \equiv m\lambda^2 + c\lambda + k - ue^{-\lambda\tau_1} - v\lambda e^{-\lambda\tau_2}. \quad (5.2.2)$$

As analyzed in Section 3.1, Eq. (5.2.1) is asymptotically stable if and only if all the roots of Eq. (5.2.2) have negative real parts.

The inequality  $u < k$  is assumed to hold hereinafter because the system free of time delay is asymptotically stable only when  $u < k$ . Otherwise, we have  $D(0, \tau_1, \tau_2) = k - u \leq 0$  and  $D(+\infty, \tau_1, \tau_2) \rightarrow +\infty$  so that Eq. (5.2.2) has at least one characteristic root with non-negative real part.

### 5.2.1 Test of Stability

Equation (5.2.2) includes two exponential functions in unknown  $\lambda$  and this fact gives rise to a great difficulty in the stability analysis. If they are replaced with any algebraic approximations, the stability analysis of Eq. (5.2.1) can be simplified. In

what follows, the Padè approximation will be used first in the case of equal time delays, and then in the case of unequal time delays.

### (1) The case of equal time delays

To get an accurate approximation of Eq. (5.2.2) in the case of  $\tau_1 = \tau_2 = \tau$ , the Padè (4, 4) approximation, see (Xu 1990), is chosen for the exponential function  $e^y$  as following

$$e^y \approx \frac{1680 + 840y + 180y^2 + 20y^3 + y^4}{1680 - 840y + 180y^2 - 20y^3 + y^4}, \quad (5.2.3)$$

with  $y = -\lambda\tau$ . The error of this approximation is estimated by

$$e^y - \frac{1680 + 840y + 180y^2 + 20y^3 + y^4}{1680 - 840y + 180y^2 - 20y^3 + y^4} = \frac{(4!)^2}{8!} y^9 + O(y^{10}), \quad (5.2.4)$$

It is about  $3.9376 \times 10^{-8}$  when  $|y| = 1$ . It increases to  $2.0156 \times 10^{-5}$  while  $|y| = 2$ . When  $|y| = 3$ , the error reaches  $7.7487 \times 10^{-4}$ .

By means of Eq. (5.2.3), Eq. (5.2.2) can be approximated as

$$\hat{D}(\lambda, \tau, \tau) \equiv a_0 \lambda^6 + a_1 \lambda^5 + a_2 \lambda^4 + a_3 \lambda^3 + a_4 \lambda^2 + a_5 \lambda + a_6, \quad (5.2.5)$$

where

$$\begin{aligned} a_0 &\equiv m\tau^4, & a_1 &\equiv 20m\tau^3 + (c-v)\tau^4, \\ a_2 &\equiv 180m\tau^2 + 20(c+v)\tau^3 + (k-u)\tau^4, \\ a_3 &\equiv 840m\tau + 180(c-v)\tau^2 + 20(k+u)\tau^3, \\ a_4 &\equiv 1680m + 840(c+v)\tau + 180(k-u)\tau^2, \\ a_5 &\equiv 1680(c-v) + 840(k+u)\tau, & a_6 &\equiv 1680(k-u). \end{aligned} \quad (5.2.6)$$

When the time delay is sufficiently short, the approximate characteristic function in Eq. (5.2.5) is in very good agreement with the original characteristic function in Eq. (5.2.2) within a certain range, say,  $|\lambda\tau| \leq 3$ .

To confirm the assertion about the agreement, we study the asymptotically stable region of the delayed dynamic systems on the plane spanned by the feedback gains  $(u, v)$ . In general, the stability boundary, defined by  $D(i\omega, \tau, \tau) = 0$ , between the stable and unstable regions on the plane of  $(u, v)$  for a given time delay may look very complicated. As shown in Subsection 3.5.1, the stability boundary may intersect with itself even many circles if the time delay is sufficiently long. Yet,

what we are concern with is the bounded, connected asymptotically stable region containing the origin  $(0, 0)$  on the plane of  $(u, v)$  as shown in Fig. 5.2.1, where the curve is the marginal stability condition  $D(i\omega, \tau, \tau)=0$  and the vertical line is the marginal stability condition  $u=k$  of the system without time delay. Such an asymptotically stable region exists provided that the time delay is short enough, say, shorter than the natural period of the system without time delay. In this case,  $\hat{D}(i\omega, \tau, \tau)$  gives a very good approximation to the marginal stability boundary of the original characteristic function.

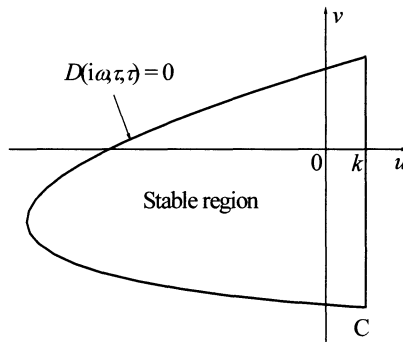


Fig. 5.2.1. Stable region on the plane of  $(u, v)$  in the case of equal time delays

From the conditions  $D(i\omega, \tau, \tau)=0$  and  $\hat{D}(i\omega, \tau, \tau)=0$  for marginal stability, it is easy to get the feedback gains of the original system on the stability boundary

$$\begin{cases} u=(k-m\omega^2)\cos\omega\tau-c\omega\sin\omega\tau, \\ v=\frac{1}{\omega}[(k-m\omega^2)\sin\omega\tau+c\omega\cos\omega\tau], \end{cases} \quad (5.2.7)$$

and those of the approximate system on its stability boundary

$$\hat{u}=\frac{p}{r}, \quad \hat{v}=\frac{q}{r}, \quad (5.2.8)$$

where

$$\begin{aligned} p \equiv & -m\omega^{10}\tau^8 + k\omega^8\tau^8 + 40c\omega^8\tau^7 + 760m\omega^8\tau^6 - 760k\omega^6\tau^6 \\ & - 8880c\omega^6\tau^5 - 69360m\omega^6\tau^4 + 69360k\omega^4\tau^4 \\ & + 369600c\omega^4\tau^3 + 1310400m\omega^4\tau^2 - 1310400k\omega^2\tau^2 \\ & - 2822400c\omega^2\tau - 2822400m\omega^2 + 2822400k, \end{aligned}$$

$$\begin{aligned}
q &= -2822400m\omega^2\tau - 1310400c\omega^2\tau^2 - 369600k\omega^2\tau^3 \\
&+ 369600m\omega^4\tau^3 + 2822400c + 2822400k\tau + 69360c\omega^4\tau^4 \\
&+ 8880k\omega^4\tau^5 - 8880m\omega^6\tau^5 - 760c\omega^6\tau^6 - 40k\omega^6\tau^7 \\
&+ 40m\omega^8\tau^7 + c\omega^8\tau^8, \\
r &= 2822400 + 100800\omega^2\tau^2 + 2160\omega^4\tau^4 + 40\omega^6\tau^6 + \omega^8\tau^8. \quad (5.2.9)
\end{aligned}$$

For a system with given  $m$ ,  $c$ ,  $k$  and  $\tau$ , it is easy to find numerically the value  $\hat{\omega}^*$ , corresponding to the point C in Fig. 5.2.1 when the stability boundary of the approximate system first intersects with  $u=k$  on the half-plane  $v < 0$ . In the following, we give an estimation of  $\hat{\omega}^*$  first.

Let  $g \equiv p - kr$ , then we define

$$g_1 \equiv g|_{\omega\tau=1} = -1580601m\omega^2 - 2461640c\omega - 1344800k, \quad (5.2.10a)$$

$$g_2 \equiv g|_{\omega\tau=2} = 1357824m\omega^2 - 2967040c\omega - 4620800k, \quad (5.2.10b)$$

$$g_3 \equiv g|_{\omega\tau=3} = 3900519m\omega^2 - 558360c\omega - 7840800k. \quad (5.2.10c)$$

Equation (5.2.10a) implies that the stability boundary on the plane of  $(u, v)$  can not intersect with  $u=k$  when  $\omega\tau=1$  since  $g_1=0$  has no positive solution  $\omega$ . Solving  $g_2=0$  for  $\omega$  gives

$$\omega_2 = \frac{1483520c + \sqrt{(1483520c)^2 + 1357824 \times 4620800mk}}{1357824m}. \quad (5.2.11a)$$

If  $0 < \tau < 2/\omega_2$ , then  $g_2 > 0$ . In this case, the stability boundary definitely intersects with  $u=k$  for some  $\omega\tau \in (1, 2)$ , and there exists  $\hat{\omega}^* \in (1/\tau, 2/\tau)$ . Similarly, from Eq. (5.2.10c), we get the unique positive root of  $g_3=0$

$$\omega_3 = \frac{279180c + \sqrt{(279180c)^2 + 3900519 \times 7840800mk}}{3900519m}. \quad (5.2.11b)$$

For all  $0 < \tau < 3/\omega_3$ , therefore, we have  $g_3 > 0$ . It follows that the stability boundary intersects with  $u=k$  for certain  $\omega\tau \in (1, 3)$ , and consequently, there exists  $\hat{\omega}^* \in (1/\tau, 3/\tau)$ . For the original system, a similar value  $\omega^*$  can also be found numerically. It is known that  $\omega^* \leq \hat{\omega}^*$ , and that  $\hat{\omega}^*$  is almost the same as  $\omega^*$ . Some numerical examples about  $\omega^*$  are given in Table 5.2.1.

**Table 5.2.1.** A number of examples for determining  $\omega^*$

System parameters	$2/\omega_2$	$3/\omega_3$	Intersection tests
$m=1.0, c=0.02, k=1.0$	1.071	2.113	$\tau=0.65, \omega^*=2.68, \omega^*\tau=1.74$
$m=1.0, c=1.50, k=1.0$	0.487	1.962	$\tau=0.65, \omega^*=3.28, \omega^*\tau=2.13$
$m=1.0, c=2.00, k=1.0$	0.396	1.913	$\tau=0.65, \omega^*=3.42, \omega^*\tau=2.22$
$m=1.0, c=5.00, k=1.0$	0.178	1.648	$\tau=0.65, \omega^*=3.92, \omega^*\tau=2.55$
$m=1.0, c=20.0, k=1.0$	0.045	0.871	$\tau=0.65, \omega^*=4.52, \omega^*\tau=2.94$

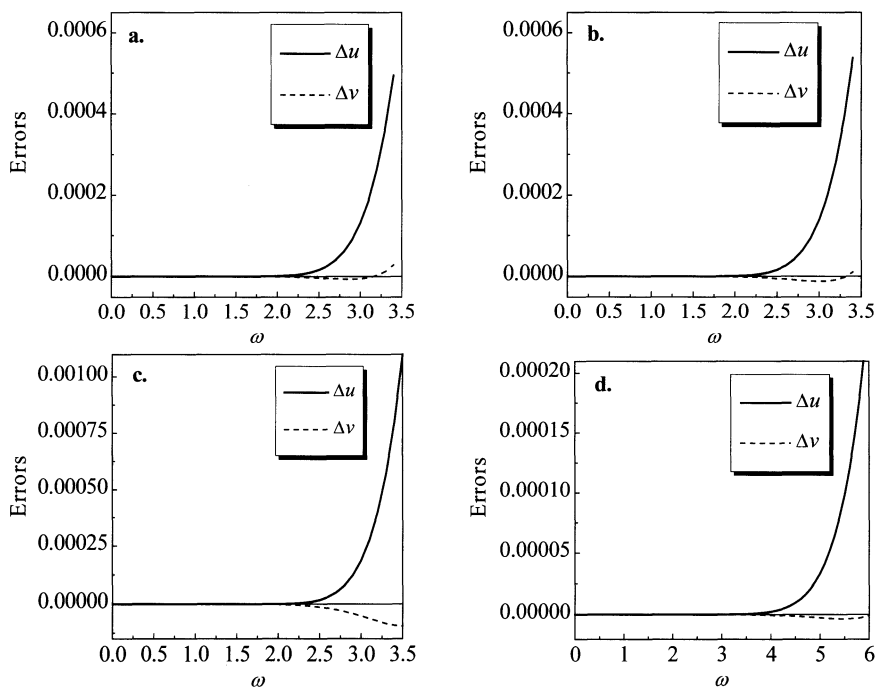


**Fig. 5.2.2.** Errors of approximation with an increase of frequency; **a.**  $c=1.5, \tau=0.65$  and  $\omega^*=3.277$ , **b.**  $c=2, \tau=0.65$  and  $\omega^*=3.415$ , **c.**  $c=5, \tau=0.65$  and  $\omega^*=3.923$ , **d.**  $c=1.5, \tau=0.3$  and  $\omega^*=6.143$

To measure the difference between the asymptotically stable regions of the approximate system and the original system, two errors are defined as

$$\Delta u \equiv u - \hat{u}, \quad \Delta v \equiv v - \hat{v}. \tag{5.2.12}$$



Once the value  $\hat{\omega}^*$  or  $\omega^*$  corresponding to the point C on the stability boundary is obtained, the approximate error curves of  $\{(\omega, \Delta u) \mid 0 \leq \omega \leq \hat{\omega}^*\}$  and  $\{(\omega, \Delta v) \mid 0 \leq \omega \leq \hat{\omega}^*\}$  can easily be figured out.

Figures 5.2.2a, 5.2.2b and 5.2.2c show the errors in three typical cases corresponding to an under-damped system, a critically damped system and an over-damped system. An additional example in Fig. 5.2.2d shows the effect of time delays on the under-damped system. Without loss of generality, the parameters  $m$  and  $k$  in these examples are set to be one. Otherwise, they can be scaled to be one by using dimensionless time and new parameters.

The above numerical examples show that the Padé approximation of the characteristic function gives excellent accuracy so that the stability boundary and the asymptotically stable region of the approximate system are almost the same as those of the original system within the concerned scopes. The errors of approximation are considerably small and come mainly from the approximation of  $u$ , and  $\hat{u} < u$  when  $\omega$  varies from some  $\omega^+$  to  $\omega^*$  with small  $\omega^* - \omega^+ \geq 0$ . This fact means that a dangerous case may happen only when the system is designed to possess a very small negative value  $v - v(\omega^*)$  and a very small positive value  $k - u$ . To avoid such a danger,  $v$  should be increased alternatively to a little bit larger value in design.

According to the Routh-Hurwitz criterion, all the roots of  $\hat{D}(\lambda, \tau, \tau)$  have negative real parts if and only if

$$a_0 > 0, \quad a_1 > 0, \quad a_2 > 0, \quad a_3 > 0, \quad a_4 > 0, \quad a_5 > 0, \quad a_6 > 0; \quad (5.2.13a)$$

$$a_1 a_2 - a_0 a_3 > 0, \quad a_1 a_2 a_3 + a_0 a_1 a_5 - a_1^2 a_4 - a_0 a_3^2 > 0; \quad (5.2.13b)$$

$$a_1 a_2 a_3 a_4 + 2a_0 a_1 a_4 a_5 + a_0 a_2 a_3 a_5 + a_1^2 a_2 a_6 - a_0 a_1 a_3 a_6 - a_1^2 a_4^2 - a_0^2 a_5^2 - a_0 a_4 a_3^2 - a_1 a_2^2 a_5 > 0; \quad (5.2.13c)$$

$$a_1 a_2 a_3 a_4 a_5 + 2a_1^2 a_2 a_5 a_6 + a_1^2 a_3 a_4 a_6 + 2a_0 a_1 a_4 a_5^2 + a_0 a_2 a_3 a_5^2 + a_0 a_3^3 a_6 - a_1 a_2 a_3^2 a_6 - a_1 a_2^2 a_5^2 - a_1^2 a_4^2 a_5 - a_1^3 a_6^2 - 3a_0 a_1 a_3 a_5 a_6 - a_0 a_3^2 a_4 a_5 - a_0^2 a_5^3 > 0. \quad (5.2.13d)$$

For given system parameters  $m$ ,  $c$ ,  $k$  and  $\tau$ , all the combinations of  $(u, v)$  subject to Eq. (5.2.13) give the stable region, which looks like that in Fig. 5.2.1, of the approximate system.

On the basis of the above analysis, a simple stability test approach is established for the dynamic system with short time delays as follows.

**Algorithm 5.2.1**

- (a) Test the stability of the approximate system by using Eq. (5.2.13).  
 (b) If the approximate system is unstable, the approach fails. Otherwise, the original system is stable for  $\tau < \min(3/\omega_3, \sqrt{k/m})$ .

**(2) The case of unequal time delays**

If the time delays are distinct, the feedback gains on the stability boundary yield

$$\begin{cases} u = \frac{1}{\cos(\omega\tau_2 - \omega\tau_1)} [(k - m\omega^2)\cos(\omega\tau_2) - c\omega\sin(\omega\tau_2)], \\ v = \frac{1}{\omega\cos(\omega\tau_2 - \omega\tau_1)} [(k - m\omega^2)\sin(\omega\tau_1) + c\omega\cos(\omega\tau_1)], \end{cases} \quad (5.2.14)$$

which depicts a more complicated curve on the plane of  $(u, v)$  than that in the case of equal time delays. However, the system has an asymptotically stable region similar to that in Fig. 5.2.1 if both  $\tau_1$  and  $|\tau_1 - \tau_2|$  are small enough. In this case, the Padè (4, 4) approximation is not appropriate since it results in a very small coefficient  $O(\tau_1^4 \tau_2^4)$  of the leading term in the characteristic equation of approximate system. To avoid this trouble, some lower order Padè approximations, say, (3, 2) or (2, 2) approximations, are more preferable. The Padè (3, 2) and (2, 2) approximations to  $e^y$ , see (Xu 1990), are respectively as following

$$e^y \approx \frac{60 + 36y + 9y^2 + y^3}{60 - 24y + 3y^2} = \frac{2!3!}{5!6!} y^6 + O(y^7), \quad (5.2.15)$$

$$e^y \approx \frac{12 + 6y + y^2}{12 - 6y + y^2} = \frac{(2!)^2}{4!5!} y^5 + O(y^6). \quad (5.2.16)$$

If the functions  $e^{-\lambda\tau_1}$  and  $e^{-\lambda\tau_2}$  in Eq. (5.2.2) are approximated by using Eqs. (5.2.15) and (5.2.16), Eq. (5.2.2) can be approximated as

$$\hat{D}(\lambda, \tau_1, \tau_2) \equiv b_0 \lambda^6 + b_1 \lambda^5 + b_2 \lambda^4 + b_3 \lambda^3 + b_4 \lambda^2 + b_5 \lambda + b_6 = 0, \quad (5.2.17)$$

where

$$b_0 \equiv 3m\tau_1^2 \tau_2^2, \quad b_1 \equiv \tau_1 \tau_2 [24m\tau_2 + 3(c-v)\tau_1 \tau_2 + 18m\tau_1 + u\tau_1^2 \tau_2],$$

$$b_2 \equiv 36m\tau_1^2 + 60m\tau_2^2 + 144m\tau_1 \tau_2 + (3k - 9u)\tau_1^2 \tau_2^2 \\ + 18(c+v)\tau_1^2 \tau_2 + 24(c-v)\tau_1 \tau_2^2 + 6u\tau_1^3 \tau_2,$$

$$\begin{aligned}
 b_3 &\equiv 288m\tau_1 + 360m\tau_2 + (24k + 36u)\tau_1\tau_2^2 + (18k - 54u)\tau_1^2\tau_2 \\
 &\quad + (c - v)(36\tau_1^2 + 60\tau_2^2) + 144(c + v)\tau_1\tau_2 + 12u\tau_1^3, \\
 b_4 &\equiv 720m + 288(c - v)\tau_1 + 360(c + v)\tau_2 + (144k + 216u)\tau_1\tau_2 \\
 &\quad + (36k - 108u)\tau_1^2 + 60(k - u)\tau_2^2, \\
 b_5 &\equiv (288k + 432u)\tau_1 + 360(k - u)\tau_2 + 720(c - v), \quad b_6 \equiv 720(k - u). \quad (5.2.18)
 \end{aligned}$$

The stability test can be made for the approximate system by using Eq. (5.2.13).

With the same argument, we can numerically find the value  $\omega^*$  of a given system for small distinct time delays  $\tau_1 \neq \tau_2$  with  $|\tau_1 - \tau_2| \ll 1$ . Usually, such a value  $\omega^*$  is almost the same as that of the corresponding system with  $\tau_2$  being the time delays in both displacement and velocity feedback paths. The accuracy of approximations in Eqs. (5.2.15) and (5.2.16) is not so good as that of Eq. (5.2.4) used in the case of equal time delays, still, the connected bounded stable region of the approximate system is in good agreement with that of the original systems.

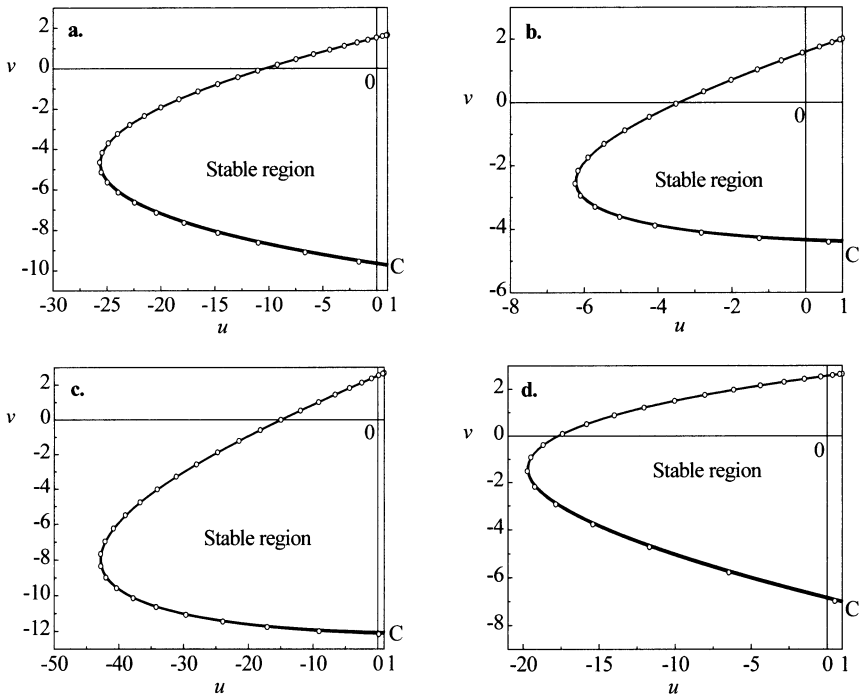


**Fig. 5.2.3.** Asymptotically Stable regions at different damping and time delays; **a.**  $c=1.5$ ,  $\tau_1=0.15$  and  $\tau_2=0.18$ , **b.**  $c=1.5$ ,  $\tau_1=0.50$  and  $\tau_2=0.45$ , **c.**  $c=2.5$ ,  $\tau_1=0.18$  and  $\tau_2=0.15$ , **d.**  $c=2.5$ ,  $\tau_1=0.45$  and  $\tau_2=0.50$ ; Key: — accurate, -○- approximate

Figure 5.2.3 illustrates four case studies where the parameters were set to be  $m=1$  and  $k=1$ . If  $|\tau_1 - \tau_2|$  is not small, the stable region may be successfully obtained as shown in Fig. 5.2.4. However, it is not always the case. Like the case of equal time delays, on the stability boundary within the scopes of concern, the velocity gain of the approximate system is almost equal to that of the original system, the main approximate error still comes from  $\hat{u}$ . A dangerous case may occur when the feedback gains are chosen as the values in the lower-right corner of the stable region of the approximate system. This case can be avoided by choosing alternatively a little bit larger value of the velocity feedback gain.

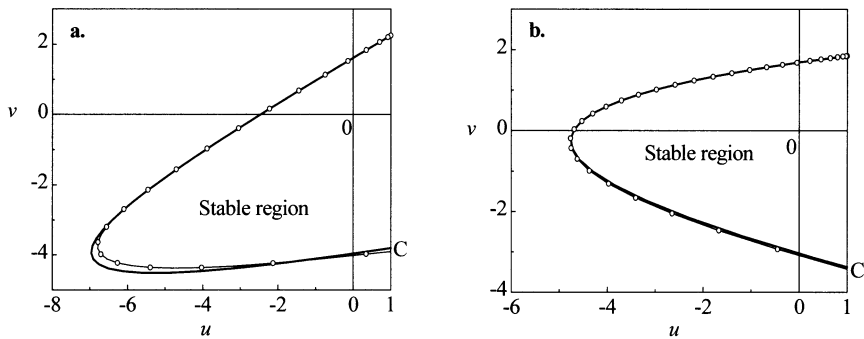


**Fig. 5.2.4.** Asymptotically stable regions when  $|\tau_1 - \tau_2|$  is not small; **a.**  $c=1.5$ ,  $\tau_1=0.75$ , and  $\tau_2=0.50$ , **b.**  $c=1.5$ ,  $\tau_1=0.35$  and  $\tau_2=0.70$ ; Key: — accurate, -o- approximate

### 5.2.2 Test of Interval Stability

In this subsection, the idea of the Padè approximation is extended to checking the interval stability of Eq. (5.2.1) with help of well-known *Kharitonov theorem* in (Kharitonov 1979). The analysis begins with the case of equal time delays  $\tau_1 \equiv \tau_2 \equiv \tau$ . Assume that the system parameters fall into the corresponding interval as following

$$\begin{aligned} 0 < \underline{m} \leq m \leq \bar{m}, & \quad 0 \leq \underline{c} \leq c \leq \bar{c}, & \quad 0 \leq \underline{k} \leq k \leq \bar{k}, \\ \underline{u} \leq u \leq \bar{u}, & \quad \underline{v} \leq v \leq \bar{v}, & \quad 0 \leq \underline{\tau} \leq \tau \leq \bar{\tau}, \end{aligned} \tag{5.2.19}$$

and define

$$\begin{aligned} \bar{\omega}_3 \equiv \max \{ \omega_3 \mid \underline{m} \leq m \leq \bar{m}, \underline{c} \leq c \leq \bar{c}, \underline{k} \leq k \leq \bar{k} \} \\ = \frac{279180\bar{c} + \sqrt{(279180\bar{c})^2 + 3900519 \times 7840800\bar{m}\bar{k}}}{3900519\bar{m}}. \end{aligned} \tag{5.2.20}$$

Then, the Padè approximation gives the boundary of asymptotically stable region of the approximate system on the plane of  $(u, v)$  for each combination of the system parameters  $0 < \underline{m} \leq m \leq \bar{m}$ ,  $0 \leq \underline{c} \leq c \leq \bar{c}$  and  $0 \leq \underline{k} \leq k \leq \bar{k}$  if  $0 < \bar{\tau} < 3/\bar{\omega}_3$ . Once the characteristic equation of the delayed dynamic system is simplified to Eq. (5.2.5) in this case, the Kharitonov Theorem can be implemented to test the interval stability. From the practical point of view, it is reasonable to assume that  $\underline{u}\bar{u} > 0$  and  $\underline{v}\bar{v} > 0$ . Then, by using Eq. (5.2.19), we have

$$\underline{a}_j \leq a_j \leq \bar{a}_j, \quad j=0,1,\dots,6, \quad (5.2.21)$$

where  $a_j$  are the coefficients in Eq. (5.2.5), and the corresponding bounds  $\underline{a}_j$  and  $\bar{a}_j$  are defined as following

$$\begin{aligned} \underline{a}_0 &\equiv \underline{m}\underline{\tau}^4, & \bar{a}_0 &\equiv \bar{m}\bar{\tau}^4, \\ \underline{a}_1 &\equiv 20\underline{m}\underline{\tau}^3 + \underline{c}\underline{\tau}^4 - \underline{v}\underline{\tau}^4, & \bar{a}_1 &\equiv 20\bar{m}\bar{\tau}^3 + \bar{c}\bar{\tau}^4 - \underline{v}\underline{\tau}^4, \\ \underline{a}_2 &\equiv 180\underline{m}\underline{\tau}^2 + 20\underline{c}\underline{\tau}^3 + \underline{k}\underline{\tau}^4 - \underline{u}\underline{\tau}^4 + 20\underline{v}\underline{\tau}^3, & \bar{a}_2 &\equiv 180\bar{m}\bar{\tau}^2 + 20\bar{c}\bar{\tau}^3 + \bar{k}\bar{\tau}^4 - \underline{u}\underline{\tau}^4 + 20\underline{v}\underline{\tau}^3, \\ \underline{a}_3 &\equiv 840\underline{m}\underline{\tau} + 180\underline{c}\underline{\tau}^2 + 20\underline{k}\underline{\tau}^3 + 20\underline{u}\underline{\tau}^3 - 180\underline{v}\underline{\tau}^2, & \bar{a}_3 &\equiv 840\bar{m}\bar{\tau} + 180\bar{c}\bar{\tau}^2 + 20\bar{u}\bar{\tau}^3 + 20\underline{u}\underline{\tau}^3 - 180\underline{v}\underline{\tau}^2, \\ \underline{a}_4 &\equiv 1680\underline{m} + 840\underline{c}\underline{\tau} + 180\underline{k}\underline{\tau}^2 - 180\underline{u}\underline{\tau}^2 + 840\underline{v}\underline{\tau}, & \bar{a}_4 &\equiv 1680\bar{m} + 840\bar{c}\bar{\tau} + 180\bar{k}\bar{\tau}^2 - 180\underline{u}\underline{\tau}^2 + 840\underline{v}\underline{\tau}, \\ \underline{a}_5 &\equiv 1680\underline{c} + 840\underline{k}\underline{\tau} + 840\underline{u}\underline{\tau} - 1680\underline{v}, & \bar{a}_5 &\equiv 1680\bar{c} + 840\bar{k}\bar{\tau} + 840\underline{u}\underline{\tau} - 1680\underline{v}, \\ \underline{a}_6 &\equiv 1680\underline{k} - 1680\underline{u}, & \bar{a}_6 &\equiv 1680\bar{k} - 1680\underline{u}, \end{aligned} \quad (5.2.22)$$

with the following simplified notions for different bounds of feedback gains and time delays

$$\overline{u\tau^j} \equiv \begin{cases} \underline{u}\bar{\tau}^j, & u \geq 0, \\ \bar{u}\underline{\tau}^j, & \bar{u} < 0, \end{cases} \quad \underline{u\tau^j} \equiv \begin{cases} \underline{u}\underline{\tau}^j, & u \geq 0, \\ \underline{u}\bar{\tau}^j, & \bar{u} < 0, \end{cases} \quad j=1,2,3,4, \quad (5.2.23a)$$

$$\overline{v\tau^j} \equiv \begin{cases} \underline{v}\bar{\tau}^j, & v \geq 0, \\ \bar{v}\underline{\tau}^j, & \bar{v} < 0, \end{cases} \quad \underline{v\tau^j} \equiv \begin{cases} \underline{v}\underline{\tau}^j, & v \geq 0, \\ \underline{v}\bar{\tau}^j, & \bar{v} < 0, \end{cases} \quad j=1,2,3,4. \quad (5.2.23b)$$

According to the Kharitonov theorem, it is sufficient to check the stability of four cases of the coefficients in Eq. (5.2.5) when testing the interval stability of Eq. (5.2.5) subject to Eq. (5.2.21). These four cases are

$$(a_0, a_1, a_2, a_3, a_4, a_5, a_6) = (\bar{a}_0, \underline{a}_1, \underline{a}_2, \bar{a}_3, \bar{a}_4, \underline{a}_5, \underline{a}_6), \quad (5.2.24a)$$

$$(a_0, a_1, a_2, a_3, a_4, a_5, a_6) = (\bar{a}_0, \bar{a}_1, \underline{a}_2, \underline{a}_3, \bar{a}_4, \bar{a}_5, \bar{a}_6), \quad (5.2.24b)$$

$$(a_0, a_1, a_2, a_3, a_4, a_5, a_6) = (\underline{a}_0, \underline{a}_1, \bar{a}_2, \bar{a}_3, \underline{a}_4, \underline{a}_5, \bar{a}_6), \quad (5.2.24c)$$

$$(a_0, a_1, a_2, a_3, a_4, a_5, a_6) = (\underline{a}_0, \bar{a}_1, \bar{a}_2, \underline{a}_3, \underline{a}_4, \bar{a}_5, \bar{a}_6). \quad (5.2.24d)$$

From the Routh-Hurwitz conditions in Eq. (5.2.13), the stability of each case can be easily tested. There follows the approach to testing the interval stability of a dynamic system governed by Eq. (5.2.1) as following.

#### Algorithm 5.2.2

(a) Check the stability of the nominal system by using Eq. (5.2.13) and compute  $\bar{\omega}_3$ . If the nominal system is asymptotically stable and  $0 < \bar{\tau} < 3/\bar{\omega}_3$ , then go to the next step.

(b) Test the stability of system in the four cases in Eq. (5.2.24) by using again Eq. (5.2.13). If the system is asymptotically stable in all of the four cases, then the interval stability is justified.

**Example 5.2.1** Consider an illustrative example of the linear dynamic system with nominal parameters  $m=1$ ,  $c=3$ ,  $k=1$ ,  $\tau = 0.55$ ,  $u=-2$ , and  $v=-3$ . It is easy to see from Eq. (5.2.13) that the system is asymptotically stable.

We check first the interval stability of the system with 25% variation in every system parameter. That is, the system parameters are allowed to vary on the following intervals

$$\begin{aligned} 0.75 \leq m \leq 1.25, \quad 2.25 \leq c \leq 3.75, \quad 0.75 \leq k \leq 1.25, \\ 0.4125 \leq \tau \leq 0.6875, \quad -2.50 \leq u \leq -1.50, \quad -3.75 \leq v \leq -2.25. \end{aligned} \quad (5.2.25)$$

Then we have  $\underline{a}_4 = -57.0867$ . By using the Kharitonov theorem, we find that the approximate systems with the parameters on the given intervals are not stable, so the method fails to test the interval stability of the original system.

If the variations in the system parameters are confined to 20%, that is

$$0.80 \leq m \leq 1.20, \quad 2.40 \leq c \leq 3.60, \quad 0.80 \leq k \leq 1.20,$$

$$0.44 \leq \tau \leq 0.66, \quad -2.40 \leq u \leq -1.60, \quad -3.60 \leq v \leq -2.40, \quad (5.2.26)$$

we have

$$0.030 \leq a_0 \leq 0.228, \quad 1.543 \leq a_1 \leq 8.266, \quad 11.36 \leq a_2 \leq 110.9,$$

$$450.5 \leq a_3 \leq 1234, \quad 318.8 \leq a_4 \leq 3407, \quad 1200 \leq a_5 \leq 12169,$$

$$4032 \leq a_6 \leq 6048, \quad \bar{\omega}_3 = 1.2642. \quad (5.2.27)$$

The Kharitonov theorem indicates that the approximate systems with the parameters on the new intervals are asymptotically stable. As  $\bar{\tau} < \min(3/\bar{\omega}_3, \sqrt{k/m})$ , the interval stability is justified.

In the case of unequal time delays, as stated in Subsection 5.2.1, the asymptotically stable region may not be as simple as shown in Fig. 5.2.1 if  $|\tau_1 - \tau_2|$  is not very small. Thus, the approach may be very poor in the test of interval stability for the systems with variable unequal time delays if  $\max(|\bar{\tau}_1 - \underline{\tau}_2|, |\bar{\tau}_2 - \underline{\tau}_1|)$  is not very small.

In practical test of asymptotic stability and interval stability, great care must be taken when the system parameters are chosen with a very small negative value  $v - v(\omega^*)$  and a very small positive value  $k - u$ . If this is the case, the negative velocity feedback gain should be increased alternatively to a little bit larger value so as to make the test result be more reliable if the given system is tested to be asymptotically stable by using the approach.

In summary, the presented approach of stability test to the delayed dynamic systems by using the Padè approximation is so simple that the stability test can be completed by using a calculator. Though this approach may not always be successful, it is an effective approach of stability test with high accuracy within the scope of concern both for the asymptotic stability and the interval stability. In addition, the idea of the Padè approximation can be extended to the study on more complicated delayed dynamic systems.

### 5.3 Dynamics of Simplified Systems via the Taylor Expansion

This section presents a study on the validity of the Taylor expansion of delayed feedback from the viewpoint of system stability. We first check the effectiveness of the Taylor expansion of delayed state feedback for a linear system, and then

study the dynamics of a nonlinear system with delayed velocity feedback through the use of singular perturbation theory.

### 5.3.1 Linear Systems with Delayed State Feedback

For simplicity, the study in this subsection is confined to a linear single-degree-of-freedom system with delayed state feedback as following

$$m\ddot{x}(t)+c\dot{x}(t)+kx(t)=ux(t-\tau_1)+v\dot{x}(t-\tau_2), \tag{5.3.1}$$

where  $m>0$ ,  $k-u>0$ ,  $c-v>0$  such that the system is asymptotically stable when the time delays totally disappear. The analysis in Subsection 5.1.1 indicates that Eq. (5.3.1) is asymptotically stable if the time delays  $\tau_1$  and  $\tau_2$  are short enough.

When the time delays are very short, it is reasonable and very popular for engineers to replace the delay terms in Eq. (5.3.1) with the following Taylor expansions

$$\begin{cases} ux(t-\tau_1)=u[x(t)-\tau_1\dot{x}(t)+\frac{1}{2}\tau_1^2\ddot{x}(t)-\frac{1}{6}\tau_1^3\dddot{x}(t)+\frac{1}{24}\tau_1^4x^{(4)}(t)+O(\tau_1^5)], \\ v\dot{x}(t-\tau_2)=v[\dot{x}(t)-\tau_2\ddot{x}(t)+\frac{1}{2}\tau_2^2\ddot{x}(t)-\frac{1}{6}\tau_2^3x^{(4)}(t)+O(\tau_2^4)]. \end{cases} \tag{5.3.2}$$

Hence, Eq. (5.3.1) can be simplified as one of the following ordinary differential equations, depending on the order of truncation

$$a_2\ddot{x}(t)+a_1\dot{x}(t)+a_0x(t)=0, \tag{5.3.3a}$$

$$a_3\ddot{x}(t)+a_2\ddot{x}(t)+a_1\dot{x}(t)+a_0x(t)=0, \tag{5.3.3b}$$

$$a_4x^{(4)}(t)+a_3\ddot{x}(t)+a_2\ddot{x}(t)+a_1\dot{x}(t)+a_0x(t)=0, \tag{5.3.3c}$$

⋮

where

$$\begin{cases} a_0=k-u, & a_1=c+u\tau_1-v, & a_2=m-\frac{1}{2}u\tau_1^2+v\tau_2, \\ a_3=\frac{1}{6}u\tau_1^3-\frac{1}{2}v\tau_2^2, & a_4=-\frac{1}{24}u\tau_1^4+\frac{1}{6}v\tau_2^3, & \dots \end{cases} \tag{5.3.4}$$

For very short time delays at the same order, Eq. (5.3.4) becomes

$$\begin{cases} a_0=k-u, & a_1=c-v+O(\tau_1), & a_2=m+O(\tau_2), \\ a_3=O(\tau_2^2), & a_4=O(\tau_2^3), & \dots \end{cases} \tag{5.3.5}$$



In what follow, we examine the efficacy of the above approximation for different truncations in the Taylor expansion from the viewpoint of stability.

If the time delays appear in the feedback, but short enough,  $a_0$ ,  $a_1$  and  $a_2$  keep positive and Eq. (5.3.3a) remains the asymptotic stability of delay free system. In this case, Eq. (5.3.3a) is topologically equivalent to Eq. (5.3.1) and the Taylor expansion is effective.

Equation (5.3.3b) is an ordinary differential equation of extended order and has a very small coefficient  $a_3$  in front of the highest order derivative. The differential equation with a very small coefficient of the highest order derivative is called the *singularly perturbed differential equation*. If Eq. (5.3.3b) is asymptotically stable, the Routh-Hurwitz criterion requires that

$$a_3 > 0, \quad a_2 > 0, \quad a_1 a_2 - a_0 a_3 > 0, \quad a_0 (a_1 a_2 - a_0 a_3) > 0. \quad (5.3.6)$$

Substituting Eq. (5.3.4) into the above inequalities gives

$$\frac{1}{6}u\tau_1^3 - \frac{1}{2}v\tau_2^2 > 0, \quad m + O(\tau_2) > 0, \quad m(c-v) + O(\tau_1, \tau_2) > 0, \quad k - u > 0. \quad (5.3.7)$$

The second, the third and the fourth inequalities in Eq. (5.3.7) always hold true for very short time delays. The first inequality, however, indicates that the Eq. (5.3.3b) may become unstable and topologically different from Eq. (5.3.1) when

$$a_3 = \frac{1}{6}u\tau_1^3 - \frac{1}{2}v\tau_2^2 > 0 \quad (5.3.8)$$

does not hold. If this is the case, the Taylor expansion of higher orders does not work for Eq. (5.3.1).

For Eq. (5.3.3c), the Routh-Hurwitz criterion imposes another condition

$$a_4 = -\frac{1}{24}u\tau_1^4 + \frac{1}{6}v\tau_2^3 > 0. \quad (5.3.9)$$

The Taylor expansion for delayed feedback, therefore, is only effective under certain conditions.

Hence, great care must be taken in the stability analysis of simplified differential equations of extended order when the Taylor expansion of higher orders is used to reduce the truncation errors, since these differential equations are singularly perturbed and may feature totally different dynamics.

For instance, Eq. (3.1.34) indicates that Eq. (5.3.1) in the case of small damping  $c < \sqrt{2mk}$  and equal time delays  $\tau_1 \equiv \tau_2 \equiv \tau$  is delay-independent stable if the absolute values of feedback gains are so small that

$$\frac{u^2}{k^2} + \left(\frac{c^2 - v^2}{2mk} - 1\right)^2 < 1. \quad (5.3.10)$$

From Eq. (5.3.8), however, the asymptotic stability of Eq. (5.3.3b) requires that

$$u\tau - 3v > 0. \quad (5.3.11)$$

If no displacement feedback is used, the velocity feedback should be negative. This is an additional requirement owing to the Taylor expansion of higher orders for the delayed feedback.

Furthermore, when Eq. (5.3.3c) is implemented to predict the system stability, Eq. (5.3.9) requires that

$$u\tau - 4v < 0. \quad (5.3.12)$$

If no displacement feedback is involved, Eqs. (5.3.11) and (5.3.12) are contradictory. This contradiction indicates again that the Taylor expansion of higher orders for the delayed feedback does not give correct analysis of system stability if the simplified differential equations are singularly perturbed.

The effect of a short time delay on the simplified model governed by the singularly perturbed differential equations will be further discussed in next subsection through an example of the Duffing oscillator with delayed velocity feedback.

### 5.3.2 Nonlinear Systems with Delayed Velocity Feedback

This subsection deals with a nonlinear autonomous system with delayed velocity feedback as following

$$\ddot{x}(t) + p(x(t), \dot{x}(t)) = v\dot{x}(t - \tau), \quad v \neq 0, \quad \tau \geq 0. \quad (5.3.13)$$

For a very short time delay  $\tau$ , the truncated Taylor expansions of different orders for the delayed velocity feedback in Eq. (5.3.13) give different simplified ordinary differential equations as following

$$\ddot{x}(t) + p(x(t), \dot{x}(t)) = v[\dot{x}(t) - \tau\ddot{x}(t)], \quad (5.3.14a)$$

$$\ddot{x}(t) + p(x(t), \dot{x}(t)) = v\left[\dot{x}(t) - \tau\ddot{x}(t) + \frac{\tau^2}{2}\ddot{\ddot{x}}(t)\right], \quad (5.3.14b)$$

⋮

The dynamics of Eq. (5.3.14a) is clear if  $\tau$  is so short that the condition  $1 + v\tau > 0$  holds. Thus, attention hereinafter is paid to Eq. (5.3.14b), which is a sin-

gularly perturbed differential equation. By using the state variables  $y_1 \equiv x$ ,  $y_2 \equiv \dot{x}$ ,  $y_3 \equiv \ddot{x}$ , Eq. (5.3.14b) can be recast as a set of differential equations

$$\begin{cases} \dot{y}_1 = y_2, \\ \dot{y}_2 = y_3, \\ \varepsilon^2 \dot{y}_3 = \frac{2}{\nu} [p(y_1, y_2) - \nu y_2 + (1 + \nu \varepsilon) y_3] \equiv g(y_1, y_2, y_3, \varepsilon), \end{cases} \quad (5.3.15)$$

where  $\varepsilon = \tau \ll 1$  is a small, non-negative parameter.

If  $\varepsilon = 0$ , Eq. (5.3.15) degenerates to a set of ordinary differential equations

$$\begin{cases} \dot{y}_1 = y_2, \\ \dot{y}_2 = y_3, \end{cases} \quad (5.3.16a)$$

which is subject to an algebraic constraint

$$0 = \frac{2}{\nu} [p(y_1, y_2) - \nu y_2 + y_3] = g(y_1, y_2, y_3, 0). \quad (5.3.16b)$$

Solving Eq. (5.3.16b) for  $y_3$  yields

$$y_3 \equiv h(y_1, y_2) = -p(y_1, y_2) + \nu y_2. \quad (5.3.17)$$

Obviously,  $h(y_1, y_2)$  is an invariant manifold of Eq. (5.3.16) in  $R^3$ . That is, any trajectory of Eq. (5.3.16) starting from  $h(y_1, y_2)$  does not leave  $h(y_1, y_2)$  forever. Because the time scale used here is slow compared with the fast one used later,  $h(y_1, y_2)$  is called the *slow manifold*. Substituting it into Eq. (5.3.16a) gives

$$\begin{cases} \dot{y}_1 = y_2, \\ \dot{y}_2 = -p(y_1, y_2) + \nu y_2. \end{cases} \quad (5.3.18)$$

Eq. (5.3.18) is called the differential equation of *reduced system* in the theory of singularly disturbed differential equations. It governs the motion of reduced system on the slow manifold. Here, the reduced system is a system without time delay.

In the study of singularly perturbed differential equations, it is helpful to introduce a new time scale

$$s = \frac{t}{\varepsilon^2}. \quad (5.3.19)$$

Because  $\varepsilon$  is very small,  $s$  varies much faster than  $t$ . Hence, the variables  $t$  and  $s$  are usually referred to as the *slow time* and the *fast time*, respectively. To distinguish the derivatives with respect to different time scales, the prime is used to represent the differentiation with respect to the fast time  $s$ . Substituting  $t$  in Eq. (5.3.15) by  $s$  yields

$$\begin{cases} y_1' = \varepsilon^2 y_2, \\ y_2' = \varepsilon^2 y_3, \\ y_3' = \frac{2}{\nu} [p(y_1, y_2) - \nu y_2 + (1 + \nu \varepsilon) y_3] \equiv g(y_1, y_2, y_3, \varepsilon). \end{cases} \quad (5.3.20)$$

For Eq. (5.3.20), any point  $(y_1, y_2, h(y_1, y_2))$  is an equilibrium when  $\varepsilon=0$  since  $g(y_1, y_2, h(y_1, y_2), 0)=0$ . However, this is not true for Eq. (5.3.15) because Eqs. (5.3.15) and (5.3.20) are not equivalent if  $\varepsilon=0$ .

The dynamics of Eq. (5.3.20) with  $\varepsilon=0$  is characterized by a one-dimensional differential equation

$$y_3' = \frac{2}{\nu} [f(y_1, y_2) - \nu y_2 + y_3] = g(y_1, y_2, y_3, 0), \quad (5.3.21)$$

where  $(y_1, y_2)$  can be regarded as constant parameters since  $y_1'=0$  and  $y_2'=0$ . Given a pair of  $(y_1, y_2)$ , Eq. (5.3.21) governs a fast motion approaching to the slow manifold  $h(y_1, y_2)$  if  $\nu < 0$ . This motion is usually called the *fast manifold* for short.

Now, it is clear that Eqs. (5.3.21) and (5.3.18) govern two kinds of extreme dynamics associated with Eq. (5.3.15) respectively when  $\varepsilon=0$ . That is, the fast manifold approaching to the slow manifold if  $\nu < 0$  and the motion, which may be simple or very complicated, on the slow manifold. The aim of further study is to gain an insight into the dynamics of Eq. (5.3.15) for very small  $\varepsilon$  from the knowledge of the asymptotic behavior of two "limit" Eqs. (5.3.18) and (5.3.21).

**Example 5.3.1** To demonstrate how to analyze the dynamics of Eq. (5.3.15), we study the dynamics of a Duffing oscillator under delayed velocity feedback around its equilibrium. Following Eq. (1.1.13), let

$$p(x, \dot{x}) = x + \mu x^3 + 2\zeta \dot{x}, \quad (5.3.22)$$

where  $\zeta \geq 0$ . In what follows, attention is paid to the case when  $\mu \geq 0$ .

If  $\varepsilon=0$ , Eq. (5.3.15) becomes

$$\begin{cases} \dot{y}_1 = y_2, \\ \dot{y}_2 = y_3, \end{cases} \quad (5.3.23a)$$

with an algebraic constraint

$$y_3 = -(y_1 + \mu y_1^3 + 2\zeta y_2) + \nu y_2. \quad (5.3.23b)$$

Figure 5.3.1 illustrates the slow manifold (5.3.23b), where a trajectory of Eq. (5.3.23a) spirally approaches to the equilibrium, when  $\mu=0.1$ ,  $\zeta=0$  and  $\nu=-0.2$ .

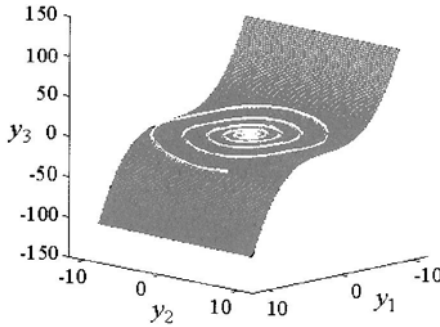


Fig. 5.3.1. A trajectory on the slow manifold

When  $\varepsilon \neq 0$ , Eq. (5.3.15) becomes

$$\begin{cases} \dot{y}_1 = y_2, \\ \dot{y}_2 = y_3, \\ \varepsilon^2 \dot{y}_3 = \frac{2}{\nu} [y_1 + \mu y_1^3 + (2\zeta - \nu)y_2 + (1 + \nu\varepsilon)y_3]. \end{cases} \quad (5.3.24)$$

As it is difficult to deal with this singularly perturbed differential equation, we turn to its equivalent form in the fast time scale, namely,

$$\begin{cases} y_1' = \varepsilon^2 y_2, \\ y_2' = \varepsilon^2 y_3, \\ y_3' = \frac{2}{\nu} [y_1 + \mu y_1^3 + (2\zeta - \nu)y_2 + (1 + \nu\varepsilon)y_3]. \end{cases} \quad (5.3.25)$$

Unfortunately, the asymptotic stability theorem in the theory of singularly perturbed differential equations, see (Isidori 1995), can not be applied directly to this

equation. The analysis below will be based on the center manifold theorem of ordinary differential equations, see (Guckenheimer and Holmes 1983).

Let  $\varepsilon$  be a function in  $s$  and rewrite Eq. (5.3.25) as following

$$\begin{cases} \varepsilon' = 0, \\ y_1' = \varepsilon^2 y_2, \\ y_2' = \varepsilon^2 y_3, \\ y_3' = \frac{2}{v} [y_1 + \mu y_1^3 + (2\zeta - v)y_2 + (1 + v\varepsilon)y_3]. \end{cases} \quad (5.3.26)$$

Equation (5.3.26) has a unique equilibrium  $(0,0,0,0)$  since  $\mu \geq 0$ . According to the following Jacobian of Eq. (5.3.26) at  $(0,0,0,0)$

$$J = \begin{bmatrix} 0 & 0 & 0 & 0 \\ 0 & 0 & 0 & 0 \\ 0 & 0 & 0 & 0 \\ 0 & \frac{2}{v} & \frac{2(2\zeta - v)}{v} & \frac{2}{v} \end{bmatrix}, \quad (5.3.27)$$

it is easy to confirm that the equilibrium is asymptotically stable if and only  $v < 0$ .

Now we study the local dynamics of Eq. (5.3.26) around the equilibrium. Using the center manifold theorem, we can prove the following fact. That is, for Eq. (5.3.26), there exists  $\varepsilon^* > 0$  and an invariant manifold

$$y_3 = H(y_1, y_2, \varepsilon), \quad (5.3.28)$$

which is passing through the point  $(0,0,0,0)$  and tangent to the super-plane of  $y_3 = 0$  at  $(0,0,0,0)$  such that for each  $\varepsilon \in [0, \varepsilon^*]$  and all  $y_1^2 + y_2^2 < r^2$

$$H(y_1, y_2, \varepsilon) - h(y_1, y_2) = O(\varepsilon), \quad (5.3.29)$$

where  $h(y_1, y_2) = H(y_1, y_2, 0)$ . The invariant manifold in Eq. (5.3.28) is also called a *slow manifold*. On each of such a manifold, Eq. (5.3.26) can be simplified as

$$\begin{cases} \varepsilon' = 0, \\ y_1' = \varepsilon^2 y_2, \\ y_2' = \varepsilon^2 H(y_1, y_2, \varepsilon). \end{cases} \quad (5.3.30)$$

The local dynamics of Eq. (5.3.26) around  $(0,0,0,0)$  is fully determined by the motion on the slow manifold  $H(y_1, y_2, \varepsilon)$ .

In what follow, the slow manifold and Eq. (5.3.30) are determined. Differentiating Eq. (5.3.28) at both sides with respect to  $s$  leads to

$$y_3' = \frac{\partial H}{\partial y_1} y_1' + \frac{\partial H}{\partial y_2} y_2'. \quad (5.3.31)$$

Substituting Eq. (5.3.26) into the Eq. (5.3.31) gives the governing equation of the slow manifold  $H(y_1, y_2, \varepsilon)$

$$\varepsilon^2 \left[ \frac{\partial H}{\partial y_1} y_2 + \frac{\partial H}{\partial y_2} y_3 \right] = \frac{2}{v} [y_1 + \mu y_1^3 + (2\zeta - v)y_2 + (1 + v\varepsilon)H(y_1, y_2, \varepsilon)]. \quad (5.3.32)$$

In general, it is impossible to solve this partial differential equation for  $H(y_1, y_2, \varepsilon)$ . So, we turn to looking for an approximate solution of Eq. (5.3.32) as following

$$H(y_1, y_2, \varepsilon) = h_0(y_1, y_2) + h_1(y_1, y_2)\varepsilon + h_2(y_1, y_2)\varepsilon^2 + \dots \quad (5.3.33)$$

Substituting Eq. (5.3.33) into Eq. (5.3.32) and equating the same power of  $\varepsilon$ , we obtain

$$h_0(y_1, y_2) = -[y_1 + \mu y_1^3 + (2\zeta - v)y_2], \quad (5.3.34a)$$

$$h_1(y_1, y_2) = v[y_1 + \mu y_1^3 + (2\zeta - v)y_2], \quad (5.3.34b)$$

$$h_2(y_1, y_2) = -\frac{1}{2}v\{y_2 + (3v - 2\zeta)[y_1 + \mu y_1^3 + (2\zeta - v)y_2]\}. \quad (5.3.34c)$$

Substituting Eqs. (5.3.33) and (5.3.34) into Eq. (5.3.30) gives the differential equation of reduced system

$$\begin{cases} \varepsilon' = 0, \\ y_1' = \varepsilon^2 y_2, \\ y_2' = -\varepsilon^2 [y_1 + \mu y_1^3 + (2\zeta - v)y_2] + \varepsilon^3 v [y_1 + \mu y_1^3 + (2\zeta - v)y_2] + O(\varepsilon^4). \end{cases} \quad (5.3.35)$$

It is easy to find that if  $\varepsilon > 0$ , the unique equilibrium  $(0, 0)$  is asymptotically stable when  $v < 0$ . According to the analysis above, we conclude that the equilibrium  $(0, 0, 0)$  is asymptotically stable if and only if  $v < 0$  and  $\varepsilon > 0$  small enough.

Given  $\varepsilon = 0.3$ , the slow manifold and a phase trajectory of Eq. (5.3.24) are shown in Fig. 5.3.2 for  $\mu = 0.1$ ,  $\zeta = 0$ ,  $v = -0.2$ . Worthy of mention is that the two slow manifolds in Figs. 5.3.1 and 5.3.2 are different though they look very similar. Figure 5.3.2 illustrates that the trajectory starting from a state point above the slow manifold goes down to the slow manifold very rapidly and then approaches to the equilibrium along a spiral on the slow manifold. It is interesting that  $\varepsilon$  taken here is not very small.

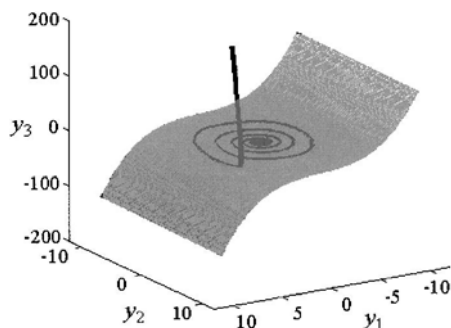


**Fig. 5.3.2.** A trajectory approaching to the slow manifold first and then to equilibrium

As a result, the dynamics of a nonlinear autonomous oscillator with the negative velocity feedback involving a short time delay includes two stages. The first is a very fast decay, and the second is very close to the vibration of delay free system around the equilibrium. Here, the negative gain of velocity feedback guarantees the rapid decay owing to the singularly perturbed term  $v\tau^2\ddot{x}(t)/2$  in Eq. (5.3.14b).

If the condition of  $v < 0$  is released, Eq. (5.3.14b) fails to predict the proper dynamics of Eq. (5.1.13). As will be seen in Section 7.3, for instance, the Duffing oscillator with delayed velocity feedback may exhibit very abundant nonlinear dynamics apart from the decaying to the equilibrium.



## 6 Dimensional Reduction of Nonlinear Delay Systems

Time delays usually give rise to great difficulty in the dynamic analysis of controlled mechanical systems. The difficulty increases so dramatically with an increase of system dimensions that the analytical results for the dynamics of delay systems of high dimensions are considerably few. So, it is highly demanded to develop some techniques for the reduction of system dimensions.

As stated in Section 2.3, the state space of a delay differential equation is a kind of Banach space and the dimension of solution space is infinite. To simplify the delayed dynamic systems, great efforts have been made for the reduction of system dimensions. The available approaches include the truncated Taylor expansion, the Padè approximation in (Lam 1993) and (Wang and Hu 1999b), the Hankel operator based method in (Ohta and Kojima 1999), and the center manifold method in (Faria and Magalhaes 1995) and (Diekmann et al. 1995), or referred to as the integral manifold approach alternatively in (Hale 1977). As analyzed in Sections 2.3 and 5.3, the truncated Taylor expansion method, albeit very simple, may give rise to wrong dynamics in general. The Hankel operator method can be used only for linear systems. The center manifold reduction is essentially a nonlinear method. In the implementation of this method, it is necessary to determine whether the system has a finite number of characteristic roots with zero real parts and the remaining characteristic roots have negative real parts. This is usually a hard task to complete for the high dimensional systems with time delays. To avoid this tough problem, the special features of system should be made advantage of.

In engineering, a great number of mechanical systems are composed of two kinds of subsystems, one is relatively stiff and has a high fundamental natural frequency, while the other is relatively soft and has a low fundamental natural frequency. Such a kind of systems is usually referred to as the *stiff-soft systems*. Examples of those systems include the ground vehicles discussed in Subsection 1.1.2, where the vehicle body is supported by soft front and rear suspensions and harder tires, the buckled viscoelastic beam supported by stiff vertical columns, etc. For the delay-free dynamic systems composed of stiff and soft subsystems, the

equations of motion can be formulated, by introducing a small singular parameter defined as the ratio of the fundamental natural frequencies of two subsystems, as singular perturbation of the equations of motion of the soft subsystem. Then, the theory of geometric singular perturbation in (Frenichel 1979) offers a natural analytic-geometric tool to deal with the dynamics of systems involving stiff-soft subsystems. Based on the singular perturbation approach, the so called *slow invariant manifold* and *fast invariant manifold* can be introduced so that the dominant dynamics of a stiff-soft system is studied on the slow invariant manifold, the dimension of which is identical to that of the phase space of soft subsystem. This case has been intensively studied, see (Bajaj et al. 1997) and (Georgiou et al. 1998). To the best knowledge of the authors, however, no such results are available for the dimensional reduction of delayed dynamic systems involving stiff and soft subsystems.

In this chapter, some basic facts on the decomposition of the state space are presented first. Then, an outline of the center manifold reduction is given for general functional differential equations in critical cases. Afterwards, the center manifold reduction is presented for the delayed dynamic systems involving stiff and soft subsystems governed by singularly perturbed differential equations. As an application of the proposed approach, the stability analysis is made for a quarter car model with active chassis.

## 6.1 Decomposition of State Space of Linear Delay Systems

This section deals with the linear delay differential equations in the frame of linear functional differential equations. For this purpose, given a positive number  $\tau$ , let  $C \equiv C([- \tau, 0], R^n)$  be the Banach space of continuous functions mapping  $[- \tau, 0]$  into  $R^n$ . For each  $\phi \in C$ , the norm  $\|\phi\|_C \equiv \sup_{-\tau \leq \theta \leq 0} \|\phi(\theta)\|$  is defined. Here,  $\|\cdot\|$  is any norm in  $R^n$ . As done in Subsection 2.2.1, the linear autonomous differential equation with a time delay can be cast as a functional differential equation in  $C$  as following

$$\dot{\mathbf{x}}(t) = \mathbf{L}(\mathbf{x}_t), \quad \mathbf{x} \in R^n, \quad t > 0, \quad (6.1.1)$$

where  $\mathbf{x}_t(\theta) \equiv \mathbf{x}(t + \theta)$  for  $-\tau \leq \theta \leq 0$ ,  $\mathbf{L}$  is a linear operator defined as

$$\mathbf{L}(\phi) \equiv \int_{-\tau}^0 [d\eta(\theta)] \phi(\theta), \quad (6.1.2)$$

through a bounded variation matrix function  $\eta(\theta)$ . The proof of the main results in this section can be found in (Hale 1977) and (Hale and Lunel 1993).

To focus on the effect of initial function  $\phi \in C$ , let  $x_t(\theta, \phi)$  denote the solution of Eq. (6.1.1) starting from  $x_0(\theta) \equiv \phi$ . Define a mapping  $T(t): C \rightarrow C$  as

$$T(t)(\phi) \equiv x_t(\theta, \phi). \quad (6.1.3)$$

It can be shown that  $T(t)$  has the following properties.

(a)  $T(0) = I$ .

(b)  $T(t+s) = T(t)T(s)$  for all  $t \geq 0$  and  $s \geq 0$ .

(c)  $T(t)$  is bounded for each  $t \geq 0$  and is strongly continuous on  $[0, +\infty)$ , i.e.,  $\lim_{s \rightarrow t} \|T(t)\phi - T(s)\phi\| = 0$  for  $t \geq 0$  and  $\phi \in C$ .

(d)  $T(t)$  is completely continuous (compact) for  $t \geq \tau$ . That is,  $T(t)$ ,  $t \geq \tau$  is continuous and maps any bounded set into a precompact set.

Therefore,  $T(t)$ ,  $t > 0$  is a strongly continuous semi-group of linear operators in  $C$  on  $[0, +\infty)$ , and the infinitesimal generator  $A$  of  $T(t)$  can be defined as

$$A(\phi) \equiv \lim_{t \rightarrow 0^+} \frac{1}{t} [T(t)(\phi) - \phi], \quad (6.1.4)$$

provided that the limit exists. It can be shown that the domain  $D(A)$  of  $A$  is dense in  $C$ , and the range  $R(A)$  is in  $C$ . Here, a set  $S_1$  is said to be *dense* in the set  $S_2$  if any point  $s \in S_2$  is the limit of a point sequence of  $S_1$ . Direct computation shows that for all  $\phi \in D(A)$ , we have

$$A(\phi) = \begin{cases} \frac{d\phi(\theta)}{d\theta}, & \theta \in [-\tau, 0), \\ L(\phi), & \theta = 0, \end{cases} \quad (6.1.5)$$

and

$$\frac{d}{dt} T(t)(\phi) = T(t)A(\phi) = AT(t)(\phi). \quad (6.1.6)$$

To decompose the state space, we need the concept of adjoint operator of  $A$ . For this purpose, let  $C^* \equiv C([0, \tau], R^{*n})$ , where  $R^{*n}$  is the  $n$ -dimensional vector space of row vectors. For  $\alpha(s) \in C^*$ ,  $0 \leq s \leq \tau$  and  $\beta(\theta) \in C$ ,  $-\tau \leq \theta \leq 0$ , define the *bilinear form* of  $\alpha(s)$  and  $\beta(\theta)$  as following

$$(\alpha, \beta) \equiv \alpha(0)\beta(0) - \int_{-\tau}^0 \int_0^\theta \alpha(\xi - \theta) [d\eta(\theta)] \beta(\xi) d\xi. \quad (6.1.7)$$

**Definition 6.1.1** The adjoint operator  $A^*$  of  $A$  is defined in  $D(A^*) \subseteq C^*$  such that for all  $\phi \in D(A)$  and  $\psi \in D(A^*)$ , the following bilinear form holds

$$(\psi, A(\phi)) = (A^*(\psi), \phi). \tag{6.1.8}$$

It is straightforward to derive that  $A^*$  is in the form

$$A^*(\psi) = \begin{cases} -\frac{d\psi(s)}{ds}, & s \in (0, \tau], \\ \int_{-\tau}^0 \psi(-\theta) d\eta(\theta), & s = 0, \end{cases} \tag{6.1.9}$$

and  $D(A^*)$  is dense in  $C^*$ .

### 6.1.1 Spectrum of a Linear Operator

To proceed further, we need the definition of the spectrum of a linear operator defined in a Banach space.

**Definition 6.1.2** For a linear operator  $A: X \rightarrow X$  defined in a Banach space  $X$ , the *resolvent set*  $\rho(A)$  of  $A$  is defined as a set on the complex plane as below

$$\rho(A) \equiv \{ \lambda \mid (\lambda I - A) \text{ has a bounded inverse with the domain dense in } X \}. \tag{6.1.10}$$

The *spectrum* of  $A$  is the complement of  $\rho(A)$  and is denoted by  $\sigma(A)$ .

Now, we consider the linear operator  $A$  in Eq. (6.1.5), the domain of which is dense in Banach space  $C$ . Then, there is a constant  $\lambda \in \rho(A)$  if and only if

$$(A - \lambda I)\phi = \psi \tag{6.1.11}$$

has a solution  $\phi$  in  $D(A)$  for every  $\psi$  in a dense set in  $C$ , and the solution depends continuously upon  $\psi$ . Hence,

$$\dot{\phi}(\theta) - \lambda\phi(\theta) = \psi(\theta), \quad -\tau \leq \theta < 0. \tag{6.1.12}$$

Solving Eq. (6.1.12) gives

$$\phi(\theta) = e^{\lambda\theta} b + \int_0^\theta e^{\lambda(\theta-\xi)} \psi(\xi) d\xi, \quad b \equiv \phi(0). \tag{6.1.13}$$

It follows that  $\phi$  is in  $D(A)$  if and only if  $\dot{\phi} \in C$  and

$$\dot{\phi}(0) = L(\phi) = \int_{-\tau}^0 [d\eta(\theta)]\phi(\theta). \tag{6.1.14}$$

Thus, we have

$$\lambda \mathbf{b} + \boldsymbol{\psi}(0) = \int_{-\tau}^0 d\boldsymbol{\eta}(\theta) [e^{\lambda\theta} \mathbf{b} + \int_0^\theta e^{\lambda(\theta-\xi)} \boldsymbol{\psi}(\xi) d\xi]. \quad (6.1.15)$$

Define the characteristic matrix  $\mathbf{A}(\lambda)$  as

$$\mathbf{A}(\lambda) \equiv \lambda \mathbf{I} - \int_{-\tau}^0 e^{\lambda\theta} d\boldsymbol{\eta}(\theta). \quad (6.1.16)$$

Then, Eq. (6.1.15) gives

$$\mathbf{A}(\lambda) \mathbf{b} = \lambda \mathbf{b} - \int_{-\tau}^0 e^{\lambda\theta} [d\boldsymbol{\eta}(\theta)] \mathbf{b} = -\boldsymbol{\psi}(0) + \int_{-\tau}^0 d\boldsymbol{\eta}(\theta) \left[ \int_0^\theta e^{\lambda(\theta-\xi)} \boldsymbol{\psi}(\xi) d\xi \right]. \quad (6.1.17)$$

Thus, for each  $\boldsymbol{\psi} \in C$ , there exists a unique  $\mathbf{b}$  if and only if  $\det \mathbf{A}(\lambda) \neq 0$ . Therefore, Eq. (6.1.11) has a solution  $\boldsymbol{\phi}$  for every  $\boldsymbol{\psi} \in C$  if and only if  $\det \mathbf{A}(\lambda) \neq 0$ , namely,  $\lambda$  is not a characteristic root. If  $\det \mathbf{A}(\lambda) = 0$  holds, Eqs. (6.1.13) and (6.1.17) imply that there exists a nonzero solution of Eq. (6.1.11) for  $\boldsymbol{\psi} = 0$ . This means that  $\lambda \in \sigma(\mathbf{A})$  holds.

The above analysis can be summarized as the following theorem.

**Theorem 6.1.1** For the linear operator  $\mathbf{A}$  in Eq. (6.1.5), we have

$$\rho(\mathbf{A}) = \{ \lambda \mid \det \mathbf{A}(\lambda) \neq 0 \}, \quad \sigma(\mathbf{A}) = \{ \lambda \mid \det \mathbf{A}(\lambda) = 0 \}. \quad (6.1.18)$$

Theorem 6.1.1 shows that the spectrum of  $\mathbf{A}$  is just the same set of characteristic roots of Eq. (6.1.1). A complex number  $\lambda \in \sigma(\mathbf{A})$  is also called the *eigenvalue* of  $\mathbf{A}$ . For  $\lambda \in \sigma(\mathbf{A})$ , the set of all  $\boldsymbol{\phi} \in C$  satisfying  $(\mathbf{A} - \lambda \mathbf{I})\boldsymbol{\phi} = 0$  is called the *eigenspace*.

**Definition 6.1.3** The *null space*  $N(\mathbf{A} - \lambda \mathbf{I})$  of  $\mathbf{A} - \lambda \mathbf{I}$  is the set of all  $\boldsymbol{\phi} \in C$  under  $(\mathbf{A} - \lambda \mathbf{I})\boldsymbol{\phi} = 0$ . For  $\lambda \in \sigma(\mathbf{A})$ , the *generalized eigenspace* of  $\lambda$ , denoted by  $M_\lambda(\mathbf{A})$ , is the smallest subspace in the state space  $C$  containing all  $\boldsymbol{\phi} \in C$  such that  $(\mathbf{A} - \lambda \mathbf{I})^k \boldsymbol{\phi} = 0$  holds for some  $k = 1, 2, \dots$

Because  $\mathbf{A}$  is a closed operator, the generalized eigenspace of each  $\lambda \in \sigma(\mathbf{A})$  is the same as  $N(\mathbf{A} - \lambda \mathbf{I})^k$  for certain  $k$ . In addition,  $\det \mathbf{A}(\lambda)$  is an entire function in  $\lambda$  on the complex plane and hence has roots of finite order. The dimension of  $N(\mathbf{A} - \lambda \mathbf{I})^k$  is equal to the multiplicity of root  $\lambda$  of  $\det \mathbf{A}(\lambda)$ . Therefore, the dimension of every generalized eigenspace is finite.

The operator  $\mathbf{A}^*$  has similar properties to those of  $\mathbf{A}$ . For example, we have

**Theorem 6.1.2**  $\lambda \in \sigma(\mathbf{A})$  if and only if  $\lambda \in \sigma(\mathbf{A}^*)$ .

**Theorem 6.1.3** The null space  $N(\mathbf{A} - \lambda \mathbf{I})^k$ , namely the generalized eigenspace  $M_\lambda(\mathbf{A})$  for  $\lambda \in \sigma(\mathbf{A})$ , is composed of

$$\boldsymbol{\phi}(\theta) = \sum_{j=1}^{k-1} \boldsymbol{\gamma}_{j+1} \frac{\theta^j}{j!} e^{\lambda\theta}, \quad -\tau \leq \theta \leq 0, \quad (6.1.19)$$

where  $\gamma \equiv [\gamma_1 \ \gamma_2 \ \cdots \ \gamma_k]^T$  yields  $A_k \gamma = 0$  with

$$A_k \equiv \begin{bmatrix} p_1 & p_2 & \cdots & p_k \\ 0 & p_1 & \cdots & p_{k-1} \\ \vdots & \vdots & \ddots & \vdots \\ 0 & 0 & \cdots & p_1 \end{bmatrix}, \quad p_{j+1} \equiv \frac{A^{(j)}(\lambda)}{j!}. \quad (6.1.20)$$

Similarly,  $N(A^* - \lambda I)^k$  consists of

$$\psi(s) = \sum_{j=1}^k \beta_j \frac{(-s)^{k-j}}{(k-j)!} e^{-\lambda s}, \quad 0 \leq s \leq \tau, \quad (6.1.21)$$

where  $\beta \equiv [\beta_1 \ \beta_2 \ \cdots \ \beta_k]$  yields  $\beta A_k = 0$ .

### 6.1.2 Decomposition of State Space

The generalized eigenspace  $M_\lambda(A)$  is invariant under the operator  $A$ , and  $T(t)$  as well. That is,  $AM_\lambda(A) \subseteq M_\lambda(A)$  and  $T(t)M_\lambda(A) \subseteq M_\lambda(A)$ , because  $\phi$  in  $M_\lambda(A)$  implies that  $(A - \lambda I)^k \phi = 0$  holds for some integer  $k$ , and  $A$ , as well as  $T(t)$ , is commutable with  $(A - \lambda I)^k$ . Denote a set of basis vectors for  $M_\lambda(A)$  by  $\phi_1^\lambda, \phi_2^\lambda, \dots, \phi_d^\lambda$ , and let

$$\Phi_\lambda \equiv [\phi_1^\lambda \ \phi_2^\lambda \ \cdots \ \phi_d^\lambda]. \quad (6.1.22)$$

Then, there is a  $d \times d$  matrix  $B_\lambda$  so that  $A\Phi_\lambda = \Phi_\lambda B_\lambda$  since  $AM_\lambda(A) \subseteq M_\lambda(A)$ . From the definition of  $A$ , we have

$$\Phi_\lambda(\theta) = \Phi_\lambda(0) \exp(B_\lambda \theta), \quad -\tau \leq \theta \leq 0. \quad (6.1.23)$$

Thus, for  $t \geq 0$  we have

$$[T(t)\Phi_\lambda](\theta) = \Phi_\lambda(0) \exp(B_\lambda(t+\theta)), \quad -\tau \leq \theta \leq 0. \quad (6.1.24)$$

Therefore, on the generalized eigenspace corresponding to a  $\lambda \in \sigma(A)$ , the functional differential equation (6.1.1) has the same structure as an ordinary differential equation. Through repeated applications of the above process, we know that if  $A \equiv \{\lambda_1, \lambda_2, \dots, \lambda_s\}$  is a set of eigenvalues of Eq. (6.1.1), and

$$\Phi_A \equiv [\Phi_{\lambda_1} \ \Phi_{\lambda_2} \ \cdots \ \Phi_{\lambda_s}], \quad B_A \equiv \text{diag}[B_{\lambda_1}, B_{\lambda_2}, \dots, B_{\lambda_s}], \quad (6.1.25)$$

where  $\Phi_{\lambda_j}$  is a basis matrix for  $M_{\lambda_j}(A)$ , and  $B_{\lambda_j}$  is the matrix defined by  $A\Phi_{\lambda_j} \equiv \Phi_{\lambda_j} B_{\lambda_j}$ ,  $j=1, 2, \dots, s$ , then the only eigenvalue of  $B_{\lambda_j}$  is  $\lambda_j$ . Moreover, we have the following theorem.

**Theorem 6.1.4** The subspace

$$P_A \equiv \{ \phi \in C \mid \phi = \Phi_A \mathbf{b} \text{ for some vectors } \mathbf{b} \} \quad (6.1.26)$$

is invariant under  $A$  and  $T(t)$ , and there exists an invariant subspace  $Q_A$  such that

$$C = P_A \oplus Q_A. \quad (6.1.27)$$

Theorem 6.1.4 gives a very clear picture of the solutions of Eq. (6.1.1). In fact, on generalized eigenspaces, Eq. (6.1.1) behaves essentially as an ordinary differential equation and the decomposition of space  $C$  into two subspaces invariant under  $A$  and  $T(t)$  enables one to separate out the dynamics of Eq. (6.1.1) on the eigenspaces from the other type of behavior. The above decomposition of  $C$  allows one to introduce a direct sum decomposition that plays the same role as the Jordan canonical form in ordinary differential equations.

The decomposition of the Banach space  $C$  can be completed provided that the projection operator defined by this decomposition can be explicitly characterized. For  $\lambda \in \sigma(A)$ , let  $\Psi_\lambda \equiv [\psi_1^T \ \psi_2^T \ \dots \ \psi_d^T]^T$  and  $\Phi_\lambda \equiv [\phi_1 \ \phi_2 \ \dots \ \phi_d]$  be the basis matrices for  $M_\lambda(A^*)$  and  $M_\lambda(A)$ , respectively. Then, the  $d \times d$  matrix  $(\Psi_\lambda, \Phi_\lambda) \equiv [(\psi_i, \phi_j)]$  is nonsingular. In addition, it can be normalized as an identity matrix by properly selecting  $\psi_i$  or  $\phi_i$ ,  $i=1, 2, \dots, d$  such that  $(\Psi_\lambda, \Phi_\lambda) = [\delta_{ij}]$  with  $\delta_{ii}=1$  and  $\delta_{ij}=0$ ,  $i \neq j$ . Then, for any  $\phi \in C$ , we have the decomposition

$$\phi = \phi^{P_\lambda} + \phi^{Q_\lambda}, \quad \phi^{P_\lambda} \equiv \Phi_\lambda (\Psi_\lambda, \phi) \in P_\lambda, \quad \phi^{Q_\lambda} \equiv \phi - \phi^{P_\lambda} \in Q_\lambda, \quad (6.1.28)$$

where

$$(\Psi, \phi) \equiv [(\psi_1, \phi) \ (\psi_2, \phi) \ \dots \ (\psi_d, \phi)]^T, \quad (6.1.29a)$$

$$P_\lambda \equiv M_\lambda(A) = \{ \phi \in C \mid \phi = \Phi_\lambda \mathbf{b} \text{ for some vector } \mathbf{b} \}, \quad (6.1.29b)$$

$$Q_\lambda \equiv \{ \phi \in C \mid (\Psi, \phi) = 0 \}. \quad (6.1.29c)$$

This decomposition can be extended to the case of multiple eigenvalues. Let  $A = \{\lambda_1, \lambda_2, \dots, \lambda_s\}$ , and let  $P_A$  be the linear extension of the  $M_{\lambda_j}(A)$ ,  $j=1, 2, \dots, s$ . We refer to this set as the generalized eigenspace of  $A$  associated with  $A$ . Similarly, we define  $P_A^*$  as the generalized eigenspace of  $A^*$  associated with  $A$ .

Then, we have

**Theorem 6.1.5** Assume that  $\Phi_A$  and  $\Psi_A$  are respectively the basis matrices of  $P_A$  and  $P_A^*$  such that  $(\Psi_A, \Phi_A) = I$ . Then, we have  $P_A = \{\phi \in C \mid \phi = \Phi_A b \text{ for some vector } b\}$  and  $Q_A = \{\phi \in C \mid (\Psi, \phi) = 0\}$  such that

$$C = P_A \oplus Q_A. \quad (6.1.30)$$

More precisely, for any  $\phi \in C$ , we have

$$\phi = \phi^{P_A} + \phi^{Q_A}, \quad \phi^{P_A} = \Phi_A(\Psi_A, \phi) \in P_A, \quad \phi^{Q_A} = \phi - \phi^{P_A} \in Q_A. \quad (6.1.31)$$

**Example 6.1.1** Consider the scalar delay differential equation

$$\dot{x}(t) = -\frac{\pi}{2}x(t-1) \equiv \int_{-1}^0 [d\eta(\theta)]x(t+\theta), \quad (6.1.32)$$

where

$$\eta(\theta) \equiv \begin{cases} -\frac{\pi}{2}, & \theta \in (-1, 0], \\ 0, & \theta = -1. \end{cases} \quad (6.1.33)$$

We study the dynamics of Eq. (6.1.32) by decomposing its state space.

The bilinear form defined by Eq. (6.1.7) is

$$(\psi, \phi) = \psi(0)\phi(0) - \frac{\pi}{2} \int_{-1}^0 \psi(\xi+1)\phi(\xi)d\xi, \quad (6.1.34)$$

and the linear operators  $A$  and  $A^*$  are given by

$$[A\phi](\theta) = \begin{cases} \dot{\phi}(\theta), & \theta \in [-1, 0], \\ -\frac{\pi}{2}\phi(-1), & \theta = 0, \end{cases} \quad (6.1.35a)$$

$$[A^*\psi](s) = \begin{cases} -\dot{\psi}(s), & s \in (0, -1], \\ -\frac{\pi}{2}\psi(1), & s = 0. \end{cases} \quad (6.1.35b)$$

Moreover,  $\phi$  is in  $N(\lambda I - A)$  if and only if  $\phi(\theta) = e^{\lambda\theta}b$ ,  $-1 \leq \theta \leq 0$ , where  $b$  is a constant and  $\lambda$  yields

$$\lambda + \frac{\pi}{2}e^{-\lambda} = 0. \quad (6.1.36)$$

Also,  $\psi$  falls into  $N(\lambda I - A^*)$  if and only if  $\psi(s) = e^{-\lambda s}c$ ,  $0 \leq s \leq 1$ , where  $c$  is a constant and  $\lambda$  yields Eq. (6.1.35).



It is easy to find that Eq. (6.1.35) has a pair of pure imaginary roots  $\pm i\pi/2$  and the remaining roots have negative real parts. Let  $\Lambda = \{i\pi/2, -i\pi/2\}$ . It becomes immediately obvious that

$$\Phi = [\phi_1 \ \phi_2] \tag{6.1.37}$$

is a set of basis vectors for the generalized eigenspace  $P = P_\Lambda$  of  $A$  associated with  $\Lambda$ , where

$$\phi_1(\theta) = \sin \frac{\pi\theta}{2}, \quad \phi_2(\theta) = \cos \frac{\pi\theta}{2}, \quad -1 \leq \theta \leq 0, \tag{6.1.38}$$

and that

$$\Psi^* = [\psi_1^* \ \psi_2^*]^T \tag{6.1.39}$$

is a basis matrix for the generalized eigenspace  $P_\Lambda^*$  of  $A^*$  associated with  $\Lambda$ , where

$$\psi_1^*(s) = \sin \frac{\pi s}{2}, \quad \psi_2^*(s) = \cos \frac{\pi s}{2}, \quad 0 \leq s \leq 1. \tag{6.1.40}$$

Noting that the matrix  $B$  subject to  $A\Phi = \Phi B$  is in the form

$$B = \begin{bmatrix} 0 & -\pi/2 \\ \pi/2 & 0 \end{bmatrix}, \tag{6.1.41}$$

we have

$$T(t)\Phi = \Phi \exp(Bt). \tag{6.1.42}$$

Now, we decompose the space  $C$  by  $\Lambda$ . The transformations are simpler if  $(\Psi^*, \Phi) = [(\psi_i^*, \phi_j)]$  is an identity matrix. However, it is not the identity matrix now. Therefore, we define a new basis matrix  $\Psi$  for  $P_\Lambda^*$  by  $\Psi = (\Psi^*, \Phi)^{-1} \Psi^*$ , and then have  $(\Psi, \Phi) = I$ . The explicit expression for the basis matrix  $\Psi$  is

$$\Psi = [\psi_1 \ \psi_2]^T, \tag{6.1.43}$$

where

$$\psi_1 = 2\mu \left( \sin \frac{\pi s}{2} + \frac{\pi}{2} \cos \frac{\pi s}{2} \right), \quad \psi_2 = 2\mu \left( \cos \frac{\pi s}{2} - \frac{\pi}{2} \sin \frac{\pi s}{2} \right), \quad \mu = \frac{1}{1 + \pi^2/4}. \tag{6.1.44}$$

If we decompose  $C$  by  $\Lambda$  and let  $Q = Q_\Lambda$  for simplicity in notation, then any  $\phi \in C$  can be written as

$$\phi = \phi^P + \phi^Q, \quad \phi^P = \Phi b, \quad b = [b_1 \ b_2]^T \equiv (\Psi, \phi), \tag{6.1.45}$$

where

$$\begin{cases} b_1 = \mu\pi\phi(0) - \mu\pi \int_{-1}^0 \left(\cos\frac{\pi s}{2} - \frac{\pi}{2}\sin\frac{\pi s}{2}\right)\phi(s)ds, \\ b_2 = 2\mu\phi(0) + \mu\pi \int_{-1}^0 \left(\frac{\pi}{2}\cos\frac{\pi s}{2} + \sin\frac{\pi s}{2}\right)\phi(s)ds. \end{cases} \quad (6.1.46)$$

The explicit expressions for  $b_1$  and  $b_2$  can be determined by substituting the expression for  $\Psi$  into Eq. (6.1.35b).

In the subspace  $P$ , we have  $T(t)\phi = \Phi \exp(Bt)b$ . The elements  $\phi_1$  and  $\phi_2$  of  $\Phi$  serve as a frame of coordinates in  $P$ . For any initial value  $\Phi b$  in  $P$ , we have

$$T(t+4)\Phi b = T(t)\Phi b, \quad (6.1.47)$$

since  $\exp[B(t+4)] = \exp(Bt)$ . In particular, we have  $T(4)\Phi b = \Phi b$ . This implies that the trajectories of Eq. (6.1.32) in  $C$  on  $P$  are closed curves. As a result, everything is clear in space  $C$  even though it is quite difficult to visualize the trajectories of Eq. (6.1.32) on the plane of  $(x, t)$ .

## 6.2 Dimensional Reduction for Stiff-soft Systems

This section is devoted to the problem of dimensional reduction for nonlinear delay systems composed of stiff and soft subsystems. We consider again the quarter car model of active suspension with a time delay in the state feedback as discussed in Subsection 3.6.1. Regarding to the vertical motion, the vehicle of concern can be considered as a stiff-soft system, where the soft subsystem is composed of the vehicle body and the suspension, while the stiff subsystem the tire and the unsprung mass. By introducing a proper time scale and a small singular parameter, the system dynamics can be described by a set of singularly perturbed differential equations with a time delay. Furthermore, this set of equations can be transformed into the standard form in critical cases. Then, the center manifold reduction is used to simplify the equation. The approach enables one to reduce a delayed stiff-soft system in the infinite dimensional solution space to a low order dynamic system without time delay, the dimension of which is identical to that of the state space of soft subsystems. It is essentially a nonlinear method and is more flexible in applications compared with the direct use of the center manifold reduction.

### 6.2.1 A quarter Car Model as a Singularly Perturbed System

As discussed in Subsection 1.1.2, the linearized dynamic equation of a quarter car model of active suspension reads

$$\begin{cases} m_b \ddot{x}_b(t) + c_s [\dot{x}_b(t) - \dot{x}_t(t)] + k_s [x_b(t) - x_t(t)] + g(t) = 0, \\ m_t \ddot{x}_t(t) + c_s [\dot{x}_t(t) - \dot{x}_b(t)] + k_s [x_t(t) - x_b(t)] + k_t [x_t(t) - z(t)] - g(t) = 0, \end{cases} \quad (6.2.1)$$

where  $x_b$  and  $x_t$  are the vertical displacements of the vehicle body of mass  $m_b$  and the unsprung mass  $m_t$ ,  $k_t$  is the linear stiffness of the tire. The vehicle body and the unsprung mass are connected through a passive suspension of stiffness  $k_s$  and damping  $c_s$ , as well as a hydraulic actuator capable of generating a control force  $g(t)$ . The control force  $g(t)$  yields the linear partial state feedback of vehicle body and includes a time delay  $\tau$  owing to the hydraulic actuator as following

$$g(t) = \tilde{u}x_b(t-\tau) + \tilde{v}\dot{x}_b(t-\tau). \quad (6.2.2)$$

The road disturbance denoted by  $z$  in Eq. (6.2.1) is the external excitation and can be set to be zero when the stability analysis is concerned with.

The quarter car model of vehicle suspensions always features that the natural frequency  $\omega_s \equiv \sqrt{k_s/m_b}$  of vehicle body with the unsprung mass clamped is much lower than the natural frequency  $\omega_t \equiv \sqrt{(k_s+k_t)/m_t}$  of the unsprung mass with the vehicle body clamped. Hence, it is a typical stiff-soft system.

To simplify the analysis, both the time  $t$  and the time delay  $\tau$  are substituted with the dimensionless ones

$$\omega_s t \rightarrow t, \quad \omega_s \tau \rightarrow \tau, \quad (6.2.3)$$

with help of the following dimensionless parameters

$$\varepsilon \equiv \frac{\omega_s}{\omega_t} \ll 1, \quad m \equiv \frac{m_b}{m_t}, \quad k \equiv \frac{k_t}{k_s}, \quad c \equiv \frac{c_s}{\sqrt{m_b k_s}}, \quad u \equiv \frac{\tilde{u}}{k_s}, \quad v \equiv \frac{\tilde{v}}{\sqrt{m_b k_s}}, \quad (6.2.4)$$

such that Eq. (6.2.1) can be recast into a set of singularly perturbed differential equations with a time delay

$$\begin{cases} \dot{\mathbf{x}}(t) = \mathbf{A}_{s0} \mathbf{x}(t) + \mathbf{B}_{s0} \mathbf{y}(t) + \mathbf{A}_{sd} \mathbf{x}(t-\tau), \\ \varepsilon \dot{\mathbf{y}}(t) = \mathbf{A}_{f0} \mathbf{x}(t) + \mathbf{B}_{f0} \mathbf{y}(t) + \mathbf{A}_{fd} \mathbf{x}(t-\tau), \end{cases} \quad (6.2.5)$$

where the dot represents the derivative with respect to the new time  $t$ , and

$$\mathbf{x} \equiv \begin{bmatrix} x_1 \\ x_2 \end{bmatrix} \equiv \begin{bmatrix} x_b \\ \dot{x}_b \end{bmatrix}, \quad \mathbf{y} \equiv \begin{bmatrix} y_1 \\ y_2 \end{bmatrix} \equiv \begin{bmatrix} x_t / \varepsilon^2 \\ \dot{x}_t / \varepsilon \end{bmatrix},$$

$$\begin{aligned}
 A_{s0} &\equiv \begin{bmatrix} 0 & 1 \\ -1 & -c \end{bmatrix}, & B_{s0} &\equiv \begin{bmatrix} 0 & 0 \\ 1 & c \\ m(1+k) & \sqrt{m(1+k)} \end{bmatrix}, & A_{sd} &\equiv \begin{bmatrix} 0 & 0 \\ -u & -v \end{bmatrix}, \\
 A_{f0} &\equiv \begin{bmatrix} 0 & 0 \\ m & mc \end{bmatrix}, & B_{f0} &\equiv \begin{bmatrix} 0 & 1 \\ -1 & -\frac{c\sqrt{m}}{\sqrt{1+k}} \end{bmatrix}, & A_{fd} &\equiv \begin{bmatrix} 0 & 0 \\ \mu u & \mu v \end{bmatrix}.
 \end{aligned} \tag{6.2.6}$$

In general, a stiff-soft system with delayed control can be described by a set of singularly perturbed differential equations with time delays if a small singular parameter is properly chosen. For simplicity, the attention in this section is paid to the following form of delay differential equations

$$\begin{cases} \dot{\mathbf{x}}(t) = \mathbf{f}(\mathbf{x}(t), \mathbf{y}(t), \mathbf{x}(t-\tau), \mathbf{y}(t-\tau)), \\ \varepsilon \dot{\mathbf{y}}(t) = \mathbf{g}(\mathbf{x}(t), \mathbf{y}(t), \mathbf{x}(t-\tau), \mathbf{y}(t-\tau)), \end{cases} \tag{6.2.7}$$

where  $0 < \varepsilon \ll 1$ ,  $\mathbf{f}, \mathbf{g} \in C^p$ ,  $p \geq 1$ ,  $\mathbf{f}(0,0,0,0) = 0$ ,  $\mathbf{g}(0,0,0,0) = 0$ ,  $\mathbf{x} \in R^m$  and  $\mathbf{y} \in R^n$  are the state vectors of soft subsystem and stiff subsystem, respectively.

In the next two subsections, an outline of the center manifold reduction is given first for the general functional differential equations in critical cases. Then, the center manifold reduction is presented for the singularly perturbed differential equation with a time delay.

## 6.2.2 Center Manifold Reduction in Critical Cases

Similar to the study in Section 6.1, a nonlinear differential equation with a time delay  $\tau$  can be written as a functional differential equation

$$\dot{\mathbf{x}}(t) = \mathbf{L}(\mathbf{x}_t) + \mathbf{N}(\mathbf{x}_t), \quad \mathbf{x} \in R^n, \quad t > 0, \tag{6.2.8}$$

where  $\mathbf{x}_t(\theta) \equiv \mathbf{x}(t+\theta)$  for  $-\tau \leq \theta \leq 0$ ,  $\mathbf{L}(\mathbf{x}_t)$  and  $\mathbf{N}(\mathbf{x}_t)$  represent the linear and nonlinear parts, respectively. Equation (6.2.8) is not in the standard form of a state equation, so the decomposition  $C = P_\Lambda \oplus Q_\Lambda$  in Theorem 6.1.5 for the Banach space  $C$  can not be directly used to the system reduction. To solve this problem, Eq. (6.2.8) is converted into the following differential equation of operators

$$\dot{\mathbf{x}}_t = \mathbf{A}(\mathbf{x}_t) + \Theta \cdot \mathbf{N}(\mathbf{x}_t), \tag{6.2.9}$$

where

$$\begin{aligned}
 A(\phi(\theta)) &\equiv \begin{cases} \frac{d\phi}{d\theta}, & \theta \in [-\tau, 0), \\ L(\phi), & \theta = 0, \end{cases} \\
 \Theta(\theta) &\equiv \begin{cases} 0, & \theta \in [-\tau, 0), \\ I, & \theta = 0. \end{cases} \quad (6.2.10)
 \end{aligned}$$

If the adjoint operator of  $L$  is denoted by  $L^*$ , the adjoint operator  $A^*$  of  $A$  reads

$$A^*(\psi(s)) = \begin{cases} -\frac{d\psi}{ds}, & s \in (0, \tau], \\ L^*(\psi), & s = 0. \end{cases} \quad (6.2.11)$$

Let  $\Lambda \equiv \{\lambda \mid \det \Delta(\lambda) = 0, \operatorname{Re} \lambda = 0\}$ , where  $\Delta(\lambda)$  is the characteristic matrix defined in Eq. (6.1.16). Assume that  $\Lambda$  has  $m$  (finite) elements, then the Banach space  $C$  can be decomposed by  $\Lambda$  as  $C = P \oplus Q$ , where  $P$  and  $Q$  are two invariant subspaces of  $C$  under  $A$  and  $T(t)$ . The subspace  $P$  is an  $m$ -dimensional subspace spanned by the eigenvectors associated with all  $\lambda$  in  $\Lambda$ . As done in Section 6.1, let  $\Phi \equiv [\phi_1 \ \phi_2 \ \cdots \ \phi_m]$  be a basis matrix for  $P$ ,  $\Psi \equiv [\psi_1^T \ \psi_2^T \ \cdots \ \psi_m^T]^T$  be a basis matrix for the dual space  $P^*$  of  $P$  in  $C^*$ , subject to  $(\Psi, \Phi) \equiv [(\psi_i, \phi_j)] = I$ . Then, for each  $t$ ,  $x_t$  can be decomposed as  $x_t = \Phi u + v$  with  $u \in R^m$  and  $v \in Q$ . Let matrix  $E$  be the solution of matrix equation  $\dot{\Phi} = \Phi E$ , direct computation shows, see (Faria and Magalhaes 1995), that  $u$  and  $v$  are governed by the following ordinary differential equations

$$\begin{cases} \dot{u} = E u + \Psi(0) N(\Phi u + v), \\ \dot{v} = A v + \Theta N(\Phi u + v) - \Phi \Psi(0) N(\Phi u + v). \end{cases} \quad (6.2.12)$$

Here the operator  $A$  in the second equation of Eq. (6.2.12) is in fact the restriction of  $A$  on the subspace  $Q$ .

The center manifold theorem in (Hale 1971) states that there exists an  $m$ -dimensional center manifold of Eq. (6.2.8) given by

$$M_c \equiv \{\phi \in C \mid \phi = \Phi u + v\} \quad (6.2.13)$$

for some  $v = h(u) \in Q$  with  $x$  in a neighborhood of the origin of  $R^n$ . The flow on the center manifold is given by  $x_t = \Phi u + v$ . The function  $h$  can be determined from

$$\begin{aligned}
 &A(h(u)) + \Theta N(\Phi u + h(u)) - \Phi \Psi(0) N(\Phi u + h(u)) \\
 &= Dh(u)[Eu + \Psi(0)N(\Phi u + h(u))], \quad (6.2.14)
 \end{aligned}$$

where  $Dh(\mathbf{u})$  is the Jacobian of  $\mathbf{h}(\mathbf{u})$  with respect to  $\mathbf{u}$ . More explicitly we have

$$\begin{aligned} & \frac{d}{d\theta} \mathbf{h}(\mathbf{u}) - \Phi \Psi(0) N(\Phi \mathbf{u} + \mathbf{h}(\mathbf{u})) \\ & = D\mathbf{h}(\mathbf{u}) [E\mathbf{u} + \Psi(0) N(\Phi \mathbf{u} + \mathbf{h}(\mathbf{u}))] \end{aligned} \tag{6.2.15a}$$

for  $\theta \in [-\tau, 0)$  and the following boundary condition

$$\begin{aligned} & [L(\mathbf{h}(\mathbf{u})) + N(\Phi \mathbf{u} + \mathbf{h}(\mathbf{u})) - \Phi \Psi(0) N(\Phi \mathbf{u} + \mathbf{h}(\mathbf{u}))] \Big|_{\theta=0} \\ & = D\mathbf{h}(\mathbf{u}) [E\mathbf{u} + \Psi(0) N(\Phi \mathbf{u} + \mathbf{h}(\mathbf{u}))] \Big|_{\theta=0}. \end{aligned} \tag{6.2.15b}$$

Thus, it is necessary to solve a series of boundary value problems in order to find out the elements of vector function  $\mathbf{h}$  since  $L(\phi)$  and  $N(\phi)$  are in terms of  $\phi(0)$  and  $\phi(-\tau)$ . Compared with the case of ordinary differential equations, it is more difficult to obtain an explicit series approximation of  $\mathbf{v}=\mathbf{h}(\mathbf{u})$  in terms of  $\mathbf{u}$ .

Once the vector function  $\mathbf{h}$  is found, the dominant dynamics of the original system in a neighborhood of the origin of  $R^n$  is governed by the first equation in Eq. (6.2.12).

### 6.2.3 Reduction for Singularly Perturbed Differential Equations

By introducing a fast time  $\eta \equiv t/\varepsilon$  and the corresponding time delay  $r \equiv \tau/\varepsilon$ , and denoting  $\mathbf{x}(\varepsilon\eta)$  and  $\mathbf{y}(\varepsilon\eta)$  by  $\mathbf{x}(\eta)$  and  $\mathbf{y}(\eta)$  respectively, Eq. (6.2.5) can be recast as

$$\begin{cases} \mathbf{x}'(\eta) = \varepsilon \mathbf{f}(\mathbf{x}(\eta), \mathbf{y}(\eta), \mathbf{x}(\eta-r), \mathbf{y}(\eta-r)), \\ \mathbf{y}'(\eta) = \mathbf{g}(\mathbf{x}(\eta), \mathbf{y}(\eta), \mathbf{x}(\eta-r), \mathbf{y}(\eta-r)), \end{cases} \tag{6.2.16}$$

where the prime represents the derivative with respect to the fast time  $\eta$ . According to  $\mathbf{g}(0,0,0,0)=0$ ,  $\mathbf{g}(\mathbf{x}(\eta), \mathbf{y}(\eta), \mathbf{x}(\eta-r), \mathbf{y}(\eta-r))$  can be written as

$$\mathbf{g} = A_{21}\mathbf{x}(\eta) + A_{22}\mathbf{y}(\eta) + B_{21}\mathbf{x}(\eta-r) + B_{22}\mathbf{y}(\eta-r) + \text{h.o.t.} \tag{6.2.17}$$

Let  $\mathbf{z} \equiv [\mathbf{x}^T \ \varepsilon \ \mathbf{y}^T]^T \in R^{m+l+1}$  and  $\mathbf{z}_\eta(\theta) \equiv \mathbf{z}(\eta+\theta)$  for  $-r \leq \theta \leq 0$ . Denote by  $C \equiv C([-r, 0], R^{m+l+1})$  the Banach space of continuous functions mapping  $[-r, 0]$  into  $R^{m+l+1}$  with the previously defined norm. Then, Eq. (6.2.16) can be written in the form of differential equation of operators

$$\mathbf{z}'_\eta = L(\mathbf{z}_\eta) + N(\mathbf{z}_\eta), \tag{6.2.18}$$

where

$$L(\phi) = \begin{bmatrix} 0 & 0 & 0 \\ A_{21} & 0 & A_{22} \end{bmatrix} \phi(0) + \begin{bmatrix} 0 & 0 & 0 \\ B_{21} & 0 & B_{22} \end{bmatrix} \phi(-r) \equiv L_1(\phi(0)) + L_2(\phi(-r)),$$

$$N(\phi) = \begin{bmatrix} \phi_{m+1}(0) f \left( \begin{bmatrix} \phi_1(0) \\ \vdots \\ \phi_m(0) \end{bmatrix}, \begin{bmatrix} \phi_{m+2}(0) \\ \vdots \\ \phi_{m+l+1}(0) \end{bmatrix}, \begin{bmatrix} \phi_1(-r) \\ \vdots \\ \phi_m(-r) \end{bmatrix}, \begin{bmatrix} \phi_{m+2}(-r) \\ \vdots \\ \phi_{m+l+1}(-r) \end{bmatrix} \right) \\ 0 \\ G \left( \begin{bmatrix} \phi_1(0) \\ \vdots \\ \phi_m(0) \end{bmatrix}, \begin{bmatrix} \phi_{m+2}(0) \\ \vdots \\ \phi_{m+l+1}(0) \end{bmatrix}, \begin{bmatrix} \phi_1(-r) \\ \vdots \\ \phi_m(-r) \end{bmatrix}, \begin{bmatrix} \phi_{m+2}(-r) \\ \vdots \\ \phi_{m+l+1}(-r) \end{bmatrix} \right) \end{bmatrix} \equiv \begin{bmatrix} N_1(\phi) \\ N_2(\phi) \end{bmatrix}, \tag{6.2.19}$$

with  $N_1 \in R^{m+1}$  and  $N_2 \in R^l$ .

In practice, it is almost impossible for an engineering system to be neutrally stable. Thus, it is very natural to assume that the dynamic equation of the stiff subsystem has no characteristic roots with zero real parts when the inertial of soft subsystem is clamped. That is, the free vibration of the stiff subsystem with the soft subsystem clamped either converges or diverges with an increase of time. Mathematically speaking, the characteristic equation

$$\det(\lambda I - A_{22} - B_{22} e^{-\lambda r}) = 0 \tag{6.2.20}$$

is assumed to have no pure imaginary roots. Then, Eq. (6.2.16) has  $m+1$  repeated zero characteristic roots and the remaining characteristic roots do not have zero real parts. This fact enables one to use the center manifold theorem.

In this case, the matrix function  $\eta(\theta)$  in Eq. (6.1.1) takes the form, see (Qin et al. 1989) and (Stépan 1989),

$$\eta(\theta) = \begin{cases} -L_2, & \theta = -r, \\ 0, & \theta \in (-r, 0), \\ L_1, & \theta = 0, \end{cases} \tag{6.2.21}$$

and the bilinear form defined in Eq. (6.1.7) reads

$$(\psi, \phi) = \psi(0)\phi(0) + \int_{-r}^0 \psi(s+r)L_2\phi(s) ds. \tag{6.2.22}$$

Let  $C = P \oplus Q$  be the decomposition by the  $m+1$  repeated zero eigenvalue of the state space  $C = C([-r, 0], R^{m+l+1})$ . Then, it is necessary to find out a basis matrix  $\Phi$  for  $P$  and a basis matrix  $\Psi$  for  $P^*$  satisfying  $(\Psi, \Phi) = I$ .

It is easy to show that the generalized eigenspace corresponding to zero eigenvalues coincides with the corresponding eigenspace. In fact, the characteristic matrix is in the form  $A(\lambda)=\lambda I-L_1-L_2e^{-\lambda r}$ . As shown in (Diekmann et al. 1995), a vector set  $[\alpha_0, \alpha_1, \dots, \alpha_{k-1}]$  is a Jordan chain of  $A(\lambda)$  at  $\lambda_0=0$  if and only if  $\alpha_0 \neq 0$  and

$$A(\lambda)[\alpha_0+(\lambda-\lambda_0)\alpha_1+\dots+(\lambda-\lambda_0)^{k-1}\alpha_{k-1}]=O((\lambda-\lambda_0)^k). \tag{6.2.23}$$

There follows immediately  $k=1$ . That is, the subspace  $P$  is composed of the eigenvectors associated with  $m+1$  repeated zero eigenvalues of  $A$ .

Each eigenvector  $z$  of  $A$  corresponding to  $\lambda = 0$  yields

$$\frac{dz}{d\theta}=0 \quad \text{and} \quad L_1(z(0))+L_2(z(-r))=0. \tag{6.2.24}$$

Hence,  $z$  is a constant vector. Let  $z \equiv [z_1 \dots z_m \dots z_{m+l+1}]^T$ , then  $(L_1+L_2)z=0$  gives

$$(A_{21}+B_{21}) \begin{bmatrix} z_1 \\ \vdots \\ z_m \end{bmatrix} + (A_{22}+B_{22}) \begin{bmatrix} z_{m+2} \\ \vdots \\ z_{m+l+1} \end{bmatrix} = 0. \tag{6.2.25}$$

Because  $\lambda=0$  is not a root of Eq. (6.2.20),  $A_{22}+B_{22}$  is invertible and hence

$$\begin{bmatrix} z_{m+2} \\ \vdots \\ z_{m+l+1} \end{bmatrix} = -(A_{22}+B_{22})^{-1}(A_{21}+B_{21}) \begin{bmatrix} z_1 \\ \vdots \\ z_m \end{bmatrix}. \tag{6.2.26}$$

When the vector  $[z_1 \dots z_m]^T$  is taken as the standard unit vectors in  $R^m$  respectively, the rest entries in vector  $z$  can be determined. Therefore, the basis matrix  $\Phi$  can be chosen as  $\Phi=[I \quad \Phi_1^T]^T$ .

Similarly, the eigenvector  $z$  in  $C^*$  of  $A^*$  corresponding to the eigenvalue  $\lambda=0$  satisfies  $dz/d\theta=0$  and  $L_1^T(z(0))+L_2^T(z(r))=0$ . That is, the sub-vector of  $z$  yields  $(A_{22}+B_{22})^T[z_{m+2} \dots z_{m+l+1}]^T=0$ . There follows  $[z_{m+2} \dots z_{m+l+1}]=0$  since the matrix  $A_{22}+B_{22}$  is invertible. Thus,  $\Psi=[I \quad 0]$  yields  $(\Psi, \Phi)=I$ .

Let  $z_\eta \in C=P \oplus Q$ , then we have  $z_\eta = \Phi u + v$  with  $u \equiv [u_1 \ u_2 \ \dots \ u_{m+1}]^T \in P$  and  $v \equiv [v_1 \ v_2 \ \dots \ v_{m+l+1}]^T \in Q$ . Thus, we can convert Eq. (6.2.12) into

$$\begin{cases} \dot{u} = N_1(\Phi u + v), \\ \dot{v} = Av + \Theta \cdot N(\Phi u + v) - \Phi \cdot N_1(\Phi u + v), \end{cases} \tag{6.2.27}$$



where the dot represents the derivative with respect to the fast time  $\eta$ . Noting that the  $(m+1)$ -th entry is zero in the vector  $N_1(\Phi \mathbf{u} + \mathbf{v})$ , which is equal to  $\Psi(0)N(\Phi \mathbf{u} + \mathbf{v})$ , we have  $du_{m+1}/d\eta=0$  and  $dv_{m+1}/d\eta=0$ . Because  $\varepsilon = u_{m+1} + v_{m+1}$ , it is natural to set  $u_{m+1} \equiv \varepsilon$  and  $v_{m+1} \equiv 0$ . Thus, in terms of the original time scale, the dominant dynamics of the Eq. (6.2.16) yields

$$\begin{bmatrix} \dot{u}_1 \\ \vdots \\ \dot{u}_m \end{bmatrix} = \mathbf{f}(\Phi \begin{bmatrix} u_1 \\ \vdots \\ u_m \\ \varepsilon \end{bmatrix} + \mathbf{h}(\begin{bmatrix} u_1 \\ \vdots \\ u_m \\ \varepsilon \end{bmatrix})), \quad (6.2.28)$$

according to the center manifold theorem. Here  $\mathbf{f}(\mathbf{x}, \mathbf{y}, \mathbf{x}(\eta-r), \mathbf{y}(\eta-r))$  is denoted by  $\mathbf{f}(\mathbf{z}_\eta)$  for simplicity.

Compared with the direct use of the center manifold reduction in the analysis on the Hopf bifurcation of delay differential equations, see (Hale 1977) and (Stépán 1989), this approach is more flexible to the high dimensional dynamic systems with time delays. Here, it is not necessary to check whether the original system of high dimensions has finite number of characteristic roots with zero real parts and all remaining characteristic roots have nonzero real parts. Instead, it is sufficient to check whether the stiff subsystem has no characteristic roots with zero real parts. In addition, the computational cost is lower because the two basis matrices  $\Phi$  and  $\Psi$  are independent of  $\theta$  in the present case. The approach is also applicable to the stability analysis of linear delay systems as seen in the next section, since it works for various problems of local dynamics.

### 6.3 Stability Analysis of an Active Suspension

This section presents an application of the dimensional reduction in Section 6.2 to the quarter car model with active suspension described by Eq. (6.2.5). The objective is to find the conditions that render the system asymptotically stable. As a special case, the stability of an undamped quarter car model with active suspension was studied in (Palkovics and Venhovens 1992) by using the method of  $D$ -subdivision. A detailed analysis has been made in Subsection 3.6.1 on the delay-independent stability of a type of damped quarter car models with active suspension by using the generalized Sturm theory. For a given time delay, however, no analytical results are available for the stability analysis of this system with respect to any system parameters. Now, the approach presented in previous sections is used to analyze the stability of this system.

### 6.3.1 Center Manifold Reduction

To study the stability of Eq. (6.2.5), we first introduce a fast time scale  $\eta \equiv t/\varepsilon$  and corresponding time delay  $r \equiv \tau/\varepsilon$ , and transform Eq. (6.2.5) into a set of delay differential equations in terms of the fast time scale

$$\begin{cases} \mathbf{x}'(\eta) = \varepsilon[\mathbf{A}_{s0}\mathbf{x}(\eta) + \mathbf{B}_{s0}\mathbf{y}(\eta) + \mathbf{A}_{sd}\mathbf{x}(\eta-r)], \\ \varepsilon'(\eta) = 0, \\ \mathbf{y}'(\eta) = \mathbf{A}_{f0}\mathbf{x}(\eta) + \mathbf{B}_{f0}\mathbf{y}(\eta) + \mathbf{A}_{fd}\mathbf{x}(\eta-r), \end{cases} \quad (6.3.1)$$

where the prime represents the derivative with respect to the fast time scale  $\eta$ . In the state space  $C([-r, 0], R^5)$  with the notations used in Section 6.1, we have

$$\begin{aligned} \mathbf{L}_1 &= \begin{bmatrix} 0 & 0 & 0 \\ \mathbf{A}_{f0} & 0 & \mathbf{B}_{f0} \end{bmatrix}, \quad \mathbf{L}_2 = \begin{bmatrix} 0 & 0 & 0 \\ \mathbf{A}_{fd} & 0 & 0 \end{bmatrix}, \quad \Phi_1 = \begin{bmatrix} m(1+u) & m(c+v) & 0 \\ 0 & 0 & 0 \end{bmatrix} \\ \mathbf{N}_1(\phi) &= \begin{bmatrix} \phi_3(0)(\mathbf{A}_{s0} \begin{bmatrix} \phi_1(0) \\ \phi_2(0) \end{bmatrix} + \mathbf{B}_{s0} \begin{bmatrix} \phi_4(0) \\ \phi_5(0) \end{bmatrix} + \mathbf{A}_{sd} \begin{bmatrix} \phi_1(-r) \\ \phi_2(-r) \end{bmatrix}) \\ 0 \end{bmatrix}, \quad \mathbf{N}_2(\phi) = 0. \end{aligned} \quad (6.3.2)$$

To investigate the local dynamics of the quarter car model with active suspension on the center manifold, it is necessary to make an approximation to the function  $\mathbf{v} = \mathbf{h}(\mathbf{u})$  determined by the center manifold theorem. This work can be completed with help of a polynomial approximation  $\mathbf{h}(\mathbf{u}) \approx \sum_{i+j+k=2,3} \mathbf{h}_{ijk}(\theta) u_1^i u_2^j u_3^k$ . For the stability analysis of the trivial solution, it is sufficient to assume the form of  $\mathbf{h}(\mathbf{u})$  as following

$$\begin{aligned} \mathbf{h}(\mathbf{u}) &\approx [\mathbf{h}_{11}(\theta)u_3 + \mathbf{h}_{12}(\theta)u_3^2]u_1 + [\mathbf{h}_{21}(\theta)u_3 + \mathbf{h}_{22}(\theta)u_3^2]u_2 \\ &= [\mathbf{h}_{11}(\theta)\varepsilon + \mathbf{h}_{12}(\theta)\varepsilon^2]u_1 + [\mathbf{h}_{21}(\theta)\varepsilon + \mathbf{h}_{22}(\theta)\varepsilon^2]u_2, \end{aligned} \quad (6.3.3)$$

where

$$\mathbf{h}_{ij}(\theta) \equiv [h_{ij}^1(\theta) \ h_{ij}^2(\theta) \ 0 \ h_{ij}^4(\theta) \ h_{ij}^5(\theta)]^T. \quad (6.3.4)$$

Then, we arrive at the dynamic equation on the center manifold

$$\begin{bmatrix} \dot{u}_1 \\ \dot{u}_2 \\ \dot{u}_3 \end{bmatrix} = u_3 \begin{bmatrix} (a_{11}u_3 + a_{12}u_3^2)u_1 + (a_{20} + a_{21}u_3 + a_{22}u_3^2)u_2 \\ (b_{10} + b_{11}u_3 + b_{12}u_3^2)u_1 + (b_{20} + b_{21}u_3 + b_{22}u_3^2)u_2 \\ 0 \end{bmatrix} \equiv \mathbf{N}_1, \quad (6.3.5)$$

where the coefficients  $a_y$  and  $b_y$  are determined as follows

$$\begin{aligned}
a_{20}=1, \quad a_{ij}=h_{ij}^2(0), \quad b_{10}=-\frac{k(1+u)}{1+k}, \quad b_{20}=-\frac{k(c+v)}{1+k}, \\
b_{ij}=-h_{ij}^1(0)-uh_{ij}^1(-r)-ch_{ij}^2(0)-vh_{ij}^2(-r) \\
+\frac{h_{ij}^4(0)}{m(1+k)}+\frac{ch_{ij}^5(0)}{\sqrt{m(1+k)}}, \quad i, j=1,2.
\end{aligned} \tag{6.3.6}$$

### 6.3.2 Computation of the Approximated Center Manifold

In what follows, attention is paid to determining the functions  $h_{ij}^k(\theta)$  in Eq. (6.3.3), which are characterized by a series of boundary value problems in Eq. (6.2.15).

With help of MAPLE, we can readily obtain the following ordinary differential equations and the corresponding boundary conditions by separating the coefficients of the terms  $u_1u_3^i$ ,  $u_2u_3^i$  in Eqs. (6.2.15a) and (6.2.15b). After some necessary substitutions, the boundary problems are converted into the following initial problems

$$\begin{aligned}
\frac{d}{d\theta}h_{11}^1(\theta)=0, \quad \frac{d}{d\theta}h_{21}^1(\theta)=1, \\
h_{11}^1(0)=0, \quad h_{21}^1(0)=0;
\end{aligned} \tag{6.3.7a}$$

$$\begin{aligned}
\frac{d}{d\theta}h_{11}^2(\theta)=b_{10}, \quad \frac{d}{d\theta}h_{21}^2(\theta)=b_{20}, \\
h_{11}^2(0)=0, \quad h_{21}^2(0)=0;
\end{aligned} \tag{6.3.7b}$$

$$\begin{aligned}
\frac{d}{d\theta}h_{12}^1(\theta)=b_{10}h_{21}^1(\theta)+h_{11}^2(0), \quad \frac{d}{d\theta}h_{22}^1(\theta)=b_{20}h_{21}^1(\theta)+h_{11}^1(\theta)+h_{21}^2(0), \\
h_{12}^1(0)=0, \quad h_{22}^1(0)=0;
\end{aligned} \tag{6.3.7c}$$

$$\begin{aligned}
\frac{d}{d\theta}h_{12}^2(\theta)=b_{10}h_{21}^2(\theta)+b_{11}, \quad \frac{d}{d\theta}h_{22}^2(\theta)=b_{20}h_{21}^2(\theta)+h_{11}^2(\theta)+b_{21}, \\
h_{12}^2(0)=0, \quad h_{22}^2(0)=0;
\end{aligned} \tag{6.3.7d}$$

$$\frac{d}{d\theta}h_{11}^4(\theta)=-\frac{mk(1+u)(c+v)}{1+k}, \quad \frac{d}{d\theta}h_{21}^4(\theta)=m(1+u)-\frac{mk(c+v)^2}{1+k},$$

$$h_{11}^4(0) = (1+u) \left[ \frac{mkvr}{1+k} + \frac{ck(c+v)\sqrt{m^3}}{\sqrt{(1+k)^3}} \right],$$

$$h_{21}^4(0) = \frac{mkv(c+v)r}{1+k} - mur + \frac{c(1+u)\sqrt{m}}{\sqrt{1+k}} - \frac{ck(c+v)^2\sqrt{m^3}}{\sqrt{(1+k)^3}}; \quad (6.3.7e)$$

$$\frac{d}{d\theta} h_{11}^5(\theta) = 0, \quad \frac{d}{d\theta} h_{21}^5(\theta) = 0,$$

$$h_{11}^5(0) = -\frac{mk(1+u)(c+v)}{1+k}, \quad h_{21}^5(0) = mk(c+v)^2 + m(1+u). \quad (6.3.7f)$$

Though the differential equations for  $h_{12}^4(\theta)$ ,  $h_{22}^4(\theta)$ ,  $h_{12}^5(\theta)$ , and  $h_{22}^5(\theta)$  are simple, for example,

$$\frac{d}{d\theta} h_{12}^4(\theta) = b_{10} h_{21}^4(\theta) + m(1+u) h_{11}^2(0) + b_{11} m(c+v),$$

$$\frac{d}{d\theta} h_{22}^4(\theta) = b_{20} h_{21}^4(\theta) + h_{11}^4(\theta) + m(1+u) h_{21}^2(0) + b_{21} m(c+v), \quad (6.3.7g)$$

$$\frac{d}{d\theta} h_{12}^5(\theta) = b_{10} h_{21}^5(\theta), \quad \frac{d}{d\theta} h_{22}^5(\theta) = b_{20} h_{21}^5(\theta) + h_{11}^5(\theta), \quad (6.3.7h)$$

the expressions of  $h_{12}^4(0)$ ,  $h_{22}^4(0)$ ,  $h_{12}^5(0)$ , and  $h_{22}^5(0)$  are somewhat lengthy as follows.

$$\frac{h_{12}^4(0)}{1+u} = \frac{ckr\sqrt{m^3} [(3vk(c+v) - u(1+k))]}{\sqrt{(1+k)^5}}$$

$$+ \frac{mk^2 \{ (3v^2 - u + cv)r^2 + 2[1+u - (c+v)^2] \}}{2(1+k)^2}$$

$$+ mk \frac{mc^2 [2(c+v)^2 - (1+u)] + (1+u)(1 - c^2m) - ur^2}{(1+k)^3},$$

$$h_{22}^4(0) = \frac{ckr\sqrt{m^3} [3kv(c+v)^2 - 2(1+k)(v + cu + 2uv)]}{\sqrt{(1+k)^5}}$$

$$+ mk^2 r^2 \frac{(vc^2 + 4v^2 + 3v^3)}{2(1+k)^2} - mkr^2 \frac{cu + 4uv + v}{2(1+k)}$$

$$\begin{aligned}
& -mk^2c^2 \frac{c+3v}{(1+k)^2} + mk^2 \frac{(2-3v^2+2u)c+2v-v^3+2uv}{(1+k)^2} \\
& + mk \frac{(2-3mc^2)(1+u)(c+v)}{(1+k)^2} \\
& + m^2k^2c^2 \frac{2c^3+6c^2v+6cv^2+2v^3}{(1+k)^3}, \tag{6.3.7g'}
\end{aligned}$$

$$\begin{aligned}
\frac{h_{12}^5(0)}{1+u} &= \frac{mkr[u(1+k)-2vk(c+v)]}{(1+k)^2} - \frac{2ck^2\sqrt{m^3}(c+v)^2}{\sqrt{(1+k)^5}} + \frac{ck\sqrt{m^3}(1+u)}{\sqrt{(1+k)^3}}, \\
h_{22}^5(0) &= -\frac{kr\sqrt{m^3}[2vk(c+v)^2-(1+k)(v+2cu+3uv)]}{(1+k)^2} \\
& - \frac{2ck^2\sqrt{m^3}[(c^3+v^3)+3cv(c+v)]}{\sqrt{(1+k)^5}} + \frac{3ck\sqrt{m^3}(1+u)(c+v)}{\sqrt{(1+k)^3}}. \tag{6.3.7h'}
\end{aligned}$$

It is now an easy task to obtain the functions  $h_{ij}^k(\theta)$ . For example, we can readily write out

$$\begin{aligned}
h_{11}^1(\theta) &= 0, \quad h_{12}^1(\theta) = \frac{b_{10}\theta^2}{2}, \\
h_{11}^2(\theta) &= b_{10}\theta, \quad h_{12}^2(\theta) = b_{11}\theta + \frac{b_{10}b_{20}\theta^2}{2}, \\
h_{21}^1(\theta) &= \theta, \quad h_{22}^1(\theta) = \frac{b_{20}\theta^2}{2}, \\
h_{21}^2(\theta) &= b_{20}\theta, \quad h_{22}^2(\theta) = b_{21}\theta + \frac{(b_{10}+b_{20}^2)\theta^2}{2}. \tag{6.3.8}
\end{aligned}$$

In terms of the original time scale  $t$ , Eq. (6.3.5) is now in the form

$$\begin{bmatrix} \dot{u}_1 \\ \dot{u}_2 \end{bmatrix} = \begin{bmatrix} u_2 \\ (b_{10}+b_{11}\varepsilon+b_{12}\varepsilon^2)u_1 + (b_{20}+b_{21}\varepsilon+b_{22}\varepsilon^2)u_2 \end{bmatrix}, \tag{6.3.9}$$

where all the coefficients are in terms of the system parameters.

### 6.3.3 Stability Analysis

As proved in (Hale 1971), if the trivial solution  $u=0$  of the first equation in Eq. (6.2.12) is asymptotically stable (or unstable), so is the trivial solution  $x=0$  of Eq. (6.2.9). From the above analysis, it is easy to see that the trivial solution of Eq. (6.2.1) is asymptotically stable if the zero solution of the reduced Eq. (6.3.9) is asymptotically stable. From the Routh-Hurwitz criterion, the trivial solution of Eq. (6.2.1) is asymptotically stable if

$$b_{10} + b_{11}\varepsilon + b_{12}\varepsilon^2 < 0 \quad \text{and} \quad b_{20} + b_{21}\varepsilon + b_{22}\varepsilon^2 < 0. \tag{6.3.10}$$

On the other hand, if the characteristic function of Eq. (6.2.1) is denoted as  $D(\lambda)$ ,  $D(0) = p(1+u)$  holds for a positive number  $p$ , and  $D(+\infty) \rightarrow +\infty$ . Thus, if  $1+u \leq 0$ ,  $D(\lambda)$  has a non-negative root, which renders the system unstable. Therefore, the inequality  $1+u > 0$  should hold true if the system is asymptotically stable. Note from the expressions  $h_{ij}^k(0)$  and  $b_{ij}$  in Eqs. (6.3.6) and (6.3.7) that there is a common factor  $1+u$  in the term of  $b_{10} + b_{11}\varepsilon + b_{12}\varepsilon^2$  because

$$\begin{cases} b_{11} = b_{10}vr + \frac{h_{11}^4(0)}{m(1+k)} + \frac{c \cdot h_{11}^5(0)}{\sqrt{m(1+k)}}, \\ b_{12} = -\frac{b_{10}ur^2}{2} + v(b_{11}r - \frac{b_{10}b_{20}r^2}{2}) + \frac{h_{12}^4(0)}{m(1+k)} + \frac{c \cdot h_{12}^5(0)}{\sqrt{m(1+k)}}. \end{cases} \tag{6.3.11}$$

Thus, the factor  $1+u$  can be dropped from the stability conditions in Eq. (6.3.10).

To demonstrate the effectiveness of the dimensional reduction, a comparison is made for the asymptotically stable regions determined by using this approach and the method of  $D$ -subdivision on the plane of  $(u, v)$  for the following parameters

$$\begin{aligned} m_b = 290 \text{ kg}, \quad m_t = 59 \text{ kg}, \quad k_s = 16,812 \text{ N/m}, \quad k_t = 190,000 \text{ N/m}, \\ c_s = 0 \sim 980 \text{ Ns/m}, \quad \tau = 0 \sim 0.4 \text{ s}, \end{aligned} \tag{6.3.12}$$

or equivalently for the following dimensionless parameters

$$m = 4.9153, \quad k = 11.301, \quad c = 0 \sim 0.4453, \quad r = 0 \sim 0.1699. \tag{6.3.13}$$

Given the combination of dimensionless feedback gains

$$(u, v) \in [-0.95, 0.95] \times [-0.95, 0.95], \tag{6.3.14}$$

we look at the following four case studies: (a)  $c=0.05$  and  $r=0.01$ ; (b)  $c=0.05$  and  $r=0.05$ ; (c)  $c=0.25$  and  $r=0.08$ ; (d)  $c=0.30$  and  $r=0.10$ .

As shown in Fig. 6.3.1 the asymptotically stable regions determined by using the approach of dimensional reduction are in good agreement with those obtained by using the method of  $D$ -subdivision.

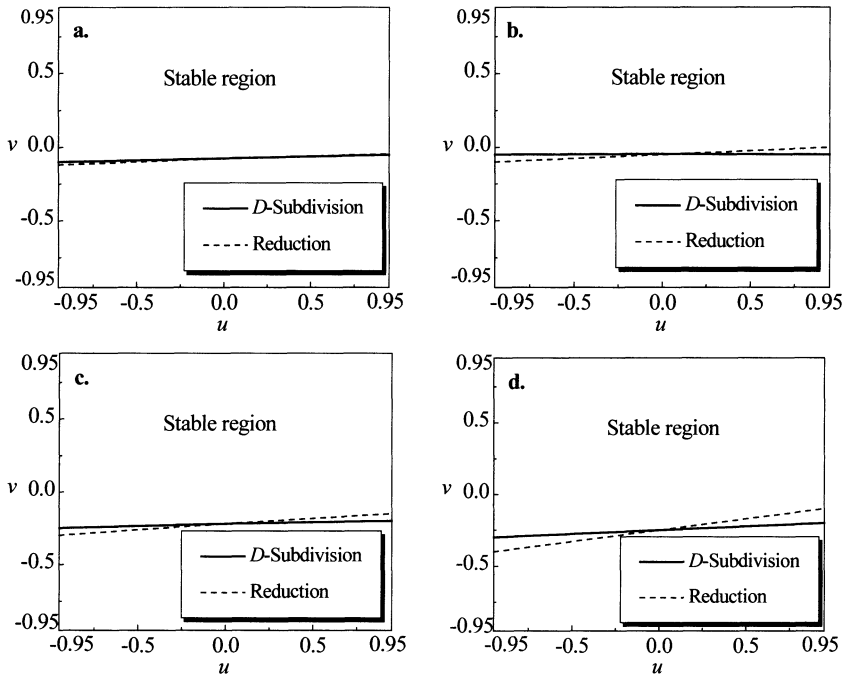


**Fig. 6.3.1.** Asymptotically stable region on the plane of  $(u, v)$ ; **a.**  $c=0.05$  and  $r=0.01$ , **b.**  $c=0.05$  and  $r=0.05$ , **c.**  $c=0.25$  and  $r=0.08$ , **d.**  $c=0.3$  and  $r=0.10$

Another application of the approach of dimensional reduction is to the local bifurcation analysis. The approach, possibly combined with the computational techniques for the normal form, see (Faria and Magalhaes 1995), enables one to complete the local bifurcation analysis of the stiff-soft systems with a time delay in a way similar to the case of the ordinary differential equations.

Even though many practical systems exhibit the behavior consistent with singularly perturbed differential equations, most of them are not in the standard form of singularly perturbed differential equations. For those systems, it is very important to have a proper physical insight when the singular parameters and transformations are chosen. It is still an open problem whether any heuristic ideas could be followed for choosing the proper small parameters and transformations when the physical insight is not obvious.

## 7 Periodic Motions of Nonlinear Delay Systems

The study on nonlinear delayed dynamic systems is a tough problem. Only a few theoretical results have been available for those that can model engineering systems. Among the available results, the existence and determination of periodic motions of nonlinear delayed dynamic systems have drawn great attention.

In theory, the existence of periodic motions can be studied by using the fixed-point theorems and the Lyapunov methods, see, for example, (Hale 1977) and (Li and Wen 1987). A very skilful approach proposed by (Kaplan and Yorke 1974) has been developed over the past two decades to construct the periodic solutions of delay differential equations via a sort of ordinary differential equations, see (Liu and Li 1996). These studies, however, are still limited to very simple delay differential equations. In practice, the periodic motions have to be determined by using approximate techniques, such as the Poincaré-Lindstedt approach in (Casal and Freeman 1980), the method of harmonic balancing in (McDonald 1995), and the method of multiple scales in (Hu et al. 1998a).

Physically speaking, there are two important causes for the emergence of a periodic motion if the system is nonlinear. One is the well-known Hopf bifurcation at the equilibrium of an autonomous system, and the other is the either external or parametric periodic excitation in a non-autonomous system. This chapter will discuss the periodic motions of nonlinear delayed dynamic systems owing to these two sources respectively.

### 7.1 The Hopf Bifurcation of Autonomous Systems

As well known in the case of ordinary differential equations, one of the simplest ways in which a non-constant periodic solution emerges is through the *Hopf bifurcation*. This occurs when, as a real parameter  $\alpha$  in the equation is passing through a critical value  $\alpha_0$ , a pair of conjugate eigenvalues of the linear operator (namely a pair of conjugate characteristic roots of the characteristic quasi-polynomial) is crossing the imaginary axis on complex plane from the left to the right. Generally



speaking, the theorem of Hopf bifurcation assumes only the local existence of periodic solutions when they arise. This case will be discussed later.

To undergo a Hopf bifurcation, the dynamic system governed by a set of ordinary differential equations must be at least two-dimensional. However, a first order delay differential equation with a single time delay may undergo the Hopf bifurcation or more complicated bifurcations such as the Hopf-Hopf bifurcation, and even exhibits chaotic behaviour. For a single-degree-of-freedom system with delayed feedback control, it does undergo complicated bifurcations, see, for example, (Shayer and Campbell 2000) and the references therein.

The theorem of Hopf bifurcations enables one to obtain the local existence of a periodic solution. To establish the global existence, it is often to resort to some kind of fixed point theorems associated with the mapping  $\mathcal{A}$  defined in a cone shaped subset  $K$  in the state space  $C$ . Here, the cone  $K$  plays the role of the Poincaré section and the mapping  $\mathcal{A}$  is usually similar to the Poincaré mapping for ordinary differential equations. A comprehensive description of this method is beyond the scope of this book. It is referred to (Hale 1977), (Kuang 1993) and (Hale and Lunel 1993).

### 7.1.1 Theory of the Hopf Bifurcations

As proved in (Hale 1977) or (Hale and Lunel 1993), a general theory is available for the Hopf bifurcation of delay differential equations. The theory is presented hereinafter for a one-parameter family of nonlinear delay differential equations

$$\dot{x}(t) = f(\alpha, x_t), \tag{7.1.1}$$

where  $x_t(\theta) \equiv x(t+\theta)$  is defined for  $\theta \in [-\tau, 0]$ ,  $f(\alpha, \phi)$  has the continuous first and second derivatives with respect to  $\alpha$  and  $\phi$  for  $\alpha \in R$  and  $\phi \in C([-\tau, 0], R^n)$ , where  $C \equiv C([-\tau, 0], R^n)$  is equipped with the norm  $\|\phi\|_C \equiv \sup_{\theta \in [-\tau, 0]} \|\phi(\theta)\|$  as before. Assume that  $f(\alpha, 0) = 0$  holds for all  $\alpha \in R$ . That is, the system has a fixed trivial solution  $x = 0$  for all values of  $\alpha$ . Furthermore, define a linear operator  $L_\alpha: R \times C \rightarrow R^n$  with parameter  $\alpha$  by

$$L_\alpha \phi = D_\phi f(\alpha, 0) \phi, \tag{7.1.2}$$

where  $D_\phi f(\alpha, 0)$  is the Jacobian of  $f(\alpha, \phi)$  with respect to  $\phi$  at  $\phi = 0$  and can be expressed by  $L_\alpha \phi = \int_{-\tau}^0 [d\eta(\theta)] \phi(\theta)$  for some bounded variation matrix function  $\eta$ . In addition, define

$$N_\alpha \phi = f(\alpha, \phi) - L_\alpha \phi, \tag{7.1.3}$$

for the nonlinear part of the right-hand side of Eq. (7.1.1) and assume that  $\|N_\alpha \phi\|_c = o(\|\phi\|_c)$  as  $\|\phi\|_c \rightarrow 0$ .

Suppose that the characteristic root  $\lambda(\alpha)$  of  $L_\alpha$  has a continuous derivative  $\lambda'(\alpha)$  with respect to  $\alpha$ . Given a specific value  $\alpha_0$ , say,  $\alpha_0 = 0$  without loss of generality, of  $\alpha$ , the trivial solution  $x=0$  is asymptotically stable for  $\alpha_0$  if all the eigenvalues of  $L_{\alpha_0}$  have negative real parts. If there exist any eigenvalues with positive real roots, then the trivial solution  $x=0$  is unstable.

In what follows, the trivial solution  $x=0$  of Eq. (7.1.1) is assumed to undergo an instability when the parameter  $\alpha$  increases and arrives at  $\alpha_0 = 0$ . That is, a pair of conjugate complex eigenvalues of  $L_\alpha$  goes from the open left half-plane into the open right half-plane as  $\alpha$  increases and passes through  $\alpha_0$ . After such a transition, an arbitrary small disturbance near the trivial solution may evolve into an oscillatory solution.

More precisely, a theorem is presented on the basis of following two assumptions.

**(H1)** For a small  $\alpha$ , the linear operator  $L_\alpha$  has a pair of simple conjugate imaginary eigenvalues  $\gamma(\alpha) \pm i\omega(\alpha)$ , which yields

$$\gamma(0) = 0, \quad \omega_0 \equiv \omega(0) \neq 0, \tag{7.1.4}$$

and  $L_0$  has no other pure imaginary eigenvalues which are multiples of  $i\omega_0$ .

**(H2)** The pair of conjugate eigenvalues is crossing the imaginary axis at  $\alpha = 0$ , namely

$$\gamma'(0) \neq 0. \tag{7.1.5}$$

**Theorem 7.1.1.** Suppose that  $f(\alpha, \phi)$  has the first two continuous derivatives with respect to  $\alpha$  and  $\phi$ , and  $F(\alpha, 0) = 0$  holds for all  $\alpha \in R$ . In addition, assume that the hypotheses (H1) and (H2) are true. Then there are constants  $\xi_0 > 0$ ,  $\alpha_0 > 0$ ,  $\delta_0 > 0$ , continuously differentiable functions  $\alpha(\xi) \in R$ ,  $\omega(\xi) \in R$ , and an  $\omega(\xi)$ -periodic function  $x^*(\xi)$  in  $\xi$  for  $\|\xi\|_c < \xi_0$  such that

$$x^*(\xi) = x_0^*(\xi)^{p_\alpha} + x_0^*(\xi)^{q_\alpha} \tag{7.1.6a}$$

is a solution of Eq. (7.1.1) with the following decompositions

$$x_0^*(\xi)^{p_\alpha} = \Phi_{\alpha(\xi)} y^*(\xi), \quad x_0^*(\xi)^{q_\alpha} = z_0^*(\xi), \tag{7.1.6b}$$

where  $y^*(\xi) = (\xi, 0)^T + o(\|\xi\|_c)$  and  $z_0^*(\xi) = o(\|\xi\|_c)$  as  $\|\xi\|_c \rightarrow 0$ . Furthermore, for  $\|\xi\|_c < \xi_0$  and  $|\omega - (2\pi/\omega_0)| < \delta_0$ , every  $\omega$ -periodic solution of Eq. (7.1.1) with  $\|x_t\|_c < \delta_0$  must be of this type except for a translation in phase.

Similar to the theory of the Hopf bifurcations of ordinary differential equations, Theorem 7.7.1 indicates two important points. One is that the existence of the Hopf bifurcation is governed by the properties of the eigenvalues of the linear operator. The other is that the asymptotic behaviour of the non-constant bifurcating periodic solution is dominated by its projection on the center manifold of original system.

**Example 7.1.1** Consider the Hopf bifurcation of a nonlinear delayed system, the characteristic function of the linearized system of which reads

$$D(\lambda, \tau) \equiv P(\lambda) + Q(\lambda)e^{-\lambda\tau}, \tag{7.1.7}$$

where  $P(\lambda)$  and  $Q(\lambda)$  are two polynomials in  $\lambda$ , with  $\deg P(\lambda) = n > \deg Q(\lambda)$ . Now, we look for the necessary condition of the Hopf bifurcation when the time delay  $\tau$  is taken as the bifurcation parameter.

As discussed in Subsection 3.5.1,  $F(\omega) \equiv |P(i\omega)|^2 - |Q(i\omega)|^2$  is a  $2n$ -th order polynomial in  $\omega$  and contains only the terms of even orders. If  $D(\lambda, 0)$  is Hurwitz stable and  $F(\omega)$  has a unique pair of simple real roots  $\pm\omega_0$ , we can determine the minimal time delay  $\tau = \tau_0$  from

$$\sin \omega_0 \tau = \frac{Q_R(\omega_0)P_I(\omega_0) - P_R(\omega_0)Q_I(\omega_0)}{Q_R^2(\omega_0) + Q_I^2(\omega_0)}, \tag{7.1.8a}$$

$$\cos \omega_0 \tau = \frac{P_R(\omega_0)Q_R(\omega_0) + Q_I(\omega_0)P_I(\omega_0)}{Q_R^2(\omega_0) + Q_I^2(\omega_0)}. \tag{7.1.8b}$$

In the case of  $F'(\omega_0) \neq 0$ , the nonlinear system of concern undergoes a Hopf bifurcation at  $\tau = \tau_0$  due to the following two facts. First, all the characteristic roots of the quasi-polynomial  $D(\lambda, \tau)$  stay on the open left half-plane for  $0 \leq \tau < \tau_0$ . Second, the characteristic function  $D(\lambda, \tau_0)$  has a pair of conjugate pure imaginary roots  $\lambda_{1,2} = \pm i\omega_0$  and the condition  $d\text{Re}(\lambda_{1,2})/d\tau \neq 0$  holds at  $\tau = \tau_0$  since Theorem 3.5.2 states that  $\text{sgn}[d\text{Re}(\lambda_{1,2})/d\tau|_{\tau=\tau_0}] = \text{sgn}[F'(\omega_0)]$ . If  $F(\omega)$  has two or more than two pairs of simple real roots, the system may undergo more complicated bifurcation.

For example, the four-wheel-steering vehicle discussed in Subsection 3.6.2 undergoes the Hopf bifurcation in the vicinity of the origin of the phase space when the parameter pair  $(L, U)$  falls into the given region

$$\Delta = \{(L, U) \mid 10 \leq L \leq 120, 5 \leq U \leq 40\}, \tag{7.1.9}$$

since there is a proper value of time delay for each pair  $(L, U)$  so that the two conditions of the Hopf bifurcation hold true, and the corresponding polynomial  $F(\omega)$  has exactly one pair of real roots  $\pm\omega$  at such values of parameters.

To make a detailed analysis on the dynamics of delay differential equations on the center manifold, a similar procedure can be followed as done for ordinary differential equations. In the next subsection, attention will be paid to the decomposition of the bifurcating solution, though it has been presented in Section 6.1 in terms of real functions.

### 7.1.2 Decomposition of Bifurcating Solution

Suppose that Eq. (7.1.1) undergoes the Hopf bifurcation at  $\tau = \tau_0$ . More precisely, let  $\alpha \equiv \tau - \tau_0$  be the bifurcation parameter and assume that a pair of conjugate simple eigenvalues  $\lambda(\alpha)$  and  $\bar{\lambda}(\alpha)$  of the linearized equation at  $x=0$  is crossing the imaginary axis as  $\alpha$  passes through zero, and no other eigenvalues stay on the imaginary axis.

Following Section 6.1, it is possible to decompose the system dynamics near the Hopf bifurcation into two parts. One governs the system dynamics on the center manifold, and the other is the complementary part, which plays a less important role in understanding system dynamics. Now we present the decomposition procedure in a more direct way. In fact, we can recast Eq. (7.1.1) as

$$\dot{x}(t) = L_\alpha x_t + N_\alpha(x_t), \tag{7.1.10}$$

or equivalently

$$\dot{x}_t = A_\alpha(x_t) + \Theta N_\alpha(x_t), \tag{7.1.11}$$

where

$$A(\phi(\theta)) \equiv \begin{cases} \frac{d\phi}{d\theta}, & \theta \in [-\tau, 0), \\ L_\alpha(\phi), & \theta = 0, \end{cases} \quad \Theta(\theta) \equiv \begin{cases} 0, & \theta \in [-\tau, 0), \\ I, & \theta = 0. \end{cases} \tag{7.1.12a}$$

In the sense of  $(A_\alpha^* \psi, \phi) = (\psi, A_\alpha \phi)$ , the adjoint operator  $A_\alpha^*$  of  $A$  reads

$$A_\alpha^*(\psi(s)) = \begin{cases} -\frac{d\psi}{ds}, & s \in (0, \tau], \\ L_\alpha^*(\psi) \equiv \int_{-\tau}^0 \psi(-\theta) d\eta(\theta), & s = 0, \end{cases} \tag{7.1.12b}$$

where the bilinear form is given as following

$$(\psi, \phi) = \psi(0)\phi(0) - \int_{-\tau}^0 \int_0^\theta \psi(\xi - \theta) d\xi [d\eta(\theta)] \phi(\xi). \quad (7.1.13)$$

Assume that  $\zeta$  and  $\zeta^*$  are the eigenvectors of  $A_\alpha$  and  $A_\alpha^*$  corresponding to  $\lambda(\alpha)$  so that

$$(\zeta^*, \zeta) - 1 = (\zeta^*, \bar{\zeta}) = 0, \quad (7.1.14)$$

where  $\bar{\zeta}$  represents the complex conjugate of  $\zeta$ . As the real solutions of Eq. (7.1.10) are of concern, we decompose the bifurcating solution  $x_t$  into a real-valued summation

$$x_t = a(t)\zeta + \bar{a}(t)\bar{\zeta} + v(t), \quad (\zeta^*, v) = 0. \quad (7.1.15)$$

Then, we have

$$[\dot{a} - \lambda(\alpha)a]\zeta + [\dot{\bar{a}} - \bar{\lambda}(\alpha)\bar{a}]\bar{\zeta} + \frac{dv}{dt} = A_\alpha v + \Theta N_\alpha(a(t)\zeta + \bar{a}(t)\bar{\zeta} + v(t)). \quad (7.1.16)$$

From Eq. (7.1.14) and

$$(\zeta^*, \frac{dv}{dt}) = \frac{d}{dt}(\zeta^*, v) = 0, \quad (\zeta^*, A_\alpha v) = (A_\alpha^* \zeta^*, v) = \lambda(\alpha)(\zeta^*, v) = 0, \quad (7.1.17)$$

we have

$$\dot{a} - \lambda(\alpha)a = (\zeta^*, \Theta N_\alpha(a\zeta + \bar{a}\bar{\zeta} + v)) = \zeta^* N_\alpha(a\zeta + \bar{a}\bar{\zeta} + v)|_{\theta=0}, \quad (7.1.18a)$$

as well as a similar equation for  $\bar{a}$ , and

$$\begin{aligned} \frac{dv}{dt} = & A_\alpha v + [\Theta N_\alpha(a(t)\zeta + \bar{a}(t)\bar{\zeta} + v(t)) \\ & - (\zeta^* N_\alpha(a\zeta + \bar{a}\bar{\zeta} + v))|_{\theta=0}]\zeta - (\bar{\zeta}^* \bar{N}_\alpha(a\zeta + \bar{a}\bar{\zeta} + v))|_{\theta=0}\bar{\zeta}. \end{aligned} \quad (7.1.18b)$$

When the linearized equation of Eq. (7.1.11) at  $x=0$  has a pair of complex-conjugate simple eigenvalues  $\lambda(\alpha)$  and  $\bar{\lambda}(\alpha)$  while  $\alpha$  passing through zero, and all the other eigenvalues remain on the open left-half complex plane, we can prove that  $\|v\|_c \rightarrow 0$  as  $t \rightarrow +\infty$ . Thus, the complementary part  $v(t)$  plays a simple role in the local dynamics analysis.

### 7.1.3 Bifurcating Solutions in Normal Form

In a neighbourhood of the origin of  $R^n$ , there exists  $v=g(\alpha,a,\bar{a})$  for Eq. (7.1.18) according to the center manifold theorem. Once the function  $g(\alpha,a,\bar{a})$  is found, the delay differential equation can be transformed into a planar differential equation free of time delays. This reduction enables one to determine the direction of the Hopf bifurcation, namely, to answer whether the bifurcating periodic solution exists locally for  $\alpha>\alpha_0\equiv 0$  (*supercritical Hopf bifurcation*) or  $\alpha<\alpha_0$  (*subcritical Hopf bifurcation*), as well as the stability of the bifurcating solutions. The problem is that it is difficult to determine the center manifold in general. As discussed in Section 6.3, a series of boundary problems of ordinary differential equations have to be solved first so as to achieve the expression of the flow on the center manifold, and then the normal form of the reduced system has to be calculated. Hence, a lot of computational efforts are required in this procedure. In (Faria and Magalhaes 1995), however, a method was proposed for the reduced differential equation on the center manifold in the normal form without computing the manifold. A similar method to estimate the direction of Hopf bifurcation was presented in (Stech 1985) by using the Lyapunov-Schmidt reduction.

Following the work in (Faria and Magalhaes 1995), we have the reduced ordinary differential equation on the center manifold in the polar coordinates  $(\rho, \xi)$

$$\begin{cases} \dot{\rho}=\alpha\gamma'(0)\rho+K_2\rho^3+\dots+K_{2p}\rho^{2p+1}+O(\alpha\rho|(\rho,\alpha)|+|(\rho,\alpha)^{2p+2}|), \\ \dot{\xi}=-\omega+O(|\alpha,\rho|). \end{cases} \quad (7.1.19)$$

Because  $\gamma'(0)\neq 0$  holds, the sign of constant  $K\equiv K_2$  governs the direction of the Hopf bifurcation. If  $\gamma'(0)>0$ , the condition  $K>0$  corresponds to a subcritical bifurcation and  $K<0$  to a supercritical bifurcation. For a scalar delay differential equation in  $C([-\tau, 0],R)$  in the form of Eq. (7.1.1), (Faria and Magalhaes 1995) gave the expression for  $K$  as following

$$K=\text{Re}\left[\frac{1}{1-L_0(\theta e^{i\omega\theta})}\left(B_{(2,1,0,0)}-\frac{B_{(1,1,0,0)}B_{(1,0,1,0)}}{L_0(1)}+\frac{B_{(2,0,0,0)}B_{(0,1,0,1)}}{2i\omega-L_0(e^{2i\omega\theta})}\right)\right], \quad (7.1.20)$$

where the constants  $B_{(2,1,0,0)}$ ,  $B_{(1,1,0,0)}$  and so on are the coefficients in the following expansion

$$\begin{aligned} f(0,x_1e^{i\omega\theta}+x_2e^{-i\omega\theta}+x_31+x_4e^{2i\omega\theta}) \\ =B_{(2,0,0,0)}x_1^2+B_{(1,1,0,0)}x_1x_2+B_{(1,0,1,0)}x_1x_3+B_{(0,1,0,1)}x_2x_4 \\ +B_{(2,1,0,0)}x_1^2x_2+\dots \end{aligned} \quad (7.1.21)$$

If  $K \neq 0$ , the periodic solution, bifurcating from the origin  $\rho=0$  at  $\alpha=0$ , of the delay differential equation reads

$$\begin{cases} \rho(t) = \sqrt{-\frac{\gamma'(0)\alpha}{K}} + O(\alpha), \\ \xi(t) = -\omega t + O(\sqrt{|\alpha|}). \end{cases} \tag{7.1.22}$$

For the non-constant periodic solution of Eq. (7.1.1), main results are as follows.

**Theorem 7.1.2** Assume that the hypotheses (H1) and (H2) are true for Eq. (7.1.1). If  $\gamma'(0)K < 0$  (or  $\gamma'(0)K > 0$ ), a unique non-trivial periodic solution exists in the neighbourhood of  $\rho=0$  for  $\alpha > 0$  (or  $\alpha < 0$ ), and no non-trivial periodic solution exists for  $\alpha < 0$  (or  $\alpha > 0$ ). The corresponding non-trivial periodic solution is asymptotically stable if  $K < 0$  and unstable if  $K > 0$ .

If  $K=0$ , the normal form has to be calculated up to the first non-vanishing coefficients  $K_{2p}$  in order to study the system dynamics.

In the following example, an outline for the Hopf bifurcation of a delay differential equation is given to demonstrate the above process. For detailed analysis, it is referred to (Hale and Lunel 1993) and (Faria and Magalhaes 1995).

**Example 7.1.2** Study the Hopf bifurcation and the corresponding periodic solution of the well-known *Wright equation*

$$\dot{x}(t) = ax(t-1)[1+x(t)], \quad x \in \mathbb{R}, \tag{7.1.23}$$

at  $x=0$  with the variation of parameter  $a$ .

The characteristic quasi-polynomial  $\lambda - ae^{-\lambda}$  of the linearized delay differential equation has a pair of simple imaginary roots  $\pm i\omega$  if and only if  $a = a_k$  and  $\omega = \omega_k$  with

$$a_k = (-1)^{k+1} \omega_k, \quad \omega_k = \frac{\pi}{2} + k\pi \quad \text{for } k=0,1,2,\dots \tag{7.1.24}$$

The implicit function theorem indicates that the characteristic quasi-polynomial has a unique pair of conjugate complex roots  $\lambda(a)$  and  $\bar{\lambda}(a)$  close to  $i\omega_k$  and  $-i\omega_k$  for  $a$  in the neighbourhood of  $a_k$ , and that for  $\lambda(a) = \gamma(a) \pm i\omega(a)$  with  $\gamma(a), \omega(a) \in \mathbb{R}$ , we have

$$\gamma'(a_k) = -\frac{a_k}{1+a_k^2} \neq 0. \tag{7.1.25}$$

Thus, Eq. (7.1.23) undergoes the Hopf bifurcation at  $a = a_k, k=0,1,2,\dots$ .

Now, we look at the bifurcating periodic solutions close to  $x=0$  and  $a=a_k$ ,  $k=0,1,2,\dots$ . Let  $\alpha \equiv a - a_k$ . The right-hand side of Eq. (7.1.23), together with the corresponding linear and nonlinear operators, is in the form

$$f(\alpha, \phi) = (a_k + \alpha)\phi(0)\phi(-1), \quad (7.1.26a)$$

$$L_0 x_t = a_k x_t(-1), \quad (7.1.26b)$$

$$N_\alpha(x_t) = (a_k + \alpha)x_t(0)x_t(-1). \quad (7.1.26c)$$

Direct computation gives

$$\begin{aligned} & f(0, x_1 e^{i\omega_k \theta} + x_2 e^{-i\omega_k \theta} + x_3 1 + x_4 e^{2i\omega_k \theta}) \\ &= a_k (x_1 + x_2 + x_3 + x_4)(x_1 e^{-i\omega_k} + x_2 e^{i\omega_k} + x_3 1 + x_4 e^{-2i\omega_k}) \\ &= a_k [(-1)^{k+1} i x_1^2 + 0 x_1 x_2 + (1 + (-1)^{k+1} i) x_1 x_3 \\ & \quad + (-1 + (-1)^k i) x_2 x_4 + 0 x_1^2 x_2 + \dots]. \end{aligned} \quad (7.1.27)$$

Thus, the non-trivial periodic solution on the center manifold is asymptotically stable since we have

$$K = \frac{\omega_k}{5(1 + \omega_k^2)} [(-1)^k - 3\omega_k] < 0, \quad k=0,1,2,\dots \quad (7.1.28)$$

Theorem 7.1.2 implies that Eq. (7.1.23) undergoes the Hopf bifurcation, which is supercritical if  $k$  is odd and is subcritical if  $k$  is even. The periodic solution in the polar coordinates  $(\rho, \xi)$  is in the form

$$\begin{cases} \rho(t) = \sqrt{\frac{5|a - a_k|}{3\omega_k + (-1)^{k+1}}} + O(|a - a_k|), \\ \xi(t) = -\omega_k t + O(\sqrt{|a - a_k|}). \end{cases} \quad (7.1.29)$$

As noted in (Hale 1977), there exist the characteristic roots with positive real part at the critical values  $a = a_k$ ,  $k=1,2,\dots$  for the Hopf bifurcation of the Wright equation so that the bifurcating periodic solutions, albeit asymptotically stable in the center manifold, are unstable in the state space. Only at  $a = a_0 = -\pi/2$ , the characteristic quasi-polynomial has a unique pair of pure simple imaginary roots and the other characteristic roots have negative real parts such that the periodic solution arising from the subcritical Hopf bifurcation at  $a = -\pi/2$  is asymptotically stable. This stable periodic solution on the center manifold reads



$$\begin{cases} \rho(t) = \sqrt{\frac{10|a+\pi/2|}{3\pi-2}} + O\left(a + \frac{\pi}{2}\right), \\ \xi(t) = -\frac{\pi}{2}t + O\left(\sqrt{|a+\pi/2|}\right). \end{cases} \quad (7.1.30)$$

In the state space, the corresponding periodic solution of the Wright equation, see (Faria and Magalhaes 1995), is as following

$$x(t) = 2\rho(t)\cos\xi(t) + O\left(\sqrt{|a+\pi/2|}\right) = 2\sqrt{\frac{10|a+\pi/2|}{3\pi-2}}\cos\left(-\frac{\pi}{2}t\right) + O\left(a + \frac{\pi}{2}\right). \quad (7.1.31)$$

## 7.2 Computation of Bifurcating Periodic Solutions

There are basically two kinds of approaches available for constructing the bifurcating periodic solutions of a delay differential equation. One kind is based on the center manifold theorem in Section 7.1, where the solution is first projected onto the center manifold and then is determined in the form of power series. The other kind is the power series approximation in the state space with respect to a properly selected small parameter. This kind of approaches has two routines to follow. The first is the *Fredholm alternative* (Iooss and Joseph 1980), where the solution is expanded into the power series first and then is projected onto the center manifold so as to determine the power series easily. The second routine includes the well-known perturbation method and its varieties, such as the averaging method, the method of multiple scales, and so forth. This section presents respectively the method of Fredholm alternative and the method of perturbation, together with the their applications to the Wright equation discussed in Subsection 7.1.3.

### 7.2.1 Method of the Fredholm Alternative

We first write the delay differential equation as a functional differential equation on the Banach space  $C([- \tau, 0], R^n)$  in the form

$$\frac{dx_t}{dt} = f(\alpha, x_t), \quad \alpha \in R, \quad x_t \in C([- \tau, 0], R^n), \quad f(\alpha, 0) = 0. \quad (7.2.1)$$

Let  $u(t) \equiv x_t(\theta)$  and assume that Eq. (7.2.1) undergoes the Hopf bifurcation at  $\alpha=0$  and the frequency of bifurcating periodic solution is  $\omega(\varepsilon)$ , where  $\varepsilon$  is a

small positive parameter, characterizing the small deviation of  $\alpha$  from zero or the small amplitude of periodic solution bifurcating just from the trivial solution.

The objective of this subsection is to construct the bifurcating periodic solution. If we introduce a new time scale  $s = \omega(\varepsilon)t$ , the task becomes to determine a  $2\pi$ -periodic solution  $\mathbf{u}(s)$ , which yields

$$\omega(\varepsilon) \frac{d\mathbf{u}}{ds} = \mathbf{f}(\alpha(\varepsilon), \mathbf{u}), \tag{7.2.2a}$$

$$\mathbf{u}(s, \varepsilon) = \mathbf{u}(s + 2\pi, \varepsilon), \quad \mathbf{u}(s, 0) = 0, \quad \alpha(0) = 0, \quad \omega(0) = \omega_0. \tag{7.2.2b}$$

We expand the solution of concern as

$$\begin{bmatrix} \mathbf{u}(s, \varepsilon) \\ \alpha(\varepsilon) \\ \omega(\varepsilon) - \omega_0 \end{bmatrix} = \sum_{j=1}^{\infty} \frac{\varepsilon^j}{j!} \begin{bmatrix} \mathbf{u}_j(s) \\ \alpha_j \\ \omega_j \end{bmatrix}, \tag{7.2.3}$$

then the coefficients  $\mathbf{u}_j(s)$ ,  $\alpha_j$  and  $\omega_j$ ,  $j=1,2,\dots$  need to be determined. For this purpose, substituting Eq. (7.2.3) into Eq. (7.2.2) and equating the same power of  $\varepsilon$ , we have a set of linear differential equations

$$\mathbf{J}_0 \mathbf{u}_1 = 0, \tag{7.2.4a}$$

$$\mathbf{J}_0 \mathbf{u}_2 - 2\omega_1 \frac{d\mathbf{u}_1}{ds} + 2\alpha_1 f_{u\alpha}(0|\mathbf{u}_1) + f_{uu}(0|\mathbf{u}_1|\mathbf{u}_1) = 0, \tag{7.2.4b}$$

$$\begin{aligned} \mathbf{J}_0 \mathbf{u}_3 - 3\omega_1 \frac{d\mathbf{u}_2}{ds} + 3\alpha_1 f_{u\alpha}(0|\mathbf{u}_2) - 3\omega_2 \frac{d\mathbf{u}_1}{ds} \\ + 3\alpha_2 f_{u\alpha}(0|\mathbf{u}_1) + 3\alpha_1 f_{u\alpha\alpha}(0|\mathbf{u}_1|\mathbf{u}_1) + 3\alpha_1^2 f_{u\alpha\alpha}(0|\mathbf{u}_1) \\ + 3f_{uu}(0|\mathbf{u}_1|\mathbf{u}_2) + f_{uuu}(0|\mathbf{u}_1|\mathbf{u}_1|\mathbf{u}_1) = 0, \end{aligned} \tag{7.2.4c}$$

where

$$\mathbf{J}_0 \equiv -\omega_0 \frac{d}{ds} + \mathbf{A}_0, \quad \mathbf{A}_0 \equiv f_u(0|\cdot), \tag{7.2.5}$$

whereas

$$f_u(\alpha|\mathbf{x}) \equiv \left. \frac{\partial f(\alpha, \delta_1 \mathbf{x})}{\partial \delta_1} \right|_{\delta_1=0}, \tag{7.2.6a}$$

$$f_{uu}(\alpha|\mathbf{x}|\mathbf{y}) = f_{uu}(\alpha|\mathbf{y}|\mathbf{x}) \equiv \left. \frac{\partial^2 f(\alpha, \delta_1 \mathbf{x} + \delta_2 \mathbf{y})}{\partial \delta_1 \partial \delta_2} \right|_{\delta_1=\delta_2=0} \tag{7.2.6b}$$

are a linear operator and a bilinear operator carrying vectors into vectors, respectively.

The notations  $f_u(\alpha|x)$ ,  $f_{uu}(\alpha|x|y)$ ,  $f_{uuu}(\alpha|x|y|z)$ , ... here are in fact the Gateaux derivatives, see, (Debnath and Mikusinski 1999). What follows is the example to show how to compute the Gateaux derivatives of the right-hand side of a delay differential equation.

**Example 7.2.1** Consider again the Wright equation in the form

$$\dot{x}(t) = -\left(\frac{\pi}{2} + \alpha\right)x(t-1)[1+x(t)]. \quad (7.2.7)$$

Note that

$$\frac{dx(t+\theta)}{dt} = \begin{cases} \frac{dx(t+\theta)}{d\theta}, & \theta \in [-1, 0), \\ -\left(\frac{\pi}{2} + \alpha\right)x(t-1)[1+x(t)], & \theta = 0, \end{cases} \quad (7.2.8)$$

we have

$$f(\alpha, \phi) = \begin{cases} \frac{d\phi}{d\theta}, & \theta \in [-1, 0), \\ -\left(\frac{\pi}{2} + \alpha\right)\phi(-1)[1+\phi(0)], & \theta = 0, \end{cases} \quad (7.2.9)$$

if Eq. (7.2.7) is in the form of Eq. (7.2.1) on the Banach space  $C([-1, 0], \mathbb{R})$ . From

$$f(\alpha, \delta_1 x + \delta_2 y) = \begin{cases} \frac{d(\delta_1 x + \delta_2 y)}{d\theta}, & \theta \in [-1, 0), \\ -\left(\frac{\pi}{2} + \alpha\right)[\delta_1 x(-1) + \delta_2 y(-1)][1 + \delta_1 x(0) + \delta_2 y(0)], & \theta = 0, \end{cases} \quad (7.2.10)$$

we have

$$f_u(0|x) = \begin{cases} \frac{dx}{d\theta}, & \theta \in [-1, 0), \\ -\frac{\pi}{2}x(-1), & \theta = 0, \end{cases} \quad (7.2.11a)$$

$$f_{ua}(0|x) = \begin{cases} 0, & \theta \in [-1, 0), \\ -x(-1), & \theta = 0, \end{cases} \quad (7.2.11b)$$

$$f_{uu}(0 | x | y) = \begin{cases} 0, & \theta \in [-1, 0), \\ -\frac{\pi}{2}[x(-1)y(0) + x(0)y(-1)], & \theta = 0. \end{cases} \quad (7.2.11c)$$

Now, we discuss how to solve Eq. (7.2.4), each equation of which is in a unified form as following

$$(J_0 u)(s) = g(s), \quad g(s) = g(s + 2\pi). \quad (7.2.12)$$

In general, it is impossible to determine any solution of Eq. (7.2.12) unless function  $g(s)$  yields some conditions, each of which is usually referred to as a *Fredholm alternative*. To introduce the concept of the Fredholm alternative, denote by  $P_{2\pi}$  and  $P_{2\pi}^*$  the subspace of  $C([-\tau, 0], R^n)$  composed of all continuous  $2\pi$ -periodic functions in  $s$  and the subspace of all continuous  $2\pi$ -periodic functions in the dual space of  $C([-\tau, 0], R^n)$ , respectively. Note that the functions in  $P_{2\pi}$  are those in  $s \in [-\tau, 0]$ , and the functions in  $P_{2\pi}^*$  are in  $s \in [0, \tau]$ , we define a new bilinear form

$$[a, b] = \frac{1}{2\pi} \int_0^{2\pi} (a(s), b(s))_0 ds, \quad a \in P_{2\pi}^*, \quad b \in P_{2\pi}, \quad (7.2.13)$$

where  $(\cdot, \cdot)_0$  is the bilinear form in the usual sense at the bifurcating point  $\alpha = 0$ . The adjoint operator  $J_0^*$  of  $J_0$  in the sense of  $[J_0^* \psi, \phi] = [\psi, J_0 \phi]$  reads

$$J_0^* = \omega_0 \frac{d}{ds} + A_0^*. \quad (7.2.14)$$

At the bifurcating point  $\alpha = 0$ , we solve the eigenvalue problem  $f_u(0|\zeta_0) = i\omega_0 \zeta_0$  and its adjoint eigenvalue problem  $f_u^*(0|\zeta_0^*) = i\omega_0 \zeta_0^*$  under the condition  $(\zeta_0^*, \zeta_0)_0 - 1 = (\zeta_0^*, \bar{\zeta}_0)_0 = 0$ . Let  $\chi(s) = e^{is} \zeta_0$ , then  $\chi$  and  $\bar{\chi}$  are in  $P_{2\pi}$  and satisfy

$$J_0 \chi = J_0 \bar{\chi} = 0. \quad (7.2.15a)$$

Similarly, we can also find a  $\chi^*(s) = e^{-is} \zeta_0^* \in P_{2\pi}^*$  such that

$$J_0^* \chi^* = J_0^* \bar{\chi}^* = 0. \quad (7.2.15b)$$

With this vector  $\chi^*(s)$ , we have

$$[\chi^*, u_1] = 1, \quad \text{and} \quad [\chi^*, u_j] = 0 \quad \text{for all } j \geq 2 \quad (7.2.16a)$$

if we define

$$\varepsilon = [\chi^*, u]. \quad (7.2.16b)$$

As shown in (Debnath and Mikusinski 1999) or (Zeidler 1995), we have the theorem of Fredholm alternative as following.

**Theorem 7.2.1** Equation (7.2.12) is solvable if and only if

$$[\chi^*, \mathbf{g}] = [\bar{\chi}^*, \mathbf{g}] = 0. \quad (7.2.17)$$

When  $\mathbf{g}(s)$  is a real function, the solvability condition is given by two real equations. Then,  $\alpha_j$  and  $\omega_j$  in Eq. (7.2.3) can be selected through condition (7.2.17) so that each equation in Eq. (7.2.4) is solvable.

The solution  $\mathbf{u}_1$  of Eq. (7.2.4a) is in the form  $\mathbf{u}_1 = ce^{is}\zeta_0 + \bar{c}e^{-is}\bar{\zeta}_0$ . As the origin of  $s$  is indeterminate, we may just as well use another transformation  $s \rightarrow s + \delta$  so that  $ce^{i\delta} = \tilde{c}$  is real-valued. Without loss of generality, we have

$$\mathbf{u}_1 = \tilde{c}(\chi + \bar{\chi}) = \chi + \bar{\chi}, \quad (7.2.18)$$

where  $\tilde{c} = 1$  is determined from Eq. (7.2.16a). According to the definitions, we have  $[\chi^*, \chi] - 1 = [\chi^*, \bar{\chi}] = 0$  because  $(\zeta_0^*, \zeta_0)_0 - 1 = (\zeta_0^*, \bar{\zeta}_0)_0 = 0$ . Thus, we obtain  $[\chi^*, f_{u\alpha}(0|\bar{\chi})] = [\zeta_0^*, e^{-2is} f_{u\alpha}(0|\bar{\zeta}_0)] = 0$ , and  $[\chi^*, f_{uu}(0|\chi + \bar{\chi}|\chi + \bar{\chi})] = 0$ . As a result, the solvability condition (7.2.4b) gives

$$-2i\omega_1 + 2\alpha_1[\chi^*, f_{u\alpha}(0|\chi)] = 0. \quad (7.2.19)$$

By differentiating the eigenvalue problem  $f_u(\alpha|\zeta_\alpha) = \lambda\zeta_\alpha$  with respect to  $\alpha$  and evaluating the result at  $\alpha = 0$ , we have

$$\lambda'(0)\zeta'_0 + i\omega_0\zeta'_0 = f_u(0|\zeta'_0) + f_{u\alpha}(0|\zeta_0), \quad (7.2.20)$$

where the prime represents the derivative respect to  $\alpha$ . According to the Fredholm alternatives, the above differential equation is solvable if and only if

$$\lambda'(0) = (\zeta_0^*, f_{u\alpha}(0|\zeta_0)) = [\chi^*, f_{u\alpha}(0|\chi)]. \quad (7.2.21)$$

As the theorem of Hopf bifurcations assumes  $\lambda'(0) \neq 0$ , we have  $\alpha_1 = 0$  and  $\omega_1 = 0$ . By using mathematical induction in (Iooss and Joseph 1980), we show that

$$\alpha_{2j+1} = 0, \quad \omega_{2j+1} = 0, \quad j = 0, 1, 2, \dots \quad (7.2.22)$$

This fact, together with Eq. (7.2.3), indicates that the bifurcation parameter  $\alpha$  and the vibrating frequency  $\omega$  are in the following form

$$\alpha = \frac{\varepsilon^2}{2}\alpha_2 + O(\varepsilon^4), \quad \omega = \omega_0 + \frac{\varepsilon^2}{2}\omega_2 + O(\varepsilon^4), \quad (7.2.23)$$

where the coefficients  $\alpha_2$  and  $\omega_2$  can be determined through the following condition

$$\begin{aligned} &3[-i\omega_2 + \alpha_2 \lambda'(0)] + 3[\chi^*, f_{uu}(0|\chi + \bar{\chi}|u_2)] \\ &+ [\chi^*, f_{uuu}(0|\chi + \bar{\chi}|\chi + \bar{\chi}|\chi + \bar{\chi})] = 0. \end{aligned} \quad (7.2.24)$$

### 7.2.2 Stability of Bifurcating Periodic Solutions

Let  $\mathbf{u}(s)$  with  $s = \omega(\varepsilon)t$  be the bifurcating periodic solution of Eq. (7.2.2) and  $\mathbf{v}(t)$  be a small disturbance of  $\mathbf{u}$  such that  $\mathbf{u}(s, \varepsilon) + \mathbf{v}(t)$  also satisfies Eq. (7.2.2). Then,  $\mathbf{v}(t)$  yields

$$\frac{d\mathbf{v}}{dt} = \mathbf{f}(\alpha, \mathbf{u} + \mathbf{v}) - \mathbf{f}(\alpha, \mathbf{u}). \quad (7.2.25)$$

The following linearized differential equation governs the stability of the bifurcating solution

$$\frac{d\mathbf{v}}{dt} = \mathbf{f}_u(\alpha(\varepsilon), \mathbf{u}(s, \varepsilon)|\mathbf{v}), \quad (7.2.26)$$

where  $\mathbf{f}_u(\alpha(\varepsilon), \mathbf{u}(s, \varepsilon)|\mathbf{v})$  is periodic in  $s$ . On the basis of the Floquet theory, let

$$\mathbf{v}(t) \equiv e^{\beta s} \boldsymbol{\xi}(s), \quad s = \omega(\varepsilon)t, \quad \boldsymbol{\xi}(s) \equiv \boldsymbol{\xi}(s + 2\pi) \text{ for all } s \in \mathbb{R}. \quad (7.2.27)$$

Then, we have

$$\omega(\varepsilon) \frac{d\boldsymbol{\xi}}{ds} + \beta \boldsymbol{\xi} = \mathbf{f}_u(\alpha(\varepsilon), \mathbf{u}|\boldsymbol{\xi}). \quad (7.2.28)$$

A similar procedure used in the previous subsection gives the following theorem.

**Theorem 7.2.2** For sufficiently small parameter  $\varepsilon$ , the following estimations are true

$$\beta(\varepsilon) = -\alpha'(\varepsilon), \quad \rho = \operatorname{Re} \lambda'(0). \quad (7.2.29)$$

Thus, the bifurcating periodic solution  $\mathbf{u}$  is asymptotically stable if  $\alpha_2 \rho > 0$  and unstable if  $\alpha_2 \rho < 0$ .

The proof of this theorem is referred to, for example, (Iooss and Joseph 1980).

**Example 7.2.2** Consider again the Wright equation in the form of Eq. (7.2.7). Example 7.1.2 indicates that the trivial solution of the Wright equation undergoes the Hopf bifurcation at  $\alpha = 0$  and the frequency of the bifurcating periodic solution is  $\omega_0 = \pi/2$ . In what follows, the method of Fredholm alternative is used to

determine the approximate periodic solution. On the Banach space  $C([-1, 0], R)$ , the following notations are defined first

$$[u(t)](\theta) \equiv x_t(\theta) = x(t + \theta), \tag{7.2.30a}$$

$$[A_\alpha \phi](\theta) = [f_u(\alpha|\phi)](\theta) \equiv \begin{cases} \frac{d\phi(\theta)}{d\theta}, & \theta \in [-1, 0), \\ -(\frac{\pi}{2} + \alpha)\phi(-1), & \theta = 0, \end{cases} \tag{7.2.30b}$$

$$[\Theta N_\alpha \phi](\theta) \equiv (\frac{\pi}{2} + \alpha) \begin{cases} 0, & \theta \in [-1, 0), \\ -\phi(0)\phi(-1), & \theta = 0. \end{cases} \tag{7.2.30c}$$

Then, Eq. (7.2.8) can be written as

$$\frac{du}{dt} = A_\alpha u + \Theta N_\alpha(u). \tag{7.2.31}$$

The adjoint operator  $A_\alpha^*$ , on  $C([0, 1], R)$ , of  $A_\alpha$ , is given in the form

$$[A_\alpha^* \psi](\theta) = [f_u^*(\alpha|\psi)](\theta) \equiv \begin{cases} -\frac{d\psi(\theta)}{d\theta}, & \theta \in (0, 1], \\ -(\frac{\pi}{2} + \alpha)\psi(1), & \theta = 0, \end{cases} \tag{7.2.32}$$

with respect to the inner product

$$(\psi, \phi)_\alpha = \psi(0)\phi(0) - (\frac{\pi}{2} + \alpha) \int_{-1}^0 \psi(s+1)\phi(s) ds. \tag{7.2.33}$$

Solving the dual eigenvalue problems

$$f_u(0|\zeta_0) = i\frac{\pi}{2}\zeta_0, \quad f_u^*(0|\zeta_0^*) = i\frac{\pi}{2}\zeta_0^*, \quad (\zeta_0^*, \zeta_0)_0 - 1 = (\zeta_0^*, \bar{\zeta}_0)_0 = 0, \tag{7.2.34}$$

gives

$$\zeta_0(\theta) = \exp(i\frac{\pi\theta}{2}), \quad \zeta_0^*(\theta) = \frac{1}{1+i(\pi/2)} \exp(-i\frac{\pi\theta}{2}), \tag{7.2.35a}$$

and

$$\chi = \zeta_0(\theta)e^{is}, \quad \chi^* = \zeta_0^*(\theta)e^{-is}. \tag{7.2.35b}$$

Now we use the Fredholm alternative to compute the power series of the bifurcating periodic solution. Because  $\alpha_1 = 0$  and  $\omega_1 = 0$ , we have

$$[u_1(s)](\theta) = \zeta_0(\theta)e^{is} + \bar{\zeta}_0(\theta)e^{-is}, \tag{7.2.36}$$

$$\omega_0 \frac{du_2}{ds} = f_u(0|u_2) + e^{2is} f_{uu}(0|\zeta_0|\zeta_0) + e^{-2is} f_{uu}(0|\bar{\zeta}_0|\bar{\zeta}_0). \tag{7.2.37}$$

Equation (7.2.37) indicates that  $u_2$  is in the form

$$[u_2(s)](\theta) = \zeta_2(\theta)e^{2is} + \bar{\zeta}_2(\theta)e^{-2is}. \tag{7.2.38}$$

Substituting Eq. (7.2.38) into Eq. (7.2.37), we have

$$\frac{\pi}{2} [2ie^{2is} \zeta_2(\theta) - 2ie^{-2is} \bar{\zeta}_2(\theta)] = e^{2is} \dot{\zeta}_2(\theta) + e^{-2is} \dot{\bar{\zeta}}_2(\theta), \quad \theta \in [-1, 0], \tag{7.2.39a}$$

and

$$\begin{aligned} & 2ie^{2is} \zeta_2(0) - 2ie^{-2is} \bar{\zeta}_2(0) \\ &= -[e^{2is} \zeta_2(-1) + e^{-2is} \bar{\zeta}_2(-1)] - 2[e^{2is} \zeta_0(-1) + e^{-2is} \bar{\zeta}_0(-1)]. \end{aligned} \tag{7.2.39b}$$

Equation (7.2.39a) gives  $\dot{\zeta}_2(\theta) = i\pi \zeta_2(\theta)$ . So, we have  $\zeta_2(\theta) = \zeta_2(0)e^{i\pi\theta}$  and  $\zeta_2(-1) = -\zeta_2(0)$ . Hence, we find the coefficient  $\zeta_2(\theta)$  in  $[u_2(s)](\theta)$

$$\zeta_2(\theta) = \frac{4-2i}{5} e^{i\pi\theta}. \tag{7.2.40}$$

Furthermore, straightforward computation gives

$$-i\omega_2 + \alpha_2 \lambda'(0) = -[\chi^*, f_{uu}(0|\chi + \chi^*|u_2)] = \frac{\pi[(2-3\pi) - (6+\pi)i]}{10(1+\pi^2/4)}, \tag{7.2.41a}$$

$$\lambda'(0) = [\chi^*, f_{u\alpha}(0|\chi)] = \frac{2\pi+4i}{4+\pi^2} \neq 0. \tag{7.2.41b}$$

By the way, the implicit differentiation can also lead to Eq. (7.2.41b). Solving Eq. (7.2.41) for  $\alpha_2$  and  $\omega_2$  gives

$$\alpha_2 = \frac{3\pi-2}{5} > 0, \quad \omega_2 = -\frac{2}{5}. \tag{7.2.42}$$

In summary, the bifurcating periodic solution of Eq. (7.2.7) at  $\alpha=0$  reads

$$\begin{aligned} x(t) &= [u(\omega t)](0) = 2\varepsilon \cos \omega t + \varepsilon^2 \operatorname{Re}\left(\frac{4-2i}{5} e^{2i\omega t}\right) + O(\varepsilon^3) \\ &= 2\varepsilon \cos \omega t + \frac{2\varepsilon^2}{5} (2\cos 2\omega t + \sin 2\omega t) + O(\varepsilon^3), \end{aligned} \tag{7.2.43a}$$

$$\alpha(\varepsilon) = \frac{\varepsilon^2}{2} \alpha_2 + O(\varepsilon^4) = \frac{3\pi-2}{10} \varepsilon^2 + O(\varepsilon^4), \tag{7.2.43b}$$



$$\omega(\varepsilon) = \omega_0 + \frac{\varepsilon^2}{2}\omega_2 + O(\varepsilon^4) = \frac{\pi}{2} - \frac{1}{5}\varepsilon^2 + O(\varepsilon^4). \tag{7.2.43c}$$

If  $\alpha$  is taken as the bifurcation parameter, we can express  $\varepsilon$  and  $\omega$  as

$$\varepsilon \approx \sqrt{\frac{10\alpha}{3\pi-2}}, \quad \omega \approx \frac{\pi}{2} - \frac{2\alpha}{3\pi-2}, \tag{7.2.44}$$

so that the solution in Eq. (7.2.43a) reads

$$\begin{aligned} x(t) \approx & 2\sqrt{\frac{10\alpha}{3\pi-2}} \cos\left[\left(\frac{\pi}{2} - \frac{2\alpha}{3\pi-2}\right)t\right] \\ & + \frac{4\alpha}{3\pi-2} \left\{ 2\cos\left[\left(\pi - \frac{4\alpha}{3\pi-2}\right)t\right] + \sin\left[\left(\pi - \frac{4\alpha}{3\pi-2}\right)t\right] \right\}. \end{aligned} \tag{7.2.45}$$

The bifurcating periodic solution at  $\alpha=0$  is asymptotically stable since Eqs. (7.2.41b) and (7.2.42) give  $\rho = \text{Re} \lambda'(0) > 0$  and  $\alpha_2 > 0$ . Obviously, Eq. (7.2.45) offers a more accurate approximation than Eq. (7.1.31) for the solution of the Wright equation.

### 7.2.3 Perturbation Method

A large number of perturbation methods have been well developed to deal with the engineering systems governed by nonlinear ordinary differential equations. In this subsection, the perturbation method is briefly described only for a type of functional differential equations. It is necessary to mention that the secular terms may also appear as in the case of ordinary differential equations. If this is the case, they must be eliminated from the functional differential equation of concern to ensure that the equation has a uniformly bounded solution. For this purpose, it is usually to re-scale the time before the perturbation method is applied.

To demonstrate the perturbation method as simple as possible, we consider a second order scalar autonomous delay differential equation

$$\begin{cases} \ddot{x}(t) = F(x, \dot{x}, \alpha), \\ x_t(\theta) \equiv x(t+\theta), \quad \dot{x}_t(\theta) \equiv \dot{x}(t+\theta), \quad \theta \in [-\tau, 0], \end{cases} \tag{7.2.46}$$

with sufficiently smooth right-hand side and  $\tau > 0$ , though the following procedure and the results are valid for more general scalar autonomous delay differential equations of higher orders.

Assume that  $F(0,0,\alpha)=0$  holds for all parameter values of  $\alpha$  and there is an  $\alpha_0$  such that for  $\alpha < \alpha_0$  all the roots of the characteristic quasi-polynomial associ-

ated with the linearized operator stay on the open left half-plane, whereas a unique pair of roots of the characteristic quasi-polynomial is crossing the imaginary axis at  $\pm i\omega_0$  when  $\alpha=\alpha_0$ . If this is the case, Eq. (7.2.46) undergoes the Hopf bifurcation.

To construct the bifurcating periodic solution, we first introduce a new time  $\sigma$  through  $t=c(\alpha)\sigma$  with  $c(\alpha_0)=1$  such that the period of solution is fixed for the new time  $\sigma$ . Let  $y(\sigma)\equiv x(c\sigma)$ , then Eq. (7.2.46) is equivalent to

$$\begin{cases} \ddot{y}(\sigma)=c^2 F(y_\sigma, c^{-1}\dot{y}_\sigma, \alpha), \\ y_\sigma(\theta)=y(\sigma+\theta), \quad \dot{y}_\sigma(\theta)=\dot{y}(\sigma+\theta), \quad \theta\in[-\tau/c, 0], \end{cases} \quad (7.2.47)$$

where the dot now represents the derivative respect to the new time  $\sigma$ . At  $\alpha=\alpha_0$ , the linearized differential equation has the solution  $y(\sigma)=\varepsilon\cos\omega_0\sigma$ , where  $\varepsilon$  is related to  $\alpha$  and  $\varepsilon|_{\alpha=\alpha_0}=0$ . Now, we look for the periodic solution of Eq. (7.2.47) in the form (up to time shift)

$$y(\sigma)=\varepsilon\cos\omega_0\sigma+\varepsilon^2 y_2(\sigma)+\varepsilon^3 y_3(\sigma)+\dots \quad (7.2.48)$$

for small  $|\varepsilon|$ . Because the change  $\varepsilon\rightarrow-\varepsilon$  is equivalent to a phase shift of the oscillation by projection, which preserves the invariance of the cycle and hence does not change the values of  $\alpha$  and  $c$ . Thus, we need to study the following forms of  $\alpha$  and  $c$

$$c=1+c_2\varepsilon^2+c_4\varepsilon^4+\dots, \quad (7.2.49a)$$

$$\alpha=\alpha_0+\alpha_2\varepsilon^2+\alpha_4\varepsilon^4+\dots. \quad (7.2.49b)$$

Substituting Eqs. (7.2.48) and (7.2.49) into Eq. (7.2.47), expanding the right-hand side in terms of  $\varepsilon$  and equating the same powers of  $\varepsilon$ , we have a series of equations with respect to  $y_j(\sigma)$  that can be solved successively as in the case of ordinary differential equations. The coefficients  $c_j$  and  $\alpha_j$  are chosen such that no secular terms are involved. The periodic solution of Eq. (7.2.46) can be achieved by using the following scheme involving indefinite steps

$$(y_1, c_0, \alpha_0) \rightarrow y_2 \rightarrow (c_2, \alpha_2) \rightarrow y_3 \rightarrow y_4 \rightarrow (c_4, \alpha_4) \rightarrow \dots \quad (7.2.50)$$

As for the Hopf bifurcation, we have the following theorem, see (Kolmanovskii and Myshkis 1999).

**Theorem 7.2.3** Assume that the conditions associated with the characteristic quasi-polynomial that governs the existence of Hopf bifurcation hold, and that  $\alpha_2 \neq 0$  holds in Eq. (7.2.49b). If  $\alpha_2 > 0$  (or  $\alpha_2 < 0$ ) and  $\alpha$  increases (or decreases) and passes through  $\alpha=\alpha_0$ , then exactly one periodic solution (up to the time shift)

of Eq. (7.2.46) occurs near the trivial solution of the same equation. This solution is asymptotically stable (unstable), and has an asymptotic representation as  $\alpha \rightarrow \alpha_0^+$  (or  $\alpha \rightarrow \alpha_0^-$ )

$$x(t) = \sqrt{\frac{\alpha - \alpha_0}{\alpha_2}} \cos \frac{\omega_0}{c} t + O(|\alpha - \alpha_0|), \quad (7.2.51a)$$

$$c = 1 + \frac{c_2}{\alpha_2} (\alpha - \alpha_0) + O(|\alpha - \alpha_0|^2). \quad (7.2.51b)$$

In addition, any solution of Eq. (7.2.45) on the entire  $t$ -axis and sufficiently close to zero tends asymptotically to either zero or the periodic solution as  $t \rightarrow +\infty$  and  $t \rightarrow -\infty$ .

**Example 7.2.3** Consider again the Wright equation in the form

$$\dot{x}(t) = -bx(t-1)[1+x(t)]. \quad (7.2.52)$$

As shown in Example 7.1.2, Eq. (7.2.52) undergoes a Hopf bifurcation at  $b = \pi/2$  and the bifurcating periodic solution is asymptotically stable. We are now interested in an explicit approximate form of the bifurcating periodic solution. It is easy to verify that the periodic solution of the linearized equation of Eq. (7.2.52) is in the form

$$x_1(t) = a \cos\left(\frac{\pi}{2}t + \varphi\right), \quad (7.2.53)$$

where  $a$  and  $\varphi$  are two constants. Thus, we look for the periodic solution of Eq. (7.2.52) in the following form

$$x(t) = \varepsilon \cos \frac{\pi \sigma}{2} + \varepsilon^2 x_2(\sigma) + \varepsilon^3 x_3(\sigma) + \dots, \quad (7.2.54a)$$

$$t = (1 + c_2 \varepsilon^2 + c_4 \varepsilon^4 + \dots) \sigma, \quad (7.2.54b)$$

$$b = \frac{\pi}{2} + b_2 \varepsilon^2 + b_4 \varepsilon^4 + \dots, \quad (7.2.54c)$$

for a small positive parameter  $\varepsilon$ . We have

$$\begin{aligned} x(t-1) &= \varepsilon \cos \frac{\pi}{2} [\sigma - (1 + c_2 \varepsilon^2 + c_4 \varepsilon^4 + \dots)^{-1}] \\ &\quad + \varepsilon^2 x_2(\sigma - (1 + c_2 \varepsilon^2 + c_4 \varepsilon^4 + \dots)^{-1}) \\ &\quad + \varepsilon^3 x_3(\sigma - (1 + c_2 \varepsilon^2 + c_4 \varepsilon^4 + \dots)^{-1}) + \dots \end{aligned} \quad (7.2.55)$$

since  $t-1=c\sigma-1=c(\sigma-c^{-1})$ . Substituting Eqs. (7.2.54) and (7.2.55) into Eq. (7.2.52) and equating the coefficients at equal powers of  $\varepsilon$  give the following equations.

$$\dot{x}_2(\sigma) = -\frac{\pi}{2}x_2(\sigma-1) - \frac{\pi}{2}\sin\frac{\pi\sigma}{2}\cos\frac{\pi\sigma}{2}, \quad (7.2.56a)$$

$$\begin{aligned} \dot{x}_3(\sigma) = & -\frac{\pi}{2}x_3(\sigma-1) - \frac{\pi}{2}[x_2(\sigma-1)\cos\frac{\pi\sigma}{2} + x_2(\sigma)\sin\frac{\pi\sigma}{2}] \\ & - \frac{\pi^2}{4}c_2\cos\frac{\pi\sigma}{2} - \frac{\pi}{2}c_2\sin\frac{\pi\sigma}{2} - b_2\sin\frac{\pi\sigma}{2}. \end{aligned} \quad (7.2.56b)$$

Solving Eq. (7.2.56a), we have

$$x_2(\sigma) = \frac{1}{5}\cos\pi\sigma + \frac{1}{10}\sin\pi\sigma. \quad (7.2.57)$$

Substituting Eq. (7.2.57) into Eq. (7.2.56b) yields

$$\begin{aligned} \dot{x}_3(\sigma) = & -\frac{\pi}{2}x_3(\sigma-1) + \left(\frac{\pi}{40} - \frac{\pi^2}{4}c_2\right)\cos\frac{\pi\sigma}{2} + \left(\frac{3\pi}{40} - \frac{\pi}{2}c_2 - b_2\right)\sin\frac{\pi\sigma}{2} \\ & + \frac{3\pi}{40}\cos\frac{3\pi\sigma}{2} - \frac{\pi}{40}\sin\frac{3\pi\sigma}{2}. \end{aligned} \quad (7.2.58)$$

Eliminating the resonant terms  $\cos(\pi\sigma/2)$  and  $\sin(\pi\sigma/2)$  in the right-hand side of Eq. (7.2.58), we find

$$c_2 = \frac{1}{10\pi}, \quad b_2 = \frac{3\pi}{40} - \frac{1}{20} > 0. \quad (7.2.59)$$

Substituting Eqs. (7.2.57) and (7.2.59) into Eq. (7.2.54) gives the periodic solution of the Wright equation

$$x(t) = \varepsilon\cos\frac{\pi\sigma}{2} + \frac{\varepsilon^2}{10}[2\cos\pi\sigma + \sin\pi\sigma] + O(\varepsilon^3), \quad (7.2.60a)$$

$$t = \left[1 + \frac{\pi}{10}\varepsilon^2 + O(\varepsilon^4)\right]\sigma, \quad (7.2.60b)$$

$$b = \frac{\pi}{2} + \left(\frac{3\pi}{40} - \frac{1}{20}\right)\varepsilon^2 + O(\varepsilon^4). \quad (7.2.60c)$$

Taking  $b$  as the bifurcation parameter, we solve Eq. (7.2.54c) for  $\varepsilon$  by neglecting the higher order terms and then obtain

$$\varepsilon \approx \sqrt{\frac{b-\pi/2}{b_2}} = 2\sqrt{\frac{10(b-\pi/2)}{3\pi-2}}, \quad \sigma \approx t\left(1 - \frac{\varepsilon^2}{10\pi}\right) = t\left[1 - \frac{4(b-\pi/2)}{\pi(3\pi-2)}\right]. \quad (7.2.61)$$

There follows

$$\begin{aligned} x(t) \approx & 2\sqrt{\frac{10(b-\pi/2)}{3\pi-2}} \cos\left\{\left[\frac{\pi}{2} - \frac{2(b-\pi/2)}{3\pi-2}\right]t\right\} \\ & + \frac{4(b-\pi/2)}{3\pi-2} \left\{2\cos\left\{\left[\pi - \frac{4(b-\pi/2)}{3\pi-2}\right]t\right\} + \sin\left\{\left[\pi - \frac{4(b-\pi/2)}{3\pi-2}\right]t\right\}\right\}. \end{aligned} \quad (7.2.62)$$

Theorem 7.2.2 indicates that the bifurcating periodic solution from the trivial solution is asymptotically stable. It is easy to see that this solution is the same as what we have had in Example 7.2.2 if the bifurcation parameter  $b - \pi/2$  is substituted with  $\alpha$ .

Examples 7.2.2 and 7.2.3 demonstrate how to determine the bifurcating solution of a delay differential equation on the original state space by using two different methods, while Example 7.1.2 deals with the bifurcating solution of the same equation on the center manifold. Among these methods, the perturbation method looks the simplest in solving the Wright equation. As well known, the perturbation method has a great number of varieties, say, the averaging method, the method of multiple scales, etc. They are also applicable to the delay differential equations. The next two sections will demonstrate the method of multiple scales through the examples of the Duffing oscillator with delayed feedback.

### 7.3 Periodic Motions of a Duffing Oscillator with Delayed Feedback

This section deals with the free vibration of a Duffing oscillator with delayed velocity feedback. It begins with the analysis on the stability switches of equilibrium, and then presents how to determine the bifurcating periodic motions during the stability switches by using the Fredholm alternative and the method of multiple scales, respectively.

As discussed in Subsection 1.1.1, the re-scaled dynamic equation of the oscillator reads

$$\ddot{x}(t) + 2\zeta \dot{x}(t) + x(t) + \mu x^3(t) = v\dot{x}(t-\tau), \quad (7.3.1)$$

where the condition  $2\zeta - \nu > 0$  is assumed to hold such that the linearized system is asymptotically stable when the time delay  $\tau$  disappears. For simplicity, the study is confined to the case when  $\mu > 0$ .

### 7.3.1 Stability Switches of Equilibrium

The system of concern has a unique equilibrium  $x=0$  since  $\mu > 0$ . The perturbed motion  $\Delta x(t)$  near the equilibrium yields a linear delay differential equation

$$\Delta \ddot{x}(t) + 2\zeta \Delta \dot{x}(t) + \Delta x(t) = \nu \Delta \dot{x}(t - \tau). \tag{7.3.2}$$

The corresponding characteristic equation of Eq. (7.3.2) reads

$$D(\lambda, \tau) \equiv \lambda^2 + 2\zeta\lambda + 1 - \nu\lambda e^{-\lambda\tau} = 0. \tag{7.3.3}$$

Obviously,  $\lambda=0$  is not the root of Eq. (7.3.3). When Eq. (7.3.3) has any pure imaginary root  $\lambda=i\omega$  with  $\omega > 0$ , it becomes

$$D(i\omega, \tau) = (1 - \omega^2) + 2i\zeta\omega - i\nu\omega e^{-i\omega\tau} = 0. \tag{7.3.4}$$

There follow the corresponding real and imaginary parts

$$\begin{cases} \text{Re}[D(i\omega, \tau)] \equiv (1 - \omega^2) - \nu\omega \sin\omega\tau = 0, \\ \text{Im}[D(i\omega, \tau)] \equiv 2\zeta\omega - \nu\omega \cos\omega\tau = 0. \end{cases} \tag{7.3.5}$$

The second equation in Eq. (7.3.5) requires that  $2\zeta/|\nu| \leq 1$ . This, together with the assumption  $2\zeta - \nu > 0$ , gives  $\nu < -2\zeta < 0$ . Hence, we have

$$\begin{cases} \sin\omega\tau = \frac{1 - \omega^2}{\nu\omega} = \frac{\omega^2 - 1}{|\nu|\omega}, \\ \cos\omega\tau = \frac{2\zeta}{\nu} = -\frac{2\zeta}{|\nu|}. \end{cases} \tag{7.3.6}$$

Eliminating the harmonic terms in Eq. (7.3.6) yields

$$F(\omega) \equiv (1 - \omega^2)^2 + (2\zeta\omega)^2 - (\nu\omega)^2 = \omega^4 + p\omega^2 + 1 = 0, \tag{7.3.7}$$

where  $p \equiv 4\zeta^2 - \nu^2 - 2$ . Equation (7.3.7) has two positive roots

$$\omega_{1,2} = \sqrt{\frac{1}{2}(-p \pm \sqrt{p^2 - 4})}, \tag{7.3.8}$$

because  $p < 0$  and  $p^2 - 4 \geq 0$ . At these two roots, the following inequality holds

$$\left. \frac{dF}{d\omega} \right|_{\omega=\omega_{1,2}} = \pm 2\omega_{1,2} \sqrt{p^2 - 4} > 0 \quad (< 0). \quad (7.3.9)$$

It is easy to see that  $\omega_1^2 > 1$  and  $\omega_2^2 < 1$ . For each of these two roots, hence, Eq. (7.3.6) gives a series of critical time delays as following

$$\tau_{1,k} = \frac{1}{\omega_1} \left[ \arccos\left(-\frac{2\zeta}{|\nu|}\right) + 2k\pi \right], \quad k=0,1,2,\dots \quad (7.3.10a)$$

$$\tau_{2,k} = \frac{1}{\omega_2} \left[ 2\pi - \arccos\left(-\frac{2\zeta}{|\nu|}\right) + 2k\pi \right], \quad k=0,1,2,\dots \quad (7.3.10b)$$

As shown in Subsection 3.5.1, a pair of roots is crossing the imaginary axis from the left to the right when  $\tau = \tau_{1,k}$ , and from the right to the left when  $\tau = \tau_{2,k}$ .

More specifically, we look at a case study when  $\zeta = 0$ ,  $\nu = -0.5$ . Now, Eq. (7.3.8) gives  $\omega_{1,2} = (\sqrt{17} \pm 1)/4$  and there follow the critical time delays from Eq. (7.3.10)

$$\tau_{1,k} = \frac{4}{\sqrt{17} + 1} \left( \frac{\pi}{2} + 2k\pi \right) = 1.226, 6.132, 11.04, 15.94, \dots \quad (7.3.11a)$$

$$\tau_{2,k} = \frac{4}{\sqrt{17} - 1} \left( \frac{3\pi}{2} + 2k\pi \right) = 6.035, 14.08, 22.13, 30.17, \dots \quad (7.3.11b)$$

which can be ranked as

$$0 < \tau_{1,0} < \tau_{2,0} < \underline{\tau_{1,1}} < \tau_{1,2} < \tau_{2,2} < \tau_{1,3} < \dots \quad (7.3.12)$$

As analyzed in Subsection 3.5.1, this sequence of critical time delays indicates that the equilibrium  $x=0$  is asymptotically stable for  $\tau \in [0, \tau_{1,0})$  and  $\tau \in (\tau_{2,0}, \tau_{1,1})$ , but unstable for  $\tau \in (\tau_{1,0}, \tau_{2,0})$  and  $\tau \in (\tau_{1,1}, +\infty)$ . As a result, the equilibrium undergoes three stability switches with an increase of time delay.

At each critical time delay, Example 7.1.1 and Eq. (7.3.9) imply that a non-degenerate Hopf bifurcation occurs when the time delay crosses the critical value. Given the system parameters, if there exist certain  $k$  and  $j$  such that  $\tau_{1,k} = \tau_{2,j}$ , then the system has two pairs of conjugate pure imaginary roots and undergoes the Hopf-Hopf bifurcation at such a critical time delay. This complicated phenomenon is out of the scope of this book. In the next two subsections, both methods of Fredholm alternative and multiple scales are respectively used to determine the periodic motions owing to the Hopf bifurcation.

### 7.3.2 Periodic Motion Determined by Method of Fredholm Alternative

This subsection presents the computation procedure for the periodic solution, which arises from a Hopf bifurcation at the critical time delay  $\tau_0$ , of Eq. (7.3.1) in three steps by using the method of Fredholm alternative.

#### (1) Computation of eigenvectors

Let  $\alpha \equiv \tau - \tau_0$  denote the bifurcation parameter. By using the transformations  $\tau t \rightarrow t$ ,  $x(\tau t) \rightarrow z_1(t)$ ,  $\dot{x}(\tau t) \rightarrow z_2(t)$ , we recast Eq. (7.3.1) as the following functional differential equation

$$\dot{z}_t = f(\alpha, z_t), \tag{7.3.13}$$

where  $z = [z_1 \ z_2]^T \in R^2$ ,  $z_t(\theta) \equiv z(t + \theta) \in C([-1, 0], R^2)$  for  $-1 \leq \theta \leq 0$ , and

$$f(\alpha, \phi) \equiv \begin{cases} \frac{d\phi}{d\theta}, & \theta \in [-1, 0), \\ \begin{bmatrix} 0 & 1 \\ -(\tau_0 + \alpha)^2 & -2\zeta(\tau_0 + \alpha) \end{bmatrix} \phi(0) + \begin{bmatrix} 0 & 0 \\ 0 & \nu(\tau_0 + \alpha) \end{bmatrix} \phi(-1), & \theta = 0. \end{cases} \tag{7.3.14}$$

The operators  $f_u(\alpha|\cdot)$ ,  $f_{u\alpha}(\alpha|\cdot)$ ,  $f_{uu}(\alpha|\cdot|\cdot)$  and  $f_{uuu}(\alpha|\cdot|\cdot|\cdot)$  are as following

$$f_u(\alpha|x) \equiv \begin{cases} \frac{dx}{d\theta}, & \theta \in [-1, 0), \\ \begin{bmatrix} 0 & 1 \\ -(\tau_0 + \alpha)^2 & -2\zeta(\tau_0 + \alpha) \end{bmatrix} x(0) + \begin{bmatrix} 0 & 0 \\ 0 & \nu(\tau_0 + \alpha) \end{bmatrix} x(-1), & \theta = 0, \end{cases} \tag{7.3.15a}$$

$$f_{u\alpha}(\alpha|x) \equiv \begin{cases} 0, & \theta \in [-1, 0), \\ \begin{bmatrix} 0 & 0 \\ -2(\tau_0 + \alpha) & -2\zeta \end{bmatrix} x(0) + \begin{bmatrix} 0 & 0 \\ 0 & \nu \end{bmatrix} x(-1), & \theta = 0, \end{cases} \tag{7.3.15b}$$

$$f_{uu}(\alpha|x|y) \equiv 0, \tag{7.3.15c}$$

$$f_{uuu}(\alpha|x|y|z) \equiv \begin{cases} 0, & \theta \in [-1, 0), \\ \begin{bmatrix} 0 \\ -6\mu(\tau_0 + \alpha)^2 x_1(0)y_1(0)z_1(0) \end{bmatrix}, & \theta = 0. \end{cases} \tag{7.3.15d}$$



Moreover, the adjoint operator  $f_u^*(0|\cdot)$  of  $f_u(0|\cdot)$  reads

$$f_u^*(\alpha|\psi) \equiv \begin{cases} -\frac{d\psi}{d\theta}, & \theta \in (0, 1], \\ \psi(0) \begin{bmatrix} 0 & 1 \\ -(\tau_0 + \alpha)^2 & -2\zeta(\tau_0 + \alpha) \end{bmatrix} + \psi(1) \begin{bmatrix} 0 & 0 \\ 0 & \nu(\tau_0 + \alpha) \end{bmatrix}, & \theta = 0. \end{cases} \quad (7.3.16)$$

It is easy to compute the eigenvector  $\zeta_0(\theta)$  of the eigenvalue problem:  $f_u(0|\zeta_0) = i\omega\zeta_0$ . This relation implies that

$$\frac{d\zeta_0}{d\theta} = i\omega\zeta_0, \quad \theta \in [-1, 0), \quad (7.3.17a)$$

$$\begin{bmatrix} 0 & 1 \\ -\tau_0^2 & -2\zeta\tau_0 \end{bmatrix} \zeta_0(0) + \begin{bmatrix} 0 & 0 \\ 0 & \nu\tau_0 \end{bmatrix} \zeta_0(-1) = i\omega\zeta_0(0). \quad (7.3.17b)$$

Equation (7.3.17a) makes it possible to assume

$$\zeta_0(\theta) \equiv \begin{bmatrix} 1 \\ B \end{bmatrix} e^{i\omega\theta}. \quad (7.3.17c)$$

Substituting Eq. (7.3.17c) into Eq. (7.3.17b) yields  $B = i\omega$ .

The adjoint eigenvalue problem  $f_u^*(0|\zeta_0^*) = i\omega\zeta_0^*$  gives

$$\frac{d\zeta_0^*(\theta)}{d\theta} = -i\omega\zeta_0^*(\theta), \quad \theta \in (0, 1], \quad (7.3.18a)$$

$$\zeta_0^*(0) \begin{bmatrix} 0 & 1 \\ -\tau_0^2 & -2\zeta\tau_0 \end{bmatrix} + \zeta_0^*(1) \begin{bmatrix} 0 & 0 \\ 0 & \nu\tau_0 \end{bmatrix} = i\omega\zeta_0^*(0). \quad (7.3.18b)$$

Thus,  $\zeta_0^*$  is in the form

$$\zeta_0^*(\theta) \equiv D[C \ 1] e^{-i\omega\theta}, \quad (7.3.18c)$$

with  $C = i\tau_0^2/\omega$ . It is possible to choose the constant  $D$  such that  $(\zeta_0^*, \zeta_0) = 1$  under the following bilinear form

$$(\psi, \phi) \equiv \psi(0)\phi(0) + \int_{-1}^0 \psi(s+1) \begin{bmatrix} 0 & 0 \\ 0 & \nu\tau_0 \end{bmatrix} \phi(s) ds. \quad (7.3.19)$$

There follows

$$D = \frac{\omega}{i(\tau_0^2 + \omega^2) + i\nu\tau_0\omega^2 e^{-i\omega}}. \quad (7.3.20)$$

With help of the constant  $D$ , it is easy to prove that  $(\zeta_0^*, \bar{\zeta}_0) = 0$ .

## (2) Computation of the power series of the bifurcating solutions

Now, the Fredholm alternative is used to determine the bifurcating periodic solution in a power series. For simplicity, a time transformation  $s = \tilde{\omega}(\varepsilon)t$  is introduced such that the task becomes to seek a  $2\pi$ -periodic solution in terms of a properly selected small parameter  $0 < \varepsilon \ll 1$ . This solution yields

$$\tilde{\omega}(\varepsilon) \frac{d\mathbf{u}}{ds} = \mathbf{f}(\alpha(\varepsilon), \mathbf{u}), \quad (7.3.21a)$$

$$\mathbf{u}(s, \varepsilon) = \mathbf{u}(s + 2\pi, \varepsilon), \quad \mathbf{u}(s, 0) = 0, \quad \alpha(0) = 0, \quad \tilde{\omega}(0) = \omega. \quad (7.3.21b)$$

Substituting the following candidate solution

$$\begin{aligned} \mathbf{u}(s, \varepsilon) &= \varepsilon \mathbf{u}_1(s) + \frac{\varepsilon^2}{2!} \mathbf{u}_2(s) + \frac{\varepsilon^3}{3!} \mathbf{u}_3(s) + O(\varepsilon^4), \\ \alpha(\varepsilon) &= \varepsilon \alpha_1 + \frac{\varepsilon^2}{2} \alpha_2 + O(\varepsilon^3), \\ \tilde{\omega}(\varepsilon) &= \omega + \varepsilon \omega_1 + \frac{\varepsilon^2}{2} \omega_2 + O(\varepsilon^3), \end{aligned} \quad (7.3.22)$$

into Eq. (7.3.13) and equating the same power of  $\varepsilon$ , we have a set of linear differential equations like Eq. (7.2.4)

$$\omega \frac{d\mathbf{u}_1}{ds} = \mathbf{f}_u(0|\mathbf{u}_1); \quad (7.3.23a)$$

$$\omega \frac{d\mathbf{u}_2}{ds} = \mathbf{f}_u(0|\mathbf{u}_2) + \mathbf{g}_1(\mathbf{u}_1),$$

$$\mathbf{g}_1(\mathbf{u}_1) \equiv -2\omega_1 \frac{d\mathbf{u}_1}{ds} + 2\alpha_1 \mathbf{f}_{u\alpha}(0|\mathbf{u}_1) + \mathbf{f}_{uu}(0|\mathbf{u}_1|\mathbf{u}_1); \quad (7.3.23b)$$

$$\omega \frac{d\mathbf{u}_3}{ds} = \mathbf{f}_u(0|\mathbf{u}_3) + \mathbf{g}_2(\mathbf{u}_1, \mathbf{u}_2),$$

$$\begin{aligned} \mathbf{g}_2(\mathbf{u}_1, \mathbf{u}_2) \equiv & -3\omega_1 \frac{d\mathbf{u}_2}{ds} + 3\alpha_1 f_{u\alpha}(0|\mathbf{u}_2) - 3\omega_2 \frac{d\mathbf{u}_1}{ds} \\ & + 3\alpha_2 f_{u\alpha}(0|\mathbf{u}_1) + 3\alpha_1 f_{uu\alpha}(0|\mathbf{u}_1|\mathbf{u}_1) + 3\alpha_1^2 f_{u\alpha\alpha}(0|\mathbf{u}_1) \\ & + 3f_{uu}(0|\mathbf{u}_1|\mathbf{u}_2) + f_{uuu}(0|\mathbf{u}_1|\mathbf{u}_1|\mathbf{u}_1). \end{aligned} \quad (7.3.23c)$$

Equation (7.3.23a) has a real solution

$$[\mathbf{u}_1(s)](\theta) = \zeta_0(\theta)e^{is} + \bar{\zeta}_0(\theta)e^{-is}. \quad (7.3.24)$$

Substituting it, together with  $f_{uu}(\alpha|x|y)=0$ , into Eq. (7.3.23b), we have

$$\begin{aligned} \mathbf{g}_1(\mathbf{u}_1) = & -2\omega_1 [i\zeta_0(\theta)e^{is} - i\bar{\zeta}_0(\theta)e^{-is}] \\ & + 2\alpha_1 [e^{is} f_{u\alpha}(0|\zeta_0) + e^{-is} f_{u\alpha}(0|\bar{\zeta}_0)]. \end{aligned} \quad (7.3.25)$$

Using the condition  $(\zeta_0^*, \zeta_0) - 1 = (\zeta_0^*, \bar{\zeta}_0) = 0$  results in

$$[\chi^*, \mathbf{g}_1(\mathbf{u}_1)] = \frac{1}{2\pi} \int_0^{2\pi} \chi^*, \mathbf{g}_1(\mathbf{u}_1) ds = 2[-i\omega_1 + \alpha_1 \lambda'(0)], \quad (7.3.26)$$

where  $\chi^* = \zeta_0^* e^{-is}$ . The Fredholm alternative gives  $\alpha_1 = 0$  and  $\omega_1 = 0$ , thus  $\mathbf{g}_1(\mathbf{u}_1) = 0$  holds.

Now, Eq. (7.3.23b) degenerates to Eq. (7.3.23a) and there exists a  $\hat{\zeta}_0(\theta)$  such that

$$[\mathbf{u}_2(s)](\theta) = \hat{\zeta}_0(\theta)e^{is} + \overline{\hat{\zeta}_0}(\theta)e^{-is}. \quad (7.3.27)$$

According to Eq. (7.3.15b), as well as  $\alpha_1 = 0$  and  $\omega_1 = 0$ , we have

$$\mathbf{g}_2(\mathbf{u}_1, \mathbf{u}_2) = -3\omega_2 \frac{d\mathbf{u}_1}{ds} + 3\alpha_2 f_{u\alpha}(0|\mathbf{u}_1) + f_{uuu}(0|\mathbf{u}_1|\mathbf{u}_1|\mathbf{u}_1). \quad (7.3.28)$$

In order to evaluate the right-hand side of Eq. (7.3.28), we write  $\mathbf{u}_1$  as  $\mathbf{u}_1 \equiv [u_{1,1} \ u_{1,2}]^T$ , where  $[u_{1,1}(s)](\theta) = e^{i\omega\theta+is} + e^{-i\omega\theta-is}$ . Substituting this expression into Eq. (7.3.15d) gives

$$f_{uuu}(0|\mathbf{u}_1|\mathbf{u}_1|\mathbf{u}_1) = \begin{cases} 0, & \theta \in [-1, 0), \\ \begin{bmatrix} 0 \\ -6\mu\tau_0^2 u_{1,1}^3(0) \end{bmatrix} = \begin{bmatrix} 0 \\ -6\mu\tau_0^2 (e^{is} + e^{-is})^3 \end{bmatrix}, & \theta = 0. \end{cases} \quad (7.3.29)$$

Thus, we have

$$\begin{aligned}
 (\chi^*, f_{uuu}(0|\mathbf{u}_1|\mathbf{u}_1|\mathbf{u}_1)) &= e^{-is} D[C-1] \begin{bmatrix} 0 \\ -6\mu\tau_0^2(e^{is}+e^{-is})^3 \end{bmatrix} \\
 &= -6\mu\tau_0^2 D(e^{is}+e^{-is})^3 e^{-is},
 \end{aligned} \tag{7.3.30a}$$

$$\begin{aligned}
 [\chi^*, f_{uuu}(0|\mathbf{u}_1|\mathbf{u}_1|\mathbf{u}_1)] &= \frac{1}{2\pi} \int_0^{2\pi} (\chi^*, f_{uuu}(0|\mathbf{u}_1|\mathbf{u}_1|\mathbf{u}_1)) ds \\
 &= -18\mu\tau_0^2 D.
 \end{aligned} \tag{7.3.30b}$$

Using the Fredholm alternative condition  $[\chi^*, \mathbf{g}_2(\mathbf{u}_1, \mathbf{u}_2)] = 0$ , we have

$$3[-i\omega_2 + \alpha_2 \lambda'(0)] - 18\mu\tau_0^2 D = 0, \tag{7.3.31}$$

whereby we obtain

$$\begin{aligned}
 \alpha_2 &= \frac{6\mu\omega^3 \tau_0^3 v \sin \omega}{\rho_R [(\tau_0^2 + \omega^2)^2 + v^2 \omega^4 \tau_0^2 + 2\omega^2 \tau_0 (\omega^2 + \tau_0^2) v \cos \omega]} \\
 &= \frac{-6\mu\omega^2 \tau_0^2 (\omega^2 - \tau_0^2)}{\rho_R [(\omega^2 - \tau_0^2)^2 + \omega^2 (4\zeta \tau_0^3 + 4\zeta \omega^2 \tau_0 + v^2 \omega^2 \tau_0^2)]},
 \end{aligned} \tag{7.3.32a}$$

$$\begin{aligned}
 \omega_2 &= \frac{6\mu\omega\tau_0^2 [\rho_R (\tau_0^2 + \omega^2 + \omega^2 \tau_0 v \cos \omega) + \rho_I \omega^2 \tau_0 v \sin \omega]}{\rho_R [(\tau_0^2 + \omega^2)^2 + v^2 \omega^4 \tau_0^2 + 2\omega^2 \tau_0 (\omega^2 + \tau_0^2) v \cos \omega]} \\
 &= \frac{6\mu\omega\tau_0^2 [(\omega^2 + \tau_0^2 + 2\zeta \omega^2 \tau_0) \rho_R - \omega(\omega^2 - \tau_0^2) \rho_I]}{\rho_R [(\omega^2 - \tau_0^2)^2 + \omega^2 (4\zeta \tau_0^3 + 4\zeta \omega^2 \tau_0 + v^2 \omega^2 \tau_0^2)]},
 \end{aligned} \tag{7.3.32b}$$

where  $\rho_R \equiv \text{Re} \lambda'(0)$  and  $\rho_I \equiv \text{Im} \lambda'(0)$ . By using implicit differentiation or computing  $(\zeta_0^*, f_{u\alpha}(0|\zeta_0))$ , we obtain

$$\lambda'(0) = \frac{i\omega(\omega^2 + \tau_0^2)}{\tau_0 [\omega^2 + \tau_0^2 + 2\zeta \omega^2 \tau_0 + i\omega(\omega^2 - \tau_0^2)]}, \tag{7.3.33}$$

as well as

$$\begin{aligned}
 \rho_R &= \frac{\omega^2 (\omega^2 + \tau_0^2) (\omega^2 - \tau_0^2)}{\tau_0 [(\omega^2 + \tau_0^2 + 2\zeta \omega^2 \tau_0)^2 + (\omega^3 - \tau_0^2 \omega)^2]}, \\
 \rho_I &= \frac{\omega (\omega^2 + \tau_0^2) (\omega^2 + \tau_0^2 + 2\zeta \tau_0 \omega^2)}{\tau_0 [(\omega^2 + \tau_0^2 + 2\zeta \omega^2 \tau_0)^2 + (\omega^3 - \tau_0^2 \omega)^2]}.
 \end{aligned} \tag{7.3.34}$$

Using the condition of marginal stability, it is easy to show that except for the factors  $\rho_R$  and  $\tau_0$ , the denominators in Eqs. (7.3.32) and (7.3.34) are the same. Thus, we simplify Eq. (7.3.32) to

$$\begin{cases} \alpha_2 = \frac{-6\mu\tau_0^3}{\omega^2 + \tau_0^2} = \frac{-12\mu\tau_0}{(v^2 + 4 - 4\zeta^2) \mp \sqrt{(v^2 - 4\zeta^2)(v^2 + 4 - 4\zeta^2)}}, \\ \omega_2 = 0. \end{cases} \quad (7.3.35)$$

In summary, the bifurcating periodic solution reads

$$\begin{aligned} z(t) &= z_1(0) = [u(\omega t)](0) \\ &= [\varepsilon \zeta_0(0) + \frac{\varepsilon^2}{2} \hat{\zeta}_0(0)] e^{i\omega t} + [\varepsilon \bar{\zeta}_0(0) + \frac{\varepsilon^2}{2} \bar{\hat{\zeta}}_0(0)] e^{-i\omega t} + O(\varepsilon^3), \end{aligned} \quad (7.3.36a)$$

$$\alpha = \frac{\varepsilon^2}{2} \alpha_2 + O(\varepsilon^3), \quad (7.3.36b)$$

$$\tilde{\omega} = \omega + O(\varepsilon^3). \quad (7.3.36c)$$

In fact, Eq. (7.2.22) gives  $\alpha = \varepsilon^2 \alpha_2 / 2 + O(\varepsilon^4)$  and  $\tilde{\omega} = \omega + O(\varepsilon^4)$ . As done in Subsection 7.2.1, it is also possible to substitute Eq. (7.3.35) into Eqs. (7.3.36b) and (7.3.36c) so that the periodic solution given by Eq. (7.3.36) is in term of the bifurcation parameter  $\alpha$ .

### (3) Stability of the bifurcating solutions

As stated in Theorem 7.2.2, the bifurcating periodic solutions are asymptotically stable when  $\Delta \equiv \alpha_2 \rho_R > 0$ , or unstable when  $\Delta < 0$ . From Eq. (7.3.32a), we have

$$\operatorname{sgn} \Delta = -\operatorname{sgn}[\mu(\omega^2 - \tau_0^2)], \quad \operatorname{sgn} \alpha_2 = -\operatorname{sgn} \mu \quad (7.3.37)$$

Note that the new time in Eq. (7.3.13) is the product of  $\tau_0$  and the original time, and that the vibrating frequency  $\omega$  obtained here is the product of  $\tau_0$  and the vibrating frequency obtained in Subsection 7.3.1. Keeping these facts in mind, we see that  $\operatorname{sgn} \Delta = -\operatorname{sgn} \mu < 0$  at  $\tau = \tau_{1,k}$  and  $\operatorname{sgn} \Delta = \operatorname{sgn} \mu > 0$  at  $\tau = \tau_{2,k}$ . That is, the periodic motions bifurcating at  $\tau = \tau_{1,k}$  are unstable, and those bifurcating at  $\tau = \tau_{2,k}$  are asymptotically stable.

Consider again the case when  $\zeta = 0$ ,  $v = -0.5$ ,  $\mu = 0.1$ . Subsection 7.3.1 indicates that  $\omega_1 = 1.281$  and  $\omega_2 = 0.7808$ , together with the critical time delays  $\tau_{1,k}$  and  $\tau_{2,k}$ . Simple computation gives

$$\Delta = -0.1187, \quad (\omega/\tau_0, \tau_0) = (\omega_1, \tau_{1,0}) = (1.281, 1.226), \quad (7.3.38a)$$

$$\Delta = 0.8705, \quad (\omega/\tau_0, \tau_0) = (\omega_2, \tau_{2,0}) = (0.781, 6.035), \quad (7.3.38b)$$

$$\Delta = -0.7345, \quad (\omega/\tau_0, \tau_0) = (\omega_1, \tau_{1,1}) = (1.281, 6.132), \quad (7.3.38c)$$

$$\Delta = -0.8635, \quad (\omega/\tau_0, \tau_0) = (\omega_1, \tau_{1,2}) = (1.281, 11.04), \quad (7.3.38d)$$

$$\Delta = 1.3470, \quad (\omega/\tau_0, \tau_0) = (\omega_2, \tau_{2,1}) = (0.781, 14.08). \quad (7.3.38e)$$

As a result, the periodic motions bifurcating at  $\tau = \tau_{1,k}$  are unstable and those at  $\tau = \tau_{2,k}$  are asymptotically stable. Noting the sign of  $\alpha_2$ , we know that the system undergoes the subcritical Hopf bifurcations at  $\tau = \tau_{2,0}$ ,  $\tau = \tau_{2,1}$  and so on.

### 7.3.3 Periodic Motion Determined by Method of Multiple Scales

#### (1) Approximate periodic solution

To simplify the computation of the periodic motions of Eq. (7.3.1), the study in this subsection is confined to the case of small damping, weak nonlinearity and weak velocity feedback. That is,

$$\zeta = \varepsilon \hat{\zeta}, \quad \nu = \varepsilon \hat{\nu}, \quad \mu = \varepsilon \hat{\mu}, \quad (7.3.39)$$

where

$$0 < \varepsilon \ll 1, \quad \hat{\zeta} = O(1), \quad \hat{\nu} = O(1), \quad \hat{\mu} = O(1). \quad (7.3.40)$$

Because Eq. (7.3.1) is an autonomous system, the period  $\omega$  of a bifurcating motion is an unknown, and can be denoted by

$$\omega^2 = 1 + \varepsilon \sigma, \quad (7.3.41)$$

where  $\sigma = O(1)$  is the detuning frequency. Upon the this assumption, Eq. (7.3.1) can be written as a linear ordinary differential equation subject to a small perturbation of both nonlinearity and delayed feedback

$$\ddot{x}(t) + \omega^2 x(t) = \varepsilon [\alpha x(t) - \hat{\mu} x^3(t) - 2\hat{\zeta} \dot{x}(t) + \hat{\nu} \dot{x}(t - \tau)]. \quad (7.3.42)$$

Now, we try to find the following expansion of two time scales for the solution of Eq. (7.3.42)

$$x(t) = x_0(T_0, T_1) + \varepsilon x_1(T_0, T_1) + O(\varepsilon^2), \quad T_0 \equiv t, \quad T_1 \equiv \varepsilon t. \quad (7.3.43)$$

For this purpose, it is helpful to use the following differential operators defined in (Nayfeh and Mook, 1979)

$$\begin{cases} \frac{d}{dt} = \frac{\partial}{\partial T_0} + \varepsilon \frac{\partial}{\partial T_1} + O(\varepsilon^2) \equiv D_0 + \varepsilon D_1 + O(\varepsilon^2), \\ \frac{d^2}{dt^2} = D_0^2 + 2\varepsilon D_0 D_1 + O(\varepsilon^2). \end{cases} \quad (7.3.44)$$

Substituting Eqs. (7.3.43) and (7.3.44) into Eq. (7.3.42) and equating the same power of  $\varepsilon$ , we obtain a set of linear partial differential equations

$$D_0^2 x_0(T_0, T_1) + \omega^2 x_0(T_0, T_1) = 0, \quad (7.3.45a)$$

$$\begin{aligned} D_0^2 x_1(T_0, T_1) + \omega^2 x_1(T_0, T_1) = & -2D_0 D_1 x_0(T_0, T_1) + \sigma x_0(T_0, T_1) - \hat{\mu} x_0^3(T_0, T_1) \\ & - 2\hat{\zeta} D_0 x_0(T_0, T_1) + \hat{\nu} D_0 x_0(T_0 - \tau, T_1). \end{aligned} \quad (7.3.45b)$$

Solving Eq. (7.3.45a) for  $x_0(T_0, T_1)$ , we have

$$x_0(T_0, T_1) = A(T_1) e^{i\omega T_0} + cc, \quad (7.3.46)$$

where  $cc$  denotes the conjugate term and

$$A(T_1) \equiv \frac{1}{2} \alpha(T_1) e^{i\beta(T_1)}. \quad (7.3.47)$$

Substituting Eq. (7.3.47) into Eq. (7.3.45b) yields

$$\begin{aligned} D_0^2 x_1(T_0, T_1) + \omega^2 x_1(T_0, T_1) = & -2i\omega D_1 A e^{i\omega T_0} + \sigma A e^{i\omega T_0} \\ & - \hat{\mu} (A^3 e^{3i\omega T_0} + 3A^2 \bar{A} e^{i\omega T_0}) \\ & - 2i\hat{\zeta} \omega A e^{i\omega T_0} + i\hat{\nu} \omega e^{-i\omega \tau} A e^{i\omega T_0} + cc. \end{aligned} \quad (7.3.48)$$

To eliminate the secular term in the right-hand side of Eq. (7.3.48), let

$$i\omega(2D_1 + 2\hat{\zeta} - \hat{\nu} e^{-i\omega \tau}) A - \sigma A + 3\hat{\mu} A^2 \bar{A} = 0. \quad (7.3.49)$$

Substituting Eqs. (7.3.47), (7.3.39) and (7.3.41) into Eq. (7.3.49) and separating the real part and the imaginary part, we have a set of autonomous differential equations that govern the amplitude  $\alpha(T_1)$  and the phase  $\beta(T_1)$

$$\begin{cases} 2\varepsilon D_1 \alpha = (-2\hat{\zeta} + \nu \cos \omega \tau) \alpha, \\ 2\varepsilon \omega \alpha D_1 \beta = -(\omega^2 - 1 + \nu \omega \sin \omega \tau) \alpha + \frac{3\mu}{4} \alpha^3. \end{cases} \quad (7.3.50)$$

Thus, the first order approximation of periodic motion is

$$x(t) = \alpha(\varepsilon t) \cos[\omega t + \beta(\varepsilon t)] + o(\varepsilon). \quad (7.3.51)$$

To determine the steady state motion, let  $D_1\alpha=0$  and  $D_1\beta=0$  in Eq. (7.3.50). For the equilibrium  $\alpha=0$ , it is easy to see from the first equation in Eq. (7.3.50) that it is asymptotically stable if and only

$$-2\zeta + v\cos\omega\tau < 0. \quad (7.3.52)$$

This stability condition offers the same information as the critical condition (7.3.6). Because the behavior of equilibrium is clear, we pay attention to the case when  $\alpha \neq 0$  hereafter. In this case,  $\alpha$  yields

$$\begin{cases} -2\zeta + v\cos\omega\tau = 0, \\ (\omega^2 - 1 + v\omega\sin\omega\tau) - \frac{3\mu}{4}\alpha^2 = 0. \end{cases} \quad (7.3.53)$$

Eliminating the harmonic terms in Eq. (7.3.53) gives the amplitude-frequency equation

$$(\omega^2 - 1 - \frac{3\mu\alpha^2}{4})^2 + (4\zeta^2 - v^2)\omega^2 = 0. \quad (7.3.54)$$

Noting that  $|v| \geq 2\zeta$ , we have two branches of solution

$$\alpha_{1,2} = \sqrt{\frac{4}{3\mu}(\omega^2 - 1 \mp v\omega\sqrt{v^2 - 4\zeta^2})}. \quad (7.3.55)$$

From the second equation in Eq. (7.3.53) and Eq. (7.3.54), we have

$$\sin\omega\tau = \frac{1}{v\omega}(\omega^2 - 1 - \frac{3\mu\alpha_{1,2}^2}{4}) = \pm \frac{1}{|v|}\sqrt{v^2 - 4\zeta^2}. \quad (7.3.56)$$

Given a time delay  $\tau$ , solving the first equation in Eq. (7.3.53) for  $\omega$  under condition (7.3.56) gives the frequency corresponding to each branch of solution

$$\omega = \frac{1}{\tau} \cos^{-1}\left(\frac{\zeta}{v}\right) = \begin{cases} \frac{1}{\tau} [\arccos(-\frac{2\zeta}{|v|}) + 2k\pi], & \alpha = \alpha_1, \\ \frac{1}{\tau} [2\pi - \arccos(-\frac{2\zeta}{|v|}) + 2k\pi], & \alpha = \alpha_2. \end{cases} \quad (7.3.57)$$

Here  $k=0,1,2,\dots$  imply an infinite number of frequencies and corresponding periodic motions as well. However, the assumption in Eq. (7.3.41) may hold only when  $k=0$ .

One may wonder the asymptotic stability of the periodic motion. Unfortunately, it is not possible to check the stability by linearizing Eq. (7.3.50) at the steady



state motion because the small perturbation  $\Delta\alpha$  near the steady state motion yields

$$2\varepsilon D_1 \Delta\alpha = 0. \tag{7.3.58}$$

In fact, the stability of a bifurcating periodic motion has to be determined through the higher order approximation in Eq. (7.3.43).

**(2) A case study**

Now, we look at the case when  $\zeta=0, \nu=-0.5, \mu=0.1$  again. Substituting these parameters into Eqs. (7.3.57) and (7.3.55) yields

$$\alpha_1 = \sqrt{\frac{4}{0.3}[(\frac{\pi}{2\tau})^2 - 0.5(\frac{\pi}{2\tau}) - 1]}, \quad \alpha_2 = \sqrt{\frac{4}{0.3}[(\frac{3\pi}{2\tau})^2 + 0.5(\frac{3\pi}{2\tau}) - 1]}, \tag{7.3.59}$$

where  $\tau \in (0, \tau_{1,0}) = (0, 1.226)$  is for the unstable branch  $\alpha_1$  and  $\tau \in (0, \tau_{2,0}) = (0, 6.035)$  for the asymptotically stable branch  $\alpha_2$ . Figure 7.3.1 gives the relation between a given time delay and the frequency of periodic motion. Figure 7.3.2 shows the amplitude of periodic motion versus the time delay, together with the numerical results obtained by using the Runge-Kutta approach.

As shown in Fig. 7.3.2, the system has an asymptotically stable equilibrium, an asymptotically stable periodic motion and an unstable periodic motion if  $\tau \in (0, \tau_{1,0})$ . When  $\tau \in (\tau_{1,0}, \tau_{2,0})$ , the equilibrium becomes unstable and the unstable periodic motion disappears, only the stable periodic motion remains. When  $\tau > \tau_{2,0} = 6.035$ , the equilibrium becomes asymptotically stable again, but loses stability soon when  $\tau > \tau_{1,1} = 6.132$ . Hence, the equilibrium undergoes the Hopf bifurcations at  $\tau_{1,0} = 1.266$  and  $\tau_{2,0} = 6.035$ , respectively.

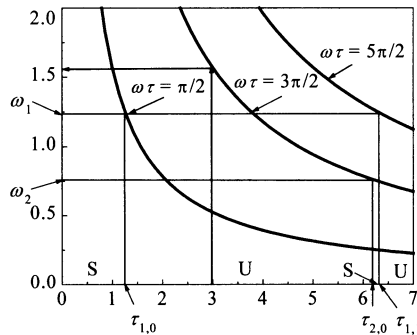


Fig. 7.3.1. Delay-frequency relation of periodic motions

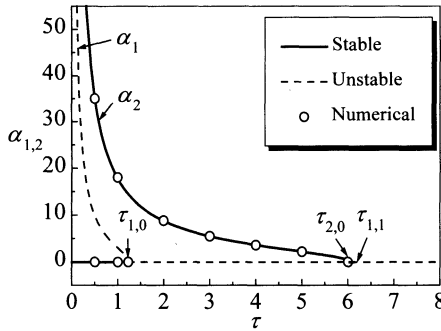


Fig. 7.3.2. Delay-amplitude relation of periodic motions

Figure 7.3.3 presents two trajectories of the system with time delay  $\tau=1$ . The phase trajectory initiating from  $x(t)=1+t+2.5t^2, t \in [-1, 0]$  approaches the asymptotically stable equilibrium, while the phase trajectory initiating from  $x(t)=10+10t+25t^2, t \in [-1, 0]$  approaches an asymptotically stable periodic motion of fundamental frequency  $\omega=4.713$  rapidly. This numerical result coincides very well with the approximate solution given by Eqs. (7.3.55) and (7.3.57), where  $\alpha \rightarrow 17.73$  and  $\omega \rightarrow 3\pi/2 \approx 4.713$  with an increase of time.

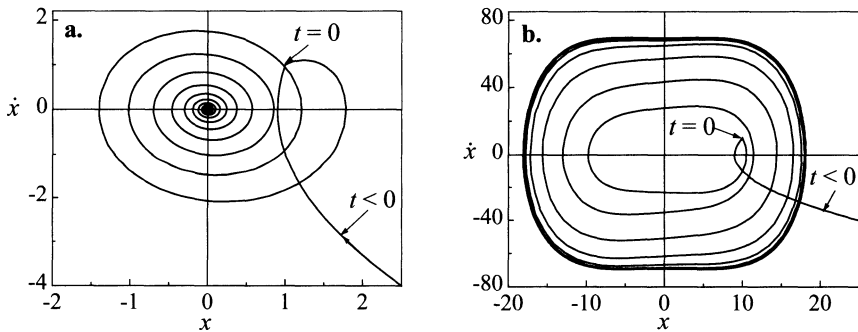


Fig. 7.3.3. Two trajectories of system when  $\tau=1$ ; a. a trajectory approaching equilibrium, b. a trajectory approaching limit circle

It should be emphasized that the Duffing oscillator with strong negative feedback of delayed velocity always exhibits a periodic motion for appropriate initial condition even if the time delay is very short. However, the approximate system on the basis of Taylor expansion in Section 5.3 does not keep this property.

One may wonder how the system behaves when  $\tau > \tau_{1,1} = 6.132$  since the system equilibrium in this case is unstable. As discussed in Subsection 7.3.2, the unstable

equilibrium may still bifurcate an asymptotically stable periodic motion. However, the basin of attraction of the bifurcating periodic motion may be very small, and falls into a “narrow” subspace of the Banach space  $C[-\tau, 0]$ . The numerical integration from a great number of initial conditions often fails to capture the periodic motion. For instance, Fig. 7.3.4 gives the time history and Fourier spectrum of a motion when  $\tau=6.2$ . They look quite chaotic. To confirm the chaotic feature behind the motion, a Poincaré section was introduced in the case study as following

$$\Sigma = \{(x, \dot{x}) \mid \dot{x} \text{ is local maximum}\}, \tag{7.3.59}$$

and the steady state motion was recorded on the Poincaré section in Fig. 7.3.5. Undoubtedly, this is a typical Poincaré section of strange attractor.

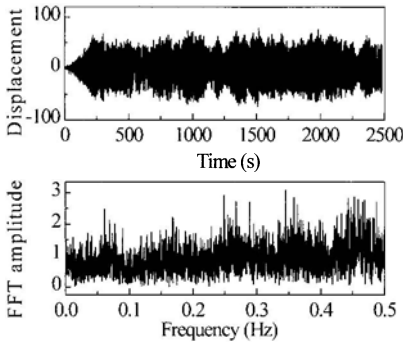


Fig. 7.3.4. Time history and FFT spectrum of a chaotic motion when  $\tau=6.2$

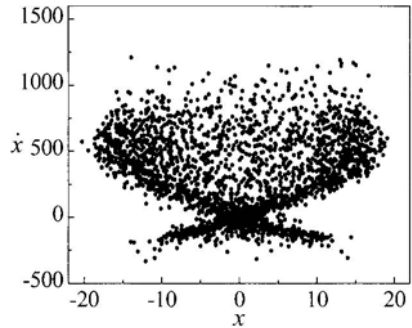


Fig. 7.3.5. Chaotic attractor on the Poincaré section when  $\tau=6.2$

### 7.4 Periodic Motions of a Forced Duffing Oscillator with Delayed Feedback

The objective of this section is to show how to analyze the periodic motions of non-autonomous nonlinear systems with a time delay through an illustrative example, a harmonically forced Duffing oscillator with linear delayed state feedback. As discussed in Subsection 1.1.1, the delay differential equation of concern, after re-scaled, can be written as

$$\ddot{x}(t) + 2\zeta \dot{x}(t) + x(t) + \mu x^3(t) = ux(t-\tau) + v\dot{x}(t-\tau) + f \cos \lambda t, \tag{7.4.1}$$

For simplicity, the study is confined to the case of small damping, weak cubic nonlinearity and weak state feedback. That is,

$$\zeta=O(\varepsilon), \quad \mu=O(\varepsilon), \quad u=O(\varepsilon), \quad v=O(\varepsilon), \quad (7.4.2)$$

where  $0<\varepsilon\ll 1$ . In what follows, the primary resonance and 1/3 subharmonic resonance of Eq. (7.4.1) will be studied respectively by using the method of multiple scales.

### 7.4.1 Primary Resonance

The primary resonance of Eq. (7.4.1) always occurs when  $\lambda\approx 1$  even though the amplitude of excitation may be very small. That is,

$$f=O(\varepsilon), \quad \lambda=1+\varepsilon\sigma, \quad (7.4.3)$$

where  $\sigma=O(1)$  is the detuning frequency. In this case, Eq. (7.4.1) becomes

$$\ddot{x}(t)+x(t)=-2\zeta\dot{x}(t)-\mu x^3(t)+ux(t-\tau)+v\dot{x}(t-\tau)+f\cos(1+\varepsilon\sigma)t. \quad (7.4.4)$$

Now, we look for an expansion of two scales for the solution of Eq. (7.4.4)

$$x(t)\equiv x_0(T_0, T_1)+\varepsilon x_1(T_0, T_1)+O(\varepsilon^2), \quad T_r\equiv\varepsilon^r t, \quad r=0,1, \quad (7.4.5)$$

Substituting Eq. (7.4.5) into Eq. (7.4.4) and equating the same power of  $\varepsilon$ , and the same order quantities as well, we obtain a set of linear partial differential equations

$$D_0^2 x_0(T_0, T_1)+x_0(T_0, T_1)=0, \quad (7.4.6a)$$

$$\begin{aligned} \varepsilon[D_0^2 x_1(T_0, T_1)+x_1(T_0, T_1)]&=-2\varepsilon D_0 D_1 x_0(T_0, T_1)-2\zeta D_0 x_0(T_0, T_1) \\ &-\mu x_0^3(T_0, T_1)+ux_0(T_0-\tau, T_1)+vD_0 x_0(T_0-\tau, T_1)+f\cos(T_0+\sigma T_1), \end{aligned} \quad (7.4.6b)$$

where the differential operators  $D_0$  and  $D_1$  are defined in Eq. (7.3.44).

Solving Eq. (7.4.6a) for  $x_0(T_0, T_1)$ , we have

$$x_0(T_0, T_1)=A(T_1)e^{iT_0}+cc, \quad (7.4.7)$$

where  $cc$  denotes the conjugate term and

$$A(T_1)\equiv\frac{1}{2}\alpha(T_1)e^{i\beta(T_1)}. \quad (7.4.8)$$

Substituting Eq. (7.4.7) into Eq. (7.4.6b) yields

$$\begin{aligned} \varepsilon[D_0^2 x_1(T_0, T_1) + x_1(T_0, T_1)] = & -2i\varepsilon D_1 A e^{i\tau_0} - 2i\zeta A e^{i\tau_0} \\ & - \mu(A^3 e^{3i\tau_0} + 3A^2 \bar{A} e^{i\tau_0}) + u e^{-i\tau} A e^{i\tau_0} + i v e^{-i\tau} A e^{i\tau_0} \\ & + \frac{f}{2} e^{i\sigma T_1} e^{i\tau_0} + \text{cc}. \end{aligned} \tag{7.4.9}$$

To eliminate the secular term in Eq. (7.4.9), let

$$-i(2\varepsilon D_1 + 2\zeta - v e^{-i\tau}) A + u A e^{-i\tau} - 3\mu A^2 \bar{A} + \frac{f}{2} e^{i\sigma T_1} = 0. \tag{7.4.10}$$

By substituting Eq. (7.4.11) into Eq. (7.4.10) and separating the real part and the imaginary part, we obtain a set of autonomous differential equations that govern the amplitude  $\alpha(T_1)$  and the phase  $\varphi(T_1)$

$$\begin{cases} 2\varepsilon D_1 \alpha = -(2\zeta + u \sin \tau - v \cos \tau) \alpha + f \sin \varphi, \\ 2\varepsilon \alpha D_1 \varphi = (2\varepsilon \sigma + u \cos \tau + v \sin \tau) \alpha - \frac{3\mu}{4} \alpha^3 + f \cos \varphi, \end{cases} \tag{7.4.11}$$

where

$$\varphi(T_1) \equiv \sigma T_1 - \beta(T_1). \tag{7.4.12}$$

### (1) Steady state primary resonance

From Eq. (7.4.11), we have a set of algebraic equations for the amplitude  $\hat{\alpha}$  and the phase  $\hat{\varphi}$  of the steady-state primary resonance by setting  $D_1 \alpha = 0$  and  $D_1 \varphi = 0$

$$\begin{cases} -(2\zeta + u \sin \tau - v \cos \tau) \hat{\alpha} + f \sin \hat{\varphi} = 0, \\ (2\lambda - 2 + u \cos \tau + v \sin \tau) \hat{\alpha} - \frac{3\mu}{4} \hat{\alpha}^3 + f \cos \hat{\varphi} = 0, \end{cases} \tag{7.4.13}$$

whereby we derive the frequency response relation between  $\hat{\alpha}$  and  $\lambda$ , and that between  $\hat{\varphi}$  and  $\lambda$

$$\begin{cases} [(2\zeta + u \sin \tau - v \cos \tau)^2 + (2\lambda - 2 + u \cos \tau + v \sin \tau - \frac{3\mu}{4} \hat{\alpha}^2)^2] \hat{\alpha}^2 - f^2 = 0, \\ \tan \hat{\varphi} + \frac{2\zeta + u \sin \tau - v \cos \tau}{2\lambda - 2 + u \cos \tau + v \sin \tau - \frac{3\mu}{4} \hat{\alpha}^2} = 0. \end{cases} \tag{7.4.14}$$

Given a specific value of  $\hat{\alpha}$ , it is easy to solve the first equation in Eq. (7.4.14) for  $\lambda$ , and then obtain  $\hat{\varphi}$  from the second equation. Hence, we have the first order approximation of the steady-state primary resonance

$$x(t) = \hat{\alpha} \cos(\lambda t - \hat{\varphi}) + O(\varepsilon). \tag{7.4.15}$$

Figure 7.4.1 shows the frequency-amplitude relations of the primary resonance for the uncontrolled system, the controlled system without time delay, and the controlled system with different time delays, respectively.

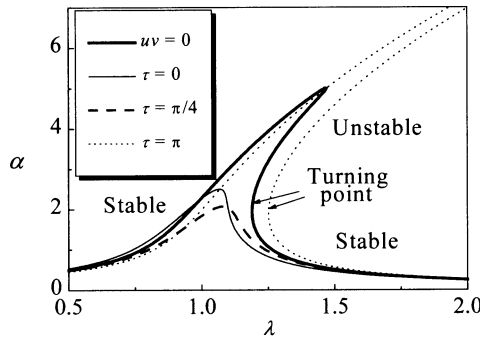


**Fig. 7.4.1.** Amplitude of frequency response of the primary resonance at different time delays when  $\zeta=0.05$ ,  $\mu=0.05$ ,  $f=0.5$ ,  $u=0$  and  $v=0$  (or  $u=0.1$  and  $v=-0.1$ )

**(2) Stability analysis**

To analyze the stability of the steady-state primary resonance, we linearize Eq. (7.4.11) at  $(\hat{\alpha}, \hat{\varphi})$  with respect to  $\alpha$  and  $\varphi$

$$\begin{cases} 2\varepsilon D_1 \Delta \alpha = -(2\zeta + u \sin \tau - v \cos \tau) \Delta \alpha + f \cos \hat{\varphi} \Delta \varphi, \\ 2\varepsilon D_1 \Delta \varphi = -\left(\frac{3\mu}{2} \hat{\alpha}^2 + \frac{f}{\hat{\alpha}^2} \cos \hat{\varphi}\right) \Delta \alpha - \frac{f}{\hat{\alpha}} \sin \hat{\varphi} \Delta \varphi. \end{cases} \tag{7.4.16}$$

The characteristic equation of Eq. (7.4.16), thus, reads

$$\det \begin{bmatrix} -(2\zeta + u \sin \tau - v \cos \tau) - 2\varepsilon & f \cos \hat{\varphi} \\ -\left(\frac{3\mu}{2} \hat{\alpha}^2 + \frac{f}{\hat{\alpha}^2} \cos \hat{\varphi}\right) & -\frac{f}{\hat{\alpha}} \sin \hat{\varphi} - 2\varepsilon \end{bmatrix} = 0. \tag{7.4.17}$$

According to Eq. (7.4.13), we simplify Eq. (7.4.17) to

$$(\varepsilon \varsigma)^2 + 2a(\varepsilon \varsigma) + b = 0, \tag{7.4.18}$$

where

$$\begin{cases} a \equiv \zeta + \frac{u}{2} \sin \tau - \frac{v}{2} \cos \tau, \\ b \equiv \left(\frac{a}{2}\right)^2 + \left(\lambda - 1 + \frac{u}{2} \cos \tau + \frac{v}{2} \sin \tau - \frac{3\mu}{8} \hat{\alpha}^2\right) \left(\lambda - 1 + \frac{u}{2} \cos \tau + \frac{v}{2} \sin \tau - \frac{9\mu}{8} \hat{\alpha}^2\right). \end{cases} \tag{7.4.19}$$

The Routh-Hurwitz criterion indicates that the steady-state vibration is asymptotically stable if and only if the following two inequalities hold simultaneously

$$\begin{cases} a = \zeta + \frac{u}{2} \sin \tau - \frac{v}{2} \cos \tau > 0, \\ b = \left(\frac{a}{2}\right)^2 + \left(\lambda - 1 + \frac{u}{2} \cos \tau + \frac{v}{2} \sin \tau - \frac{3\mu}{8} \hat{\alpha}^2\right) \left(\lambda - 1 + \frac{u}{2} \cos \tau + \frac{v}{2} \sin \tau - \frac{9\mu}{8} \hat{\alpha}^2\right) > 0. \end{cases} \quad (7.4.20)$$

The first condition in Eq. (7.4.20) is independent of the nonlinearity, the resonance amplitude and the excitation. As a matter of fact, it serves as the stability condition for the free vibration of the linear system with delayed state feedback. Letting

$$\frac{da}{d\tau} = \frac{u}{2} \cos \tau + \frac{v}{2} \sin \tau = 0, \quad (7.4.21)$$

we obtain an infinite number of time delays

$$\tau_r = \tan^{-1}\left(-\frac{u}{v}\right) + r\pi, \quad r = 0, 1, 2, \dots \quad (7.4.22)$$

at which  $a$  arrives at the extreme values

$$a_{\min} = \zeta - \frac{\sqrt{u^2 + v^2}}{2}, \quad a_{\max} = \zeta + \frac{\sqrt{u^2 + v^2}}{2}. \quad (7.4.23)$$

This implies that if the feedback gains are so small that  $\sqrt{u^2 + v^2} < 2\zeta$ , the stability of the free vibration of the linear system is independent of the time delay in the state feedback. This condition carries the same information as Eq. (3.1.33) if the higher order terms such as  $v^4$ ,  $\zeta^4$  and  $v^2\zeta^2$  are neglected there.

By calculating the condition  $d\lambda/d\hat{\alpha} = 0$ , we can readily find that the critical case of  $b = 0$  corresponds to the turning points in Fig. 7.4.1. Thus, the stability of the primary resonance of the Duffing oscillator with delayed state feedback is qualitatively the same as that of the Duffing oscillator free of time delay. When the time delay yields Eq. (7.4.21), the second condition in Eq. (7.4.20) becomes

$$b = \left(\zeta \pm \frac{\sqrt{u^2 + v^2}}{2}\right)^2 + \left(\lambda - 1 - \frac{3\mu}{8} \hat{\alpha}^2\right) \left(\lambda - 1 - \frac{9\mu}{8} \hat{\alpha}^2\right) > 0. \quad (7.4.24)$$

### (3) Amplitude peak and equivalent damping

Substituting Eq. (7.4.23) into the first equation in Eq. (7.4.14) yields

$$\left[(2\zeta \pm \sqrt{u^2 + v^2})^2 + \left(2\lambda - 2 - \frac{3\mu}{4} \hat{\alpha}^2\right)\right] \hat{\alpha}^2 - f^2 = 0. \quad (7.4.25)$$

Hence, the amplitude peak of the primary resonance reads

$$\hat{\alpha}_{\max} = \frac{f}{2\zeta \pm \sqrt{u^2 + v^2}}. \quad (7.4.26)$$

This implies that if the time delay is appropriately chosen so that  $a = a_{\max} = \zeta + \sqrt{u^2 + v^2}/2$ , the amplitude peak can be reduced to a minimum by the state feedback. On the other hand, the state feedback will greatly increase the amplitude peak if the time delay makes  $a = a_{\min} = \zeta - \sqrt{u^2 + v^2}/2$ . This property enables one to design an appropriate time delay in the state feedback in order to enhance the control performance.

It is interesting that the quantity  $a$  defined in Eq. (7.4.19) plays a role of the damping ratio in the harmonically forced Duffing oscillator. That is, it governs not only the stability of the resonance, but also the amplitude peak of the primary resonance. For simplicity, we refer to  $a$  as the *equivalent damping ratio* of the system with delayed state feedback. For the case shown in Fig. 7.4.1, the equivalent damping ratios at the time delay  $\tau = \pi/4 \approx 0.786$  and  $\tau = \pi \approx 3.142$  are  $a = a_{\max} \approx 0.1207$  and  $a = a_{\min} \approx 0$ , respectively. The corresponding peaks of the displacement amplitude reach the minimum and the positive infinity, respectively. Furthermore, when  $a$  happens to vanish, the system response will include the free vibration that does not decay. This may result in a quasi-periodic motion if the frequency ratio of the free vibration and the forced vibration is not a rational number. Anyhow, this case should be avoided from the viewpoint of vibration control, for the critically stable response is very dangerous.

Now we consider the case of negative velocity feedback, i.e.,  $v < 0$ , which is widely used to reduce the steady-state vibration in engineering. In this case, Eq. (7.4.22) gives  $\tau_r = r\pi$  since  $u = 0$ . The optimal control performance, hence, can be realized only when there is no time delay or there is a long time delay, say,  $\tau = 2\pi$  in the velocity feedback. If displacement feedback is introduced, we have the following linear approximation of Eq. (7.4.19) for a short time delay

$$a \approx \zeta + \frac{|v| + u\tau}{2} + o(\tau). \quad (7.4.27)$$

This implies that the control performance can be better than the optimal one of the velocity feedback only, if the displacement feedback gain  $u$  is positive.



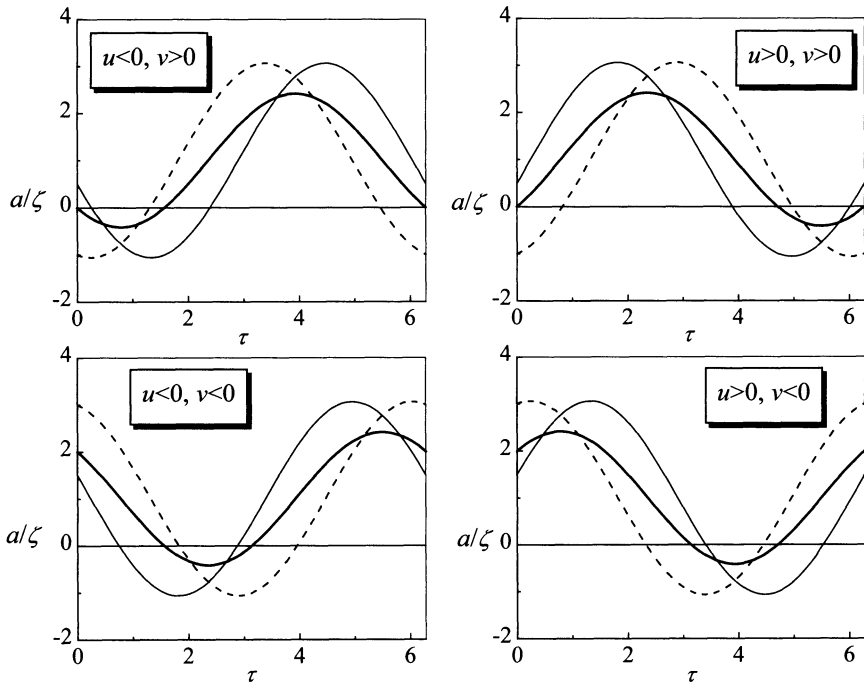


**Fig. 7.4.2.** Relations between ratio  $a/\zeta$  and delay  $\tau$  at various feedback gains  $u$  and  $v$ ; Key: thick solid:  $|u|=|v|=2\zeta$ , thin solid:  $|u|=\zeta, |v|=\zeta$ , dashed:  $|u|=\zeta, |v|=4\zeta$

Figure 7.4.2 shows the variation of ratio  $a/\zeta$  with an increase in time delay  $\tau$  under different combinations of the feedback gains. It is easy to see from Fig. 7.4.2 that the equivalent damping ratio is optimal when the feedback gains satisfy  $u > 0$  and  $v < 0$ , because it is the largest when the time delay is short, and decreases to zero at a relatively long time delay. This shows again that the positive displacement feedback will improve the vibration control performance of the negative velocity feedback.

### 7.4.2 1/3 Subharmonic Resonance

As well known, a harmonically forced Duffing oscillator may undergo a 1/3 subharmonic resonance when the excitation frequency is near the tripled fundamental natural frequency of linearized oscillator and the excitation amplitude is large enough. This subsection will show that a harmonically forced Duffing oscillator under linear state feedback with time delay may also have a 1/3 subharmonic resonance if some conditions hold.

To study the 1/3 subharmonic resonance of the controlled system, we confine ourselves to the case when

$$\lambda - 3 = \varepsilon\sigma, \quad \sigma = O(1), \tag{7.4.28}$$

but release the excitation from the small magnitude. Rewrite Eq. (7.4.1) as

$$\ddot{x}(t) + x(t) = -2\zeta \dot{x}(t) - \mu x^3(t) + ux(t - \tau) + v\dot{x}(t - \tau) + f \cos(3 + \varepsilon\sigma)t. \tag{7.4.29}$$

Substituting Eq. (7.4.5) into Eq. (7.4.29) and equating the same power of  $\varepsilon$ , as well as the same order quantities, we obtain

$$D_0^2 x_0(T_0, T_1) + x_0(T_0, T_1) = f \cos(3T_0 + \sigma T_1) \tag{7.4.30a}$$

$$\begin{aligned} \varepsilon[D_0^2 x_1(T_0, T_1) + x_1(T_0, T_1)] = & -2\varepsilon D_0 D_1 x_0(T_0, T_1) - 2\zeta D_0 x_0(T_0, T_1) \\ & - \mu x_0^3(T_0, T_1) + ux_0(T_0 - \tau, T_1) + vD_0 x_0(T_0 - \tau, T_1). \end{aligned} \tag{7.4.30b}$$

By solving Eq. (7.4.30a) for  $x_0(T_0, T_1)$ , we have

$$x_0(T_0, T_1) = A(T_1)e^{i7_0} + Ge^{i(3T_0 + \sigma T_1)} + cc, \quad G \equiv \frac{f}{2(1 - \lambda^2)}. \tag{7.4.31}$$

Substituting Eq. (7.4.31) into Eq. (7.4.30b) yields

$$\begin{aligned} \varepsilon[D_0^2 x_1(T_0, T_1) + x_1(T_0, T_1)] = & (-2i\varepsilon D_1 A - 2i\zeta A - 6\mu A G^2 - 3\mu A^2 \bar{A} + ue^{-ir} A + ive^{-ir} A)e^{i7_0} \\ & - 3\mu \bar{A}^2 G e^{i(7_0 + \sigma T_1)} + \dots \end{aligned} \tag{7.4.32}$$

The secular term of Eq. (7.4.32) vanishes if and only if

$$i(2\varepsilon D_1 A + 2\zeta A - ve^{-ir} A) - ue^{-ir} A + 6\mu A G^2 + 3\mu A^2 \bar{A} + 3\mu \bar{A}^2 G e^{i\sigma T_1} = 0. \tag{7.4.33}$$

Substituting Eq. (7.4.8) into Eq. (7.4.33) and separating the real part and the imaginary part, we obtain a set of autonomous differential equations governing the amplitude and phase of the 1/3 subharmonic resonance

$$\begin{cases} 2\varepsilon D_1 \alpha = -(2\zeta + u \sin \tau - v \cos \tau) \alpha - \frac{3\mu G \alpha^2}{2} \sin \phi, \\ 2\varepsilon D_1 \phi = (2\varepsilon \sigma + 3u \cos \tau + 3v \sin \tau - 18\mu G^2) - \frac{9\mu}{4} \alpha^2 - \frac{9\mu G \alpha}{2} \cos \phi, \end{cases} \tag{7.4.34}$$

where

$$\phi(T_1) \equiv \sigma T_1 - 3\beta(T_1). \tag{7.4.35}$$

**(1) Steady state subharmonic resonance**

From Eq. (7.4.34), we get a set of algebraic equations that governs the amplitude  $\hat{\alpha}$  and the phase  $\hat{\phi}$  of the steady-state 1/3 subharmonic resonance

$$\begin{cases} (2\zeta + u\sin\tau - v\cos\tau)\hat{\alpha} = -\frac{3\mu G\hat{\alpha}^2}{2}\sin\hat{\phi}, \\ (2\lambda - 6 + 3u\cos\tau + 3v\sin\tau - 18\mu G^2) - \frac{9\mu}{4}\hat{\alpha}^2 = \frac{9\mu G\hat{\alpha}}{2}\cos\hat{\phi}, \end{cases} \quad (7.4.36)$$

whereby we have the frequency response relation between  $\hat{\alpha}$  and  $\lambda$ , and that between  $\hat{\phi}$  and  $\lambda$

$$\begin{cases} 9(2\zeta + u\sin\tau - v\cos\tau)^2 + (2\lambda - 6 + 3u\cos\tau + 3v\sin\tau - 18\mu G^2 - \frac{9\mu}{4}\hat{\alpha}^2)^2 \\ - (\frac{9\mu G\hat{\alpha}}{2})^2 = 0, \\ \tan\hat{\phi} + \frac{3(2\zeta + u\sin\tau - v\cos\tau)}{2\lambda - 6 + 3u\cos\tau + 3v\sin\tau - 18\mu G^2 - \frac{9\mu}{4}\hat{\alpha}^2} = 0. \end{cases} \quad (7.4.37)$$

The first order approximation for the steady-state 1/3 subharmonic resonance reads

$$x(t) = \hat{\alpha}\cos\left(\frac{\lambda t - \hat{\phi}}{3}\right) + \frac{f}{1 - \lambda^2}\cos\lambda t. \quad (7.4.38)$$

We can expand the first equation in Eq. (7.4.37) as

$$\hat{\alpha}^4 - 2P\hat{\alpha}^2 + Q = 0, \quad (7.4.39)$$

and solve it for  $\hat{\alpha}$

$$\hat{\alpha} = \sqrt{P \pm \sqrt{P^2 - Q}}, \quad (7.4.40)$$

where

$$\begin{cases} P \equiv \frac{4}{9\mu}(2\lambda - 6 + 3u\cos\tau + 3v\sin\tau) - 6G^2, \\ Q \equiv \frac{16}{81\mu^2}[9(2\zeta + u\sin\tau - v\cos\tau)^2 \\ + (2\lambda - 6 + 3u\cos\tau + 3v\sin\tau - 18\mu G^2)^2]. \end{cases} \quad (7.4.41)$$

Equation (7.4.40) requires  $P > 0$  and  $P^2 > Q$  since  $Q > 0$ . Substituting Eq. (7.4.41) into these inequalities gives

$$\left\{ \begin{array}{l} \frac{27\mu}{4} G^2 < (\lambda - 3 + \frac{3u}{2} \cos \tau + \frac{3v}{2} \sin \tau), \\ \left| \frac{63\mu}{4} G^2 - (\lambda - 3 + \frac{3u}{2} \cos \tau + \frac{3v}{2} \sin \tau) \right| \\ \leq \sqrt{(\lambda - 3 + \frac{3u}{2} \cos \tau + \frac{3v}{2} \sin \tau)^2 - 63(\zeta + \frac{u}{2} \sin \tau - \frac{v}{2} \cos \tau)^2}. \end{array} \right. \quad (7.4.42)$$

It is easy to prove that the second inequality covers the first, and hence gives the existence condition of the  $1/3$  subharmonic resonance. We can readily convert this condition into the form with respect to the dimensionless excitation amplitude  $f$  and excitation frequency  $\lambda$ .

Figure 7.4.3 shows the existence regions of the  $1/3$  subharmonic resonance on the plane of  $(\lambda, f)$  for the uncontrolled system, the controlled system without time delay, and those with time delays corresponding to  $a \approx a_{\max}$  and  $a \approx 0$ , respectively. Figure 7.4.4 gives the frequency-amplitude relations of the  $1/3$  subharmonic resonance for these systems subject to the same level of excitation. Obviously, the equivalent damping ratio governs the threshold of the excitation amplitude and frequency for the occurrence of the  $1/3$  subharmonic resonance, so does the time delay. However, it is not so effective to reduce the amplitude of the  $1/3$  subharmonic resonance as in the control of primary resonance by choosing a proper time delay.

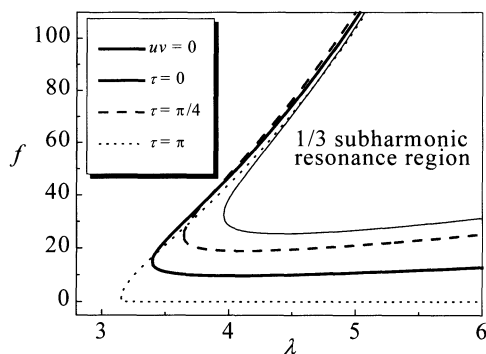


**Fig. 7.4.3.** Amplitude and frequency of threshold excitation at different time delays when  $\zeta=0.05$ ,  $\mu=0.05$ ,  $u=0$  and  $v=0$  or ( $u=0.1$  and  $v=-0.1$ )

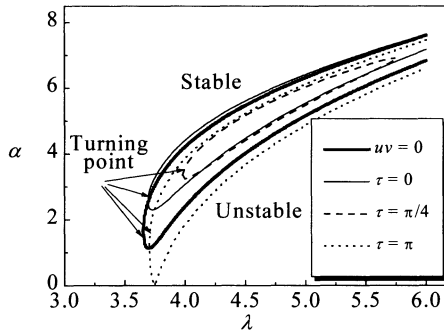


**Fig. 7.4.4.** Amplitude of frequency response of 1/3 subharmonic resonance at different time delays when  $\zeta=0.05$ ,  $\mu=0.05$ ,  $f=30$ ,  $u=0$  and  $v=0$  (or  $u=0.1$  and  $v=-0.1$ )

**(2) Stability analysis**

To analyze the stability of the steady-state subharmonic resonance, we linearize Eq. (7.4.34) at  $(\hat{\alpha}, \hat{\phi})$  with respect to  $\alpha$  and  $\phi$

$$\begin{cases} 2\varepsilon D_1 \Delta\alpha = -(2\zeta + u\sin\tau - v\cos\tau + 3\mu G \hat{\alpha} \sin\hat{\phi}) \Delta\alpha - \frac{3\mu G \hat{\alpha}^2}{2} \cos\hat{\phi} \Delta\hat{\phi}, \\ 2\varepsilon D_1 \Delta\phi = -\frac{9\mu}{2} (\hat{\alpha} + G \cos\hat{\phi}) \Delta\alpha + \frac{9\mu G \hat{\alpha}}{2} \sin\hat{\phi} \Delta\phi. \end{cases} \quad (7.4.43)$$

The corresponding characteristic equation in  $\varepsilon s$  reads

$$\det \begin{bmatrix} -(2\zeta + u\sin\tau - v\cos\tau + 3\mu G \hat{\alpha} \sin\hat{\phi}) - 2\varepsilon s & -\frac{3\mu G \hat{\alpha}^2}{2} \cos\hat{\phi} \\ -\frac{9\mu}{2} (\hat{\alpha} + G \cos\hat{\phi}) & -\frac{9\mu G \hat{\alpha}}{2} \sin\hat{\phi} - 2\varepsilon s \end{bmatrix} = 0. \quad (7.4.44)$$

Applying Eq. (7.4.36) and the first equation in Eq. (7.4.41) to Eq. (7.4.44) gives

$$(\varepsilon s)^2 + 2a(\varepsilon s) + d = 0, \quad (7.4.45)$$

where

$$a \equiv \zeta + \frac{u}{2} \sin\tau - \frac{v}{2} \cos\tau, \quad d \equiv -\frac{27\mu^2 \hat{\alpha}^2}{32} (P - \hat{\alpha}^2). \quad (7.4.46)$$

Hence, the 1/3 subharmonic resonance is asymptotically stable if and only if

$$a > 0, \quad \hat{\alpha}^2 > P. \quad (7.4.47)$$

The first inequality here shows that the equivalent damping ratio takes an important role again in the stability of the subharmonic resonance. The second inequality

ity implies that the upper branch solution in Eq. (7.4.40) is asymptotically stable, while the lower branch solution shown as the dashed curve in Fig. 7.4.4 is unstable.

In summary, the method of multiple scales proves to be a powerful tool to gain an insight into the primary resonance and subharmonic resonance of the harmonically forced Duffing oscillator when the nonlinearity and gains of delayed feedback are weak. The method is also applicable to the super-harmonic resonance and combined resonance of this type of oscillators, and even the harmonically forced oscillators with two feedback time delays. Furthermore, the method of multiple scales here can be replaced by other techniques for weakly nonlinear differential equations, see, for example, the average method used in (Nguyen 1999). The primary resonance and the  $1/3$  subharmonic resonance of the harmonically forced Duffing oscillator with delay state feedback are qualitatively the same as those of the uncontrolled Duffing oscillator subject to harmonic excitation when the dimensionless feedback gains are the same order as the small linear damping ratio. From the viewpoint of vibration control, however, the time delay plays an important role in providing active damping, which governs the resonance stability and the amplitude peak. The combination of positive displacement feedback and negative velocity feedback is the most advantageous one for attenuating those resonances. Furthermore, a proper choice of time delay can enhance the control performance.

## 7.5 Shooting Scheme for Locating Periodic Motions

This section presents how to compute the periodic solutions of a nonlinear delayed dynamic numerically in order to verify the approximate results in Section 7.4. As shown in Section 7.4, more than one periodic motion may co-exist at certain range of excitation frequency if the primary resonance or  $1/3$  subharmonic resonance occurs. If this is the case, one of the periodic motions is unstable. Thus, the shooting technique, rather than the direct numerical integration, such as the Runge-Kutta approach, will be discussed in order to determine the co-existing periodic motions, including the unstable ones.

### 7.5.1 Basic Concepts and Computation Scheme

We first consider the initial value problem of a 2-dimensional non-autonomous delay differential equation as following

$$\begin{cases} \dot{\mathbf{y}}(t) = \mathbf{f}(\mathbf{y}(t), \mathbf{y}(t-\tau), t), & t > t_0 \in \mathbb{R}, \quad \mathbf{y} \in \mathbb{R}^2, \\ \mathbf{y}(t) = \mathbf{y}_0(t), & t \in [t_0 - \tau, t_0]. \end{cases} \quad (7.5.1)$$

As discussed in Section 2.1, the initial condition now must be a given function vector  $\mathbf{y}_0(t)$  on the time interval  $[t_0 - \tau, t_0]$ , rather than a single initial state  $\mathbf{y}_0(t_0)$  at the moment of  $t = t_0$ . For the harmonically forced Duffing oscillator with delayed state feedback in Section 7.4, let

$$\mathbf{y}(t) \equiv [x(t) \quad \dot{x}(t)]^T, \quad \mathbf{y}_0(t) \equiv [x_0(t) \quad \dot{x}_0(t)]^T, \quad (7.5.2)$$

$$\mathbf{f}(\mathbf{y}(t), \mathbf{y}(t-\tau), t) \equiv \begin{bmatrix} \dot{x}(t) \\ -x(t) - \mu x^3(t) - 2\zeta \dot{x}(t) + ux(t-\tau) + \dot{v}(t-\tau) + f \cos \lambda t \end{bmatrix}. \quad (7.5.3)$$

In what follows, we study how to locate the solution of Eq. (7.5.1) with the period  $T \equiv 2l\pi/\lambda$ , where  $l$  is a positive integer. For simplicity, we assume that the time delay yields  $0 \leq \tau < T$ .

Now, we recall the Poincaré section and the Poincaré mapping, which conceptually simplify the task of finding a periodic solution  $\Gamma$  of the ordinary differential equation to locating the corresponding fixed point  $\mathbf{y}_F$ . In the case of non-autonomous ordinary differential equations, especially those with harmonic inhomogeneous terms, the Poincaré section  $\Sigma_0$  is often defined as a fixed excitation phase  $\psi_0$  in the 3-dimensional expanded state space  $(x, \dot{x}, \psi)$ , where  $\psi = \text{mod}(\lambda t, 2\pi)$ , and the corresponding Poincaré mapping  $\mathbf{P}_0: \Sigma_0 \rightarrow \Sigma_0$  establishes a unique correspondence between the periodic orbit  $\Gamma$  and the fixed point  $\mathbf{y}_F \in \Sigma_0$ . For the delay differential equations, however, it may be impossible to determine the unique periodic solution  $\Gamma$  of Eq. (7.5.1) from the fixed point  $\mathbf{y}_F \in \Sigma_0$  of the Poincaré mapping  $\mathbf{P}_0$ . This is because there exist an infinite number of trajectories that start from  $\mathbf{y}_F \in \Sigma_0$ , whereas the periodic orbit  $\Gamma$  should be the one that coincides with the piece of itself on the previous phase interval  $[\psi_0 - \lambda\tau, \psi_0]$ , not only at the fix point  $\mathbf{y}_F \in \Sigma_0$ .

To establish a one-to-one correspondence between the fixed point  $\mathbf{y}_F$  of Poincaré mapping and the periodic solution  $\Gamma$  of Eq. (7.5.1), we intuitively generalize the Poincaré section to the “Poincaré Plate”  $\Sigma_\tau$  with the thickness of  $\tau$ , as shown in Fig. 7.5.1. The corresponding Poincaré mapping  $\mathbf{P}_\tau: \Sigma_\tau \rightarrow \Sigma_\tau$  is an infinite dimensional mapping, which maps a function  $\mathbf{y}(t) \in C \equiv C([t_0 - \tau, t_0], \mathbb{R}^2)$  to the function  $\mathbf{P}_\tau(\mathbf{y}(t)) \in C$ , where  $t_0 \equiv \psi_0/\lambda$ . The original fixed point  $\mathbf{y}_F \in \Sigma_0$  under the Poincaré mapping  $\mathbf{P}_0$  should be generalized to a “Fixed Arc”  $\mathbf{y}_F(t) \in \Sigma_\tau$  under the infinite dimensional Poincaré mapping  $\mathbf{P}_\tau$ . Here,  $\mathbf{y}_F(t) \in \Sigma_\tau$  represents the

segment of the periodic orbit  $\Gamma$  intersecting with the Poincaré plate, namely,  $y_F(t) \equiv \Gamma \cap \Sigma_\tau$ .

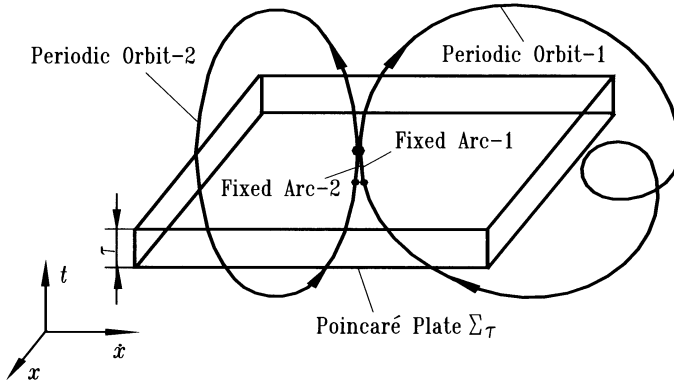


**Fig. 7.5.1.** Generalization of the Poincaré section and the fixed point for locating the periodic orbit of a delayed nonlinear system

The task of shooting a periodic orbit of Eq. (7.5.1) now is to locate the fixed arc  $y_F(t) \in \Sigma_\tau$ . A straightforward extension of the current shooting scheme is to approximate the candidate arc  $y(t), t \in [t_0 - \tau, t_0]$  in shooting by using  $N$  line segments and to shoot the  $N + 1$  nodes of these segments. No doubt that the longer the time delay  $\tau$ , the more line segments must be used in the shooting procedure.

Specifically, let  $z \equiv [y_1^T \ y_2^T \ \dots \ y_{N+1}^T]^T$  denote the vector of node coordinates on the candidate arc  $y(t), t \in [t_0 - \tau, t_0]$ . Here,

$$y_1 \equiv y(t_0), \quad y_{i+1} \equiv y(t_i), \quad t_i \equiv t_0 - \frac{(i-1)\tau}{N-1}, \quad i=1, 2, \dots, N. \quad (7.5.4)$$

The shooting procedure based on the Newton-Raphson iteration is as below

$$z_{k+1} = z_k - [DP(z_k) - I]^{-1} [P(z_k) - z_k], \quad k=0, 1, 2, \dots, \quad (7.5.5)$$

where  $P: z \rightarrow z$  is the  $N$ -dimensional approximate mapping for  $P_\tau$  and  $DP$  is its Jacobian. In the following, we present how to compute  $P(z_k)$  and  $DP(z_k)$  in Eq. (7.5.5). For the sake of simplicity, let the subscript of  $z_k$  be omitted.

The computation of mapping  $P(z)$  is actually the numerical integration for the following differential equations through the successive use of available codes such as the Runge-Kutta scheme until  $t \geq t_0 + T$

$$\dot{y}_{j+1}(t) = f(y_{j+1}(t), y_j(t-\tau), t), \quad t \in [t_0 + (j-1)\tau, t_0 + j\tau], \quad j=0, 1, 2, \dots \quad (7.5.6)$$

If the ratio  $T/\tau$  is an integer, we happen to obtain



$$P(z)=[y^T(t_0+T) \ y^T(t_1+T) \ \dots \ y^T(t_N+T)]^T. \tag{7.5.7}$$

Otherwise, it is necessary to interpolate every  $y(t_i+T)$ ,  $i=0,1,\dots,N$  in Eq. (7.5.7) from its two neighbors.

The Jacobian  $DP$  is the solution matrix  $Z(T)$  of the initial value problem of the following set of linear delay differential equations

$$\begin{cases} \dot{Z}(t)=D_1 f(z(t),z(t-\tau),t)Z(t)+D_2 f(z(t),z(t-\tau),t)Z(t-\tau), & t>t_0, \\ Z(t)=\text{diag}[\delta(t-t_i)], & t\in[t_0-\tau, t_0], \end{cases} \tag{7.5.8}$$

$0\leq i\leq N$

where

$$z(t)\equiv[x(t_0+t) \ x(t_1+t) \ \dots \ x(t_N+t)]^T, \tag{7.5.9}$$

$$\delta(t)\equiv\begin{cases} 1, & t=0, \\ 0, & t\neq 0, \end{cases} \tag{7.5.10}$$

$D_1$  and  $D_2$  are the derivative operators with respect to  $z(t)$  and  $z(t-\tau)$ , respectively. To obtain the Jacobian  $DP$ , Eq. (7.5.8) should be simultaneously integrated with Eq. (7.5.1) by using the codes for computing  $P(z)$ .

The shooting procedure can be incorporated with the parametric continuation technique to determine the unknown periodic orbits of the nonlinear delay system from a known periodic orbit of the simplified systems. For instance, it is possible to start from the periodic orbit of the delay-free system, and to take the time delay  $\tau$  as the continuation parameter.

### 7.5.2 Case Studies

#### (1) Primary resonance

Figure 7.5.2 shows the amplitudes of primary resonance versus the excitation frequency obtained by the method of multiple scales in Subsection 7.5.1 and the shooting scheme for four typical parametric combinations as shown in Fig. 7.4.1. Here, the results of the shooting scheme can be considered as the exact resonance amplitudes including the higher order terms of  $O(\varepsilon)$  neglected in Subsection 7.4.1. It is obvious that the approximate analytical results coincide with the exact results very well, except in the lower frequency range when the equivalent damping ratio is large. The comparison supports the assertion that the properly

selected time delay increases the equivalent damping ratio so that the primary resonance can be attenuated effectively.

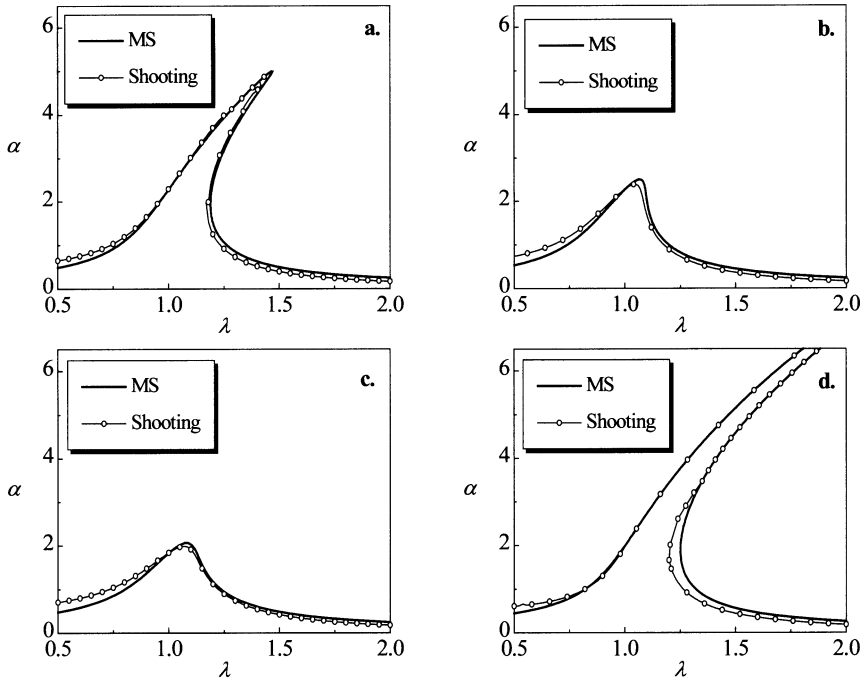


**Fig. 7.5.2.** Amplitudes of primary resonance computed by the method of multiple scales (MS) and shooting method when  $\zeta=0.05$ ,  $\mu=0.05$  and  $f=0.5$ ; **a.**  $u=0.0$  and  $v=0$ , **b.**  $u=0.1$ ,  $v=-0.1$  and  $\tau=0$ , **c.**  $u=0.1$ ,  $v=-0.1$  and  $\tau=\pi/4$ , **d.**  $u=0.1$ ,  $v=-0.1$  and  $\tau=\pi$

## (2) 1/3 subharmonic resonance

In Fig. 7.5.3 are shown the vibration amplitudes of the 1/3 subharmonic resonance versus the excitation frequency obtained by the two methods for four typical parametric combinations. It should be noted that the amplitude here is the maximal value of the displacement, instead of the amplitude of 1/3 harmonic component only. Of course, the self-intersections of the amplitude curves only mean the amplitudes of the asymptotically stable motion and the unstable motion are the same at a specific excitation frequency, rather than any bifurcation, because the phases of these two motions are totally different.

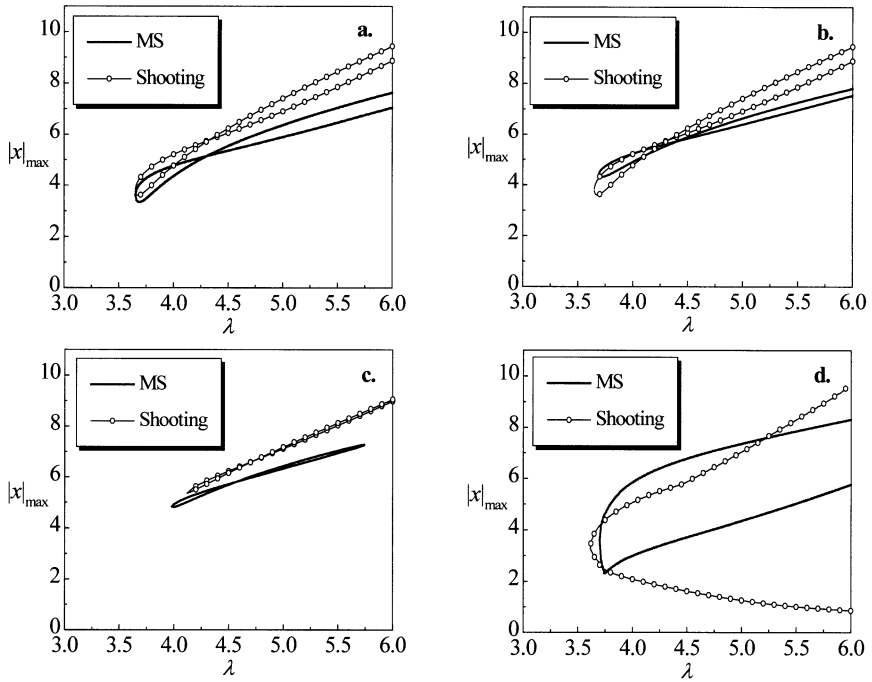


**Fig. 7.5.3.** Amplitudes of  $1/3$  subharmonic resonance computed by the method of multiple scales (MS) and the shooting method when  $\zeta=0.05$ ,  $\mu=0.05$  and  $f=30$ ; **a.**  $u=0.0$  and  $v=0$ , **b.**  $u=0.1$ ,  $v=-0.1$  and  $\tau=0$ , **c.**  $u=0.1$ ,  $v=-0.1$  and  $\tau=\pi/4$ , **d.**  $u=0.1$ ,  $v=-0.1$  and  $\tau=\pi$

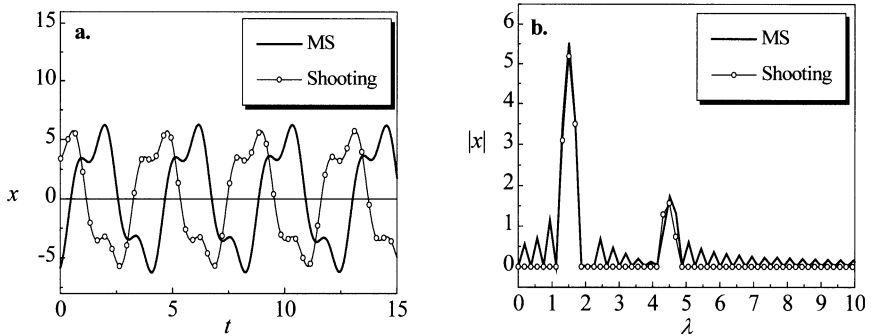


**Fig. 7.5.4.**  $1/3$  subharmonic resonance computed by the method of multiple scales (MS) and the shooting method when  $\zeta=0.05$ ,  $\mu=0.05$ ,  $f=30$ ,  $\lambda=4.5$ ,  $u=0.1$ ,  $v=-0.1$  and  $\tau=\pi/4$ ; **a.** time history, **b.** amplitude of the Fourier spectrum

Compared with the primary resonance, the subharmonic resonance given by the method of multiple scales substantially deviates from the exact result, but is still acceptable for most engineering applications. As shown in Fig. 7.5.4, the subharmonic and harmonic amplitudes obtained by the two methods are almost the same, while the phase difference between the results causes the above mentioned deviation. The numerical result in the case of  $\tau = \pi/4 \approx 0.786$  supports again the important role that the proper time delay plays in removing the occurrence of the 1/3 subharmonic resonance.

## 8 Delayed Control of Dynamic Systems

In previous chapters, attention is mainly paid to the effect of unavoidable feedback time delays on the dynamics of systems. As mentioned time to time, the time delays can be utilized to improve the control performance of dynamic systems. In this case, the time delay plays a favorable and important role in control. This chapter will present a number of control strategies of delayed feedback from the viewpoints of both vibration reduction and system stabilization.

### 8.1 Delayed Linear Feedback for Linear Systems

#### 8.1.1 Delayed Linear Feedback and Artificial Damping

Consider a linear, harmonically forced, single-degree-of-freedom system with delayed state feedback as following

$$m\ddot{x}(t)+c\dot{x}(t)+kx(t)=ux(t-\tau_1)+v\dot{x}(t-\tau_2)+f_0\sin\omega t, \quad (8.1.1)$$

where  $m>0$ ,  $c\geq 0$ ,  $k\geq 0$ ,  $f_0\geq 0$ ,  $\omega\geq 0$ ,  $\tau_1\geq 0$  and  $\tau_2\geq 0$  are constant parameters. We choose the feedback gains  $u$  and  $v$  such that the steady state motion of system is asymptotically stable. In this case, the transient motion of system is damped out and the forced vibration becomes a steady state motion as follows

$$x(t)=a\sin(\omega t+\varphi), \quad (8.1.2)$$

where  $a$  and  $\varphi$  are constants. Substituting Eq. (8.1.2) into Eq. (8.1.1) yields

$$\begin{aligned} (k-m\omega^2)a\sin(\omega t+\varphi)+c\omega a\cos(\omega t+\varphi) \\ =u\sin[\omega(t-\tau_1)+\varphi]+v\omega a\cos[\omega(t-\tau_2)+\varphi]+f_0\sin\omega t. \end{aligned} \quad (8.1.3)$$

We can recast Equation (8.1.3) as the following harmonic balancing equation corresponding to an uncontrolled system

$$[k_e(\omega)-m\omega^2]a\sin(\omega t+\varphi)+c_e(\omega)\omega a\cos(\omega t+\varphi)=f_0\sin\omega t, \quad (8.1.4)$$

where

$$\begin{cases} k_e(\omega) = k - u \cos \omega \tau_1 - v \omega \sin \omega \tau_2, \\ c_e(\omega) = c + u \sin \omega \tau_1 / \omega - v \cos \omega \tau_2. \end{cases} \quad (8.1.5)$$

We refer to these two parameters as the *equivalent stiffness* and the *equivalent damping* of system (8.1.1), respectively.

Now, four control parameters  $u$ ,  $v$ ,  $\tau_1$  and  $\tau_2$  are available to adjust the dynamic performance of system through the equivalent stiffness and damping. To see the fact more explicitly, recast Eq. (8.1.5) as

$$\begin{bmatrix} \cos \omega \tau_1 & \omega \sin \omega \tau_2 \\ -\sin \omega \tau_1 / \omega & \cos \omega \tau_2 \end{bmatrix} \begin{bmatrix} u \\ v \end{bmatrix} = \begin{bmatrix} k - k_e(\omega) \\ c - c_e(\omega) \end{bmatrix}. \quad (8.1.6)$$

Given a pair of  $c_e(\omega)$  and  $k_e(\omega)$ , it is possible to solve Eq. (8.1.6) for  $u$  and  $v$  provided that

$$\det \begin{bmatrix} \cos \omega \tau_1 & \omega \sin \omega \tau_2 \\ -\sin \omega \tau_1 / \omega & \cos \omega \tau_2 \end{bmatrix} = \cos \omega (\tau_1 - \tau_2) \neq 0. \quad (8.1.7)$$

If Eq. (8.1.7) holds true, we have

$$\begin{bmatrix} u \\ v \end{bmatrix} = \frac{1}{\cos \omega (\tau_1 - \tau_2)} \begin{bmatrix} \cos \omega \tau_2 & -\omega \sin \omega \tau_2 \\ \sin \omega \tau_1 / \omega & \cos \omega \tau_1 \end{bmatrix} \begin{bmatrix} k - k_e(\omega) \\ c - c_e(\omega) \end{bmatrix}. \quad (8.1.8)$$

Theoretically speaking, two control parameters are enough in order to adjust the above equivalent stiffness and damping if they are properly chosen. The simplest example is the state feedback without any time delays. In this case, Eq. (8.1.8) becomes

$$\begin{bmatrix} u \\ v \end{bmatrix} = \begin{bmatrix} 1 & 0 \\ 0 & 1 \end{bmatrix} \begin{bmatrix} k - k_e \\ c - c_e \end{bmatrix}. \quad (8.1.9)$$

Hence, the feedback paths of displacement and velocity alter the equivalent stiffness and damping of system, or equivalently, the resonant frequency and resonant peak of system, respectively.

Now, we consider the delayed displacement feedback. Imposing  $v=0$  in Eq. (8.1.5) yields

$$\begin{cases} k_e(\omega) = k - u \cos \omega \tau_1, \\ c_e(\omega) = c + u \sin \omega \tau_1 / \omega, \end{cases} \quad (8.1.10)$$

whereby we have

$$u = \pm \sqrt{[k - k_e(\omega)]^2 + \omega^2 [c - c_e(\omega)]^2}, \quad \tau_1 = \frac{1}{\omega} \tan^{-1} \left\{ \frac{\omega [c_e(\omega) - c]}{k - k_e(\omega)} \right\}. \quad (8.1.11)$$

Equation (8.1.11) implies that properly selected displacement feedback with a time delay can achieve any given equivalent stiffness and damping of system.

This fact has found two direct applications, that is, the artificial damping and tunable vibration absorbers. In what follows, the artificial damping will be briefly discussed, while the tunable vibration absorber will be presented in the next subsection.

**Example 8.1.1** As a well-known concept in vibration control, the artificial damping can be realized through the use of negative velocity feedback. According to Eq. (8.1.11), however, it can also be achieved by means of the delayed displacement feedback. For instance, if the natural frequency of system is fixed and the equivalent damping is expected to be larger than the original damping, that is,  $k_e(\omega) = k$  and  $c_e(\omega) > c$ , the control parameters of delayed displacement feedback can be chosen as

$$u = \omega [c_e(\omega) - c] > 0, \quad \tau_1 = \frac{\pi}{2\omega}. \quad (8.1.12)$$

The physical meaning behind Eq. (8.1.12) is obvious. That is, the phase delay  $\pi/2$  in the displacement happens to be the negative velocity since the forced steady state vibration of system is harmonic. Hence, the displacement delayed by time  $\tau_1 = \pi/2\omega$  serves as a negative velocity feedback by nature.

### 8.1.2 Delayed Resonator: A Tunable Vibration Absorber

The second application of delayed displacement feedback is in active vibration absorption. As well known, the classical vibration absorber is an undamped oscillator. At its natural frequency in frequency domain, the vibration absorber produces an anti-resonance for the attached location on a primary system. The active vibration absorber, hence, is expected to have no damping, but adjustable natural frequency. This task can be completed through the use of an adjustable mass or stiffness coefficient. For the same purpose, the concept of *delayed resonator* was proposed in (Olgac and Holm-Hansen 1995). A delayed resonator is a linear oscillator with delayed displacement feedback. It is designed such that the equivalent damping vanishes and the natural frequency always coincides with the excitation frequency. That is,  $c_e(\omega) = 0$  and  $k_e(\omega) = m\omega^2$ . Substituting these requirements into Eq. (8.1.11) yields

$$u = \pm \sqrt{(k - m\omega^2)^2 + (c\omega)^2}, \quad \tau_1 = \frac{1}{\omega} \tan^{-1} \left( \frac{c\omega}{m\omega^2 - k} \right). \quad (8.1.13)$$

Because the oscillator is asymptotically stable when the displacement feedback has no time delay,  $\tau_1$  should be taken as the smallest positive value so that only a pair of eigenvalues is pure imaginary numbers and all other eigenvalues have negative real parts. That is, the delayed resonator is marginally stable.

To determine the sign and the shortest time delay in Eq. (8.1.13), we first look at a special case when the excitation frequency  $\omega = \sqrt{k/m}$ . In this case, the minimal positive time delay yields  $\tau_1 = \pi / (2\omega)$  and the displacement delayed by phase  $\pi/2$  is the negative velocity. Hence, the displacement feedback plays a role in balancing the damping force only, and the feedback gain should be  $u = -c\omega < 0$ . Figure 8.1.1 shows the dimensionless displacement feedback gain  $u/k$  and the time delay  $\tau_1$  versus the dimensionless excitation frequency  $\lambda = \omega / \sqrt{k/m}$  at the different damping ratio  $\zeta = c / \sqrt{4mk}$ .

In general, the control law of delayed resonator should be

$$u = -\sqrt{(k - m\omega^2)^2 + (c\omega)^2}, \quad \tau_1 = \frac{1}{\omega} \left[ \arctan \left( \frac{c\omega}{m\omega^2 - k} \right) + l\pi \right], \quad (8.1.14)$$

where

$$l = \begin{cases} 0, & m\omega^2 - k \geq 0, \\ 1, & m\omega^2 - k < 0. \end{cases} \quad (8.1.15)$$

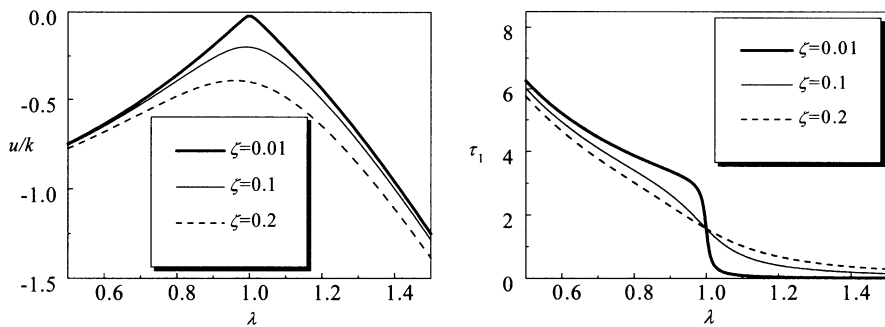


Fig. 8.1.1. Desirable displacement feedback gain and time delay in the delayed resonator versus dimensionless excitation frequency at different damping ratios

As an oscillator, the delayed resonator has an adjustable resonant frequency and an infinite resonant peak. Theoretically speaking, if such a delayed resonator is attached to a linear primary system subject to a harmonic excitation, the forced vi-



bration at the attached location of primary system can be totally attenuated no matter how the excitation frequency varies. Hence, the delayed resonator can be used as a tunable vibration absorber.

**Example 8.1.2** As shown in Fig. 8.1.2, the delayed resonator is attached to a primary system of single degree of freedom to reduce the vibration of primary system subject to a harmonica force  $f(t)=\sin\omega t$ . The dynamic equation of this combined system reads

$$\begin{cases} m_1\ddot{x}_1(t)+c_1\dot{x}_1(t)+k_1x_1(t)+c_2[\dot{x}_1(t)-\dot{x}_2(t)]+k_2[x_1(t)-x_2(t)] \\ =u[x_1(t-\tau_1)-x_2(t-\tau_1)]+\sin\omega t, \\ m_2\ddot{x}_2(t)+c_2[\dot{x}_2(t)-\dot{x}_1(t)]+k_2[x_2(t)-x_1(t)] \\ =u[x_2(t-\tau_1)-x_1(t-\tau_1)], \end{cases} \quad (8.1.16)$$

where  $m_1=1.0, k_1=1.0, c_1=0.10, m_2=0.1, k_2=0.1, c_2=0.02$  are fixed,  $u$  and  $\tau_1$  are determined from Eq. (8.1.13) for given excitation frequency  $\omega$ .

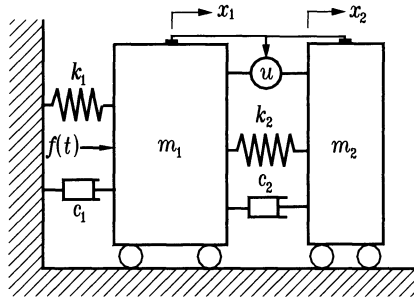


**Fig. 8.1.2.** A primary system with a delayed resonator as tunable absorber

Before the control is put into use, the vibration absorber only works near  $\omega=1$  and the primary system has two resonance peaks at  $\omega_{n1}\approx 0.8543$  and  $\omega_{n2}\approx 1.1705$ . Figure 8.1.3 shows the displacements of both primary system and vibration absorber under the excitation  $f(t)=\sin 1.1705t$  before and after the control is actuated. In this case study, Eq. (8.1.14) gives  $u=-0.0438$  and  $\tau_1=0.482$ , and the tunable vibration absorber works well.

It should be noticed that the time delay  $\tau_1$  given in Eq. (8.1.14) may not be able to ensure the stability of combined systems because it is derived from the critically stability of vibration absorber under the assumption that the primary system does not move at all. Thus, the feasible time delay in feedback has to be subject to the stability limitation of combined system. As shown in Fig. 8.1.1, the time delay  $\tau_1$  given by Eq. (8.1.14) increases very rapidly with decrease of excitation frequency  $\omega$  when  $\omega < \sqrt{k/m}$ , and may exceeds the stability threshold of

combined system. Therefore, the delayed resonator may work only at a narrow frequency range when  $\omega < \sqrt{k/m}$ . In the above case study, for instance, the delayed resonator can not attenuate the resonance at  $\omega=0.8543$  because the combined system becomes unstable when  $\omega \approx 0.892$ , which requires  $\tau_1 = 2.7173$ .

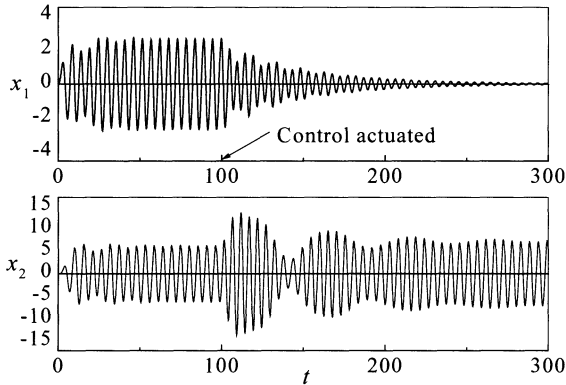


**Fig. 8.1.3.** Displacements of primary system and vibration absorber before and after the control is actuated

To guarantee the robustness of controlled systems, it is better to keep a small equivalent damping in the delayed resonator at the cost of an increase in residual vibration of primary system. In addition, the time delay  $\tau_1$  in Eq. (8.1.14) becomes very sensitive to any small change of excitation frequency when  $\omega \rightarrow \sqrt{k/m}$  as shown in Fig. 8.1.1 if the oscillator is very slightly damped. To reduce the sensitivity, the damping coefficient  $c$  should be large enough. However, the larger the damping coefficient  $c$ , the longer the time delay  $\tau_1$  in Eq. (8.1.14). Hence, the excessive damping coefficient  $c$  may indirectly arouse instability.

Finally, it is worthy to mention that a similar analysis can also be made for the delayed velocity feedback. For instance, it is almost the same procedure to construct the control strategy of delayed velocity feedback for a delayed resonator. However, the implementations of delayed displacement feedback and delayed velocity feedback may need quite different cost of hardware in practice.

## 8.2 Stabilization to Critically Stable Nonlinear Systems

Stabilization to nonlinear systems in a critical case has received great attention over the past decade. The critical case here means that the linearized nonlinear

system at its equilibrium has at least one eigenvalue on the imaginary axis, whereas the remaining eigenvalues remain on the left half-plane. The center manifold reduction has become a powerful tool to stabilize nonlinear systems of this kind, see, for example, (Steiner et al. 1995), (Liaw and Abed 1990), (Liaw 1998), and (Behtash and Sastry 1988). By using the technique of center manifold reduction, Steiner and his colleagues studied how to stabilize a tethered satellite system, for which the linearized equation possesses an uncontrollable pair of pure imaginary eigenvalues. Liaw gave a general design frame of stabilization law for nonlinear systems in critical cases in 1998. Yet, those studies focused on the nonlinear systems without time delays only.

As mentioned before, the time delays in controllers and actuators are usually unavoidable in controlled mechanical systems, especially in those related to tethered satellites, hydraulic actuators, and so on. Thus, great efforts have been made to develop the control strategies for stabilizing delayed dynamic systems. For instance, a memoryless, full state observer was designed in (Chen 1997) to stabilize uncertain dynamic systems with time delay. His design procedure requires solving two linear matrix inequalities. A linear transform was proposed and studied in (Fiagdedzi and Pearson 1986), and (Phoojaruenchanachai et al. 1998) to simplify the delay differential systems to ordinary differential systems. This approach involves solving a matrix equation of exponential type. Hence, it is not easy to apply these approaches to nonlinear systems with any time delay.

To stabilize nonlinear dynamic systems, a two-step design procedure was suggested in (Su and Chu 1998) for control law of delayed state feedback. The first step is to simplify the nonlinear systems to linear systems by using an appropriate nonlinear transform, and the second step is to stabilize the simplified linear controllable system with time delay in control path by means of a controller with memory. To authors' knowledge, no approach is available to the stabilization of critical cases by delayed state feedback.

The aim of this section is to present a methodological frame for the local stabilization of a dynamic system in critical case by delayed state feedback. To simplify the analysis, we assume the time delay in controller or actuator to be short. This is the case in most applications. As previously analyzed in Sections 2.3 and 5.3, a delayed dynamic system may behave completely different from the model simplified by using the Taylor approximation or by neglecting the time delay even if the time delay is very short. So, the effect of time delay on the system dynamics should be taken into account.

### 8.2.1 Statement of Problem

Consider a problem of the local stabilization, through a delayed feedback, of an  $n$ -dimensional nonlinear system in the form

$$\dot{\mathbf{x}}(t) = \mathbf{p}(\mathbf{x}(t)) + \mathbf{b}u(t-\tau), \quad (8.2.1)$$

where  $\mathbf{x} \in R^n$ ,  $\mathbf{b} \in R^n$ ,  $u \in R$ , and  $\tau > 0$  is the time delay in the control path. We assume that  $\mathbf{p}(\mathbf{x})$  is smooth enough and  $\mathbf{x} = 0$  represents the equilibrium of the system. Following the popular notations, we partition the spectrum of matrix  $\mathbf{A} \equiv \mathbf{D}_x \mathbf{p}(0)$ , the Jacobian of  $\mathbf{p}(\mathbf{x})$  at  $\mathbf{x} = 0$ , as

$$\sigma(\mathbf{A}) = \sigma^c(\mathbf{A}) \cup \sigma^s(\mathbf{A}) \cup \sigma^u(\mathbf{A}), \quad (8.2.2)$$

where

$$\begin{cases} \sigma^c(\mathbf{A}) \equiv \{\lambda \in \sigma(\mathbf{A}) \mid \operatorname{Re}(\lambda) = 0\}, \\ \sigma^s(\mathbf{A}) \equiv \{\lambda \in \sigma(\mathbf{A}) \mid \operatorname{Re}(\lambda) < 0\}, \\ \sigma^u(\mathbf{A}) \equiv \{\lambda \in \sigma(\mathbf{A}) \mid \operatorname{Re}(\lambda) > 0\}. \end{cases} \quad (8.2.3)$$

Obviously, we can transform Eq. (8.2.1) into the following form

$$\begin{bmatrix} \dot{\hat{\mathbf{x}}}_1 \\ \dot{\hat{\mathbf{x}}}_2 \\ \dot{\hat{\mathbf{x}}}_3 \end{bmatrix} = \begin{bmatrix} \hat{\mathbf{A}}_{11} & 0 & 0 \\ 0 & \hat{\mathbf{A}}_{22} & 0 \\ 0 & 0 & \hat{\mathbf{A}}_{33} \end{bmatrix} \begin{bmatrix} \hat{\mathbf{x}}_1 \\ \hat{\mathbf{x}}_2 \\ \hat{\mathbf{x}}_3 \end{bmatrix} + \begin{bmatrix} \hat{\mathbf{F}}(\hat{\mathbf{x}}_1, \hat{\mathbf{x}}_2, \hat{\mathbf{x}}_3) \\ \hat{\mathbf{G}}(\hat{\mathbf{x}}_1, \hat{\mathbf{x}}_2, \hat{\mathbf{x}}_3) \\ \hat{\mathbf{H}}(\hat{\mathbf{x}}_1, \hat{\mathbf{x}}_2, \hat{\mathbf{x}}_3) \end{bmatrix} + \begin{bmatrix} \hat{\mathbf{b}}_1 \\ \hat{\mathbf{b}}_2 \\ \hat{\mathbf{b}}_3 \end{bmatrix} u(t-\tau), \quad (8.2.4)$$

where

$$\begin{cases} \sigma(\hat{\mathbf{A}}_{11}) = \{\lambda \in C \mid \operatorname{Re}(\lambda) = 0\}, \\ \sigma(\hat{\mathbf{A}}_{22}) = \{\lambda \in C \mid \operatorname{Re}(\lambda) < 0\}, \\ \sigma(\hat{\mathbf{A}}_{33}) = \{\lambda \in C \mid \operatorname{Re}(\lambda) > 0\}. \end{cases} \quad (8.2.5)$$

Equation (8.2.4) is linearly stabilizable if and only if the matrices  $[\hat{\mathbf{A}}_{11} \ \hat{\mathbf{b}}_1]$  and  $[\hat{\mathbf{A}}_{33} \ \hat{\mathbf{b}}_3]$  are completely controllable.

This section will concentrate on the following critical case, where the critical eigenvalues are completely uncontrollable, i.e.,  $\hat{\mathbf{b}}_1 = 0$ , while the remaining eigenvalues are linearly controllable. The task of this section is to construct a feedback such that the equilibrium  $\mathbf{x} = 0$  is asymptotically stable. For this purpose, it may be necessary to use some quadratic or cubic terms of  $\hat{\mathbf{x}}_1$  to stabilize the system.

## 8.2.2 Analysis on Stabilization

Now, we recast Equation (8.2.4) as a more compact form

$$\begin{cases} \dot{\mathbf{x}}_c = \mathbf{A}_c \mathbf{x}_c + \mathbf{b}_1 u(t-\tau) + \mathbf{F}(\mathbf{x}_c, \mathbf{x}_r), \\ \dot{\mathbf{x}}_r = \mathbf{A}_r \mathbf{x}_r + \mathbf{b}_2 u(t-\tau) + \mathbf{G}(\mathbf{x}_c, \mathbf{x}_r), \end{cases} \quad (8.2.6)$$

where  $\mathbf{x}_c \in R^{n_c}$ ,  $\mathbf{x}_r \in R^{n_r}$ ,  $\mathbf{A}_c$  has only pure imaginary eigenvalues and  $\mathbf{A}_r$  has only those with non-zero real part. As assumed,  $\mathbf{b}_1 = 0$  holds here, but the pair  $[\mathbf{A}_r, \mathbf{b}_2]$  is linearly controllable. The analysis on the system stabilization includes following two steps.

### (1) Simplification of the system equation

We first convert Equation (8.2.6) into

$$\begin{cases} \dot{\mathbf{x}}_c = \mathbf{A}_c \mathbf{x}_c + \mathbf{F}(\mathbf{x}_c, \tilde{\mathbf{x}}_r - \int_{t-\tau}^t \exp[\mathbf{A}_r(t-\tau-s)] \mathbf{b}_2 u(s) ds), \\ \dot{\tilde{\mathbf{x}}}_r = \mathbf{A}_r \tilde{\mathbf{x}}_r + \tilde{\mathbf{b}}_2 u + \mathbf{G}(\mathbf{x}_c, \tilde{\mathbf{x}}_r - \int_{t-\tau}^t \exp[\mathbf{A}_r(t-\tau-s)] \mathbf{b}_2 u(s) ds), \end{cases} \quad (8.2.7)$$

by using a transformation

$$\tilde{\mathbf{x}}_r = \mathbf{x}_r + \int_{t-\tau}^t \exp[\mathbf{A}_r(t-\tau-s)] \mathbf{b}_2 u(s) ds, \quad (8.2.8)$$

where  $\tilde{\mathbf{b}}_2 \equiv \exp(-\mathbf{A}_r \tau) \mathbf{b}_2$ . It is easy to verify that the pair  $[\mathbf{A}_r, \tilde{\mathbf{b}}_2]$  is controllable owing to a controllable pair  $[\mathbf{A}_r, \mathbf{b}_2]$ , as well as the following full rank matrix

$$[\tilde{\mathbf{b}}_2, \mathbf{A}_r \tilde{\mathbf{b}}_2, \dots, \mathbf{A}_r^{n_r-1} \tilde{\mathbf{b}}_2] = \exp(-\mathbf{A}_r \tau) [\mathbf{b}_2, \mathbf{A}_r \mathbf{b}_2, \dots, \mathbf{A}_r^{n_r-1} \mathbf{b}_2]. \quad (8.2.9)$$

The theorem of pole assignment in control theory indicates that there exists a gain vector  $\mathbf{c} \in R^{n_r}$  such that the matrix  $\mathbf{A}_r - \tilde{\mathbf{b}}_2 \mathbf{c}^T$  is Hurwitz stable. Without loss of generality, we assume  $\mathbf{A}_r$  Hurwitz stable hereinafter.

Moreover, it is easy to show that the zero solution of Eq. (8.2.7) is also asymptotically stable if the zero solution of Eq. (8.2.8) is asymptotically stable under the linear or nonlinear control  $u = u(\mathbf{x}_c, \tilde{\mathbf{x}}_r)$  with  $u(0,0) = 0$  since

$$\begin{aligned} \mathbf{x}_r(t) &= \tilde{\mathbf{x}}_r(t) + \int_{t-\tau}^t \exp[\mathbf{A}_r(t-\tau-s)] \mathbf{b}_2 u(\mathbf{x}_c, \tilde{\mathbf{x}}_r) ds \\ &= \tilde{\mathbf{x}}_r(t) + \int_{-\tau}^0 \exp[\mathbf{A}_r(-\tau-\xi)] \mathbf{b}_2 u(\mathbf{x}_c, \tilde{\mathbf{x}}_r) d\xi, \end{aligned} \quad (8.2.10a)$$

$$\begin{aligned} \|\mathbf{x}_r(t)\| &\leq \|\tilde{\mathbf{x}}_r(t)\| \\ &+ \tau \|u(\mathbf{x}_c, \tilde{\mathbf{x}}_r)\| \cdot \max_{-\tau \leq \xi \leq 0} (\|\exp[-\mathbf{A}_r(\tau + \xi)]\|) \rightarrow 0, \quad t \rightarrow +\infty. \end{aligned} \tag{8.2.10b}$$

To complete the design of local stabilization, some approximation should be used to simplify the integral in Eq. (8.2.7). From a practical point of view, a feasible choice is to assume that the time delay is very short, then

$$\begin{aligned} \int_{t-\tau}^t \exp[\mathbf{A}_r(t-\tau-s)] \mathbf{b}_2 u(s) ds &= \exp(-\mathbf{A}_r \tau) \int_{-\tau}^0 \exp(-\mathbf{A}_r \xi) \mathbf{b}_2 u(t+\xi) d\xi \\ &= (\tau u + \frac{\dot{u} - \mathbf{A}_r u}{2} \tau^2 + \dots) \tilde{\mathbf{b}}_2. \end{aligned} \tag{8.2.11}$$

Thus, Eq. (8.2.7) can be recast in the following form

$$\begin{cases} \dot{\mathbf{x}}_c = \mathbf{A}_c \mathbf{x}_c + \mathbf{F}(\mathbf{x}_c, \tilde{\mathbf{x}}_r - \tau \tilde{\mathbf{b}}_2 u) + \tau^2 \mathbf{\Delta}_F, \\ \dot{\tilde{\mathbf{x}}}_r = \mathbf{A}_r \tilde{\mathbf{x}}_r + \tilde{\mathbf{b}}_2 u + \mathbf{G}(\mathbf{x}_c, \tilde{\mathbf{x}}_r - \tau \tilde{\mathbf{b}}_2 u) + \tau^2 \mathbf{\Delta}_G, \end{cases} \tag{8.2.12}$$

where  $\mathbf{\Delta}_F$  and  $\mathbf{\Delta}_G$  are the nonlinear terms with respect to  $\tilde{\mathbf{x}}_r, \mathbf{x}_c, u, \dot{u}, \dots$ . As the time delay  $\tau$  is short,  $\tau^2 \mathbf{\Delta}_F$  and  $\tau^2 \mathbf{\Delta}_G$  can be neglected when the local stabilization is concerned with.

In summary, if the time delay is short, the local stabilization related to Eq. (8.2.7) can be simplified to the local stabilization problem as following

$$\begin{cases} \dot{\mathbf{x}}_c = \mathbf{A}_c \mathbf{x}_c + \mathbf{F}(\mathbf{x}_c, \mathbf{x}_s - \tau \tilde{\mathbf{b}}_2 u), \\ \dot{\mathbf{x}}_s = \mathbf{A}_s \mathbf{x}_s + \tilde{\mathbf{b}}_2 u + \mathbf{G}(\mathbf{x}_c, \mathbf{x}_s - \tau \tilde{\mathbf{b}}_2 u), \end{cases} \tag{8.2.13}$$

where  $\mathbf{A}_c$  has only the pure imaginary eigenvalues and  $\mathbf{A}_s$  is Hurwitz stable. In this case, the integral in Eq. (8.2.8) can be regarded as an approximation of rectangle quadrature.

**(2) Stabilization to the simplified nonlinear system**

Now, we focus on the local stabilization of Eq. (8.2.13) by using feedback. Let the control force be in the form, see, (Liaw and Abed 1990), (Liaw 1998) and (Behash and Sastry 1988),

$$u = -\mathbf{k}_c^T \mathbf{x}_c + q(\mathbf{x}_c), \tag{8.2.14}$$

where  $q(\mathbf{x}_c)$  is a nonlinear function in  $\mathbf{x}_c$ . Then, we have

$$\begin{cases} \dot{\mathbf{x}}_c = \mathbf{A}_c \mathbf{x}_c + \tilde{\mathbf{F}}(\mathbf{x}_c, \mathbf{x}_s), \\ \dot{\mathbf{x}}_s = \mathbf{A}_s \mathbf{x}_s + \mathbf{B} \mathbf{x}_c + \tilde{\mathbf{G}}(\mathbf{x}_c, \mathbf{x}_s), \end{cases} \quad (8.2.15)$$

with

$$\begin{cases} \mathbf{B} = -\tilde{\mathbf{b}}_2 \mathbf{k}_c^\top, \\ \tilde{\mathbf{F}}(\mathbf{x}_c, \mathbf{x}_s) = \mathbf{F}(\mathbf{x}_c, \mathbf{x}_s - \tau \tilde{\mathbf{b}}_2 [-\mathbf{k}_c^\top \mathbf{x}_c + q(\mathbf{x}_c)]), \\ \tilde{\mathbf{G}}(\mathbf{x}_c, \mathbf{x}_s) = \mathbf{G}(\mathbf{x}_c, \mathbf{x}_s - \tau \tilde{\mathbf{b}}_2 [-\mathbf{k}_c^\top \mathbf{x}_c + q(\mathbf{x}_c)]). \end{cases} \quad (8.2.16)$$

As stated in (Huang 1984), for any matrices  $\mathbf{A}$ ,  $\mathbf{B}$  and  $\mathbf{C}$ , the matrix equation

$$\mathbf{A}\mathbf{X} + \mathbf{X}\mathbf{B} = \mathbf{C} \quad (8.2.17)$$

is equivalent to a linear equation

$$(\mathbf{A} \otimes \mathbf{I} + \mathbf{I} \otimes \mathbf{B}^\top) \mathbf{vec}(\mathbf{X}) = \mathbf{vec}(\mathbf{C}), \quad (8.2.18)$$

where  $\otimes$  is the *Kronecker product*, and  $\mathbf{vec}(\mathbf{X})$  is the vector composed of the columns of  $\mathbf{X}$  taken in order. Eq. (8.2.17) has a unique solution  $\mathbf{X}$  if and only if none of the eigenvalues  $\lambda_i(\mathbf{A}) + \mu_j(\mathbf{B})$  of  $\mathbf{A} \otimes \mathbf{I} + \mathbf{I} \otimes \mathbf{B}^\top$  are zeros, where  $\lambda_i(\mathbf{A})$  and  $\mu_j(\mathbf{B})$  are the  $i$ -th and  $j$ -th eigenvalues of  $\mathbf{A}$  and  $\mathbf{B}$ , respectively. For  $\mathbf{A}_s, \mathbf{A}_c$  and  $\mathbf{B}$  in Eq. (8.2.15), thus, there exists a unique matrix  $\mathbf{E}$  such that

$$\mathbf{A}_s \mathbf{E} - \mathbf{E} \mathbf{A}_c = -\mathbf{B}, \quad (8.2.19)$$

because  $\lambda_i(\mathbf{A}_s) + \mu_j(-\mathbf{A}_c) \neq 0$  holds for all possible  $i$  and  $j$ .

Let  $\mathbf{y} \equiv \mathbf{x}_c$  and  $\mathbf{z} \equiv \mathbf{x}_s - \mathbf{E} \mathbf{x}_c$ . Then, we cast Eq. (8.2.15) as

$$\begin{cases} \dot{\mathbf{y}} = \mathbf{A}_c \mathbf{y} + \mathbf{f}(\mathbf{y}, \mathbf{z}), \\ \dot{\mathbf{z}} = \mathbf{A}_s \mathbf{z} + \mathbf{g}(\mathbf{y}, \mathbf{z}), \end{cases} \quad (8.2.20)$$

where

$$\begin{cases} \mathbf{f}(\mathbf{y}, \mathbf{z}) \equiv \tilde{\mathbf{F}}(\mathbf{y}, \mathbf{E}\mathbf{y} + \mathbf{z}), \\ \mathbf{g}(\mathbf{y}, \mathbf{z}) \equiv \tilde{\mathbf{G}}(\mathbf{y}, \mathbf{E}\mathbf{y} + \mathbf{z}) - \mathbf{E} \cdot \tilde{\mathbf{F}}(\mathbf{y}, \mathbf{E}\mathbf{y} + \mathbf{z}). \end{cases} \quad (8.2.21)$$

As stated in the center manifold theorem, there exists a local invariant manifold  $\mathbf{z} = \mathbf{h}(\mathbf{y})$ , which yields the following equation

$$\mathbf{D}\mathbf{h}(\mathbf{y})[\mathbf{A}_c \mathbf{y} + \mathbf{f}(\mathbf{y}, \mathbf{h}(\mathbf{y}))] = \mathbf{A}_s \mathbf{h}(\mathbf{y}) + \mathbf{g}(\mathbf{y}, \mathbf{h}(\mathbf{y})), \quad (8.2.22)$$

where  $\mathbf{D}\mathbf{h}(\mathbf{y})$  is the Jacobian of  $\mathbf{h}$  with respect to  $\mathbf{y}$ , and  $\mathbf{h}(\mathbf{y})$  yields  $\mathbf{h}(0) = 0$  and  $\mathbf{D}\mathbf{h}(0) = 0$ . The flow on the center manifold satisfies

$$\dot{\mathbf{y}} = \mathbf{A}_c \mathbf{y} + \mathbf{f}(\mathbf{y}, \mathbf{h}(\mathbf{y})). \quad (8.2.23)$$

Therefore, to stabilize Eq. (8.2.13), we need to choose  $u$  in the form of Eq. (8.2.14) such that the zero solution of Eq. (8.2.23) is asymptotically stable.

Now, it is possible to use the standard stability criteria for autonomous ordinary differential equations, see (Behtash and Sastry 1988) and (Guckenheimer and Holmes 1983), so as to check the stability of Eq. (8.2.23). For example, the zero solution of a two-dimensional differential equation in the form

$$\begin{bmatrix} \dot{x} \\ \dot{y} \end{bmatrix} = \begin{bmatrix} 0 & \omega_0 \\ -\omega_0 & 0 \end{bmatrix} \begin{bmatrix} x \\ y \end{bmatrix} + \begin{bmatrix} f(x,y) \\ g(x,y) \end{bmatrix} \quad (8.2.24)$$

is asymptotically stable if the following condition holds

$$\frac{1}{16\omega_0} [\omega_0 (f_{xxx} + f_{xyy} + g_{xxy} + g_{yyx}) + f_{xy} (f_{xx} + f_{yy}) - g_{xy} (g_{xx} + g_{yy}) - f_{xx} g_{xx} + f_{yy} g_{yy}] \Big|_{(x,y)=(0,0)} < 0. \quad (8.2.25)$$

### 8.2.3 Case Studies

**Example 8.2.1** To demonstrate the approach, consider a three-dimensional system with a short time delay in the control path as following

$$\begin{cases} \dot{x}(t) = y(t) - x^3(t) + x(t)y^2(t) - 2y(t)z(t), \\ \dot{y}(t) = x^3(t) + x(t)z(t), \\ \dot{z}(t) = -5z(t) + u(t-\tau). \end{cases} \quad (8.2.26)$$

When  $u=0$  and  $z=0$ , the system state  $[x \ y]^T$  is not asymptotically stable at  $(0,0)$ . By using the transform

$$\eta = z + \int_{t-\tau}^t \exp[-5(t-\tau-s)]u(s)ds, \quad (8.2.27)$$

we arrive at

$$\begin{cases} \dot{x} = y - x^3 + xy^2 - 2y\{\eta - \int_{t-\tau}^t \exp[-5(t-\tau-s)]u(s)ds\}, \\ \dot{y} = x^3 + x\{\eta - \int_{t-\tau}^t \exp[-5(t-\tau-s)]u(s)ds\}, \\ \dot{\eta} = -5\eta + \exp(5\tau)u. \end{cases} \quad (8.2.28)$$

Applying the rectangle quadrature to Eq. (8.2.28) gives



$$\begin{cases} \dot{x}=y-x^3+xy^2-2y(\eta-\tau e^{5\tau}u), \\ \dot{y}=x^3+x(\eta-\tau e^{5\tau}u), \\ \dot{\eta}=-5\eta+e^{5\tau}u, \end{cases} \quad (8.2.29)$$

where the delayed term has disappeared. To stabilize the simplified system, we implement a nonlinear control force in the form

$$u=\alpha x^2+\beta xy+\gamma y^2. \quad (8.2.30)$$

Suppose that the center manifold is truncated to order 2, namely,

$$h(x,y)=ax^2+bxy+cy^2+\text{h.o.t.} \quad (8.2.31)$$

Substituting Eqs. (8.2.30) and (8.2.31) into Eq. (8.2.22) first and then equating the coefficients of the state variables, we have the following relationship

$$\begin{bmatrix} 5 & 0 & 0 \\ 2 & 5 & 0 \\ 0 & 1 & 5 \end{bmatrix} \begin{bmatrix} a \\ b \\ c \end{bmatrix} = e^{5\tau} \begin{bmatrix} \alpha \\ \beta \\ \lambda \end{bmatrix}. \quad (8.2.32)$$

The flow on the center manifold yields

$$\begin{cases} \dot{x}=y-x^3+xy^2-2y[ax^2+bxy+cy^2-\tau e^{5\tau}(\alpha x^2+\beta xy+\gamma y^2)]+\text{h.o.t} \\ \dot{y}=x^3+x[ax^2+bxy+cy^2-\tau e^{5\tau}(\alpha x^2+\beta xy+\gamma y^2)]+\text{h.o.t} \end{cases} \quad (8.2.33)$$

which is locally stabilizable at  $(0,0)$ . Denote the nonlinear terms in the right-hand side of Eq. (8.2.33) by  $f(x,y)$  and  $g(x,y)$  respectively, the coefficients  $a, b, c$  and  $\alpha, \beta, \lambda$  should be chosen to meet the stability conditions, see (Behtash and Sastry 1988),

$$\frac{1}{3}g_{xxx}+(f_{xx})^2|_{(x,y)=(0,0)}<0, \quad \text{namely,} \quad 1+a-5a\tau<0, \quad (8.2.34)$$

and

$$g_{xy}+f_{xx}-f_{xx}\cdot(f_{xy}+g_{yy})|_{(x,y)=(0,0)}<0, \quad \text{namely,} \quad b-(2a+5b)\tau-3<0. \quad (8.2.35)$$

For  $\tau=0.05$ , a choice for the parameters of center manifold to stabilize Eq. (8.2.33) is  $a=-2.568$ ,  $b=-11.81$  and  $c=2.363$ , while the corresponding control parameters are  $\alpha=-10$ ,  $\beta=-50$  and  $\gamma=0$ . Thus, the control force is

$$u=-10x^2-50xy, \quad (8.2.36)$$

and the corresponding center manifold is in the form

$$h = -2.568x^2 - 11.81xy + 2.363y^2 + \text{h.o.t.} \tag{8.2.37}$$

Figure 8.2.1 shows the phase portrait of the flow on the center manifold starting from (0.1, -0.1) when  $\tau = 0.05$ ,  $\alpha = -10$ ,  $\beta = -50$  and  $\gamma = 0$ .

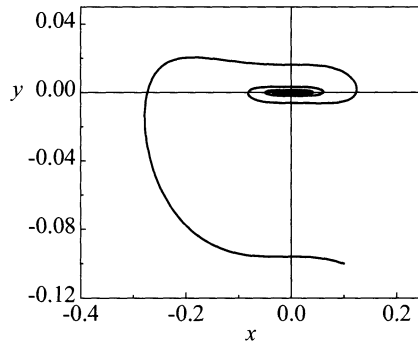


**Fig. 8.2.1.** A phase portrait of the flow on the center manifold when  $\tau=0.05$ ,  $\alpha=-10$ ,  $\beta=-50$  and  $\gamma=0$

### 8.2.4 Discussions on Approximate Integrals

In the design of stabilization strategy in Subsection 8.2.3, the rectangle quadrature has been used to simplify the integral in the system equation. In this subsection, the feasibility of truncated Eq. (8.2.8) to Eq. (8.2.14) is discussed through a few illustrative examples in Subsection 8.2.3. To approximate the integral, either the rectangle quadrature or the trapezoidal quadrature, or the Simpson quadrature can be implemented if the time delay is short. The approximations of the trapezoidal quadrature and the Simpson quadrature to the integral in Eq. (8.2.28) are respectively given as following

$$\int_{t-\tau}^t \exp(-5(t-\tau-s))u(s)ds = \frac{\tau}{2}[e^{5\tau}u(t)+u(t-\tau)], \tag{8.2.38}$$

$$\int_{t-\tau}^t \exp[-5(t-\tau-s)]u(s)ds = \frac{\tau}{16}[u(t)e^{5\tau} + 4e^{5\tau/2}u(t-\frac{\tau}{2}) + u(t-\tau)]. \tag{8.2.39}$$

In the following two examples, a comparison is made between the phase portraits of  $[x \ y]^T$  computed by the rectangle quadrature and the Simpson quadrature with variable steps, respectively.

**Example 8.2.2** Consider again the case when  $\alpha = -10$ ,  $\beta = -50$  and  $\gamma = 0$ . For  $\tau = 0.05$ , we can hardly observe the difference between the two trajectories in Fig.

8.2.2a. If we increase the time delay to  $\tau=0.1$ , the difference between the two trajectories increases, but is still acceptable. However, when the time delay increases to 0.15, the difference becomes unacceptable, see, Fig. 8.2.2b. In this case, the rectangle quadrature is not appropriate for the approximation when the time delay is long. However, the two trajectories determined by using the trapezoidal quadrature and the Simpson quadrature look almost the same as shown in Fig. 8.2.2b.

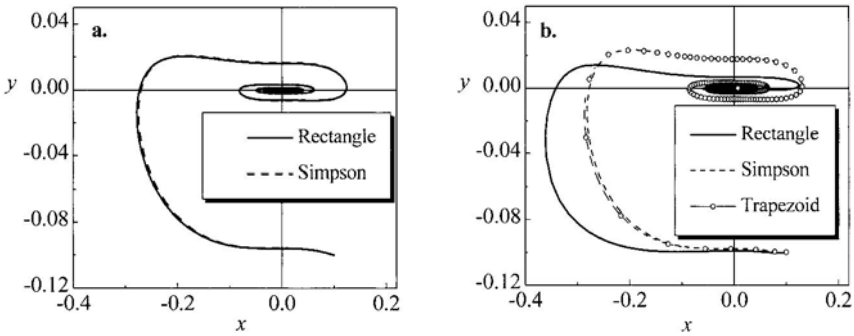


**Fig. 8.2.2.** Comparison between the states  $[x \ y]^T$  of Eq. (8.2.28) computed by different quadratures for  $\alpha=-10$ ,  $\beta=-50$  and  $\gamma=0$ ; **a.**  $\tau=0.05$ , **b.**  $\tau=0.15$

**Example 8.2.3** Consider the case when  $\alpha=-10$ ,  $\beta=-4$  and  $\gamma=0$ . We have the similar results as those in Example 8.2.2. Figure 8.2.3 shows the differences between the phase portraits of  $[x \ y]^T$  for  $\tau=0.05$  and 0.1, respectively.

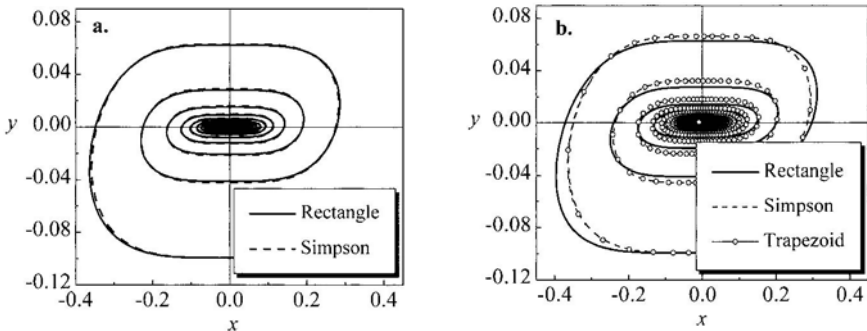


**Fig. 8.2.3.** Comparison between the states  $[x \ y]^T$  of Eq. (8.2.28) computed by different quadratures for  $\alpha=-10$ ,  $\beta=-4$  and  $\gamma=0$ ; **a.**  $\tau=0.05$ , **b.**  $\tau=0.1$

The above examples indicate that when the time delay is considerably short, the approximation by the rectangle quadrature gives excellent accuracy for the local stabilization. If the time delay is not so short, the approach may result in a wrong stability prediction. In this case, it is necessary to implement more accurate quadratures, such as the trapezoidal quadrature and the Simpson quadrature. As shown in Eqs. (8.2.38) and (8.2.39), the controlled system in this case yields a set of delay differential equations.

In summary, when the time delay in control path is short, the local stabilization, by means of delayed state feedback, for ordinary differential systems in critical cases can be completed in two steps. The key step is to convert the dynamic system under delayed control into a slightly perturbed dynamic system governed by a set of ordinary differential equations. Once the simplified system equation is obtained, the center manifold technique can be applied to the local stabilization. The analysis and numerical examples indicate that the approach gives the approximation excellent accuracy if the time delay is short enough, and consequently, the center manifold reduction to the local stabilization works effectively. However, if the time delay is long, the approach may not predict the stabilization correctly.

### 8.3 Controlling Chaotic Motion

The early studies on controlling chaos mainly focused on the attenuation of chaotic motion through the use of available techniques in control engineering until Ott, Grebogi and Yorke proposed their seminal control strategy, see (Ott et al. 1990). The idea of this control strategy, usually referred to as *OGY control*, is quite interesting. One of the infinite number of unstable periodic motions embedded in the chaotic attractor is chosen as the target first, then the chaotic motion, as soon as it wanders into the neighborhood of target, is directed to the stable invariant manifold of the target and stabilized. Compared with previous studies, OGY control makes use of the features of chaos, and thus needs very little control energy and small structural modification. Over the past decade, OGY control has received great attention and had many varieties. Among them, the delayed linear feedback control proposed in (Pyragas 1992) is a simple, but effective one. This subsection presents the delay control of Pyragas through an example of controlling the chaotic motion of a harmonically forced Duffing oscillator, and addresses an open problem in the design of delayed feedback.

### 8.3.1 Basic Idea

Consider an  $n$ -dimensional non-autonomous system described by

$$\dot{z}(t) = f(z(t), t), \quad z \in R^n, \quad (8.3.1)$$

where  $f: R^{n+1} \rightarrow R^n$  is of period  $T$  with respect to  $t$ . Suppose that the system has a chaotic attractor, where an infinite number of unstable periodic orbits are embedded. Among them, an unstable motion  $z_p(t)$  of period  $\tau = mT$  is selected as the target of control, where  $m$  is a positive integer. To direct a chaotic motion  $z(t)$  near  $z_p(t)$  to  $z_p(t)$ , a control force  $g(t)$  is introduced into the system. More specifically, Eq. (8.3.1) with the control force  $g(t)$  is partitioned as

$$\begin{cases} \dot{x}(t) = p(x(t), y(t), t), \\ \dot{y}(t) = q(x(t), y(t), t) + g(t), \end{cases} \quad (8.3.2)$$

where  $y \in R$  is an observable and controllable state variable and  $x \in R^{n-1}$  is the vector of remaining state variables which are not available or not of interest for observation. As suggested in (Pyragas 1992), the control force can be a delayed linear feedback as following

$$g(t) = v[y(t) - y(t - \tau)], \quad (8.3.3)$$

where  $v$  is an experimentally adjustable feedback gain. The objective of control now is to reduce the Lyapunov exponents of system through the use of delayed linear feedback such that the unstable periodic motion  $z_p(t)$  becomes stable. When  $z(t)$  arrives at  $z_p(t)$ ,  $g(t) = 0$  holds. That is, the introduced control force  $g(t)$  does not change the target of control. The control force  $g(t)$  can be actuated again whenever the motion  $z(t)$  deviates from the target  $z_p(t)$  to a certain extent.

**Example 8.3.1** To demonstrate the efficacy of delayed linear feedback, we consider a harmonically forced Duffing oscillator as follows

$$\begin{cases} \dot{x}(t) = y(t), & x \in R, \\ \dot{y}(t) = x(t) - x^3(t) - 0.02y(t) + 2.5\cos t. \end{cases} \quad (8.3.4)$$

Fig. 8.3.1a shows a chaotic motion of the oscillator obtained in the numerical simulation, and the corresponding chaotic attractor embeds an infinite number of unstable periodic orbits. Among them, a period-1 orbit shown in Fig. 8.3.1b was taken as the target of control so that the delayed linear feedback became

$$g(t) = v[y(t) - y(t - 2\pi)], \quad (8.3.5)$$

where  $\nu$  was set to  $-0.25$  after a few tests. The forced motion of oscillator without control exhibited chaotic behavior within the first 30 circles of excitation, namely,  $t \leq 60\pi \approx 188.5s$ , and then became periodic gradually after the delayed feedback control was put to use. Figure 8.3.2 shows the time histories of both displacement and control force of the above process. When the forced motion of oscillator looked periodic, the control force approached to zero.

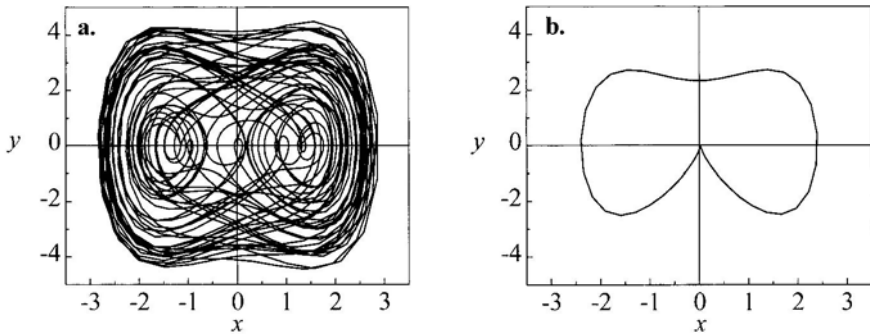


Fig. 8.3.1. Phase portraits of Eq. (8.3.4); a. a chaotic motion, b. a period-1 motion

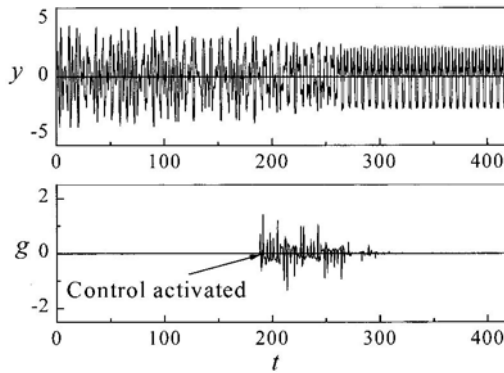


Fig. 8.3.2. Controlling process of a chaotic motion

### 8.3.2 Choice of Feedback Gain

The success of delayed linear feedback relies on a proper choice of feedback gain. To acquire a good understanding of this problem, we look at the stabilization of unstable  $z_p(t)$  of period  $\tau$  by using a full state feedback, so that Eq. (8.3.1) becomes

$$\dot{z}(t) = f(z(t), t) + U[z(t) - z(t - \tau)], \quad (8.3.6)$$

where  $U$  is the constant matrix of state feedback gain.

The small perturbation  $\Delta z(t)$  near the unstable periodic motion  $z_p(t)$  yields a set of linear delay differential equations with periodic coefficients as following

$$\Delta \dot{z}(t) = D_z f(z_p(t), t) \Delta z(t) + U[\Delta z(t) - \Delta z(t - \tau)]. \quad (8.3.7)$$

The Floquet theory extended in (Hale 1977) indicates that  $\Delta z(t)$  should be in the form

$$\Delta z(t) = \exp[(A + i\Omega)t] u(t), \quad (8.3.8)$$

where  $A$  and  $\Omega$  are the diagonal matrices for real and imaginary parts of the Floquet exponents of Eq. (8.3.7), and  $u(t)$  is a function vector of period  $\tau$ . Substituting Eq. (8.3.8) into Eq. (8.3.7) yields

$$\begin{aligned} \dot{u}(t) + (A + i\Omega)u(t) &= \{D_z f(z_p(t), t) + U\{I - \exp[-(A + i\Omega)\tau]\}\} u(t) \\ &\equiv A(U, t)u(t). \end{aligned} \quad (8.3.9)$$

Let  $\Gamma_A(U)$  be the matrix of the Floquet exponents of matrix  $A(U, t)$ , depending on the matrix  $U$  of feedback gain. That is,

$$A + i\Omega = \Gamma_A(U). \quad (8.3.10)$$

When  $U = 0$ , we have  $\Gamma_A(0) = A_0 + i\Omega_0$ , representing the diagonal matrix of the Floquet exponents of Eq. (8.3.1) evaluated at the unstable periodic motion  $z_p(t)$ . In this case, at least one Floquet exponent in  $A_0$  is positive. The task of stabilization of  $z_p(t)$ , thus, is to choose the matrix  $U$  of state feedback gain properly so that all entries in  $A$  are negative.

Unfortunately, it is only possible to determine  $\Gamma_A(U)$  approximately or numerically. In (Just et al. 1997), for instance,  $\Gamma_A(U)$  was written as the Taylor expansion truncated to the first order and the choice of  $U$  was discussed for some special cases. Even in this approximation, it is still an open problem to determine the Jacobian  $D_U \Gamma_A(0)$  for the Taylor expansion.

In practice, therefore, it seems only possible to determine the feedback gain experimentally, rather than theoretically. To get rid of the difficulty in the try-and-error process, the possibility of automatic adjustment of time delay and feedback gain was explored in (Kittle et al. 1995) and (Nakajima et al. 1997). If the control strategy is numerically simulated in advance, then the continuation technique can be used to determine the feedback gain according to the variation of the largest Lyapunov exponent of calculated phase trajectory.

## References

- Arusawatwung S (1996) Stability of retarded delay differential systems. *International Journal of Control* **65**: 347-367
- Bai EW, Chyng DH (1993) Improving delay estimates derived from least-square algorithms and Pade approximations. *International Journal of Systems Science* **24**: 745-756
- Bajaj AK, Georgiou IT, Corless M (1997) Dynamics of singular perturbed nonlinear systems with two degrees-of-freedom. In: van Campen DH (ed) *Proceedings of IUTAM symposium on interaction between dynamics and control in advanced mechanical systems*. Kluwer Academic Publishers, Amsterdam, pp9-16
- Barmish BR, Shi ZH (1989) Robust stability of perturbed systems with time delays. *Automatica* **25**: 321-328
- Bartlett AC, Hollot CV, Huang L (1988) Root locations of an entire polytope of polynomials: It suffices to check the edges. *Mathematics of Control, Signals, and Systems* **1**: 61-71
- Behtash S, Sastry S (1988) Stabilization of nonlinear systems with uncontrollable linearization. *IEEE Transactions on Automatic Control* **33**: 585-590
- Belair J, Campbell SA (1994) Stability and bifurcation of equilibria in a multi-delayed differential equation. *SIAM Journal on Applied Mathematics* **54**: 1402-1424
- Bhattacharyya SP, Chapellat H, Keel L (1995) *Robust control: the parametric approach*. Prentice-Hall, New York
- Blondel VD, Tsitsiklis JN (2000) A survey of computational complexity results in systems and control. *Automatica* **36**: 1249-1274
- Casal A, Freeman MA (1980) Poincaré-Lindstedt approach to bifurcation problem for differential delay equations. *IEEE Transactions on Automatic Control* **25**: 967-973
- Chen J (1995) On computing the maximal delay intervals for stability of linear delay systems. *IEEE Transactions on Automatic Control* **40**: 1087-1093
- Chen JC (1997) Designing stabilizing controllers and observers for uncertain linear systems with time-varying delay. *IEE Proceedings, Control Theory and Applications* **144**: 331-333
- Debnath L, Mikusinski P (1999) *Introduction to Hilbert spaces with applications*, 2nd edn. Academic Press, San Diego
- Diekmann O, van Gils SA, Verduyn Lunel SM, Walther HO (1995) *Delay equations, functional-, complex-, and nonlinear analysis*. Springer-Verlag, New York
- Dixon AL (1908) The eliminant of three quantics in two independent variables. *Proceedings of London Mathematical Society* **6**: 468-478
- Elnaggar A, Dumont GA, Elshafei AL (1989) Recursive estimation for system of unknown delay. In: *Proceedings of the 28th conference on decision and control*. Tampa, Florida, pp1809-1810
- Eykhoff P (1961) Process-parameter estimation using an analog model. In: *Proceedings of 3rd international analog computation meeting*. Opatija, Yugoslavia, pp276-290



- Faria F, Magalhaes LT (1995) Normal forms for retarded functional differential equations and applications to Bogdanov-Takens singularity. *Journal of Differential Equations* **122**: 201-224
- Ferretti G, Maffezzoni C, Scattolini R (1991) Recursive estimation of time delay in sampled systems. *Automatica* **27**: 653-661
- Ferretti G, Maffezzoni C, Scattolini R (1996) On the identifiability of the time delay with least-squares methods. *Automatica* **32**: 449-453
- Fiagbedzi YA, Pearson AE (1986) Feedback stabilization of linear autonomous time lag systems. *IEEE Transactions on Automatic Control* **31**: 847-855
- Frenichel N (1979) Geometric singular perturbation theory for ordinary differential equations. *Journal of Differential Equations* **31**: 53-98
- Fu MY, Olbrot AW, Polis MP (1989) Robust stability for time-delay systems: the edge theorem and graphical tests. *IEEE Transactions on Automatic Control* **34**: 813-820
- Gawthrop PJ, Nihtila MT (1985) Identification of time delays using a polynomial identification method. *Systems and Control Letters* **5**: 267-271
- Georgiou IT, Bajaj AK, Corless M (1998) Slow and fast invariant manifolds, and normal modes in a two degree-of-freedom structural dynamical systems with multiple equilibrium states. *International Journal of Non-Linear Mechanics* **33**: 275-300
- Gopalsamy K (1992) *Stability and oscillations in delay differential equations of population dynamics*. Kluwer Academic Publishers, Dordrecht
- Guckenheimer J, Holmes P (1983) *Nonlinear oscillations, dynamical systems, and bifurcations of vector fields*. Springer-Verlag, New York
- Hale JK (1971) Critical cases for neutral functional differential equations. *Journal of Differential Equations* **10**: 59-82
- Hale JK (1977) *Theory of functional differential equations*. Springer-Verlag, New York
- Hale JK, Lunel SMV (1993) *Introduction to functional differential equations*. Springer-Verlag, New York
- Hassard B (1997) Counting roots of the characteristic equation for linear delay-differential systems. *Journal of Differential Equations* **136**: 222-235
- Hassard B, Kazarinoff N, Wan YH (1981) *Theory and applications of Hopf bifurcations*. Cambridge University Press, London
- Heck A (1996) *Introduction to MAPLE*. Springer-Verlag, New York
- Heiden U, Walter HO (1983) Existence of chaos in control system with delayed feedback. *Journal of Differential Equations* **47**: 273-295
- Hsia TC (1968) Identification of parameters in linear systems with transport lags. In: *Proceedings of the 11th midwest symposium on circuit theory*. University of Notre Dame, Notre Dame, pp62-69
- Hsu CS (1970) Application of the  $\tau$ -decomposition method to dynamical systems subject to the retarded follower forces. *Journal of Applied Mechanics* **37**: 258-266
- Ho KC, Ching PC (1993) Statistical performance analysis of a fast stochastic gradient for constrained adaptive time delay estimation. *Circuits, Systems and Signal Processing* **12**: 453-464
- Hu HY, Wang ZH (1998) Stability Analysis of damped SDOF systems with two time delays in state feedback. *Journal of Sound and Vibration* **214**: 213-225
- Hu HY, Wang ZH (2000) Nonlinear dynamics of controlled mechanical systems with time delays. *Progress in Natural Sciences* **10**: 801-811

- Hu HY, Wu ZQ (2000) Stability and Hopf bifurcation of four-wheel-steering vehicles involving driver's delay. *Nonlinear Dynamics* **22**: 361-374
- Hu HY, Dowell EH, Virgin LN (1998a) Resonance of a harmonically forced Duffing oscillator with time delay feedback control. *Nonlinear Dynamics* **15**: 311-327
- Hu HY, Dowell EH, Virgin LN (1998b) Stability estimation of high dimensional vibrating systems under state delay feedback control. *Journal of Sound and Vibration* **214**: 497-511
- Huang L (1984) *Linear Algebra in System and Control Theory*. Science Press, Beijing
- Huang L (1992) *Stability theory*. Press of Peking University, Beijing
- Iooss G, Joseph DD (1980) *Elementary stability and bifurcation theory*, Springer-Verlag, New York
- Isidori A (1985) *Nonlinear control systems*. Springer-Verlag, New York
- Just W, Bernard T, Ostheimer M, Reibold E, Benner H (1997) Mechanism of time-delayed feedback control of chaos. *Physical Review Letters* **78**: 203-207
- Kaplan JL, Yorke JA (1974) Ordinary differential equations which yield periodic solutions of differential delay equations. *Journal of Mathematical Analysis and Applications* **48**: 317-324
- Kapur D, Saxena T, Yang L (1994) Algebraic and geometric reasoning using Dixon resultants. ACM international symposium on symbolic and algebraic computation, preprint.
- Kharitonov VL (1979) Asymptotic stability of an equilibrium position of a family of systems of linear differential equations. *Differential Equations* **14**: 1483-1485
- Kharitonov VL, Zhabko AP (1994) Robust stability of time-delay systems. *IEEE Transactions on Automatic Control* **39**: 2388-2397
- Kittel A, Parisi J, Pyragas K (1995) Delayed feedback control of chaos by self-adapted delay time. *Physics Letters A* **198**: 433-436
- Kogan J, Leizarowitz A (1995) Exponential stability of linear systems with commensurate time-delays. *Mathematics of Control, Signals, and Systems* **8**: 65-81
- Kolmanovskii V, Myshkis A (1999) *Introduction to the theory and applications of functional differential equations*. Kluwer Academic Publishers, Dordrecht
- Kuang Y (1993) *Delay differential equations with applications to population dynamics*. Academic Press, New York
- Kurz H, Goedcke W (1981) Digital parameter adaptive control of processes with unknown dead time. *Automatica* **17**: 245-252
- Lam J (1993) Model reduction of delay systems using Padé approximation. *International Journal of Control* **57**: 377-391
- Li SL, Wen LZ (1987) *Functional differential equations (in Chinese)*. Hunan Press of Science and Technology, Changsha
- Liang DF, Christensen GS (1976) New estimation algorithms for discrete non-linear systems and observations with multiple time delays. *International Journal of Control* **23**: 613-625
- Liaw DC (1998) Application of center manifold reduction to nonlinear system stabilization. *Applied Mathematics and Computation* **91**: 243-258
- Liaw DC, Abed EH (1990) Stabilization of tethered satellites during station keeping. *IEEE Transactions on Automatic Control* **35**: 1186-1196
- Liu ZR, Li JB (1996) *Hamiltonian systems and periodic solutions of retarded differential equations (in Chinese)*. Science Press, Beijing

- Manitius AZ (1984) Feedback controllers for a wind tunnel model involving a delay: analytical design and numerical simulation. *IEEE Transactions on Automatic Control* **29**: 1058-1068
- Marshall JE, Gorecki H, Walton K and Korytowski (1992) Time-delay systems: stability and performance criteria with applications. Ellis Horwood, New York.
- McDonald N (1995) Harmonic balance in delay-differential equations. *Journal of Sound and Vibration* **186**: 649-656
- Moiola JL, Chen G (1997) Hopf bifurcation analysis: a frequency domain approach. World Scientific, Singapore
- Moiola JL, Chiacchiarini HG, Desages AC (1996) Bifurcations and Hopf degeneracies in nonlinear feedback systems with time delay. *International Journal of Bifurcations and Chaos* **6**: 661-672
- Mori T, Kokame H (1989) Stability of  $\dot{x}(t) = Ax(t) + Bx(t - \tau)$ . *IEEE Transactions on Automatic Control* **34**: 460-462
- Nagai M, Mitschke M (1987) An adaptive control model of a car-driver and computer simulation of the closed-loop system. In: Proceedings of 10th IAVSD symposium, Prague
- Naimark L, Zeheb E (1997) All constant gain stabilizing controllers for an interval delay system with uncertain parameters. *Automatica* **33**: 1669-1675
- Nakajima H, Ito H, Ueda Y (1997) Automatic adjustment of delay time and feedback gain in delayed feedback control of chaos. *IEICE Transactions on Fundamentals of Electronics, Communications and Computer Sciences*, **E80-A**: 1554-1559
- Nayfeh AH, Mook DT (1979) Nonlinear oscillations. John Wiley, New York
- Nayfeh AH, Chin CM, Pratt J (1997) Perturbation methods in nonlinear dynamics: applications to machining dynamics. *Journal of Manufacture Science and Technology* **119**: 485-493
- Nguyen VD (1999) Nonlinear oscillators under delay control. *Vietnam Journal of Mechanics* **21**: 75-88
- Ohta Y, Kojima A (1999) Formulas for Hankel singular values and vectors for a class of input delay systems. *Automatica* **35**: 201-215
- Olgac N, Holm-Hansen B (1995) Tunable active vibration absorber: the delayed resonator. *Journal of Dynamic Systems, Measurement, and Control* **117**: 513-519
- Ott E, Grebogi C, Yorke JA (1990) Controlling chaos. *Physical Review Letters* **64**: 1196-1199
- Pacejka H (1989) A new tyre model with an application in vehicle dynamics studies. SAE Paper No.89007
- Palkovics L, Venhovens PJ Th (1992) Investigation on stability and possible chaotic motions in the controlled wheel suspension system. *Vehicle System Dynamics* **21**: 269-296
- Phoojaruenchanachai S, Uahchinkul K, Prempraneerach Y (1998) Robust stabilization of a state delayed system. *IEE Proceedings, Control Theory and Applications* **145**: 87-91
- Plaut RH, Hsieh JC (1987) Non-linear structural vibrations involving a time delay in damping. *Journal of Sound and Vibration* **117**: 497-510
- Pyragas K (1992) Continuous control of chaos by self-controlling feedback. *Physics Letters A* **170**: 421-428
- Qin YX, Liu YQ, Wang L, Zheng ZX (1989) Stability of dynamic systems with delays (in Chinese) 2nd edn. Science Press, Beijing

- Robinson WR, Soundack AC (1970) A method for the identification of time delays in linear system. *IEEE Transactions on Automatic Control* **15**: 97-101
- Shayer L, Campbell SA (2000) Stability, bifurcation, and multi-stability in a system of two coupled neurons with multiple time delays. *SIAM Journal of Applied Mathematics* **61**: 673-700.
- Stech H W (1985) Hopf bifurcation calculations for functional differential equations. *Journal of Mathematical Analysis and Applications* **109**: 472-491
- Steiner W, Steindl A, Troger H (1995) Center manifold approach to the control of a tethered satellite system. *Applied Mathematics and Computation* **70**: 315-327
- Stépán G (1989) Retarded dynamical systems: stability and characteristic functions. Longman Scientific and Technical, Essex
- Su HY, Chu J (1998) Stabilizing controller design for a class of nonlinear time-delay systems. *Acta Automatica Sinica* **24**: 30-35
- Su JH, Fong IK, Tseng CL (1994) Stability analysis of linear systems with time delay. *IEEE Transactions on Automatic Control* **39**: 1341-1344
- Tissir E, Hmamed A (1996) Further results on stability of  $\dot{x} = Ax(t) + Bx(t - \tau)$ . *Automatica* **32**: 1723-1726
- Tsytkin YZ, Fu MY (1993) Robust stability of time-delay systems with an uncertain time-delay constant. *International Journal of Control* **57**: 865-879
- Tuch J, Feuer A, Palmor ZJ (1994) Time delay estimation in continuous linear time-invariant systems. *IEEE Transactions on Automatic control* **39**: 823-827
- Van Den Hof PMJ, De Vries DK, Schoen P (1992) Delay structure conditions for identifiability of closed loop systems. *Automatica* **28**: 1047-1050
- Wang L, Wang MQ (1993) On Lyapunov functionals in stability theory of systems with time lag. In: Liao ST (ed) *Dynamic systems*. World Scientific, Singapore, pp248-263
- Wang RJ, Wang WJ (1996)  $\alpha$ -stability analysis of perturbed systems with multiple non-commensurate time delays. *IEEE Transactions on Circuits and Systems -I* **43**: 349-352
- Wang ZH, Hu HY (1998) Stability of linear time variant dynamic systems with multiple time delays. *Acta Mechanica Sinica* **14**: 274-282
- Wang ZH, Hu HY (1999a) Delay-independent stability of retarded dynamic systems of multiple degrees of freedom. *Journal of Sound and Vibration* **226**: 57-81
- Wang ZH, Hu HY (1999b) Robust stability test for retarded dynamic systems by using Padé approximation. *Nonlinear Dynamics* **18**: 275-287
- Wang ZH, Hu HY (1999c) Stabilization to nonlinear systems with short time delays in state feedback. In: *Proceedings of 17th ASME biennial conference on mechanical vibration and noise, Las Vegas, DETC99/VIB-8029*
- Wang ZH, Hu HY (2000) Stability switches of time-delayed dynamic systems with unknown parameters. *Journal of Sound and Vibration* **233**: 215-233
- Wang ZH, Hu HY (2001) Dimensional reduction for delayed dynamic systems composed of stiff and soft substructures. *Nonlinear Dynamics*, **25**: 317-331
- Xu XY (1990) Introduction to the Padé approximation (in Chinese). Shanghai Scientific and Technological Education Publishing House, Shanghai
- Yang L, Hou XR, Zeng ZB (1996a) A complete discrimination system for polynomial. *Sciences in China, Series E* **26**: 424-441
- Yang L, Zhang JZ, Hou XR (1996b) Nonlinear algebraic equation system and automated theorem proving (in Chinese). Shanghai Scientific and Technological Education Publishing House, Shanghai

- Yang ZJ, Hachino T, Tsuji T (1997) On-line identification of continuous time-delay systems combining least-squares techniques with a genetic algorithm. *International Journal of Control* **66**: 23-42
- Zeidler E (1995) *Applied functional analysis*. Springer-Verlag, New York
- Zhang L, Yang CY, Chajes MJ, Cheng AH (1993) Stability of active-tendon structural control with time delay. *ASCE Journal of Engineering Mechanics* **119**: 1017-1024
- Zhang WF (2002) *Nonlinear dynamics of the active chassis for ground vehicles*. Ph. D. dissertation, Nanjing University of Aeronautics and Astronautics
- Zhang WF, Hu HY (2001) Parametric estimation of nonlinear dynamic systems with time delays (in Chinese). *Journal of Vibration Engineering* **14**: 314-318
- Zhang WF, Weng JS, Hu HY (1999) Effect of time delay on active vehicle suspensions equipped with "sky-hook" damper (in Chinese). *Journal of Vibration Engineering* **12**: 486-491
- Zheng WX, Feng CB (1990) Identification of stochastic time lag systems in the presence of colored noise. *Automatica* **26**: 769-779
- Zheng WX, Feng CB (1991) Optimizing search-based identification of stochastic time-delay systems. *International Journal of Systems Science* **22**: 783-792

# Index

- Active suspension, 4, 102, 199, 205
- Active tendon, 3, 82
- Adjoint eigenvalue problem, 152
- Adjoint operator, 192, 201, 217, 238
- Asymptotically stable, 38
  
- Banach space, 28, 41, 54, 189, 190, 195, 200, 201, 202, 222, 228
- Bezout matrix, 73
- Bilinear form, 191, 203, 218, 238
  
- Center manifold, 206, 219
  - reduction, 198, 206
  - theorem, 201, 203, 205, 206
- Chaotic
  - attractor, 283
  - motion, 282
- Characteristic
  - equation, 43
  - function, 35
  - root, 36, 43
- Commensurate time delays, 98, 135, 140
- Convex combination, 116
- Crossover, 16
  
- Decomposition, 194, 215
- Delayed resonator, 269
- Delay-independent stable, 46, 61, 65
- Dense, 191
- Discrimination matrix, 73
- Discrimination sequence, 74
- Dixon's
  - reduced polynomial, 131
  - reduced polynomial equations, 133
  - resultant, 133
  - resultant elimination, 130
- $D$ -stability, 115, 136
- Duffing oscillator, 3, 234, 248, 260, 283
  
- Edge of polytope, 126
- Edge theorem, 115, 127
  
- Eigenspace, 193, 204
- Eigenvalue, 193
- Equivalent
  - damping, 253, 257, 268
  - stiffness, 268
- Exponential asymptotic stability, 38
  
- Fast
  - invariant manifold, 190
  - manifold, 184
  - time, 184, 202
- Finite time delays, 86
- Fitness
  - function, 17
  - number, 15
- Fixed Arc, 260
- Flatness of solution, 33
- Floquet exponents, 285
- Floquet theory, 227
- Four-wheel-steering vehicle, 6, 109, 216
- Fredholm alternative, 222, 225, 239
- Frequency response function, 10
- Frequency-amplitude relation, 251, 257
- Functional differential equation, 41, 190, 194, 222
- Fundamental solutions, 36
  
- Gateaux derivatives, 224
- Gauss elimination, 133, 138, 139
- General solution, 35
- Generalized eigenspace, 193
- Generalized Sturm criterion, 75
- Generators, 126
- Genetic algorithms, 14
- Global asymptotic stability, 38
- Gronwall inequality, 33
  
- Hassard theorem, 47
- Hopf bifurcation, 213, 231, 237, 246
  - subcritical, 219, 243
  - supercritical, 219

- Hurwitz stable, 40, 117
- Impedance difference, 23
- Impulse response function, 35
- Interval stable, 115
- Kharitonov theorem, 176, 178
- Kronecker product, 277
- Laplace transform, 35
- Lyapunov, 37
  - exponent, 285
  - function, 38
  - functional, 41
  - method, 38
- Magic formula, 7, 110
- MAPLE routine *discr*, 74, 98, 104, 111
- Method of characteristic function, 38
- Method of step-by-step, 28
- Michailov's criterion, 51
- Modified sign table, 74
- Most dangerous eigenvalues, 155
- Multiple scales, 243, 249, 259
- Mutation, 16
- Neutral type, 27
- Newton-Raphson iteration, 157, 166
- Null space, 193
- Nyquist diagram, 53, 117, 128, 147
- OGY control, 282
- Over-steered, 110, 113
- Padé approximation, 10, 168, 189
- Perceptual delay, 8
- Perturbation, 157, 230
- Poincaré
  - mapping, 260
  - plate, 260
  - section, 248, 260
- Pole assignment, 275
- Polytope, 124
- Pontryakin Theorem, 45
- Quarter car model, 4, 102, 199, 205
- Quasi-polynomial, 43
- Rayleigh quotient, 156
- Razumikhin condition, 39
- Reduced system, 183
- Reproduction, 15
- Resolvent set, 192
- Resonance
  - primary, 249, 251, 262
  - subharmonic, 249, 254, 263
- Retarded type, 27
- Robust stability, 115
- Rouche's theorem, 45, 154
- Routh-Hurwitz
  - criterion, 60, 103, 111, 173, 181, 210
  - stability condition, 83, 98, 112, 133
- Runge-Kutta approach, 246
- Schur stability, 136, 138
- Secular term, 230, 231, 244, 250, 255
- Sequence of sub-resultants, 74
- Shooting technique, 259
- Sign table of the sequence, 70
- Singularly perturbed differential equation, 181
- Sky-hook damper, 5, 102
- Slow
  - invariant manifold, 190
  - manifold, 183
  - time, 184
- Spectrum, 192
- Stability switch, 91, 102, 235
- Stabilization, 272, 284
- Stable, 38
- Stiff-soft system, 189, 198
- Sturm
  - criterion, 71
  - sequence, 71
- Taylor expansion, 10, 13, 56, 156, 168, 179, 181, 189, 285
- Under-steered, 110, 112
- Uniformly asymptotic stability, 38
- Value set, 126
- Vertex quasi-polynomials, 124, 126
- Wright equation, 220, 224, 227, 232